Springer Protocols

Methods in Molecular Biology 639

Plant Stress Tolerance

Methods and Protocols

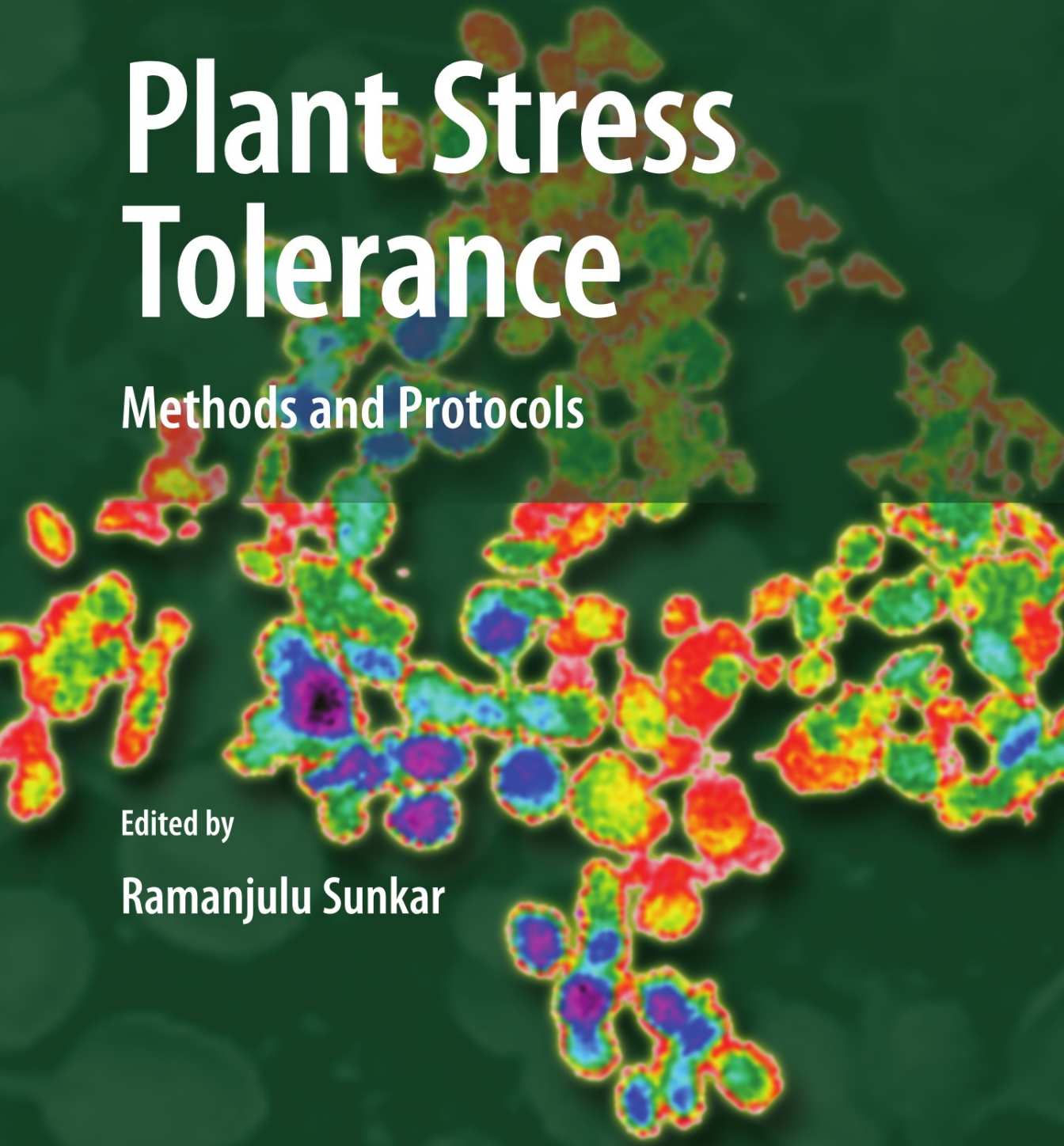

Edited by

Ramanjulu Sunkar

Humana Press

METHODS IN MOLECULAR BIOLOGY™

Series Editor
John M. Walker
School of Life Sciences
University of Hertfordshire
Hatfield, Hertfordshire, AL10 9AB, UK

For other titles published in this series, go to
www.springer.com/series/7651

Plant Stress Tolerance

Methods and Protocols

Edited by

Ramanjulu Sunkar

Oklahoma State University, Stillwater, OK, USA

Humana Press

Editor
Ramanjulu Sunkar
Department of Biochemistry &
Molecular Biology
Oklahoma State University
246 NRC-D
Stillwater, OK 74078
USA
ramanjulu.sunkar@okstate.edu

ISSN 1064-3745 e-ISSN 1940-6029
ISBN 978-1-60761-701-3 e-ISBN 978-1-60761-702-0
DOI 10.1007/978-1-60761-702-0
Springer New York Dordrecht Heidelberg London

Library of Congress Control Number: 2010923200

Cover illustration: Infrared thermal imaging of Arabidopsis plants. Visible light and infrared image of young Arabidopsis plants with differences in their surface temperature. Red color indicates higher, blue and violet indicates lower temperature than average (green). From Figure 2 of Chapter 7.

Printed on acid-free paper

Humana Press is part of Springer Science+Business Media (www.springer.com)

Preface

A number of abiotic factors such as drought, salinity, extreme temperatures (very low and very high), low or high light intensity, deficiency or toxic levels of nutrients have huge impacts on crop productivity. In the last few decades, we are witnessing tremendous efforts to understand the molecular, biochemical, and physiological basis of stress tolerance, but it is also critical that the available techniques be applied in an effective manner by the research community. This volume is not intended to cover every minor technique available for understanding plant stress tolerance, but it does cover the most important widely used techniques including the most recent ones. *Plant Stress Tolerance: Methods and Protocols* includes a wide range of protocols catering to the needs of plant physiologists, biochemists, and molecular biologists interested in probing plant stress tolerance.

This volume begins with chapters on dehydration tolerance (Mel Oliver, John Cushman and colleagues), salinity tolerance (Rana Munns), cold tolerance (Chinnusamy and Sunkar), and oxidative stress (Karl-Josef Dietz), which introduces the concepts, mechanisms, and current knowledge in these areas. Following these chapters are two overview chapters covering the microarray analysis of stress-associated transcriptomes (Sreenivasulu and colleagues) and the importance of glyoxalase (Sopory and colleagues) during plant response to abiotic stress.

At the molecular level, identification of stress-responsive genes is an initial step toward understanding plant stress tolerance. Protocols describing the identification of stress-regulated genes using diverse approaches such as genetic screens (Szabados and colleagues), tiling arrays (Seki and colleagues), subtractive suppression hybridization (Mahalingam and colleagues), and yeast one-hybrid and two-hybrid assays (Karl-Josef Dietz) are provided. Next is a chapter devoted to the functional characterization of stress-responsive genes by VIGS (Senthil-Kumar and colleagues). Identification of stress-regulated proteins at a global level is a complementary approach, and two chapters (proteome analysis using DIGE by Jenny Renaut and redox proteomics by Karl-Josef Dietz and colleagues) describe the relevant protocols. Small regulatory RNAs have emerged as new players in plant stress regulatory networks. Two chapters deal with the identification of stress-regulated microRNAs from plants exposed to stress by cloning (Sunkar and collaborators) and/or using microRNA arrays (Guiliang Tang and colleagues).

Oxidative stress is a commonly observed secondary stress as a consequence of diverse primary stresses (drought, salinity, low temperature, heavy metals, air pollution, biotic stress, etc.). The changes in reactive oxygen species (ROS), damage to the lipids, and membrane dysfunctions are well-characterized biochemical changes in response to stress. Niranjani Jambunathan provides commonly used protocols to determine the levels of ROS, lipid peroxidation, and ion leakage. Superoxide dismutases, catalase, peroxidase, etc., are protective enzymes during oxidative stress, and determination of their activity is an important assay to evaluate tolerance potential of the plant species. Sathya Elavarthi and Bjorn Martin contributed a detailed protocol on assaying those enzymes. Hans-Hubert Kirch provided a protocol to assay aldehyde dehydrogenases, which are an important part of oxidative stress regulatory networks.

Accumulation of compatible solutes (proline, sugars, glycine betaine, and some of the inorganic ions such as K^+) is often observed in plants subjected to drought and salt stress, and the phenomenon is referred to as osmotic adjustment. Chapters devoted to measuring the osmotic adjustment (Paul Verslues), proline levels (László Szabados), enzymes involved in proline metabolism (Arnould Savouré), and sugar (Niels Maness) are provided. Finally, a chapter on measuring Na^+, K^+, and Cl^- content critical for assessing salt tolerance is provided (Rana Munns).

I thank Prof. John Walker, chief editor, for providing me this opportunity and all contributors for making it possible to bring together this useful collection of methods for all of us who are working in this discipline. I also thank Dr. Gary Thompson, Head, department of Biochemistry and Microbiology, Oklahoma State University, for his encouragement to take up this task and Dr. B. Ravi Prasad Rao for his assistance in formatting these chapters.

Ramanjulu Sunkar

Contents

Contributors

Edit Ábrahám • *Institute of Plant Biology, Biological Research Center, Szeged, Hungary*

Catalina Arenas-Huertero • *Department Biologia Molecular de Plantas, Instituto de Biotecnologia, Universidad Nacional Autonoma de Mexico, Cuernavaca, Morelos, Mexico*

Marianne Bordenave • *Université Pierre et Marie Curie, PCMP, UR5 EAC7180 CNRS, Paris, France*

Viswanathan Chinnusamy • *Department of Botany and Plant Sciences, University of California, Riverside, CA, USA*

Françoise Cochet • *Université Pierre et Marie Curie-Paris6, CNRS, PCMP, Paris, France*

Timothy D. Colmer • *School of Plant Biology, The University of Western Australia, Crawley, WA, Australia*

John C. Cushman • *Department of Biochemistry & Molecular Biology, University of Nevada, Reno, NV*

Karl-Josef Dietz • *Biochemistry and Physiology of Plants, Faculty of Biology, Bielefeld University, Bielefeld, Germany*

Sathya Elavarthi • *Department of Plant and Soil Sciences, Oklahoma State University, Stillwater, OK, USA*

Takaho A. Endo • *Bioinformatics and Systems Engineering Division, RIKEN Yokohama Institute, Yokohama, Japan*

László Erdei • *Department of Plant Physiology, University of Szeged, Szeged, Hungary*

Mohamed Ali Ghars • *Borj Cedria, Adaptation des Plantes aux Stress Abiotiques, Hamman Lif, Tunisia*

Cecile Hourton-Cabassa • *UPMC-Univ Paris 06, PCMP, Paris, France*

Junko Ishida • *Plant Genomic Network Research Team, Plant Functional Genomics Research Group, RIKEN Plant Science Center, Yokohama, Japan*

Niranjani Jambunathan • *Department of Biochemistry and Molecular Biology, Oklahoma State University, Stillwater, OK, USA*

Xiaoyun Jia • *Department of Plant and Soil Sciences and KTRDC, University of Kentucky, Lexington, KY, USA*

Mary Prathiba Joseph • *Institute of Plant Biology, Biological Research Center, Szeged, Hungary*

Eli Kaminuma • *Bioinformatics and Systems Engineering Division, RIKEN Yokohama Institute, Yokohama, Japan*

Shuji Kawaguchi • *Bioinformatics and Systems Engineering Division, RIKEN Yokohama Institute, Yokohama, Japan*

Makiko Kawashima • *Plant Genomic Network Research Team, Plant Functional Genomics Research Group, RIKEN Plant Science Center, Yokohama, Japan*

Jong-Myong Kim • *Plant Genomic Network Research Team, Plant Functional Genomics Research Group, RIKEN Plant Science Center, Yokohama, Japan*

HANS-HUBERT KIRCH • *Institute of Molecular Physiology and Biotechnology of Plants (IMBIO), University of Bonn, Bonn, Germany*
PETER KLEIN • *Biochemistry and Physiology of Plants, Faculty of Biology, Bielefeld University, Bielefeld, Germany*
NORIO KOBAYASHI • *Bioinformatics and Systems Engineering Division, RIKEN Yokohama Institute, Yokohama, Japan*
KAREN L. KOSTER • *Department of Biology, The University of South Dakota, Vermillion, SD, USA*
YUKIO KURIHARA • *Plant Genomic Network Research Team, Plant Functional Genomics Research Group, RIKEN Plant Science Center, Yokohama, Japan*
ANNE-SOPHIE LEPRINCE • *Université Pierre et Marie Curie, PCMP, UR5 EAC7180 CNRS, Paris, France*
JEFFREY LEUNG • *Institut des Sciences du Vegetal, CNRS, Gif sur Yvette, France*
RAMAMURTHY MAHALINGAM • *Department of Biochemistry and Molecular Biology, Oklahoma State University, Stillwater, OK, USA*
NIELS MANESS • *Horticulture and Landscape Architecture Department, Oklahoma State University, Stillwater, OK, USA*
BJORN MARTIN • *Department of Plant and Soil Sciences, Oklahoma State University, Stillwater, OK, USA*
AKIHIRO MATSUI • *Plant Genomic Network Research Team, Plant Functional Genomics Research Group, RIKEN Plant Science Center, Yokohama, Japan*
VENUGOPAL MENDU • *Department of Plant and Soil Sciences and KTRDC, University of Kentucky, Lexington, KY, USA*
YOSHIKI MOCHIZUKI • *Bioinformatics and Systems Engineering Division, RIKEN Yokohama Institute, Yokohama, Japan*
TAEKO MOROSAWA • *Plant Genomic Network Research Team, Plant Functional Genomics Research Group, RIKEN Plant Science Center, Yokohama, Japan*
RANA MUNNS • *CSIRO Plant Industry, Canberra, ACT, Australia*
ANANDA MUSTAFIZ • *Plant Molecular Biology, International Centre for Genetic Engineering and Biotechnology, New Delhi, India*
MEENAKUMARI MUTHURAMALINGAM • *Biochemistry and Physiology of Plants, Faculty of Biology, Bielefeld University, Bielefeld, Germany*
KIRANKUMAR S. MYSORE • *Plant Biology Division, The Samuel Roberts Noble Foundation, Ardmore, OK, USA*
KENTARO NAKAMINAMI • *Plant Genomic Network Research Team, Plant Functional Genomics Research Group, RIKEN Plant Science Center, Yokohama, Japan*
MASANORI OKAMOTO • *Plant Genomic Network Research Team, Plant Functional Genomics Research Group, RIKEN Plant Science Center, Yokohama, Japan*
MELVIN J. OLIVER • *USDA-ARS Plant Genetics Research Unit, University of Missouri, Columbia, MO, USA*
CSABA PAPDI • *Institute of Plant Biology, Biological Research Center, Szeged, Hungary*
ELODIE PARRE • *Université Pierre et Marie Curie, PCMP, UR5 EAC7180 CNRS, Paris, France*
LILA PEAL • *Department of Biochemistry and Molecular Biology, Oklahoma State University, Stillwater, OK, USA*
MICHAEL PUCKETTE • *Department of Biochemistry and Molecular Biology, Oklahoma State University, Stillwater, OK, USA*

Jenny Renaut • *Department of Environment and Agrobiotechnologies (EVA), Proteomics Platform, Centre de Recherche Public – Gabriel Lippmann, Belvaux, Luxembourg*
Jose Luis Reyes • *Department Biologia Molecular de Plantas, Instituto de Biotecnologia, Universidad Nacional Autonoma de Mexico, Cuernavaca, Morelos, Mexico*
Luc Richard • *Université Pierre et Marie Curie, PCMP, UR5 EAC7180 CNRS, Paris, France*
Horst Röhrig • *Institute of Molecular Physiology and Biotechnology of Plants (IMBIO), University of Bonn, Bonn, Germany*
Khirod K. Sahoo • *Plant Molecular Biology, International Centre for Genetic Engineering and Biotechnology, New Delhi, India*
Imma Perez Salamó • *Institute of Plant Biology, Biological Research Center, Szeged, Hungary*
Arnould Savouré • *Université Pierre et Marie Curie, PCMP, UR5 EAC7180 CNRS, Paris, France*
Motoaki Seki • *Plant Genomic Network Research Team, Plant Functional Genomics Research Group, RIKEN Plant Science Center, Yokohama, Japan; Kihara Institute for Biological Research, Yokohama City University, Yokohama, Japan*
Muthappa Senthil-Kumar • *Department of Crop Physiology, University of Agricultural Sciences, GKVK, Bangalore, Karnataka, India; Plant Biology Division, The Samuel Roberts Noble Foundation, Ardmore, OK, USA*
Kazuo Shinozaki • *Gene Discovery Research Team, Gene Discovery Research Group, RIKEN Plant Science Center, Tsukuba, Japan*
Sneh L. Singla-Pareek • *Plant Molecular Biology, International Centre for Genetic Engineering and Biotechnology, New Delhi, India*
Sudhir K. Sopory • *Plant Molecular Biology, International Centre for Genetic Engineering and Biotechnology, New Delhi, India*
Nese Sreenivasulu • *Leibniz Institute of Plant Genetics and Crop Plant Research (IPK), Gatersleben, Germany*
Marc Strickert • *Leibniz Institute of Plant Genetics and Crop Plant Research (IPK), Gatersleben, Germany*
Elke Ströher • *Biochemistry and Physiology of Plants, Faculty of Biology, Bielefeld University, Bielefeld, Germany*
Ramanjulu Sunkar • *Department of Biochemistry and Molecular Biology, Oklahoma State University, Stillwater, OK, USA*
László Szabados • *Institute of Plant Biology, Biological Research Center, Szeged, Hungary*
Maho Tanaka • *Plant Genomic Network Research Team, Plant Functional Genomics Research Group, RIKEN Plant Science Center, Yokohama, Japan*
Guiliang Tang • *Department of Plant and Soil Sciences and KTRDC, University of Kentucky, Lexington, KY, USA*
Natasha L. Teakle • *School of Plant Biology and Center for Ecohydrology, The University of Western Australia, Crawley, WA, Australia*
Taiko Kim To • *Plant Genomic Network Research Team, Plant Functional Genomics Research Group, RIKEN Plant Science Center, Yokohama, Japan*
Tetsuro Toyoda • *Bioinformatics and Systems Engineering Division, RIKEN Yokohama Institute, Yokohama, Japan*
Makarla Udayakumar • *Department of Crop Physiology, University of Agricultural Sciences, GKVK, Bangalore, Karnataka India*

PAUL E. VERSLUES • *Institute of Plant and Microbial Biology, Academia Sinica, Taipei, Taiwan*
JACQUES DE VIRVILLE • *Université Pierre et Marie Curie, PCMP, UR5 EAC7180 CNRS, Paris, France*
DELPHINE LEFEBVRE-DE VOS • *Université Pierre et Marie Curie, PCMP, UR5 EAC7180 CNRS, Paris, France*
PATRICIA A. WALLACE • *CSIRO Plant Industry, Canberra, ACT, Australia*
ULRICH WOBUS • *Leibniz Institute of Plant Genetics and Crop Plant Research (IPK), Gatersleben, Germany*
ALAIN ZACHOWSKI • *Université Pierre et Marie Curie, PCMP, UR5 EAC7180 CNRS, Paris, France*
JIAN-KANG ZHU • *Department of Botany and Plant Sciences, University of California, Riverside, CA, USA*

Part I

Reviews and Overview Chapters

Chapter 1

Dehydration Tolerance in Plants

Melvin J. Oliver, John C. Cushman, and Karen L. Koster

Abstract

Dehydration tolerance in plants is an important but understudied component of the complex phenotype of drought tolerance. Most plants have little capacity to tolerate dehydration; most die at leaf water potentials between −5 and −10 MPa. Some of the non-vascular plants and a small percentage (0.2%) of vascular plants, however, can survive dehydration to −100 MPa and beyond, and it is from studying such plants that we are starting to understand the components of dehydration tolerance in plants. In this chapter we define what dehydration tolerance is and how it can be assessed, important prerequisites to understanding the response of a plant to water loss. The metabolic and mechanical consequences of cellular dehydration in plants prelude a discussion on the role that gene expression responses play in tolerance mechanisms. We finally discuss the key biochemical aspects of tolerance focusing on the roles of carbohydrates, late embryogenesis abundant and heat shock proteins, reactive oxygen scavenging (ROS) pathways, and novel transcription factors. It is clear that we are making significant advances in our understanding of dehydration tolerance and the added stimulus of new model systems will speed our abilities to impact the search for new strategies to improve drought tolerance in major crops.

Key words: Dehydration, desiccation, drought, gene expression, LEA proteins, carbohydrates, ROS.

1. Introduction

All plants have to cope with the constant tendency of their tissues to equilibrate to the water potential (Ψ_w) of their surrounding environment, whether it is the substrate upon or within which they grow, the soil within which they are rooted, or the air that surrounds them. The gradient in water potential between the tissues of the plant and the surrounding environment determines

R. Sunkar (ed.), *Plant Stress Tolerance*, Methods in Molecular Biology 639,
DOI 10.1007/978-1-60761-702-0_1,

the direction of water flow and the steepness of the gradient that determines, in part, the speed of that flow.

Poikilohydric plants whose water content is governed directly by the water status of the surrounding environment, such as bryophytes, have few morphological safeguards for preventing water loss when free liquid water is not present. Once water is lost from the surface of the leaves they rapidly equilibrate (because the gradient is steep) to the water potential of the air, which is normally dry. If the plant can survive this event then it is considered dehydration tolerant. Many poikilohydric plants can survive moderate dehydration, to equilibrium with air between −20 and −40 MPa, representing a loss of water to approximately 10% of full turgor (relative water content (RWC)) (1). There are, however, a considerable number of poikilohydric plants that can survive dehydration to much lower water potentials and are deemed to be desiccation tolerant. All desiccation-tolerant poikilohydric plants can survive equilibration with air that has a relative humidity of 50%, which translates to a Ψ_w of approximately −100 MPa. Many of these plants can survive much lower tissue water potentials, even to a Ψ_w of −600 MPa in the case of the desiccation-tolerant moss *Tortula ruralis* (2).

The vast majority of plants species are not poikilohydric, however, and have evolved life forms, from the simple (e.g., the Selaginellas) to the complex (angiosperms), that can maintain a chronic disequilibrium between hydrated tissues and dry air (3). The evolution of this ability undoubtedly led to the radiation of plants into the vast number of ecological niches that the terrestrial habitat offers (4). With the ability to maintain hydration in a drying atmosphere, tracheophytes lost the ability to tolerate desiccation of their vegetative tissues (4). Most present-day angiosperms cannot survive the dehydration of their vegetative tissues to 20–30% of full turgor (RWC), which translates to between −5 and −10 MPa (1). The lowest reported water potential reached for an angiosperm that is not desiccation tolerant is −12.1 MPa for *Larrea divaricata*, a desert shrub (5). Most crop species are relatively sensitive to dehydration and rarely survive leaf water potentials of −4 MPa. There are plant species that are desiccation tolerant, i.e., can equilibrate to water potentials at or greater than −100 MPa, but they are relatively few in number: ~300 species or 0.1% of all angiosperms (6). These "resurrection plants" represent a minimum of eight re-evolutions of vegetative desiccation tolerance in the land plants (4).

When drought occurs, plants experience a number of stresses in combination, but the underlying condition that drives them all is a decrease in soil water availability. The decline in available soil water results in a steepening of the gradient between the Ψ_w of the soil and the Ψ_w plant and thus limits the ability of the plant to take up water; if the Ψ_w of the soil becomes low enough, the plant

will lose water from the roots. The initial response of the plant is to prevent the water content of its tissues from declining by maintaining the balance between the rate of water loss and the rate of water uptake, a stress avoidance strategy (7). Stomatal closure is the immediate and short-term mechanism that plants employ to prevent water loss in an attempt to balance water flow from the plant with uptake from the soil. If the water deficit persists then an increase in the root-to-shoot ratio (increase in root growth) and other morphological changes can be employed (7). When stomata are closed and the transpiration stream declines, the Ψ_w of the plant will equilibrate to the Ψ_w of the soil. To achieve this without an accompanying water loss the plant increases the accumulation of solutes in a process termed osmotic adjustment (8). This works because the Ψ_w of a plant cell consists of two components: the osmotic potential of the cell (Ψ_s) and the turgor pressure (pressure potential) of the cell (Ψ_p) where $\Psi_w = \Psi_s + \Psi_p$. As solutes accumulate Ψ_s decreases allowing for a change in Ψ_w without a change in the turgor pressure (Ψ_p) and thus water loss does not occur. This is a dehydration avoidance mechanism (7). As the Ψ_w of the soil continues to decrease and stress intensifies the plants can no longer avoid dehydration and thus dehydration tolerance mechanisms become critical for survival.

From an agronomic view, drought stress in crops occurs when leaf water potentials decrease to a level where physiological damage occurs and yield is reduced. This can be visualized as a series of repetitive declines in leaf water potential that increase until physiological damage and ultimately death occurs (**Fig. 1.1**). The

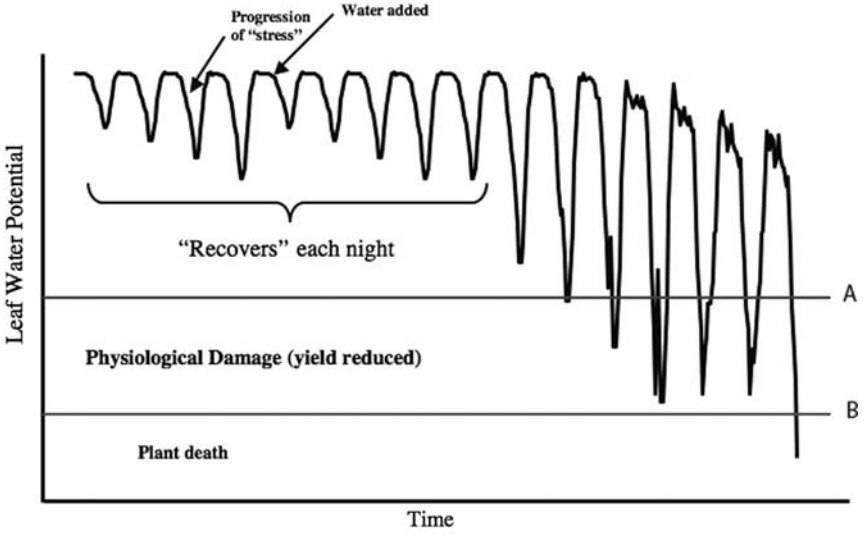

Fig. 1.1. Water stress cycle for a typical crop plant: leaf water potential vs time in field undergoing an irrigation event and a severe drought.

major physiological damage and yield reductions (delimitated by lines A and B in **Fig. 1.1**) occur when cells start to experience dehydration as whole plant water retention strategies, such as stomatal closure and osmotic adjustment, fail to prevent water loss from individual cells either in the root or in leaves. Improving dehydration tolerance lowers both the leaf water potential where physiological damage occurs and when cells die. Tolerance of dehydration, not avoidance of stress, may be especially advantageous for crop improvement, as it does not compromise allocation to photosynthetic tissues or suppress gas exchange (9).

2. Defining Dehydration and Desiccation

In assessing the response of a plant to a dehydration stress it is imperative that the extent and rate of water loss are measured and defined. For most angiosperms where dehydration tolerance is limited, the water status of a plant can be described in a number of ways. Water potential, generally of leaf tissue, is a standard measure of the level of dehydration stress a plant is experiencing, although one has to be aware of the role that osmotic adjustment may play in its value. Water potential is defined as the chemical potential of water in a system, compared to a standard of pure water at the same temperature and at atmospheric pressure (*see* (10) for details of the derivation). In brief, water potential describes the Gibbs free energy status of water molecules within the system; thus, this value governs the thermodynamic behavior of water. If the tissues are poikilohydric in nature and are dried by equilibration of the tissue to air of a known relative humidity, water potentials can be calculated from the equation: $\Psi_w = RT/V_w \ln(\%RH/100)$, where R is the gas constant, T is absolute temperature in K, and V_w is the molar volume of water (*see* (10) for a detailed explanation).

Relative water content (RWC) relates the amount of water remaining after dehydration to that found in fully turgid tissues, and so conveys information about the fractional water content of the tissue. RWC is calculated from the following equation: RWC = (Fwt–Dwt)/(FTwt–Dwt) × 100 where FTwt is the fresh weight at full turgor. This measure is frequently used in studies of vegetative desiccation tolerance (11), but is not commonly used in studies of seeds due, in part, to the confounding possibility that the seeds used to determine 100% RWC will germinate (12).

Water content measured on a weight basis commonly describes the amount of water as a fraction or percentage of either the total sample weight, e.g., g H_2O per g fw (fresh weight), or the sample dry matter, e.g., g H_2O per g dw (dry weight)

or per g dm (dry matter). Often, researchers studying moderate dehydration responses discuss water contents on a fresh weight basis. In contrast, researchers studying desiccation more frequently describe water contents on a dry matter basis, because the scale is expanded and enables a quick understanding of the number of water molecules associated with cellular structures (12, 13). This may, however, be misleading if the tissue composition is not considered (13). Tissues with high lipid contents may achieve lower water contents on a dry matter basis than tissues containing fewer lipids, simply due to the poor affinity of lipids for water. In such cases, water potential may be a more useful indicator of water status.

In addition to considering the extent of dehydration, it is important to consider whether the water is in equilibrium throughout the system or whether the water may be found in heterogeneous domains, as might occur if samples are taken and measured during the drying process. In the equilibrium system, one assumes that the water potential is the same throughout the cells and tissues. However, if samples are taken during the drying process, water molecules are in flux within the tissue, and the water potential and water content may differ at a microscopic or macroscopic scale. Measurements of water content made on a mass basis reflect the average number of water molecules throughout the tissue and fail to account for the existence of localized pools of water that may occur in non-equilibrated samples (11, 12). Even samples that may appear to be in equilibration with the surrounding air have been shown to contain microdomains of water molecules with greater mobility than those in the bulk of the tissue (e.g., 14, 15). Thus, the apparent tolerance or sensitivity to dehydration measured may not reflect all portions of the sample, but may instead reflect the tolerance of a sufficient number of cells to sustain metabolism or permit growth. This consideration is particularly important when viability is measured using assays such as regrowth.

3. Dehydration Is a Kinetic Process

The rate of water loss is a critical consideration when performing a dehydration tolerance experiment. Unfortunately, control or measurement of the rate of water loss is often neglected in experimental design; yet without knowledge of this factor, results may be difficult to interpret and the experiment impossible for other researchers to replicate. The rate of dehydration profoundly influences physiology and may, therefore, determine survival. In some cases, slow drying can improve survival because it permits

organisms to acclimate and adjust their metabolism accordingly (reviewed by 12) or, in the case of maturing orthodox seed embryos, to complete developmental programs that enable desiccation tolerance (reviewed by 16). Sufficiently slow water loss may enable cells to accumulate protective compounds (e.g., proteins, sugars, antioxidants) and to regulate the slowing of metabolism, thereby diminishing the accumulation of reactive oxygen species (ROS). In contrast, some cells and organisms that are not intrinsically tolerant of desiccation may show improved survival after rapid drying. This is thought to occur because the rapid drying rate forces cells through intermediate water contents too quickly for damaging products of uncoupled metabolism to accumulate to toxic levels (e.g., 12, 17 18). The importance of drying kinetics has been discussed by a number of authors (e.g., 12, 13, 18, 19, 23) and the interested reader is referred to them for more detailed discussions.

4. Metabolic and Mechanical Consequences of Dehydration

At relatively high water contents, cellular metabolism is altered by dehydration, and tolerant cells must be able either to regulate metabolic processes as the cell dehydrates or to repair damage from unregulated metabolism (20–25). Products of uncontrolled metabolism, in particular reactive oxygen species (ROS), have been implicated as causal agents of damage to sensitive tissues (21, 22, 25–28). Other metabolites produced by uncontrolled metabolism, such as acetaldehyde produced by fermentation, might also be damaging to desiccation sensitive cells (22). Damage due to unregulated metabolism is greatly dependent upon both the rate and the extent of drying. Prolonged time at intermediate water contents where sufficient water is available for some metabolic reactions, but not enough to maintain proper regulation of those reactions, can exacerbate this type of damage, as more time is available for damaging products to accumulate (17, 21, 23, 24). For example, desiccation sensitive (recalcitrant) embryos are typically killed by slow drying, but many can survive rapid drying, although the embryos generally do not remain viable for long periods when dried (12, 17).

Desiccation-tolerant cells, in addition to having the ability to evade and/or repair damage to metabolic systems, must also have the ability to survive the physical consequences of dehydration, including deformations of cell structure caused by tremendous changes in cell volume that occur as water is withdrawn (29, 30). Cellular membranes are particularly vulnerable to mechanical stress and can be lethally damaged by large changes

in cell volume (13, 30–32). Plasma membrane surface area must be conserved reversibly as the cells shrink so that lysis during expansion does not occur (33, 34). More extensive dehydration can bring cell membranes into close approach with one another, which leads to the development of strong hydration forces near the surfaces. Hydration forces are strongly repulsive forces that tend to resist the close approach of the hydrophilic surfaces, such as membranes and other cellular structures (35). If hydrophilic surfaces are brought close together, as occurs when cells experience moderate to severe water loss and if the extracellular water potential is low enough to overcome the resistance of the hydration force, water is sucked out from the intermembrane space. As a result of this a compressive lateral stress develops within the bilayers (36–39) causing a variety of lesions, including transitions of lipids to the gel phase, demixing of membrane components, and fusion of the membrane bilayers. Many of these lesions, such as the formation of the non-bilayer hexagonal II phase, result in the loss of membrane semipermeability, leakage of cell contents into the external environment, and death of the cell (31, 32, 36, 39, 40). The ability of cells to minimize the physical stress brought about by mechanical deformations during the process of dehydration is an important component of dehydration and desiccation tolerance.

5. Gene Expression and Dehydration

From studies using model plants that are relatively sensitive to water deficit, in particular *Arabidopsis*, we are able to enumerate the genes that are induced by water-deficit stress (41–43). We have also gained a great deal of insight into how the genetic response to water deficit is controlled by abscisic acid (ABA) and non-ABA signaling pathways (44, 45), and more recently by micro-RNAs (miRNAs) and short interfering RNAs (siRNAs) (46–49). However, even with the addition of in-depth examination of gene expression patterns using *Arabidopsis* microarrays (43, 50) we have only limited functional knowledge of the genes that respond to water deficits (51, 52) or their possible adaptive value in the establishment of dehydration tolerance mechanisms. This is not to say that such studies have not yielded useful strategies that can impact a biotechnological approach for the improvement of drought tolerance (for reviews *see* 53–56). Bartels and Sunkar (52) list 49 genes that have been engineered for use in altering abiotic stress tolerance in plants, 28 of which improve the drought tolerance of the target species. It is unclear from most of these studies as to how the tolerance is achieved and if the

transgene exerts its effect via a dehydration tolerance or avoidance mechanism. Expression of a homeodomain-START transcription factor from *Arabidopsis* in transgenic tobacco improved drought tolerance by altering root architecture and reducing the number of stomata, clearly improving the dehydration avoidance capabilities of the transgenic plant (57).

Castiglioni et al. (58) achieved improved drought tolerance in maize by overexpressing RNA chaperones under the control of the rice actin 1 promoter. However, the improved drought tolerance in these transgenic maize lines appeared to be the result of a common protection mechanism that improves transcript stability in general and under drought conditions, a mechanism that would classify as dehydration tolerance. In some cases the mechanism can be inferred from the proposed function of the transgene, as is the case for transgenics expressing late embryogenesis abundant (LEA) proteins such as HVAI (*see* below and 59) suggesting a cellular protection mechanism for tolerance of dehydration, but in general the exact nature of such mechanisms remains enigmatic. In the majority of cases the target plants are either *Arabidopsis* and/or tobacco and most have only exhibited an improved drought tolerance in growth chamber or greenhouse studies. In some cases more rigorous characterizations and drying regimes are required before improved drought tolerance can be established. Only a few transgenes have been field-tested for performance under drought conditions that would clearly enter into the range associated with cellular dehydration. These include the RNA chaperones described earlier (58), an HVA1 protein in wheat (60), and a transcription factor of the NF-Y family (61). Although the approaches so far have had some success they have tended to rely upon educated guesses as to which genes to target or have derived from large-scale screenings and serendipitous observations as to the phenotype of genes that are of interest for a reason only somewhat related to drought stress. Much progress would be made in this area if we had a full understanding of dehydration tolerance mechanisms in plants and the genes or gene networks involved.

Many of the genes induced by water deficit are unique to plants and have unknown function. Clues that these genes have adaptive function come from knowledge that these genes are also expressed in developmental processes in which desiccation tolerance is acquired, such as during the late stages of seed development, and in leaves of desiccation-tolerant plants during drying (51, 52, 62). Yet, the induction of specific genes by water-deficit stress can be misleading. It is also possible that changes in gene expression result from cellular injury. Plants subjected to water-deficit stress suffer a disruption in physiological and metabolic processes that may be interpreted as an injury response. As injury is incurred, this may trigger the up-regulation of specific genes

that indicate injury and thus are not involved in promoting adaptation to the stress. In addition, because the majority of plant species studied to date tolerate only mild water deficits, it is possible that pathways and genes important in water-deficit tolerance have yet to be revealed.

Studies on changes in gene expression in response to dehydration have led to the identification of several classes of genes whose products are suggested to play a role in adaptation to dehydration stress. In Arabidopsis, for example, 277 genes were shown to be up-regulated more than fivefold and 79 were downregulated by dehydration (63). In the general category of signaling, the largest number of induced genes encodes transcription factors. There are also genes induced whose products are involved in phosphoinositide signaling and MAP kinase signaling pathways. Categories of gene products that may have an adaptive function include enzymes that detoxify products of oxidative stress, degrade proteins, and alter the structure of the cell wall. Transport proteins, such as aquaporins, are also induced and may have a role in distribution of water in the cell and plant (64). There remain a large number of genes whose products do not have a known function. These include the lea genes, which are expressed as seeds acquire desiccation tolerance during development and during water-deficit stress in vegetative tissues (65–67). Rizhsky et al. (43) has provided a realistic look at the effects of abiotic stress on gene expression in *Arabidopsis* by attempting to administer a natural drought treatment by combining a water deficit with an increase in ambient temperature. This study revealed 454 transcripts by microarray expression profiling that were specifically expressed in response to the combination of heat and water deficit. As seen in response to dehydration in other plant systems, *Arabidopsis* accumulates sucrose and other sugars in response to the combination of heat and water stress. Proline, which accumulates in Arabidopsis as an osmoprotectant during water stress, did not accumulate in response to the combination of water stress and heat. Rizhsky et al. (43) also established that heat shock factors (HSFs) function as a network of transcription factors that control the expression of HSPs during different stresses and identified a group of HSFs that are water deficit specific. More recently, approximately 70 proteins associated with dehydration in the moss, *Physcomitrella patens* were described in which LEA proteins and reactive oxygen species-scavenging enzymes were expressed prominently (68).

ABA plays an important role in the physiological and molecular responses to dehydration and it is of interest to us how the role of ABA in dehydration tolerance has evolved. ABA content increases in response to water-deficit stress, arising from an increase in ABA biosynthesis and/or a decrease in ABA breakdown (69, 70). The genes encoding the major enzymes in the

ABA biosynthetic pathway have now been cloned in *Arabidopsis* and a few other species (71). Once ABA content increases, signaling pathways are initiated that lead to ABA responses, including changes in gene expression. Many components have been identified but a full understanding of these complex networks has yet to be achieved (44, 45, 72). Alterations in responses to ABA may occur through changes in signaling pathways or through manipulations that lead to changes in ABA accumulation. Experiments in which NCED levels are elevated result in plants with a higher ABA content and a reduced rate of water loss (73, 74).

Although relatively large gene expression databases that describe the response to water deficits in dehydration- and desiccation-sensitive species, such as Arabidopsis (42–44, 50, 67, 75), have been established, very few resources are available for desiccation-tolerant species. To date, gene expression studies of desiccation-tolerant plants have been limited to a few species: *T. ruralis* (76, 77), *Polypodium virginianum* (78), *Craterostigma plantagineum* (62, 79–81), *Sporobolus stapfianus* (82, 83), and *Xerophyta humilis* (84, 85). The latter study presents evidence that in *Xerophyta humilis,* and perhaps all desiccation-tolerant angiosperms, the mechanism for vegetative desiccation tolerance carries "footprints" of a seed-derived origin. Although the resources for desiccation-tolerant plants are at present limited, significant progress is being made in our understanding of the genetic aspects of dehydration tolerance. Gene expression appears to be programmed to respond to relatively precise levels of dehydration, almost in stages seemingly to render an ordered process that only initiates if water loss has the potential to result in desiccation. This has been reported for *T. ruralis* where a certain level of dehydration is required to induce the translational control of gene expression related to rehydration (86). In *Sporobolus stapfianus* both the accumulation of ABA and the alteration in gene expression related to dehydration happens in two distinct phases (87), one early before reaching 60% RWC and one late at 40% RWC and below. Recently, Jiang et al. (88) report a programmed regulation of protein expression triggered by changes of water status in drying *Boea hygrometrica* leaves.

The regulation of gene expression in desiccation-tolerant plants is complex but does appear in some respects similar to that seen in desiccation sensitive species. ABA plays a major role both in the genetic response but also in the acquisition of desiccation tolerance. Callus tissue derived from the leaves of *C. plantagineum* is not inherently desiccation tolerant but will become so when exposed to exogenous ABA (79). ABA accumulates in the drying leaves of *Craterostigma* and as it does there is a coordinated increase in both transcripts and proteins that are specific to drying tissues (62, 79, 89). Several bryophytes have

been shown to accumulate ABA in response to mild dehydration although this endogenous increase in ABA does not allow for tolerance to severe dehydration or desiccation (2, 90). However, application of exogenous ABA can induce desiccation tolerance in bryophytes that are normally sensitive to severe dehydration, such as *Physcomitrella patens* and *Funaria hygrometrica* (91, 92). The assumption is that ABA-induced gene expression is sufficient to acquire desiccation tolerance in these plants; however, the means by which this is achieved remains to be elucidated. In contrast, ABA appears to be not involved in the dehydration response of the desiccation-tolerant moss *T. ruralis* (93, Oliver unpublished observations).

Although ABA is clearly important in the gene expression response to dehydration there are clear indications that it is not the sole signal transduction component. In *Sporobolus stapfianus*, a desiccation-tolerant grass, changes in gene expression induced by dehydration occur before the accumulation of ABA in the leaf tissues and exogenous ABA cannot induce desiccation tolerance in detached leaves which are sensitive to drying (87). A desiccation-induced homeodomain-leucine zipper protein CPHB-1, which is expressed very early in the drying process for *Craterostigma*, is not induced by ABA (80). Recently, Hilbricht et al. (94) reported that a previously described desiccation and ABA-induced gene from *Craterostigma, CDT-1*, belongs to a family of retroelements and directs the synthesis of a 21 base pair siRNA that, in turn, can induce the expression of both desiccation- and ABA-inducible genes. Overexpression of CDT-1 in normally desiccation sensitive callus tissue resulted in the acquisition of desiccation tolerance in the absence of ABA. The discovery of this mechanism for gene expression control during the acquisition of desiccation tolerance is an exciting one and will undoubtedly lead to a major advance in our understanding of how plant cells tolerate dehydration.

6. Biochemical Aspects of Dehydration Tolerance

6.1. Carbohydrates

The accumulation of soluble sugars has long been correlated with the acquisition of desiccation tolerance in plants and other organisms (18, 23, 25). Orthodox seeds, pollen, and most plants that accumulate soluble sugars in response to desiccation utilize the disaccharide, sucrose, sometimes in combination with oligosaccharides. Correlations between high sucrose contents and desiccation tolerance were noted in resurrection plants (95, 96), seed embryos (97), and pollen (98). In *C. plantagineum*, 2-octulose stored in the hydrated leaves is converted to sucrose during

drying to such an extent that in the dried state it comprises about 40% of the dry weight (99). Sucrose also accumulates in *Sporobolus stapfianus* and *Xerophyta viscosa* during desiccation (100). Sucrose makes up approximately 10% of the dry mass of *T. ruralis* gametophytes and does not change in amount during desiccation or rehydration in the dark or light (101). The disaccharide trehalose has been correlated with desiccation tolerance in fungi (e.g., yeast) (102) and invertebrates (e.g., Artemia cysts) (103), but is not often found associated with desiccation tolerance in plants. Notable exceptions are the club mosses *Selaginella lepidophylla* and *Selaginella tamariscina*, where trehalose accumulates to relatively high levels during drying (104–106), and a North American Sporobolus species (106). Sugars contribute to a significant proportion of *S. lepidophylla* weight and their concentration varies with hydration states (104, 107). Trehalose, however, is either absent or only present in small amounts in other resurrection plants such as *Myrothamnus flabellifolius* and *Sporobolus stapfianus* (108–110). Transgenic plants that have been engineered to accumulate trehalose exhibit increased drought tolerance in the laboratory which further supports the role of sugars as cellular protectants during drying (111, 112).

Sugars are proposed to protect cellular structures from both mechanical and metabolic stresses during dehydration. Sugars and more complex polysaccharides can scavenge ROS (113, 114) and so may diminish the metabolic consequences of dehydration. Extensive studies in vitro show that sugars can also minimize the mechanical stresses that occur during drying and so can stabilize cellular structures such as membranes and proteins. The ability of sugars to stabilize these structures lies primarily in the osmotic and volumetric properties of the sugars – they act as osmotic spacers that prevent the close approach of membranes and other hydrophilic surfaces and, thereby, diminish the compressive stress that otherwise causes damage (36, 37, 39, 40, 115). The effect of sugars on phase behavior in model membranes has been qualitatively and quantitatively modeled in terms of the solutes' influence on the damaging hydration forces that arise during dehydration, and this simple physicochemical model suffices to explain the observed data (37, 39, 40, 115, 116). In many studies, the protective effects of sugars are attributed primarily to their ability to form hydrogen bonds with hydrophilic cellular structures in the near absence of water (e.g., 103, 117, 118). The ability of concentrated sugar solutions to vitrify, i.e., to enter an amorphous solid state that confers mechanical stability to the dried cell, is also cited as protective (115, 118–122). While both of these properties exist and may occur in cells at very low hydrations, we point out that the stabilizing effects of sugars on membranes can be measured at water contents far in excess of those that would promote either hydrogen bonding between sugars and membranes

or glass formation (115, 116). In addition, glass forming sugars and LEA proteins are often abundant in tissues that fail to survive dehydration (12), suggesting that vitrification, on its own, is not sufficient for dehydration tolerance. We suggest that neither hydrogen bond formation by sugars nor vitrification is necessary for dehydration tolerance, although both may occur at very low water contents. Vitrification can, however, confer additional mechanical stability to dehydrated membranes (37, 115, 120), and to cells, and has been linked to longevity of dried seeds and pollen (13, 122, 123).

6.2. Late Embryogenesis Abundant (LEA) Proteins

LEA proteins, of which there are at least five major groups, have functions that remain largely unknown, but are assumed to be important in the establishment of desiccation tolerance in seeds, and by inference, vegetative tissues (66, 67). ABA treatment of immature barley embryos results in both the accumulation of LEA proteins and the acquisition of tolerance (124). Water deficits and ABA treatments of vegetative tissues result in the accumulation of many LEA proteins to relatively high concentrations, suggesting that LEA proteins serve as protective molecules enabling cells to survive a certain level of dehydration (41, 48, 65). Although the mechanistic basis for such protection is unclear, several studies have suggested that LEA proteins may protect cells during desiccation and freezing by acting as hydration buffers (125), sequestering ions, stabilizing proteins, membranes and chromatin structure, or renaturing unfolded proteins (126, 127). A Di21 family LEA protein from Arabidopsis was shown to afford oxidative stress tolerance in yeast and possibly in Arabidopsis (128). A group 3 LEA protein expressed in pea seed mitochondria appears to act to stabilize mitochondrial matrix proteins (129) and the inner mitochondrial membranes during desiccation (130). A recent study demonstrated that the expression of two group 4 LEA proteins from *Boea hygrometrica* (a desiccation-tolerant angiosperm) appeared to improve the dehydration tolerance of transgenic tobacco by an overall improvement of membrane and protein stability during dehydration (131). Molecular models suggest some LEA proteins may form cytoskeleton-like filaments that could stabilize cellular structure during drying (126), whereas group 2 LEA proteins (dehydrins) may form amphiphilic helices that could intercalate into membrane surfaces (65, 132). Such an interaction with negatively charged liposomes has been demonstrated in vitro for dehydrins from maize (132) and *T. ruralis* (Oliver, unpublished). While some LEA proteins may confer protection via specific interactions with cellular components, Tunnacliffe and Wise (125) suggest that nonspecific effects due to their molecular volume and hydrophilic nature may allow these proteins to act as molecular shields to prevent the aggregation of labile proteins

(127, 133, 134) and liposomes (133) during desiccation in vitro. We point out that these volumetric effects would enable LEAs to serve as molecular spacers and, thus, minimize the development of damaging hydration forces in cellular structures during drying, as previously shown for sugars. Strong evidence suggests that LEA proteins also contribute to vitrification of the dehydrated cellular milieu (122, 135) and, thus, can help confer long-term mechanical stability to desiccated cells.

Wood and Oliver (136) demonstrated that LEA protein transcripts in *T. ruralis* are sequestered in mRNPs as the cells dry or accumulate in the initial phases of recovery following rehydration (77, 137). The inference is that LEA proteins in this plant are required either for protecting cellular components during recovery or are an integral part of the reconstitution process. In a recent analysis of ESTs and expression profiles for *Selaginella* exposed to 2.5 h of dehydration stress Iturriaga et al. (138) discovered an abundant transcript that encodes a hypothetical protein with weak homology to group 3 LEA proteins from *Dictyostelium discoideum*, *Chlorella vulgaris*, *Caenorhabditis elegans*, and *Deinococcus geothermalis* but is not present in angiosperms. Velten and Oliver (139) also reported a LEA-like protein from *T. ruralis* that appears to be an ancient LEA found only in present-day bryophytes. These findings demonstrate that resurrection species carry novel stress adaptive determinants.

6.3. Heat Shock Proteins (HSPs)

As described above, cellular dehydration has long been thought to impact cellular function and viability by compromising macromolecular structures, in particular membranes and proteins. Although accumulation of sugars, LEA proteins, and the process of cytoplasmic vitrification may stabilize membranes and some protein structures, protein stabilization per se may require the additional aid of chaperones to escape denaturation during drying. Heat shock proteins, many of which are chaperones, have been implicated in dehydration tolerance (52). In Arabidopsis desiccation intolerant seeds of the *abi3-6*, *fus3-3*, and *lec1-2* mutants accumulated < 2% of wild-type levels of Hsp17.4 protein where tolerant seeds have normal levels (140). HSPs have been associated with water stress in several species (141) and transgenic plants overexpressing Hsp17.7 show increased drought and salt tolerance (142).

6.4. Reactive Oxygen Scavenging Pathways

During dehydration, reactive oxygen species (ROS) (e.g., singlet oxygen, hydroxyl radicals, hydrogen peroxide, and superoxide anions) increase in plant cells and tissues (21, 22, 25–28, 113). ROS generation occurs mostly in the chloroplast and its main effect is to inhibit the repair of damage to Photosystem II and synthesis of D1 protein (143). The generation of antioxidants and the establishment of a reactive oxygen scavenging system,

involving such enzymes as superoxide dismutase, the ascorbate–glutathione cycle and catalase, counter ROS activity in plants. The efficiency of these systems is closely related to an increased resistance to abiotic stresses, in particular dehydration (27, 144). This was demonstrated elegantly for the desiccation-tolerant shrub *Myrothamnus flabellifolia,* whose ability to resurrect from dryness can be directly correlated to the state of its antioxidant defense system. The plant resurrects normally if kept in the dried state for 4 months. At 8 months, when antioxidants (i.e., ascorbate, tocopherol, glutathione) have been depleted, the plants die when watered (144). The ability of plants to resist cellular damage can be enhanced by overexpressing enzymes of antioxidant pathways in transgenic plants (143); the most notable is overexpression of MnSOD in alfalfa (145), which generated stress tolerance in the field.

6.5. Other Components

Cell wall composition undergoes significant changes during drying. In desiccation-tolerant species, specific mechanisms must limit irreversible damage to the cell wall structure and polymer organization (146). Dried leaves of *Craterostigma wilmsii* have lower glucose content and a higher xyloglucan substitution rate than hydrated leaves (147). Cell walls increase in extensibility during drying and recovery correlating with expression of three alpha-expansin genes in *C. plantagineum* (148). Resurrection plants are also a source of novel transcription factors associated with dehydration tolerance (149). These include a set of five homeodomain-leucine zipper transcription factors in *C. plantagineum* (150), and an ABA- and dehydration inducible gene family of DNA-binding proteins associated with early stages of dehydration-induced chloroplast remodeling (80, 81). This species expresses a novel Myb factor that confers dehydration and salinity tolerance when ectopically expressed in Arabidopsis (151).

7. Conclusions

As can be seen from the preceding narrative dehydration tolerance is a complex trait and in crops it is only one aspect of the even more complex phenotype of drought tolerance. We are starting to make significant inroads into our understanding of dehydration tolerance, much of which comes from the study of desiccation tolerance. We are also in an exciting era where the tools we have developed in the "omics" revolution offer us the chance to unlock some of the deeper aspects of dehydration tolerance and to discover those genes and gene networks that are truly adaptive and central to this trait. As we start to generate full genome sequences

of desiccation-tolerant plants and develop the tools we need to manipulate the phenotype the pace of discovery will increase. Of particular interest is the addition of a new and *Agrobacterium* transformable desiccation-tolerant angiosperm, *Lindernia brevidens* (152), to our list of models for dehydration tolerance. This addition promises to be more flexible than *Craterostigma* for the insertion of expression constructs and will add to the promise that the successful transformation of *Ramonda myconi* (153) brought to the field. These models, along with others that are in development, will hopefully allow for a more detailed and directed functional dissection of dehydration tolerance mechanisms.

References

1. Proctor, M.C.F. and Pence, V.C. (2002) Vegetative tissues: bryophytes, vascular resurrection plants and vegetative propagules. In *Desiccation and Survival in Plants: Drying Without Dying* (Black, M. and Pritchard, H., eds.). CABI Publishing, Oxford, pp. 207–237.
2. Oliver, M.J. (2008) Biochemical and molecular mechanisms of desiccation tolerance in bryophytes. In *Bryophyte Biology*, 2nd ed. (Shaw, J and Goffinet, B., eds.). Cambridge Press, New York, pp. 269–298.
3. Alpert, P. and Oliver, M.J. (2002) Drying without dying. In *Desiccation and Survival in Plants: Drying Without Dying* (Black, M. and Pritchard, H., eds.). CABI Publishing, Oxford, pp. 3–43.
4. Oliver, M.J., Tuba, Z., and Mishler, B.D. (2000) Evolution of desiccation tolerance in land plants. *Plant Ecol* **151**, 85–100.
5. Cunningham, G.L. and Burk, J.H. (1973) The effect of carbonate deposition layers ("Caliche") on the water status of *Larrea divericata*. *Amer Midland Nat* **90**, 474–480.
6. Porembski, S. and Barthlott, W. (2000) Genetic and gneisic outcrops (inselbergs) as centers for diversity of desiccation-tolerant vascular plants. *Plant Ecol* **151**, 19–28.
7. Verslues, P.E., Agarwal, M., Katiyar-Agarwal, S., Zhu, J., and Zhu J.-K. (2006) Methods and concepts in quantifying resistance to drought, salt, and freezing, abiotic stresses that affect plant water status. *Plant J* **45**, 523–539.
8. Zhang, L., Nguyen, H.T., and Blum, A. (1999) Genetic analysis of osmotic adjustment in crop plants. *J Exp Bot* **50**, 292–302.
9. Borrell, A.K., Hammer, G.L., and Henzell, R.G. (2000) Does maintaining green leaf area in sorghum improve yield under drought? II. Dry matter production and yield. *Crop Sci* **40**, 1037–1039.
10. Nobel, P.S. (1983) *Biophysical Plant Physiology and Ecology*. W.H. Freeman and Company, San Francisco, USA.
11. Farrant, J.M. (2002) Mechanisms of desiccation tolerance in angiosperm resurrection plants. In *Plant Desiccation Tolerance* (Jenks, M.A. and Wood, A.J., eds.). Blackwell Publishing, Iowa, USA, pp. 51–90.
12. Pammenter, N.W. and Berjak, P. (2000) Aspects of recalcitrant seed physiology. *R Bras Fisiol Veg* **12** (Edição Especial), 56–69.
13. Walters, C. and Koster, K.L. (2007) Structural dynamics and desiccation damage in plant reproductive organs. In *Plant Desiccation Tolerance* (Jenks, M.A. and Wood, A.J., eds.). Blackwell Publishing, Iowa, USA, pp. 251–280.
14. Balsamo, R.A., Vander Willigen, C., Boyko, W., and Farrant, J. (2005) Retention of mobile water during dehydration in the desiccation tolerant grass *Eragrostis nindensis*. *Physiol Plant* **124**, 336–342.
15. Leubner-Metzger, G. (2005) β-1,3-Glucanase gene expression in low-hydrated seeds as a mechanism for dormancy release during tobacco after-ripening. *Plant J* **41**, 133–145.
16. Kermode, A. and Finch-Savage, W.E. (2002) Desiccation sensitivity in orthodox and recalcitrant seeds in relation to development. In *Desiccation and Survival in Plants: Drying Without Dying* (Black, M. and Pritchard, H., eds.). CABI Publishing, Oxford, pp. 149–184.
17. Pammenter, N.W. and Berjak, P. (1999) A review of recalcitrant seed physiology in relation to desiccation-tolerance mechanisms. *Seed Sci Res* **9**, 13–37.
18. Berjak, P., Farrant, J.M., and Pammenter, N.W. (2007) Seed desiccation tolerance mechanisms. In *Plant Desiccation Tolerance*

(Jenks, M.A. and Wood, A.J., eds.). Blackwell Publishing, Iowa, USA, pp. 151–192.
19. Farrant, J.M., Cooper, K., Kruger, L.A., and Sherwin, H.W. (1999) The effect of drying rate on the survival of three desiccation-tolerant angiosperm species. *Ann Bot* **84**, 371–379.
20. Pammenter, N.W., Berjak, P., Wesley-Smith, J., and Vander Willigen, C. (2002) Experimental aspects of drying and recovery. In *Desiccation and Survival in Plants: Drying Without Dying* (Black, M. and Pritchard, H., eds.). CABI Publishing, Oxford, pp. 93–110.
21. Leprince, O., Deltour, R., Thorpe, P.C., Atherton, N.M., and Hendry, G.A.F. (1990) The role of free radicals and radical processing systems in loss of desiccation tolerance in germinating maize (*Zea mays* L.). *New Phytol* **116**, 573–580.
22. Leprince, O., Harren, F.J.M., Buitink, J., Alberda, M., and Hoekstra, F.A. (2000) Metabolic dysfunction and unabated respiration precede the loss of membrane integrity during dehydration of germinating radicles. *Plant Physiol* 122, 597–608.
23. Vertucci, C.W. and Farrant, J.M. (1995) Acquisition and loss of desiccation-tolerance. In *Seed development and germination* (Kigel, J. and Galili, G., eds.). Marcel Dekker Inc., New York, pp. 237–271.
24. Walters, C., Pammenter, N.W., Berjak, P., and Crane, J. (2001) Desiccation damage, accelerated aging, and respiration in desiccation tolerant and sensitive seeds. *Seed Sci Res* **11**, 135–148.
25. Walters, C., Farrant, J.M., Pammenter, N.W., and Berjak, P. (2002) Desiccation stress and damage. In *Desiccation and Survival in Plants: Drying Without Dying* (Black, M. and Pritchard, H., eds.). CABI Publishing, Oxford, pp. 263–291.
26. Kranner, I. and Birtic, S. (2005). A modulating role for antioxidants in desiccation tolerance. *Integr Comp Biol* **45**, 734–740.
27. Smirnoff, N. (1998) Plant resistance to environmental stress. *Curr Opin Plant Biol* **9**, 214–219.
28. Apel, K., Hurt, H. (2004) Reactive oxygen species: metabolism, oxidative stress, and signal transduction. *Annu Rev Plant Biol* **55**, 373–399.
29. Iljin, W.S. (1957) Drought resistance in plants and physiological processes. *Annu Rev Plant Physiol* **8**, 257–274.
30. Meryman, H.T. (1974) Freezing injury and its prevention in living cells. *Annu Rev Biophys Bioeng* **3**, 341–363.
31. Steponkus, P.L. (1984) Role of the plasma membrane in freezing injury and cold acclimation. *Annu Rev Plant Physiol* **35**, 543–584.
32. Steponkus, P.L. and Webb, M.S. (1992) Freeze-induced dehydration and membrane destabilization in plants. In *Water and Life: Comparative Analysis of Water Relationships at the Organismic, Cellular and Molecular Level* (Somero, G.N., et al., eds.). Springer Verlag, Berlin, Germany, pp. 338–362.
33. Gordon-Kamm, W.J. and Steponkus, P.L. (1984a) The behavior of the plasma membrane following osmotic contraction of isolated protoplasts: implications in freezing injury. *Protoplasma* **123**, 83–94.
34. Wolfe, J. and Steponkus, P.L. (1983) Mechanical properties of the plasma membrane of isolated protoplasts-mechanism of hyperosmotic and extracellular freezing injury. *Plant Physiol* **71**, 276–285.
35. Rand, R.P. and Parsegian, V.A. (1989) Hydration forces between phospholipid bilayers. *Biochim Biophys Acta* **988**, 351–376.
36. Bryant, G. and Wolfe, J. (1992) Interfacial forces in cryobiology and anhydrobiology. *Cryo-Lett* **13**, 23–36.
37. Bryant, G., Koster, K.L., and Wolfe, J. (2001) Membrane behaviour in seeds and other systems at low water content: the various effects of solutes. *Seed Sci Res* **11**, 17–25.
38. Wolfe, J. (1987) Lateral stresses in membranes at low water potential. *Aust J Plant Physiol* **14**, 311–318.
39. Wolfe, J. and Bryant, G. (1999) Freezing, drying, and/or vitrification of membrane-solute-water systems. *Cryobiol* **39**, 103–129.
40. Koster, K.L. and Bryant, G. (2006) Dehydration in model membranes and protoplasts: contrasting effects at low, intermediate and high hydrations. In *Cold Hardiness in Plants* (Chen, T.H.H., et al., eds.). CABI, Wallingford, UK, pp. 219–234.
41. Ingram, J. and Bartels, D. (1996) The molecular basis of dehydration tolerance in plants. *Annu Rev Plant Physiol Plant Mol Biol* **47**, 377–403.
42. Shinozaki, K. and Yamaguchi-Shinozaki, K. (1999) Gene expression and signal transduction in water-stress response. *Plant Physiol* **115**, 327–334.
43. Rizhsky, L., Liang, H., Shuman,J., Shulaev, V., Davletova, S., and Mittler, R. (2004) When defense pathways collide. The response of *Arabidopsis* to a combination of drought and heat stress. *Plant Physiol* **134**, 1683–1696.
44. Zhu, J.K. (2002) Salt and drought stress signal transduction in plants. *Annu Rev Plant Biol* **53**, 247–273.

45. Wasilewska, A., Vlad, F., Sirichandra, C., Redko, Y., Jammes, F., Valon, C., Frie dit Frey, N., and Leung, J. (2008) An update on abscisic acid signaling in plants and more... *Mol Plant* **1**, 198–217.
46. Sunkar, R., and Zhu, J.-K. (2004) Novel and stress-regulated microRNAs and other small RNAs from *Arabidopsis*. *Plant Cell* **16**, 2001–2019.
47. Sunkar, R., Chinnusamy, V., Zhu, J., and Zhu, J.-K. (2007) Small RNAs as big players in plant abiotic stress responses and nutrient deprivation. *Trends Plant Sci* **12**, 301–309.
48. Phillips, J.R., Dalmay, T., and Bartels, D. (2007) The role of small RNAs in abiotic stress. *FEBS Letters* **581**, 3592–3597.
49. Zhao, B., Liang, R., Ge, L., Li, W., Xiao, H., Lin, H., Ruan, K., and Jin, Y. (2007) Identification of drought-induced microRNAs in rice. *Biochem Biophys Res Comm* **354**, 585–590.
50. Seki, M., Narusaka, M., Abe, H., Kasuga, M., Yamaguchi-Shinozaki, K., Carninci, P., Hayashizaki, Y., and Shinozaki, K. (2001) Monitoring the expression pattern of 1300 *Arabidopsis* genes under drought and cold stresses using a full-length cDNA microarray. *Plant Cell* **13**, 61–72.
51. Sunkar, R. and Bartels, D. (2002) Drought- and desiccation-induced modulation of gene expression in plants. *Plant Cell Environ* **25**, 141–151.
52. Bartels, D. and Sunkar, R. (2005) Drought and salt tolerance in plants. *Crit Rev Plant Sci* **24**, 23–58.
53. Umezawa, T., Fujita, M., Fujita, Y., Yamaguchi-Shinozaki, K., and Shinozaki, K. (2006) Engineering drought tolerance in plants: discovering and tailoring genes to unlock the future. *Curr Opin Biotech* **17**, 113–122.
54. Valliyodan, B., and Nguyen, H. T. (2006) Understanding regulatory networks and engineering for enhanced drought tolerance in plants. *Curr Opin Plant Biol* **9**, 189–195.
55. Vinocur, B., and Altman, A. (2005) Recent advances in engineering plant tolerance to abiotic stress: achievements and limitations. *Curr Opin Biotech* **16**, 123–132.
56. Parry, M.A.J., Flexas, J., and Medrano, H. (2005) Prospects for crop production under drought: research priorities and future directions. *Ann Appl Biol* **147**, 211–226.
57. Yu, H., Chen, X., Hong, Y.-Y., Wang, Y., Xu, P., Ke, S.-D., Liu, H.-Y., Zhu, J.-K., Olive, D.J., and Xiang, C.-B. (2008) Activated expression of an *Arabidopsis* HD-START protein confers drought tolerance with improved root system and reduced stomatal density. *Plant Cell* **20**, 1134–1151.
58. Castiglioni, P., Warner, D., Bensen, R.J., Anstrom, D.C., Harrison, J., Stoecker, M., Abad, M., Kumar, G., Salvador, S., D′Ordine, R., Navarro., S., Back, S., Fernandes, M., Targolli, J., Dasgupta, S., Bonin, C., Leuthy, M.H., and Heard, J.E. (2008) Bacterial RNA chaperones confer abiotic stress tolerance in plants and improved grain yield in maize under water-limited conditions. *Plant Physiol* **147**, 446–455.
59. Xu, D., Duan, X., Wang, B., Hong, B., Ho, T.-H.D., and Wu, R. (1996) Expression of a late embryogenesis abundant protein gene, HVA1, from barley confers tolerance to water deficit and salt stress in transgenic rice. *Plant Physiol* **110**, 249–257.
60. Bahieldina, A., Mahfouza, H.T., Eissaa, H.F., Salehc, O.M., Ramadana, A.M., Ahmedd, I.A., Dyere, W.E., El-Itribya, H.A., and Madkour, M.A. (2005) Field evaluation of transgenic wheat plants stably expressing the HVA1 gene for drought tolerance. *Physiol Plant* **123**, 421–427.
61. Nelson, D.E., Repetti, P.P., Adams, T.R., Creelman, R.A., Wu, J., Warner, D.C., Anstrom, D.C., Bensen, R.J., Castiglioni, P.P., Donnarummo, M.G., Hinchey, B.S., Kumimoto, W.R., Maszle, D.R., Canales, R.D., Krolikowski, K.A., Dotson, S.B., Gutterson, N., Ratcliffe, O.J., and Heard, J.E. (2007) Plant nuclear factor Y (NF-Y) B subunits confer drought tolerance and lead to improved corn yields on water-limited acres. *Proc Natl Acad Sci USA* **104**, 16450–16455.
62. Bartels, D., Phillips, J., and Chandler, J. (2007) Desiccation tolerance: gene expression, pathways, and regulation of gene expression. In *Plant Desiccation Tolerance* (Jenks, M.A. and Wood, A.J., eds.). Blackwell Publishing, Iowa, USA, pp. 115–148.
63. Seki, M., Narusaka, M., Ishida, J., Nanjo, T., Fujita, M., Oono, Y., Kamiya, A., Nakajima, M., Enju, A., Sakurai, T., Satou, M., Akiyama, K., Taji, T., Yamaguchi-Shinozaki, K., Carninci, P., Kawai, J., Hayashizaki, Y. and Shinozaki, K. (2002) Monitoring the expression profiles of 7000 *Arabidopsis* genes under drought, cold, and high-salinity stresses using a full-length cDNA microarray. *Plant J* **31**, 279–292.
64. Maurel, C., Verdoucq, L., Luu, D.-T., and Santoni, V. (2008) Plant aquaporins: membrane channels with multiple integrated functions. *Annu Rev Plant Biol* 59, 595–624.
65. Close, T.J. (1996) Dehydrins: emergence of a biochemical role of a family of plant dehydration proteins. *Physiol Plant* **97**, 795–803.

66. Hundertmark, M. and Hincha, D.K. (2008) LEA (Late Embryogenesis Abundant) proteins and their encoding genes in *Arabidopsis thaliana*. *BMC Genomics* **9**, 118.
67. Battaglia, M., Olvera-Carrillo, Y., Garciarrubio, A., Campos, F., and Covarrubias, A.A. (2008) The enigmatic LEA proteins and other hydrophilins. *Plant Physiol* **148**, 6–24.
68. Wang, X.Q., Yang, P.F., Liu, Z., Liu, W.Z., Hu, Y., Chen, H., Kuang, T.Y., Pei, Z.M. Shen, S.H., and He, Y.K. (2009) Exploring the mechanism of *Physcomitrella patens* desiccation tolerance through a proteomic strategy. *Plant Physiol* February 11, 2009; 10.1104/pp.108.131714.
69. Zeevaart, J.A.D. (1999) Abscisic acid metabolism and its regulation. In *Biochemistry and Molecular Biology of Plant Hormones* (Hooykaas, P.J.J., et al., eds.). Elsevier Science, Amsterdam, the Netherlands, pp. 189–207.
70. Xiong, L. and Zhu, J.-K. (2003) Regulation of abscisic acid biosynthesis. *Plant Physiol* **133**, 29–36.
71. Seo, M. and Koshiba, T. (2002) Complex regulation of ABA biosynthesis in plants. *Trends Plant Sci* **7**, 41–48.
72. Finkelstein, R.R., Gampala, S.S.L., and Rock, C.D. (2002) ABA signaling in seeds and seedlings. *Plant Cell* **13**, S15–S45.
73. Qin, X.Q. and Zeevaart, J.A.D. (2002) Overexpression of a 9-cis-epoxycarotenoid dioxygenase gene in *Nicotiana plumbaginifolia* increases abscisic acid and phaseic acid levels and enhances drought tolerance. *Plant Physiol* **128**, 544–551.
74. Iuchi, S., Kobayashi, M., Tajo, T., Naramoto, M., Seki, M., Kato, T., Tabata, S., Kakubari, Y., Yamaguchi-Shinozaki, K., and Shinozaki, K. (2001) Regulation of drought tolerance by gene manipulation of 9-cis-epoxycarotenoid dioxygenase, a key enzyme in abscisic acid biosynthesis in *Arabidopsis*. *Plant J* **27**, 325–333.
75. Bray, E.A. (2002) Classification of genes differentially expressed during water-deficit stress in *Arabidopsis thaliana*: an analysis using microarray and differential expression data. *Ann Bot* **89**, 803–811.
76. Wood, A.J., Duff, R.J., and Oliver, M.J. (1999) Expressed sequence Tags (ESTs) from desiccated *Tortula ruralis* identify a large number of novel plant genes. *Plant Cell Physiol* **40**, 361–368.
77. Oliver, M.J., Dowd, S.E., Zaragoza, J. Mauget, S., and Payton, P.R. (2004) The rehydration transcriptome of the desiccation-tolerant bryophyte *Tortula ruralis*: transcript classification and analysis. *BMC Genomics* **5**, 1–49.
78. Reynolds, T.L. and Bewley, J.D. (1993) Characterization of protein synthetic changes in a desiccation-tolerant fern, *Polypodium virginianum*. Comparison of the effects of drying, rehydration and abscisic acid. *J Expt Bot* **44**, 921–928.
79. Bartels, D., Schneider, K., Terstappen, G., Piatkowski, D., and Salamini, F. (1990) Molecular cloning of abscisic acid-modulated genes which are induced during desiccation of the resurrection plant *Craterostigma plantagineum*. *Planta* **181**, 27–34.
80. Frank, W., Phillips, J., Salamini, F., and Bartels, D. (1998) Two dehydration-inducible transcripts from the resurrection plant *Craterostigma plantagineum* encode interacting homeodomain–leucine zipper proteins. *Plant J* **15**, 413–421.
81. Phillips, J.R., Hilbricht, T., Salamini, F., and Bartels, D. (2002) A novel abscisic acid- and dehydration-responsive gene family from the resurrection plant *Craterostigma plantagineum* encodes a plastid-targeted protein with DNA-binding activity. *Planta* **215**, 258–266.
82. Neale, A.D., Blomstedt, C.K., Bronson, P., Le, T.-N., Guthridge, K., Evans, J., Gaff, D.F., and Hamill, J.D. (2000) The isolation of genes from the resurrection grass *Sporobolus stapfianus* which are induced during severe drought stress. *Plant Cell Environ* **23**, 265–277.
83. O'Mahony, P. and Oliver, M.J. (1999) Characterization of a desiccation-responsive small GTP-binding protein (Rab2) from the desiccation-tolerant grass *Sporobolus stapfianus*. *Plant Mol Biol* **39**, 809–821.
84. Collett, H., Shen, A., Gardner, M., Farrant, J.M., Denby, K.J., and Illing, N.A. (2004) Towards transcript profiling of desiccation tolerance in *Xerophyta humilis*: construction of a normalized 11 k X. humilis cDNA set and microarray expression analysis of 424 cDNAs in response to dehydration. *Physiol Plant* **122**, 39–53.
85. Illing, N., Denby, K., Collett, H., Shen, A., and Farrant, J.M. (2005) The signature of seeds in resurrection plants: a molecular and physiological comparison of desiccation tolerance in seeds and vegetative tissues. *Integr Comp Biol* **45**, 771–787.
86. Oliver, M.J. (1991) Influence of protoplasmic water loss on the control of protein synthesis in the desiccation-tolerant moss *Tortula ruralis*: ramifications for a repair-based mechanism of desiccation tolerance. *Plant Physiol* **97**, 1501–1511.

87. Kuang, J., Gaff, D.F., Gianello, R.D., Blomstedt, C.K., Neale, A.D., and Hamill, J.D. (1995) Changes in vivo protein complements in drying leaves of the desiccation-tolerant grass *Sporobolus stapfianus* and the desiccation-sensitive grass *Sporobolus pyramidalis*. *Aust J Plant Physiol* **22**, 1027–1034.
88. Jiang, G., Wang, Z., Shang, H., Yang, W., Hu, Z., Phillips, J., Deng, X. (2007) Proteome analysis of leaves from the resurrection plant *Boea hygrometrica* in response to dehydration and rehydration. *Planta* **225**, 1405–1420.
89. Piatkowski, D., Schneider, K., Salamini, F., and Bartels, D., (1990) Characterization of five abscisic acid-responsive cDNA clones from the desiccation-tolerant plant *Craterostigma plantagineum* and their relationship to other water-stress genes. *Plant Physiol* **94**, 1682–1688.
90. Proctor, M.C.F., Oliver, M.J., Wood, A.J., Alpert, P., Stark, L.R., Cleavitt, N., and Mishler, B.D. (2007) Desiccation tolerance in bryophytes: a review. *The Bryologist* **110**, 595–621.
91. Werner, O., Espin, R.M.R., Bopp, M., and Atzorn, R. (1991) Abscisic-acid-induced drought tolerance in *Funaria hygrometrica* Hedw. *Planta* **186**, 99–103.
92. Cuming, A.C., Cho, S.H., Kamisugi, Y., Graham, H., and Quatrano, R.S. (2007). Microarray analysis of transcriptional responses to abscisic acid and osmotic, salt, and drought stress in the moss, *Physcomitrella patens*. *New Phytol* **176**, 275–287.
93. Bewley, J.D., Reynolds, T.L., and Oliver, M.J. (1993) Evolving strategies in the adaptation to desiccation. *In Plant Responses to Cellular Dehydration During Environmental Stress. Current Topics in Plant Physiology: American Society of Plant Physiologists Series Vol. 10* (Close, T.J., and Bray, E.A. eds.). ASPB Publishers, Rockville, MD, pp. 193–201.
94. Hilbricht, T., Varotto, S., Sgaramella, V., Bartels, D., Salamini, F., and Furini, A. (2008) Retrotransposons and siRNA have a role in the evolution of desiccation tolerance leading to resurrection of the plant *Craterostigma plantagineum*. *New Phyto* **179**, 877–887.
95. Schwab, K.B. and Heber, U. (1984) Thylakoid membrane stability in drought-tolerant and drought-sensitive plants. *Planta* **161**, 37–45.
96. Kaiser, K., Gaff, D.F. and Outlaw, Jr., W.H. (1985) Sugar contents of leaves of desiccation-sensitive and desiccation-tolerant plants. *Naturwissenschaften* **72**, 608–609.
97. Koster, K.L. and Leopold, A.C. (1988) Sugars and desiccation tolerance in seeds. *Plant Physiol* **88**, 829–832.
98. Hoekstra, F.A. and van Roekel, T. (1988) Desiccation tolerance of *Papaver dubium* L. pollen during its development in the anther: possible role of phospholipid composition and sucrose content. *Plant Physiol* **88**, 626–632.
99. Bianchi, G., Gamba A., Murelli C., Salamini F., and Bartels, D. (1991) Novel carbohydrate metabolism in the resurrection plant *Craterostigma plantagineum*. *Plant J* **1**, 355–359.
100. Whittaker, A., Bochicchio, A., Vazzana, C., Lindsey, G., and Farrant, J. (2001) Changes in leaf hexokinase activity and metabolite levels in response to drying in the desiccation-tolerant species *Sporobolus stapfianus* and *Xerophyta viscosa*. *J Exp Bot* **52**, 961–969.
101. Bewley, J.D., Halmer, P., Krochko, J.E., and Winner W.E. (1978) Metabolism of a drought-tolerant and a drought-sensitive moss: respiration, ATP synthesis and carbohydrate status. In *Dry biological systems* (Crowe, J.H. and Clegg, J.S., eds.). Academic Press, New York, pp. 185–203.
102. Wiemken, A. (1990) Trehalose in yeast, stress protectant rather than reserve carbohydrate. *Antonie van Leeuwenhoek* **58**, 209–217.
103. Clegg, J.S. (1986) The physical properties and metabolic status of *Artemia* cysts at low water contents: the water replacement hypothesis. In *Membranes, Metabolism and Dry Organisms*. (Leopold, A.C., ed.). Cornell University Press, Ithaca, NY, pp. 169–187.
104. Adams, R.P., Kendall, E., and Kartha, K.K. (1990) Comparison of free sugars in growing and desiccated plants of *Selaginella lepidophylla*. *Biochem Syst Ecol* **18**, 107–110.
105. Iturriaga, G., Gaff, D.F., and Zentella, R. (2000) New desiccation-tolerant plants, including a grass, in the central highlands of Mexico, accumulate trehalose. *Aust J Bot* **48**, 153–158.
106. Lui, M.-S., Chien, C.-T, and Lin T.-P. (2008) Constitutive components and induced gene expression are involved in the desiccation tolerance of *Selaginella tamariscina*. *Plant Cell Physiol* **49**, 653–663.
107. Figueroa-Soto, C.G., Iturriaga, G., and Valenzuela-Soto, E.M. (2004) Actividad de trehalosa 6-fosfato sintasa en respuesta a hidratación y desecación en plantas de *Selaginella lepidophylla*. *Rev Fitotéc Mex* **27**, 17–22.
108. Bianchi, G., Gamba, A., Limiroli, R., Pozzi, N., Elster, R., Salamini, F., and Bartels, D.

(1993) The unusual sugar composition in leaves of the resurrection plant *Myrothamnus flabellifolia*. *Physiol Plant* **87**, 223–226.
109. Drennan, P.M., Smith, M.T., Goldsworthy, D., and van Staden, J. (1993) The occurrence of trehalose in the leaves of the desiccation-tolerant angiosperm *Myrothamnus flabellifolius* Welw. *J Plant Physiol* **142**, 493–496.
110. Albini, F.M., Murelli, C., Patritti, G., Rovati, M., Zienna, P., Finzi, P.V. (1994) Low-molecular weight substances from the resurrection plant *Sporobolus stapfianus*. *Phytochem* **37**, 137–142.
111. Holmström, K.O., Mantyla, E., Welin, B., Mandal, A., and Palva, E.T. (1996) Drought tolerance in tobacco. *Nature* **379 (6567)**, 683–684.
112. Jang, I.-C., Oh, S.-J., Seo, J.-S., Choi, W.-B, Song, S.I., Kim, C.H. Kim,Y.S., Seo, H.-S., Choi, Y.D., Nahm, B.H., and Kim, J.K. (2003) Expression of a bifunctional fusion of the *Escherichia coli* genes for trehalose-6-phosphate synthase and trehalose-6-phosphate phosphatase in transgenic rice plants increases trehalose accumulation and abiotic stress tolerance without stunting growth. *Plant Physiol* **131**, 516–524.
113. Smirnoff, N. (1993) Role of active oxygen in the response of plants to water deficit and desiccation. *New Phytol* **125**, 27–58.
114. Van den Ende, W. and Valluru, R. (2009) Sucrose, sucrosyl oligosaccharides, and oxidative stress: scavenging and salvaging? *J Exp Bot* **60**, 9–18.
115. Koster, K.L., Lei, Y.P., Anderson, M., Martin, S., and Bryant, G. (2000) Effects of vitrified and non-vitrified sugars on phosphatidylcholine fluid-to-gel phase transitions. *Biophys J* **78**, 1932–1946.
116. Lenné, T., Bryant, G., Holcomb, R., and Koster, K.L. (2007) How much solute is needed to inhibit the fluid-gel membrane phase transition at low hydration? *Biochim Biophys Acta* **1768**, 1019–1022.
117. Crowe, J.H., Crowe, L.M., and Chapman, D. (1984) Preservation of membranes in anhydrobiotic organisms: the role of trehalose. *Science* **223**, 701–703.
118. Crowe, J.H. (2007) Trehalose as a "chemical chaperone": fact and fantasy. In *Molecular Aspects of the Stress Response: Chaperones, Membranes and Networks* (Csermely, P. and Vigh, L., eds.), Springer, New York, pp 143–158.
119. Koster, K.L. (1991) Glass formation and desiccation tolerance in seeds. *Plant Physiol* **96**, 302–304.
120. Koster, K.L., Webb, M.S., Bryant, G., and Lynch, D.V. (1994) Interactions between soluble sugars and POPC (1-palmitoyl-2-oleoylphosphatidylcholine) during dehydration: vitrification of sugars alters the phase behavior of the phospholipid. *Biochim Biophys Acta* **1193**, 143–150.
121. Sun, W., Irving, T.C., and Leopold, A.C. (1994) The role of sugar, vitrification and membrane phase transition in seed desiccation tolerance. *Physiol Plant* **90**, 621–628.
122. Buitink, J. and Leprince, O. (2004) Glass formation in plant anhydrobiotes: survival in the dry state. *Cryobiol* **48**, 215–228.
123. Walters, C., Hill, L.M., and Wheeler, L.J. (2005) Dying while dry: kinetics and mechanisms of deterioration in desiccated organisms. *Integr Comp Biol* **45**, 751–758.
124. Bartels, D., Singh M., and Salamini F. (1988) Onset of desiccation-tolerance during development of the barley embryo. *Planta* **175**, 485–492.
125. Tunnacliffe, A. and Wise, M.J. (2007) The continuing conundrum of the LEA proteins. *Naturwiss* **94**, 791–812.
126. Wise, M.J., and Tunnacliffe. A (2004) POPP the question: What do LEA proteins do? *Trends Plant Sci* **9**, 13–17.
127. Goyal, K., Walton, L.J., and Tunnacliffe, A. (2005) LEA proteins prevent protein aggregation due to water stress. *Biochem. J* **388**, 151–157.
128. Mowla, S.B., Cuypers, A., Driscoll, S.P., Kiddle, G., Thomson, J., Foyer, C.H., and Theodoulou, F.L. (2006) Yeast complementation reveals a role for an *Arabidopsis thaliana* late embryogenesis abundant (LEA)-like protein in oxidative stress tolerance. *Plant J* **48**, 743–756.
129. Grelet, J., Benamar, A., Teyssier, E., Avelange-Macherel, M.-H., Grunwald, D., and Macherel, D. (2005) Identification in pea seed mitochondria of a late-embryogenesis abundant protein able to protect enzymes from drying. *Plant Physiol* **137**, 157–167.
130. Tolleter, D., Jaquinod, M., Mangavel, C., Passirani, C., Saulnier, P., Manon, S., Teyssier, E., Payet, N., Avelange-Macherel, M.-H., and Macherel, D (2007) Structure and function of a mitochondrial late embryogenesis abundant protein are revealed by desiccation. *Plant Cell* **19**, 1580–1589.
131. Lui, X., Wanga, Z., Wanga, L., Wua, R., Phillips, J., and Deng, X. (2009) LEA 4 group genes from the resurrection plant *Boea hygrometrica* confer dehydration tolerance in transgenic tobacco. *Plant Sci* **176**, 90–98.

132. Koag, M.-C., Fenton, R.D., Wilkens, S., and Close, T.J. (2003) The binding of maize DHN1 to lipid vesicles. Gain of structure and lipid specificity. *Plant Physiol* **131**, 309–316.
133. Pouchkina-Stantcheva, N.N., McGee, B.M., Boschetti, C., Tolleter, D., Chakrabortee, S., Popova, A.V., Meersman, F., Macherel, D., Hincha, D.K., and Tunnacliffe, A. (2007) Functional divergence of former alleles in an ancient asexual invertebrate. *Science* **318**, 268–271.
134. Chakrabortee, S., Boschetti, C., Walton, L.J., Sarkar, S., Rubinsztein, D.C., and Tunnacliffe, A. (2007) Hydrophilic protein associated with desiccation tolerance exhibits broad protein stabilization function. *Proc Natl Acad Sci USA* **104**, 18073–18078.
135. Wolkers, W.F., McCready, S., Brandt, W., Lindsey, G.G., and Hoekstra, F.A. (2001) Isolation and characterization of a D-7 LEA protein from pollen that stabilizes glasses in vitro. *Biochim Biophys Acta* **1544**, 196–206.
136. Wood, A.J. and Oliver, M.J. (1999) Translational control in plant stress: the formation of messenger ribonucleoprotein particles (mRNPs) in response to desiccation of *Tortula ruralis* gametophytes. *Plant J* **18**, 359–370.
137. Oliver, M.J., Velten, J., and Mishler B.D. (2005) Desiccation tolerance in bryophytes: a reflection of the primitive strategy for plant survival in dehydrating habitats? *Integr Comp Biol* **45**, 788–799.
138. Iturriaga, G., Cushman, M.A.F., and Cushman, J.C. (2006) An EST catalogue from the resurrection plant *Selaginella lepidophylla* reveals abiotic stress-adaptive genes. *Plant Biol* **170**, 1173–1184.
139. Velten, J., Oliver, M.J. (2001) Tr288: a rehydrin with a dehydrin twist. *Plant Mol Biol* **45**, 713–722.
140. Wehmeyer, N. and Vierling, E. (2000) The expression of small heat shock proteins in seeds responds to discrete developmental signals and suggests a general protective role in desiccation tolerance. *Plant Physiol* **25**, 1347–1357.
141. Wang, W., Vinocur, B., Shoseyov, O., and Altman, A. (2004) Role of plant heat shock proteins and molecular chaperones in the abiotic stress response. *Trends Plant Sci* **9**, 244–252.
142. Sun, W., Bernard, C., van de Cotte., van Montague, M., and Verbruggen, N. (2001) At-HSP17.6A, encoding a small heat shock protein in *Arabidopsis*, can enhance osmotolerance upon overexpression. *Plant J* **27**, 407–415.
143. Allen, R. (1995). Dissection of oxidative stress tolerance using transgenic plants. *Plant Physiol* **107**, 1049–1054.
144. Kranner, I., Beckett, R.P, Wornik, S., Zorn, M., and Pfeifhofer, H.W. (2002) Revival of a resurrection plant correlates with its antioxidant status. *Plant J* **31**, 13–24.
145. McKersie, B.D., Bowley, S.R., Harjanto, E., and Leprince, O. (1996) Water-deficit tolerance and field performance of transgenic alfalfa overexpressing superoxide dismutase. *Plant Physiol* **124**, 153–162.
146. Moore, J.P., Vicre-Gibouin, M., Farrant, J.M., and Driouich, A. (2008) Adaptations of higher plant cell walls to water loss: drought vs desiccation. *Physiol Plant.* **134**, 237–245
147. Vicré, M., Lerouxel, O., Farrant, J., Lerouge, P., and Driouich, A. (2004) Composition and desiccation-induced alterations of the cell wall in the resurrection plant *Craterostigma wilmsii*. *Physiol Plant* **120**, 229–239.
148. Jones, L. and McQueen-Mason, S. (2004) A role for expansins in dehydration and rehydration of the resurrection plant *Craterostigma plantagineum*. *FEBS Lett* **559**, 61–65.
149. Hilbricht, T., Salamini, F., and Bartels, D. (2002) CpR18, a novel SAP-domain plant transcription factor, binds to a promoter region necessary for ABA mediated expression of the CDeT27-45 gene from the resurrection plant *Craterostigma plantagineum* Hochst. *Plant J* 31, 293–303.
150. Deng, X., Phillips, J., Meijer, A.H., Salamini, F., and Bartels, D. (2002) Characterization of five novel dehydration-responsive homeodomain leucine zipper genes from the resurrection plant *Craterostigma plantagineum*. *Plant Mol Biol* **49**, 601–610.
151. Villalobos, M.A., Bartels, D., and Iturriaga, G. (2004) Stress tolerance and glucose insensitive phenotypes in *Arabidopsis* overexpressing the CpMYB10 transcription factor gene. *Plant Physiol* **135**, 309–324.
152. Smith-Espinoza, C., Bartels, D., and Phillips, J. (2007) Analysis of a LEA gene promoter via Agrobacterium-mediated transformation of the desiccation tolerant plant *Lindernia brevidens*. *Plant Cell Rep* **26**, 1681–1688.
153. Toth, S., Kiss, C., Scott, P., Kovacs, G., Sorvari, S., and Toldi, O. (2006) Agrobacterium-mediated genetic transformation of the desiccation tolerant resurrection plant *Ramonda myconi* (L.) Rchb. *Plant Cell Rep* **25**, 442–449.

Chapter 2

Approaches to Identifying Genes for Salinity Tolerance and the Importance of Timescale

Rana Munns

Abstract

Soil salinity reduces the ability of plants to take up water, and this quickly causes reductions in the rate of cell expansion in growing tissues. The slower formation of photosynthetic leaf area in turn reduces the flow of assimilates to the meristematic and growing tissues of the plant. Later, salt may exert an additional effect on growth. If excessive amounts of Na^+ or Cl^- enter the plant it may rise to toxic levels in the older transpiring leaves. This injury, added to an already reduced leaf area, will then further limit the flow of carbon compounds to meristems and growing zones in leaves. This chapter analyses the various plant responses over time, to provide a conceptual framework on which the different approaches to gene discovery can be based. Knowledge of the physiological processes that are important in the tolerance response, and the time frame in which they act, will enable further progress in understanding of the molecular regulation of salt tolerance.

Key words: Gene expression, salinity, salt tolerance, Na^+ accumulation.

1. Introduction

Salinity affects about 6% of the world's land area, much of which is important to agriculture. Over 800 million ha of land throughout the world are salt affected either by salinity or by the associated condition of sodicity (1). Most of this salinity, and all of the sodicity, is natural. However, a significant proportion of recently cultivated agricultural land has become saline due to clearing of natural vegetation or irrigation. Of the current 230 million ha of irrigated land, 45 million ha are salt affected (1). Irrigated land is only 15% of total cultivated land, but as irrigated land has at least twice the productivity of rain-fed land, it produces one-third of the world's food.

R. Sunkar (ed.), *Plant Stress Tolerance*, Methods in Molecular Biology 639,
DOI 10.1007/978-1-60761-702-0_2,

Yield of essential food and forage crops is limited by soil salinity in many of these regions, so genetic improvements in salt tolerance are essential to sustain global food production. The ability to grow and reproduce in saline soil differs widely between species, due to differences in the ability to control salt uptake from the soil and to compartmentalise it effectively at the cellular level (2). Yet, even in the most salt-tolerant species, growth rates are greatly reduced by salinity, due to the osmotic stress of the salt in the soil. Maintaining turgor through osmotic adjustment is essential to counter the osmotic stress. Turgor maintenance through osmotic adjustment is a mechanism that contributes to the salt tolerance of halophytes (3).

The genetic control of the tolerance response is complex. There are a number of transporters involved in the regulation of Na^+ uptake and transport (2), and a number of signalling pathways involved in the growth response to the perturbation of the osmotic stress outside the roots (4). However, it is difficult to distinguish critical genes that determine the tolerance or susceptibility of the plant, from those 'downstream' of the perturbation, the so-called housekeeping genes. Genes controlling the level of reactive oxygen species are an example of these housekeeping genes (2).

This chapter aims to distinguish the osmotic and salt-specific parts of the response, so that candidate genes can be more clearly discerned. Growth reductions are predominantly due to the osmotic stress, but in species that have a high rate of salt uptake, or cannot compartmentalise salt effectively in vacuoles, salt-specific effects develop with time, impose an additional stress on the plant through failing capacity to produce photoassimilate, and give rise to the category of 'salt-sensitive'. This chapter does not focus on individual genes, but on the general process in which they are operating. These are basically the maintenance of cell turgor and volume, the control of ion transport, and the control of cell growth by hormone action or by carbon supply. Individual genes that are important in the tolerance mechanism have been covered in several recent reviews (2, 5, 6). This chapter attempts to construct a whole plant framework and to suggest the time and place in which gene expression should be investigated. An understanding of the tissue- or cell-specific nature of the response, and the whole plant phenotype associated with individual gene action, is essential in the identification of important genes.

2. Growth Processes at Different Timescales

Table 2.1 summarises the sequence of events in a plant when exposed to salinity. In the first few seconds or minutes, cells lose water and shrink. Over hours, cells regain their original turgor and

Table 2.1
The effect of salinity on plant growth at different timescales and the cellular and metabolic events involved. The species indicated as 'sensitive' have poor exclusion by roots or inadequate compartmentation within leaves, although this would occur in all species if the salinity was high enough

	Observed effect on growth	Cellular events	Metabolic events
Seconds to minutes	Instant reduction in leaf and root elongation rate then rapid partial recovery	Shrinkage of cell volume then restoration due to regaining turgor	Osmotic adjustment
Hours	Steady reduced rate of leaf and root elongation	Changed rheology of cell wall	Signalling pathways
Days	Reduced rate of leaf emergence; increase in root:shoot ratio	Cell production rate and primordia development inhibited	Signalling pathways and carbohydrate supply
Weeks	Reduced branch or tiller formation	Apical development program altered	Signalling pathways and carbohydrate supply
Weeks – sensitive species	*Old leaves die*	*Na^+ and/or Cl^- accumulates excessively in cells*	*Ion toxicity in mature leaves*
Months	Altered flowering time, reduced seed production	Reproductive development program altered	Signalling pathways and carbohydrate supply
Months – sensitive species	*Plant dies before maturity*	*Inadequate capacity for assimilate production to support further growth*	*Carbohydrate deficit*

volume but cell elongation rates in growing tissues are reduced, leading to lower rates of leaf and root growth. Over days, lower rates of leaf and root growth can be seen. Over weeks, gross changes in vegetative development are apparent, such as reduced formation of lateral shoots, and over months changes in reproductive development. In salt-sensitive species, which are often those less able to control the uptake and internal transport of salt, leaves die prematurely and the plant may be unable to produce sufficient photosynthate to complete its life cycle.

The different responses occur over different timescales, from changes in water relations that occur as soon as the roots encounter a saline soil solution to complex controls at the whole plant level involving long-distance signalling and the supply of assimilates. Salt toxicity affects growth in the longer term. Salt toxicity occurs in plants growing in salinities too high for them to adequately control the uptake of salt by roots, its transport

to leaves, and compartmentalisation of the salt within cells. Salts accumulate in the older transpiring leaves over time, and if reaching toxic concentrations will inhibit growth of the younger leaves by reducing the supply of carbohydrates to the growing cells.

2.1. Timescale of Seconds to Minutes – The Transient Phase

Cell expansion rates change suddenly in both leaves and roots. With a sudden change in salinity there are rapid, virtually instantaneous, shrinking of cells in both roots and leaves and cessation of cell expansion. Several minutes after the initial decline of leaf and root growth, a gradual recovery is observed that may take 30 minutes or more before reaching a new steady rate. This response has been recorded for both roots and leaves in many different species (7–9) and shown for barley in **Fig. 2.1**.

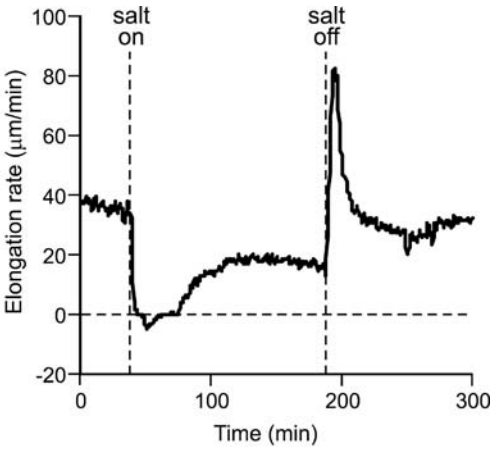

Fig. 2.1. Effect of changes in soil salinity (75 mM NaCl) on leaf elongation rate of a barley leaf. *Vertical broken lines* mark the times at which the soil solution was changed. Adapted from (7) [http://www.publish.csiro.au/journals/fpb; DOI: 10.1071/PP99193].

These rapid and transient changes in growth are due to changes in cell–water relations alone. Evidence for this comes from experiments in which leaf water status was maintained as the soil was made saline by a pressurisation technique, which prevented a drop in leaf water status and completely prevented the transient changes shown in **Fig. 2.1** (9). A water relations explanation is supported by the findings that different osmotica produce the same rapid and transient decline (10). In roots also, there are rapid and transient reductions in growth rates, which are due to changed water relations, as indicated by the similar effect of non-ionic osmotica (10).

2.2. Timescale of Hours – The Recovery Phase

Leaf growth recovers to a large extent within one or more hours after a sudden change in salinity, settling down to a new steady rate that is considerably less than the original one (**Fig. 2.1**). The time taken to recover and the new steady rate depend on the

concentration of the salt solution (7). Other osmotica have the same effect (10).

Root growth, in contrast to leaf growth, recovers remarkably well. With moderate levels of osmotic stress the recovery is essentially complete within 1 h, but with a larger osmotic shock this may take 24 h (10). In a study with maize roots comparing the effects of a salt shock versus a gradual increase, Rodriguez et al. (11) found that salt had no effect on root growth at concentrations up to 100 mM NaCl (about 0.5 MPa) as long as the concentration was increased gradually. The deleterious effects of a salt shock are presumably associated with the plasmolysis of root cells that would ensue if there was a single-step increase in osmotic pressure of more than 0.4 MPa (as the turgor of root cells is about 0.4 MPa), and the plasma membranes would take some time to repair (10).

The new steady rate of growth is unlikely to be determined by salt toxicity, as other osmotica such as KCl and mannitol have the same effect. It is also unlikely to be due to water relations or a hydraulic message from the roots, as turgor is regained in roots (7) and probably also in leaves. Complex signalling pathways are regulating root and leaf growth.

2.3. Timescale of Days – The Adjustment Phase

Over the timescale of days, in addition to a reduced rate of leaf expansion, there is a reduced meristematic activity, with delayed emergence of new leaves and lateral buds. Leaf growth is often more affected than root growth, resulting in an increased shoot:root ratio. This is an adaptive response as reduced leaf area would lessen the depletion of soil water and therefore the rate at which the salt concentration in the soil rises. Plants exclude at least 90% of the salt from the solution they take up (12), which results in a concentration of the salt around the roots, so a reduction in water use is beneficial in the long term.

The slower growth rate is not due to water relations, as shown by the fact that the leaves have regained turgor (13), and that leaf expansion of plants in saline soil does not respond to an increase in leaf water status (14). Photosynthesis of expanded leaves is reduced due to stomatal closure (15, 16); however, growth does not seem to be limited simply by carbon supply as carbohydrate status of the plant is still high (14). This means that the slower growth is regulated by signalling pathways, which includes the transmission of a message from the roots to the shoots.

Salt-specific effects are unlikely at this stage, as it is unlikely that salt ever builds up to toxic concentrations in the growing cells themselves. For instance, in the rapidly elongating tissue of leaves of wheat grown in 120 mM NaCl, Na^+ averaged only 15 mM and Cl^- averaged 50 mM (17). Fricke (18) found no correlation between the rate of barley leaf elongation and Na^+ concentrations in the growing zone. The rapid expansion of the growing

cells would keep the salt from building up to high concentrations. As long as it can be sequestered in rapidly expanding vacuoles, salt uptake at this stage of cell development is advantageous for osmotic adjustment.

Antioxidant activity is increased in order to maintain reactive oxygen species (ROS) at the levels required for their role in various signal transduction cascades. Leaves have surplus capacity to produce antioxidants to prevent ROS reaching toxic levels, the latter occurring only in a controlled oxidative burst that signals programmed cell death (19).

2.4. Timescale of Weeks – The Phase of Rapid Vegetative Development

After a week, developmental changes appear in the shoot. A marked reduction in the number of lateral shoots can occur. For example, the number of tillers of wheat growing in 150 mM NaCl was reduced by two-thirds (20), which accounted for the two-thirds reduction in leaf area. Leaf anatomy changes, so that leaves are smaller in area but thicker, resulting in a higher concentration of chlorophyll per unit area. Leaves are often visibly greener. For this reason, photosynthetic rate per unit area may be little affected (15), although photosynthetic rate per leaf and certainly per plant is reduced.

The mechanism by which salinity affects these developmental processes is unknown. It is unlikely to be by an effect of Na^+ or Cl^- in the meristematic tissues themselves, as concentrations there are probably quite low (20). Lateral bud development is influenced by the supply of carbohydrate, as elevated CO_2 increased the number of tillers of wheat plants in saline soil and reversed the effect of salinity (20). However, the carbohydrate status of the growing tissues was not reduced by salinity (20) indicating that signalling pathways are regulating the growth rate to keep a positive carbon balance between source and sink, i.e. between supply and demand.

Extra changes are seen in sensitive species. In this timescale of weeks, the sensitive genotypes show marked injury in older leaves. It is due to salts accumulating in transpiring leaves to excessive levels, exceeding the ability of the cells to compartmentalise salts in the vacuole. Salts then rapidly build up in the cytoplasm and inhibit enzyme activity. Salts eventually build up to high concentrations in the transpiring leaves and cause premature senescence.

In very sensitive species, leaves die at a fast rate. The rate at which they die becomes the crucial issue determining the survival of the plant. If new leaves are continually produced at a rate greater than that at which old leaves die, then there is enough photosynthetic surface for the plant to produce flowers and seeds. However, if the rate of leaf death exceeds the rate at which new leaves are produced, then the proportion of leaves that are injured starts to increase. There is then a race against time to initiate

flowers and form seeds while there are still an adequate number of green leaves left to supply the necessary photosynthate.

This is illustrated in an experiment with two wheat genotypes with contrasting rate of Na^+ transport to leaves, and resultant contrast in salt tolerance in the long term (21). A period of a month elapsed during which growth rates of both genotypes were equally reduced by salinity, even though leaf injury appeared on one more than the other. After a month, the growth rate of the injured genotype started to slow down, and within 2 weeks many individual plants had died (**Fig. 2.2**). This experiment indicated that the major effect on growth was osmotic, but after time, salt toxicity exerted an additional effect.

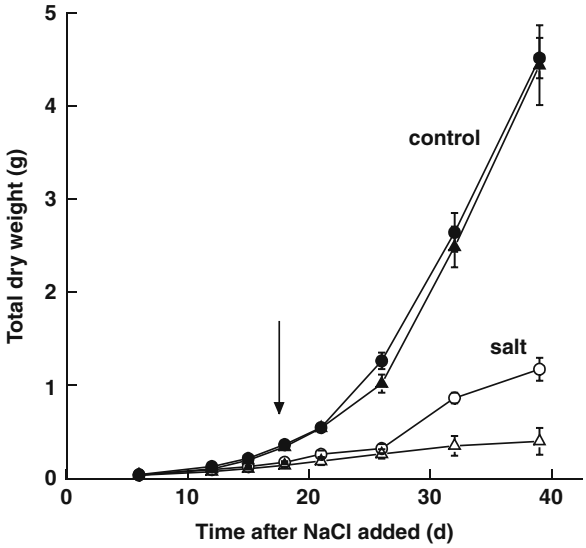

Fig. 2.2. Two accessions of the diploid wheat progenitor *Triticum tauschii* in control solution (*closed symbols*) and in 150 mM NaCl with supplemental Ca^{2+} (*open symbols*). *Circles* denote the tolerant accession and *triangles* the sensitive one. The *arrow marks* denote the time at which symptoms of salt injury could be seen on the sensitive accession; at that time the proportion of dead leaves was 10% for the sensitive and 1% for the tolerant accession. Adapted from (21) [http://www.publish.csiro.au/nid/102/paper/PP9950561.htm].

2.5. Timescale of Months – The Reproductive Phase

After a month there can be obvious effects of salinity on the development of reproductive organs. Salinity reduced the number of florets per ear in barley and wheat and altered the time of flowering (22).

The mechanisms by which salinity might affect the formation of reproductive organs are not clear. Similar phenomena occur under drought. It is probable that it is controlled by signalling pathways that affect the expression of genes switching on developmental programs, again influenced by the supply of carbohydrate but not wholly determined by it. A salt-specific effect is

an unlikely cause of altered reproductive development in the relatively salt-tolerant species like wheat and barley; Na^+ and Cl^- are present in the reproductive primordia (22), but at concentrations too low to affect metabolism. In tomato, another relatively salt-tolerant species, microanalysis of Na^+ concentrations and carbohydrate concentrations in various floral tissues at critical times indicated that the floral abortion was more likely due to the supply of carbohydrates to the inflorescence than to accumulation of ions to toxic levels (23).

In salt-sensitive plants like rice, in which salt has built up to excessive levels in leaves and the vacuoles can no longer contain the incoming salt, significant amounts of salt can be transported in the phloem to the reproductive organs. High levels of Na^+ were found in pollen and stigmas of rice grown at 50 mM NaCl, and stigmatic receptivity was reduced as well as pollen viability (24). These authors concluded that the high degree of sterility was probably due to Na^+ toxicity in the reproductive tissues. This may be peculiar to rice and explain why the yield of rice is particularly sensitive to salinity: the grain yield was only 10% of controls, whereas the straw weight was 80% of controls (24).

In summary, there is a two-phase growth response to salinity. The first phase of growth reduction is quickly apparent and is due to the salt outside the roots. It can be called a water stress or osmotic phase. The second phase of growth reduction, which takes time to develop, results from internal injury. It is due to salts accumulating in transpiring leaves to excessive levels, exceeding the ability of the cells to compartmentalise salts in the vacuole. The osmotic stress affects growing leaves and salt toxicity affects old leaves.

3. Measurement of Salt Tolerance

Salt tolerance is usually assessed as the percent biomass production in saline versus control conditions over a prolonged period of time. Screening methods that avoid the need to grow controls are desirable, as a large amount of space is needed to grow controls under optimum light levels and to obtain sufficient replication as the environmental influences on growth rate are large (25). When comparing landraces versus cultivars, or wild types versus mutants, there is likely to be large genotypic differences in height or leaf area, and space is needed to prevent shading of smaller genotypes by larger ones.

Specific screening methods that avoid the need for comparison with plants in control conditions are summarised in **Table 2.2**. These methods have been used to screen natural vari-

Table 2.2
Techniques used to screen large numbers of genotypes for salinity tolerance in glasshouses or controlled environments. Comments indicate whether a control (non-saline) treatment is necessary, particular advantages of the technique that relate to its experimental feasibility, whether the responses measured are due to the osmotic or the salt-specific effect of the salinity treatment, and how long the treatment needs to be imposed. Avoiding the need to grow controls plants is a major advantage

Technique[a]	Controls needed	Advantages	Osmotic or salt-specific effect	Length of treatment (weeks)
Screening techniques for tolerance to moderate salinity (50–150 mM NaCl)				
Measurements of growth				
Root elongation	Yes	Can be used with very young seedlings	Osmotic	1
Leaf elongation	Yes	Not destructive	Osmotic	2
Biomass	Yes	More likely to relate to field	Both	4
Yield	Yes	Most likely to relate to field	Both	16
Measurements of injury				
Leakage from leaf discs	No*	Not destructive	Either	3–4
Chlorophyll content	No*	Not destructive and quick (using hand-held meter)	Either	3–4
Chlorophyll fluorescence	No*	Not destructive	Either	3–4
Specific traits				
Na^+ exclusion	No	Not destructive, and a single easy analysis	Salt-specific	1–2
K^+/Na^+discrimination	No	Not destructive	Salt-specific	1–2
Cl^- exclusion	No	Not destructive	Salt-specific	1–2
Screening techniques for tolerance to high salinity (200–300 mM NaCl)				
Germination	Yes	Very large numbers easily handled	Osmotic	1
Survival	No*	Limited experimental period, as can adjust the salinity. Highly tolerant genotypes stand out	Either	2–8, depending on salinity

Reproduced from (25) with kind permission of Springer Science and Business Media.
*Assumes all genotypes under control conditions have no leakage, the same leaf chlorophyll concentration per unit area, fluorescence parameters typical of healthy plants, and 100% survival.
[a]Not listed are photosynthesis, transpiration efficiency, osmotic adjustment, enzyme activity, gene expression, compatible solutes, ABA, ethylene, as these are not feasible screening techniques. These measurements can be made on only small numbers of genotypes at one time.

ation, but can also be useful for screening mutant populations if the numbers can be reduced to a feasible level. Destructive harvests can be replaced by non-destructive harvests if an automated imaging system is available (26).

Survival is sometimes used as an index of salt tolerance, when dealing with large numbers of genotypes. Survival can be measured as the percent of plants alive after a given period of time at a given salinity. Alternatively, if there is a range of salinities, survival can be measured as the salinity at which 50% of the plants have died. The drawback of this index is that it gives little idea of how well a plant can actually *grow* in saline conditions.

Realistic experimental design should avoid large osmotic shocks, avoid salt-induced Ca deficiency, optimise ambient conditions especially if controls are grown, and ensure roots are not constrained by small pots that are waterlogged at the base.

It is not possible to be prescriptive about the length of time that plants should be grown before genotypic differences in salt tolerance can be seen. The second phase will start earlier in plants that are poor excluders of Na^+, such as lupins or beans, and when salinities are higher. It will also start earlier when root temperatures are higher. For plants such as rice that are grown at high temperatures, 10–15 days in salinity is sufficient to generate genotypic differences in biomass that correlate well with differences in yield (27).

4. Identifying Important Genes

Genes so far identified as being important in salt tolerance fall under the categories of ion transporters, compatible solutes or osmolytes, and transcription factors involved in growth regulation. Genes that regulate ion transport in salt-affected plants are listed in Table 3 of Munns (12) and summarised in Munns and Tester (2). Genes that synthesize osmoprotectants are listed in Table 2 of Chinnusamy et al. (6) and Table 4 of Munns (12). Signalling pathways involved in hormonal transduction and likely to be regulating cell growth under abiotic stress are reviewed by Xiong et al. (4).

Various approaches have been used successfully to identify candidate genes for salinity tolerance (**Table 2.3**):

1. A trait-based approach is built upon knowledge about function and forward genetics using a specific phenotype and Mendelian genetics. This approach has been successful in the discovery of sodium transporters of the HKT family from QTLs (*Q*uantitative *T*rait *Lo*ci) for Na^+ exclusion, namely, *SKC1*, *Nax1*, *Nax2*, and *Kna1*. The phenotype is the Na^+

Table 2.3
Different approaches for identifying genes for salinity tolerance. The first approach is based on physiological and mechanistic understanding, the next two assume no prior physiological knowledge. Candidate genes used in the last approach are based on prior knowledge of the gene function in other organisms or the outputs from approaches 1, 2, and 3

	Starting point	Material	Method	Result	Next step
1.	Knowledge of important trait	Natural variation	Phenotype	QTL	Fine mapping and cloning
2.	Molecular genetics	Mutant population	High-throughput screen	Candidate gene	Go to 4
3.	Technical advances in 'Omics'	Contrasting genotypes or treatments	Transcriptomics (microarray), proteomics, metabolomics	Candidate gene or metabolic pathway	Go to 4
4.	Candidate gene	Overexpression and null transformants	Phenotype	Proof of function	Cross with high yielding cultivar

concentration in a given leaf after a given time in salinity. In rice, fine mapping of the *SKC1* locus yielded the sodium transporter OsHKT1;5 (28). In wheat the *Nax1* locus yielded the sodium transporter TmHKT1;4 (29), the *Nax2* locus revealed TmHKT1;5 (30), and the *Kna1* locus revealed TaHKT1;5 (30).

2. High-throughput mutant screens based on clever assays have discovered new and important genes, the most significant being the plasma membrane Na^+/H^+ antiporter SOS1 (31) and the Na^+ transporter AtHKT1 (32).
3. 'Omics' approaches require no prior knowledge about traits or phenotypes. Salinity-related changes in gene expression (transcriptomics), protein levels (proteomics), or metabolite concentrations (metabolomics) can be detected (33) using genotype or treatment comparisons. Comparisons can be made between closely related genotypes with known differences in salinity tolerance, e.g. *Arabidopsis thaliana* versus *Thellungiella halophila* (34), transgenics with overexpression of a candidate gene (35), or different treatments with the same genotype (36). Comparison of different abiotic stresses (salt, cold, dehydration) can reveal salt-specific effects. Studies done at short periods of time after a sudden exposure to NaCl concentrations of over 50 mM, such as 1 or 3 h, are unlikely to reveal useful information as the cells are still recovering from the shrinkage (*see* **Fig. 2.1**).

4. Functional or candidate gene-based approach uses knowledge of the function of a metabolite or transporter in halophytic species, particularly microorganisms or model systems. Notable examples are the K^+ transporter HKT1 (37), the vacuolar Na^+/H^+ antiporter NHX1 (38), the Na^+-ATPase PpENA (39), and the osmoprotectant glycine betaine (40).

Tissue selection is a critical part of experimental design, particularly for the 'omics' approaches (12). Genes involved in growth regulation can be best detected by comparing growing versus non-growing tissues. The growing zones in roots and in leaves of monocotyledonous species have a very well-defined growing zone, and the different tissues that are affected by salinity in cereal leaves are well known (17, 41).

5. Conclusions

Salinity can affect growth in a number of ways. First, the presence of salt in the soil reduces the ability of the plant to take up water, and this quickly causes reductions in the rate of leaf and root elongation. This is the first phase of the growth response, due to the osmotic effect of the salt in the soil solution, and produces a suite of effects identical to those of water stress caused by drought. Later, there may be an additional effect on growth; if excessive amounts of salt enter the plant they will eventually rise to toxic levels in the older transpiring leaves. The reduced photosynthetic capacity of the plant will reduce the amount of assimilate transported to the growing tissues, which may further limit growth. This is the second phase of the growth response and is the phase that clearly separates species and genotypes that differ in the ability to tolerate saline soil.

Many genes are important in adapting plants to grow and yield well in saline soil. The concern about future food shortages makes it imperative to better understand the genetic control of salt tolerance and to use this knowledge to increase the salt tolerance of important crops and pasture species. Various approaches can be taken to discover genes for salinity tolerance. An understanding of the physiological mechanisms in which the genes operate will accelerate their application for improving salt tolerance of crops.

Acknowledgements

I thank Mark Tester and Stuart Roy for critical comments on the chapter.

References

1. FAO. (2009) FAO Land and Plant Nutrition Management Service. http://www.fao.org/ag/agl/agll/spush
2. Munns, R. and Tester, M. (2008) Mechanisms of salinity tolerance. *Annu Rev Plant Biol* **59**, 651–681.
3. Flowers, T.J. and Colmer, T.D. (2008) Salinity tolerance in halophytes. *New Phytol* **179**, 945–963.
4. Xiong, L.M., Schumaker, K.S., and Zhu, J.K. (2002) Cell signaling during cold, drought and salt stress. *Plant Cell*, **14**, S165–S183.
5. Bartels, D. and Sunkar, R. (2005) Drought and salt tolerance in plants. *CRC Crit Rev Plant Sci* **24**, 23–58.
6. Chinnusamy, V., Jagendorf, A., and Zhu, J.K. (2005) Understanding and improving salt tolerance in plants. *Crop Science* **45**, 437–448.
7. Cramer, G.R. and Bowman, D.C. (1991) Kinetics of maize leaf elongation. I. Increased yield threshold limits short-term, steady-state elongation rates after exposure to salinity. *J Exp Bot* **42**, 1417–1426.
8. Frensch, J. and Hsiao, T.C. (1995) Rapid response of the yield threshold and turgor regulation during adjustment of root growth to water stress in *Zea mays*. *Plant Physiol* **108**, 303–312.
9. Passioura, J.B. and Munns, R. (2000) Rapid environmental changes that affect leaf water status induce transient surges or pauses in leaf expansion rate. *Aust J Plant Physiol* **27**, 941–948.
10. Munns, R. (2002) Comparative physiology of salt and water stress. *Plant, Cell & Environ* **25**, 239–250.
11. Rodríguez, H.G., Roberts, J.K.M., Jordan, W.R., and Drew, M.C. (1997) Growth, water relations, and accumulation of organic and inorganic solutes in roots of maize seedlings during salt stress. *Plant Physiol* **113**, 881–893.
12. Munns R. (2005) Genes and salt tolerance: bringing them together. *New Phytologist* **167**, 645–663.
13. Boyer, J.S., James, R.A., Munns, R., Condon, A.G., and Passioura, J.B. (2008) Osmotic adjustment may lead to anomalously low estimates of relative water content in wheat and barley. *Funct Plant Biol* **35**, 1172–1182.
14. Munns, R., Guo, J., Passioura, J.B., and Cramer, G.R. (2000) Leaf water status controls day-time but not daily rates of leaf expansion in salt-treated barley. *Aust J Plant Physiol* **27**, 949–957.
15. James, R.A., Rivelli, A.R., Munns, R., and von Caemmerer, S. (2002) Factors affecting CO_2 assimilation, leaf injury and growth in salt-stressed durum wheat. *Funct Plant Biol* **29**, 1393–1403.
16. James, R.A., von Caemmerer, S., Condon, A.G., Zwart, A.B., and Munns, R. (2008) Genetic variation in tolerance to the osmotic stress component of salinity stress in durum wheat. *Funct Plant Biol* **35**, 111–123.
17. Hu, Y. and Schmidhalter, U. (1998) Spatial distributions and net deposition rates of mineral elements in the elongating wheat (*Triticum aestivum* L.) leaf under saline soil conditions. *Planta* **204**, 212–219.
18. Fricke, W. (2004) Rapid and tissue-specific accumulation of solutes in the growth zone of barley leaves in response to salinity. *Planta* **219**, 515–525.
19. Foyer, C.H. and Noctor, G. (2005) Oxidant and antioxidant signalling in plants: a re-evaluation of the concept of oxidative stress in a physiological context. *Plant Cell Environ* **28**, 1056–1071.
20. Nicolas, M.E., Munns, R., Samarakoon, A.B., and Gifford, R.M. (1993) Elevated CO_2 improves the growth of wheat under salinity, *Aust J Plant Physiol* **20**, 349–360.
21. Munns, R., Schachtman, D.P., and Condon, A.G. (1995) The significance of a two-phase growth response to salinity in wheat and barley, *Aust J Plant Physiol* **22**, 561–569.
22. Munns, R. and Rawson, H.M. (1999) Effect of salinity on salt accumulation and reproductive development in the apical meristem of wheat and barley, *Aust J Plant Physiol* **26**, 459–464.
23. Ghanem, M.E., van Elteren, J., Albacete, A., Quinet, M., Martínez-Andújar, C., Kinet, J.M., Pérez-Alfocea, F., and Lutts, S. (2008) Impact of salinity on early reproductive physiology of tomato (*Solanum lycopersicum*L.) in relation to a heterogeneous distribution of toxic ions in flower organs. *Funct Plant Biol* **36**, 125–136.
24. Khatun, S., Rizzo, C.A., and Flowers, T.J. (1995) Genotypic variation in the effect of salinity on fertility in rice. *Plant Soil* **173**, 239–250.
25. Munns, R. and James, R.A. (2003) Screening methods for salinity tolerance: a case study with tetraploid wheat. *Plant Soil* **253**, 201–218.
26. Rajendran, K., Tester, M., and Roy, S.J. (2008) Quantifying the three main components of salinity tolerance in cereals. *Plant Cell & Environ* **32**, 237–249.

27. Aslam, M., Qureshi, R.H., and Ahmed, N. (1993) A rapid screening technique for salt tolerance in rice (*Oryza sativa* L.). *Plant Soil* **150**, 99–107.
28. Ren, Z.H., Gao, J.P., Li, L.G., Cai, H.L., Huang, W., Chao, D.Y., Zhu, M.Z., Wang, Z.Y., Luan, S., and Lin, H.X. (2005) A rice quantitative trait locus for salt tolerance encodes a sodium transporter *Nature Genet* **37**, 1141–1146.
29. Huang, S., Spielmeyer, W., Lagudah, E.S., James, R.A., Platten, J.D., Dennis, E.S., and Munns, R. (2006) A sodium transporter (HKT7) is a candidate for *Nax1*, a gene for salt tolerance in durum wheat. *Plant Physiol* **142**, 1718–1727.
30. Byrt, C.S., Platten, J.D., Spielmeyer, W., James, R.A., Lagudah, E.S., Dennis, E.S., Tester, M., and Munns, R. (2007) HKT1;5-like cation transporters linked to Na^+ exclusion loci in wheat, *Nax2* and *Kna1*. *Plant Physiol* **143**, 1918–28.
31. Wu, S.J., Lei, D., and Zhu, J.K. (1996) *SOS1*,a genetic locus essential for salt tolerance and potassium acquisition. *Plant Cell* **8**, 617–627.
32. Rus, A., Yokoi, S., Sharkhuu, A., Reddy, M., Lee, B.H., Matsumoto, T.K., Koiwa, H., Zhu, J.K., Bressan, R.A., and Hasegawa, P.M. (2001) AtHKT1 is a salt tolerance determinant that controls Na^+ entry into plant roots. *Proc Natl Acad Sci USA* **98**, 14150–14155.
33. Sanchez, D.H., Siahpoosh, M., Roessner, U., Udvardi, M., and Kopka, J. (2007) Plant metabolomics reveals conserved and divergent metabolic responses to salinity. *Physiol Plant* **132**, 209–219.
34. Gong, Q.Q., Li, P.H., Ma, S.S., Rupassara, S.I., and Bohnert, H.J. (2005) Salinity stress adaptation competence in the extremophile *Thellungiella halophila* in comparison with its relative *Arabidopsis thaliana*. *Plant J* **44**, 826–39.
35. Jacobs, A., Lunde, C., Bacic, A., Tester, M., and Roessner, U. (2007) The impact of constitutive heterologous expression of a moss Na^+ transporter on the metabolomes of rice and barley. *Metabolomics* **3**, 307–317.
36. Walia, H., Wilson, C., Wahid, A., Condamine, P., Cui, X.P., and Close, T.J. (2006) Expression analysis of barley (*Hordeum vulgare* L.) during salinity stress. *Funct Integr Genomics* **6**, 143–156.
37. Schachtman, D.P. and Schroeder, J.I. (1994) Structure and transport mechanism of a high-affinity potassium uptake transporter from higher plants. *Nature* **370**, 655–658.
38. Apse, M.P., Aharon, G.S., Snedden, W.A., and Blumwald, E. (1999) Salt tolerance conferred by overexpression of a vacuolar Na^+/H^+ antiport in Arabidopsis. *Science* **285**, 1256–1258.
39. Benito, B. and Rodriguez-Navarro, A. (2003) Molecular cloning and characterization of a sodium-pump ATPase of the moss *Physcomitrella patens*. *Plant J* **36**, 382–389.
40. Chen, T.H.H. and Murata, N. (2008) Glycinebetaine: an effective protectant against abiotic stress in plants. *Trends Plant Sci* **13**, 499–505.
41. Bernstein, N., Silk, W.K., and Läuchli, A. (1993) Growth and development of sorghum leaves under conditions of NaCl stress. Spatial and temporal aspects of leaf growth inhibition. *Planta* **191**, 433–439.

Chapter 3

Gene Regulation During Cold Stress Acclimation in Plants

Viswanathan Chinnusamy, Jian-Kang Zhu, and Ramanjulu Sunkar

Abstract

Cold stress adversely affects plant growth and development and thus limits crop productivity. Diverse plant species tolerate cold stress to a varying degree, which depends on reprogramming gene expression to modify their physiology, metabolism, and growth. Cold signal in plants is transmitted to activate CBF-dependent (C-repeat/drought-responsive element binding factor-dependent) and CBF-independent transcriptional pathway, of which CBF-dependent pathway activates CBF regulon. CBF transcription factor genes are induced by the constitutively expressed ICE1 (inducer of CBF expression 1) by binding to the *CBF* promoter. ICE1–CBF cold response pathway is conserved in diverse plant species. Transgenic analysis in different plant species revealed that cold tolerance can be significantly enhanced by genetic engineering CBF pathway. Posttranscriptional regulation at pre-mRNA processing and export from nucleus plays a role in cold acclimation. Small noncoding RNAs, namely micro-RNAs (miRNAs) and small interfering RNAs (siRNAs), are emerging as key players of posttranscriptional gene silencing. Cold stress-regulated miRNAs have been identified in *Arabidopsis* and rice. In this chapter, recent advances on cold stress signaling and tolerance are highlighted.

Key words: Cold stress, second messengers, CBF regulon, CBF-independent regulation, ICE1, posttranscriptional gene regulation.

1. Introduction

Temperature profoundly influences the metabolism of organisms and thus is a key factor determining the growing season and geographical distribution of plants. Cold stress can be classified as chilling (<20°C) and freezing (<0°C) stress. Temperate plants have evolved a repertoire of adaptive mechanisms such as seed and bud dormancy, photoperiod sensitivity, vernalization,

R. Sunkar (ed.), *Plant Stress Tolerance*, Methods in Molecular Biology 639,
DOI 10.1007/978-1-60761-702-0_3,

supercooling (prevention of ice formation in xylem parenchyma cells up to homogenous ice nucleation temperature, −40°C), and cold acclimation. In cold acclimation, plants acquire freezing tolerance on prior exposure to suboptimal, low, nonfreezing temperatures. The molecular basis of cold acclimation and acquired freezing tolerance in *Arabidopsis* and winter cereals has been studied extensively. Plants modify their metabolism and growth to adapt to cold stress by reprogramming gene expression during cold acclimation (1, 2). This chapter briefly covers cold stress signaling, transcriptional and posttranscriptional regulation of gene expression in cold acclimation process, and the genetic engineering of crops with enhanced cold tolerance.

2. Cold Stress Sensing

Thus far, the identity of stress sensor in plants is unknown. The fluid mosaic physical state of the plasma membrane is vital for the structure and function of cells, as well as to sense temperature stress. The plasma membrane undergoes phase transitions, from a liquid crystalline to a rigid gel phase at low temperature and to a fluid state at high temperature. Thus, a decrease in temperature can rapidly induce membrane rigidity at microdomains. Further, protein folding is influenced by temperature changes. Temperature-induced changes in the physical state of membranes and proteins are expected to change the metabolic reactions and thus the metabolite concentrations. Therefore, plant cells can sense cold stress through membrane rigidification, protein/nucleic acid conformation, and/or metabolite concentration (a specific metabolite or redox status).

In alfalfa and *Brassica napus*, cold stress-induced plasma membrane rigidification leads to actin cytoskeletal rearrangement, induction of Ca^{2+} channels, and increased cytosolic Ca^{2+} level. These events induce the expression of *cold-responsive* (*COR*) genes and cold acclimation. Further, a membrane rigidifier (DMSO) can induce *COR* genes even at 25°C, whereas a membrane fluidizer (benzyl alcohol) prevents *COR* gene expression even at 0°C (3, 4). Genetic evidence for plants sensing cold stress through membrane rigidification is from the study of the *fad2* mutant impaired in the oleic acid desaturase gene of *Arabidopsis*. In wild-type *Arabidopsis* plants, diacylglycerol (DAG) kinase is induced at 14°C. The *fad2* mutant (more saturated membrane) and transgenic *Arabidopsis* overexpressing linoleate desaturase gene showed the expression of DAG kinase at 18 and 12°C, respectively (5).

3. Second Messengers and Signaling

Cytosolic Ca^{2+}levels act as second messenger of the cold stress signal (6). Calcium may be imported into the cell or released from intracellular calcium stores. Patch-clamp studies of cold-induced potential changes of the plasma membrane in *Arabidopsis* mesophyll protoplasts showed the cold-activated calcium-permeable channel involved in the regulation of cytosolic Ca^{2+}signatures (7). Membrane rigidification induced cytosolic Ca^{2+}signatures; and *COR* gene expression was impaired by gadolinium, a mechanosensitive Ca^{2+} channel blocker, which suggests the involvement of mechanosensitive Ca^{2+} channels in cold acclimation (4). Pharmocological studies implicated cyclic ADP-ribose- and inositol-1,4,5-triphosphate (IP_3)-activated intracellular calcium channels in *COR* gene expression (4). Calcium influx into the cell appears to activate phospholipase C (PLC) and D (PLD), which produce IP_3 and phosphatidic acid, respectively. IP_3 can further amplify Ca^{2+}signatures by activation of IP_3-gated calcium channels (8). Genetic analysis revealed that loss-of-function mutants of *FIERY1* (*FRY1*) inositol polyphosphate 1-phosphatase show significantly higher and sustained levels of IP_3 instead of the transient increase observed in wild-type plants. This situation leads to higher induction of *COR* genes and CBFs, the upstream transcription factors (9). In addition, the *ca*lcium e*x*changer 1 (*cax1*) mutant of *Arabidopsis*, which is defective in a vacuolar Ca^{2+}/H^+ antiporter, exhibited enhanced expression of C-repeat binding factor/dehydration responsive element binding (*CBF/DREB*) proteins and their target *COR* genes (10). Therefore, cytosolic Ca^{2+} signatures are upstream of the expression of *CBFs* and *COR* genes in cold stress signaling.

Cold acclimation induces accumulation of ROS such as H_2O_2, both in chilling-tolerant *Arabidopsis* and chilling-sensitive maize plants. ROS can act as a signaling molecule to reprogram transcriptome probably through induction of Ca^{2+} signatures and activation of mitogen-activated protein kinases (MAPKs) (11) and redox-responsive transcription factors. *Arabidopsis frostbite1* (*fro1*) mutant, which is defective in the mitochondrial Fe-S subunit of complex I (NADH dehydrogenase) of the electron transfer chain, shows a constitutively high accumulation of ROS. This high accumulation of ROS in *fro1* results in reduced *COR* gene expression and hypersensitivity to freezing stress, probably because of desensitization of cells by the constitutively high ROS expression (12).

Cold stress-induced second messenger signatures can be decoded by different pathways. Calcium signatures are sensed by calcium sensor family proteins, namely calcium-dependent

protein kinases (CDPKs), calmodulins (CaMs), and salt overly sensitive 3-like (SOS3-like) or calcineurin B-like (CBL) proteins. In a transient expression system in maize leaf protoplast, a constitutively active form of an *Arabidopsis* CDPK (AtCDPK1) activated the expression of barley *HVA1* ABA-responsive promoter::*LUC* reporter gene suggesting that AtCDPK is a positive regulator in stress-induced gene transcription (13). Genetic and transgenic analyses implicated CDPKs as positive regulators, but a calmodulin, a SOS3-like or a CBL calcium binding protein, and a protein phosphatase 2C (AtPP2CA) are negative regulators of gene expression and cold tolerance in plants. Components of MAPK cascades are induced or activated by cold and other abiotic stresses. Genetic and transgenic analyses showed that MAPKs act as a converging point in abiotic stress signaling. ROS accumulation under these stresses might be sensed through a MAPK cascade (14). ROS activates the AtMEKK1/ANP1 (MAPKKK)–AtMKK2 (MAPKK)–AtMPK4/6 (MAPK) MAPK cascade, which positively regulates cold acclimation in plants (11). Many of these phosphorylated proteins show activation or induction of gene expression under multiple stress conditions, and genetic modification results in alteration of multiple stress responses. These results suggest that the proteins act as connecting nodes of stress signal networks. Identification of the target proteins or transcription factors of protein kinase or phosphatase cascades will shed further light on stress signaling.

4. Transcriptional Regulation

Chilling-tolerant plants reprogram their transcriptome in response to acclimation temperature. Cold-regulated genes constitute about 4–20% of the genome in *Arabidopsis* (15). The promoter region of many *COR* genes of *Arabidopsis* contains C-repeat (CRT)/DREs, initially identified in the promoter of *r*esponsive to *d*ehydration *29A* (*RD29A/COR78/LTI78*). As well, ABA-responsive elements are present in many cold-induced genes. Genetic screens using dehydration and cold stress-responsive promoter-driven *LUCIFERASE* (*RD29A::LUC* and *CBF3::LUC*) led to the isolation of mutants, which unraveled cold-responsive transcriptional networks.

4.1. CBF Regulons and Cold Tolerance

Yeast one-hybrid screens to identify CRT/DRE binding proteins led to the identification of CRT/DREBs (CBFs/DREBs) in *Arabidopsis*. CBFs belong to the ethylene-responsive element binding factor/APETALA2 (ERF/AP2)-type transcription factor family. *Arabidopsis* encodes three *CBF* genes (*CBF1/DREB1B*, *CBF2/DREB1C*, and *CBF3/DREB1A*), which are induced within a short period of exposure to cold stress. CBFs bind to

CRT/DRE cis-elements in the promoters of *COR* genes and induce their expression (16, 17). Ectopic expression of *CBFs* in transgenic *Arabidopsis* induced the expression of *COR* genes at warm temperatures and induced constitutive freezing tolerance. These transgenic *Arabidopsis* plants were also tolerant to salt and drought stresses (17–19). Microarray analysis of *CBF*-overexpressing transgenic plants identified several CBF target genes involved in signaling, transcription, osmolyte biosynthesis, ROS detoxification, membrane transport, hormone metabolism, and stress response (20, 21). Transgenic overexpression of *Arabidopsis* CBFs is sufficient to induce cold tolerance in diverse plant species (**Table 3.1**). Further, CBF homologs have been identified

Table 3. 1
Abiotic stress tolerance of transgenic plants overexpressing CBFs

Gene	Transgenic plant	Stress tolerance of transgenic plants	References
AtCBF1/2/3	*Brassica napus*	Constitutive overexpression enhanced both basal and acquired freezing tolerance	(22)
AtCBF1	Tomato	Constitutive overexpression enhanced oxidative stress tolerance under chilling stress; enhanced tolerance to water-deficit stress	(23, 24)
AtDREB1A/CBF3	Tobacco	Transgenic plants expressing *RD29A::DREB1A* exhibited enhanced chilling and drought tolerance	(25)
AtDREB1A/CBF3	Wheat	Transgenic plants expressing *RD29A* promoter::*AtDREB1A* gene showed delayed water stress symptoms	(26)
AtCBF3	Rice	Constitutive overexpression resulted in enhanced tolerance to drought and high salinity and a marginal increase in chilling tolerance	(27)
AtDREB1A/CBF3	Maize	*RD29A::CBF3* transgenic plants are more tolerant to cold, drought, and salinity	(28)
AtCBF1	Potato	Constitutive or stress-inducible expression of *CBF1* or *CBF3* but not *CBF2* conferred improved freezing tolerance to frost-sensitive *Solanum tuberosum*	(29)
OsDREB1	*Arabidopsis*	Overexpression in *Arabidopsis* induced target *COR* genes and conferred enhanced tolerance to freezing and drought stresses	(30)
OsDREB1A/B	Rice	Constitutive expression conferred improved tolerance to cold, drought, and salinity	(31)
ZmDREB1	*Arabidopsis*	Overexpression in *Arabidopsis* induced *COR* genes and conferred tolerance to freezing and drought	(32)
BnCBF5 and BnCBF 17	*B. napus*	Overexpression led to increased constitutive freezing tolerance, increased photochemical efficiency and photosynthetic capacity	(33)

from several chilling-tolerant and chilling-sensitive plant species and transgenic analysis confirmed their pivotal role in cold acclimation (**Table3.1**).

These evidences suggest that a CBF transcription network plays a pivotal role in cold acclimation of evolutionarily diverse plant species. Transcriptome analysis of transgenic tomato and *Arabidopsis* plants overexpressing *LeCBF1* and *AtCBF3* revealed that CBF regulons from freezing-tolerant and freezing-sensitive plant species differ significantly (35).

Constitutive overexpression of CBFs under the transcriptional control of the 35S cauliflower mosaic virus promoter in transgenic plants resulted in severe growth retardation under normal growth conditions in diverse plant species such as *Arabidopsis* (18, 19, 34, 36), *B. napus* (22), tomato (23, 24), potato (29), and rice (31). Inhibition of metabolism and change in growth-regulating hormones appears to be important causes of the growth inhibition of CBF-overexpressing plants. Reduction in the expression of photosynthetic genes appears to reduce photosynthesis and growth under cold stress. Transgenic plants constitutively overexpressing *CBFs* showed higher induction of the *STZ/ZAT10* zinc finger transcription factor gene, which appears to repress genes involved in photosynthesis and carbohydrate metabolism and thus reduce the growth of these transgenic plants (21). Microarray analysis revealed that cold stress regulates several genes involved in biosynthesis or signaling of hormones such as ABA, gibberellic acid (GA), and auxin, which suggests the importance of these hormones in coordinated regulation of cold tolerance and plant development (15). GA promotes important processes in plant growth and development, such as seed germination, growth through elongation, and floral transition. Growth retardation of transgenic tomato plants constitutively overexpressing *AtCBF1* was reversed by GA_3 treatment (24). This finding suggested a link between CBFs and GA in cold stress-induced growth retardation. During cold stress, growth retardation appears to be regulated by CBFs through nuclear-localized DELLA proteins, which repress growth in *Arabidopsis*. GA stimulates the degradation of DELLA proteins and promotes growth. CBFs enhance the expression of GA-inactivating GA2-oxidases, and thus allow the accumulation of the DELLA protein repressor of GA1-like 3 (RGL3), which leads to dwarfism and late flowering. Further, mutant plants of *DELLA* genes encoding GA-insensitive [GAI] repressor of GA1-3 [RGA] were significantly less freezing tolerant than were wild-type plants after cold acclimation. This finding suggests that DELLAs might contribute significantly to cold acclimation and freezing tolerance (37).

4.2. Regulators of CBF Expression

Transcription of CBF genes is induced by cold stress. Hence, constitutive transcription factors present in the cell at normal

growth temperatures may induce the expression of CBFs on activation by cold stress. A systematic genetic analysis by *CBF3::LUC* bioluminescent genetic screening led to the identification of a constitutively expressed and nuclear-localized transcription factor, *i*nducer of *C*BF *e*xpression 1 (ICE1) in *Arabidopsis*. *ICE1* encodes a MYC-type basic helix-loop-helix (bHLH) transcription factor, can bind to MYC recognition elements in the *CBF3* promoter, and induces the expression of *CBF3* during cold acclimation. The *ice1* mutant is defective in both chilling and freezing tolerance, whereas transgenic *Arabidopsis* overexpressing *ICE1* showed enhanced freezing tolerance (38). Transcriptome analysis revealed the dominant *ice1* mutant with impaired expression of about 40% of cold-regulated genes, in particular 46% of cold-regulated transcription factor genes (15). Therefore, ICE1 is a master regulator that controls CBF and many other cold-responsive regulons. Overexpression analysis showed that ICE2 (At1g12860, a homolog of ICE1) induces the expression of CBF1 and confers enhanced freezing tolerance in *Arabidopsis* after cold acclimation (39). In wheat, the ICE1 homologs *TaICE141* and *TaICE187* are constitutively expressed and activate the wheat CBF group IV, which are associated with freezing tolerance. Overexpression of *TaICE141* and *TaICE187* in *Arabidopsis* enhanced *CBF* and *COR* gene expression and enhanced freezing tolerance only after cold acclimation. This finding suggests that similar to *Arabidopsis* ICE1, wheat ICE1 also needs to be activated by cold acclimation (40).

ICE1 appears to negatively regulate the expression of MYB15 (an R2R3-MYB family protein) in *Arabidopsis*. MYB15 is an upstream transcription factor that negatively regulates *CBF* expression. Transgenic *Arabidopsis* overexpressing *MYB15* showed reduced expression of *CBFs* and freezingtolerance, whereas *myb15* T-DNA knockout mutants showed enhanced cold induction of *CBFs* and enhanced freezing tolerance. In a yeast two-hybrid system, ICE1 interacted with MYB15 (41). Further, the expression of MYB15 is increased in *ice1* mutants (R236H and K393R) (41, 42). Thus, the ICE1–MYB15 interaction appears to play a role in regulating CBF expression levels during cold acclimation (41).

Although ICE1 is expressed constitutively, only on exposure to low temperature does it induce transcription of the CBF and other cold stress-responsive genes (38, 40). Posttranslational modifications play a key role in regulating the activity of ICE1 under cold stress. Cold stress activates ICE1 sumoylation (42) and negatively regulates ICE1 levels by targeted proteolysis (43). The *Arabidopsis High expression of Osmotically responsive* gene 1 (*HOS1*) encodes a RING finger ubiquitin E3 ligase. The nuclear localization of *HOS1* is enhanced by cold stress. HOS1 physically interacts with ICE1 and targets ICE1 for polyubiquitination and

proteolysis of ICE1 after 12 h of cold stress. Overexpression of HOS1 in transgenic *Arabidopsis* results in a substantial reduction in level of ICE1 protein and that of its target genes, as well as hypersensitivity to freezing stress. Thus, HOS1 mediates ubiquitination of ICE1 and plays a critical role in maintaining the level of ICE1 target genes in the cell during cold acclimation (43). Sumoylation of proteins prevents the proteasomal degradation of target proteins. The null mutant of *Arabidopsis* SUMO E3 ligase, *SIZ1* (SAP and Miz1), exhibits reduced cold induction of *CBFs* and the target *COR* genes, as well as hypersensitivity to chilling and freezing stresses. SIZ1 catalyzes SUMO conjugation to K393 of ICE1 during cold acclimation and thus reduces polyubiquitination of ICE1. Mutation in a K393 residue of ICE1 impairs its activity (42). Hence, SIZ1-mediated sumoylation facilitates ICE1 stability and activity, whereas HOS1 mediation reduces ICE1 protein levels during cold acclimation.

Stomata play a crucial role in regulating photosynthesis and transpiration. Recently, the *scream-D* dominant mutant and *ice1* mutant were found to be the same as R236H, which results in constitutive stomatal differentiation in the epidermis, and the entire epidermis differentiates into stomata. Thus, ICE1 is required for controlled stomatal development. ICE1protein interacts and forms a dimer with other bHLH transcription factors, SPEECHLESS (SPCH), MUTE, and FAMA, which regulate stomatal development. ICE1 may act as a link between the formation of stomata and the plant response to environmental cues (44).

Recently, members of the calmodulin binding transcription activator (CAMTA) family proteins have been identified as transcriptional regulators of *CBF2* expression. Cold-induced expression of CBF2 was considerably lower in *camta3* mutant as compared to WT plants. The CAMTA3 protein binds to conserved DNA motifs present in *CBF2* promoter and regulates *CBF2* expression. The *camta1/camta3* double mutant exhibited hypersensitivity to freezing stress as compared to WT plants. Since CAMTA proteins can interact with calmodulins, cold-induced calcium signals may regulate *CBFs* expression through CAMTA proteins (45).

4.3. CBF1, CBF2, and CBF3 Play Different Roles in Cold Acclimation

Microarray analysis revealed that CBFs regulate about 12% of the cold-responsive transcriptome. Overexpression of CBFs enhances osmolyte accumulation, reduces growth, and enhances abiotic stress tolerance (**Table 3.1**). Constitutive overexpression studies of transgenic *Arabidopsis* suggested that CBF1, CBF2, and CBF3 have redundant functional activities (36). However, the *ice1* mutant, impaired mainly in *CBF3* but not *CBF1* and *CBF2*, showed chilling and freezing hypersensitivity (38). Studies of the *cbf2* T-DNA insertion mutant of *Arabidopsis* revealed that CBFs

have different functions in cold acclimation. *cbf2* null mutants showed increased expression of *CBF1* and *CBF3* and enhanced tolerance to freezing (with or without cold acclimation), dehydration, and salt stresses. Further, *CBFs* show a temporal difference in expression, with the cold-induced expression of *CBF1* and *CBF3* preceding that of *CBF2*. These results suggest that CBF2 negatively regulates *CBF1* and *CBF3* to optimize the expression of downstream target genes (45). In potato (*Solanum tuberosum*), overexpression of *AtCBF2* failed to confer freezing tolerance (29). Transgenic analysis of *CBF1* and *CBF3* RNAi lines revealed that both CBF1 and CBF3 are required for the full set of CBF regulon expression and freezing tolerance (46).

Besides CBF2, the C2H2 zinc finger transcription factor *ZAT12* negatively regulates the expression of *CBF1*, *CBF2*, *and CBF3* during cold stress. *Arabidopsis* transgenic plants overexpressing *ZAT12* showed decreased expression of *CBFs* under cold stress (47). *los2* mutant plants showed an enhanced and more sustained induction of *ZAT10/STZ* during cold stress and enhanced cold sensitivity. *LOS2* encodes a bifunctional enolase that negatively regulates the expression of *ZAT10* (48).

Transgenic *Arabidopsis* plants overexpressing *AtMKK2* showed constitutive expression of *CBF2*, which suggests that the *CBF2* expression is probably positively regulated by a MAPK signaling cascade (11). *Arabidopsis FIERY2* (*FRY2*), which encodes an RNA polymerase II C-terminal domain (CTD) phosphatase, appears to act as a negative regulator of *CBFs* and their target *COR* genes because the *fry2* mutant showed enhanced expression of *CBFs* and *COR* genes under cold stress and ABA. Since the *fry2* mutant is hypersensitive to freezing despite enhanced expression of *CBFs*, FRY2 may positively regulate the expression of certain genes critical for freezing tolerance (49). The maintenance of an optimal level of CBFs at an appropriate time is necessary, because constitutive overexpression affects growth and development significantly. Further, *CBF* expression is under the control of a circadian clock. The maximal cold-induced increase in transcription of *CBFs* occurs when cold stress is imposed 4 h after dawn. Transgenic plants overexpressing arrhythmic CCA1 showed no temporal difference in the cold induction of *CBF* expression (50).

4.4. CBF-Independent Regulons

Genetic and transgenic analyses revealed that several classes of transcription factors besides CBFs play an important role in cold acclimation. The *eskimo1* (*esk1*) mutant of *Arabidopsis* was identified through freezing tolerance genetic screening. The *esk1* mutant accumulated constitutively high levels of proline and exhibited constitutively freezing tolerance. *ESK1* is constitutively expressed and encodes the protein domain of unknown function (23). Transcriptome comparison of CBF2-overexpressing plants

and *esk1* mutants showed that different sets of genes are regulated by CBF2 and ESK1. However, the mechanism of action of ESK1 in freezing tolerance has yet to be revealed (51).

P_{RD29A}*::LUC* reporter gene-based genetic screening led to the identification of two constitutively expressed transcription factors, HOS9 (a homeodomain protein) and HOS10 (an R2R3-type MYB), which are necessary for cold tolerance in *Arabidopsis*. *hos9* and *hos10* mutants are less freezing tolerant than wild-type *Arabidopsis* (52, 53). Transcriptome analysis revealed distinct CBF and HOS9 regulons (52). HOS10 probably regulates ABA-dependent cold acclimation pathways, because HOS10 positively regulates *NCED3* (9-*cis*-epoxycarotenoid dioxygenase) and thus ABA accumulation during cold stress (53).

Gene expression analysis revealed several transcription factors induced during cold acclimation. Transgenic analysis of cold-inducible transcription factors helped in validation of functions of some transcription factors in cold tolerance. Constitutive overexpression of the soybean C2H2-type zinc finger protein SCOF1 in *Arabidopsis* transgenic plants enhanced the expression of *COR* genes and conferred constitutive freezing tolerance. SCOF1 interacts with soybean G-box binding factor 1 (SGBF1) and may enhance the DNA binding activity of the SGBF1. *SGBF1* is induced by both cold and ABA (54). Overexpression of the cold-regulated rice transcription factors *MYB4* (an R2R3-type MYB) and *OsMYB3R-2* (an R1R2R3 MYB) enhanced freezing tolerance of *Arabidopsis* (55, 56).

Some members of the abiotic, plant hormone, and pathogen-inducible ERF family play a crucial role in abiotic and biotic stress tolerance. The pepper ERF/AP2-type transcription factor, *Capsicum annuum* pathogen and freezing tolerance-related protein 1 (*CaPF1*) is induced by cold, osmotic stress, ethylene, and jasmonic acid. Transgenic *Arabidopsis* overexpressing *CaPF1* showed induction of pathogen-responsive as well as *COR* genes and exhibited enhanced tolerance to stress by freezing and to pathogens (*Pseudomonas syringae* pv *tomato* DC3000) (57). Similarly, *Triticum aestivum ERF1* (*TaERF1*) was induced by cold, drought salinity, ABA, ethylene, salicylic acid, and infection by *Blumeria graminis f.* sp. *Tritici* pathogen in wheat. Transgenic *Arabidopsis* overexpressing *TaERF1* exhibited enhanced tolerance to cold, salt, and drought stresses, as well as pathogens (58). Genes encoding the A-5 subgroup AP2 domain protein from *Physcomitrella patens* (PpDBF1) (59) and soybean (GmDREB3) (60) are cold induced, and overexpression of these genes conferred enhanced cold tolerance.

In wheat, *w*heat *l*ow-*t*emperature-*i*nduced *protein* 19 (WLIP19), encoding a basic-region leucine zipper protein, is induced by cold, drought, and ABA. WLIP19 activates the expression of *COR* genes in wheat. Transgenic tobacco

overexpressing *Wlip19* showed significant freezing tolerance. WLIP19 was found to interact and form a heterodimer with *T. aestivum ocs*-element *b*inding *f*actor 1 (*TaOBF1*), a bZIP transcription factor (61). The plant-specific transcription factor NAC (NAM, ATAF, and CUC) family plays a key role in stress response. Overexpression of cold stress-inducible rice *SNAC2* in transgenic rice resulted in high cell membrane stability under cold stress. Microarray analysis showed upregulation of several stress-regulated genes in *SNAC2*-overexpressing plants (62). These results suggest that several transcriptional networks operate during cold acclimation and cold stress tolerance of plants.

5. Posttranscriptional Gene Regulation

Posttranscriptional regulation at pre-mRNA processing, mRNA stability, and export from nucleus plays critical roles in cold acclimation and cold tolerance (2).

5.1. Messenger RNA Processing

Pre-mRNA processing and exports constitute important mechanisms of regulation of gene expression in eukaryotes. Pre-mRNA undergoes various nuclear processes such as the addition of a 5′ methyl cap and poly(A) tail and intron splicing. Splicing is necessary to remove introns and to synthesize translationally competent mRNAs. Primary transcripts with more than one intron can undergo alternative splicing to produce functionally different proteins from a single gene. In plants, about 20% of genes undergo alternative splicing. Although most alternative splicing events are uncharacterized in plants, but it appears to play an important role in the regulation of photosynthesis, flowering, grain quality in cereals, and plant defense response. Recent studies have implicated intron splicing in abiotic stress response. In wheat, cold stress induction of two early cold-regulated (e-cor) genes coding for a ribokinase (7H8) and a C3H2C3 RING finger protein (6G2) undergo stress-dependent splicing. Both of these genes are regulated by intron retention under cold stress, whereas 6G2 intron retention is also regulated by drought stress. However, homologs of these genes did not show stress-regulated intron retention in *Arabidopsis*. Interestingly, barley homologs of 7H8 and 6G2 showed stress-dependent intron retention under cold stress, whereas barley albino mutants defective in chloroplast development failed to retain introns in these genes under cold stress (63). The *Arabidopsis COR15A* gene encoding a chloroplast stromal protein with cryoprotective activity plays an important role in conferring freezing tolerance to chloroplasts (64). The *Arabidopsis stabilized1* (*sta1*) mutant is defective in the

splicing of the cold-induced *COR15A* pre-mRNA and is hypersensitive to chilling, ABA, and salt stresses. *STA1* encodes a nuclear pre-mRNA splicing factor and is upregulated by cold stress. STA1 catalyzes splicing of *COR15A*, which is necessary for cold tolerance (65). Further, pre-mRNA of serine/arginine-rich (SR) proteins, which are involved in the regulation or execution of mRNA splicing, undergo alternate splicing under cold and heat stresses in *Arabidopsis* (66). Further, in addition to a change in splicing pattern, expression levels of *AtSR45a* and *AtSR30*, SF2/ASF-like SR proteins, are also increased by high light and salinity stresses in *Arabidopsis* (67). Thus, the stress-regulated alternate splicing machinery may in turn change the splicing pattern of some of the stress-responsive genes.

5.2. Small RNAs

Small noncoding RNAs, namely micro-RNAs (miRNAs) and small interfering RNAs (siRNAs), act as ubiquitous repressors of gene expression in animals and plants. Small RNAs are incorporated into the argonaute (AGO) family of proteins containing the RNA-induced silencing complex (RISC) or RNA-induced transcriptional silencing (RITS) complex. The RISC-containing miRNA/siRNA induces posttranscriptional gene silencing by cleavage of mRNA and translational repression. Transcriptional gene silencing is mainly mediated by siRNAs. Cold stress-upregulated and -downregulated miRNAs have been identified in *Arabidopsis*. Abiotic stress-induced or -upregulated small RNAs can downregulate their target genes, which are likely negative regulators and/or determinants of the stress response. In contrast, stress-downregulated small RNAs can upregulate their target mRNAs, which are likely positive regulators and/or determinants of stress tolerance (68).

Accumulation of ROS is induced by abiotic stresses. Superoxide dismutases catalyze conversion of the superoxide radical into H_2O_2, which is then detoxified by ascorbate peroxidase. The miR398 expression is reduced and that of its target genes *CSD1* and *CSD2* enhanced under oxidative stress in *Arabidopsis*. Under normal conditions, miR398 targets the *CSD* mRNAs for cleavage, and thus stress-induced reduction in miR398 expression results in accumulation of CSD transcripts. Because miR398 and its target sequence on the *CSD* mRNAs are conserved across plant species, miR398 appears to play a ubiquitous role in ROS detoxification under abiotic stresses (69). siRNAs derived from double-stranded RNAs (dsRNAs) formed from the mRNAs encoded by a natural *cis*–antisense gene pair are called natural antisense transcript-derived siRNAs (nat-siRNAs). One of the nat-siRNAs derived from a *cis*–nat pair of *SRO5* and *P5CDH* (Δ1-pyrroline-5-carboxylate dehydrogenase) regulates oxidative stress and osmolyte accumulation under salt stress in *Arabidopsis*. Salt stress-induced expression of *SRO5* leads to SRO5-P5CDH

dsRNA, which is then processed by DCL2, RDR6, SGS3, and DNA-dependent RNA polymerase IV (NRPD1A) to generate a 24-nt nat-siRNA. The 24-nt nat-siRNA targets the cleavage of P5CDH and thus accumulation of proline. Oxidative stress also induces the expression of *SRO5* and the 24-nt SRO5-P5CDH nat-siRNA and decreases P5CDH transcript levels (70, 71). These results suggest that small RNAs play a key role in gene regulation in the cold and other abiotic stress response of *Arabidopsis*.

6. Conclusions and Perspectives

Significant progress has been made to unravel the molecular basis of cold acclimation in model plant *Arabidopsis* and winter cereals. During cold acclimation, plants reprogram their gene expression through transcriptional, posttranscriptional, and posttranslational mechanisms. The ICE1–CBF transcriptional cascade plays crucial role in cold acclimation in diverse plant species. Transgenic analysis revealed that genetic engineering of CBF pathway can improve cold tolerance across plant species. Recently, several components of CBF-independent transcriptional pathway of cold acclimation have been identified. Besides transcriptional regulation, plants employ diverse posttranscriptional regulatory mechanisms to regulate their gene expression during cold acclimation. Several cold stress-regulated miRNAs have been identified in *Arabidopsis* and rice. Characterization of cold-regulated miRNAs will help understand the role of posttranscriptional regulation of mRNA stability in cold stress response of plants. Cold-induced transcriptome differs significantly among leaf, root, and reproductive (pollen) tissues. Most of the mechanisms of cold acclimation were studied in vegetative stages of *Arabidopsis*. Further studies on transcriptional networks in reproductive tissues will identify key regulators of cold tolerance. Epigenetic processes play a key role in the regulation of plant development and stress responses. Further studies on the function of epigenetic processes, such as DNA methylation and chromatin modifications, and epigenetic stress memory will be necessary.

References

1. Yamaguchi-Shinozaki, K., and Shinozaki, K. (2006). Transcriptional regulatory networks in cellular responses and tolerance to dehydration and cold stresses. *Annu Rev Plant Biol* **57**, 781–803.
2. Chinnusamy, V., Zhu, J., and Zhu, J.K. (2007). Cold stress regulation of gene expression plants. *Trends Plant Sci* **12**, 444–451.
3. Orvar, B.L., Sangwan, V., Omann, F., and Dhindsa, R. (2000). Early steps in cold sensing by plant cells: the role of actin cytoskeleton and membrane fluidity. *Plant J* **23**, 785–794.

4. Sangwan, V., Foulds, I., Singh, J., and Dhindsa, R.J. (2001). Cold activation of *Brassica napus* BN115 promoter is mediated by structural changes in membranes and cytoskeleton, and requires Ca^{2+} influx. *Plant J* **27**, 1–12.
5. Vaultier, M.N., Cantrel, C., Vergnolle, C., Justin, A.-M., Demandre, C., Benhassaine-Kesri, G., Cicek, D., Zachowski, A., and Ruelland, E. (2006) Desaturase mutants reveal that membrane rigidification acts as a cold perception mechanism upstream of the diacylglycerol kinase pathway in *Arabidopsis* cells. *FEBS Lett* **580**, 4218–4223.
6. Knight, M.R. (2002). Signal transduction leading to low-temperature tolerance in *Arabidopsis thaliana*. *Philos Trans R Soc Lond B Biol Sci* **357**, 871–875.
7. Carpaneto, A., Ivashikina, N., Levchenko, V., Krol, E., Jeworutzki, E., Zhu, J.K., and Hedrich, R. (2007). Cold transiently activates calcium-permeable channels in *Arabidopsis* mesophyll cells. *Plant Physiol* **143**, 487–494.
8. Vergnolle, C., Vaultier, M.N., Taconnat, L., Renou, J.P., Kader, J.C., Zachowski, A., and Ruell, E. (2005). The cold-induced early activation of phospholipase C and D pathways determines the response of two distinct clusters of genes in *Arabidopsis* cell suspensions. *Plant Physiol* **139**, 1217–1233.
9. Xiong, L., Lee, B.H., Ishitani, M., Lee, H., Zhang, C., and Zhu, J.K. (2001). FIERY1 encoding an inositol polyphosphate 1-phosphatase is a negative regulator of abscisic acid and stress signaling in *Arabidopsis*. *Genes Dev* **15**, 1971–1984.
10. Catala, R., Santos, E., Alonso, J.M., Ecker, J.R., Martinez-Zapater, J.M., and Salinas, J. (2003). Mutations in the Ca^{2+}/H^{+} transporter CAX1 increase *CBF/DREB1* expression and the cold-acclimation response in *Arabidopsis*. *Plant Cell* **15**, 2940–2951.
11. Teige, M., Scheikl, E., Eulgem, T., Doczi, R., Ichimura, K., Shinozaki, K., Dangl, J.L., and Hirt, H. (2004) The MKK2 pathway mediates cold and salt stress signaling in *Arabidopsis*. *Mol Cell* **15**, 141–152.
12. Lee, B.H., Lee, H., Xiong, L., and Zhu, J.K. (2002). A mitochondrial complex I defect impairs cold-regulated nuclear gene expression. *Plant Cell 14*, 1235–1251.
13. Sheen, J. (1996). Specific Ca^{2+}-dependent protein kinase in stress signal transduction. *Science* **274**, 1900–1902.
14. Pitzschke, A. and Hirt, H. (2006). Mitogen-activated protein kinases and reactive oxygen species signaling in plants.*Plant Physiol* **141**, 351–356.
15. Lee, B.H., Henderson, D.A., and Zhu, J.K. (2005). The *Arabidopsis* cold-responsive transcriptome and its regulation by ICE1. *Plant Cell* **17**, 3155–3175.
16. Stockinger, E.J., Gilmour, S.J., and Thomashow, M.F. (1997). Arabidopsis thaliana CBF1 encodes an AP2 domain-containing transcription activator that binds to the C repeat/DRE, a cis-acting DNA regulatory element that stimulates transcription in response to low temperature and water deficit. *Proc Natl Acad Sci USA* **94**, 1035–1040.
17. Liu, Q., Kasuga, M., Sakuma, Y., Abe, H., Miura, S., Yamaguchi-Shinozaki, K., and Shinozaki, K. (1998). Two transcription factors, DREB1 and DREB2, with an EREBP/AP2 DNA-binding domain separate two cellular signal transduction pathways in drought- and low-temperature-responsive gene expression in *Arabidopsis*. *Plant Cell* **10**, 1391–1406.
18. Jaglo-Ottosen, K.R., Gilmour, S.J., Zarka, D.G., Schabenberger, O., and Thomashow, M.F. (1998). *Arabidopsis CBF1* overexpression induces COR genes and enhances freezing tolerance. *Science* **280**, 104–106.
19. Kasuga, M., Liu, Q., Miura, S., Yamaguchi-Shinozaki, K., and Shinozaki, K. (1999). Improving plant drought, salt, and freezing tolerance by gene transfer of a single stress inducible transcription factor. *Nat Biotech* **17**, 287–291.
20. Fowler, S. and Thomashow, M.F. (2002). *Arabidopsis* transcriptome profiling indicates that multiple regulatory pathways are activated during cold acclimation in addition to the CBF cold response pathway. *Plant Cell* **14**, 1675–1690.
21. Maruyama, K., Sakuma, Y., Kasuga, M., Ito, Y., Seki, M., Goda, H., Shimada, Y., Yoshida, S., Shinozaki, K., and Yamaguchi-Shinozaki, K. (2004). Identification of cold-inducible downstream genes of the *Arabidopsis* DREB1A/CBF3 transcriptional factor using two microarray systems. *Plant J* **38**, 982–993.
22. Jaglo, K.R., Kleff, S., Amundsen, K.L., Zhang, X., Haake, V., Zhang, J.Z., Deits, T., and Thomashow, M.F. (2001). Components of the *Arabidopsis* C-repeat/dehydration responsive element binding factor cold-response pathway are conserved in *Brassica napus*and other plant species. *Plant Physiol* **127**, 910–917.
23. Hsieh, T.H., Lee, J.T., Charng, Y.Y., and Chan, M.T. (2002). Tomato plants ectopically expressing *Arabidopsis* CBF1 show enhanced resistance to water deficit stress. *Plant Physiol* **130**, 618–26.

24. Hsieh, T.H., Lee, J.T., Yang, P.T., Chiu, L.H., Charng, Y.Y., Wang, Y.C., and Chan, M.T. (2002). Heterology expression of the *Arabidopsis* C-repeat/dehydration response element binding factor 1 gene confers elevated tolerance to chilling and oxidative stresses in transgenic tomato. *Plant Physiol* **129**, 1086–1094.
25. Kasuga, M., Miura, S., Shinozaki, K., and Yamaguchi-Shinozaki, K. (2004). A combination of the A*rabidopsis DREB1A* gene and stress-inducible *RD29A* promoter improved drought- and low-temperature stress tolerance in tobacco by gene transfer. *Plant Cell Physiol* **45**, 346–350.
26. Pellegrineschi, A., Reynolds, M., Pacheco, M., Brito, R.M., Almeraya, R., and Yamaguchi-Shinozaki, K., Hoisington, D. (2004). Stress-induced expression in wheat of the *Arabidopsis thaliana DREB1A* gene delays water stress symptoms under greenhouse conditions. *Genome* **47**, 493–500.
27. Oh, S.J., Song, S.I., Kim, Y.S., Jang, H.J., Kim, S.Y., Kim, M, Kim, Y.K., Nahm, B.H., and Kim, J.K. (2005). *Arabidopsis CBF3/DREB1A* and *ABF3* in transgenic rice increased tolerance to abiotic stress without stunting growth. *Plant Physiol* **138**, 341–351.
28. Al-Abed, D., Madasamy, P., Talla, R., Goldman, S., and Rudrabhatla, S. (2007). Genetic engineering of maize with the *Arabidopsis DREB1A/CBF3* gene using split-seed explants. *Crop Sci* **47**, 2390–2402.
29. Pino, M.T., Skinner, J.S., Park, E.J., Jeknic Z, Hayes, P.M., Thomashow, M.F., and Chen, T.H.H (2007). Use of a stress inducible promoter to drive ectopic *AtCBF* expression improves potato freezing tolerance while minimizing negative effects on tuber yield. *Plant Biotechnology J.* **5**, 591–604.
30. Dubouzet, J.G., Sakuma, Y., Ito, Y., Kasuga, M., Dubouzet, E.G., Miura, S., Seki, M., Shinozaki, K., and Yamaguchi-Shinozaki, K. (2003). *OsDREB* genes in rice, *Oryza sativa* L., encode transcription activators that function in drought-, high-salt- and cold-responsive gene expression. *Plant J* **33**, 751–763.
31. Ito, Y., Katsura, K., Maruyama, K., Taji, T., Kobayashi, M., Seki, M., Shinozaki, K., and Yamaguchi-Shinozaki, K. (2006) Functional analysis of rice DREB1/CBF-type transcription factors involved in cold-responsive gene expression in transgenic rice. *Plant Cell Physiol* **47**, 141–153.
32. Qin, F, Sakuma, Y, Li, J., Liu, Q, Li, Y-Q, Shinozaki, K, and Yamaguchi-Shinozaki, K (2004). Cloning and functional analysis of a novel *DREB1/CBF* transcription factor involved in cold-responsive gene expression in *Zea mays. Plant Cell Physiol* **45**, 1042–1052.
33. Savitch, L.V., Allard G., Seki M., Robert, L.S., Tinker, N.A., Huner, N.P., Shinozaki K., and Singh, J. (2005). The effect of overexpression of two Brassica CBF/DREB1-like transcription factors on photosynthetic capacity and freezing tolerance in *Brassica napus. Plant Cell Physiol* **46**, 1525–1539.
34. Welling, A., and Palva, E.T. (2008). Involvement of CBF transcription factors in winter hardiness in birch. *Plant Physiol* **147**, 1199–1211.
35. Zhang X., Fowler, S.G., Cheng H., Lou Y., Rhee, S.Y., Stockinger, E.J., and Thomashow, M.F. (2004). Freezing-sensitive tomato has a functional CBF cold response pathway, but a CBF regulon that differs from that of freezing-tolerant *Arabidopsis. Plant J* **39**, 905–919.
36. Gilmour, S.J., Fowler, S.G., and Thomashow, M.F. (2004). *Arabidopsis* transcriptional activators CBF1, CBF2, and CBF3 have matching functional activities. *Plant Mol Biol* **54**, 767–781.
37. Achard, P., Gong, F., Cheminant, S., Alioua, M., Hedden, P., and Genschik, P. (2008). The cold-inducible CBF1 factor-dependent signaling pathway modulates the accumulation of the growth-repressing DELLA proteins via its effect on gibberellin metabolism. *Plant Cell* **20**, 2117–2129.
38. Chinnusamy, V., Ohta, M., Kanrar, S., Lee B.-h, Hong, X., Agarwal, M., and Zhu, J.K. (2003). ICE1, a regulator of cold induced transcriptome and freezing tolerance in *Arabidopsis. Genes Dev* **17**, 1043–1054.
39. Fursova, O.V., Pogorelko, G.V., and Tarasov, V.A. (2009). Identification of ICE2, a gene involved in cold acclimation which determines freezing tolerance in *Arabidopsis thaliana. Gene* **429**, 98–103.
40. Badawi, M., Reddy, Y.V., Agharbaoui, Z., Tominaga, Y., Danyluk, J., Sarhan, F., and Houde, M. (2008). Structure and functional analysis of wheat ICE (Inducer of CBF Expression) genes. *Plant Cell Physiol* **49**, 1237–1249.
41. Agarwal, M., Hao, Y., Kapoor, A., Dong, C.H., Fujii, H., Zheng, X., and Zhu, J.K. (2006). A R2R3 type MYB transcription factor is involved in the cold regulation of *CBF* genes and in acquired freezing tolerance. *J Biol Chem* **281**, 37636–37645.
42. Miura, K., Jin, J.B., Lee, J., Yoo, C.Y., Stirm, V., Miura, T., Ashworth, E.N., Bressan, R.A., Yun, D.J., and Hasegawa, P.M. (2007).

SIZ1-mediated sumoylation of ICE1 controls *CBF3/DREB1A* expression and freezing tolerance in *Arabidopsis*. *Plant Cell* **19**, 1403–1414.

43. Dong, C.H., Agarwal, M., Zhang, Y., Xie, Q., and Zhu, J.K. (2006). The negative regulator of plant cold responses, HOS1, is a RING E3 ligase that mediates the ubiquitination and degradation of ICE1. *Proc Natl Acad Sci USA* **103**, 8281–8286.
44. Kanaoka, M.M., Pillitteri, L.J., Fujii, H., Yoshida, Y., Bogenschutz, N.L., Takabayashi, J., Zhu, J.K., and Torii, K.U. (2008).*SCREAM/ICE1* and *SCREAM2* specify three cell-state transitional steps leading to *Arabidopsis* stomatal differentiation. *Plant Cell* **20**, 1775–1785.
45. Doherty, C.J., Van Buskirk, H.A., Myers, S.J., and Thomashow, M.F. (2009). Roles for Arabidopsis CAMTA transcription factors in cold-regulated gene expression and freezing tolerance. *Plant Cell* 21, 972–984.
46. Novillo, F., Alonso, J.M., Ecker, J.R., and Salinas, J. (2004). CBF2/DREB1C is a negative regulator of CBF1/DREB1B and CBF3/DREB1A expression and plays a central role in stress tolerance in Arabidopsis. *Proc Natl Acad Sci USA* **101**, 3985–3990.
47. Novillo, F., Medina, J., and Salinas, J. (2007). *Arabidopsis* CBF1 and CBF3 have a different function than CBF2 in cold acclimation and define different gene classes in the CBF regulon. *Proc Natl Acad Sci USA* **104**, 21002–21007.
48. Vogel, J.T., *et al.* (2005) Roles of the CBF2 and ZAT12 transcription factors in configuring the low temperature transcriptome of *Arabidopsis*. *Plant J* **41**, 195–211.
49. Lee, H., Guo, Y., Ohta, M., Xiong, L., Stevenson, B., and Zhu, J.K. (2002b). *LOS2*, a genetic locus required for cold responsive transcription encodes a bi-functional enolase. *EMBO J.* **21**, 2692–2702.
50. Xiong, L., Lee, H., Ishitani, M., Tanaka, Y., Stevenson, B., Koiwa, H., Bressan, R.A., Hasegawa, P.M., and Zhu, J.K.. (2002) Repression of stress-responsive genes by FIERY2, a novel transcriptional regulator in *Arabidopsis*. *Proc Natl Acad Sci USA* **99**, 10899–10904.
51. Fowler, S.G., Cook, D., and Thomashow, M.F. (2005) Low temperature induction of Arabidopsis CBF1, 2 and 3 is gated by the circadian clock. *Plant Physiol* **137**, 961–968.
52. Xin, Z., Mandaokar, A., Chen, J., Last, R.L., and Browse, J. (2007). *Arabidopsis ESK1* encodes a novel regulator of freezing tolerance. *Plant J.* **49**, 786–799.
53. Zhu, J., Shi, H., Lee, B.H., Damsz, B., Cheng, S., Stirm, V., Zhu, J.K., Hasegawa, P.M., and Bressan, R.A. (2004). An *Arabidopsis* homeodomain transcription factor gene, *HOS9*, mediates cold tolerance through a CBF-independent pathway. *Proc Natl Acad Sci USA* **101**, 9873–9878.
54. Zhu, J., Verslues, P.E., Zheng, X., Lee, B.H., Zhan, X., Manabe, Y., Sokolchik, I., Zhu, Y., Dong, C.H., Zhu, J.K., Hasegawa, P.M., and Bressan, R.A. (2005). *HOS10* encodes an R2R3-type MYB transcription factor essential for cold acclimation in plants. *Proc Natl Acad Sci USA* **102**, 9966–9971.
55. Kim, J.C., Lee, S.H., Cheong, Y.H., Yoo, C.M., Lee, S.I., Chun, H.J., Yun, D.J., Hong, J.C., Lee, S.Y., Lim, C.O., and Cho, M.J. (2001) A novel cold-inducible zinc finger protein from soybean, SCOF-1, enhances cold tolerance in transgenic plants. *Plant J* **25**, 247–259.
56. Vannini, C., Locatelli, F., Bracale, M., Magnani, E., Marsoni, M., Osnato, M., Mattana, M., Baldoni, E., and Coraggio, I. (2004). Overexpression of the rice *Osmyb4* gene increases chilling and freezing tolerance of *Arabidopsis thaliana* plants. *Plant J* **37**, 115–127.
57. Dai, X., Xu, Y., Ma, Q., Xu, W., Wang, T., Xue, Y., and Chong, K. (2007). Overexpression of a *R1R2R3 MYB* gene, *OsMYB3R-2*, increases tolerance to freezing, drought, and salt stress in transgenic *Arabidopsis*. *Plant Physiol* **143**, 1739–1751.
58. Yi, S.Y., Kim, J.H., Joung, Y.H., Lee, S., Kim, W.T., Yu, S.H., and Choi, D. (2004). The pepper transcription factor *CaPF1* confers pathogen and freezing tolerance in *Arabidopsis*. *Plant Physiol* **136**, 2862–2874.
59. Xu, Z.S., Xia, L.Q., Chen, M., Cheng, X.G., Zhang, R.Y., Li, L.C., Zhao, Y.X., Lu, Y., Ni, Z.Y., Liu, L., Qiu, Z.G., and Ma, Y.Z. (2007). Isolation and molecular characterization of the *Triticum aestivum* L. ethylene-responsive factor 1 (*TaERF1*) that increases multiple stress tolerance. *Plant Mol Biol* **65**, 719–732.
60. Liu, N., Zhong, N.Q., Wang, G.L., Li, L.J., Liu, X.L., He, Y.K., and Xia, G.X. (2007). Cloning and functional characterization of PpDBF1 gene encoding a DRE-binding transcription factor from *Physcomitrella patens*. *Planta* **226**, 827–838.
61. Chen, M., Xu, Z., Xia, L., Li, L., Cheng, X., Dong, J., Wang, Q., and Ma, Y. (2009). Cold-induced modulation and functional analyses of the DRE-binding transcription factor gene, GmDREB3, in soybean (*Glycine max* L.). *J Exp Bot* **60**, 121–135.

62. Kobayashi, F., Maeta, E., Terashima, A., Kawaura, K., Ogihara, Y., and Takumi, S. (2008). Development of abiotic stress tolerance via bZIP-type transcription factor LIP19 in common wheat. *J Exp Bot* **59**, 891–905.
63. Hu, H., You, J., Fang, Y., Zhu, X., Qi, Z., and Xiong L (2008) Characterization of transcription factor gene *SNAC2* conferring cold and salt tolerance in rice. *Plant Mol Biol* **67**, 169–181.
64. Mastrangelo, A.M., Belloni, S., Barilli, S., Ruperti, B., Fonzo, N.D., Stanca, A.M., and Cattivelli, L. (2005). Low temperature promotes intron retention in two *e-cor* genes of durum wheat. *Planta* **221**, 705–715.
65. Nakayama, K., Okawa, K., Kakizaki, T., Honma, T., Itoh, H., and Inaba, T. (2007). *Arabidopsis* Cor15am is a chloroplast stromal protein that has cryoprotective activity and forms oligomers. *Plant Physiol* **144**, 513–523.
66. Lee, B.H., Kapoor, A., Zhu, J., and Zhu, J.K. (2006). STABILIZED1, a stress-upregulated nuclear protein, is required for pre-mRNA splicing, mRNA turnover, and stress tolerance in *Arabidopsis. Plant Cell* **18**, 1736–1749.
67. Palusa, S.G., Ali, G.S., and Reddy, A.S.N. (2007). Alternative splicing of pre-mRNAs of *Arabidopsis* serine/arginine-rich proteins: regulation by hormones and stresses. *Plant J.* **49**, 1091–1107.
68. Tanabe, N., Yoshimura, K., Kimura, A., Yabuta, Y., and Shigeoka, S. (2007). Differential expression of alternatively spliced mRNAs of Arabidopsis SR protein homologs, atSR30 and atSR45a, in response to environmental stress. *Plant Cell Physiol* **48**, 1036–1049.
69. Sunkar, R., Chinnusamy, V., Zhu, J., and Zhu, J.K. (2007). Small RNAs as big players in plant abiotic stress responses and nutrient deprivation. *Trends Plant Sci* **12**, 301–309.
70. Sunkar, R., Kapoor, A., and Zhu, J.K. (2006). Posttranscriptional induction of two Cu/Zn superoxide dismutase genes in *Arabidopsis* is mediated by downregulation of miR398 and important for oxidative stress tolerance. *Plant Cell* **18**, 2051–2065.
71. Borsani, O, Zhu, J., Verslues, P.E., Sunkar, R., and Zhu, J.K. (2005). Endogenous siRNAs derived from a pair of natural *cis*-antisense transcripts regulate salt tolerance in *Arabidopsis. Cell* **123**, 1279–1291.

Chapter 4

Redox-Dependent Regulation, Redox Control and Oxidative Damage in Plant Cells Subjected to Abiotic Stress

Karl-Josef Dietz

Abstract

Stress development intricately involves uncontrolled redox reactions and oxidative damage to functional macromolecules. Three phases characterize progressing abiotic stress and the stress strength; in the first phase redox-dependent deregulation in metabolism, in the second phase detectable development of oxidative damage and in the third phase cell death. Each phase is characterized by traceable biochemical features and specific molecular responses that reflect on the one hand cell damage but on the other hand indicate specific regulation and redox signalling aiming at compensation of stress impact.

Key words: Abiotic stress, redox regulation, cell death, reactive oxygen species, oxidative stress.

1. Introduction

Each plant is able to acclimate to changing environmental conditions within its given genetic potential. In addition, the adaptation ability of plants has been widened during evolution by genotypic variation and phylogenetic radiation. If the acclimation potential is surpassed by environmental constraints ('stressors'), plants encounter metabolic imbalances, disturbance of development, yield losses and eventually cell and plant death. According to the general stress concept, an initial moderate stress impact often is important to trigger hardening responses and only then the full acclimation potential can be exploited by the plant (1). Early events in most stress responses are alterations in the cellular redox environment and late events the development of progressive oxidative damage up to the extent of chlorosis and

R. Sunkar (ed.), *Plant Stress Tolerance*, Methods in Molecular Biology 639,
DOI 10.1007/978-1-60761-702-0_4,

necrosis formation. The mutual relationship between redox imbalance, oxidative stress and stress sensitivity and, in turn, maintenance of redox homeostasis and stress tolerance has been established for many abiotic stress types (2–4). The initiation of hardening processes and the expression of appropriate acclimation responses depend on mechanisms that (i) sense the deteriorating growth conditions, (ii) transmit the information to regulators and (iii) allow the plant to establish the specific biochemical mechanism needed to counter the adverse stress effects. In a simplified view aiming at classifying components involved in the first step of sensing, one can distinguish specific and non-specific stress sensors. Specific sensors directly or indirectly, e.g. mediated through specific metabolic reactions, monitor the chemical or physical 'environment' and thus eventually the advent of a stress stimulus.

Heat-induced conformational changes of heat shock factor proteins (5) and Cd-induced activation of phytochelatin synthase (PCS) (6) are two examples of direct and stress-specific activation of responses. In the first case temperature-dependent decrease of the activation energy barrier facilitates a conformational switch which according to a widely discussed hypothesis enables the trimerization of heat shock factors, translocation of the complex to the nucleus and transcription of early heat stress-responsive genes (7, 8). In the second case, thiol and glutamate groups within PCS are responsible for metal-mediated activation of PCS which synthesizes phytochelatins, a $(\gamma$-glutamylcysteine$)_n$-glycine, from glutathione by its γ-glutamylcysteinyl-transpeptidase activity (9, 10). Accumulating PCs bind certain metals such as Cd^{2+}, Cu^{2+} and Zn^{2+} and also enable their transport to the vacuole. On the other hand not each stressor is sensed by specific sensory mechanisms. With increased strength the stressor gradually alters the metabolic state and progressively dis-regulates the otherwise finely tuned cellular processes. This is immediately plausible for xenobiotics, rare toxic metals or nutrient deprivation, stressors which are either little abundant in nature or chemically highly variable, or where transition from adequate to limiting supply and to severe stress occurs in a gradual fashion. Such structural and functional alterations and deviations are countered by established regulatory mechanisms to regain homeostasis and by activation of general defence systems to minimize damage development. Redox regulation and antioxidant defence usually are often assigned to the category of secondary stress responses (5).

It appears quite clear that the assignment of redox disequilibria as solely secondary stress effects inadequately describes the principle relationship between redox regulation and acclimation. Literature presents a vast set of publications on the effect of various stressors on the cell redox state which in its totality

suggests that redox sensing is intricately involved in primary stress defence. A small part of the available information is summarized in this contribution. In addition it is attempted to substantiate the hypothesis that redox deregulation and its readjustment are prime events in stress response.

1.1. Players in Oxidative Stress

Cell metabolism comprises many redox reactions embedded in metabolic pathways or electron transport processes. Reduction–oxidation reactions often show very large changes in Gibbs free energy and a very high reduction potential of involved metabolites corresponding to a very negative redox midpoint potential, e.g. the conversion of pyruvate to acetate with an E_m of −0.7 V (11). The substrates and products of these reactions are harmless as long as the reactions proceed in a controlled manner, and the rate of reducing power release is adjusted to the needs of the cell. However, if the tight control fails and specific intermediates such as ferredoxin and other Fe–S centres, quinones and flavins turn highly reduced, the propensity of electron transfer from these donors to O_2 increases. The single electron transfer to dioxygen generates superoxide $O_2^{\cdot -}$, a reactive oxygen species (ROS). The midpoint redox potential of the redox couple $O_2 + e^- \rightarrow O_2^{\cdot -}$ is −0.33 mV (12). $O_2^{\cdot -}$ reacts with many cellular compounds

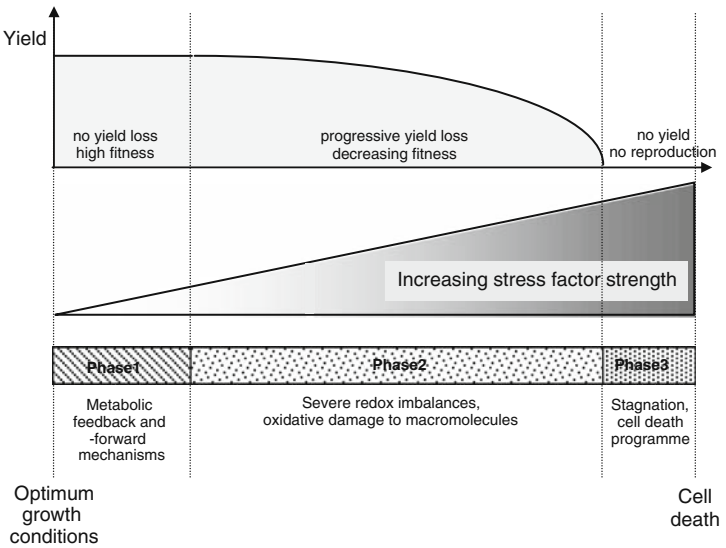

Fig. 4.1. Schematic depiction of the phases of redox deregulation and oxidative damage development during progressive impact of an environmental factor that if present above a certain threshold causes abiotic stress. During phase 1, regular metabolic regulation is efficient and no yield loss occurs. Plant fitness in terms of reproductive units is maximal. In phase 2, severe redox imbalances and oxidative stress coincide with increasing yield loss. In phase 3, the stress level has reached a level that strongly inhibits growth up to stagnation and suppresses the development of reproductive structures and may even cause cell death.

of the cell, e.g. ascorbate, glutathione, unsaturated lipids and protein thiols, with reaction constants between 10^3 and 10^7 L mol^{-1} s^{-1} (13). Reaction of $O_2^{\cdot -}$ with double bonds in lipids causes lipid peroxidation. For comparison, superoxide dismutase (SOD) increases the rate constant of $O_2^{\cdot -}$ dismutation to a diffusion limited rate of 2×10^9 L $mol^{-1}\cdot s^{-1}$. Spontaneously occurring or SOD-catalyzed dismutation of $O_2^{\cdot -}$ releases H_2O_2 which is less reactive than $O_2^{\cdot -}$ but may be converted by reduction to highly toxic hydroxyl radical (OH·). OH· abstracts electrons from organic compounds which may be present in close vicinity and thereby modifies and damages target molecules such as proteins and nucleic acids within diffusion distance of the generation site. Reactive nitrogen species (RNS) including NO and peroxynitrite and other radicals such as thioyl and peroxyl also participate in potentially uncontrolled redox metabolism in the cell. If the redox imbalance is progressively manifested severe oxidative damage and induction of cell death programmes may ultimately cause cell death (**Fig. 4.1**).

2. Phases of Redox Deregulation and Cell Death

The short outline of potential hazards of uncontrolled redox reactions and accumulation of reactive redox species (RRS) substantiates the view that the primary goal of cellular regulation is the readjustment of metabolic homeostasis under conditions of increasing redox imbalances. Deviations from redox equilibrium of central redox intermediates must be sensed prior to oxidative damage development. This information must be transduced into appropriate compensatory responses. The necessity of redox sensing and redox regulation may explain why redox sensitive cysteinyl residues are widely present in proteins, and why thiol modifications modulate many cellular activities (14). Analysis of the redox proteome and its alteration upon stress are important to understand the cellular regulatory state and the response to stress. During the last years diverse proteomics methods have been developed to address this topic. Thioredoxin (Trx) and glutaredoxin (Grx) trapping by chromatography of Trx- and Grx-targets (15, 16), differential fluorescence labelling of thiol proteins and their separation in 2D gels (17) and diagonal redox gel analysis (18, 19) have allowed to identify hundreds of potential dithiol/disulfide transition proteins involved in virtually all functional categories of the cell covering metabolism, transport, transcription, translation and signalling (19). For part of the identified proteins the significance of changing redox state has been proven by functional tests under reducing and oxidizing conditions, for

most others not. The thiol–disulfide proteins are woven into a network consisting of redox input elements, redox transmitters, redox targets and redox sensors (14). The state of this redox network under normal growth conditions and during abiotic stress is poorly understood. However, it is likely that stress-related redox changes are sensed on this level of the thiol–disulfide redox proteome and converted to early responses of compensatory readjustment of metabolic fluxes. In context of retrograde signalling from the chloroplast to the nucleus, the plastoquinone redox state provides also information on the state of the photosynthetic electron transport chain via protein kinases such as Stn7 and Stn8 in *Arabidopsis thaliana* for short- and long-term light acclimation (20–22). Chloroplasts also function in stress sensing since photosynthesis amplifies environmentally caused metabolic imbalances and retrograde signalling can transmit this information to the other cell compartments (23). Retrograde signals from the plastid to the nucleus as from the mitochondrion to the nucleus also reflect photosynthetic redox states and involve redox as well as ROS signals. The redox cues derive (i) either from the photosynthetic electron transport (PET) chain itself such as the redox state of the plastoquinone pool, (ii) the acceptor site of photosystem I such as the NADPH or thioredoxin system, or are (iii) signals linked to singlet oxygen, $O_2^{\cdot -}$, H_2O_2 and lipid peroxides (24). Abiotic stresses affect the retrograde signalling by modifying the balance between energy provision through the light reaction and the energy-consuming activities of the anabolic metabolism and growth.

In a more progressed stress state of redox imbalance, ROS and RNS accumulate above the normally very low levels due to stress-stimulated high rates of ROS and RNS generation with insufficient detoxification activity. This second phase is characterized by a large set of cell responses and metabolic alterations (**Fig. 4.2**) which are intensely studied in different plants and with diverse stresses. Phase 2-associated stress effects are ROS

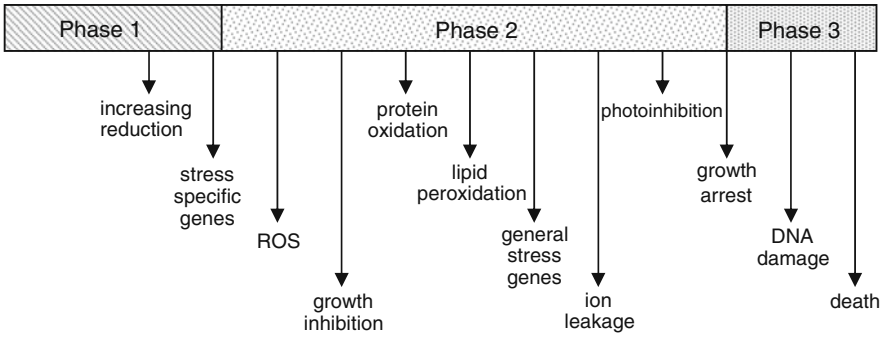

Fig. 4.2. Tentative assignment of regulatory features, metabolic events and damage symptoms to the different phases of redox deregulation.

generation, e.g. determined by diaminobenzidine (DAB) and nitroblue tetrazolium (NBT) staining for histochemical detection of H_2O_2 and $O_2^{\cdot -}$, respectively, e.g. in Cd^{2+}-exposed pea plants (25). Both methods do not quantify the accumulated levels of ROS but rather determine a mixed signal of concentration and ongoing rate of production. Other imaging methods for measuring accumulating ROS in cells involve dichlorofluorescein diacetate. Using this single cell method ROS generation was shown to increase in tobacco with decreased levels of alternative oxidase in mitochondria (26). New imaging methods such as counting of biophotons emitted during ROS reactions in vivo which depend on the availability of sophisticated machinery (27) and novel molecular probes are only used at a small scale until now. Another typical indicator of phase 2 is the accumulation of malondialdehyde as a consequence of non-enzymatic or enzymatic lipid peroxidation (28). Oxidation of unsaturated fatty acids at a low level is a normal reaction in living cells. Enzymatic oxidation is catalyzed by lipoxygenases whose transcript levels are high in young leaves, while stereo-random lipid peroxidation products accumulate in senescent leaves indicating the predominance of non-enzymatic lipid peroxidation reactions (28).

The third phase of damage development corresponds to growth stagnation, failure to reproduce and tissue and plant death (**Fig. 4.2**). Some stressors such as microbial pathogens that induce not only the hypersensitive response but also ozone exposure, heat and excessive salt stress cause lesions in tissues and cause cell death by necrosis or programmed cell death.

2.1. Phase 1: Redox-Dependent Deregulation in Abiotic Stress

The cause for any deviation from cell redox equilibrium is an imbalance between energy supply and consumption. Such imbalances in metabolism occur if substrate provision, activity of committed steps and other exergonic reactions of the energy providing metabolic pathways either remain more active or run with lower efficiency than demanded by downstream pathways that consume energy in growth and development. Under normal conditions, feedback regulation adjusts the upstream and downstream activities. However, under stress, such regulatory mechanisms frequently fail. As a consequence, the redox states of $NADH/NAD^+$ and $NADPH/NADP^+$ may shift to a more reduced or a more oxidized state. Plant cells maintain highly active pathways to oxidize excessively formed NADPH and NADH. The mitochondrial external NAD(P)H dehydrogenase (eNDH) in conjunction with alternative oxidase and uncoupling protein allow for dissipation of reducing power without the concomitant generation of proton motive force and ATP (29).

The alternative oxidases (AOXs) belong to two groups, AOX1 and AOX2, of which the AOX1 group strongly responds to various stress treatments such as oxidative stress. Interest-

ingly one particular NAD(P)H dehydrogenase (*ndb1*) is highly coregulated with *aox1a* (30) suggesting a coordinated function in over reduction control. Recently it was shown that the NADPH redox poise feeds back to the photosynthetic electron transport chain as well (31). Two transgenic tobacco lines with either reduced levels of ferredoxin-dependent $NADP^+$ reductase (FNR), linking electron transport to $NADP^+$ reduction, or reduced levels of glyceraldehyde 3-phosphate dehydrogenase (GAPDH), catalyzing the NADPH consuming reaction in the Calvin cycle, showed a similar degree of inhibition of carbon fixation and lowered electron transport. Interestingly the GAPDH knock down plants revealed no visible signs of stress, while the FNR plants were chlorotic and oxidatively stressed. The authors propose that increased NADPH reduction activates a regulatory mechanism that protects the photosynthetic apparatus (31). This mechanism is not activated in the FNR plants causing stress symptoms to develop. These examples show high redundancy in regulation aiming at adjusting an adequate cellular NAD(P)H redox poise. Via NADPH-dependent thioredoxin reductase and NADPH-dependent glutathione reductase, the NADPH redox poise feeds into the thiol protein redox network (14). More than 300 thiol proteins have been identified by diverse proteomics approaches that either interact with thioredoxin (15), with glutaredoxin (16) or undergo major conformational changes upon shifting from a reduced to an oxidized state (19). The energization level of illuminated leaves and the NADP-reduction state often increase under stress. For example under nutrient deprivation caused by S- or P-deficiency the assimilatory force F_A which is the product of phosphorylation potential and state of the NADP system $F_A = \frac{[ATP]}{[ADP][P_i]} \frac{[NADPH][H^+]}{[NADP^+]} = k\frac{[DHAP]}{[PGA]}$ (where P_i is inorganic phosphate, DHAP dihydroxyacetone phosphate and PGA 3-phosphoglyerate) increased in spinach leaves (32). Since the [ATP]/[ADP]-ratio decreased, this increased F_A likely indicates increased reduction potential. Changes in the NADPH redox state via coupling to the thioredoxin and glutathione/glutaredoxin systems will modify the redox state of target proteins. New cell imaging methods using roGFP allow monitoring the redox state of the glutathione system (33).

The almost full reduction of roGFP2 in vivo corresponds to only 1% oxidized glutathione under normal conditions, i.e. at a total cytosolic glutathione concentration of 2.5 mmol/L only 25 nmol/L would be present in the oxidized glutathione disulfide form (GSSG) (33). The rapid equilibration of the roGFP redox state with the glutathione pool is realized by coupling to glutaredoxin activity (34). Thus the first phase of stress-mediated redox imbalances will be reflected by altered thiol redox states and activities of thiol-regulated target proteins (35), which will affect diverse levels of cell activities reaching from metabolism to

translation and transcription. Comprehensive studies to describe this state under stress are unavailable. However, the experiment performed by Kolbe et al. (36) by administering dithiothreitol (DTT) to intact leaves might be a first approximation of the altered cell state under conditions of increasing reduction without concomitant generation of reactive oxygen species. Synthesis of starch, organic acid, amino acid, protein and cell wall increased in the presence of 5 mmol/L DTT, while carbohydrate metabolism including sucrose synthesis decreased (36). This study shows the power and significance of redox-dependent readjustment of cell activities after redox deregulation during abiotic stress (37).

2.2. Phase 2: Development of Oxidative Damage During Abiotic Stress

If the readjustment of cell redox norm by compensatory reactions in phase 1 fails excessively available electrons are transferred to oxygen as described above, primarily generating reactive oxygen species and secondarily other radicals and reactive metabolites by subsequent reactions of ROS. This second phase is subsumed as oxidative stress which is considered to be a major cause of stress-associated decline in biomass production and yield (38). Cells maintain an antioxidant defence system to eliminate toxic reactive intermediates. The detoxification is mostly achieved by dismutation, reduction or conjugation of the reactive intermediates. The reduction reaction is linked to NAD(P)H, glutathione and glutathione/glutaredoxins or thioredoxins as exemplified in the following: (i) Aldehyde dehydrogenases (ALDH) reduce reactive aldehydes by using NAD(P)H as cofactor. If not detoxified these aldehydes may initiate lipid peroxidation during stress. Many ALDH transcripts respond to stress. Overexpression of At-ALDH3-gene in *A. thaliana* resulted in a significant increase in tolerance to NaCl−, Cd−, Cu−, H_2O_2− and methyl viologen-linked stress with concomitant decrease in malondialdehyde formation as compared to wild-type plants (39). (ii) In the Halliwell–Asada cycle ascorbate peroxidase reduces H_2O_2 to water and oxidizes ascorbate. Regeneration of ascorbate by dehydroascorbate reductase is coupled to glutathione and glutathione reductase (40). (iii) Peroxide reduction by peroxiredoxins is either linked to the glutathione/GRX system (41) or the thioredoxin system (42, 43).

Proteins are prone to oxidative and nitrosative modification. Amino acid side chains that are targeted by this type of reaction in particular are cysteine, methionine, tyrosine and tryptophan. Such oxidative reactions are used to generate functional cofactors in some enzymes (44). In other cases oxidative modifications play a regulatory role of protein activity, e.g. the sulfinic acid form of typical 2-Cys peroxiredoxins that is rereduced by sulfiredoxins (45). Or they are irreversible and mark proteins for degradation (46).

In addition to their potentially damaging effect, ROS serve as important signalling messengers in cells and between cells. Altered accumulation of singlet oxygen in chloroplasts (47), decreased hydrogen peroxide detoxification in peroxisomes by catalase suppression (48) or in mitochondria by knockout of the mitochondrial PrxII F (49) trigger specific changes in nuclear gene expression as derived from transcriptomics analyses. The signalling effect depends on sensoric systems that reversibly detect changes in ROS levels. That is where phase 1 and phase 2 mechanisms of the redox regulatory network converge: Oxidative modification of thiol target proteins which alter their activity in dependence on the redox state is controlled by electron drainage from the redox network by ROS and reduction by the electron input elements (14). H_2O_2 is assumed to play a crucial role in electron drainage from the redox regulatory network.

Extracellular generation of reactive oxygen species is implicated in processes such as crosslinking and loosening of cell wall constituents, respectively, by production of H_2O_2 or OH· (50), initiation of hypersensitive response as incompatible pathogen–host interaction (51) and in systemic signalling, e.g. after illuminating leaves with excess excitation energy (52). Systemic signalling is the spreading of a signal to communicate the occurrence of stress in a particular plant tissue to distant non-stressed tissue and involves a plasma membrane NADPH dehydrogenase that generates $O_2^{\cdot -}$ (53). The lesion simulating disease 1 (lsd1) mutant of *A. thaliana* is deregulated in its excess excitation energy acclimation response. Data from a detailed analysis of hormone-, plastoquinone- and ROS-dependent signalling suggest that programmed cell death, light acclimation and many other defence responses are linked and initiated, at least in part, by redox changes of the PQ pool (54).

In addition to oxygen-dependent modifications, protein nitrosylation and nitration also strongly affect cell functions. In a screening approach to identify defence mechanisms involved in heat stress tolerance, two *A. thaliana* mutants with missense alleles of nitrosoglutathione reductase were identified (55). Seedlings with the missense alleles do not acclimate to heat stress in the dark, while the null alleles can acclimate to heat in the light. Since nitrosoglutathione is a substrate of S-nitrosylation of proteins its decomposition is essential to reduce nitrosative stress. The data of this study signify the important role of nitrosoglutathione reductase-dependent NO homeostasis in abiotic stress and plant development (55).

2.3. Phase 3: Cell death, Reactive Oxygen Species and Abiotic Stress

Developmental cues, biotic interactions and abiotic environmental factors affect cell fate and also may initiate cell death. Necrosis describes a rapid cell death with cell swelling due to collapse of cell membrane integrity and loss of osmoregulation. It occurs

when a sudden overwhelming stress impacts on the plant cells. Alternatively, apoptotic cell death involves the activation of a biochemical programme that causes the cell to die and consists of specific steps. Often mitochondria are involved as ROS source, cytosolic caspase-like proteases are activated, DNA is cleaved and, in a terminal phase, the cell shrinks by cytoplasmic condensation (56). The oxidative state and the overproduction of ROS are intricately involved in cell death. Severe heat stress is a well-studied abiotic stress leading to programmed cell death. After treatment at 55°C for about 10 min tobacco Bright Yellow-2 (BY-2) suspension cultured cells accumulate increasing amounts of H_2O_2 in a biphasic kinetics and also malondialdehyde over a period of 48 h after the transient stress treatment, while the control cells treated with a mild heat stress of 35°C for 10 min generated H_2O_2 only transiently. DNA fragmentation and cytoplasmic condensation in dying 55°C-treated cells indicate the involvement of an apoptosis-like programmed cell death (PCD) (2). The severely stressed cells also accumulated NO. A balanced accumulation of H_2O_2 and NO is required for inducing PCD in plant cells (57, 58). Ascorbate and glutathione levels increased in the 55°C-treated cell, while their reduction state decreased. Total ascorbate peroxidase activity fell to about one-third of the pre-stress value within 1 h.

Locato et al. (2) hypothesize that the collapse in APX activity coincides with PCD. Interestingly the induction of PCD in cadmium-treated BY-2 cell cultures depends on the cell cycle phase (59). Cd application induced apoptosis-like PCD in the S and G2 cells as indicated by pronounced DNA fragmentation, while Cd administration to cells in the G1 and M phase underwent slow non-lytic cell death. The authors hypothesize that the biological significance of the PCD in the S and G2 phases might reflect the necessity of removing defective and massively stressed meristematic cells, while the slow autophagic type mechanism in the G1 phase might be a mechanism to delay cell death in adult cells and tissues where no rapid cell death is required and maintenance of cell functions as long as possible is advantageous (59). Plant-specific PCD regulators and signalling pathways have been identified in mutant screens, e.g. for lesion-mimic mutants with more than 37 independent loci (51). Examples are the vtc-mutants (vitamin c-deficient), where an ascorbate deficiency fosters ozone-induced lesion formation (60), and the rcd-mutants (rcd: radical induced cell death) (61). In the *Arabidopsis* mutant sos1 that is hypersensitive to salt, moderate salinity induces biochemical and cytological changes typical for lysigenous PCD (62). Salinity stress and abscisic acid whose synthesis is enhanced under salt stress cause accumulation of reactive oxygen species. By a screen for increased salt tolerance, a first candidate gene product that links these cell responses has been identified and encodes ITN1, a transmembrane protein with an

ankyrin repeat motif apparently involved in the control of ROS generation by NADPH oxidase (3). These examples show the intricate relationship between oxidative stress, hormonal control of cell responses and induction of cell death programme (63).

3. Conclusions

An abstract text mining search in scientific databases for the combinations of abiotic stresses, e.g. salt stress or cadmium stress, and oxidative stress, retrieves thousands of references across all phylogenetic kingdoms. Apparently redox imbalances, generation of reactive species, oxidative modifications to cell structures and in the most severe case cell death are part of the cell response to adverse environmental conditions. In the light of this strict interrelation, the distinction between primary stress effects as defined by immediate impact of the stressor on cell functions and secondary stress effects, namely osmotic and oxidative stress, appears not to be well substantiated (64). As pointed out above the stressor-induced damage to cell structures is possibly always or at least in most cases the consequence of unfavourable oxidation reactions involving ROS and RNS. Thus the analysis of redox proteins, redox linked regulation, quantification of oxidative stress at the level of specific individual and sensitive macromolecules, and the stress-tailored activation of antioxidant mechanisms counteracting the development of oxidative stress will remain a major topic of abiotic stress research. Species that are tolerant, e.g. to heavy metal regularly have an enhanced antioxidant capacity (for review *see* [4]). On the other hand, the tolerance mechanisms at first hand must involve biochemical reactions such as transport that specifically reduce the stress strength in plasmatic compartments of the plants or strengthen the stability of sensitive sides.

References

1. Lichtenthaler, H.K. (1996) Vegetation stress: an introduction to the stress concept in plants. *J Plant Physiol* **148**, 4–14.
2. Locato, V., Gadaleta, C., De Gara, L., and De Pinto, M.C. (2008) Production of reactive species and modulation of antioxidant network in response to heat shock: a critical balance for cell fate. *Plant Cell Environ* **31**, 1606–1619.
3. Sakamoto, H., Matsuda, O., and Iba, K. (2008) ITN1, a novel gene encoding an ankyrin-repeat protein that affects the ABA-mediated production of reactive oxygen species and is involved in salt-stress tolerance in Arabidopsis thaliana. *Plant J* **56**, 411–422.
4. Sharma, S.S. and Dietz, K.J. (2009) The relationship between metal toxicity and cellular redox imbalance. *Trends Plant Sci* **14**, 43–50.
5. Wang, W., Vinocur, B., Shoseyov, O., and Altman, A. (2004) Role of plant heat-shock proteins and molecular chaperones in the abiotic stress response. *Trends Plant Sci* **9**, 244–252.
6. Ha, S.B., Smith, A.P., Howden, R., Dietrich, W.M., Bugg, S., O′Connell, M.J., Goldsbrough, P.B., and Cobbett, C.S. (1999)

Phytochelatin synthase genes from Arabidopsis and the yeast, *Schizosaccharomyces* pombe. *Plant Cell* **11**, 1153–1164.
7. Sorger, P.K. and Nelson, H.C. (1989) Trimerization of a yeast transcriptional activator via a coiled-coil motif. *Cell* **59**, 807–813.
8. Miller, G. and Mittler, R. (2006) Could heat shock transcription factors function as hydrogen peroxide sensors in plants? *Ann Bot* **98**, 279–288.
9. Maier, T., Yu, C., Küllertz, G., and Clemens, S. (2003) Localization and functional characterization of metal-binding sites in phytochelatin synthases. *Planta* **218**, 300–308.
10. Vatamaniuk, O.K., Mari, S., Lu, Y.P., and Rea, P.A. (2000) Mechanism of heavy metal ion activation of phytochelatin (PC) synthase: blocked thiols are sufficient for PC synthase-catalyzed transpeptidation of glutathione and related thiol peptides. *J Biol Chem* **275**, 31451–31459.
11. Segel, I.H. (1976) Biochemical calculations. John Wiley & Sons, New York.
12. Elstner, E.F. (1990) Der Sauerstoff. BI Wissenschaftsverlag, Mannheim.
13. Asada, K., Takahashi, M., Tanaka, K., and Nakano, Y. (1977) Formation of active oxygen and its fate in chloroplasts. *In* Biochemical and Medical Aspects of Active Oxygen (Hayaishi, O. & Asada, K., eds.), pp. 45–63, Japan Scientific Society Press, Tokyo. ISBN 0-8391-1204-1.
14. Dietz, K.J. (2008) Redox signal integration: from stimulus to networks and genes. *Physiol Plant* **133**, 459–468.
15. Motohashi, K., Kondoh, A., Stumpp, M.T., and Hisabori, T. (2001) Comprehensive survey of proteins targeted by chloroplast thioredoxin. *Proc Natl Acad Sci USA* **98**, 11224–11229.
16. Rouhier, N., Villarejo, A., Srivastava, M., Gelhaye, E., Keech, O., Droux, M., Finkemeier, I., Samuelsson, G., Dietz, K.J., Jacquot, J.P., and Wingsle, G. (2005) Identification of plant glutaredoxin targets. *Antiox Redox Signal* **7**, 919–929.
17. Yano, H., Wong, J.H., Cho, M.J., and Buchanan, B.B. (2001) Redox changes accompanying the degradation of seed storage proteins in germinating rice. *Plant Cell Physiol* **42**, 879–883.
18. Winger, A.M., Taylor, N.L., Heazlewood, J.L., Day, D.A., and Millar, A.H. (2007) Identification of intra- and intermolecular disulphide bonding in the plant mitochondrial proteome by diagonal gel electrophoresis. *Proteomics* **7**, 4158–4170.
19. Ströher, E. and Dietz, K.J. (2008) The dynamic thiol-disulphide redox proteome of the Arabidopsis thaliana chloroplast as revealed by differential electrophoretic mobility. *Physiol Plant* **133**, 566–583.
20. Ihnatowicz, A., Pesaresi, P., Lohrig, K., Wolters, D., Müller, B., and Leister, D. (2008) Impaired photosystem I oxidation induces STN7-dependent phosphorylation of the light-harvesting complex I protein Lhca4 in Arabidopsis thaliana. *Planta* **227**, 717–722.
21. Rochaix, J.D. (2007) Role of thylakoid protein kinases in photosynthetic acclimation. *FEBS Lett* **581**, 2768–2775.
22. Wagner, R., Dietzel, L., Bräutigam, K., Fischer, W., and Pfannschmidt, T. (2008) The long-term response to fluctuating light quality is an important and distinct light acclimation mechanism that supports survival of *Arabidopsis thaliana* under low light conditions. *Planta* **228**, 573–587.
23. Fey, V., Wagner, R., Bräutigam, K., and Pfannschmidt, T. (2005) Photosynthetic redox control of nuclear gene expression. *J Exp Bot* **56**, 1491–1498.
24. Baier, M. and Dietz, K.J. (2005) Chloroplasts as source and target of cellular redox regulation: a discussion on chloroplast redox signals in the context of plant physiology. *J Exp Bot* **56**, 1449–1462.
25. Romero-Puertas, M.C., Rodriguez-Serrano, M., Corpas, F.J., Gomez, M., Del Rio, L.A., and Sandalio, L.M. (2004) Cadmium-induced subcellular accumulation of $O_2^{\cdot -}$ and H_2O_2 in pea leaves. *Plant Cell Environ* **27**, 1122–1134.
26. Maxwell, D.P., Wang, Y., and McIntosh, L. (1999) The alternative oxidase lowers mitochondrial reactive oxygen production in plant cells. *Proc Natl Acad Sci USA* **96**, 8271–8276.
27. Kobayashi, M., Sasaki, K., Enomoto, M., and Ehara, Y. (2007) Highly sensitive determination of transient generation of biophotons during hypersensitive response to cucumber mosaic virus in cowpea. *J Exp Bot* **58**, 465–472.
28. Berger, S., Weichert, H., Porzel, A., Wasternack, C., Kuhn, H., and Feussner, I. (2001) Enzymatic and non-enzymatic lipid peroxidation in leaf development. *Biochim Biophys Acta* **1533**, 266–276.
29. Clifton, R., Millar, A.H., and Whelan, J. (2006) Alternative oxidases in Arabidopsis: a comparative analysis of differential expression in the gene family provides new insights into function of non-phosphorylating bypasses. *Biochim Biophys Acta* **1757**, 730–741.
30. Clifton, R., Lister, R., Parker, K.L., Sappl, P.G., Elhafez, D., Millar, A.H., Day, D.A.,

and Whelan, J. (2005) Stress-induced co-expression of alternative respiratory chain components in Arabidopsis thaliana. *Plant Mol Biol* **58**, 193–212.
31. Hald, S., Nandha, B., Gallois, P., and Johnson, G.N. (2008) Feedback regulation of photosynthetic electron transport by NADP(H) redox poise. *Biochim Biophys Acta* **1777**, 433–440.
32. Dietz, K.J. and Heilos, L. (1990) Carbon metabolism in spinach leaves as affected by leaf age and phosphorus and sulphur nutrition. *Plant Physiol* **93**, 1219–1225.
33. Meyer, A.J., Brach, T., Marty, L., Kreye, S., Rouhier, N., Jacquot, J.P., and Hell, R. (2007) Redox-sensitive GFP in Arabidopsis thaliana is a quantitative biosensor for the redox potential of the cellular glutathione redox buffer. *Plant J* **52**, 973–986.
34. Gutscher, M., Pauleau, A.L., Marty, L., Brach, T., Wabnitz, G.H., Samstag, Y., Meyer, A.J., and Dick, T.P. (2008) Real-time imaging of the intracellular glutathione redox potential. *Nat. Methods* **5**, 553–559.
35. Buchanan, B.B. and Balmer, Y. (2005) Redox regulation: a broadening horizon. *Annu Rev Plant Biol* **56**, 187–220.
36. Kolbe, A., Oliver, S.N., Fernie, A.R., Stitt, M., van Dongen, J.T., and Geigenberger, P. (2006) Combined transcript and metabolite profiling of Arabidopsis leaves reveals fundamental effects of the thiol-disulfide status on plant metabolism. *Plant Physiol* **141**, 412–422.
37. Oelze, M.L., Kandibinder, A., and Dietz, K.J. (2008) Redox regulation and overreduction control in the photosynthesizing cell: Complexity in redox regulatory networks. *Biochim Biophys Acta* **1780**, 1261–1270.
38. Van Breusegem, F., Bailey-Serres, J., and Mittler, R. (2008) Unraveling the tapestry of networks involving Reactive Oxygen Species in plants. *Plant Physiol* **147**, 978–984.
39. Sunkar, R., Bartels, D., and Kirch, H.H. (2003) Overexpression of a stress-inducible aldehyde dehydrogenase gene from Arabidopsis thaliana in transgenic plants improves stress tolerance. *Plant J* **35**, 452–464.
40. Dalton, D.A., Russell, S.A., Hanus, F.J., Pascoe, G.A., and Evans, H.J. (1986) Enzymatic reactions of ascorbate and glutathione that prevent peroxide damage in soybean root nodules. *Proc Natl Acad Sci USA* **83**, 3811–3815.
41. Rouhier, N., Gelhaye, E., Sautiere, P.E., Brun, A., Laurent, P., Tagu, D., Gerard, J., de Faÿ, E., Meyer, Y., and Jacquot, J.P. (2001) Isolation and characterization of a new peroxiredoxin from poplar sieve tubes that uses either glutaredoxin or thioredoxin as a proton donor. *Plant Physiol* **127**, 1299–1309.
42. Collin, V., Issakidis-Bourguet, E., Marchand, C., Hirasawa, M., Lancelin, J.M., Knaff, D.B., and Miginiac-Maslow, M. (2003) The Arabidopsis plastidial thioredoxins: new functions and new insights into specificity. *J Biol Chem* **278**, 23747–23752.
43. Collin, V., Lamkemeyer, P., Miginiac-Maslow, M., Hirasawa, M., Knaff, D.B., Dietz, K.J., and Issakidis-Bourguet, E. (2004) Characterization of plastidial thioredoxins from Arabidopsis belonging to the new y-type. *Plant Physiol* **136**, 4088–4095.
44. Davidson, V.L. (2007) Protein-derived cofactors. Expanding the scope of post-translational modifications. *Biochemistry* **46**, 5283–5292.
45. Biteau, B., Labarre, J., and Toledano, M.B. (2003) ATP-dependent reduction of cysteine-sulphinic acid by S-cerevisiae sulphiredoxin. *Nature* **425**, 980–984.
46. Ghezzi, P. and Bonetto, V. (2003) Redox proteomics: identification of oxidatively, modified proteins. *Proteomics* **3**, 1145–1153.
47. op den Camp, R.G., Przybyla, D., Ochsenbein, C., Laloi, C., Kim, C., Danon, A., Wagner, D., Hideg, E., Göbel, C., Feussner, I., Nater, M., and Apel, K. (2003) Rapid induction of distinct stress responses after the release of singlet oxygen in Arabidopsis. *Plant Cell* **15**, 2320–2332.
48. Vandenabeele, S., Van Der Kelen, K., Dat, J., Gadjev, I., Boonefaes, T., Morsa, S., Rottiers, P., Slooten, L., Van Montagu, M., Zabeau, M., Inze, D., and Van Breusegem, F. (2003) A comprehensive analysis of hydrogen peroxide-induced gene expression in tobacco. *Proc Natl Acad Sci USA* **100**, 16113–16118.
49. Finkemeier, I., Goodman, M., Lamkemeyer, P., Kandlbinder, A., Sweetlove, L.J., and Dietz, K.J. (2005) The mitochondrial type II peroxiredoxin F is essential for redox homeostasis and root growth of Arabidopsis thaliana under stress. *J Biol Chem* **280**, 12168–12180.
50. Liszkay, A., van der Zalm, E., and Schopfer, P. (2004) Production of reactive oxygen intermediates ($O_2^{\cdot-}$, H_2O_2, and $^{\cdot}OH$) by maize roots and their role in wall loosening and elongation growth. *Plant Physiol* **136**, 3114–3123.
51. Lorrain, S., Vailleau, F., Balaque, C., and Roby, D. (2003) Lesion mimic mutants: keys for deciphering cell death and defense pathways in plants? *Trends Plant Sci* **8**, 263–271.

52. Karpinski, S., Reynolds, H., Karpinska, B., Wingsle, G., Creissen, G., and Mullineaux, P. (1999) Systemic signaling and acclimation in response to excess excitation energy in Arabidopsis. *Science* **284**, 654–657.
53. Bechtold, U., Richard, O., Zamboni, A., Gapper, C., Geisler, M., Pogson, B., Karpinski, S., and Mullineaux, P.M. (2008) Impact of chloroplastic- and extracellular-sourced ROS on high light-responsive gene expression in Arabidopsis. *J Exp Bot* **59**, 121–133.
54. Mühlenbock, P., Szechynska-Hebda, M., Plaszczyca, M., Baudo, M., Mullineaux, P.M., Parker, J.E., Karpinska, B., and Karpinski, S. (2008) Chloroplast signaling and LESION SIMULATING DISEASE1 regulate crosstalk between light acclimation and immunity in Arabidopsis. *Plant Cell* **20**, 2339–2356.
55. Lee, U., Wie, C., Fernandez, B.O., Feelisch, M., and Vierling, E. (2008) Modulation of nitrosative stress by S-nitrosoglutathione reductase is critical for thermotolerance and plant growth in Arabidopsis. *Plant Cell* **20**, 786–802.
56. Reape, T.J. and McCabe, P.F. (2008) Apoptotic-like programmed cell death in plants. *New Phytol* **180**, 13–26.
57. Delledonne, M., Zeier, J., Marocco, A., and Lamb, C. (2001) Signal interactions between nitric oxide and reactive oxygen intermediates in the plant hypersensitive disease resistance response. *Proc Natl Acad Sci USA* **98**, 13454–13459.
58. de Pinto, M.C., Tommasi, F., and De Gara, L. (2002) Changes in the antioxidant systems as part of the signaling pathway responsible for the programmed cell death activated by nitric oxide and reactive oxygen species in tobacco Bright-Yellow 2 cells. *Plant Physiol* **130**, 698–708.
59. Kuthanova, A., Fischer, L., Nick, P., and Opatrny, Z. (2008) Cell cycle phase-specific death response of tobacco BY-2 cell line to cadmium treatment. *Plant Cell Environ* **31**, 1634–1643.
60. Conklin, P.L., Williams, E.H., and Last, R.L. (1996) Environmental stress sensitivity of an ascorbic acid-deficient Arabidopsis mutant. *Proc Natl Acad Sci USA* **93**, 9970–9974.
61. Overmyer, K., Brosche, M., and Kangasjarvi, J. (2003) Reactive oxygen species and hormonal control of cell death. *Trends Plant Sci* **8**, 335–342.
62. Huh, G.H., Damsz, B., Matsumoto, T.K., Reddy, M.P., Rus, A.M., Ibeas, J.I., Narasimhan, M.L., Bressan, R.A., and Hasegawa, P.M. (2002) Salt causes ion disequilibrium-induced programmed cell death in yeast and plants. *Plant J* **29**, 649–659.
63. Overmyer, K., Tuominen, H., Kettunen, R., Betz, C., Langebartels, C., Sandermann, H., and Kangasjarvi, J. (2000) Ozone-sensitive Arabidopsis rcd1 mutant reveals opposite roles for ethylene and jasmonate signaling pathways in regulating superoxide-dependent cell death. *Plant Cell* **12**, 1849–1862.
64. Wang, W.X., Vinocur, B., and Altman, A. (2003) Plant responses to drought, salinity and extreme temperatures, towards genetic engineering for stress tolerance. *Planta* **218**, 1–14.

Chapter 5

Array Platforms and Bioinformatics Tools for the Analysis of Plant Transcriptome in Response to Abiotic Stress

Nese Sreenivasulu, Ramanjulu Sunkar, Ulrich Wobus, and Marc Strickert

Abstract

Current microarray technologies allow high-density in situ synthesis of oligonucleotides or ex situ spotting of target molecules (cDNA) for conducting genome-wide comparative gene expression profiling studies. The avalanche of available microarray gene expression data from model plant species covering cell-related, tissue-specific, and developmental events, as well as perturbations to a variety of environmental stimuli has triggered many activities regarding the development of adequate bioinformatics tools for the analysis of these complex data sets. In this chapter we summarize the technical issues of different microarray technologies, discuss the availability of bioinformatics tools, and present approaches to extract biologically meaningful knowledge. For case studies of abiotic stress transcriptome analysis we highlight the unprecedented opportunities provided by these high-throughput technologies to understand networks of regulatory and metabolic pathway responses of plant cells to the application of abiotic stress stimuli.

Key words: Array technology, microarrays, macroarrays, transcriptome analysis, bioinformatics tools, abiotic stress.

1. Introduction

The recent technology-driven and fast evolving development of genome analysis instruments has revolutionized animal and plant genomics. Presently a variety of platforms are available to perform gene expression profiling for the quantification of transcript abundance in cells, tissues, or organs and their responses to environmental stimuli such as biotic and abiotic stress. For addressing transcriptome-related biological questions the researcher can

R. Sunkar (ed.), *Plant Stress Tolerance*, Methods in Molecular Biology 639,
DOI 10.1007/978-1-60761-702-0_5,

choose between different platforms: (a) techniques mostly confined to binary comparisons: differential displays (1) and representational difference AFLP analysis (2); (b) latest revolutionary cost-effective sequencing approaches to identify transcripts from specific libraries including transcript-enriched tag identification through sequencing (SAGE–serial analysis of gene expression) (3); and (c) hybridization-based approaches, especially microarray technologies, which allow comprehensive transcriptome analyses of any given cell type and its response to external perturbations like abiotic stress. In this chapter we focus on the wide potential of array-based hybridization platforms.

Lately a number of reviews were published, which address genomic aspects of plant responses to abiotic stress (4–7). Here, we focus on technical aspects. We first provide an overview of array platforms and discuss their advantages and disadvantages. Furthermore, a summary of existing databases for these platforms is given. Second, bioinformatics approaches are discussed that help turning raw experimental data into biologically meaningful data, thereby addressing questions about necessary steps of normalization for faithful comparisons with reference data and about the use of dimension reduction techniques and clustering algorithms for extracting differentially expressed genes under abiotic stress treatments. Software tools for the identification of metabolic pathways linked to differentially expressed gene sets are discussed as well as possibilities for reaching insights into stress-related transcriptional dependencies by interpreting these complex data in the context of networks. Third, a case study of transcriptome profiling is given describing the influence of terminal drought on barley seed metabolism. In addition to that, future directions of plant genomics are outlined by extrapolating tools and data available for the model plant *Arabidopsis thaliana* to more important crop plants. Finally, the relevance of integrative and systems approaches as applied to stress biology will be discussed.

2. Array-Based Technology Platforms for Transcriptome Studies

In order to produce arrays for whole-transcript gene expression analyses, available EST or cDNA sequences from libraries are used to first amplify cDNA fragments by the polymerase chain reaction (PCR) using vector- or gene-specific primers. The amplified and purified fragment collections can then be spotted on the surface of nylon membranes with a density of 12,600 fragments with duplicated spots on an 11 × 22 cm filter (macroarray) using a spotting robot or the EST collection can be printed onto a microscopic

glass slide (microarray), which can accommodate 30,000 amplified cDNA fragments (8). Details of design and fabrication as well as probe synthesis and hybridization of macroarrays using ^{33}P-labeled nucleotides (9) and of microarrays using Cy3 and Cy5 fluorescent probes (10) have been described. Hybridizations have to be performed under stringent, high-temperature conditions in order to avoid cross-hybridizations among closely related sequences as much as possible. Macro- and microarray technologies allow a great deal of flexibility in terms of design under moderate costs. Therefore, such a technology has often been the method of choice for academic research on gene discovery and transcriptome studies. The use of Cy3 and Cy5 fluorescent dyes in microarray hybridizations allows to differentially label mRNA populations from control and abiotic stress-treated tissues and eventually to hybridize them under competitive binding conditions to the array probes. The hybridized array is then read at wavelengths specific to Cy3 (~550/570 nm) and Cy5 fluorescent (~650/670 nm) dyes, and the measured ratio of transcript levels is determined and used to identify down- or up-regulated gene sets in a given abiotic stress treatment. Conducting labeling experiments by combining both dyes on arrays and counting Cy3/Cy5 ratios might be problematic in summer months due to a rise in ozone levels beyond/up to 25 parts per billion (ppb), since the exposition of Cy5 dye to 5–10 ppb ozone levels for 10–30 s leads to its degradation. Use of the Cy3 dye alone is more stable which could sustain ozone levels up to 100 ppb. Although such experimental designs are cost-effective, the obtained results can often not be integrated in the analyses of larger experimental series due to technical limitations.

Furthermore, in these kinds of ex situ spotted (cDNA) arrays the possibility of undesired cross-hybridization between closely related gene family members always exists. This issue is particularly important given the fact that most organisms contain multigene families whose members possess a high degree of sequence similarity but are often expressed in a cell-specific manner. To tackle this problem, oligonucleotides (60–100 mers) may be amplified from unique parts of transcripts often found in the 3′-untranslated region of messengers. Such sequences can potentially differentiate between gene family members as well as splice variants thus allowing designation of a specific transcript level to an individual gene family member. This option is especially recommendable when whole genome sequence information is available as for rice (http://rice.plantbiology.msu.edu/index.shtml), *Arabidopsis* (http://www.tigr.org/tdb/e2k1/ath1/) and a few other plant species (11).

The recently advanced combination of powerful robotics approaches and in situ oligonucleotide synthesis technologies enables an effective production of oligo arrays as important

genomics tools. Commercially fabricated arrays of the Agilent, NimbleGen, and Affymetrix platforms allow relatively straightforward data generation due to well-described experimental procedures covering RNA sample preparation, probe labeling, hybridization, and signal detection procedures (*see* the available review by 12). These procedures can also be outsourced to companies. Hence, we focus on aspects relevant to deciding which technology should be used in a given experimental set-up.

The Agilent platform (http://www.chem.agilent.com/en-US/products/instruments/dnamicroarrays/pages/default.aspx) and NimbleGen arrays allow spotting of longer oligonucleotides (60–100 mers) at a higher density through ink-jet and maskless array synthesizer technologies, respectively. The Agilent and NimbleGen platforms are also flexible, efficient, and relatively cost-effective. Agilent allows researchers to test their DNA sequences to find the best oligos using the eArray platform provided by Agilent free of charge and to design arrays which could accommodate 244,000 oligos (1 × 244 K) on a standard 1 × 3 in. glass slide. Alternatively, the design allows freedom to choose different formats as, for instance, 2 × 105 K, 4 × 44 K, and 8 × 15 K, depending on the number of available target sequences from a given crop plant. Likewise, NimbleGen allows multiplex arrays 12 × 135 K to run several replicates on the same array (http://www.nimblegen.com/products/lit/expression_brochure_2008_10_31.pdf). For labeling it is recommended to use one color Cy3 fluorescent probes (see above). Detailed protocols for cRNA synthesis, purification, hybridization, washing, scanning, and feature selection are provided by the Agilent Company (http://www.chem.agilent.com/Library/usermanuals/Public/G4140-90041_One-Color_Tecan.pdf). Printing of multiplex microarrays (4-plex or 8-plex arrays) with a feature of 60-mer oligos helps to achieve high specificity and sensitivity with a need of only small probe volumes. These technological features are beneficial for obtaining reliable quantitative information on transcript abundances even from small amounts of RNA used for amplification by in vitro transcription with T7 polymerase. Such small amounts are typically obtained from micro-dissected tissue samples of control and stress-treated plant material.

The other major platform based on oligonucleotides is provided by Affymetrix (http://www.affymetrix.com/). It has been well accepted to study genome-wide gene expression patterns also in different crop plant species subjected to diverse stress (http://www.ncbi.nlm.nih.gov/geo/; https://www.genevestigator.com/gv/index.jsp) treatments. For this platform Fodor et al. (13) implemented a photolithographic technology which allows to spatially addressing approximately 300,000 spots/cm^{2}resulting in an extremely high oligo density. The

procedure allows a realization of at least 11 short (20–25mer) oligos as perfectly matching and mismatching probes from a chosen mRNA reference sequence typically derived from the most unique part of the 5′-untranslated region of the transcript. The feature of perfect match and mismatch probes enables a statistically powerful comparison of signals obtained from different arrays (14). The described salient features of the Affymetrix chip design compensate for the limitations of shorter oligos known to yield less specific hybridization data and reduced sensitivity in comparison to longer oligos (60 mers and longer). For the production of custom arrays additional design costs will be included. Hence, the technology is usually inaccessible to academic laboratories for performing large series of experiments.

In order to get a comprehensive overview of stress regulation mechanisms, researchers usually need to utilize a combination of expression platforms: (i) custom-made arrays to perform detailed experiments covering stress responses from diverse time points during development. These experiments also allow selecting samples of special interest which are then (ii) subjected to genome-wide expression analyses using Affymetrix or Agilent chips. Such analyses are necessary, since a single developmental time point is insufficient for the identification of differential gene expression processes between control and stress-treated samples due to the fact that developmental cues and stress perception can be different at different developmental stages.

To compare data obtained from different platforms, a number of critical issues related to hybridization specificity and signal sensitivity discussed above have to be considered with care before interpreting the results in a biologically relevant manner. The Microarray Quality Control study (MAQC) incorporating data from seven microarray platforms and three alternative technologies highlighted that oligo-based microarray technology data are comparable and well reproduced (14). Among them, the Affymetrix technology turned out to yield expression data of superior quality with better reproducibility between the arrays, in particular for low-expressed genes (http://www.affymetrix.com/support/technical/technotes/expression_comparison_technote.pdf), whereas the Agilent platform shows improved sensitivity with a significant detection of higher numbers of genes above background level due to high-fidelity DNA synthesis (http://www.chem.agilent.com/Library/technicaloverviews/Public/5989-5805EN_LO.pdf). There are several data repositories available. Among them the Gene Expression Omnibus (GEO) database allows storage of unprocessed and processed gene expression data in different formats of arrays according to the standards of Minimum Information About a Microarray Experiment (MIAME) (15).

3. Bioinformatics Approaches for Data Processing and for the Inference of Metabolic and Regulatory Gene Networks from Transcriptome Studies

The full potential of high-throughput array technologies can only be exploited in tight combination with suitable computational data analysis tools. Complementary to sequence search jobs that can be highly parallelized into separate tasks on a cluster computer, array data analysis puts higher demands on fast accessible memory capacity. Data matrix operations necessary for clustering and statistical analysis do strongly profit from symmetric multiprocessing (SMP) computer architectures with several processors/cores connected to the same, possibly large, main memory. On such machines, programming languages like Java provide easy support for multithreaded program execution, and mathematic libraries for parallel evaluation of shared data can be effectively used by bioinformatics tools.

The array data have to be evaluated at two levels, first by pre-processing the data to control for quality checks and eventually post-processing the data to infer the biological significance of the transcriptome study results. The detailed steps involved in pre-processing of microarray data obtained from different platforms have lately been reviewed by Durinck (16). Also the R packaging system (http://www.r-project.org) has been utilized effectively to develop open source software for assessing quality checks of microarray data in Bioconductor (http://www.bioconductor.org). For Affymetrix data analysis the Robin platform has been developed (http://bioinformatics.mpimp-golm.mpg.de/projects/own/robin).

In this chapter, we concentrate on the array data post-processing pipeline (**Fig. 5.1B–E**), which is summarized as follows. After quality checks, the array data are normalized to reach best comparability of the experiments. At first dimension reduction techniques help to visualize the obtained multi- and high-dimensional data sets and to identify general data groupings and outliers. More accurate groupings and better characterization of gene expression patterns are achieved by clustering methods. Thereby, the choice of data similarity measure usually has a strong impact. For identification of stress-regulated gene sets, potentially interesting candidate genes triggered by the application of stress conditions are discovered by statistical analysis. To widen the scope from individual genes to families of functionally related genes, a combination of functional annotations and statistical tools is an essential approach for creating an in-depth understanding of biochemical metabolic pathways and regulatory networks responsive to stress treatments as part of systems regulation processes and their interaction structures. The individual steps of the data processing pipeline are discussed in the following sections.

3.1. Normalization Makes Array Data Comparable

Normalization is an important data transformation step to turn a collection of data records by an information-maintaining operation into well-comparable data sets (17). Only after strong efforts have been undertaken to make measurements as similar as possible between the arrays, the remaining differences indicate a set of candidate markers explaining biologically meaningful differences corresponding to the experimental design, including stress treatments, time points, and so forth. Thereby, the normalization method must be chosen according to subsequent analysis targets (18). For example, a logarithmic transform or a *z*-score transformation might be needed to prepare data sets for the application of Student's *t*-test which requires normal distributed data. It should be noted that normalization of arrays (columns represented by different samples/experiments) will be distorted if an additional normalization of genes (rows represented by genes) is conducted and vice versa (see also below).

Two elementary modes of normalization exist, within-sample normalization and between-sample normalization. Median centering, i.e., subtracting the median value, from an array is a typical within-sample operation which does not require information from other data samples. On one hand, this makes within normalization usually quite fast, whereas between arrays (samples) normalization needs to be redone for the whole data sets even after adding only a single new array. On the other hand, higher computational efforts of between-sample normalization usually are rewarded by better comparability of the data sets and more reliable identification of, in our case, stress-related genes. In this respect, quantile normalization is a fast and robust approach to normalize gene expression data tables (17). The arrays are normalized in such a way that all genes belonging to the same sorting rank are set to their overall average value. This is a generalization of median centering which yields identical values only for the midmost value of sorted arrays. Each quantile value, including minimum, median, and maximum, is replaced by its average across the respective quantile of all arrays, this way, making the data distributions of all arrays identical. Quantile normalization is the central step of the robust multiarray average analysis (rma) which was shown to provide more reliable sets of candidate genes for microarray data than the MAS5 method provided by the genechip manufacturer (19).

In transcript data a naturally higher variation is found in high-intensity levels than in low-intensity levels assuming intensities being reliably above the noise level. In practice, a specific fold change of a repeated measurement is thus more likely to occur in high-intensity signals than in low-intensity signals, which might lead to undesired effects in fold-change-based analyses. Variance stabilizing normalization is a method for creating a similar variability across the whole range of values (20). Since the

computational demands of the data transformation are quite high, an application to massive data sets must be considered with care. The main target of application of this normalization procedure is data preparation for differential analysis of small data sets involving fold-change criteria. As a consequence, fold changes between stress and control experiments get comparable for whole data sets, regardless of differences between average expressions levels of the genes.

3.2. Dimension Reduction Provides Access to Complex Data Tables

The complexity of large data tables can be substantially reduced by mapping data points of high dimensionality to points located in a two-dimensional plane or even on a one-dimensional real-value interval (21). This way scatter plots can be created where mapped data proximities reflect proximities in the high-dimensional data space. Mappings to intervals can be used to impose a well-defined ordering of the associated data vectors, i.e., high-dimensional data tables can be sorted according to the mapping values, thereby providing smooth transitions between subsequent expression vectors. Ideally, experiments of the same stress treatment or a given developmental time point are projected to nearby locations, helping to identify outliers and to confirm the consistency of the available experiments (22). Principal component analysis (PCA) is one of the most often used methods for a dimension reduction mapping, targeting directions in the data space along maximum variance (23). Although PCA can be calculated quickly, it is limited by the linear mapping approach which, in strict sense, is only applicable to data vectors compared by Euclidean distance. Alternatively, self-organizing maps (SOM) are commonly utilized for mapping gene expression vectors in a non-linear way onto a one- or two-dimensional grid of data cluster centers (24). Thereby, a SOM realizes neighborhood preservation such that neighbored prototypes in the grid tend to be similar to each other, which allows an easy navigation along major shapes of expression vectors. On the pro-side, a flexible choice of data similarity measures is possible; on the con-side, the grid size and some parameters of the algorithm need to be well specified by the researcher. Also in case of few available data points or if proper data densities should be displayed, SOM is not the best choice, because of its built-in clustering procedure.

Faithful non-linear one-to-one mappings of possibly non-Euclidean input data are realized by multidimensional scaling (MDS) techniques which only require few parameters, if any. High-throughput multidimensional scaling (HiT-MDS) is a recent high-performance formulation of this dimension-reduction principle that helps to generate scatter plots from general similarity matrices describing relationships between expression vectors (25). MDS outperforms PCA for visual data representation, but unlike PCA, MDS cannot be used for factor

analysis, because covariance between data attributes, necessary for PCA, is not applicable to non-Euclidean similarity measures.

3.3. Clustering Untangles Prominent Expression Patterns

Complementary to visual data inspection discussed in the previous paragraph, a more rigorous grouping and identification of characteristic gene expression patterns is obtained by computing methods for the clustering of high-dimensional data. The most frequently used clustering approaches applied to gene expression data, in the order of computational demands, are *k*-means clustering, self-organizing maps (SOM), and hierarchical clustering (HC) (26, 27) (**Table 5.1**). The *k*-means method iteratively assigns a number of *k* data centroids to the centers of gravity of the data vectors to which they are closest (28). This competition for optimum representation of local data centers finally leads to the detection of the *k* most prominent gene expression patterns. While no natural ordering of these *k* patterns is induced, this is different for the SOM method that creates a navigable grid of locally similar patterns. As a consequence, empty SOM clusters (idle nodes) may occur and complicate the analysis. This can be solved by switching to an appropriate visualization of the relationships by means of the U-matrix (24). The benefit of SOM is its ability to create a one-dimensional chain of cluster centers, allowing a tabular ordering of clusters and their associated gene expression vectors. A similar, but computationally much more expensive clustering alternative is brought about by hierarchical clustering (29). First of all, groups of pair wise similar expression patterns can be obtained. Depending on the chosen type of data cluster linkage different connectivity's can be emphasized, ranging from single linkage via average linkage to complete linkage, for better representing strongly connected data clouds, partially connected clouds and disconnected clouds, respectively. Although single-link clustering is fastest, average linkage and complete linkage are preferred for robustly dealing with natural noise in gene expression data.

Tree plots resulting from any type of hierarchical clustering are often misleading, because the calculated subtrees usually appear in arbitrary rotation. Subtree rotation does not affect the grouping of the data that they represent is thus not optimized during clustering. As a consequence, nearby objects at the leaves of a cluster tree plot might belong to very distant subtrees. However, if an ordering procedure is applied to the leaves of the hierarchical tree, i.e., to individual gene expression vectors, non-specific rotations of cluster-subtrees are turned into an equivalent arrangement such that maximum similarity between all adjacent leaves is reached in the reordered tree (30). The time complexity of the reordering operation is slightly higher than the clustering itself. If time permits, it is generally recommended to apply leaf ordering for creating unique and convincing hierarchical cluster

Table 5.1
List of software used for spot detection, quality check, and clustering gene expression data

Name	URL	Function
AIDA (C)	http://www.raytest.de/bio_imaging	Spot scoring
ArrayVision (C)	http://www.gelifesciences.com/	Spot scoring
Microarray Suit (C)	http://www.affymetrix.com/	Spot scoring
ScanAlyze (A)	http://rana.lbl.gov/EisenSoftware.htm	Spot scoring
SPOT (A)	http://www.hca-vision.com/product_spot.html	Spot scoring
Spotfinder (A)	http://www.tm4.org/spotfinder.html	Spot scoring
Genepix Pro (C)	http://www.moleculardevices.com/pages/software/gn_genepix_pro.html	Spot scoring
UCSF spot (A)	http://jainlab.ucsf.edu/	Spot scoring
BASE	http://base.thep.lu.se/	Integrated gene expression tool
CyberT (A)	http://www.research.ibm.com/journal/sj/402/mangalam.html	Integrated gene expression tool
R/BioConductor (A)	http://www.bioconductor.org/	Quality check
RMAExpress (A)	http://rmaexpress.bmbolstad.com/	Quality check
ROBIN (A)	http://bioinformatics.mpimp-golm.mpg.de/projects/own/robin	Quality check Affymetrix
Genemaths XT (C)	http://www.applied-maths.com/products.htm	Integrated gene expression tool
GenePattern (A)	http://www.broad.mit.edu/cancer/software/genepattern/	Integrated gene expression tool
Genowiz (C)	http://www.ocimumbio.com/	Integrated gene expression tool
Genespring GX (C)	http://www.chem.agilent.com/en-US/products/software/lifesciencesinformatics/genespringgx/Pages/default.aspx	Integrated gene expression tool
Cluster & Treeview (A)	http://rana.lbl.gov/EisenSoftware.htm	Clustering

MeV (A)	http://www.tm4.org/mev.html	Clustering
MIDAS (A)	http://www.tm4.org/midas.html	Clustering
HiT-MDS (A)	http://hitmds.webhop.net/	Clustering
J-Express Pro (C)	http://www.molmine.com/	Clustering
Xcluster (A)	http://fafner.stanford.edu/~sherlock/cluster.html	Clustering
BRB array tool (A)	http://linus.nci.nih.gov/BRB-ArrayTools.html	Statistical tool
SAM (A)	http://www-stat.stanford.edu/~tibs/SAM/index.html	Statistical tool
EDGE (A)	http://www.genomine.org/edge/	Significance test, clustering
Microarray explorer (A)	http://www.lecb.ncifcrf.gov/MAExplorer/	Significance test, clustering

A: free for academic use; C: commercial product.

trees. In transcriptome studies, depending on the noise level and the number of differentially regulated genes, stress and control plants should occur systematically arranged in the ordered cluster trees, such as stress-related samples on one side, controls on the other side.

3.4. Distance Measures Determine Clustering Structures

Clustering procedures are mainly determined by the underlying data similarity measure (31). Expression vectors of similar expression levels are best represented by Euclidean distance. If general trends of co-expressions are of interest, it is better to switch to a one-minus-correlation measure. Strict Euclidean data representation, such as by *k*-means clustering, requires many more clusters than for representing the subset of most prominent shapes of co-expression with the same method and accuracy. Many available tools offer a choice between linear Pearson correlation and Spearman rank correlation. While Pearson correlation is more sensitive to outliers, the Spearman correlation is less sensitive to real pattern changes, and no general recommendation on a proper choice can be given. Interestingly, for efficient computation one-minus-Pearson correlation can be expressed by squared Euclidean distance applied to *z*-score transformed and rescaled data vectors, and Spearman rank correlation can be expressed by converting the expression data vectors first into sorting ranks and then applying Pearson correlation. Euclidean distance itself is just one instance of general Minkowski metrics, corresponding to a Minkowski parameter of two. If this parameter is set to one, these results in the Manhattan distance which is more robust against outliers and which is also offered in many tools for gene expression analysis.

3.5. Statistical Analysis Highlights Stress-Related Candidate Genes

The identification of differentially expressed genes from transcriptome studies is one major goal in research on plant reactions to stress. Intensity-based color table views of clustered gene expression data reveal specific gene expression patterns and provide first hints on differentially expressed genes from arrays representing different experimental conditions. A possibly improved identification of gene expression patterns associated with certain stress conditions can be obtained by using a simultaneous clustering of experiments and genes, the so-called biclustering (32). Even more rigorous results are provided by multifactor statistical analysis aiming at detecting significant differences between factor-specific average gene expression levels. For two experimental factors, such as stress and control conditions, Student's *t*-test is most frequently used in the literature. In order to get reliable results, a good number of repetitions should be carried out for a proper estimation of average gene expression levels. These gene expression values are assumed to be normally distributed. Furthermore, to justify the use of a common significance level for all genes, the

variance is assumed to be independent of expression intensity, and all genes are considered as being regulated independently of each other. By using a significance level correction like the Bonferroni method these strong constrains can be slightly relaxed (33). The analysis of variance (ANOVA) is a generalization of the *t*-test to more than two factors. A more specific situation occurs for paired observations of two conditions; then a paired *t*-test can be applied to test for a significant deviation of the average differences from zero. Despite of the strong prerequisites of ANOVA approaches, they are still useful for generating lists of candidate genes ordered according to their *p* value.

For two-factor analysis a commonly used more robust, yet less sensitive, test is the Mann–Whitney *U* test, based on ranks of ordered observations. The multifactor counterpart of this non-parametric test is the Kruskal–Wallis *H* test (34). More recently, a sensitive optimal discovery procedure was developed and integrated into the easy-to-use EDGE software for the extraction of differential gene expression for various types of experimental designs (35).

Proper statistics should also be applied to find stress-regulated gene sets from individual developmental stages, and eventually the differentially expressed gene sets identified across all developmental points are subjected to the above-described clustering procedures. Such a combinatory procedure easily excludes non-regulated gene set including noise data and subsequently helps to effectively improve the clustering procedures in order to find tightly co-expressed gene sets regulated under abiotic stress treatments. A list of publicly available software used in different levels of gene expression data processing is provided in **Table 5.1**.

3.6. Functional Annotation Reveals Novel Regulatory Mechanisms

Although statistical identification of differentially expressed genes is one important aspect of stress-related studies, more comprehensive insights at the level of relevant regulatory processes can only be reached by the incorporation of careful gene annotations. The sequences spotted on the array need to be annotated through computational-assisted approaches based on homology search analysis programs, domain scans, signal retention predictions for predicting protein localizations, and structural element predictions for putative enzymes, transcription factors, kinases, etc. The challenge here is to collect the biologically relevant data from different databases, to manually curate the annotations and to assign functional pathways in a defined vocabulary according to MapMan (36), Gene Ontology (37), MIPS (38) or KEGG (39) databases. To automate the annotation pipeline it is required to develop specific software tools to alleviate the presently labor-intensive procedure. The assignment of functional categories to each of the probed genes allows binning of whole sets of homologous and inter-related genes for testing differential enrichment

of functional categories. This way, systemic reactions to stress applications can be unraveled. For control versus stress conditions between two experiments the MapMan software enables a mapping of functional annotation of significantly differentially expressed gene set onto known pathways (36, 40). By means of the pathway visualization module an overview of relevant biological processes is provided, allowing the researcher to create new hypotheses about regulation cascades. Also significant overrepresentation of functional categories under abiotic stimuli can be profiled in time course studies by using the PageMan tool (41). Likewise, there are a number of tools available for model species. Some representative examples include Cytoscape (42) and Osprey (43) for creating gene networks and Genevestigator, a web-based online tool to search for biomarkers in stress- or hormone-regulated gene sets of *Arabidopsis*, rice and barley (44). All these tools support the visualization of ontology-based gene networks helping to gain first-hand information of global alterations at the transcriptome level. For a comprehensive list of publicly available software used for mapping gene expression data onto metabolic pathways and for finding interesting gene networks see **Table 5.2**.

4. A Case Study: Drought Stress Tolerance in Spring Barley

A macroarray design combining 12,590 seed-specific and development-related ESTs was used for assessing differential gene expression in the spring barley variety "Brenda" exposed to drought stress. Homogenized seed material collected from control and drought treatments covering three time points at 12, 16, and 20 days after flowering was used for total RNA isolation and radioactive probes labeled as described previously (45). Subsequently the probes were hybridized onto the cDNA membranes (**Fig. 5.1**). An independent repetition was carried out.

An exposition time of 12 hours was used to create 12 high-contrast images. In macroarray experiments, the exposed imaging plates are scanned with a phosphorimager at a resolution chosen to reveal spots at a fixed radius between 10 and 20 pixels, typically at a depth of 16 bits, i.e., 65,536 intensity levels. A compromise between the level of detail and file size is usually found at a resolution between 10 μm^2 and 100 μm^2. A scanning resolution of 50 μm^2 produced bitmaps of 5000×4000 pixels, a size for which the spot detection was carried out by a customized algorithm taking into account spatial correlations for a faithful estimation of background signals. One critical task is the proper alignment of a pre-defined grid structure to the signal-carrying spots of scanned

Table 5.2
List of software used for finding functional enriched groups, mapping gene expression data onto pathway tools, and gene networks from transcriptome data

Name	URL	Function
Gene Ontology based Expression tools (A)	http://www.geneontology.org/GO.tools.microarray.shtml	Tools make use of GO for expression mapping
AraCyc: Pathway tool Omics Viewer (A)	http://www.plantcyc.org:1555/expression.html	Pathway tool for visualizing omics data
MAPMAN (A)	http://www.gabipd.org/projects/MapMan/	Pathway tool for visualizing omics data
KaPPA-View (A)	http://kpv.kazusa.or.jp/kappa-view/	Pathway tool for visualizing omics data
Reactome (A)	http://www.arabidopsisreactome.org/	Pathway tool for visualizing omics data
VANTED (A)	http://vanted.ipk-gatersleben.de/	Pathway tool for visualizing omics data
Osprey (C)	http://biodata.mshri.on.ca/osprey/servlet/Index	Networks for omics data
CSB.DB (A)	http://csbdb.mpimp-golm.mpg.de/	Networks for omics data
Cytoscape (A)	http://www.cytoscape.org/	Networks for omics data
Pathway Express (A)	http://vortex.cs.wayne.edu/	Networks for omics data
PathSys (A)	http://biologicalnetworks.net/PathSys/index.php	Networks for omics data
ONDEX (A)	http://ondex.sourceforge.net/	Networks for omics data
MultiGO (A)	http://ekhidna.biocenter.helsinki.fi/poxo/multigo	Stress transcriptome networks for omics data
Genevestigator (A)	https://www.genevestigator.ethz.ch/gv/index.jsp	Biomarker identification reference expression data
PAGEMAN (A)	http://mapman.mpimp-golm.mpg.de/pageman/	Overrepresentation funcat identification across temporal stages

A: free for academic use; C: commercial product.

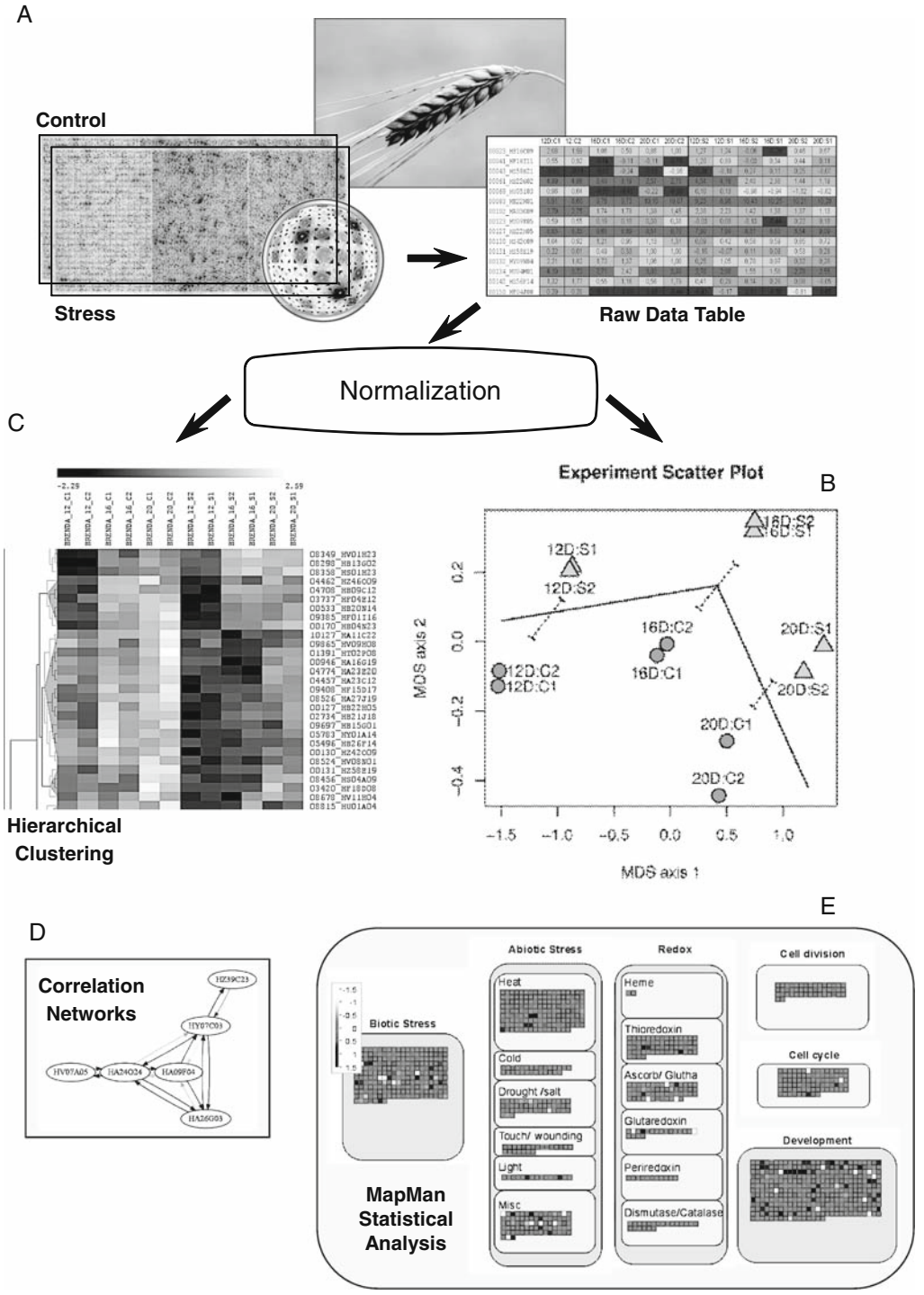

Fig. 5.1. Conceptual data analysis pipeline in transcriptome studies. Raw data acquisition is obtained from extracted plant mRNA probes of control and stress plants, exemplified by cDNA membrane technology (**a**). After data normalization, visual experiment validation may be obtained by principal component analysis (PCA) or by multidimensional scaling (MDS) (**b**), and global patterns of gene expression are extracted by hierarchical clustering (**c**). Correlation analysis of genes highlights common networks of regulations (**d**), and statistical identification of significantly enriched subsets of genetically altered functional categories sheds light on general regulatory processes taking place in stress-treated plants (**e**).

images (46). Tools like ArrayVision® allow a semi-automatic grid alignment after providing an initial grid positioning for resolving rotational components. Once a grid is successfully brought in good accordance with the underlying spots, intensity information is gathered separately for each spot and the signal values are mapped onto the list of spotted ESTs for which the locations are fixed by design. Double spotted ESTs provide an internal control of the quality of the extracted intensities. Spare spots help to estimate local hybridization background signals which should be subtracted from the nearby EST spots. After all, intensities of probed ESTs together with their corresponding background are written to file, one per experiment. Each image of an array provides a record of several thousand gene expression values, and the data matrix of all hybridized arrays is the target of subsequent analysis. Therein the matrix rows correspond to gene expressions and the columns to the experiments. A development-specific quantile normalization method is used for data processing which involves only those stress and control experiments from both repetitions belonging to the same time point. If all three time points were mixed by a single overall normalization, the dynamic range of the transformed expression data would have been substantially reduced to temporally averaged values, and this would complicate later ratio-based differential comparisons. After a log2 transformation, the median of the whole data table is subtracted from each value for centering purposes.

For illustration, a pair wise *t*-test between stress and control at a significance level of 0.01 leads to a reduction to 716 potentially interesting genes. **Figure. 5.1B** shows an MDS scatter plot of the experiments, projecting down from these 716 significant genes to two dimensions in the plane. The plot reveals several data properties. The repetitions C1/C2 (C: control, experiment repetitions 1 and 2), S1/S2 (S: stress, experiment repetitions 1 and 2) indicate a good reproducibility of the experiments, including slightly increased variability at the time point of 20 days (20 D). A systematic separation of time (along the solid line) and of conditions (dashed lines) can be stated. This plot supports the hypothesis of consistently differentially expressed genes within the set of 716 genes.

A detailed view on the individual genes can be obtained by tools like the multiexperiment viewer (MeV). After the built-in hierarchical clustering, using complete link and optimum leaf ordering, the gene representation in **Fig. 5.1C** is obtained. Rows are organized according to similar gene expression patterns related to the subtree structure on the left, and clear differences between control plants and stress plants become obvious. Corresponding genes can be looked up on the right. The list of differentially expressed genes between control plants and drought-treated plants is re-organized by similarity-based

hierarchical clustering adding optimum leaf ordering as post-processing step. The six columns on the left represent three time points of control plants, including repeats, and the six columns on the right represent corresponding stress plants. Dark to light shades indicate low to high gene expression levels, respectively. This list of differentially expressed genes depicting major gene expression patterns is further processed by MapMan to infer the altered metabolic and regulatory networks. As an example we highlight here the altered transcriptome of functional bins connected to abiotic and biotic stress response and from development-related bins covering storage protein transcripts and desiccation-related LEA gene sets (**Fig. 5.1E**). Furthermore, we compared macroarray gene expression data with Affymetrix gene expression data from 20 DAF. Nearly 73% of sequences present on 12 K macroarray had overlapping sequences on the 22 K Affymetrix array. When we compared transcriptome of control versus drought stress seed samples we found that more than 94% of the identified differentially expressed gene sets were identical between the two array formats. In the remaining cases the Affymetrix data showed improved sensitivity for the above laid technical arguments.

5. Genome-Wide Expression Profiling to Study Abiotic Stress Response in Model Species – *Arabidopsis thaliana*

Using 7,000 full-length clone inserts (47) (multistress interactions of abiotic stress treatments were studied to find overlapping responses as well as to identify genes of potential interest to salt, drought, and cold responses). Multistress interactions of abiotic stress treatments were also studied by Kreps et al. (48) using an oligonucleotide array containing 8,100 genes. The availability of AtGenExpress for *Arabidopsis* genome-wide gene expression data obtained by the Affymetrix platform and covering comprehensive plant responses to drought, salinity, cold, oxidative stress from different tissues, organs, and developmental stages in a defined genetic background offers the unique opportunity to identify regulatory networks operative under abiotic stress stimuli (49). Lately, altered transcriptional responses to abiotic stress stimuli in defined cell layers of *Arabidopsis* roots have been studied and cell-type-specific transcription profiles were generated using a fluorescence-activated cell-sorting technique (50). Genes specifically induced by salt in longitudinal and radial zones were enriched in known drought-responsive (DRE) and abscisic acid-responsive elements (ABRE). In another *Arabidopsis* study genes up-regulated in response to saline, drought and cold stress conditions were also enriched with DRE-related and

ABRE core motifs (47, 51). The available *Arabidopsis* expression data is deposited in several online repositories such as GEO (15), NASCArrays (52), PLEXdb (53), ArrayExpress (54). With the availability of large-scale gene expression data sets covering a variety of stress responses of various plant systems, a number of clustering algorithms and bioinformatics tools such as Genevestigator (44), *Arabidopsis* Co-expression Data Mining Tools (55) and Plant Gene Expression Database (56) have been developed for the identification of stress regulons (*see* **Tables 5.1** and **5.2**). Using these publicly available Affymetrix expression data more systematic studies have been initiated to identify the characteristic transcriptome responses to abiotic stress stimuli (57), and co-expression gene networks have been derived using a graphical Gaussian model (58). By combining the analysis of stress-dependent expression profiles and tissue-/cell-specific expressions nearly 197 genes belong to GO ontology responses to wounding, osmotic stress, ABA stimulus, salt stress, ethylene stimulus, JA stimulus, salicylic acid stimulus, MAPK signaling, calcium, reactive oxygen species, phospholipids, apoptosis, and protein degradation are found to be universally induced in common tissue-/cell-specific stress responses of *Arabidopsis* (57). Interestingly among the down-regulated gene sets responding to osmotic and salinity stresses in roots the MYCATERD1 motif (CATGTG) and the SORLRP3AT motif (TGTATATAT) were identified. Lately, a more comprehensive study has been launched to define GO terms overrepresentation for regulons identified using a Markov chain graph clustering method from 963 microarray chips covering a wide variety of environmental stimuli and developmental and genetic perturbations (59). With these systematic efforts "stress regulons," i.e., sets of genes regulated in a similar fashion in response to abiotic stress stimuli, have been identified. Along with these defined stress regulons transcription factors induced or repressed by a range of abiotic stresses were found. However, mere expression patterns do not allow verifying the roles of these co-expressed transcription factors acting in certain networks (regulons) in stress tolerance. In order to obtain a comprehensive picture of complex regulatory networks, Weston et al. (60) used a combination of weighted gene co-expression networks along with the genomic signature concept to define an abiotic stress transcriptome with common and specific pathways associated to the underlying phenotypic response. As a result an ankyrin, calcium, and calmodulin signaling hub has been identified as a common abiotic stress module (60). Recently, using TILING arrays, the effects of osmotic, salt, cold, heat stress, and ABA-induced changes in the *Arabidopsis* transcriptome have been studied and revealed approximately 900 new probe features which have not been seen earlier in the Affymetrix array (61). In particular pseudogenes and retrotransposons are found to be

transcriptionally activated by abiotic stress stimuli, providing evidence for additional regulatory roles of these elements. Such integrative studies are expected to yield more increasing valuable insights into the regulatory mechanisms of abiotic stress tolerance.

6. Outlook

The systematic analysis of large-scale gene expression data provides a rational way to increase the knowledge of stress perception and stress tolerance by identifying key target genes (62, 4, 57). The identification of transcription factors and their target genes corresponding to abiotic stress responses using expression profiling platforms is the crucial step toward the development of transgenic plants that are capable of coping with harsh environmental conditions. At the same time identifying other levels of gene expression regulation, including the role of micro-RNA and epigenetic-based chromatin remodeling and modification in abiotic stress responses, would provide a more holistic view of regulation. Microarrays can be used for multidisciplinary approaches, such as chromatin immunoprecipitation on chip and chromatin remodeling, to identify binding sites of transcription factors and histones, respectively, using TILING arrays (**Fig. 5.2**). Also for conducting genome-wide epigenome studies array platforms

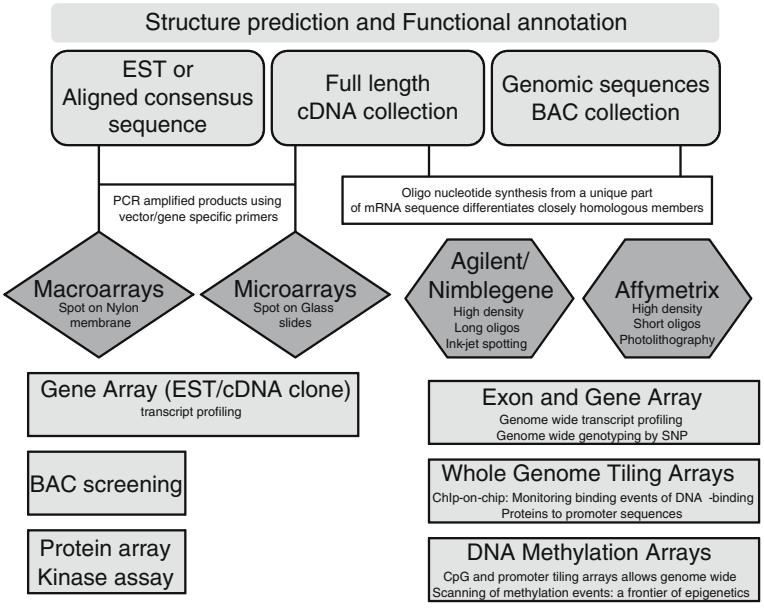

Fig. 5.2. Application of microarray technology for multidisciplinary approaches beyond transcriptome.

can be used to scan for CpG islands (63) and to look for an altered DNA methylation status of interesting loci corresponding to changes of steady-state mRNA levels associated with stress responses. In addition, microarray platforms can be used for the identification of stress-regulated micro-RNAs (64). All in all, a combinatory use of these powerful technologies will eventually yield a global understanding of the complex regulatory networks operative in abiotic stress responses.

Acknowledgments

This work was supported by the Federal Ministry of Education and Research (BMBF; GABI-GRAIN grant FKZ: 0315041A) to NS and Oklahoma Agricultural Experiment Station to RS.

References

1. Liang, P. and Pardee, A.B. (1992) Differential display of eukaryotic messenger RNA by means of the polymerase chain reaction. *Science* **257**, 967–971.
2. Kato, K. (1995) Description of the entire mRNA population by a 3′ end cDNA fragment generated by class IIS restriction enzymes. *Nucleic Acids Res* **23**, 3685–3690.
3. Velculescu, V.E., Zhang, L., Vogelstein, B., and Kinzler, K.W. (1995) Serial analysis of gene expression. *Science* **270**, 484–487.
4. Sreenivasulu, N., Sopory, S.K., and Kishor, P.B.K. (2007) Deciphering the regulatory mechanisms of abiotic stress tolerance in plants by genomic approaches. *Gene* **388**, 1–13.
5. Yamaguchi-Shinozaki, K. and Shinozaki, K. (2005) Organization of cis-acting regulatory elements in osmotic- and cold-stress-responsive promoters. *Trends Plant Sci* **10**, 88–94.
6. Bohnert, H.J., Gong, Q., Li, P., and Ma, S. (2006) Unraveling abiotic stress tolerance mechanisms-getting genomics going. *Curr Opin Plant Biol* **9**, 180–188.
7. Hazen, S.P., Wu, Y., and Kreps, J.A. (2003) Gene expression profiling of plant responses to abiotic stress. *Funct Integr Genomics* **3**, 105–111.
8. Berger, D.K., Crampton, B.G., Hein, I., and Vos, W. (2007) Screening of cDNA libraries on glass slide microarrays. *Methods Mol Biol* **382**, 177–203.
9. Sreenivasulu N., Kishor, P.B.K., Varshney, R.K., and Altschmied, L. Mining functional information from cereal genomes - the utility of expressed sequence tags. *Current Sci* **83**, 965–973.
10. Chou, C.C. and Peck, K. (2007) Design and fabrication of spotted long oligonucleotide microarrays for gene expression analysis. *Methods Mol Biol* **381**, 213–225.
11. Lister, R., Gregory, B.D., and Ecker, J.R. (2009) Next is now: new technologies for sequencing of genomes, transcriptomes, and beyond. *Curr Opin Plant Biol* **12**, 107–118.
12. Lescallett, J., Chicurel, M.E., Lipshutz, R., and Dalma-Weiszhausz, D.D. (2004) Monitoring eukaryotic gene expression using oligonucleotide microarrays. *Methods Mol Biol* **258**, 71–94.
13. Fodor, S.P., Read, J.L., Pirrung, M.C., Stryer, L., Lu, A.T., and Solas, D. (1991) Light-directed, spatially addressable parallel chemical synthesis. *Science* **251**,*767–773*.
14. Shi, L., Reid, L.H., Jones, W.D., Shippy, R., Warrington, J.A., Baker, S.C., et al. (2006) The MicroArray Quality Control (MAQC) project shows inter- and intraplatform reproducibility of gene expression measurements. *Nat Biotechnol* **24**, 1151–1161.
15. Barrett, T. and Edgar, R. (2006) Gene expression omnibus: microarray data storage, submission, retrieval, and analysis. *Methods Enzymol* **411**, 352–369.

16. Durinck, S. (2008) Pre-processing of microarray data and analysis of differential expression. *Methods Mol Biol* **452**, 89–110.
17. Bolstad, B., Irizarry, R., Astrand, M., and Speed, T. (2003) A comparison of normalization methods for high density oligonucleotide array data based on variance and bias. *Bioinformatics* **19**, 185–193.
18. Knudsen, S. (2004) *Guide to Analysis of DNA Microarray Data*, Wiley.
19. Irizarry, R., Bolstad, B., Collin, F., Cope, L., Hobbs, B., and Speed, T. (2003) Summaries of Affymetrix GeneChip probe level data. *Nucl Acids Res* **31**, e15.
20. Durbin, B., Hardin, J., Hawkins, D., and Rocke, D. (2002) A variance-stabilizing transformation for gene-expression microarray data. *Bioinformatics* **18**, S105–110.
21. Lee, J. and Verleysen, M. (2007) *Nonlinear Dimension Reduction*, Springer.
22. Azuaje, F. and Dopazo, J. (2005) *Data Analysis and Visualization in Genomics and Proteomics*, Wiley, Chichester, England.
23. Yeung, K. and Ruzzo, W. (2001) Principal component analysis for clustering gene expression data. *Bioinformatics* **17**, 763–774.
24. Ultsch, A. and Kämpf, D. (2004) Knowledge discovery in DNA microarray data of cancer patients with emergent self organizing maps. *In* M. Verleysen (ed.), *Proceedings of the European Symposium on Artificial Neural Networks (ESANN 2004). D-side Publications*, Evere, Belgium, pp. 501–506.
25. Strickert, M., Sreenivasulu, N., Usadel, B., and Seiffert, U. (2007) Correlation-maximizing surrogate gene space for visual mining of gene expression patterns in developing barley endosperm tissue. *BMC Bioinformatics* **8**(165).
26. de Hoon, M., Imoto, S., Nolan, J., and Miyano, S. (2004) Open source clustering software. *Bioinformatics* **20**, 1453–1454.
27. Eisen, M., Spellman, P., Brown, P., and Botstein, D. (1998) Cluster analysis and display of genome-wide expression patterns. *Proc Natl Acad Sci USA* **95**, 14863–14868.
28. Cover, T. and Hart, P. (1967) Nearest neighbor pattern classification. *IEEE Transactions on Information Theory* **13**, 21–27.
29. McQuitty, L.L. (1966) Similarity analysis by reciprocal pairs for discrete and continuous data. *Educational and Psychological Measurement* **26**, 825–831.
30. Bar-Joseph, Z., Gifford, D., and Jaakkola, T. (2001) Fast optimal leaf ordering for hierarchical clustering. *Bioinformatics* **17**, S22–29.
31. Balasubramaniyan, R., Hüllermeier, E., Weskamp, N., and Kämper, J. (2005) Clustering of gene expression data using a local shape-based similarity measure. *Bioinformatics* **21**, 1069–1077.
32. Cheng, Y. and Church, G. (2000) Biclustering of expression data. *In* P. Bourne et al. (ed.), Proceedings of the 8th International Conference on Intelligent Systems for Molecular Biology (ISMB 2000). AAAI Press, pp. 93–103.
33. Abdi, H. (2007) *Bonferroni and Sidak corrections for multiple comparisons.* In *Encyclopedia of Measurement and Statistics* (Salkind, N.J., ed.). Sage, Thousand Oaks, CA, pp. 1–9.
34. Mack, G.A. and Wolfe, D.A. (1981) K-Sample Rank Tests for Umbrella Alternatives. *Journal of the American Statistical Association* 76, 175–181.
35. Leek, J., Monsen, E., Dabney, A., and Storey, J. (2006) EDGE: extraction and analysis of differential gene expression. *Bioinformatics* **22**, 507–508.
36. Thimm, O., Blasing, O., Gibon, Y., Nagel, A., Meyer, S., Krüger, P., Selbig, J., Müller, L., Rhee, S., and Stitt, M. (2004) MAPMAN: A user-driven tool to display genomics data sets onto diagrams of metabolic pathways and other biological processes. *Plant J.* **37**, 914–939.
37. Fontana, P., Cestaro, A., Velasco, R., Formentin, E., and Toppo, S. (2009) Rapid annotation of anonymous sequences from genome projects using semantic similarities and a weighting scheme in gene ontology. *PLoS ONE* **4**, e4619.
38. Spannagl, M., Noubibou, O., Haase, D., Yang, L., Gundlach, H., Hindemitt, T., Klee, K., Haberer, G., Schoof, H., and Mayer, K. F. X. (2007) MIPS Plants DB—plant database resource for integrative and comparative plant genome research. *Nucleic Acids Res* 35, Database issue D834–D840.
39. Zhang, J.D. and Wiemann, S. (2009) KEGGgraph: a graph approach to KEGG PATHWAY in R and Bioconductor. *Bioinformatics.* **25**(11), 1470–1471.
40. Sreenivasulu, N., Usadel, B., Winter, A., Radchuk, V., Scholz, U., Stein, N. et al. (2008) Barley grain maturation and germination: metabolic pathway and regulatory network commonalities and differences highlighted by new MapMan/PageMan profiling tools. *Plant Physiol* **146**, 1738–1758.
41. Usadel, B., Nagel, A., Steinhauser, D., Gibon, Y., Blasing, O., Redestig, H. et al. (2006) PageMan: An interactive ontology tool to generate, display, and annotate overview graphs for profiling experiments. *BMC Bioinformatics* 7, 1436–1452.

42. Bell, G.W. and Lewitter, F. (2006) Visualizing networks. *Methods Enzymol* **411**, 408–421.
43. Breitkreutz, B.-J., Stark, C., and Tyers, M. (2003) Osprey: a network visualization system. *Genome Biol* **4**, R22.
44. Zimmermann, P., Hirsch-Hoffmann, M., Hennig, L., and Gruissem, W. (2004) GENEVESTIGATOR. *Arabidopsis* microarray database and analysis toolbox. *Plant Physiol* **136**, 2621–2632.
45. Sreenivasulu, N., Altschmied, L., Panitz, R., Hähnel, U., Michalek, W., Weschke, W., and Wobus, U. (2002) Identification of genes specifically expressed in maternal and filial tissues of barley caryopses: a cDNA array analysis. *Mol Genet Genomics* **266**, 758–767.
46. Xie, Y., Cutler, A., Weimer, B., and Parfionovas, A. (2002) Statistical Methods for Spot Detection with Macroarray Data. *In* Proceedings of the 35th Symposium on the Interface of Computing Science and Statistics. The Interface Foundation.
47. Seki, M., Narusaka, M., Ishida, J., Nanjo, T., Fujita, M., Oono, Y., et al. (2002) Monitoring the expression profiles of 7000 *Arabidopsis* genes under drought, cold and high-salinity stresses using a full-length cDNA microarray. *Plant J* **31**, 279–292.
48. Kreps, J.A., Wu, Y.J., Chang, H.S., Zhu, T., Wang, X., and Harper, J.F. (2002) Transcriptome changes for *Arabidopsis* in response to salt, osmotic, and cold stress. *Plant Physiol* **130**, 2129–2141.
49. Kilian, J., Whitehead, D., Horak, J., Wanke, D., Weinl, S., Batistic, O., et al. (2007) The AtGenExpress global stress expression data set: protocols, evaluation and model data analysis of UV-B light, drought and cold stress responses. *Plant J* **50**, 347–363.
50. Dinneny, J.R., Long, T.A., Wang, J.Y., Jung, J.W., Mace, D., Pointer, S., et al. (2008) Cell identity mediates the response of *Arabidopsis* roots to abiotic stress. *Science* **320**, 942–945.
51. Seki, M., Narusaka, M., Abe, H., Kasuga, M., Yamaguchi-Shinozaki, K., Carninci, P., et al. (2001) Monitoring the expression pattern of 1300 *Arabidopsis* genes under drought and cold stresses by using a full-length cDNA microarray. *Plant Cell* **13**, 61–72.
52. Craigon, D.J., James, N., Okyere, J., Higgins, J., Jotham, J., and May, S. (2004) NASCArrays: a repository for microarray data generated by NASC's transcriptomics service. *Nucleic Acids Res* **32**, D575–577.
53. Wise, R.P., Caldo, R.A., Hong, L., Shen, L., Cannon, E., and Dickerson, J.A. (2007) BarleyBase/PLEXdb. *Methods Mol Biol* **406**, 347–363.
54. Parkinson, H., Kapushesky, M., Kolesnikov, N., Rustici, G., Shojatalab, M., Abeygunawardena, N., et al. (2009) ArrayExpress update-from an archive of functional genomics experiments to the atlas of gene expression. *Nucleic Acids Res* **37**, D868–872.
55. Manfield, I.W., Jen, C.H., Pinney, J.W., Michalopoulos, I., Bradford, J.R., Gilmartin, P.M., and Westhead, D.R. (2006) *Arabidopsis* Co-expression Tool (ACT): web server tools for microarray-based gene expression analysis. *Nucleic Acids Res* **34**, W504–509.
56. Horan, K., Jang, C., Bailey-Serres, J., Mittler, R., Shelton, C., Harper, J.F., et al. (2008) Annotating genes of known and unknown function by large-scale coexpression analysis. *Plant Physiol* **147**, 41–57.
57. Ma, S. and Bohnert, H.J. (2007) Integration of *Arabidopsis* thaliana stress-related transcript profiles, promoter structures, and cell-specific expression. *Genome Biol* **8**, R49.
58. Ma, S., Gong, Q., and Bohnert, H.J. (2007) An *Arabidopsis* gene network based on the graphical Gaussian model. *Genome Res* **17**, 1614–1625.
59. Mentzen W.I. and Wurtele E.S. (2008) Regulon organization of *Arabidopsis. BMC Plant Biol* **8**, 99.
60. Weston, D.J., Gunter, L.E., Rogers, A., and Wullschleger, S.D. (2008) Connecting genes, coexpression modules, and molecular signatures to environmental stress phenotypes in plants. *BMC Syst Biol* **2**, 16.
61. Zeller, G., Henz, S.R., Widmer, C.K., Sachsenberg, T., Rätsch, G., Weigel, D., and Laubinger, S. (2009) Stress-induced changes in the *Arabidopsis* thaliana transcriptome analyzed using whole-genome tiling arrays. *Plant J* **58**, 1068–1082.
62. Denby, K. and Gehring, C. (2005) Engineering drought and salinity tolerance in plants: lessons from genome-wide expression profiling in *Arabidopsis. Trends in Biotechnol* **23**, 547–552.
63. Aceituno, F.F., Moseyko, N., Rhee, S.Y., and Gutiérrez, R.A. (2008) The rules of gene expression in plants: Organ identity and gene body methylation are key factors for regulation of gene expression in *Arabidopsis thaliana. BMC Genomics* **9**, 438.
64. Sunkar, R., Chinnusamy, V., Zhu, J., Zhu, J.K. (2007) Small RNAs as big players in plant abiotic stress responses and nutrient deprivation. *Trends Plant Sci* **12**, 301–309.

Chapter 6

Metabolic Engineering of Glyoxalase Pathway for Enhancing Stress Tolerance in Plants

Ananda Mustafiz, Khirod K. Sahoo, Sneh L. Singla-Pareek, and Sudhir K. Sopory

Abstract

Glyoxalase system consists of two enzymes glyoxalase I (Gly I) and glyoxalase II (Gly II). Gly I detoxifies methylglyoxal (MG), a cytotoxic byproduct of glycolysis, to S-lactoylglutathione (SLG) where it uses one molecule of reduced glutathione. Subsequently, SLG is converted to lactate by Gly II and one molecule of reduced glutathione is recycled back into the system. The level of MG, which is produced ubiquitously in all living organisms, is enhanced upon exposure to different abiotic stresses in plants. Overexpression of glyoxalase pathway genes in transgenic plants has been found to keep a check on the MG level under stress conditions, regulate glutathione homeostasis, and the transgenic plants are able to survive and grow under various abiotic stresses.

Key words: Glutathione, glyoxalase I, glyoxalase II, S-lactoylglutathione, methylglyoxal.

1. Introduction

Plants are exposed to several abiotic and biotic stress factors which individually and in totality decide on their overall growth and yield performance. Plants have developed unique strategies for responding to ever-changing environmental conditions, exhaustively monitoring their surroundings, and adjusting their metabolic systems to maintain homeostasis. The severity of stress and the genetic background of the plant are the basic determining factors for the ultimate survival or death of plants. In fact these factors dictate the destiny of any individual. The genome–environment interaction is, therefore, an essential focus for the elucidation of the nature of phenotypic variation leading to the successful response of plants to environmental stress. Plants

R. Sunkar (ed.), *Plant Stress Tolerance*, Methods in Molecular Biology 639,
DOI 10.1007/978-1-60761-702-0_6,

acclimate to abiotic stresses by triggering a cascade or network of events that starts with stress perception and ends with the expression of a battery of target genes. The function of these gene products are classified into those that are involved in stress tolerance, such as chaperones, late embryogenesis abundant (LEA) proteins, enzymes for osmolyte biosynthesis, and detoxification enzymes and those that are involved in signal transduction in abiotic stress response, such as protein kinases, transcription factors, and enzymes of phospholipid metabolism (1). The genes encoding glyoxalase pathway would fall in the former category. Glyoxalase pathway consists of two enzymes, glyoxalase I (Gly I) and glyoxalase II (Gly II). Gly I uses one molecule of reduced glutathione to convert methylglyoxal (MG) to S-D-lactoylglutathione (SLG). Gly II then converts SLG to D-lactate and one molecule of reduced glutathione is recycled back into the system. The D-lactate is then translocated to mitochondria through a D-lactate/H^+ symporter and then metabolized to pyruvate by a flavoprotein D-lactate dehydrogenase (D-LDH) (2) (**Fig. 6.1**).

Both Gly I and Gly II enzymes have been extensively studied in the microbial and animal system (3, 4) but in plants these enzymes have only recently been studied in some detail (5). In our own studies we have shown that by manipulating the

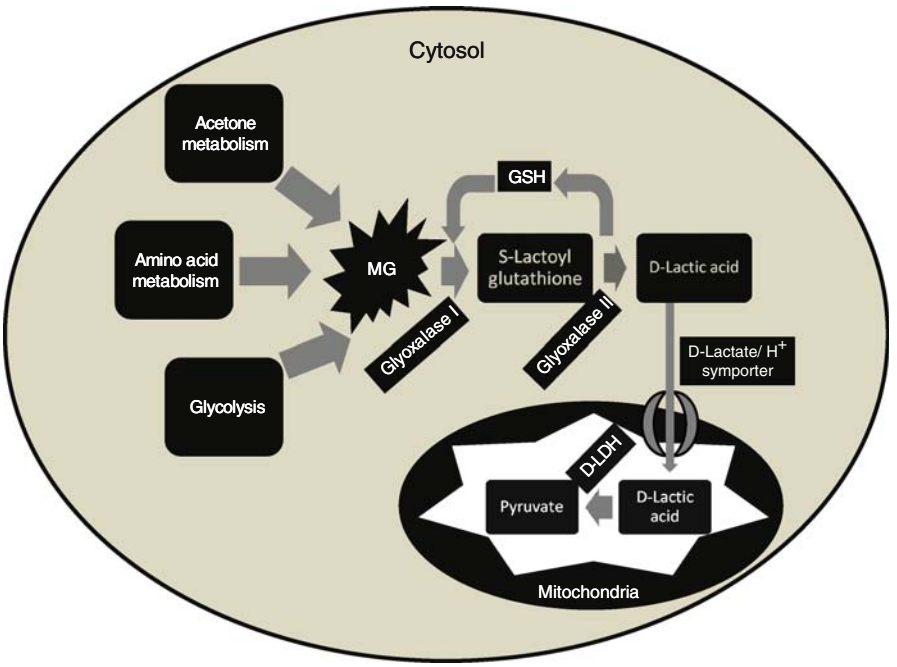

Fig. 6.1. Synthesis of methylglyoxal (MG) and its detoxification by glyoxalase system. Methylglyoxal, a byproduct of glycolysis, amino acid metabolism, and acetone metabolism, is converted to D-lactic acid by glyoxalase I and glyoxalase II. In the process, one molecule of reduced GSH is utilized which is recycled back into the system at the end of the reaction. D-lactate is transported to mitochondria by D-Lactate/H^+ symporter, where it is converted to pyruvate by D-lactate dehydrogenase.

expression of two enzymes of glyoxalase pathway, Gly I and Gly II we could engineer salinity-tolerant and heavy metal-tolerant plants (6, 7).

1.1. Glyoxalase I

The Gly I activity was documented for the first time in Douglas fir needles (8), but later it was detected from various monocots as well as from dicot plant species (9–13). Though the presence of Gly I in all types of cells, tissues, and organs has been shown, in some systems it is preferentially accumulated in phloem and sieve cells (14–16). Recently, Gly I was also found to be conserved in tubers among different potato variants (17).

The Gly I enzyme encoding gene has been cloned from tomato (14), *Brassica juncea* (18), and soybean (19). The Gly I transcript levels were found to increase upto two- to threefold in roots, stems, and leaves of plants in response to NaCl, mannitol, and abscisic acid (14). Similarly *Gly I* expression analysis in *Brassica* showed it to be upregulated in response to salt, water, and heavy metal stresses (18). Upregulation of *Gly I* transcript under abiotic stress conditions has indicated its role in stress tolerance.

1.2. Glyoxalase II

In comparison to Gly I, very little information is available for Gly II of plants. In recent years, *Gly II* has been cloned from few organisms including humans (20), yeast (21), and African *Trypanosomes* (22). In plants, partial purification of Gly II has been reported from *Aloe vera* and spinach (10, 23) and detailed characterization has been done only in *Arabidopsis thaliana* (24, 25), *Brassica* (26), and rice (5). The purified Gly II from *Zea mays* is an acidic protein (p*I* 4.5) of about 26 kDa relative molecular mass (27). The Gly II from *Aloe vera*, purified as three proteins, is also an acidic protein (p*I* 4.7, 4.8, and 5.0) (10). Electrophoretic and isoelectric focusing studies on spinach leaf proteins have revealed the existence of Gly II in multiple forms, viz. cytosolic (p*I* 5.3, 5.8, and 6.2) and mitochondrial (p*I* 4.8), and exist as a monomer showing a relative molecular mass of about 26 kDa (23). In plants, the presence of specific forms of Gly II in mitochondria has been observed as shown earlier in mammalian systems. The structural and functional similarities between Gly II from *A. thaliana* and humans further suggest a common evolutionary origin for this enzyme (25). Recently recombinant Gly II of rice was expressed and purified from *Escherichia coli* and biochemically characterized (5).

The transcript of *Gly II* has been shown to be inducible by various abiotic stresses like heat, cold, salinity, desiccation, and air drying at different time points. Also in response to abscisic acid and salicylic acid, *Gly II* transcript gets upregulated at different time points (5).

1.3. Methylglyoxal

MG is produced during normal metabolism of glucose. This aldehyde is extremely cytotoxic and inhibits growth of cells in all types

of organisms, be it lower microorganisms or higher eukaryotes. All organisms have an inbuilt capacity to detoxify MG though the efficiency may vary from system to system. One of the most important pathways for MG detoxification is mediated by the glyoxalase system. In response to abiotic stresses in plants especially drought, salinity, and cold stress, MG levels have been found to increase by two- to sixfolds (28). Overexpression of glyoxalase system in the transgenic plants might help to detoxify the increased amount of MG.

1.4. GSH

GSH, reduced glutathione, is a tripeptide (γ-Glu-Cys-Gly). It is the most abundant reducing equivalent of a cell and is found in two forms: reduced (GSH) and oxidized (GSSG) state. Synthesis of GSH is catalyzed by two enzymes, which are ATP-dependent, gamma-glutamylcysteine synthetase (γ-ECS, EC; 6.3.2.2) and glutathione synthetase (EC; 6.3.2.3) (29, 30).

Various studies on total foliar glutathione levels in higher plants have now indicated that it is in the range of 0.1–1.5 mM and principally found as GSH (31, 32). GSH is utilized in various cellular processes like in ascorbate–glutathione cycle for quenching of ROS and during this it undergoes oxidation generating GSSG. In MG detoxification also, GSH plays a vital role. For each molecule of MG, one reduced glutathione molecule is utilized which is recycled back into the system upon completion of glyoxalase pathway.

1.5. Generating Transgenic Tobacco and Rice Overexpressing Gly I and Gly II

The *Gly I* gene from *Brassica* was overexpressed in tobacco plants and the transgenic plants showed significant tolerance against high concentrations of salt and MG as compared to the wild-type plants. This study suggested that Gly I may have an important role during stress conditions (18). Furthermore, the overexpression of both *Gly I* and *Gly II* genes together in tobacco transgenic plants provided improved salinity tolerance as compared to either G*ly I* or *Gly II* overexpressing plants (6). Further, ionic measurements in the transgenic lines revealed higher accumulation of Na^+ in old leaves and negligible accumulation in seeds as compared to the WT plants. Comparison of various growth parameters and seed production demonstrated that there is hardly any yield penalty in the double transgenics under non-stress conditions and that these plants suffered only 5% loss in total productivity when grown in 200 mM NaCl. Recently, it has been shown that overexpression of *Brassica* Gly I under Cestrum yellow leaf curling viral promoter provided salinity tolerance to blackgram (*Vigna mungo* L. Hepper) (33). The enhancement of salinity tolerance in transgenic rice overexpressing Gly II has also been demonstrated (7). These findings have established the potential of manipulation of glyoxalase pathway for enhanced salinity tolerance without affecting yield in crop plants.

2. Materials

2.1. Glyoxalase I

2.1.1. Glyoxalase I Assay

1. Extraction buffer: 0.1 M sodium phosphate buffer, pH 7.0; 50% glycerol; 16 mM $MgSO_4$, 0.2 mM PMSF, and 0.2% PVPP.
2. Bradford reagent (available commercially from BioRad or Sigma).
3. Enzyme assay mixture: 0.1 M sodium phosphate buffer, pH 7.5; 3.5 mM MG; 1.7 mM GSH; 16 mM $MgSO_4$. Depending on the type of Gly I, metal ions like Zn^{+2}, Ni^{+2}, Mg^{+2} are added in the assay buffer. Prepare freshly before the assay.
4. UV spectrophotometer.

2.1.2. Cloning and Purification of Recombinant Glyoxalase I

1. Restriction enzymes; *EcoRI* (20 unit/μL), *XhoI* (20 unit/μL) (New England Biolabs).
2. pET28a expression vector (Novagen).
3. Chemically competent BL21 (DE3) pLysE *E. coli* cells.
4. LB broth, Miller (Luria-Bertani) media.
5. 1 M IPTG (isopropyl-1-thio-β-D-galactopyranoside) stock solution.
6. 1 mL Ni-NTA agarose (Qiagen).

2.1.3. Transcript Analysis of Gly I

1. Healthy seeds.
2. Yoshida solution (34).

2.1.3.1. Preparation of Material

2.1.3.2. Isolation of Total RNA

1. Trizol (Invitrogen).
2. Chloroform.
3. Isopropanol.
4. RNAse-free distilled water: Add 0.1% DEPC (Diethyl pyrocarbonate) to distilled water. Stir and autoclave.
5. 80% ethanol prepared in RNAse-free distilled water.

2.1.3.3. Northern Blot Analysis

1. 10X MOPS: Dissolve 41.2 g 3-(N-morpholino)propanesulfonic acid (MOPS), 10.9 g sodium acetate 3-hydrate, 3.7 g EDTA sodium salt in 800 mL nuclease free water; pH adjusted to 7.0 with NaOH; filter sterilized.
2. 20x SSC (88.23 g trisodium citrate, 175.32 g NaCl in 1 L distilled water).
3. Formaldehyde.

4. Agarose.
5. Whatman sheet no.3.
6. Filter paper.
7. 2x RNA loading dye (Fermentas).
8. Hexa label DNA labeling Kit (Fermentas).
9. Hybridization buffer 1 L contains: 20x SSC 250 mL; 50% dextran sulfate 100 mL; 1.0 M sodium phosphate pH 7.2 50 mL; 50x Denhardt's solution 100 mL; 0.5 M EDTA 5 mL; 20% SDS 20 mL.

2.2. Glyoxalase II

2.2.1. Cloning and Purification of Recombinant Glyoxalase II

1. Restriction enzyme; *EcoRI* (20 unit/μL), *XhoI* (20 unit/μL) (New England Biolabs).
2. pET28a expression vector (Novagen).
3. Chemically competent BL21 (DE3) pLysE *E. coli* cells.
4. LB broth, Miller (Luria-Bertani) media.
5. 1 M IPTG (isopropyl-1-thio-β-D-galactopyranoside) stock solution.
6. 1 mL Ni-NTA agarose (Qiagen).

2.2.2. Assay of Glyoxalase II

1. Enzyme assay mixture: 50 mM Tris–HCl (pH 7.2), 300 μM SLG.
2. UV-visible spectrophotometer.

2.2.3. Transcript Analysis of Gly II

Similar to transcript analysis of GLY1 (*see* **Section 2.1.3**)

2.3. Methylglyoxyl

2.3.1. Spectrophotometric Assay of MG

1. Perchloric acid.
2. Charcoal.
3. Saturated solution of potassium carbonate: Dissolve potassium carbonate in water in excess amount so that some amount of the solute remains undissolved in the solution.
4. 1, 2-diaminobenzene.
5. Methylglyoxal (Sigma).

2.3.2. Methylglyoxal Estimation Using HPLC

1. Methylglyoxal (Sigma).
2. 1,2-diaminobenzene.
3. 2,3-dimethylquinoxaline (DMQ).
4. Ammonium formate.
5. Methanol.
6. HPLC column (μBondapak 3.9X 300 mm, RP-18C, Waters, Division of Millipore).

2.4. Glutathione

2.4.1. Estimation of Total, Oxidized, and Reduced Glutathione

1. NADPH.
2. DTNB (5,5′-dithiobis (2-nitrobenzoic acid)), known as Ellman's Reagent.
3. Phosphate buffer, pH 7.4, containing 7 mM EDTA.
4. Glutathione reductase (50 units/mL).
5. 2-vinylpyridine.

2.5. Generating Transgenic Tobacco and Rice Overexpressing Gly I and Gly II

2.5.1. Cloning of Gly I and Gly II in Plant Transformation Vector

1. Typical reagents required for plasmid isolation using alkaline lysis method.
2. Reagents for PCR: Taq polymerase (with proof reading activity), buffer supplied with the Taq polymerase, dNTP, primers specific for the amplicon.
3. Restriction enzymes: XbaI (20 unit/μL) and SacI (20 unit/μL) (New England Biolabs).
4. Agarose.
5. Gel extraction columns (Qiagen).
6. T4 DNA ligase and buffer for ligation.
7. DH5-α chemical competent cells.
8. Kanamycin (50 μg/mL) containing LB agar plate.

2.5.2. Transformation of Agrobacterium with Gly I and Gly II Gene Construct

1. *Agrobacterium* (LBA4404) competent cells.
2. YEM media (yeast extract 0.4 g/L, mannitol 10 g/L, NaCl 0.1 g/L, $MgSO_4 \cdot 7H_2O$ 0.2 g/L, K_2HPO_4 0.5 g/L).
3. LB agar media containing streptomycin (25 mg/L), rifampicin (10 mg/L), kanamycin (50 mg/L).

2.5.3. Agrobacterium tumefaciens-Mediated Transformation of Tobacco Leaf Discs

1. 50% bleach made in autoclaved distilled water.
2. 70% ethanol.
3. MS media solid: MS salts, 3% sucrose, 0.8% agar, pH 5.7.
4. MS media liquid: MS salts, 3% sucrose, pH 5.7.

2.5.3.1. Germination of Wild-Type Tobacco Seeds

2.5.3.2. Preparation of Agrobacterium Culture

1. YEM medium.
2. Antibiotics (streptomycin, 25 mg/mL, rifampicin 10 mg/mL, kanamycin 50 mg/mL stock solution).
3. MS media liquid: MS salts, 3% sucrose, pH 5.7.

2.5.3.3. Infection and Co-cultivation

1. Whatman paper.
2. Co-cultivation media (MS salts, 3% sucrose, 1 mL/L B5 vitamin, 1 mg/L BAP, 0.1 mg/L NAA, 0.8% agar, pH 5.7).

3. Sterile tissue paper.
4. Selection media (MS salts, 3% sucrose, 1 mL/L B5 vitamin, 1 mg/L BAP, 0.1 mg/L NAA, 0.8% agar pH 5.7 with antibiotics for plant selection and 250 mg/L cefotaxime).
5. Antibiotics: kanamycin (50 mg/mL stock), hygromycin (50 mg/mL).
6. Rooting media (MS salts, 3% sucrose, 0.8% agar, pH 5.7, with 25 mg/L hygromycin and 250 mg/L cefotaxime).
7. Red extract and amp kit (Sigma).

2.5.4. Agrobacterium tumefaciens-Mediated Transformation of Rice (cv. PB1) Calli

1. Healthy seeds of PB1 rice.
2. Acetosyringone (100–150 μM).
3. Autoclaved Whatman paper.

2.5.4.1. Sterilization of Seeds and Callus Formation

4. Callus induction media: MS salts, 3% maltose, 0.03% casein hydrolysate, 2.5 mg/L 2,4-D, 0.2 mg/L BAP, 0.3% phytagel.

2.5.4.2. Preparation of Agrobacterium Culture

1. YEP (10 g/L bactopeptone, 10 g/L yeast extract, 5 g/L sodium chloride, pH 7.0).
2. Streptomycin (25 mg/L), rifampicin (10 mg/L), kanamycin (50 mg/L).

2.5.4.3. Infection and Co-cultivation

1. Sterile conical flask.
2. MS salts, 3% maltose, 1.0% glucose, 2.5 mg/L 2,4-D, 0.2 mg/L BAP, 0.3% phytagel, pH 5.2, 100 μM acetosyringone).

2.5.4.4. Selection and Regeneration of Transformed Microcalli

1. Selection medium: MS salts, 3% maltose, 0.03% casein hydrolysate, 2.5 mg/L 2,4-D, 0.2 mg/L BAP, 0.3% phytagel, pH 5.8, 250 mg/L cefotaxime and 50 mg/L hygromycin.
2. Regeneration medium: MS salts, 3.0% maltose, 2.5 mg/L BAP, 1.0 mg/L kinetin, 0.5 mg/L NAA, 0.3% phytagel, pH 5.8, 250 mg/L cefotaxime and 30 mg/L hygromycin.
3. Rooting medium: half strength MS salts, 3.0% sucrose, 0.3% phytagel, 250 mg/L cefotaxime and 40 mg/L hygromycin.
4. Vermiculite.
5. Polythene bag.

2.6. Stress Tolerance Test

1. 80% acetone.
2. NaCl.

2.6.1. Leaf Senescence Test and Chlorophyll Estimation

3. MG.

2.6.2. Seed Germination

1. Healthy seeds.
2. Germination paper or MS media.

2.6.3. Salt Stress in Pot Cultures

1. Solution to mimic natural saline stress (50 mM NaCl, 3.75 mM $MgCl_2$, 15 mM $MgSO_4$, 6.25 mM $CaCl_2$) (EC 15–20 dS m^{-1}).

3. Methods

3.1. Glyoxalase I

*3.1.1. Glyoxalase I Assay (See **Notes 1 and 2**)*

1. Fresh plant tissues are weighed (~200 mg) and powdered with a mortar and pestle in the presence of liquid nitrogen.
2. The powdered tissues are transferred into centrifuge tubes and mixed by vortexing with 1:2 (w/v) of extraction buffer.
3. The extract is centrifuged at 12,000×g for 30 min at 4°C.
4. The supernatant is kept on ice and the protein is quantified using Bradford method.
5. After quantification, the supernatant is immediately used for Gly I activity assay.
6. A standard enzyme assay mixture is prepared with 0.1 M sodium phosphate buffer, pH 7.5; 3.5 mM MG; 1.7 mM GSH; 16 mM $MgSO_4$. Depending on the type of Gly I, metal ions like Zn^{+2}, Ni^{+2}, Mg^{+2} are added in the assay buffer.
7. The mixture is incubated in the dark for at least 7 min, so that the substrate hemithioacetal can be formed.
8. The crude or purified protein is added to the mixture in a final volume of 1 mL and a time scan is performed spectrophotometrically, taking the OD_{240} at every 10 s within a timescale that shows a linear increase in absorbance.
9. The molar absorption coefficient of SLG at 240 nm is 3,370 $m^{-1}cm^{-1}$.
10. The specific activity of the enzyme is expressed in units/mg of protein (35).

*3.1.2. Cloning and Purification of Recombinant Glyoxalase I (See **Notes 3–5**)*

1. The full-length *Gly I* cDNA is amplified and cloned in the vector pET28a (Novagen) at *EcoRI* and *XhoI* site.
2. The construct is then transformed into BL21 (DE3) pLysE *E. coli* cells.
3. The transformed cells are grown in LB medium till the OD_{600} reaches about 0.5 and induced with 0.05 mM IPTG for 4 h.

4. The recombinant protein is then purified using Ni-NTA affinity chromatography as per manufacturer's instructions.

3.1.3. Transcript Analysis of Gly I

3.1.3.1. Preparation of Material

1. About 7–10 days old seedlings growing in hydroponics are given appropriate abiotic stress treatments like heat, cold, salinity, oxidative stress, etc.
2. Salt stress, oxidative stress (with methylviologen or hydrogen peroxide) is given by making the particular solution in the nutrient media where the plants are already growing. For example, for salt stress 200 mM NaCl is added in Yoshida solution.
3. At specific time point following stress treatment, plant tissues are cut, weighed, and packed in aluminum foil; labeled properly; and then frozen in liquid nitrogen.
4. These tissues can be stored up to 6 months in −80°C freezer or in liquid nitrogen.

3.1.3.2. Isolation of Total RNA

Total RNA is isolated by using Trizol (Invitrogen) as per the manufacturer's protocol (*see* **Notes 6–10**).

3.1.3.3. Northern Blot Analysis

1. RNA gel blot is prepared where 20 μg of total RNA is loaded for each sample (*see* **Note 11**)
2. The blot is taken in a hybridization bottle (depending on the size of the blot) in such a way so that the RNA side is inside and in touch with the pre-hybridization buffer.
3. The pre-hybridization buffer is pre-warmed at 65°C and added in the hybridization bottle. The buffer should cover about 30% of the total volume of the bottle.
4. 200 μL (5 mg/mL) of heat denatured salmon sperm DNA is added in the hybridization bottle.
5. Pre-hybridization is done for 4–8 h.
6. The specific probe for Gly I is prepared using Hexa Label DNA Labeling Kit (Fermentas) using manufacturer's protocol.
7. The specific radiolabeled probe is boiled for 10 min, snap cooled in ice, and added.
8. The blot is hybridized at 62°C for 18–24 h.
9. After hybridization the blot is washed in the following way:
   a) Rinsed briefly in 2x SSC, 0.1% (w/v) SDS.
   b) Washed twice, 5 min each, 2x SSC, 0.1% SDS.
   c) Washed twice, 10 min each, 1x SSC, 0.1% SDS.
   d) Washed four times, 5 min each, 2x SSC, 0.1% SDS.

8. The blot is removed from the last stringency wash, drained, and wrapped in saran wrap and exposed to X-ray film or phosphorimager cassette.
9. The blot is kept moist if it is to be reprobed.
10. The blot is scanned in phosphorimager after 4–24 h, depending on the signal obtained or the expression level of the particular gene.
11. All the band intensity values are then normalized with the value of the corresponding 28S or 18S rRNA band and the expression level can be compared with the control.
12. The RNA blot is probed with particular *Gly I*-specific cDNA probe which is labeled with dCTPα^{32}P.
13. The hybridized blot is then exposed to X-ray film or phosphorimager cassette.
14. The obtained signal for each sample is then normalized with 18S or 28S rRNA band of the corresponding gel and the transcript level is quantified.

3.2. Glyoxalase II

*3.2.1. Cloning and Purification of Recombinant Glyoxalase II (See **Notes 3–5**)*

1. The full-length *Gly II* cDNA is cloned in the vector pET28a (Novagen) at NdeI and BamHI sites.
2. The construct is then transformed into BL21 (DE3) pLysE *E. coli* cells.
3. The transformed cells are grown in LB medium till the OD_{600} reaches about 0.5 and induced with 0.5 mM IPTG for 4 h.
4. The recombinant protein is then purified using Ni-NTA affinity chromatography as per manufacturer's instructions (Invitrogen) (5).

*3.2.2. Assay of Glyoxalase II (See **Notes 1** and **2**)*

1. The assay mixture contains 50 mM Tris–HCl (pH 7.2), 300 μM SLG.
2. Crude protein extract or purified protein is added and a total 1 mL volume is made.
3. The rate of hydrolysis of SLG at 240 nm is monitored using a UV-visible spectrophotometer.
4. The molar absorption coefficient of SLG at 240 nm is 3,370 $m^{-1}cm^{-1}$.
5. The specific activity of the enzyme is expressed in units/mg of protein.

*3.2.3. Transcript Analysis of Gly II (See **Notes 6–11**)*

Similar to **Section 3.1.3**, except use *Gly II* cDNA probe labeled with dCTPα^{32}P.

3.3. MG

3.3.1. Spectrophotometric Assay of MG

1. Fresh plant tissue is weighed (250 mg) and crushed in the mortar pestle in the presence of liquid nitrogen.
2. 2.5 mL 0.5 M perchloric acid is added and mixed well. The mixture is transferred in a microcentrifuge tube and incubated for 15 min on ice.
3. The extract is centrifuged for 10 min at 11,000×*g* at 4°C.
4. The supernatant is transferred to a fresh tube. Charcoal (10 mg/mL) is added to decolorize the supernatant if colored; the solution is mixed well with charcoal and kept at room temperature for 15 min. The mixture is centrifuged for 10 min at 11,000×*g*. The clear supernatant is taken in fresh microcentrifuge tube. An additional spin can be given to remove residual charcoal from the solution.
5. The solution is neutralized using saturated potassium carbonate which should be added gradually (initially 20–30 μL should be added, and then one should add 2 μL of saturated K_2CO_3 at a time) and the pH of the supernatant should be checked using a pH paper time to time. With each addition of K_2CO_3, the solution should be mixed properly and the bubbles of CO_2 gas should be allowed to come out.
6. The extract is kept at room temperature for 15 min and centrifuge at 11,000×*g* for 10 min.
7. The supernatant is taken in fresh microcentrifuge tube and is used for MG estimation.
8. For MG estimation, 250 μL of 7.2 mM 1,2-diaminobenzene, 100 μL of 5 M perchloric acid, and 650 μL of neutralized supernatant is taken in a total volume of 1 mL.
9. The mixture is incubated at room temperature for 30 min and absorbance is taken at 336 nm.
10. A standard curve of different concentrations of MG (10, 25, 50, and 100 μM) is made using pure commercial MG (Sigma) (see **Note 12**).
11. Using the standard curve the amount of MG is estimated and expressed as μmol/g fresh weight (36).

3.3.2. Methylglyoxal Estimation Using HPLC

1. A standard curve is made using pure MG (1–10 μM) (see **Note 12**).
2. For this, a total 2 mL of reaction volume contains 1 mL MG (of desired concentration), 200 μL of 7.2 mM 1,2-

diaminobenzene, 200 μL of 5 M perchloric acid, and 100 μL of 10 μM 2,3-dimethylquinoxaline (DMQ) (as internal standard).

3. The samples are then incubated at room temperature (~25°C) for 30 min. In this reaction, MG is derivatized with 1,2-diaminobenzene to form methylquinoxaline (MQ).
4. The solid phase extraction of the quinoxaline is performed (37).
5. The mobile phase contain 80% (v/v) 25 mM ammonium formate buffer (pH 3.4) and 20% (v/v) methanol.
6. A volume of 100 μL is injected in a HPLC column (μBondapak 3.9X 300 mm, RP-18C, Waters, Division of Millipore). Flux is set at 1 mL/min.
7. The quinoxalines are detected at 320 nm. Under these conditions the retention time for MQ and DMQ is 9.9 and 13.2 min, respectively.
8. Note that with increment of MG, the height of the MQ peak will increase, whereas the height of the internal standard DMQ will remain the same.
9. For estimation of MG in vivo, plant extracts are used in the above protocol instead of pure MG (36).

3.4. Glutathione

3.4.1. Estimation of Total, Oxidized, and Reduced Glutathione

1. For the assay of total GSH equivalent, 1.4 mL of 0.3 mM NADPH is taken in a cuvette.
2. 0.2 mL of 6 mM DTNB is added.
3. 0.1 mL of the sample (suitably diluted) is added to it followed by addition of 0.28 mL of 50 mM phosphate buffer, pH 7.4, containing 7 mM EDTA.
4. Finally 20 μL of glutathione reductase (50 units/mL) is added to the cuvette and the change in absorbance is noted at 2 min interval till 6 min.
5. A reagent blank (without sample) is taken in a similar manner.
6. For GSSG assay, the GSH present in the solution is readily derivatized by adding 2 μL of neat 2-vinylpyridine for 100 μL solution, mixing it vigorously for about 1 min.
7. GSH is fully derivatized after 30 min at 25°C. The assay is performed in a similar manner as that of total GSH equivalent.
8. Total glutathione is calculated using the following formula: Total Glutathione equivalent = GSSG + GSH.

9. Reduced glutathione is taken as the standard, which gives a linear curve in the concentration range of 2.32 μmol (0.2–3.2 nmol/0.1 mL). The results are expressed as nmol/g fresh weight of tissue (38, 39).

3.5. Generating Transgenic Tobacco and Rice Overexpressing Gly I and Gly II

3.5.1. Cloning of Gly I and Gly II in Plant Transformation Vector

For cloning of *Gly I* from *B. juncea* (GenBank accession no.Y13239) in pBI121 binary vector go through the following steps.

1. Plasmid of pBI121 is isolated using alkaline lysis method.
2. The particular *Gly I* gene can be amplified using forward and reverse primer containing XbaI and SacI site, respectively.
3. The vector (pBI121 plasmid) and the insert (*Gly I* amplicon containing appropriate restriction site) are digested with *Xba*I and *Sac*I restriction enzymes.
4. The digested vector and insert is run on 0.8% agarose gel and purified using agarose gel extraction columns (Qiagen) according to the manufacturer's protocol.
5. A ligation reaction is set with 1:5 vector and insert ratio using T4 DNA ligase.
6. The ligation mixture is transformed in DH5-α chemical competent cells using heat shock method and plated on ampicillin containing agar plate.
7. The colonies are checked using colony PCR.
8. The plasmids isolated from the positive colonies are confirmed by restriction digestion.

Following the similar protocol as above, the *Gly II* gene (GenBank accession no. AY054407) is cloned into plant transformation vector pCAMBIA1304 at the *NcoI* site under CaMV 35S promoter. In pCAMBIA1304, the cloned G*ly II* gene would make a fusion with reporter gene gfp:gusA at the transcript level. However, due to a stop codon inserted at the end of *Gly II* gene, there is no fusion protein made. The details of this can be obtained in Singla-Pareek et al. (6).

3.5.2. Agrobacterium tumefaciens-Mediated Transformation of Plants

In this section, to elaborate the methodology of *Agrobacterium tumefaciens*-mediated plant transformation, we have taken the case study of transformation of tobacco (*Nicotiana tabaccum* L.) leaf discs as model system and rice (*Oryza sativa* L. *PB1*) as a crop plant.

3.5.3. Transformation of Agrobacterium with Gly I and Gly II Gene Construct

Agrobacterium strain (LBA4404) is being used for high efficiency transformation with the construct having *Gly I* and *Gly II* genes by freeze and thaw method that results in production of number of positive colonies and the protocol used is as follows:

1. The *Agrobacterium* (LBA4404) competent cells are taken out from −80°C and kept on ice for 10–15 min and 2 μg of plasmid is added into it and allowed to mix properly by incubating on ice for 30 min.
2. Cold shock is given by keeping the microcentrifuge tube in liquid nitrogen for 1 min quickly followed by heat shock at 37°C for 5 min.
3. Transfer the tube to ice and incubate for 5 min. Add 800 μL YEM and grow the culture by incubating the tube at 28°C at 200 rpm in an incubator shaker for 3 h.
4. The culture is spun down by centrifuging at 5,000×*g* 4 min. Discard 800 μL of supernatant and resuspend the bacterial pellet in remaining supernatant and spread on the LB agar media containing streptomycin (25 mg/L), rifampicin (10 mg/L), kanamycin (50 mg/L).
5. Plates are incubated at 28°C for 2 days to allow bacterial colonies to form. The colonies are checked by colony PCR with respective primers (*Vir* gene, *Gly I,* and *Gly II* gene-specific forward and reverse primer) and isolated the plasmid from PCR positive colony and digested with respective restriction enzymes (*XhoI* for *Gly I* and *NcoI* for *Gly II*) to get the desired fall out.
6. Positive colony is inoculated in YEM with appropriate selection and grown overnight at 28°C with shaking at 200 rpm. Glycerol stock is made by adding 500 μL culture and 500 μL 50% glycerol in Eppendorf tube and kept at −80°C for future use.

3.5.4. Agrobacterium tumefaciens-Mediated Transformation of Tobacco Leaf Discs

3.5.4.1. Germination of Wild-Type Tobacco Seeds

1. Treat the seeds with 50% bleach with constant shaking for 8–10 min followed by five washes with sterile distilled water.
2. Thereafter, seeds are treated with 70% ethanol for 30 s followed by five washes with sterile distilled water. Seeds are spread on plates containing (MS salts, 3% sucrose, 0.8% agar, pH 5.7).
3. Plates are incubated in dark at 26–28°C for 5–6 days until sprouting. After germination seedlings are kept in light till the plants reached the cover of the plate.
4. Individual seedlings are transferred in the jam bottle having same media for further growth.
5. Sterile tobacco leaves are cut from 4 week-old healthy tobacco plantlets grown in vitro. Midrib of the leaf is removed and the leaf discs of 1 cm^2 are cut and soaked in MS liquid media in a sterile petridish to avoid dehydration.

3.5.4.2. Preparation of Agrobacterium Culture

1. Primary culture is prepared by inoculating *Agrobacterium* glycerol stock or fresh streaked colony in 5 mL medium with suitable antibiotics (streptomycin 25 mg/L, rifampicin 10 mg/L, kanamycin 50 mg/L) and grew for 24 h at 28°C with shaking at 200 rpm, in dark inside the incubator.
2. Secondary culture is made in 100 mL YEM by adding 2% of the inoculum from the primary culture with same antibiotics for 16–24 h.
3. When the OD_{600} reached 0.6–0.8, the secondary culture is spun down at 5,000×*g* for 10 min at 4°C and the pellet is resuspended in MS liquid medium containing 3% sucrose to bring the OD to 0.4–0.5.

3.5.4.3. Infection and Co-cultivation

1. The *Agrobacterium* (transformed with *Gly I* and *Gly II* in pCAMBIA1304) culture is poured into the plate containing tobacco leaf discs. The *Agrobacterium* culture is allowed to infect the leaf tissue for 15 min with gentle shaking (*see* **Notes 13–16**).
2. After 15 min the bacterial solution is aspirated from the plate and leaf discs are dried on autoclaved Whatman paper.
3. Then the leaf discs are placed upside down on co-cultivation media and incubated for 48 h in dark inside the culture room at 26–28°C.
4. After 48 h, growth of *Agrobacterium* is checked at the edges of the leaf discs, and if bacterial growth appeared, then leaf discs are transferred to the selection medium, in case there is no growth plates are kept for one more day in same condition.
5. When the *Agrobacterium* growth is observed, leaf discs are dried by wiping with sterile tissue paper and transferred 4–5 pieces per plate on selection media (co-cultivation media with antibiotics for plant selection and 250 mg/L cefotaxime) and kept under light in culture room.
6. The single-gene (*Gly I*) transformants are selected on kanamycin (50 mg/L), whereas the double (*Gly II*) transformants were selected on the mixture of kanamycin (50 mg/L) and hygromycin (25 mg/L).
7. In the first selection, the explants which are not transformed started turning yellow and died and explants which get transformed remain green, started to swell, and the green notches appear eventually.
8. The selection media is changed after every 12–14 days up to third selection, callus is developed in the second selection, and some of the plantlets come out in the second selection.

9. In the third selection, fully developed plantlets appear which are shifted to rooting media.
10. The regenerated plantlets are transferred to rooting media and kept for 15 days under light till the fully developed roots appeared.
11. Positively transformed plants are screened by tissue PCR with red extract and amp kit (Sigma chemical company) and positive plants are transferred to vermiculite pot for hardening.

3.5.5. Agrobacterium tumefaciens-Mediated Transformation of Rice (cv. PB1) Calli

Plant transformation vectors and methodologies have been improved to increase the efficiency of plant transformation and to achieve stable expression of transgene (*Gly II*) in plants (*see* **Notes 13–16**). The naturally evolved unique ability of *Agrobacterium tumefaciens* (LBA4404) to precisely transfer defined DNA sequences to plant cells has been very effectively utilized in the design of a range of Ti plasmid-based vectors. *Agrobacterium tumefaciens* strain carrying binary vector pCAMBIA1304 was used for transformation of economically important *indica* rice (cv. PB1). High concentration of acetosyringone (100–150 μM) in the *Agrobacterium* culture and co-cultivation medium proved to be indispensable for successful transformation. Embryogenic scutellar calli are used for transformation studies.

3.5.5.1. Sterilization of Seeds and Callus Formation

1. Healthy seeds of PB1 rice are dehusked manually with care that the embryo should not be damaged.
2. Surface sterilization is carried out inside the laminar air flow hood. Seeds are treated with 70% ethanol for 1–1.5 min and then washed three to four times with autoclaved distilled water.
3. After washing, seeds are treated with 50% bleach for 35–40 min on a rotary shaker.
4. Then seeds are washed three to four times with autoclaved distilled water. Thereafter seeds are spread on autoclaved Whatman paper to soak extra water from the seeds.
5. Fourteen to fifteen seeds are inoculated in a petriplate containing the callus induction media (MS salts, 0.3% maltose, 0.03% casein hydrolysate, 2.5 mg/L 2,4-D, 0.2 mg/L BAP, 0.3% phytagel, pH 5.8) and kept in dark inside the culture room at 26–28°C.
6. The plates are checked after every 3–4 days for the growth and to remove contaminated cultures, if any. Highly embryogenic calli are developed within a period of 25–30 days.
7. After callus formation, the calli are subcultured onto the fresh callus induction medium for 4–5 days for further

growth. During this period globular embryos are developed and calli appeared friable, which are chosen for transformation with *Agrobacterium tumefaciens*.

3.5.5.2. Preparation of Agrobacterium Culture

1. Primary broth culture is prepared in 5 mL of YEP (10 g/L Bactopeptone, 10 g/L yeast extract, 5 g/L sodium chloride, pH 7.0) medium with suitable antibiotics (25 mg/L streptomycin, 10 mg/L rifampicin, 50 mg/L kanamycin) by growing for 24 h at 28°C with 200 rpm, in dark inside the incubator shaker.
2. The secondary culture is made in 100 mL of same YEP medium by adding 1% of the inoculum from the primary culture in the presence of same antibiotics for 8 h with same conditions as for primary culture.
3. When the OD_{600} reached to 0.8–1.0, spin down the culture at 5,000×*g* for 10 min at 4°C. The supernatant is discarded and pellet is resuspended with MS liquid medium (containing 1.5% sucrose) so as to bring the OD_{600} to 0.5.

3.5.5.3. Infection and Co-cultivation

1. Highly embryogenic calli are collected in a sterile conical flask. The transformation is performed by transferring the *Agrobacterium* culture in the flask containing calli for 18–20 min with continuous shaking.
2. The infected calli are transferred on an autoclaved Whatman paper and dried. After drying, calli are inoculated on co-cultivation medium (MS salts, 3% maltose, 1.0% glucose, 2.5 mg/L 2,4-D, 0.2 mg/L BAP, 0.3% phytagel, pH 5.2, 100 μM acetosyringone).
3. Incubate the infected calli in dark at 26–28°C for 2 days.

3.5.5.4. Selection and Regeneration of Transformed Microcalli

1. After enough growth of *Agrobacterium* in the co-cultivation medium is observed (~2 days), the infected calli are washed with autoclaved double distilled water for 8–10 times in a sterile conical flask.
2. Then the calli are washed with 250 mg/L cefotaxime for 15 min and dried with the help of sterile Whatman paper.
3. The dried calli are plated on first selection medium (callus induction medium containing 50 mg/L hygromycin and 250 mg/L cefotaxime) and incubated for 20 days in dark at 26–28°C (40).
4. After first selection for 20 days, black/brown calli are removed and creamish healthy calli are transferred to the fresh medium for second selection.
5. During the second selection, small microcalli started growing on the transformed calli and became white and granular.

6. Only these microcalli are chosen to be transferred to the third selection medium (same as first selection) and allowed to proliferate for another 10–15 days in dark.
7. After the third selection, black/brown microcalli are discarded and white and granular macrocalli are transferred to the regeneration medium (MS salts, 3.0% maltose, 2.5 mg/L BAP, 1.0 mg/L kinetin, 0.5 mg/L NAA, 0.3% phytagel, pH 5.8, 250 mg/L cefotaxime and 30 mg/L hygromycin) and incubated in culture room under light for 10–15 days.
8. During this period the callus started to turn green. The greenish calli are again transferred to fresh regeneration medium and incubated in culture room under light. In this medium the calli will start to regenerate into shoots.
9. Once growing shoots touch the cover of the plate, these are transferred to rooting medium (half strength MS salts, 3.0% sucrose, 0.3% phytagel, 40 mg/L hygromycin and 250 mg/L cefotaxime) and kept for 20 days in light.
10. The rooted plantlets are transferred to pots containing vermiculite and covered with polythene bag for 7 days for hardening inside green house.
11. After 7 days the polythene bags are removed and kept for another 7 days for proper shoot and root development.
12. The regenerated plants are checked by PCR with gene-specific primers and/or hygromycin-resistance gene-specific primers. PCR-positive plants are transferred to soil pot for further growth.
13. Confirmation of transgenic nature of the plants is done by Southern and Western blot analysis.

3.6. Stress Tolerance Test

The leaf disc assay is the most common way to have some primary knowledge regarding abiotic stress tolerance (*see* **Note 17**).

3.6.1. Leaf Senescence Test and Chlorophyll Estimation

1. Leaf discs of equal size are cut with a borer and floated onto the desired solution (200 mM, 400 mM NaCl and 5 mM, 10 mM MG stress) in small plates and kept inside the culture room in light. A water control should always be taken for transgenic as well as for WT plant.
2. Leaf discs are constantly observed for the loss of chlorophyll. When the contrasting response is observed the picture of the leaf discs is taken and leaf discs are harvested for the chlorophyll estimation.
3. Chlorophyll (Chl) is extracted by grinding the leaf discs in mortar pestle with 80% acetone and the extract is transferred into a microcentrifuge tube and volume is made up

to 2 mL with 80% acetone and kept on ice under dark condition.

4. The tissue debris is spun down at 10,000 rpm for 15 min at 4°C.
5. Supernatant is transferred into fresh microcentrifuge tube and kept on ice and the absorbance is taken at 645 and 663 nm for Chl a and b, respectively.
6. Total Chl, Chl a, and Chl b are calculated according to the following formulas (41).

$$\text{Chl a} = (12.7 \times A_{663} - 2.63 \times A_{645}) \times \frac{V}{1000 \times w}$$

$$\text{Chl b} = (22.9 \times A_{645} - 4.68 \times A_{663}) \times \frac{V}{1000 \times w}$$

$$\text{Total Chl} = (20.2 \times A_{645} + 8.02 \times A_{663}) \times \frac{V}{1000 \times w}$$

where

A_{663} = absorbance of chlorophyll extract at 663 nm
A_{645} = absorbance of chlorophyll extract at 645 nm
V = final volume of solution (mL)
w = fresh weight of leaf tissue in grams.

3.6.2. Seed Germination

Salt stress tolerance test of the transgenic seedlings in the medium as well as in hydroponics provide strong evidence for the tolerance conferred by expression of transgene. The seeds are germinated in half MS media containing 3% sucrose with 50 mg/L of hygromycin for selection of transgenic lines. Once germinated, the seedlings of WT and transgenic lines are transferred to MS media containing 200 mM NaCl and continue to grow. After few days, the transgenic seedlings show distinct tolerance as compared to wild types.

3.6.3. Salt Stress in Pot Cultures

1. Salt stress tolerance at maturity (when plants are in soil pot at the stage just before flowering) is the ultimate test to see the effect of transgene. To mimic the natural salinity stress in the field condition, solution of four different salts (50 mM NaCl, 3.75 mM $MgCl_2$, 15 mM $MgSO_4$, 6.25 mM $CaCl_2$) is prepared and mixed to obtain a solution of EC 15–20 dS m^{-1}.
2. Pots of transgenic plants and WT plants are initially irrigated with equal amount of salt solution and 4–5 L of same solution is added to the plastic tray underneath the soil pot at the start of the experiment.

3. The level of salt solution in the plastic tray is maintained at every 48 h till the differential effect is observed. If visual differential response is developed, then the tissues from different parts of the plant are harvested for further analysis.

3.6.4. Flowering and Seed Set Under Stress

The shoot length is recorded before applying the stress and at the completion of stress. Shoot growth of transgenic plants is compared with that of WT plant. At the end of the experiment, shoot fresh weight and dry weight are recorded. Root length, fresh weight, and dry weight of transgenic and WT plants are recorded and compared. Another most important parameter is the total yield under stress condition. The time taken to develop flower and total yield of the transgenic and WT plants is recorded under stress as well as under unstressed conditions. Yield penalty in terms of percent reduction in yield under stress as compared to under unstressed condition is recorded for transgenic and WT plants.

4. Conclusion

Methylglyoxal has been shown to present from prokaryotes to higher eukaryotes. A lot of work has been done on glyoxalase pathway enzymes and the degradation of methylglyoxal in different biological system. In our laboratory, it has been shown that in plants the methylglyoxal level correlates with the stress level in plants; and in response to different abiotic stresses the level of methyglyoxal was found to increase. We have shown that overexpressing glyoxalase pathway enzymes can help plants to tolerate abiotic stresses. It is suggested that genetic manipulation of glyoxalase pathway can be a reliable and efficient strategy to develop abiotic stress-tolerant plants.

5. Notes

1. All the steps for protein purification of Gly I and Gly II should be performed in cold condition (4°C).
2. The enzyme assay should be done using fresh protein sample and absorbance recorded immediately.
3. For cloning of the *Gly I* and *Gly II* genes, a Taq polymerase with proof reading activity should be used to avoid error during the PCR reaction.

4. After successful cloning, the vector construct should be sequenced and checked carefully for any sequence variation.
5. The glycerol stocks of all the constructs should be maintained at −80°C with proper labeling.
6. For RNA isolation, tips and microcentrifuge tubes should be treated with DEPC and autoclaved. The mortar and pestles are treated with chloroform and autoclaved.
7. The area used for RNA isolation should be clean and generally isolated from other lab area.
8. The water used for dissolving RNA and making MOPS buffer should be DEPC treated.
9. The OD_{260}/OD_{280} ratio of the RNA should be more than 2 in TE (10 mM Tris pH 7.5 and 1 mM EDTA).
10. The integrity of the RNA should be checked by running a denaturing agarose gel. The intensity of the 28S rRNA band should be twice than the intensity of the 18S ribosomal RNA band.
11. During the northern gel blotting, avoid trapping of any air bubbles beneath the gel. If there is any bubble it should be carefully removed by rolling a glass rod on top of the gel.
12. Methylglyoxal should be maintained in dark bottle and handled carefully as it is highly toxic.
13. The plant tissue culture should be done in separate laminar hood dedicated to only tissue culture work.
14. Before starting the tissue culture work, the hood should be cleaned using spirit and sterilized by UV light for 30 min.
15. Forceps and scalpels used for tissue culture should be autoclaved and flamed to red hot and cooled before using for transfer of callus/plantlets to another media.
16. All the water and media used in tissue culture should be opened only inside the laminar hood.
17. During the stress-tolerant test, leaf discs should be taken from different leaves from plants of same size and same growth stage and randomly incubated in different salt, MG, or other solutions to apply stress.

Acknowledgment

This work is supported by internal grants of ICGEB, New Delhi, and Department of Biotechnology, Government of India.

References

1. Seki, M., Umezawa, T., Urano, K., and Shinozaki, K. (2007) Regulatory metabolic networks in drought stress responses. *Curr Opin Plant Biol* **10**, 296–302.
2. Atlante, A., de Bari, L., Valenti, D., Pizzuto, R., Paventi, G., and Passarella, S. (2005) Transport and metabolism of D-lactate in Jerusalem artichoke mitochondria. *Biochim Biophys Acta* **1708,** 13–22.
3. Rhee, H., Murata, K., and Kimura, A. (1987) Molecular cloning of the *Pseudomonas putida* glyoxalase I gene in *Escherichia coli*. *Biochem Biophys Res Commun* **147**, 831–838.
4. Thornalley, P.J. (1990) The glyoxalase system: new developments towards functional characterization of a metabolic pathway fundamental to biological life. *Biochem J* **269**, 1–11.
5. Yadav, S.K., Singla-Pareek, S.L., Kumar, M., Pareek, A., Saxena, M., Sarin, N.B. et al. (2007) Characterization and functional validation of glyoxalase II from rice. *Protein Expr Purif* **51**, 126–132.
6. Singla-Pareek, S.L., Reddy, M.K., and Sopory, S.K. (2003) Genetic engineering of the glyoxalase pathway in tobacco leads to enhanced salinity tolerance. *Proc Nat Acad Sci USA* **100**,14672–14677.
7. Singla-Pareek, S.L., Yadav, S.K., Pareek, A., Reddy, M.K., and Sopory, S.K. (2008) Enhancing salt tolerance in a crop plant by overexpression of glyoxalase II. *Trans Res* **17**, 171–180.
8. Smits, M.M. and Johnson, M.A. (1981) Methylglyoxal: enzyme distributions relative to its presence in Douglas-fir needles and absence in Douglas-fir needle callus. *Arch Biochem Biophy* **208**, 431–439.
9. Chakravarty, T.N. and Sopory, S.K. (1990) Light stimulated cell proliferation and glyoxalase I activity in callus cultures of *Amaranthus paniculatus*. In *Progress in Plant Cellular and Molecular Biology*. (Nijkamp, H.J.J., Van-derplas, L.H.W., and Asrtrijk, V.J., eds.), Kluwer Academic, Dordrecht, the Netherland, pp. 379–384.
10. Norton, S.J., Talesa, V., Yuan, W.J., and Principato, G.B. (1990) Glyoxalase I and glyoxalase II from *Aloe vera*: purification, characterization and comparison with animal glyoxalases. *Biochem Int* **22**, 411–418.
11. Seraj, Z.I., Sarker, A.B., and Islam, A.S. (1992) Plant regeneration in a jute species (*C. capsularis*) and its possible relationship with glyoxalase-I. *Plant Cell Rep* **12**, 29–33.
12. Deswal, R., Chakaravarty, T.N., and Sopory, S.K. (1993) The glyoxalase system in higher plants: regulation in growth and differentiation. *Biochem Soc Trans* **21**, 527–530.
13. Paulus, C., Köllner, B., and Jacobsen, H.J. (1993) Physiological and biochemical characterization of glyoxalase I, a general marker for cell proliferation, from a soybean cell suspension. *Planta* **189**, 561–566.
14. Espartero, J., Sanchez-Aguayo, I. and Pardo, J.M. (1995) Molecular characterization of glyoxalase I from a higher plant: upregulation by stress. *Plant Mol. Biol.* **29**, 1223-1233.
15. Deswal, R. and Sopory, S.K. (1998) Biochemical and immunochemical characterization of *Brassica juncea* glyoxalase I. *Phytochemistry* **49**, 2245–2253.
16. Walz, C., Giavalisco, P., Schad, M., Juenger, M., Klose, J., and Kehr, J. (2004) Proteomics of curcurbit phloem exudate reveals a network of defence proteins. *Phytochemistry* **65**, 1795–1804.
17. Bauw, G., Nielsen, H.V., Emmersen, J., Nielsen, K.L., Jørgensen, M., and Welinder, K.G. (2006) Patatins, Kunitz protease inhibitors and other major proteins in tuber of potato cv. Kuras. *FEBS J* **273**, 3569–3584.
18. Veena, Reddy, V.S., and Sopory, S.K. (1999) Glyoxalase I from *Brassica juncea*: molecular cloning, regulation and its over-expression confer tolerance in transgenic tobacco under stress. *Plant J* **17**, 385–395 .
19. Skipsey, M., Andrews, C.J., Townson, J.K., Jepson, I., and Edwards, R. (2000) Cloning and characterization of glyoxalase I from soybean. *Arch Biochem Biophys* **374**, 261–268.
20. Cordell, P.A., Futers, T.S., Grant, P.J., and Pease, R.J. (2004) The human hydroxyacylglutathione hydrolase (HAGH) gene encodes both cytosolic and mitochondrial forms of glyoxalase II. *J Biol Chem* **279**, 28653–2866.
21. Bito, A., Haider, M., Hadler I., and Breitenbach, M. (1997) Identification and phenotypic analysis of two glyoxalase II encoding genes from *Saccharomyces cerevisiae*, GLO2 and GLO4, and intracellular localization of the corresponding proteins. *J Biol Chem* **272**, 690–694.
22. Irsch, T. and Krauth-Siegel, R.L. (2004) Glyoxalase II of African trypanosomes is trypanothione-dependent. *J Biol Chem* **279**, 22209–22217.
23. Talesa, V., Rosi, G., Contenti, S., Mangiabene, C., Lupattelli, M., Norton, S.J. et al. (1990) Presence of glyoxalase II in mitochondria from spinach leaves: comparison with the enzyme from cytosol. *Biochem. Int.* **22**, 1115-1120.

24. Maiti, M.K., Krishnasamy, S., Owen, H.A., and Makaroff, C.A. (1997) Molecular characterization of glyoxalase II from *Arabidopsis thaliana*. *Plant Mol Biol* **35**, 471–481.
25. Ridderstrom, M. and Mannervik, B. (1997) Molecular cloning and characterization of the thiolesterase glyoxalase II from *Arabidopsis thaliana*. *Biochem J* **322**, 449–454.
26. Saxena, M., Bisht, R., Roy, S.D., Sopory, S.K., and Bhalla-Sarin, N. (2005) Cloning and characterization of a mitochondrial glyoxalase II from *Brassica juncea* that is upregulated by NaCl, Zn, and ABA. *Biochem Biophys Res Commun* **336**, 813–819.
27. Norton, S.J., Principato, G.B., Talesa, V., Lupattelli, M., and Rosi, G. (1989) Glyoxalase II from *Zea mays*: properties and inhibition study of the enzyme purified by use of a new affinity ligand. *Enzyme* **42**,189–196.
28. Yadav, S.K., Singla-Pareek, S.L., Reddy, M.K., and Sopory, S.K. (2005) Transgenic tobacco plants overexpressing glyoxalase enzymes resist an increase in methylglyoxal and maintain higher reduced glutathione levels under salinity stress. *FEBS Lett* **579**, 6265–6271.
29. May, M.J. and Leaver, C.J. (1994) *Arabidopsis thaliana* c-glutamylcysteine synthetase is structurally unrelated to mammalian, yeast, and *Escherichia coli* homologs. *Proc Natl Acad Sci USA* **91**,10059–10063.
30. Ullmann, P., Gondet, L., Potier, S., and Bach, T.J. (1996) Cloning of *Arabidopsis thaliana* glutathione synthetase (GSH2) by functional complementation of a yeast gsh2 mutant. *Eur J Biochem* **236**, 662–669.
31. Noctor, G., Gomez, L., Vanacker, H., and Foyer, C.H. (2002) Interactions between biosynthesis, compartmentation and transport in the control of glutathione homeostasis and signalling. *J Exp Bot* **53**, 1283–1304.
32. Gomez, L.D., Noctor, G., Knight, M.R., and Foyer, C.H. (2004) Regulation of calcium signalling and gene expression by glutathione. *J Exp Bot* **55**, 1851–1859
33. Bhomkar, P., Upadhyay. C.P., Saxena, M., Muthusamy. A., Prakash, N. S., Pooggin, M., et al. (2008) Salt stress alleviation in transgenic *Vigna mungo* L. Hepper (blackgram) by overexpression of the glyoxalase I gene using a novel Cestrum yellow leaf curling virus (CmYLCV) promoter. *Mol Breed* **22**,169–181.
34. Yoshida, S., Forno, D.A., Cock, J.H., and Gomez, K.A. (1972) Laboratory *Manual for Physiological Studies of Rice*. International Rice Research Institute, Manila.
35. Ramaswamy, O., Guha-Mukherjee, S., and Sopory, S.K. (1983) Presence of glyoxalase I in pea. *Biochem Int* **7**, 307–318.
36. Yadav, S.K., Singla-Pareek, S.L., Ray, M., Reddy, M.K., and Sopory, S.K. (2005) Methylglyoxal levels in plants under salinity stress are dependent on glyoxalase I and glutathione. *Biochem Biophys Res Commun* **337**, 61–67.
37. Cordeiro, C. and Freire, A.P. (1996) Methylglyoxal assay in cells as 2-methylquinoxalineusing 1,2-diaminobenzene as a derivatizing reagents. *Anal Biochem* **234,** 221–224.
38. Tietze F. (1969) Enzymatic method for quantitative determination of nanogram amounts of total and oxidized glutathione: applications to mammalian blood and other tissues. *Anal Biochem* **27,** 502–522.
39. Griffith, O.W. (1980) Determination of glutathione and glutathione disulfide using glutathione reductase and 2-vinylpyridine. *Anal Biochem* **106**, 207–212.
40. Garg, A.K., Kim, J.K., Owens, T.G., Ranwala, A.P., Choi, Y.D., Kochian, L.V. et al. (2002) Trehalose accumulation in rice plants confers high tolerance levels to different abiotic stresses. *Proc Natl Acad Sci USA* **99**, 15898–15903.
41. Arnon, D.I. (1949) Copper enzymes in isolated chloroplasts. Polyphenoloxidase in *Beta vulgaris*. *Plant Physiol* **24**, 1–15.

Part II

Genome-Wide Approaches for Identification of Stress-Regulated Genes, Proteins, and Small RNAs

Chapter 7

Genetic Screens to Identify Plant Stress Genes

Csaba Papdi, Jeffrey Leung, Mary Prathiba Joseph, Imma Perez Salamó, and László Szabados

Abstract

A powerful means to learn about gene functions in a developmental or physiological context in an organism is to isolate the corresponding mutants with altered phenotypes. Diverse mutagenic agents, including chemical and biological, have been widely employed, and each comes with its own advantages and inconveniences. For *Arabidopsis thaliana*, whose genome sequence is publicly available, the reliance of reverse genetics to understand the relevant roles of genes particularly those coding for proteins in growth and development is now a common practice. Identifying multiple alleles at each locus is important because they can potentially reveal epistatic relationship in a signaling pathway or components belonging to a common signaling complex by their synergistic or even allele-specific enhancement of the phenotypic severity. In this article, we describe mutagenesis by using ethyl methanesulfonate (EMS) and transfer (T)-DNA-mediated insertion or activation tagging as applied to the most widely used genetic plant model *A. thaliana*. Also, we demonstrate the utility of several genetic screening approaches to dissect adaptive responses to various abiotic stresses.

Key words: Abscisic acid, abiotic stress tolerance, Arabidopsis, bioluminescence, genetic screen, mutagenesis, thermoluminescence.

1. Introduction

Drought, extreme temperature, high salinity, and other abiotic stresses reduce plant growth and provoke defense responses to survive and eventually to adapt to these adverse conditions if they persist. In agriculture, these abiotic stresses represent the principle limitations of productivity amounting to about 50% losses in yield world-wide (1–3). The specific physiological responses elicited by the various stresses on higher plants are relatively well described, but lacking is the molecular understanding of

R. Sunkar (ed.), *Plant Stress Tolerance*, Methods in Molecular Biology 639,
DOI 10.1007/978-1-60761-702-0_7,

the events underlying how plants sense and transmit stress stimuli and how the responses might be integrated at the cell, tissue, organ, and whole plant levels. From transcriptomic studies we know that drought, cold, and salt evoke the expression of an over-lapping sets of genes, suggesting that their signaling transduction pathways share common control points (4). Identification of the major common and distinct regulatory nodes of these pathways can be achieved by mutagenesis and isolation of such mutants by appropriate screens. Genetic dissection of regulatory processes controlling stress responses can provide entry points, leading to more detailed and better understanding of the various adaptive responses (5–7). Here we provide easy-to-follow protocols for mutagenesis (EMS or T-DNA insertion mutagenesis) and genetic screens using stress-responsive promoter-driven reporter genes (for e.g., promoter::luciferase screens) as well as isolation and characterization of mutants defective in stress tolerance or responses.

1.1. EMS Mutagenesis of Arabidopsis

Ethyl methanesulfonate (EMS) is a frequently used chemical mutagen, which predominantly generates point mutations. EMS can be used to generate mutations for both forward and reverse genetic programs in Arabidopsis and other plants (8, 9).

1.2. T-DNA Insertion Mutagenesis

Molecular and physiological characterization and genetic analysis can be efficiently connected when mutations are generated with insertions of DNA elements. For Arabidopsis, the most common insertions are the Ac/DS or En/I type transposable elements (10–12) or the T-DNA of *Agrobacterium tumefaciens* (13–16). Integration of the T-DNA of Agrobacterium into the genome of the host cell does not require sequence homology of the target genomic sequence, therefore distribution of the T-DNA integration sites in the Arabidopsis genome is nearly random (17–19). Number of T-DNA inserts in a transformed plant ranges between 1.2 and 1.8. In gene-rich chromosomal regions, T-DNA integration frequency is higher, while in centromeric regions it is lower (20, 21). More frequent T-DNA integration was found in promoter and 5′ untranslated regions of actively transcribed plant genes than in intergenic regions (20, 22, 23). Several vectors have been developed and used for Agrobacterium-mediated transformation (**Table 7.1**).

To generate a population of insertion mutants, large-scale transformation methods have to be used. In planta Agrobacterium-mediated transformation methods have been developed for Arabidopsis and are suitable to generate large number of transgenic lines without the need of tissue culture regeneration (29–31). Here we describe a simple protocol which is routinely used in our laboratory for large-scale Arabidopsis transformation.

Table 7.1
Several Agrobacterium transformation vectors used for T-DNA insertion mutagenesis

Name	Selection marker	Use	Reference
pPCV6NFHyg	Hygromycin (Hyg^R)	Promoter trap with promoterless nptII marker	(24)
pTgus	Hygromycin (Hyg^R)	Promoter trap with promoterless b-glucuronidase (GUS) marker	(24)
pTluc	Hygromycin (Hyg^R)	Promoter trap with promoterless luciferase (Ffluc)	(25)
pPCVICEn4HPT	Hygromycin (Hyg^R)	Activation tagging (4x35S enhancer)	(26)
pSKI015 pSKI074	Glufosinate	Activation tagging (35S promoter)	(27)
pROK2	Kanamycin (Km^R)	Activation taging (35S promoter)	(21)
pAC161	Sulfadiazine (SUL^R)	Activation tagging (35S promoter)	(22)
pPCV501	Hygromycin (Hyg^R)	Insertion mutagenesis	(28)
pTAc1	Hygromycin (Hyg^R)	Activation tagging (35S promoter)	(28)
pTAc16	Hygromycin (Hyg^R)	Activation tagging (Dex-inducible promoter)	(28)

1.3. Use of Bioluminescence Imaging to Identify Stress Genes

Promoters of stress-induced genes have been fused to firefly luciferase gene in several laboratories to create a reporter gene construct which faithfully reflects the activities of native genes and can be monitored in vivo by bioluminescence imaging. Screening for mutants with activation or disruption of the reporter gene construct can be used to dissect signaling pathways. Zhu and coworkers employed a high-throughput bioluminescence monitoring system (RD29A-LUC reporter gene) to identify mutants implicated in cold, drought, or salt tolerance as well as in ABA signal transduction (32). The mutants with constitutive expression of osmotically responsive genes (*cos*), low expression of osmotically responsive genes (*los*), and high expression of osmotically responsive genes (*hos*) have been isolated (5, 32, 33).

The success of the genetic screen will depend on the choice of promoter (a promoter, which is responsive highly and specifically to a particular stress will likely be suitable). Several stress-induced promoter-luciferase reporters have been constructed and used with success for mutant screens (**Table 7.2**). In order to obtain a suitable reporter line, numerous independent transgenic plants and lines have to be generated with the vector carrying the test gene construct for testing luciferase activity. Homozygous lines with single insert and with high signal/low background ratio should be employed for subsequent mutagenesis. Activities of three ABA and stress-responsive reporter gene constructs are shown in **Fig. 7.1**.

Table 7.2
Examples for luciferase gene constructs used to isolate stress signaling mutants

Reporter gene	Mutant/gene	Regulation	Reference
RD29A-LUC	cos, los, hos (constitutive-, low- or high expression of osmotically responsive genes)	Response to salt, drought, cold, ABA signal	(33, 34, 35, 36)
CBF3-LUC	*ice1* (inducer of CBF expression 1)	Response to cold stress	(37)
KIN2-LUC	*ade1* (ABA deregulated expression)	ABA signal	(38)
PR1-LUC	*adr1* (activated disease resistance 1)	Response to pathogens	(39)
ADH1-LUC	*ADH1* activation, RAP2.12	Response to osmotic stress, anoxia, ABA signal	(40)

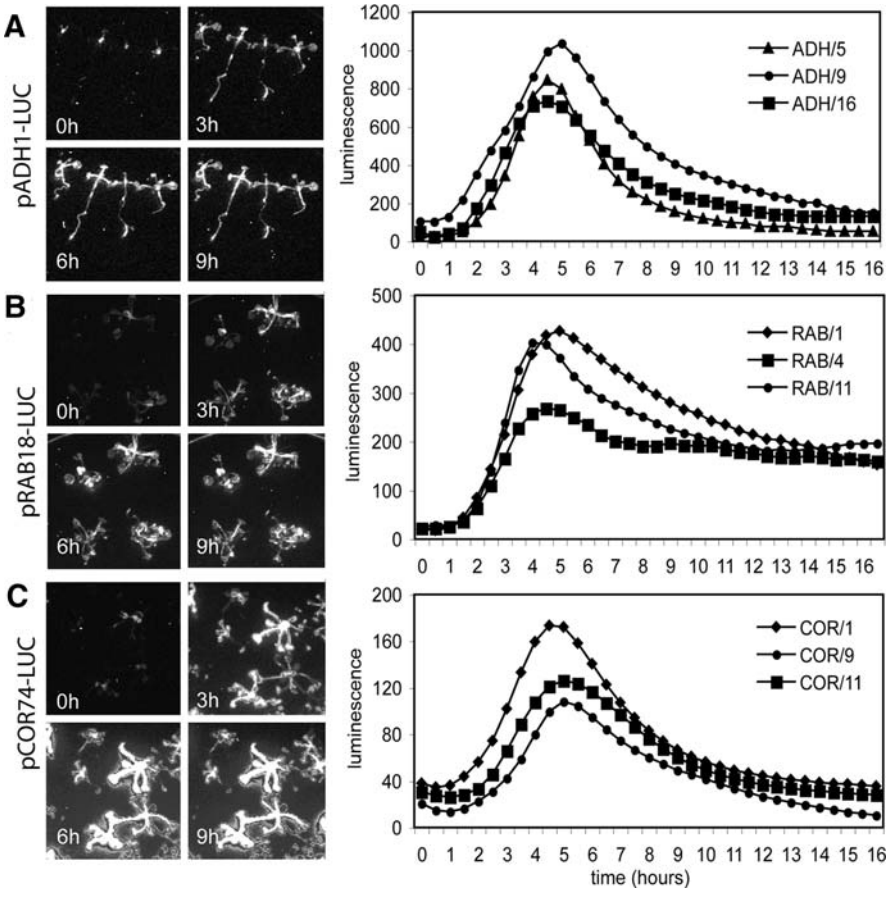

Fig. 7.1. Activation of three ABA-induced luciferase reporter genes in transgenic Arabidopsis seedlings: pADH1-LUC (**a**), pRAB18-LUC (**b**), and pCOR74-LUC (**c**). Left panels show luminescence images of four to five seedlings with each construct, which were sprayed with 50 μM ABA, and incubated for 0, 3, 6, and 9 h. *Right panels* show quantitative analysis of luminescence in three independent lines with each construct, having been sprayed with 50 μM ABA at 0 h.

1.4. Infrared Thermoluminescence Screen

Guard cells tightly regulate the pore aperture by integrating a variety of external and hormonal signals. Light stimulates stomatal opening permitting photosynthetic CO_2 uptake, whereas drought triggers closing of the pore to limit water loss through transpiration. Thus, during the day, the stomatal aperture is continuously being optimized by the plant to accommodate these conflicting needs. Guard cells thus have an impact on two of the most important agricultural traits to the plant, efficacy of photosynthesis and transpiration. Research on guard cells helps the understanding of the underlying regulatory events which have a direct bearing on agricultural productivity, management of arable land, and water resources.

Transpirational fluxes caused by stomatal movements can alter leaf temperatures. The amplitudes of temperature changes caused by stomatal conductance are in fact sufficiently large to be semi-quantifiable by infrared thermography (**Fig. 7.2**) (41). This imaging technology has been successfully exploited to identify mutants of *Arabidopsis* impaired in stomatal response to high CO_2, ozone, or drought, opening the possibility to gain insight into the adaptive mechanisms underlying the integration of external and hormonal signals in the most advanced single cell model in plants (42, 43). We developed the guard cell as a simple model system with the aim of decoding the signaling network in which the membrane transport system operates in tight relationship to components in ABA signaling (44).

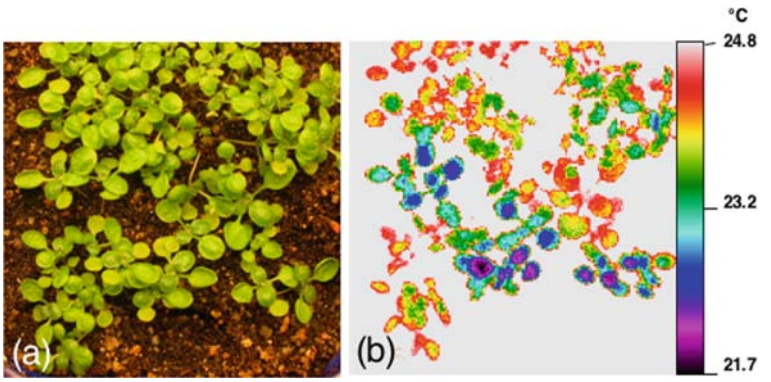

Fig. 7.2. Infrared thermal imaging of Arabidopsis plants. Visible light (a) and infrared image (b) of young Arabidopsis plants with differences in their leaf surface temperature. In (b), the dark grey color indicates colder leaf temperature (higher rate of transpiration of a mutant), while the lighter grey indicates the higher leaf temperature of the wild type plants.

There are many variables that can theoretically alter the leaf temperature. It depends obviously on stomatal conductance to water vapor but other contributing factors could be absorbed net radiation, air humidity, CO_2 levels, light quality, air temperature, stomatal circadian, and boundary layer conductance (41). Thus, it is possible that cryptic variations in the experimental conditions

could bias the identity of different subclasses of mutants. Cooling in leaves derives predominantly from convection or from transpiration influenced by stomatal density (45, 46). This also suggests that mutations affecting the cuticle structure will probably not be recovered. It is important to note that in vitro cultures alter stomatal development (as well as ABA sensitivity), thus we recommend soil-grown plantlets to be used as experimental material. Using this approach, we successfully identified mutants defective in either ABA biosynthesis or sensitivity.

2. Materials

2.1. EMS Mutagenesis of Arabidopsis

1. 100 mM phosphate buffer (pH 7.5). Prepare 100 mM phosphate buffer by mixing 70 mL of 1 M K_2HPO_4 and 20 mL 1 M KH_2PO_4 and adjust the pH to 7.5 by gradually adding 1 M KH_2PO_4 and continuous testing the pH of the solution. Dilute the 1 M phosphate buffer 10 times to obtain the required 100 mM phosphate buffer.
2. Ethyl methanesulfonate (EMS) liquid (SIGMA, M0880). Prepare 0.4% solution in 100 mM phosphate buffer (*see* **Note 1**).

2.2. T-DNA Insertion Mutagenesis

1. Arabidopsis seeds. Use either wild-type ecotypes (Col-0, LER, etc.) or the mutant of your interest.
2. Agrobacterium strain with the T-DNA vector. Our preferred strain for Arabidopsis transformation is GV3101::pMP90 (RifR, GmR). Numerous transformation vectors are available for insertion mutagenesis and some of them are listed in **Table 7.1**.
3. Germination medium: half-strength Murashige and Skoog medium (pH 5.7) (47) containing 0.5% sucrose and 0.7% agar. To prepare selection (plants with T-DNA insertions) plates, supplement germination medium with 500 mg/L Claforan and selective antibiotics, depending on the marker genes (50 mg/L kanamycin, 20 mg/L hygromycin, 5 mg/L sulfadiazine, 15 mg/L phosphinotricin).
4. YEP medium: 10 g yeast extract, 10 g Bacto Peptone, 5 g NaCl, adjust pH to 7.0, and bring final volume to 1 L with H_2O. Sterilize for 30 min using liquid cycle in an autoclave.
5. Antibiotics: for GV3101::pMP90 strain use 100 mg/L rifampicin, 25 mg/L gentamycin.
6. Infiltration medium containing 0.5% sucrose, and 0.01% Silwet L77 (Lehle Seeds, Round Rock, TX, USA).

7. Culture room or illuminated growth chamber with temperature 22–24°C and 16/8 h of light/dark cycle.
8. Greenhouse space for plants in 1,000 pots with 12 cm diameter.

2.2.1. Screening for Salt Hypersensitivity and Tolerance

1. Germination medium: Murashige and Skoog medium containing 0.5% sucrose, 0.7% agar, pH 5.7, in petri plates (9 cm diameter).
2. Low salt selection medium: Murashige and Skoog medium containing 3% sucrose, 50 mM NaCl, and 1.2% agar, pH 5.7, dispensed into square petri plates.
3. High salt selection medium: Murashige and Skoog medium containing 3% sucrose, 150 mM NaCl, and 1.2% agar, pH 5.7, dispensed into square petri plates.
4. Mutagenized Arabidopsis seeds derived either from EMS treatment or insertion mutagenesis.
5. Illuminated growth chamber with temperature 22–24°C and 16/8 h of light/dark cycle.

2.2.2. Screening for ABA Insensitivity

1. Germination medium: Murashige and Skoog medium containing 0.5% sucrose, 0.7% agar, pH 5.7.
2. Selection medium: Murashige and Skoog medium containing 0.5% sucrose, 2.5–10 μM ABA, and 0.7% agar, pH 5.7.
3. Mutagenized Arabidopsis seeds derived either from EMS treatment or insertion mutagenesis.
4. Illuminated growth chamber with temperature 22–24°C, with 16/8 h light/dark cycle.

2.3. Use of Bioluminescence Imaging to Identify Stress Genes

1. Plant material: Mutagenized Arabidopsis seeds derived from homozygous transgenics from a promoter::luciferase constructs. We routinely use in vitro germinated 5- to 10-day-old seedlings or 2- to 3-week-old plantlets.
2. Germination medium: Half-strength MS medium, containing 0.5% sucrose, 0.8% agar, pH 5.7.
3. D-luciferin solution (luciferin: Biosynth AG, Staad, Switzerland): 2 mM final concentration, containing 0.01% Triton X-100, diluted from 100 mM luciferin stock, which is dissolved in sterile water.

1. Low light camera system: The low light imaging system can be built using a cooled CCD camera connected to the controller computer with appropriate imaging software. Cameras with suitable characteristics are available from various manufacturers. The camera must have high sensitivity to detect low light intensities, should be cooled to reduce noise-signal ratio, and should have sufficient pixel resolution

to allow the generation of images containing a 15 cm diameter petri plate. The camera is placed on a dark box which can efficiently prevent light infiltration (often supplied by the manufacturer). To exclude light completely, it is advisable to place the whole setup inside a dark room. Low light cameras are available from several manufacturers:

(i) Visitron Systems GmbH, Puchheim, Germany (http://www.visitron.de/) have developed the VisiLuxx Imager, the low light imaging system for plant application, which is optimized for detecting luciferase activity (http://www.visitron.de/Products/Dark_Box_Imagers/VisiLuxx/visiluxx.html).

(ii) Princeton Instruments (USA) (http://www.princetoninstruments.com/) have developed several imaging cameras for scientific purposes, including charge-coupled devices (CCD) for low light imaging.

(iii) Hamamatsu Photonics (http://www.hamamatsu.com/) have several cameras which are suitable for low light imaging and have different technical characteristics (http://sales.hamamatsu.com/en/products/system-division/cameras).

2. Imaging software: Several computer software have been developed to acquire, process, and analyze bioluminescence images. Camera manufacturers usually deliver their instruments with basic imaging softwares. WinView software from Princeton Instruments, MetaMorph, and the cost-efficient MetaVue products from Molecular Devices are suitable for image analysis.

2.4. Infrared Thermoluminescence Screen

2.4.1. Plant Growth

1. Commercially available gardening soil (compost, peat moss, and pulverized wood fibers).
2. Sand of about 2–3 mm in diameter.
3. Vermiculite.
4. Disposable plastic gardening pots. Disposable square pots of 9–10 cm are recommended because of their lower price.
5. Mineral solution for irrigation.
6. Plant growth chambers.

2.4.2. Image Visualization, Collection, and Analysis

1. Thermacam PM250 (Inframetrics, FLIR Systems, North Billerica, MA, USA).
2. Video monitor.
3. Memory card (SiliconDrive® PC card 32 MB, Silicon Systems).
4. A support to suspend the camera over the canopy of plants.

3. Methods

3.1. EMS Mutagenesis of Arabidopsis

1. Mix 3 g Arabidopsis seeds in 40 mL 100 mM phosphate buffer and incubate them at 4°C, overnight.
2. Centrifuge seeds and replace phosphate buffer with 0.4% EMS solution. Incubate the mixture at room temperature for 8 h with occasional swirling.
3. Wash the seeds at least 10 times with water, and store them at 4°C in the dark for 3 days.
4. Transfer M1 seeds to the surface of wet soil in pots or flats and incubate them at 22°C with 16/8 h of light/dark cycle to allow the plants to flower and set seeds.
5. Harvest M2 seeds and pool them from 500–1,000 plants.

3.2. T-DNA Insertion Mutagenesis

1. Grow 5–10 wild-type Arabidopsis plants in 12 cm diameter pots in greenhouse or growth chamber using short-day illumination (8/16 h of light/dark cycle). Transfer plants with 6–8 cm rosettes to long-day illumination (16/8 h of light/dark cycle). Alternatively plants can be germinated and grown on long-day cycles. In this case grow 10–20 plants in a 12 cm diameter pot. For a large-scale experiment use 1,000 pots of Arabidopsis.
2. When bolting begins, remove the first few emerging inflorescences. Higher number of secondary inflorescences is formed in a few days.
3. Inoculate 1 L YEP medium in 3 L Erlenmeyer flask with single fresh colony of Agrobacterium and let it grow overnight, with continuous shaking (250 rpm, 28°C) until it reaches OD_{600}nm = 1.0.
4. Spin down Agrobacteria (3,000×*g*/15 min) and resuspend in infiltration medium. Adjust concentration to OD_{600}nm=1.5.
5. Submerge Arabidopsis inflorescence into the Agrobacterium solution and wait for 5 min. To prevent soil falling into the medium, cover soil with aluminum foil. Remove plants and cover them with Saran^{TM} wrap to maintain high levels of humidity. Lay the plants horizontally on a tray and cover the tray with another tray in order to maintain the plants in dark. Transfer the tray to a shaded area and keep it for a day. Then, transfer the plants to long-day illumination (16/8 h light/dark cycle).
6. Alternatively, Arabidopsis plants can be vacuum infiltrated with the Agrobacterium solution. Arabidopsis plants,

submerged into the Agrobacterium solution, are placed into vacuum for 2 min, then rapidly released.

7. Repeat infiltration again after 7 days.
8. Let plants flower and set seeds. Harvest seeds and collect them in bulk.
9. For selection of transformed plants from the seed bulk, surface sterilize 5 mL seeds in a 50 mL Falcon tube by soaking them in 70% commercial bleach or in Clorox containing 0.01% Triton X-100. Wash seeds at least five times using sterile distilled water. Keep sterilized seeds at 4°C for 2–3 days for stratification.
10. Spread seeds on the surface of selective germination medium and germinate them in growth chamber with temperature between 22–24°C and in 8/16 h of light/dark cycle. Select resistant plants, transfer them to soil, and grow them in a greenhouse to set seeds. Harvest seeds and store stocks individually.
11. For forward genetic screens bulks of seeds are prepared by mixing equal amount of T2 generation seed stocks.

3.2.1. Screening for Salt Hypersensitivity and Tolerance

Growth of Arabidopsis is inhibited by NaCl, which can be tested by monitoring seedling root elongation, cotyledon, and leaf expansion. These characters can be used as selection criteria for isolating salt hypersensitive or tolerant mutants. Root bending assay was used for the isolation of salt overly sensitive (*sos*) mutants (48). 50 mM NaCl allows root growth of wild-type Arabidopsis but can block root growth of salt hypersensitive mutants such as *sos1*. Screen is performed on vertical plates where monitoring root growth is feasible.

3.2.1.1. Procedure for Isolating Salt Hypersensitive Mutants

1. Surface sterilize Arabidopsis seeds by soaking them in 70% commercial bleach or in Clorox containing 0.01% Triton X-100. Wash seeds at least five times in sterile distilled water.
2. Transfer seeds to Petri plates containing germination medium and incubate at 4°C for 2 days for stratification.
3. Transfer the plates to a growth chamber maintained at 22–24°C with 8/16 h of light/dark cycle and let seeds germinate and develop for four days into seedlings.
4. Transfer plants and arrange them in rows on a low salt medium. Place the plates in vertical position, with the roots pointing upward, and incubate them for 4–5 days.
5. Select the mutants with impaired root growth and transfer them to germination medium to allow them to form several leaves.

6. Transfer selected plants to greenhouse, to flower, and set seeds.
7. Repeat the root bending assay on progenies of selected plants. Confirmed salt sensitive mutants are ready for further analysis.

3.2.1.2. Procedure for Isolating Salt-Tolerant Mutants

Screening for salt tolerance can be done on vertical plates with medium supplemented by inhibitory concentrations of salt (at least 150 mM NaCl). Selection of tolerant plants is based on their root growth, greening, or survival (**Fig. 7.3a**).

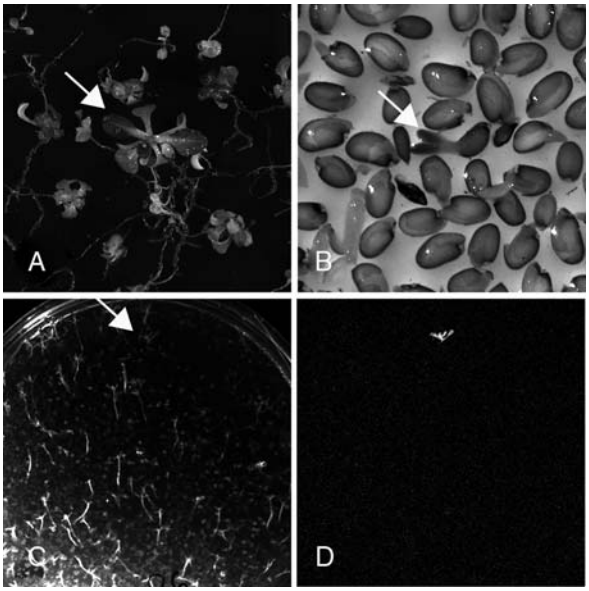

Fig. 7.3. Screening for salt tolerance, ABA insensitivity, and activation of a luciferase reporter gene construct. (**a**) Wild-type Arabidopsis plants were transformed by the COS cDNA library (40). T1 generation seedlings were selected for hygromycin resistance and the resistant seedlings were screened for salt tolerance on medium supplemented by 200 mM NaCl and 4 μM estradiol. *Arrow* show a growing, putative salt-tolerant plantlet. (**b**) To screen for ABA insensitivity, T1 generation seeds were plated on medium containing 2.5 μM ABA and 4 μM estradiol. *Arrow* indicates a germinating seed among the non-germinating seeds. (**c, d**) For activation of the *pADH1-LUC* reporter gene construct, a transgenic line was transformed by the COS library, and T1 generation seedlings were germinated on hygromycin, sprayed with 4 μM estradiol, and luminescence images were recorded with a CCD camera. *Arrow* indicates the position of a seedling (**c**) which shows luminescence (**d**).

1. Surface sterilize Arabidopsis seeds by soaking them in 70% commercial bleach or in Clorox containing 0.01% Triton X-100. Wash seeds at least five times in sterile distilled water.
2. Transfer seeds to germination medium containing petri plates and incubate at 4°C for 2 days for stratification.

3. Transfer the plates to a growth chamber maintained at 22–24°C with 8/16 h of light/dark cycle and let seeds germinate and develop seedlings for 4 days.
4. Transfer seedlings to high salt selection medium and arrange them in rows. Incubate the plates in vertical position for 5–10 days.
5. Select plantlets with superior root and leaf growth when compared to wild-type seedlings. Transfer them to germination medium for further growth.
6. Alternatively, seedlings can be transferred onto a high salt (200 mM NaCl) containing medium and incubated for at least 4 weeks. Surviving seedlings are rescued and transferred to germination medium for further growth.
7. Transfer plants to greenhouse to flower and set seeds.
8. Repeat growth assay on high salt medium to confirm the mutant phenotype.

3.2.2. Procedure for Isolating ABA Insensitive Mutants

Abscisic acid is a growth hormone which affects many aspects of plant growth and development, seed and embryo development, seed dormancy, germination, stomatal closure, tolerance to drought, and other stresses (49, 50). A number of mutants with altered ABA sensitivity have been isolated by selecting for germination in the presence of inhibitory concentrations of ABA, including *abi1*, *abi2*, and *abi3* (51). Recently dominant ABA insensitive Arabidopsis lines were selected in plant populations overexpressing two different cDNA libraries (52, 40) (**Fig. 7.3b**).

1. Surface sterilize Arabidopsis seeds by soaking them in 70% commercial bleach or in Clorox containing 0.01% Triton X-100. Wash seeds at least five times in sterile distilled water.
2. Transfer seeds onto selective medium containing 2-3 μM ABA, and incubate 4°C for 2 days for stratification.
3. Transfer the seeds to growth chamber maintained at 22–24°C with 8/16 h of light/dark cycle and let the seedlings grow for at least 2 weeks. Monitor the seedlings on a daily basis.
4. Select germinating seedlings while most seeds are blocked in their germination capacity.
5. Transfer selected seedlings to germination medium and allow the seedlings to grow and develop a few leaves.
6. Transfer plants to greenhouse to flower and set seeds.
7. Test ABA insensitive germination capacity of T2 generation seeds on media supplemented by 1–10 μM ABA. Calculate the percentage of germinating seedlings every day and compare it to germination of wild-type plants.

3.3. Bioluminescence Imaging with CCD Camera

3.3.1. Screening for Luciferase Activation in a Mutagenized Plant Population

1. Sterilize and germinate M2 generation mutagenized seeds or pooled seed stocks from insertion mutant collections on agar-solidified germination medium. Use approximately 500 seeds on a 150 mm × 15 mm petri plate.
2. Incubate plates in growth chambers at 20–22°C with 16/8 h light/dark cycle. Grow the seedlings for 7 days.
3. In order to detect upregulated reporter gene expression, spray seedlings with 2 mM luciferin solution, and wait 1–2 h before imaging (*see* **Note 2**).
4. Turn on the imaging system, and allow to cool it down until temperature of the chip reaches working temperature (−120°C in Visilux Imager).
5. Place the plate into the sample holder of the camera chamber, take a reference picture in dim light.
6. Alternatively a fluorescence image can be acquired immediately after closing the camera box (10–30 s). This image allows positioning of the seedlings.
7. Wait 5 min to reduce chlorophyll fluorescence.
8. Acquire the luminescence image. Length of the exposition can be 5–30 min, depending on the gene construct and the expected intensity of the luminescence.
9. Select seedlings with enhanced luminescence, transfer them to new plates, and grow them separately until they form abundant roots to transfer them to soil.

3.3.2. Suppression Screen

Besides activation of the luciferase reporter gene, suppression of the luminescence can be screened. The two strategies can be combined by screening the same plant population first for gene activation and subsequently for suppression. For the suppression screen the seedlings are treated by sublethal stress or hormone which activates the reporter gene in all plants. Mutants are identified based on low or missing luminescence.

1. Activate the reporter gene construct in the seedlings either by transferring them to inductive medium (e.g., 150 mM NaCl or 300 mM mannitol for salt or osmotic stress, respectively) or by spraying them with an inducer (e.g., 20 μM ABA).
2. Allow the seedlings to activate the reporter gene for 3–4 h.
3. Perform luminescence imaging, but this time select seedlings with low or no luminescence when compared to the rest of seedlings (wild-type ones).
4. Remove the selected seedlings from the inductive plates, grow the seedlings separately.

5. Transfer plants to greenhouse for selfing and collect M3 generation seed stocks for further analysis.

3.3.3. Screening for Dominant Activation of the Luciferase Reporter Gene

Screening for dominant luciferase activation in T1 generation seedlings using a promoter trap vector, transactivation of reporter gene with activation tagging, or cDNA library transfer (**Fig. 7.3c,d**).

1. Generate large number of transgenic seeds with the promoter trap vector in a Col-0 wild-type background. For reporter gene activation transform the homozygous reporter line with the activation vector or the cDNA library.
2. Germinate seeds of infiltrated plants in the presence of selection marker (e.g., hygromycin).
3. Transfer around 100 hygromycin resistant seedlings to new 15 cm diameter plates. Handling of seedlings may activate reporter genes, therefore incubate plates in standard culture conditions for 2–3 days before testing.
4. Spray seedlings with luciferin and measure luminescence as described above. Select seedlings with detectable luminescence.
5. In order to select for suppressed reporter gene activation, treat seedlings with ABA or stress (cold, heat, salinity, osmotic, etc.).
6. Incubate plates for 3–4 h.
7. Measure luminescence, select seedlings with reduced luciferase activity.
8. Transfer selected seedlings to germination medium to recover, grow separately, and transfer to greenhouse to flower and set seeds.

Screening of T2 generation, pooled seed stocks is similar, with the exception that such seeds do not need to have to be germinated first on hygromycin plates.

3.4. Infrared Thermoluminescence Screen

The screen described below is to identify mutants with reduced ability to close their stomata in response to water stress.

3.4.1. Plant Growth and Water-Deficit Conditions

1. Prepare the mixture of 50% sand and 50% commercial soil in disposable plastic pots. Thoroughly wet the substrate by subirrigation (soaking the pots in water) (*see* **Note 3**).
2. Sow mutagenized seeds onto the sand/soil substrate at a density of 1 –3 seeds/1.5 cm^2. Incubate 2 days at 4°C in darkness to remove any residual dormancy.
3. Transfer the pots containing seeds to the greenhouse to germinate and grow in water-sufficient conditions (*see* **Note 4**).

4. Submit the plantlets to drought stress when the true leaves just begin to emerge. The drought is imposed simply by transferring the plants to a growth chamber with a drier atmosphere, and withholding water for about 3–4 days (*see* **Note 5**).

3.4.2. Camera Set-Up, Thermoluminescence Screen

1. Suspend the camera approximately 40 cm above the canopy and observe leaf temperature on the color monitor relayed to the camera (*see* **Note 6**). One might need to adjust the temperature sensitivity scale of the camera for each observation of a different field of plantlets (*see* **Note 7**).
2. Remove the majority of the plantlets that register relatively higher foliar temperatures by cutting at the stems with a small pair of surgical scissors (*see* **Note 8**).
3. Save images of potential mutants as 8-bit TIFF files on the memory card of the camera.
4. After the observation, re-water the plants by subirrigation.
5. After 2–4 days, re-observe the temperatures of the remaining plants.
6. Select plants with reproducible difference in thermoluminescence.

4. Notes

1. EMS is highly hazardous solution. Use gloves, lab coat, and chemical hood for handling. Decontaminate everything that has come in contact with EMS by washing it with 1 M NaOH. Discard waste in biohazardous containers.
2. Prepare 100 mM luciferin stock solution in sterile distilled water. Prepare 100 μL aliquots and store them in −80°C freezer, in dark. Luciferin is heat and light sensitive.
3. In our hands, sand (2–3 mm diameter) was satisfactory, but plant growth tends to be variable. Water used for subirrigation should be enriched with mineral nutrients during the initial growth phase under water-replete conditions. On the other hand, commercial compost has a high water retention capacity, dries too slowly and furthermore, has a tendency to collapse to a highly compact state during drying. In our case, a mixture composed of 50% sand and 50% compost (v/v) is judged as a good compromise. To accelerate homogeneous evaporation from the soil, in practice, the bottom half of the pots are filled with pure sand or vermiculite, while the top half is filled with the sand/compost mix.

4. Our greenhouse conditions are 200 $\mu E\ m^{-2}\ s^{-1}$, 24°C, vary between 55 and 80% RH throughout the day, 16 h light. The plants are watered every 2 days from below by subirrigation in water and/or mineral solution.
5. By series of empirical tests, the optimal conditions in the growth chamber are 24–25°C, relative humidity between 40 and 50%, and ventilation to an air speed of 0.4 m/s from the sides of the growth chamber and from below the pots. This ventilation guarantees uniformity of the different environmental parameters and drying of the pots. The growth cabinet is equipped with fluorescent rather than incandescent lights (150 $\mu E/m^2/s$) to minimize the short-wave infrared background that could bias the estimation of the leaf temperature when using the 3.4–5 μm infrared band for thermal imaging. These environmental conditions are designed to maximize the difference in temperature between leaves with closed stomata and leaves with open stomata, while maintaining a homogeneous temperature response for a given transpiration rate in all the plants observed over the image field. We do not measure the absolute leaf temperatures for each plant independently in the mutagenized population, which quickly becomes unmanageable in a "saturating" genetic screen. Young plantlets at this described stage do not seem to consume much water and often 4 days or longer after water deprivation will be needed to impose sufficient water deficit to elicit a stomatal response.
6. As the technology of infrared vision rapidly evolves, interested individual should consult with manufacturers concerning the model of cameras suitable for your particular needs. In our case, thermal images are captured by the Thermacam PM250 infrared camera equipped with a 16° lens. The camera used a cooled 256 × 256 PtSi array detector responsive to the short-wave infrared (3.4–5μm band). Specified temperature resolution is below 0.1°C at room temperature based on calibration by using a black metallic object. Straight temperature images generated by the camera software on the basis of manufacturer calibration were used. Leaf emissivity is set to 1 since an accurate absolute measurement of leaf temperature is not required. The camera is connected to a color monitor to facilitate visualization of individual plants (**Fig. 7.2**), although sometimes black and white images give better resolution of the different temperatures.
7. The idea is to identify individual mutants amidst a population of wild-type plants by visualizing the differences in leaf temperature between several plants in a given image rather than by measuring the absolute leaf temperature of each individual plant independently. Even for wild-type plants,

they often show some variations in leaf temperature especially near the edges of the pots, hence continually adjusting the temperature sensitivity scale may be necessary.

8. We avoid pulling out the unwanted wild-type plantlets because it tends to up-root neighboring plants as well. Locally up-turned soil is also detected by the infrared camera as "cooler" patches, which renders observations much more difficult. For these reasons, the wild-type plants are rather removed by cutting with a small pair of scissors.

Acknowledgment

This work was supported by EU Grant no. FP6-020232-2, TéT grant no. FR-34/2008 and OTKA Grant no. K-68226.

References

1. Boyer, J.S. (1982) Plant Productivity and Environment. *Science* **218**, 443–48.
2. Flowers, T.J. (2004). Improving crop salt tolerance. *J Exp Bot* **55** 307–319.
3. Vinocur, B and Altman, A. (2005). Recent advances in engineering plant tolerance to abiotic stress: achievements and limitations. *Curr Opin Biotechnol* **16**,123–32.
4. Nakashima, K., Ito, Y., and Yamaguchi-Shinozaki, K. (2009) Transcriptional regulatory networks in response to abiotic stresses in Arabidopsis and grasses. *Plant Physiol* **149**, 88–95.
5. Zhu, J.K. (2002). Salt and drought stress signal transduction in plants. *Annu Rev Plant Biol* **53**, 247–273.
6. Alonso, J.M. and Ecker, J.R. (2006) Moving forward in reverse: genetic technologies to enable genome-wide phenomic screens in Arabidopsis. *Nat Rev Genet* **7**, 524–536.
7. Chinnusamy, V., Zhu, J., and Zhu, J.K. (2006) Salt stress signaling and mechanisms of plant salt tolerance. *Genet Eng (NY)* **27**, 141–177.
8. Rédei, G.P. and Koncz, C. (1992) Classical mutagenesis. In *Methods in Arabidopsis Research* (C. Koncz, Chua, N.-H., Schell, J., eds.), World Scientific: Singapore, pp. 16–82.
9. Kim, Y., Schumaker, K.S., and Zhu, J.K. (2006) EMS mutagenesis of Arabidopsis. *Methods Mol Biol* **323**, 101–103.
10. Bancroft, I., Bhatt, A. M., Sjodin, C., Scofield, S., Jones, J. D., and Dean, C. (1992) Development of an efficient two-element transposon tagging system in Arabidopsis thaliana. *Mol Gen Genet* **233**, 449–461.
11. Martienssen, R.A. (1998) Functional genomics: probing plant gene function and expression with transposons. *Proc Natl Acad Sci U S A* **95**, 2021–2026.
12. Wisman, E., Hartmann, U., Sagasser, M., Baumann, E., Palme, K., Hahlbrock, K., Saedler, H., and Weisshaar, B. (1998) Knock-out mutants from an En-1 mutagenized Arabidopsis thaliana population generate phenylpropanoid biosynthesis phenotypes. *Proc Natl Acad Sci U S A* **95**, 12432–12437.
13. Koncz, C., Martini, N., Mayerhofer, R., Koncz-Kalman, Z., Korber, H., Redei, G. P., and Schell, J. (1989) High-frequency T-DNA-mediated gene tagging in plants. *Proc Natl Acad Sci U S A* **86**, 8467–8471.
14. Koncz, C., Nemeth, K., Redei, G.P., and Schell, J. (1992) T-DNA insertional mutagenesis in Arabidopsis. *Plant Mol Biol* **20**, 963–76.
15. Feldmann, K.A., Marks, M.D., Christianson, M.L., and Quatrano, R.S. (1989) A dwarf mutant of Arabidopsis generated by T-DNA insertion mutagenesis. *Science* **243**, 1351–1354.
16. Azpiroz-Leehan, R. and Feldmann K.A. (1997) T-DNA insertion mutagenesis in Arabidopsis: going back and forth. *Trends Genet* **13**, 152–156.

17. Tinland, B. and Hohn, B. (1995) Recombination between prokaryotic and eukaryotic DNA: integration of *Agrobacterium tumefaciens* T-DNA into the plant genome. *Genet Eng (NY)* **17**, 209–229.
18. Hansen, G. and Chilton, M.D. (1999) Lessons in gene transfer to plants by a gifted microbe. *Curr Top Microbiol Immunol* **240**, 21–57.
19. Zupan, J., Muth, T.R., Draper, O., and Zambryski, P. (2000) The transfer of DNA from Agrobacterium tumefaciens into plants: a feast of fundamental insights. *Plant J* **23**, 11–28.
20. Szabados, L., Kovacs, I., Oberschall, A., Abraham, E., Kerekes, I., Zsigmond, L., Nagy, R., Alvarado, M., Krasovskaja, I., Gal, M., Berente, A., Redei, G. P., and Haim, A. B., Koncz, C. (2002). Distribution of 1000 sequenced T-DNA tags in the Arabidopsis genome. *Plant J* **32**, 233–242.
21. Alonso, J.M., Stepanova, A.N., Leisse, T.J., Kim, C.J., Chen, H., et al., (2003) Genome-wide insertional mutagenesis of Arabidopsis thaliana. *Science* **301**, 653–637.
22. Rosso, M.G., Li, Y., Strizhov, N., Reiss, B., Dekker, K., and Weisshaar, B. (2003) An Arabidopsis thaliana T-DNA mutagenized population (GABI-Kat) for flanking sequence tag-based reverse genetics. *Plant Mol Biol* **53**, 247–259.
23. Li, Y., Rosso, M.G., Ulker, B., and Weisshaar, B. (2006) Analysis of T-DNA insertion site distribution patterns in Arabidopsis thaliana reveals special features of genes without insertions. *Genomics* **87**, 645–652.
24. Koncz, C., Martini, N., Szabados, L., Hrouda, M., Bachmair, A., and Schell, J. (1994) Specialized vectors for gene tagging and expression studies. In *Plant Molecular Biology Manual* (S.B. Gelvin, ed.), Kluwer Academic Publishers, pp. 1–22.
25. Alvarado, M.C., Zsigmond, L.M., Kovacs, I., Cséplő, A., Koncz, C., and Szabados, L.M. (2004) Gene trapping with firefly luciferase in Arabidopsis. Tagging of stress-responsive genes. *Plant Physiol* **134**, 18–27.
26. Walden, R., Fritze, K., Hayashi, H., Miklashevichs, E., Harling, H., and Schell, J. (1994) Activation tagging: a means of isolating genes implicated as playing a role in plant growth and development. *Plant Mol Biol* **26**, 1521–1528.
27. Weigel, D., Ahn, J.H., Blazquez, M.A., Borevitz, J. O., and Christensen, S. K. (2000) Activation tagging in Arabidopsis. *Plant Physiol* **122**, 1003–1013.
28. Szabados, L. and Koncz, C. (2003) Identification of T-DNA insertions in Arabidopsis genes. In *Genomics of Plants and Fungi,* (H.J.B. R.A.Prade, ed.), Marcel Dekker Inc, New York, pp. 255–277.
29. Bechtold, N., Ellis, J., and Pelletier, G. (1993) In planta Agrobacterium mediated gene transfer by infiltration of adult Arabidopsis thaliana plants. *C.R. Acad. Sci. Paris.* **316**, 1194–1199.
30. Bechtold, N. and Pelletier, G. (1998) In planta Agrobacterium-mediated transformation of adult Arabidopsis thaliana plants by vacuum infiltration. *Methods Mol Biol* **82**, 259–266.
31. Bent, A.F. (2000) Arabidopsis in planta transformation. Uses, mechanisms, and prospects for transformation of other species. *Plant Physiol* **124**, 1540–1547.
32. Chinnusamy, V., Stevenson, B, Lee, B.H., and Zhu, J.K. (2002) Screening for gene regulation mutants by bioluminescence imaging. *Sci STKE* **140**, 1–10.
33. Ishitani, M., Xiong, L., Stevenson, B., and Zhu, J.K. (1997) Genetic analysis of osmotic and cold stress signal transduction in Arabidopsis: interactions and convergence of abscisic acid-dependent and abscisic acid-independent pathways. *Plant Cell* **9**, 1935–1949.
34. Ishitani, M., Xiong, L., Lee, H., Stevenson, B., and Zhu, J.K. (1998) HOS1, a genetic locus involved in cold-responsive gene expression in Arabidopsis. *Plant Cell* **10**, 1151–1161.
35. Lee, H., Xiong, L., Gong, Z., Ishitani, M., Stevenson, B., and Zhu, J.K. (2001) The Arabidopsis HOS1 gene negatively regulates cold signal transduction and encodes a RING finger protein that displays cold-regulated nucleo-cytoplasmic partitioning. *Genes Dev* **15**, 912–924.
36. Zhu, J., Verslues, P.E., Zheng, X., Lee, B.H.m Zhan, X., Manabe, Y., Sokolchik, I., Zhu, Y., Dong, C. H., Zhu, J.K., Hasegawa, P. M., and Bressan, R. (2005) A HOS10 encodes an R2R3-type MYB transcription factor essential for cold acclimation in plants. *Proc Natl Acad Sci U S A* **102**, 9966–9971.
37. Chinnusamy, V., Ohta, M., Kanrar, S., Lee, B.H., Hong, X., Agarwal, M., and Zhu, J.K. (2003) ICE1: a regulator of cold-induced transcriptome and freezing tolerance in Arabidopsis. *Genes Dev* **17**, 1043–1054.
38. Foster, R. and Chua, N.H. (1999) An Arabidopsis mutant with deregulated ABA gene expression: implications for negative regulator function. *Plant J* **17**, 363–372.
39. Grant, J.J., Chini, A., Basu, D., and Loake, G. J. (2003) Targeted activation tagging of the Arabidopsis NBS-LRR gene, ADR1,

conveys resistance to virulent pathogens. *Mol Plant Microbe Interact* **16**, 669–680.
40. Papdi, C., Abraham, E., Joseph, M.P., Popescu, C., Koncz, C., and Szabados, L. (2008) Functional identification of Arabidopsis stress regulatory genes using the controlled cDNA overexpression system. *Plant Physiol* **147**, 528–542.
41. Jones, H.G. (1999) Use of thermography for quantitative studies of spatial and temporal variation of stomatal conductance over leaf surfaces. *Plant, Cell, and Environ* **22**, 1043–1055.
42. Mustilli, A.C., Merlot, S., Vavasseur, A., Fenzi, F., and Giraudat, J. (2002) Arabidopsis OST1 protein kinase mediates the regulation of stomatal aperture by abscisic acid and acts upstream of reactive oxygen species production. *Plant Cell* **14**, 3089–3099.
43. Wang, Y., Holroyd, G., Hetherington, A.M., and Ng, C.K., (2004) Seeing 'cool' and 'hot'–infrared thermography as a tool for non-invasive, high-throughput screening of Arabidopsis guard cell signalling mutants. *J Exp Bot* **55**, 1187–1193.
44. Sirichandra, C., Wasilewska, A., Vlad, F., Valon, C., and Leung, J. (2009) The guard cell as a single-cell model towards understanding drought tolerance and abscisic acid action. *J Exp Bot* **60,** 1439–1463
45. Beerling, D.J., Osborne, C.P., and Chaloner, W.G. (2001) Evolution of leaf-form in land plants linked to atmospheric CO2 decline in the Late Palaeozoic era. *Nature* **410**, 352–354.
46. Hedrich, R. and Steinmeyer, R. (2001) Do drought-hardened plants suffer from fever? *Trends Plant Sci* **6**, 506; author reply 507–508.
47. Murashige, T. and Skoog, F. (1962) A revised medium for rapid growth and bio assays with tobacco tissue culture. *Physiol Plant* **15,** 473–497.
48. Wu, S.J., Ding, L., and Zhu, J.K. (1996) SOS1, a genetic locus essential for salt tolerance and potassium acquisition. *Plant Cell* **8**, 617–627.
49. Leung, J. and Giraudat, J. (1998) Abscisic Acid Signal Transduction. *Annu Rev Plant Physiol Plant Mol Biol* **49**, 199–222.
50. Finkelstein, R.R., S.S. Gampala, and C.D. (2002) Rock, abscisic acid signaling in seeds and seedlings. *Plant Cell* **14S,** 15–45.
51. Koornneef, M., Reuling, G., and Karssen, C.M., (1984) The isolation and characterization of abscisic acid-insensitive mutants of Arabidopsis thaliana. *Physiol Plant* **61**, 377–383.
52. Kuhn, J.M., Boisson-Dernier, A., Dizon, M.B., Maktabi, M.H., and Schroeder, J.I. (2006) The protein phosphatase AtPP2CA negatively regulates abscisic acid signal transduction in Arabidopsis, and effects of abh1 on AtPP2CA mRNA. *Plant Physiol* **140**, 127–39.

Chapter 8

Arabidopsis Tiling Array Analysis to Identify the Stress-Responsive Genes

Akihiro Matsui, Junko Ishida, Taeko Morosawa, Masanori Okamoto, Jong-Myong Kim, Yukio Kurihara, Makiko Kawashima, Maho Tanaka, Taiko Kim To, Kentaro Nakaminami, Eli Kaminuma, Takaho A. Endo, Yoshiki Mochizuki, Shuji Kawaguchi, Norio Kobayashi, Kazuo Shinozaki, Tetsuro Toyoda, and Motoaki Seki

Abstract

Plants respond and adapt to drought, cold, and high-salinity stresses. Stress-inducible gene products function in the stress response and tolerance in plants. Using cDNA microarrays and oligonucleotide microarrays, stress-inducible genes have been identified in various plant species so far. Recently, tiling array technology has become a powerful tool for the whole-genome transcriptome analysis. We applied the *Arabidopsis* Affymetrix tiling arrays to study the whole-genome transcriptome under drought, cold, and high-salinity stresses and identified a large number of drought, cold, and high-salinity stress-inducible genes and transcriptional units (TUs).

Key words: *Arabidopsis*, drought stress, tiling array, transcriptome analysis, stress-inducible genes.

1. Introduction

Stress-inducible gene's products function in stress response and tolerance in plants. Many stress-inducible genes encoding regulatory proteins and functional proteins have been identified using cDNA microarrays and oligonucleotide microarrays (1, 2). However, many unidentified stress-inducible genes and transcripts including non-protein-coding RNAs remained uncharacterized in *Arabidopsis* genome as of 2007.

R. Sunkar (ed.), *Plant Stress Tolerance*, Methods in Molecular Biology 639,
DOI 10.1007/978-1-60761-702-0_8,

The whole-genome tiling arrays cover genome sequence of both strands with oligo probes and is a useful tool for the analysis of whole-genome transcriptome, such as (a) mapping of transcripts including putative non-protein-coding RNAs (3–7), (b) identification of alternative splice sites (8), (c) identification of binding sites for the proteins (9–11), (d) comparative genomic hybridization (12, 13), (e) mapping of DNA methylation sites (14–16) and histone modification (17, 18) sites. Recently, we applied the *Arabidopsis* Affymetrix tiling arrays to identify drought, cold, and high-salinity stress-inducible genes and identified many new stress-inducible genes and transcriptional units (TUs) as well as the known stress-inducible genes (19). In this analysis, we used the biotin-labeled cRNAs generated after the synthesis of the first-strand and second-strand cDNAs, in vitro transcription (IVT), and biotin labeling for the hybridization to the arrays in order to reveal which DNA strand is transcribed, as described in the **Section 3**. In this chapter, we describe the protocol for *Arabidopsis* tiling array analysis to identify the drought stress-responsive genes.

2. Materials

2.1. Isolation of Total RNA from Plants

1. Isogen (Nippon Gene).
2. Agilent 2100 Bioanalyzer (Agilent Technologies).

2.2. cDNA Synthesis from Total RNA

1. Diluted Poly-A RNA control (*see* **Note 1**): Add 2 μ l of the "Poly-A Control Stock" (Affymetrix) to 38 μ L of "Poly-A Control Dil Buffer" (Affymetrix). Mix thoroughly and spin down to collect the liquid. Add 2 μL of the first dilution to 98 μL of "Poly-A Control Dil Buffer" to prepare the second dilution. Mix thoroughly and spin down to collect the liquid. Add 2 μL of the second dilution to 8 μL of "Poly-A Control Dil Buffer" to prepare the third dilution. Mix thoroughly and spin down to collect the liquid. Add 2 μL of the third dilution to 8 μg of total RNA sample (*see* **Note 2**).
2. DNase/RNase-free distilled water (Gibco). Store at room temperature.
3. One-Cycle Target Labeling and Control Reagents (Affymetrix. The following reagents and materials are supplied from the manufacturer: 2 mL collection tube, 1.5 mL collection tube, cDNA binding buffer, cDNA elution buffer, cDNA Cleanup Spin Column, 0.1 M DTT, *Escherichia coli* DNA ligase, *E. coli* DNA polymerase I,

0.5 M EDTA, cDNA wash buffer, 10 mM dNTP, RNaseH, SuperScript II, T4 DNA polymerase, 50 μM T7-Oligo(dT) primer, 5X first Strand Reaction Mix, 5X second Strand Reaction Mix, RNase-free water). Store collection tube, cDNA binding buffer, cDNA elution buffer, and cDNA wash buffer at room temperature. Store cDNA Cleanup Spin Column at 4°C. Store the other reagents at −20°C.

2.3. Synthesis of Biotin-Labeled cRNA with In Vitro Transcription (IVT) Reaction

1. Nanodrop ND-1000 Spectrophotometer (Thermo Fisher Scientific).
2. One-Cycle Target Labeling and Control Reagents (The following reagents and materials are supplied from the manufacturer Affymetrix: 10X IVT labeling buffer, IVT labeling NTP mix, IVT labeling enzyme mix, IVT cRNA Cleanup Spin Column, IVT cRNA binding buffer, IVT cRNA wash buffer). Store IVT cRNA Cleanup Spin Column at 4°C. Store IVT cRNA binding buffer and IVT cRNA Wash buffer at room temperature. Store the other reagents at −20°C.
3. Ethanol.

2.4. Fragmentation of the cRNA for Target Preparation

1. 5X Fragmentation buffer (Affymetrix). Store at room temperature.

2.5. Hybridization

1. GeneChip Hybridization Oven 640 (Affymetrix).
2. GeneChip *Arabidopsis* tiling array set (1.0F Array and 1.0R Array, Affymetrix) (*see* **Note 3**). It can be stored for 6 months at 4°C in dark.
3. 250 μL micropipette tips HR-250S (Rainin) (*see* **Note 4**). Use when applying the hybridization buffer to the tiling array.
4. 5 M NaCl (DNase/RNase-free, Ambion).
5. 0.5 M EDTA (Sigma-Aldrich). Store at room temperature.
6. 2X Hybridization buffer: Add 8.3 mL of 12X MES stock buffer, 17.7 mL of 5 M NaCl, 4 mL of 0.5 M EDTA, 0.1 mL of 10% Tween-20 to 19 mL RNase-free water, and fill up to 50 mL. Store at 4°C in dark.
7. GeneChip Eukaryotic Hybridization Control Kit (The following reagents and materials are supplied from the manufacturer Affymetrix: 3 nM Contol Oligo B2, 20X Eukaryotic Hybridization Controls). Store at −20°C.
8. 10 mg/mL Herring Sperm DNA (Promega). Store at −20°C.

9. 50 mg/mL bovine serum albumin (BSA) (Invitrogen). Store at −20°C.
10. Dimethyl sulfoxide (DMSO) (Sigma-Aldrich). Store at room temperature.

2.6. Wash and Stain

1. GeneChip Fluidics Station 450 (Affymetrix).
2. 20X SSPE (3 M NaCl, 0.2 M NaH_2PO_4, 0.02 M EDTA, Cambrex).
3. Wash Buffer A: Add 300 mL of 20X SSPE and 1 mL of 10% Tween-20 (Pierce Chemical) to 650 mL of autoclaved distilled water and fill up to 1,000 mL with autoclaved distilled water. The washing buffer A is then filtered through 0.2 μm filter. It can be stored for 3 months at 4°C in dark.
4. 12X 2-[N-morpholino] ethanesulfonic acid (MES) stock buffer: Add 3.2 g of MES free acid monohydrate (Sigma-Aldrich) and 9.7 g of MES sodium salt (Sigma-Aldrich) to 40 mL of DNase/RNase-free water (Gibco) and fill up to 50 mL with DNase/RNase-free water. 12X MES stock buffer is then filtered through 0.2 μm filter. It can be stored for 3 months at 4°C in dark.
5. Wash buffer B: Add 41.7 mL of 12X MES Stock buffer, 2.6 mL of 5 M NaCl, 0.5 mL of 10% Tween-20 to 400 mL of autoclaved distilled water and fill up to 500 mL with autoclaved distilled water. The wash buffer B is then filtered through a 0.2 μm filter. It can be stored for 3 months at 4°C in dark.
6. 10 mg/mL Goat IgG Stock: Add 50 mg of Goat IgG (Sigma-Aldrich) to 5 mL of 150 mM NaCl solution (prepared from 5 M NaCl solution). If a larger volume of the 10 mg/mL IgG stock is prepared, aliquot and store at −20°C until use. After thawing the solution, store at 4°C. Avoid repeated freezing and thawing.
7. 2X Stain Buffer: Add 41.7 mL of 12X MES Stock buffer, 92.5 mL of 5 M NaCl, 2.5 mL of 10% Tween-20 to 113.3 mL of RNase-free water. The 2X stain Buffer is then filtered through 0.2 μm filter. It can be stored at 4°C in dark.
8. Anti-streptavidin antibody (goat), biotinylated (Vector Laboratories). Store at −20°C.
9. 1 mg/mL streptavidin phycoerythrin (SAPE) solution (Molecular Probes). Store at 4°C.

2.7. Scanning of the Array

1. GeneChip Scanner 3000 7G (Affymetrix).
2. Tough-Spots (USA Scientific).

3. Methods

3.1. Isolation of Total RNA from Drought Stress-Treated and Untreated Arabidopsis Plants

1. Grow *Arabidopsis thaliana* plants (ecotype Columbia) in plastic dishes (20 plants per plastic dish) containing GM agar (0.85%) medium supplemented with 1% sucrose under 16-h-light/8-h-dark cycle (40–80 μmol photons $m^{-2}s^{-1}$, light period: A.M. 5:00 to P.M. 9:00) (*see* **Note 5**) (19).
2. Start the drought stress treatments (*see* **Note 6**) as follows: Remove 30–40 plants per one replicate grown on two dishes from the agar and perform drought stress treatment in two to three plastic dishes for 2 and 10 h at 22°C under dim light (0.9–1.2 μmol photons $m^{-2}s^{-1}$) essentially as reported previously (1).
3. Freeze the drought-treated and untreated control plants in liquid nitrogen and store at −80°C for isolation of total RNA.
4. Prepare the total RNA using Isogen (Nippon Gene) according to the instruction (*see* **Note 7**).

3.2. cDNA Synthesis from Total RNA

1. Add 2 μL of "Third Poly-A Control Dilution" and 2 μL of 50 μM "T7-Oligo(dT) Primer" to 8 μg of total RNA.
2. Adjust to a final volume of 12 μL with RNase-free water (Gibco).
3. Shake the tube gently two to three times and spin down to collect the liquid.
4. Keep the reaction for 10 min at 70°C.
5. Place the samples at 4°C for at least 2 min.
6. Spin down to collect the liquid.
7. Prepare 7 μL of "First-Strand Master Mix" which contains 4 μL of "5 × 1st Strand Reaction Mix", 2 μL of 0.1 M DTT, and 1 μL of 10 mM dNTP for each sample.
8. Transfer 7 μL of "First-Strand Master Mix" to each sample and mix.
9. Incubate for 2 min at 42°C immediately.
10. Add 1 μL of SuperScript II to each sample.
11. Incubate for 1 h at 42°C and then cool the sample for at least 2 min at 4°C.
12. For one sample, prepare the 130 μL of "Second-Strand Master Mix" that contains 91 μL of RNase-free water, 30 μL of 5× 2nd Strand Reaction Mix, 3 μL of 10 mM dNTP, 1 μL of *E. coli* DNA ligase, 4 μL of *E. coli* DNA polymerase I, and 1 μL of RNaseH.

13. Add 130 μL of "Second-Strand Master Mix" to each first-strand cDNA sample (after step 11).
14. Mix the solution gently and spin down to collect the solution.
15. Incubate for 2 h at 16°C.
16. Add 2 μL of T4 DNA polymerase to each sample and incubate for 5 min at 16°C.
17. Add 10 μL of 0.5 M EDTA (*see* **Note 8**).
18. Transfer the double-strand cDNA sample to a new 1.5 mL tube. Add 600 μL of "cDNA binding buffer" to the double-strand cDNA sample. Vortex for 3 s (*see* **Note 9**).
19. Apply 500 μL of the sample onto the cDNA Cleanup Spin Column set in a 2 mL collection tube.
20. Centrifuge for 1 min at 8,000×*g*. Discard the flow-through.
21. Apply the remaining mixture sample (after step 19) onto the cDNA Cleanup Spin Column. Centrifuge for 1 min at 8,000×*g*. Discard the flow-through and collection tube.
22. Set the spin column (after **step 21**) into new 2 mL collection tube. Apply 750 μL of the cDNA wash buffer onto the spin column. Centrifuge for 1 min at 8,000×*g*. Discard flow-through.
23. Open the cap of the spin column and centrifuge for 5 min at 20,000×*g*. Discard the flow-through and collection tube.
24. Transfer spin column into 1.5 mL collection tube and apply 14 μL of cDNA elution buffer directly onto the membrane of the spin column. Keep at room temperature for 1 min. Then elute the solution by centrifuging for 1 min at 20,000×*g*. 12 μL of the solution should be eluted.

3.3. Synthesis of Biotin-Labeled cRNA with IVT Reaction

1. Transfer the double-strand cDNA sample to RNase-free microfuge tube and add 4 μL of 10X IVT labeling buffer, 12 μL of IVT labeling NTP mix, and 4 μL of IVT labeling enzyme mix. Adjust to a final volume of 40 μL with RNase-free water.
2. Mix gently and spin down to collect the solution.
3. Incubate at 37°C for 16 h in an air incubator (*see* **Note 10**).
4. For cleanup of biotin-labeled cRNA (*see* **Note 11**), add 60 μL of RNase-free water to the IVT reaction mixture sample (after step 3) and vortex for 3 s.

5. Add 350 μL of IVT cRNA binding buffer (*see* **Note 12**) to the sample and mix by vortex for 3 s.
6. Add 250 μL of ethanol and mix well by pipetting (*see* **Note 13**).
7. Apply 700 μL of the sample onto "IVT cRNA Cleanup Spin Column" set in a 2 mL collection tube. Centrifuge for 15 s at 8,000×*g*. Discard the flow-through and the collection tube.
8. Transfer the spin column into a new 2 mL Collection tube. Apply 500 μL of "IVT cRNA wash buffer" onto the spin column. Centrifuge for 15 s at 8,000×*g*. Discard flow-through.
9. Apply 500 μL of 80% ethanol onto the spin column. Centrifuge for 15 s at 8,000×*g*. Discard the flow-through.
10. Open the cap of the spin column and centrifuge for 5 min at 20,000×*g*. Discard the flow-through and the collection tube.
11. Transfer the spin column into 1.5 mL collection tube and apply 11 μL of RNase-free water onto the membrane of the spin column. Then centrifuge for 1 min at 20,000×*g* to elute.
12. Apply 10 μL of RNase-free water onto the membrane of the spin column. Then centrifuge for 1 min at 20,000×*g*. Collect the elute.
13. Check the concentration of biotin-labeled cRNAs by measuring absorbance (*see* **Note 14**).

3.4. Fragmentation of the cRNA

1. Prepare the fragmentation buffer, containing 20 μg of cRNA (1–21 μL) and 8 μL of 5X fragmentation buffer in a 0.2 mL tube. Adjust to the final volume of 40 μL with RNase-free water.
2. Incubate at 94°C for 35 min using a thermal cycler. Put it on ice immediately after the incubation.
3. Check the fragmentation with Agilent 2100 Bioanalyzer (*see* **Note 15**).

3.5. Hybridization

1. Incubate 20X eukaryotic hybridization controls for 5 min at 65°C to dissolve the elements completely.
2. Prepare the hybridization cocktail. For each target sample, add the following reagents to 15 μg of each fragmented cRNA sample: 5 μL of 3 nM control Oligo B2 , 15 μL of 20X eukaryotic hybridization controls, 3 μL of 10 mg/mL Herring Sperm DNA, 3 μL of 50 mg/mL BSA, 150 μL

of 2X hybridization buffer, and 30 μL of DMSO. Adjust to final volume of 300 μL with RNase-free water.

3. Leave the tiling array at room temperature (*see* **Note 16**).
4. Prehybridize the array by filling through a septum with 200 μL of 1X hybridization buffer using a micropipettor (*see* **Note 17**) and incubating the array for 10 min at 45°C with rotation.
5. Heat the hybridization cocktail at 99°C for 5 min on a heat block.
6. Transfer the hybridization cocktail to 45°C on heat block and keep for 5 min.
7. Centrifuge the hybridization cocktail at 8,000×*g* for 5 min to remove any insoluble materials.
8. Remove the prehybridization buffer solution from the array and add 200 μL of the hybridization cocktail (*see* **Note 18**) onto the array.
9. Incubate the array for 18 h at 45°C with 60 rpm rotation in the hybridization oven.

3.6. Wash and Stain

1. For each target sample, prepare three tubes for SAPE solution for the first stain, antibody solution, and SAPE solution for the third stain. For each sample, prepare 1,200 μL of SAPE solution mix containing 600 μL of 2X stain buffer, 48 μL of 50 mg/mL BSA, 12 μL of 1 mg/mL streptavidin phycoerythrin (SAPE) and 540 μL of DNase/RNase-free water. Divide it into two aliquots of 600 μL. They are used for the first stain solution and the third stain solution (*see* **Note 19**).
2. For each sample, prepare 600 μL of the antibody solution mix containing 300 μL of 2X stain Buffer, 24 μL of 50 mg/mL BSA (*see* **Note 20**), 6 μL of 10 mg/mL Goat IgG Stock, 3.6 μL of 0.5 mg/mL biotinylated antibody, and 266.4 μL of DNase/RNase-free water.
3. After 18 h of hybridization, remove the hybridization cocktail from the array (*see* **Note 21**) and fill the array completely with the appropriate volume (about 250 μL) of nonstringent wash buffer A.
4. Set the wash buffer A and wash buffer B into the fluidics station. Run the protocol "Prime_450."
5. Set the SAPE solution and antibody solution into the fluidics station.
6. Select the protocol "EuKGE-ws2v4" in the fluidics station. Insert the array into the designated module of the fluidics

station, and start the run (*see* **Note 22**). Carry out washing and staining as follows:

a. Post-Hyb wash #1: 10 cycles of 2 mixes/cycle with wash buffer A at 25°C.
b. Post-Hyb wash #2: 4 cycles of 15 mixes/cycle with wash buffer B at 50°C.
c. Stain: Stain the array for 10 min in SAPE solution at 25°C.
d. Post stain wash: 10 cycles of 4 mixes/cycle with wash buffer A at 25°C.
e. Second Stain: Stain the array for 10 min in antibody solution at 25°C.
f. Third Stain: Stain the array for 10 min in SAPE solution at 25°C.
g. Final wash: 15 cycles of 4 mixes/cycle with wash buffer A at 30°C. The loading temperature is 25°C.

7. Turn on the scanner about 30 min before the end of the protocol (*see* **Note 23**). One hour and 20 min after starting the run, the sign "Eject" will appear. Then remove the array (*see* **Note 24**).

3.7. Array scanning

1. On the back of the array, wipe off excess solution around the septum. Cover the septum with the seal "Tough-Spots" and keep the surface of the seal flat (*see* **Note 25**).
2. Perform scanning using filters (570 nm) at 0.7 μm resolution using a GeneChip Scanner 3000 7G. In entering the experimental information using GCOS (GeneChip Operating Software) ver. 1.3, select "At35b_MF_v04" and "At35b_MR_v04" for 1.0F and 1.0R Array, respectively.

3.8. Computational Analyses of RNA Expression

1. Prepare the information of Arabidopsis genome sequence and annotation from *Arabidopsis* Genome Release(ftp://ftp.arabidopsis.org/home/tair/Genes/TAIR**_genome_release/; *see* **Note 26**) in the *Arabidopsis* information resource (TAIR).
2. Map the probes of each Affymetrix *Arabidopsis* whole-genome tiling array (1.0F Array or 1.0R Array) on *Arabidopsis* genomic sequence (*see* **Note 27**).
3. For the analysis of transcriptional activities in the *Arabidopsis* whole genome, normalize intensity of a total of 6.4 millions 25-nt oligonucleotide probes for each strand genomic sequence, that is, 3.2 millions perfect match (PM) and 3.2 millions mismatch (MM) probes, of individual replicates for all treated and untreated samples at the same time via quantile normalization (20) (*see* **Note 28**).

4. Calculate the intensity of (PM-MM) by subtracting the intensity of MM probes from that of PM probes and use the intensity values of (PM-MM) for all subsequent data analyses (*see* **Note 29**).
5. Evaluate whether AGI code genes and non-AGI TUs are expressed, by "*Arabidopsis* tiling array-based detection of exons (ARTADE)-based method," that uses the p-initial value or the binomial-distribution-based probability of finding the expression profile within a 750-nucleotide window scanning the whole genome during the initial evaluation process in the method (21) (*see* **Note 30**).
6. Calculate Hodges–Lehmann estimator (HLE) values (*see* **Note 31**) as the expression values of each gene and transcriptional unit (TU) (*see* **Note 32**) by use of the intensity value of 25-nt probes mapped to exons of each AGI code gene and non-AGI TUs.
7. Identify the drought stress-inducible (*see* **Note 33**) and downregulated (*see* **Note 34**) AGI code genes and non-AGI TUs by Mann–Whitney *U*-test (FDR $\alpha = 0.01$) (22, 23).

4. Notes

1. The first diluted Poly-A RNA control solution can be stored at −20°C for 6 weeks. The freeze–thaw cycle must not exceed eight times. The second and the third diluted Poly-A RNA control solution should be prepared before its use.
2. The maximal volume of the mixed solution is 10 μL.
3. Information of the tilling array platform can be found at the Gene Expression Omnibus (GEO) at NCBI (http://www.ncbi.nlm.nih.gov/geo/). The 25-nt oligonucleotides chosen from the forward strand genomic sequence is comprised in the 1.0R Array and the sequence information is the array platform GPL1979. The 25-nt oligonucleotides chosen from the reverse strand genomic sequence is comprised in the 1.0F Array and the sequence information is the array platform GPL1980. Each Affymetrix *Arabidopsis* whole-genome tiling array (1.0F Array or 1.0R Array) contains 6.4 millions 25-nt oligonucleotide probes(15). They are composed of 3.2 million perfect match (PM) probes that perfectly match genomic sequence and 3.2 million mismatch (MM) probes whose central base (positions 13 of 25) is substituted by its complement.

4. The head of the tip is ultrathin.
5. Two-week-old whole seedlings including entire aerial parts and roots are used for the stress treatments (19).
6. Start the drought stress treatment at almost the same time, 5–6 h after the start of the light period to eliminate the effect of diurnal and circadian regulation (24).
7. Isolate total RNA samples using Isogen reagent (Nippon Gene) according to the manufacturer's instructions. Examine the quality and quantity of the total RNA by spectrophotometry and gel electrophoresis using Agilent 2100 Bioanalyzer (Agilent Technologies). About 200–300 μg total RNA should be isolated from the plants (fresh weight: about 1 g) in two to three dishes. Isolate three biological replicative RNA samples (at least 16 μg per sample). For each RNA sample, use 8 μg of RNAs as the starting materials for hybridization with *Arabidopsis* tiling 1.0F Array or 1.0R Array (Affymetrix).
8. Do not keep double-strand cDNA samples at 4°C for a long time and perform the following cleanup of the double-strand cDNAs immediately.
9. The color of the mixture should be yellow. If the color is orange or purple, add 10 μL of 3 M sodium acetate (pH 5.0) to make the color yellow.
10. If the biotin-labeled cRNAs are not used for cleanup immediately, store at −20°C or −70°C.
11. Perform the cleanup of the biotin-labeled cRNAs at room temperature.
12. If precipitates are formed, the IVT cRNA binding buffer should be warmed to 30°C and then kept at room temperature before use.
13. Do not centrifuge the samples after mixing.
14. Calculate the whole quantity of the biotinylated cRNAs as follows: Whole quantity of the biotinylated cRNAs = (Whole quantity of the cRNAs recovered after the IVT reaction) × (Whole quantity of the total RNA) × (ratio of the cDNAs used for the IVT reaction). More than 30 μg of the biotinylated cRNAs should be generated. The ratio (A260/A280) should be between 1.9 and 2.1.
15. The acceptable RNA fragment size range is between 35 and 200 bases. Store the fragmented cRNA samples at −70°C before the use for hybridization.
16. Immediately after the tiling array is returned from the low temperature, the rubber of the septa will still be hard and will easily crack.

17. Use the pipetman tip "HR-250S" for pushing the septa and filling hybridization buffer through the septum. Note that the cracking of septum causes deposition of hybridization buffer.
18. Do not use the insoluble materials at the bottom of the tube. Do not add bubble onto the array.
19. Mix the SAPE solution thoroughly by tapping before its use.
20. For BSA, IgG, and antibody stocks, centrifuge the solution and use the supernatant for preparation of the antibody solution mix.
21. If the volume of the recovered hybridization cocktail is less than 170 μL, the center part of the array may not be filled with the cocktail.
22. Be sure to check that the buffer runs up and down. If the bubbles stay at the same position, stop the run, and refill the array with the wash buffer A manually. When the wrong buffer is used, the run stops.
23. The scanner should be warmed up at least 15 min before the scanning.
24. Be sure to check whether the bubble stays on the array or not. If the bubble stays on the array, the array is reset into the cartridge holder and then subjected to washing and staining. However, excess washing causes loss of the signal intensity of each probe. After being washed, the array should be subjected to scanning immediately. The remaining array is kept at room temperature in the dark before the scanning.
25. This step is done to prevent the leakage of the solution during the scanning.
26. Use of the latest version on *Arabidopsis* genome annotation is recommended. The latest version is TAIR8 (ftp://ftp.arabidopsis.org/home/tair/Genes/TAIR8_genome_release/). Check the announcement on *Arabidopsis* genome annotation from the TAIR carefully.
27. In our tiling array analysis (19), the following probes were excluded from the data analysis: (1) the PM probes which perfectly matched more than two positions and (2) the MM probes which perfectly matched the positions different from its original ones. Finally, 5.8 million PM and 5.8 million MM probes per each array were used for the data analysis. Note that the data of about 400 AGI code genes was not analyzed due to the exclusion of the probes in our previous tiling array analysis (19).

28. After the quantile normalization, intensities of all replicates representing different samples reach a common median. All normalized intensities for each expressed spot are then averaged among all replicates of the same sample to obtain a single statistic. Their data is available at OmicBrowse (http://omicspace.riken.jp/gps/group/psca1).
29. We used the intensities of (PM-MM) for the analyses, because our preliminary analyses using the intensities of (PM-MM) gave better results for identification of the stress-responsive genes than that using only PM intensities. If the intensity of (PM-MM) for some 25-nt probes is less than 1, intensity value 1 is used for our previous data analyses (19).
30. The genes or TUs whose *p*-initial value is less than $10^{-8}$are regarded as the expressed genes or TUs based on the comparison with the data obtained by "the promoter-based method" that determines the threshold levels based on the expression levels at the promoter region (1, 2).
31. HLE has strong robustness and high-efficiency properties. In our previous study (19), we regarded the HLE values as the expression values of each gene and TU and used it for the subsequent data analyses.
32. To enable a global description of the *Arabidopsis* transcriptome, we used the term TU to describe a segment of the genome from which transcripts are generated, in addition to annotated *Arabidopsis* Genome Initiative (AGI) code genes whose information is available from TAIR (http://www.arabidopsis.org/). A TU is defined by the identification of a cluster of transcripts containing a common core of genetic information (in some cases, protein-coding region) and a non-AGI TU is defined as the TU identified in unannotated intergenic regions by the bioinformatic analysis.
33. In our previous analysis (19), we regarded the following AGI code genes and non-AGI TUs as the AGI code genes and non-AGI TUs upregulated by drought stress: (1) AGI code genes and non-AGI TUs (in non-AGI code regions) identified as expressed under the drought stress treatments by the ARTADE-based method (*p*-initial value $<10^{-8}$). (2) AGI code genes and non-AGI TUs identified as drought stress-upregulated by Mann–Whitney U-test (FDR $\alpha = 0.01$). (3) Expression ratios (drought-treated/untreated) >1.8. We identified 2,421 AGI code genes and 527 non-AGI TUs as drought stress-upregulated ones (19).
34. In our previous analysis (19), we regarded the following AGI code genes and non-AGI TUs as the AGI code genes

and non-AGI TUs downregulated by drought stress: (1) AGI code genes and non-AGI TUs (in non AGI-code regions) identified as expressed under untreated condition by ARTADE-based method (p-initial value < 10^{-8}). (2) AGI code genes and non-AGI TUs identified as drought stress-downregulated by Mann–Whitney U-test (FDR α = 0.01). (3) Expression ratios (drought-treated/untreated) <5/9. We identified 2,097 AGI code genes and 80 non-AGI TUs as drought stress-downregulated ones (19).

Acknowledgments

This work was supported by a Grant-in-Aid for Scientific Research on Priority Areas "Systems Genomics" from MECSST and the President Discretionary Fund from RIKEN to M.S. It was also supported in part by a grant for Genome Research from RIKEN to K.S.

References

1. Seki, M., Narusaka, M., Ishida, J., Nanjo, T., Fujita, M., Oono, Y., et al. (2002) Monitoring the expression profiles of 7000 *Arabidopsis* genes under drought, cold, and high-salinity stresses using a full-length cDNA microarray. *Plant J* **31**, 279–292.
2. Kreps, J.A., Wu, Y., Chang, H.S., Zhu, T., Wang, X., and Harper, J.F. (2002) Transcriptome changes for *Arabidopsis* in response to salt, osmotic, and cold stress. *Plant Physiol* **130**, 2129–2141.
3. Yamada, K., Lim, J., Dale, J. M., Chen, H., Shinn, P., Palm, C. J., et al. (2003) Empirical analysis of transcriptional activity in the *Arabidopsis* genome. *Science* **302**, 842–846.
4. Stolc, V., Samanta, M.P., Tongprasit, W., Sethi, H., Liang, S., Nelson, D. C., et al. (2005) Identification of transcribed sequences in *Arabidopsis thaliana* by using high-resolution genome tiling arrays. *Proc Natl Acad Sci USA* **102**, 4453–4458.
5. Li, X., Wang, X., He, K., Ma, Y., Su, N., He, H., et al. (2008) High-resolution mapping of epigenetic modifications of the rice genome uncovers interplay between DNA methylation, histone methylation and gene expression.*Plant Cell* **20**, 259–276.
6. Hanada, K., Zhang, X., Borevitz, J. O., Li, W. H., and Shiu, S. H. (2007) A large number of novel coding small open reading frames in the intergenic regions of the *Arabidopsis thaliana* genome are transcribed and/or under purifying selection. *Genome Res* **17**, 632–640.
7. Laubinger, S., Zeller, G., Henz, S. R., Sachsenberg, T., Widmer, C. K., Naouar, N., et al. (2008) At-TAX: a whole-genome tiling array resource for developmental expression analysis and transcript identification in *Arabidopsis thaliana*. *Genome Biol* **9**, R112.
8. Clark, T. A., Sugnet, C. W., and Ares, M., Jr. (2002) Genome wide analysis of mRNA processing in yeast using splicing-specific microarrays. *Science* **296**, 907–910.
9. Katou, Y., Kanoh, Y., Bando, M., Noguchi, H., Tanaka, H., Ashikari, T., et al. (2003) S-phase checkpoint proteins Tof1 and Mrc1 form a stable replication-pausing complex. *Nature* **424**, 1078–1083.
10. Thibaud-Nissen, F., Wu, H., Richmond, T., Redman, J. C., Johnson, C., Green, R., et al. (2006) Development of *Arabidopsis* whole-genome microarrays and their application to the discovery of binding sites for the TGA2 transcription factor in salicylic acid-treated plants. *Plant J* **47**, 152–162.
11. Turck, F., Roudier, F., Farrona, S., Martin-Magniette, M. L., Guillaume, E., Buisine,

N., et al. (2007) *Arabidopsis* TFL2/LHP1 specifically associates with genes marked by trimethylation of histone H3 lysine 27. *PLoS Genet* **3**, 855–866.
12. Bignell, G. R., Huang, J., Greshock, J., Watt, S., Butler, A., West, S., et al. (2004) High-resolution analysis of DNA copy number using oligonucleotide microarrays. *Genome Res* **14**, 287–295.
13. Ishkanian, A. S., Malloff, C. A., Watson, S. K., DeLeeuw, R. J., Chi, B., Coe, B. P., et al. (2004) A tiling resolution DNA microarray with complete coverage of the human genome. *Nat Genet* **36**, 299–303.
14. Martienssen, R. A., Doerge, R. W., and Colot, V. (2005) Epigenomic mapping in *Arabidopsis* using tiling microarrays. *Chromosome Res* **13**, 299–308.
15. Zhang, X., Yazaki, J., Sundaresan, A., Cokus, S., Chan, S. W., Chen. H., et al. (2006) Genome-wide high-resolution mapping and functional analysis of DNA methylation in *Arabidopsis. Cell* **126**, 1189–1201.
16. Zilberman, D., Gehring, M., Tran, R. K., Ballinger, T., and Henikoff, S. (2007) Genome-wide analysis of *Arabidopsis thaliana* DNA methylation uncovers an interdependence between methylation and transcription. *Nat Genet* **39**, 61–69.
17. Zhang, X., Clarenz, O., Cokus, S., Bernatavichute, Y. V., Pellegrini, M., Goodrich, J., et al. (2007) Whole-genome analysis of histone H3 lysine 27 trimethylation in *Arabidopsis. PLoS Biol* **5**, 1026–1035.
18. Li, X., Wang, X., He, K., Ma, Y., Su, N., He. H., et al. (2008) High-resolution mapping of epigenetic modifications of the rice genome uncovers interplay between DNA methylation, histone methylation and gene expression. *Plant Cell* **20**, 259–276.
19. Matsui, A., Ishida, J., Morosawa, T., Mochizuki, Y., Kaminuma, E., Endo, T. A., et al. (2008) *Arabidopsis* transcriptome analysis under drought, cold, high-salinity and ABA treatment conditions using a tiling array. *Plant Cell Physiol* **49**, 1135–1149.
20. Bolstad, B. M., Irizarry, R. A., Astrand, M., and Speed, T. P. (2003) A comparison of normalization methods for high density oligonucleotide array data based on variance and bias. *Bioinformatics* **19**, 185–193.
21. Toyoda, T. and Shinozaki, K. (2005) Tiling-array-driven elucidation of transcriptional structures based on maximum likelihood and Markov models. *Plant J* **43**, 611–621.
22. Mann, H. B. and Whitney, D.R. (1947) On a test of whether one of two random variables is stochastically larger than the other. *Annals of Mathematical Statistics* **18**, 50–60.
23. Storey, J. D. and Tibshirani, R. (2003) Statistical significance for genome-wide studies. *Proc Natl Acad Sci USA* **100**, 9440–9445.
24. Bieniawska, Z., Espinoza, C., Schlereth, A., Sulpice, R., Hincha, D.K., and Hannah, M.A. (2008) Disruption of the *Arabidopsis* circadian clock is responsible for extensive variation in the cold-responsive transcriptome. *Plant Physiol* **147**, 263–279.

Chapter 9

Identification of Stress-Responsive Genes in Plants Using Suppression Subtraction Hybridization: Ozone Stress as an Example

Lila Peal, Michael Puckette, and Ramamurthy Mahalingam

Abstract

Among the open-ended techniques for identifying differentially expressed genes in response to stress, the PCR-based suppression subtraction hybridization (SSH) is widely used. The popularity of this technique stems from the ease of conducting this procedure in any laboratory set up for basic molecular biology research. Further, the availability of a comprehensive kit for conducting suppression subtractions from BD Biosciences has made this technique easy to adapt and adopt to any biological system. In this chapter we describe in detail the SSH procedure and explain the subtle changes that have been incorporated to make this technique adaptable for identifying stress-responsive genes in plants.

Key words: Adaptor, cDNAs, cloning, differential screening, driver, ligation, macroarray, tester, suppression PCR.

1. Introduction

Transcriptional gene regulation plays a crucial role in shaping the plant responses to external perturbations. As such literature is replete with identification of transcriptional responses to external insults in plants (1–5). The closed-end technologies such as microarrays and real-time PCR have gained a lot of attention in the recent years (6). However, as the name indicates these techniques are confined to only those genes that are on the microarray or restricted to organisms wherein extensive sequence information is available. There are a number of different open-ended techniques that have been developed and adapted for

R. Sunkar (ed.), *Plant Stress Tolerance*, Methods in Molecular Biology 639,
DOI 10.1007/978-1-60761-702-0_9,

the identification of differentially expressed genes in response to stresses (6). This includes differential display (7), cDNA-AFLPs (8), serial analysis of gene expression (9), massively parallel signature sequencing (10), and subtraction hybridizations (11–13). These techniques are applicable to organisms that do not have any sequence information.

Subtractive hybridization is a powerful technique for comparing two populations of messenger RNAs and obtaining genes that are differentially expressed in one population but not in the other. The population that the researcher is interested in identifying the differentially expressed genes is called the tester, while population that serves as the reference is termed as the driver. Suppression subtraction hybridization is designed to overcome several shortcomings of the traditional procedures (14). The method does not require the physical separation of the single-stranded and double-stranded molecules. Furthermore this method includes normalization and exploits the suppression PCR technology that is extremely useful for enriching rare differentially expressed genes (15).

The BD Biosciences (formerly Clontech) PCR-Select cDNA subtraction kit provides all the necessary reagents for conducting SSH. This kit is optimized for animal samples. Here we describe in detail how this kit can be adapted for conducting successful subtractions for plant samples. We also describe the methods for constructing the subtracted cDNA libraries. Finally we describe adapting the macroarray technology for rapid differential screening of subtracted cDNA libraries.

2. Materials

2.1. Plant Materials and Acute Ozone Stress Treatment

1. Plant growth chamber for raising plants (Percival).
2. Activated charcoal filters (VWR).
3. Ozone generation apparatus connected to a growth chamber.
4. Falcon screw cap tubes of 50 mL size for harvesting the tissue samples.
5. Liquid nitrogen for freezing samples and a −80°C freezer for storing the frozen tissues.

2.2. Total RNA and Messenger RNA Isolation

1. Trizol (Invitrogen).
2. DEPC water. Add 1 mL of diethyl pyrocarbonate (Sigma) (*see* **Note 1**) to 1 L of water and shake vigorously to ensure

complete mixing up. Place the bottle at 37°C overnight and then autoclave for 20 min.

3. RNase and DNase free tubes and tips.
4. Chloroform, isopropanol, and ethyl alcohol.
5. Oligotex mRNA midi kit (Qiagen).

2.3. Suppression Subtraction Hybridization

1. All the components required for processing up to seven samples can be found in the PCR-Select cDNA Subtraction Kit from BD Biosciences. For each subtraction two samples are processed in parallel.
2. Thermo cycler.
3. Heating block or water bath.
4. Primers for amplifying G3PDH gene.
5. Mini gel electrophoresis unit.

2.4. Cloning

1. TA cloning kit.
2. Water bath.
3. Large plates for plating library.
4. LB medium containing ampicillin.
5. X-gal (5-bromo-4-chloro-3-indolyl-ß-D-galactoside or 5-bromo-4-chloro-3-indolyl-ß-D-galactopyranoside).

2.5. Differential Screening

1. Differential screening kit (BD Biosciences).
2. Large electrophoresis unit with multiple rows.
3. Hybond N^+ Nylon membranes (Amersham).
4. Seiko D-TRAN robot.
5. Hybridization incubator.
6. RadPrime DNA labeling system (Invitrogen).
7. Scintillation Counter (Beckman Coulter).

3. Methods

In order to identify ozone-induced genes in Arabidopsis plants, the mRNA from plants treated with ozone will be designated as the tester sample and the mRNA from the control plants maintained in ozone-free air is referred to as the driver sample. It is also possible to identify the ozone-repressed genes between these two samples. Conducting the subtraction procedure with the mRNA isolated from control plants as the tester and using the mRNA from ozone-treated plants as the driver will enrich for genes that are repressed in response to the oxidant.

The procedures described here below are for identifying genes responsive to ozone in Arabidopsis. The same protocol can be adapted for identifying stress-responsive genes in other plant species (16, 17, 18).

3.1. Acute Ozone Treatment

1. Arabidopsis plants are grown in ozone-free chambers. Chambers are made ozone-free by placing activated charcoal strips in the chamber that will effectively absorb any ambient ozone. Plants are grown under moderate light intensity (80–100 $\mu mol/m^2s$) with 10-h light and 14-h dark period for 4 weeks, from the day of sowing seeds. Plants are grown in 1.5 in. pots and only one plant is maintained in each pot to avoid crowding.
2. About 80 plants can be accommodated in a single shelf of the small Percival chamber connected to the ozone generation apparatus. If planning to collect plants at different time points, ensure that equal number of plants is used for each time point. Always allow four to five plants to observe for ozone-related symptoms 24–48 h after the end of the treatment.
3. Since ozone is a gas maintaining the concentration precisely for several hours can be challenging. Especially if the chamber door has to be opened during the course of ozone treatment to collect samples, ensure that additional help is available. This ensures that one person can quickly remove the plants from the chamber and harvest them in labeled 50 mL falcon tubes, immediately frozen using liquid nitrogen and stored in −80°C. The other person can regulate the concentration of ozone in the chamber. When the door is opened to remove the plants, the ozone levels in the chamber will drop sharply. Raise the flow of oxygen into the ozone generator.

3.2. Total RNA and mRNA isolation

3.2.1. Total RNA Isolation

1. Grind the plant tissue to fine powder using liquid nitrogen (*see* **Note 2**).
2. Add 1 mL Trizol for every 100 mg of tissue powder.
3. Vortex for 30 s and incubate for 5 min at room temperature.
4. Add 0.2 mL chloroform for every 1 mL Trizol used and shake vigorously for 15 s.
5. Incubate for 2–3 min at room temperature and then centrifuge at 16,000×*g* for 15 min at 4°C.
6. Transfer aqueous layer to a clean tube and add 0.5 mL isopropanol for every 1 mL Trizol used.
7. Invert tube 2–5 times and incubate for 10 min at room temperature.
8. Centrifuge at 16,000×*g* for 10 min at 4°C.

9. Aspirate off the supernatant and add 1 mL of 75% ethanol (made with DEPC-treated water) per mL of Trizol used.
10. Mix by vortexing and centrifuge at 16,000×*g* for 5 min at 4°C.
11. Remove supernatant, briefly dry pellet by aspiration, and let pellet air dry for 2 min and then dissolve pellet in RNase-free water (100 μL for 100 mg of tissue).
12. Analyze the quality of the RNA preparation on a 1% agarose gel. The RNA samples are mixed with 1 μL of ethidium bromide (1 mg/mL) and the RNA loading dye (*see* **Note 3**).

3.2.2. mRNA Isolation

1. For total RNA more than 500 μg up to 1 mg, the Qiagen Oligotex mRNA Midi Kit works well. Follow the instructions in the kit carefully.
2. Determine the concentration of the mRNA using a nanodrop spectrophotometer.
3. Analyze about 100 ng of the mRNA on a 1% agarose gel to ensure that the preparation is free of ribosomal RNA.

3.3. Suppression Subtraction Hybridization

3.3.1. First-Strand cDNA Synthesis

1. For each tester and driver combine the following in a microfuge tube

Poly A^+ RNA (4–5 μg) (*see* **Note 4**)	2–4 μL
10 μM cDNA Synthesis Primer	1 μL

2. Incubate for 2 min at 70°C in a thermo cycler or a heating block.
3. Place the tubes on ice for 2 min, and then centrifuge tubes briefly.
4. Add to each tube:

5x First-strand buffer	2 μL
10 mM dNTP mix	1 μL
Sterile water	1 μL
AMV reverse transcriptase	1 μL

4. Mix gently with a pipette tip and centrifuge briefly.
5. Incubate for 1.5 h in a 42°C air incubator or heating block.
6. Place the tubes on ice to terminate the reaction.

3.3.2. Second-Strand cDNA Synthesis

1. Add to the first-strand synthesis reaction

5x Second-strand buffer	16.0 μL
10 mM dNTP mix	1.0 μL
20x Second-strand enzyme cocktail	4.0 μL
Sterile water to	80 μL

2. Mix and centrifuge briefly.
3. Incubate for 2 h at 16°C.
4. Add 2 μL of T4 DNA polymerase and mix well.
5. Incubate for 30 min at 16°C.
6. Add 4 μL of 20x EDTA/glycogen mix to terminate the reaction.
7. Add 100 μL of phenol: chloroform: isoamyl alcohol (25:24:1)
8. Vortex vigorously and centrifuge at 16,000×*g* for 10 min at room temperature.
9. Remove aqueous layer and transfer to a new tube.
10. Add 100 μL chloroform: isoamyl alcohol (24:1) to the aqueous layer.
11. Repeat steps 9–11.
12. Add 40 μL of 4 M ammonium acetate and 300 μL of 95% ethanol.
13. Vortex vigorously and centrifuge at 12,000×*g* for 20 min at room temperature.
14. Remove the supernatant and add 500 μL of 80% ethanol to the pellet.
15. Centrifuge at 12,000×*g* for 10 min.
16. Remove the supernatant and then air dry pellet for 10 min.
17. Dissolve pellet in 50 μL of water.
18. Transfer 6 μL to a new tube and store at −20°C.

3.3.3. Rsa I Digestion

1. Add the following into a microfuge tube:

Double-stranded cDNA	43.5 μL
10x *Rsa* I restriction buffer	5.0 μL
10 U/μl *Rsa* I	1.5 μL

2. Vortex and briefly centrifuge.
3. Incubate for 1.5 h at 37°C.
4. Transfer 5 μL to a new tube for analyzing efficiency of digestion (*see* **Note 5**).
5. To the rest of the reaction add 2.5 μL of 20x EDTA/glycogen mix to terminate the reaction.
6. Add 50 μL of phenol:chloroform:isoamyl alcohol (25:24:1).
7. Vortex vigorously and centrifuge at 12,000×*g* for 10 min.
8. Remove aqueous layer and transfer to a clean microfuge tube.

9. Add 50 μL chloroform:isoamyl alcohol (24:1) to the aqueous layer and vortex vigorously.
10. Centrifuge at 12,000×*g* for 10 min.
11. Remove aqueous layer and transfer to a clean microfuge tube.
12. Add 25 μL of 4 M ammonium acetate and 187.5 μL of 95% ethanol.
13. Vortex vigorously and centrifuge at 12,000×*g* for 20 min at room temperature.
14. Remove supernatant without disturbing the pellet.
15. Add 200 μL of 80% ethanol to the pellet.
16. Centrifuge at 12,000×*g* for 5 min.
17. Remove supernatant.
18. Air dry pellet for 5–10 min.
19. Resuspend pellet in 5.5 μL water and store at −20°C.

3.3.4. Adapter Ligation

1. Dilute 1.5 μL of each *Rsa* I digested experimental cDNA with 2.5 μL of water. (*see* **Note 6**)
2. Prepare a ligation Master Mix by combining the following components in a 0.5 mL tube for each reaction:

Sterile water	3 μL
5x Ligation buffer (*see* **Note 7**)	2 μL
T4 DNA ligase	1 μL

3. Set up two reactions for each tester cDNA. Label the tubes as 1-1 and 1-2 and add the following ingredients

	1-1	1-2
Diluted tester cDNA	2 μL	2 μL
10 uM Adaptor 1	2 μL	—
10 uM Adaptor 2R	—	2 μL
Master Mix	6 μL	6 μL

4. Mix 2 μL of 1-1 reaction and 2 μL of 1-2 in a new tube. This will be unsubtracted control 1-c.
5. Briefly centrifuge and leave overnight at 16°C.
6. Add 1 μL EDTA/glycogen mix to stop the reaction.
7. Heat sample for 5 min at 72°C to inactivate the ligase.
8. Briefly centrifuge the tubes.
9. Remove 1 μL of the unsubtracted tester control and dilute with 1 mL of water.
10. Store samples at −20°C.
11. Perform the ligation efficiency test (*see* **Note 8**).

3.3.5. First Hybridization

1. Combine the following in a 0.5 mL tube for each experimental subtraction. Label the tubes as 1 and 2 and add the following components

	1	2
Rsa I digested driver cDNA	1.5 μL	1.5 μL
Adaptor 1-ligated tester 1-1	1.5 μL	—
Adaptor 2R-ligated tester 1-2	—	1.5 μL
4x Hybridization buffer (*see* **Note 9**)	1.0 μL	1.0 μL

2. Overlay sample with a drop of mineral oil.
3. Briefly centrifuge tubes.
4. Incubate for 1.5 min at 98°C in a thermocycler.
5. Incubate for 8 h at 68°C.
6. Proceed to second hybridization.

3.3.6. Second Hybridization

1. Add the following to a new tube:

Driver cDNA	1 μL
4x Hybridization buffer	1 μL
Sterile water	2 μL

2. Transfer 1 μL of this above mix into a 0.5 mL tube.
3. Overlay with a drop of mineral oil.
4. Incubate at 98°C for 1.5 min in a thermocycler.
5. Remove the tube from the thermocycler.
6. Set a micropipet to 15 μL.
7. Carefully draw hybridization sample 2 part-way into the pipet tip.
8. Remove tip from tube and draw in a small amount of air.
9. Repeat steps 7 and 8 with the freshly denatured driver.
10. Transfer the contents of the pipet to the tube containing hybridization sample 1.
11. Mix by pipetting.
12. Briefly centrifuge tube.
13. Incubate overnight at 68°C.
14. Add 100 μL of dilution buffer to the tube (*see* **Note 10**).
15. Mix by pipetting.
16. Heat for 7 min at 68°C in a thermocycler.
17. Store at −20°C.

3.3.7. PCR Amplifications

1. Take 2.5 μL of the diluted cDNA and the corresponding diluted unsubtracted tester control into a labeled tube (*see* **Note 11**).

2. Prepare a Master Mix for all the primary PCRs by adding the following for each reaction:

Sterile water	18 μL
10x PCR reaction buffer	2.5 μL
10 mM dNTP	0.5 μL
10 μM PCR primer 1	1.0 μL
50x Advantage cDNA polymerase mix	0.5 μL

3. Vortex to mix and centrifuge briefly.
4. Add 22.5 μL of master mix into each of the reaction tubes.
5. Incubate for 5 min at 75°C in a thermocycler and immediately begin the PCR as follows: 94°C for 25 s followed by 27 cycles at 94°C for 30 s, 66°C for 30 s and 72°C for 1.5 min followed by a final extension at 72°C for 10 min.
6. Dilute 3 μL of each primary PCR with 27 μL water.
7. Take 1 μL of diluted primary PCR in a labeled tube.
8. Prepare a master mix for secondary PCR by adding the following for each reaction:

Sterile water	18 μL
10x PCR reaction buffer	2.5 μL
10 μM Nested PCR Primer 1	1.0 μL
10 μM Nested PCR Primer 2R	1.0 μL
10 mM dNTP Mix	0.5 μL
50x Advantage cDNA Polymerase Mix	0.5 μL (*See* **Note 12**)

9. Vortex to mix and centrifuge briefly.
10. Add 24 μL of master mix to each reaction tube.
11. Immediately begin the PCR as follows:

94°C	10 s
68°C	30 s
72°C	1.5 min

The PCR is run for 11 cycles.

12. Analyze 8 μL of the primary and secondary PCRs on a 2.0% agarose/EtBr gel. (*see* **Note 13**)
13. Store the PCR products at −20°C.
14. Conduct the subtraction efficiency analysis using the G3PDH primers that were designed for the adaptor ligation efficiency analysis (*see* **Note 14**).

3.4. Constructing Subtracted cDNA library

1. Take 2 μL freshly amplified secondary PCR products in a 0.5 mL tube.
2. Add 1 μL of the T/A cloning vector, 1 μL of 10 x ligase buffer, 5 μL of sterile distilled water, and 1 μL of the ligase enzyme.

3. Incubate the samples at 4°C overnight.
4. Use heat-shock competent DH5 alpha cells for transformation. Use 8 μL of the ligation mix for the transformation procedure.
5. Add about 1 mL of the SOC media and then plate about 200 μL aliquots of the transformation mix in large plates containing LB, X-gal, and ampicillin.
6. Incubate the plates overnight at 37°C.
7. Pick the white colonies using toothpicks and transfer them into 96-well plates containing about 100 μL of LB media with appropriate amount of ampicillin.
8. For each subtraction library pick as many white colonies as possible. We recommend at least 800–1000 colonies for each subtraction.
9. Place a seal on these plates and then incubate them in 37°C incubator with a constant agitation of 225 rpm overnight (*see* **Note 15**).

3.5. Differential Screening

1. The copy plates containing the subtracted cDNA clones are amplified using the nested PCR primers.
2. The PCR products are then analyzed on a high-density agarose gel. This is a large gel containing 3–4 rows of combs in order to analyze 48–96 PCR products simultaneously.
3. The gels are photographed and all the clones showing positive amplification and single discrete bands are selected for constructing macroarrays.
4. The PCR products are arrayed on to a nylon membrane robotically. Each membrane of the size of a 96-well plate can accommodate 480 spots. The membranes are printed in duplicates.
5. Each set of duplicate membranes are subjected to differential screening using radioactively labeled probes generated from the subtracted cDNA and unsubtracted cDNAs using the Radprime DNA labeling kit and alpha P^{32} dCTP (*see* **Note 16**).
6. Following random priming reaction the probes are cleaned using the sephadex columns.
7. An aliquot (1 μL) of the purified probe from the subtracted and unsubtracted samples are analyzed on a scintillation counter to determine the total amount of radioactivity incorporated. Equal counts of radiolabeled probes ($\sim 5 \times 10^6$ cpm) are used for the two membranes.

8. Membranes are allowed to hybridize in a rotary oven overnight at 68°C.
9. Membranes are washed twice using a solution of 2x SSC and 0.5% SDS for 10 min duration each.
10. The membranes are then covered in plastic wrap and exposed to phosphorimaging overnight.
11. The scanned images are transferred to the Imagemaster 2D platinum software (GE Healthcare) to extract the signal intensities around each spot. Clones that show a strong signal with the subtracted cDNA probe compared with the unsubtracted probe are selected for further analysis.

4. Notes

1. DEPC is carcinogenic and irritant. Wear gloves and open the DEPC containing bottle under a fume hood.
2. The finer the tissue grinding, higher will be the yield of RNA. We grind the plant tissue samples 3–5 times and then transfer the fine powder to pre-weighed 2 mL Eppendorf tubes to determine the exact weight of the samples. Approximately 1 mg of total RNA is necessary for isolating 10 μg of mRNA.
3. When viewed under the UV light, the 28S ribosomal bands must be twice the intensity of the 18S ribosomal bands.
4. The kit protocol recommends using 2 μg. In our experience with plants using 4–5 μg of mRNA gives better results. Since the average size of plant mRNA is significantly smaller compared with the animal mRNAs this change is necessary.
5. For determining the efficiency of the *Rsa* I digest, take 5 μL of digested and the undigested cDNA samples, add 1 μL of ethidium bromide and 1 μL of 6x loading buffer before loading the samples onto thin (less than 20 mL) 1% agarose mini gels. This enables to visualize the products on the gel very clearly. Run the digestion efficiency analysis gel before the phenol: chloroform cleanup procedures. The smear in the digested cDNA samples range between 100–500 bp. If the smearing in the digested samples is similar to the undigested samples, repeat the RsaI digestion again. If repeating the digestion it is advisable to use more enzymes and also extend the incubation time to 3–4 h.
6. The kit protocol recommends diluting 1 μL of the digested cDNA with 5 μL of water. Based on our experience, in

plants, we recommend using 1.5 μL of the digested cDNA and adding 2.5 μL of water for dilution.

7. It is recommended to make 10 μL aliquots of the ligase buffer. Use an aliquot and then discard the remaining. Freezing and thawing the ligase buffer will lead to the breakdown of the ATP and this in turn will reduce the ligation efficiency.
8. The G3PDH primers provided in the kit are for the mouse or human cDNA. For conducting the ligation efficiency analysis for plant samples design a forward primer and a reverse primer to amplify a housekeeping gene such as G3PDH. The designed primers should give an amplified product of about 400–500 bp and should not contain an internal *Rsa* I restriction site.
   The cDNA amplifications using the PCR primer 1 from the kit and the 3′ or the 5′ G3PDH primers should be at least 25% the intensity of the PCR amplifications using the 3′ and 5′ G3PDH primers. If the results are not as expected do not proceed to the next step. Repeat the ligations again using more concentrated cDNAs.
9. The hybridization buffer tube must be stored at room temperature.
10. Protocol recommends adding 200 μL of the dilution buffer. For the plant samples we recommend adding 100 μL of the dilution buffer.
11. The kit protocol recommends using 1 μL of the subtracted cDNA. For plant samples we found that taking 2.5 μL of the diluted subtracted cDNA gives better results.
12. The Advantage Taq polymerase can be replaced with Takara Taq polymerase. However, remember to use the appropriate polymerase buffer.
13. Mix 0.5–1 μL of ethidium bromide to the primary and secondary PCR products before running them on thin 1% agarose gel. This ensures to visualize the products clearly.
14. Subtraction efficiency analysis is conducted as described in the kit protocol except for the use of the plant-specific G3PDH primers. Instead of setting up a 30 μL reaction we recommend 50 μL volumes. This ensures that there are sufficient volumes left over when removing 5 μL aliquots of samples after 28 and 33 PCR cycles.
15. It is advisable to make copy plates from each master plate. This is done by transferring 2–3 μL of the overnight cultures growing in 96-well plates to new 96-well plates containing LB and ampicillin. Use the copy plates for conducting PCR amplifications for macroarraying or

microarraying. Add 100 μL of glycerol to the original 96-well plates, mix well, seal with a new plate seal before storing them in −80°C freezer.

16. Only licensed and trained personnel can use radioactivity. Ensure that protective clothing, gloves, eyewear are available before conducting radioactive work. It is important to conduct radioactive work behind half-inch plexi-glass shield.

Acknowledgments

This work was partially supported by the Oklahoma Agricultural Experiment Station (Project No. 2528).

References

1. Agarwal, P.K., Agarwal, P., Reddy, M.K., and Sopory, S.K. (2006) Role of DREB transcription factors in abiotic and biotic stress tolerance in plants. *Plant Cell Rep* **25,** 1263–1274.
2. Chen, W.J., and Zhu, T. (2004) Networks of transcription factors with roles in environmental stress response. *Trends Plant Sci* **9,** 591–596.
3. Chinnusamy, V., Schumaker, K., and Zhu, J.K. (2004) Molecular genetic perspectives on cross-talk and specificity in abiotic stress signalling in plants. *J Exp Bot* **55,** 225–236.
4. Umezawa, T., Fujita, M., Fujita, Y., Yamaguchi-Shinozaki, K., and Shinozaki, K. (2006) Engineering drought tolerance in plants: discovering and tailoring genes to unlock the future. *Curr Opin Biotechnol* **17,** 113–122.
5. Yamaguchi-Shinozaki, K., and Shinozaki, K. (2006) Transcriptional regulatory networks in cellular responses and tolerance to dehydration and cold stresses. *Annu Rev Plant Biol* **57**, 781–803.
6. Green, C.D., Simons, J.F., Taillon, B.E., and Lewin, D.A. (2001) Open systems: panoramic views of gene expression. *J Immunol Methods* **250**, 67–79.
7. Liang, P., and Pardee, A.B. (1992) Differential Display of Eukaryotic Messenger-RNA by Means of the Polymerase Chain Reaction. *Science* **257**, 967–971.
8. Gabriels, S.H., Takken, F.L., Vossen JH, et al. (2006) CDNA-AFLP combined with functional analysis reveals novel genes involved in the hypersensitive response. *Mol Plant Microbe Interact* **19**, 567–576.
9. Velculescu, V.E., Zhang, L., Vogelstein, B., Kinzler, K.W. (1995) Serial Analysis of Gene-Expression. *Science* **270**, 484–487.
10. Brenner, S., Johnson, M., Bridgham, J., et al. (2000) Gene expression analysis by massively parallel signature sequencing (MPSS) on microbead arrays. *Nature Biotech* **18**, 630–634.
11. Hara, E., Kato, T., Nakada, S., Sekiya, S., and Oda, K. (1991) Subtractive cDNA cloning using oligo(dT)30-latex and PCR: isolation of cDNA clones specific to undifferentiated human embryonal carcinoma cells. *Nucleic Acids Res.* **19**, 7097–7104.
12. Hedrick, S.M., Cohen, D.I., Nielsen, E.A., Davis, M.M. (1984) Isolation of cDNA clones encoding T cell-specific membrane-associated proteins. *Nature* **308**, 149–153.
13. Sargent, T.D., and Dawid, I.B. (1983) Differential gene expression in the gastrula of *Xenopus laevis. Science* **222**, 135–139.
14. Diatchenko, L., Lau, Y.F.C., Campbell. A.P, et al. (1996) Suppression subtractive hybridization: A method for generating differentially regulated or tissue-specific cDNA probes and libraries. *Proc Natl Acad Sci USA,* **93**, 6025–6030.
15. Gurskaya, N.G., Diatchenko, L., Chenchik, A., et al. (1996) Equalizing cDNA

subtraction based on selective suppression of polymerase chain reaction: Cloning of Jurkat cell transcripts induced by phytohemaglutinin and phorbol 12-myristate 13-acetate. *Anal Biochem* **240**, 90–97.
16. Mahalingam, R., Gomez-Buitrago, A., Eckardt, N, et al. (2003) Characterizing the stress/defense transcriptome of Arabidopsis. *Genome Biol* **4**, R20.
17. Puckette, M., Peal, L., Steele, J., Tang, Y., and Mahalingam, R. (2009) Ozone responsive genes in *Medicago truncatula*: Analysis by suppression subtraction hybridization. *J Plant Physiol.* **166**, 1284–1295.
18. Tomkins, J. P., Mahalingam, R., Smith, H., Goicoechea., J. L., Knap, H. T., and Wing R. A. (1999) A bacterial artificial chromosome library for soybean PI 437654 and identification of clones associated with cyst nematode resistance. *Plant Mol Biol.* **41**, 25–32.

Chapter 10

Identification of DNA-Binding Proteins and Protein-Protein Interactions by Yeast One-Hybrid and Yeast Two-Hybrid Screen

Peter Klein and Karl-Josef Dietz

Abstract

The regulation of gene activity is a crucial factor in coordinating development, growth and acclimation to environmental changes. By this means, metabolic processes are adjusted according to cellular needs by changing gene expression patterns. In the genome of the model plant *Arabidopsis thaliana*, more than 7% of the genes are estimated to encode proteins directly involved in gene regulation. Transcription factors (TFs) are able to bind to specific DNA motifs named *cis*-elements and control the expression of target genes. The regulation may be either activation, stimulation, inhibition or suppression. The activation of genes is mediated by well-coordinated protein–protein interactions between transcription factors and a various number of cofactors. The gene activation networks are still poorly understood. In order to address the involved protein–DNA and protein–protein interactions, a number of methods have been developed that efficiently address *cis*-element interacting partners. This chapter describes two powerful methods: the yeast one-hybrid system and the yeast two-hybrid system. In combination these techniques provide the ability to identify *cis*-element-binding transcription factors and their upstream interaction partners.

Key words: Protein–protein interactions, transcription factors, yeast one-hybrid system, yeast two-hybrid system.

1. Introduction

In the late 1990s Stanley Fields and Ok-kyu Song described a revolutionary method for identifying protein interaction partners, the yeast two-hybrid screen (1). The big advantage of this technique is its capability to identify a high number of protein

R. Sunkar (ed.), *Plant Stress Tolerance*, Methods in Molecular Biology 639,
DOI 10.1007/978-1-60761-702-0_10,

interaction partners in an easy straightforward approach and within a reasonable short time period.

The yeast two-hybrid system is based on the fact that many eukaryotic transcription factors contain at least two physically and functionally independent domains. For example, the well-characterized *Saccharomyces cerevisiae* GAL4 transcription factor is a 99.35-kDa protein (2). Its DNA-binding domain (BD) is encoded in the first 147 amino acids, whereas its transactivation domain (AD) is encoded in the amino acids 768–881 (3).

Fields and Song (1) showed that the separation of the BD domain from the AD domain of GAL4 transcriptional activator did not affect their activity after reconstitution. This feature was utilized to design bait and prey vectors, first expressing the GAL4 BD domain and then the GAL4 AD region. To investigate new protein–protein interactions, a known bait protein is fused to the GAL4 BD domain. The second vector contains either a cDNA library element or a gene encoding another specified protein downstream of the GAL4 AD activation domain. As selection markers, both vectors harbour genes involved in amino acid biosynthesis. The suitable *S. cerevisiae* host strain lacks the corresponding genes. Host cells expressing the marker genes that are contained on both vectors have the ability to grow on selective media lacking the appropriate amino acids.

In the case of positive interaction between the bait protein and its putative interacting partner, the fused GAL4 BD and AD are localized close enough to act as a fully functional GAL4 transcription activator (**Fig. 10.1**). The GAL4 BD interacts with specific GAL1, GAL2 and MEL1 upstream activating sequences (UASs) in the reporter gene promoter. The positioned AD domain initiates the assembly of the preinitiation complex (PIC) and causes the expression of the reporter gene (4).

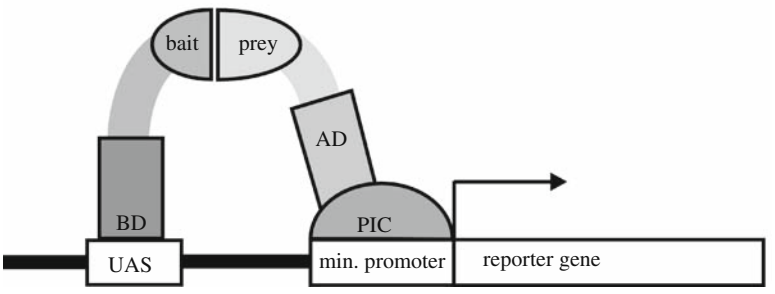

Fig. 10.1. Scheme for the activation mechanism of a reporter gene in yeast two-hybrid system. The GAL4 DNA-binding domain (BD) binds to the upstream activating sequence (UAS) upstream of the reporter gene minimal promoter. The binding of an appropriate partner protein to GAL4 activation domain (AD) mediates assembly of the preinitiation complex (PIC) and results in transcription of the reporter gene.

In subsequent work, modifications of the yeast two-hybrid system were introduced, one of which was the yeast one-hybrid system. In contrast to other descendants, this powerful technique allows researchers to identify proteins with DNA-binding properties. This special ability is utilized to investigate transcription regulation mechanisms of genes and helps to characterize transcription-regulative *cis*-elements inside promoter regions (**Fig. 10.2**). In the case of the yeast one-hybrid system also, two vectors are required. The bait carries a target DNA element upstream of a reporter gene. Similar to the yeast two-hybrid system, each one-hybrid system vector also harbours a gene for nutrient selection. The prey vector is similar to that in the two-hybrid system, except its lower copy number in yeast cells and decreased expression level of prey proteins.

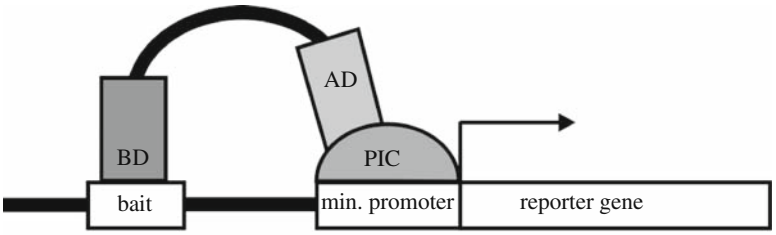

Fig. 10.2. Activation mechanism of a reporter gene in the yeast one-hybrid system. The GAL4 activation domain (AD) fused to a protein with putative DNA-binding properties interacts with the DNA bait element and arranges the GAL4 AD domain close to the minimal promoter of the reporter gene. The reporter gene activation is the result of the interaction between the AD domain and the PIC subunits.

2. Materials

2.1. cDNA Library Construction

2.1.1. First-Strand cDNA Synthesis

1. SMART III primer (Clontech)
   5′-AAGCAGTGGTATCAACGCAGAGTGGCCATTA TGGCCGGG-3′.
2. CDS III primer (Clontech)
   5′-ATTCTAGAGGCCGAGGCGGCCGACATG-$d(T)_{30}$-3′.
3. MMLV reverse transcriptase (Promega).
4. First-strand buffer (5×; Promega).
5. RNase H (NEB Biolabs).
6. DTT (dithiothreitol) (20 mM).
7. dNTP mix (10 mM each).

2.1.2. cDNA Amplification

1. 5′-PCR primer 5′-TTCCACCCAAGCAGTGGTATCAACGCAGAGTGG-3′.
2. 3′-PCR primer 5′-TATCGATGCCCACCCTCTAGAGGCCGAGGCGGCCGACA-3′.
3. GC-Melt solution (10×; Clontech).
4. Advantage 2 PCR Kit (Clontech).

2.2. One-Hybrid Screen

1. Genomic DNA containing the promoter region of interest.
2. Double-stranded cDNA library constructed with SMART technique.
3. pHIS2: bait vector with *TRP1* marker and *HIS3* reporter gene (Clontech); pGADT7-Rec2 AD: GAL4 AD domain fusion vector with *LEU2* marker.
4. pHis2 reverse primer: 5′-ATCGAGTGCTCTATCGCTAG-3′.
5. pGADT7-Rec2 prey vector: GAL4 AD fusion vector with *LEU2* selection marker (SmaI linearized).
6. *S. cerevisiae* strain Y187: *MATα, ura3–52, his3–200, ade2–101, trp1–901, leu2–3, 112, gal4Δ, gal80Δ, met–, URA3::GAL1*$_{UAS}$*–GAL1*$_{TATA}$*–LacZ MEL1.*

2.3. Two-Hybrid Screen

1. *S. cerevisiae* strain AH109: *MATa, trp1–901, leu2–3, 112, ura3–52, his3–200, gal4Δ, gal80Δ, LYS2::GAL1*$_{UAS}$*–GAL1*$_{TATA}$*–HIS3, GAL2*$_{UAS}$*–GAL2*$_{TATA}$*–ADE2, URA3::MEL1*$_{UAS}$*–MEL1*$_{TATA}$*–lacZ.*
2. pGBKT7 bait vector: GAL4 BD fusion vector with *TRP1* selection marker.
3. Available prey cDNA library from organism of interest inserted into appropriate AD fusion vector such as pAct2. For selection purposes this vector carries a *LEU2* marker.

2.4. Additional Material

1. LB (Luria–Bertani) medium (1 L): 10 g tryptone, 10 g yeast extract, 5 g NaCl [add 1.8 % (w/v) agar for solid medium].
2. Ampicillin (Sigma).
3. Kanamycin sulphate (Sigma).
4. YPDA medium (1 L): 20 g peptone, 10 g yeast extract, 15 mL of 0.2% filter-sterilized adenine hemisulphate; for plates add 20 g agar.

5. Amino acid solution (10×, 1 L): 200 mg L-adenine, 200 mg L-arginine, 200 mg L-histidine, 300 mg L-isoleucine, 1,000 mg L-leucine, 300 mg L-lysine, 200 mg L-methionine, 500 mg L-phenylalanine, 2,000 mg L-threonine, 200 mg L-tryptophan, 300 mg L-tyrosine, 200 mg L-uracil, 1,500 mg L-valine.
   Exclude amino acids to produce appropriate dropout (DO) solution.
6. Autoclaved glucose stock (40%, w/v).
7. 3-Amino-1,2,4-triazole (3-AT): filter-sterilized 1 M stock, stored at −20°C.
8. Synthetic drop out medium (SD): autoclave 0.67% yeast nitrogen base (Dofco) solution. Depending on selection, add 1:10 volume of appropriate 10× amino acid solution and 40% glucose stock solution to a final concentration of 2%. If necessary, add also the His3 inhibitor 3-AT to suppress the background growth. For plates, use the agar concentration of 2% w/v.
9. Polyethylene glycol (PEG) stock (50%, w/v): filter-sterilized 3350 PEG (Sigma).
10. TE buffer (10×): 0.1 M Tris–HCl, 10 mM EDTA, adjust to pH 7.5 and autoclave.
11. LiAc solution (10×): 1 M lithium acetate (Sigma), adjust to pH 7.5 with acetic acid and autoclave.
12. TE/LiAc solution (10 mL): 1 mL of 10× TE buffer, 1 mL of 10× LiAc solution, 8 mL sterile H_2O, prepare fresh before use.
13. PEG solution (10 mL): 1 mL of 10× TE buffer, 1 mL of 10× LiAc solution, 8 mL of 50% GEP stock, prepare before use.
14. Sheared salmon sperm DNA (Sigma): 5 mg/mL; denaturate the DNA by boiling appropriate volume at 95°C for 5 min before use and cool immediately on ice.
15. Z-buffer (1 L): 16.1 g Na_2HPO_4, 5.5 g NaH_2PO_4, 0.75 g KCl, 0.246 g $MgSO_4$, adjust to pH 7.0 and autoclave.
16. X-Gal stock: prepare an X-Gal (5-bromo-4-chloro-3-indolyl-β-D-galactopyranoside) in 20 mg/mL *N*,*N*-dimethylformamide (DMF) solution and store it at −20°C.
17. Z-buffer/X-Gal working solution: 100 mL Z-buffer, 0.27 mL β-mercaptoethanol, 1.67 mL X-Gal stock.
18. Rescue buffer: 50 mM Tris–HCl (pH 7.8), 10 mM EDTA, 0.3% β-mercaptoethanol.

19. Lysis solution: 50 mM Tris–HCl (pH 7.8), 10 mM EDTA, 0.3% β-mercaptoethanol, 2,000 U/mL β-glucuronidase from *Escherichia coli* (Sigma).
20. Wizard® Plus SV Minipreps DNA Purification System (Promega).
21. Wizard® SV Gel and PCR Clean-Up System (Promega).

3. Methods

In this chapter we provide instructions for two highly potent techniques to identify DNA–protein and protein–protein interacting partners. Both techniques essentially follow the same work flow. Once optimized, one is able to switch between one- and two-hybrid screenings without any big trouble (**Fig. 10.3**).

3.1. One-Hybrid Bait Construction

Co-expression of genes involved in the same or similar pathways can be driven by the same regulatory mechanism. The analysis of this co-regulation is one possible first step in the determination

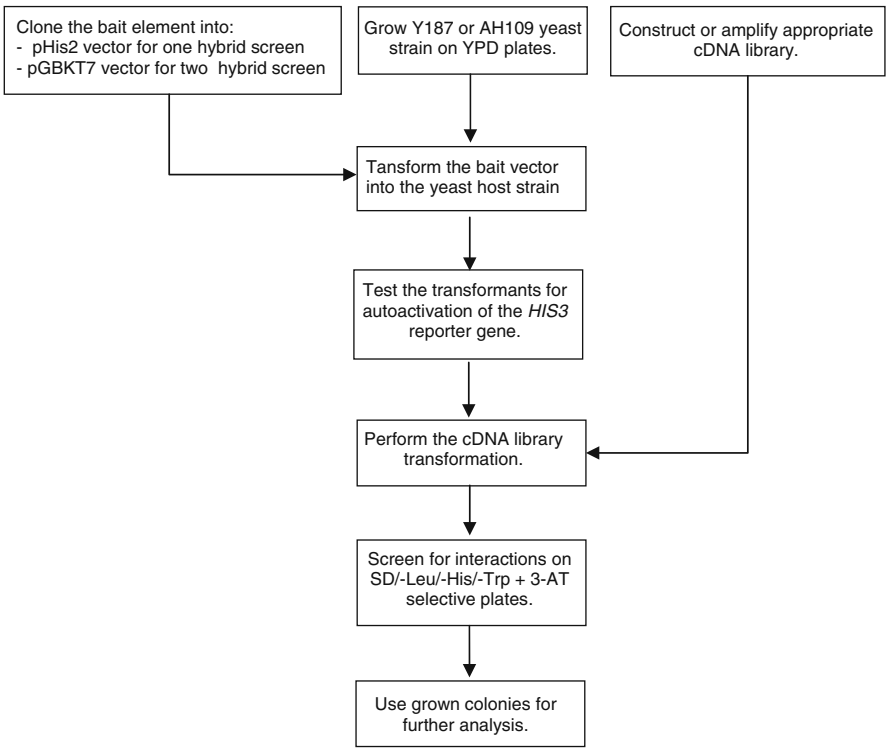

Fig. 10.3. Experimental workflow to identify DNA–protein and protein–protein interactors using the yeast one-hybrid and yeast two-hybrid system.

of bait elements. Publicly available online tools using microarray data sets are suitable tools to start with. Promoter regions of genes showing similar expression pattern must be compared and common putative *cis*-elements determined. Next step is to confirm these promoter elements in vivo by deletion experiments. Based on a combination of bioinformatics and in vivo data a promising bait element can be constructed by PCR amplification from the determined promoter section. Alternatively, a completely empirical approach may take advantage of an easily scorable trait such as the activation or the inhibition of reporter gene expression. In combination with site-directed mutagenesis, this approach allows to identify regulatory *cis*-elements within a promoter of interest.

To avoid false-positive signals, the bait pHis2 vector carries a yeast low-copy CEN6/ARS4 origin. Downstream of a *HIS3* minimal promoter it carries a *HIS3* reporter gene. The DNA element of interest should be inserted into the multiple cloning site upstream of the mentioned minimal promoter.

1. In the very beginning the DNA region of interest should be amplified with appropriate restriction sites for the insertion into the bait vector pHis2.
2. Clone the putative *cis*-element into pHis2 vector by standard cloning procedure.
3. For amplification purposes, transform the ligation reaction into *E. coli* DH5α host strain and select for clones on LB agar plates with 50 μg/mL kanamycin.
4. Identify positive clones via colony PCR by using vector-specific pHis2 reverse primer and insert specific forward primer.
5. Incubate several of these colonies overnight in 6 mL LB/kanamycin liquid media. Extract the pHis2 vector using a standard plasmid purification protocol and verify the presence as well as the right orientation of the insert by PCR reaction using purified vector as template.
6. Determine sequence of the inserted DNA showing positive PCR signal and verify the result by comparison with reported sequence in DNA database.
7. Use the small-scale transformation protocol (**Section 3.1.2**) to introduce the bait pHis2 vector into Y187 cells.
8. To get isolated colonies on selective agar medium, plate each 100 μL of 1:100 and 1:1,000 dilution, respectively, on SD/-Trp selective medium.
9. Seal the plates with parafilm and incubate them at 30°C until colonies appear.

3.1.1. Yeast Competent Cell Preparation

The lithium acetate method for preparation of highly competent *S. cerevisiae* cells is easy to handle and saves time. Additionally it provides transformation efficiency of about 10^6 colonies per 1 μg of vector DNA (5, 6). A very high transformation efficiency of competent yeast cells is required especially for yeast transformation with cDNA libraries as prey molecules since a representative coverage of all expressed genes is essential. For this efficiency reason, a large number of optimized small- and large-scale transformation protocols have been developed based on the lithium acetate method.

For best transformation results, prepare new working plates of yeast strains every 4 weeks. Use fresh yeast colonies of at least 2 mm in diameter for competent cell preparation.

1. Inoculate 5 mL YPDA or appropriate SD liquid selection media with a single yeast colony and grow the culture at 30°C with 170 rpm shaking for at least 16 h.
2. Prepare a sterile 250-mL flask with 50 mL prewarmed appropriate liquid medium and transfer sufficient volume of your overnight culture to reach an $OD_{600\ nm}$ of 0.2.
3. Incubate the culture on a shaker with 170 rpm at 30°C until the cell density reaches an $OD_{600\ nm}$ value of approximately 0.5–0.6.
4. Collect the cells in two 50-mL centrifugation tubes at room temperature by centrifugation at 700×*g* for 5 min.
5. Discard the supernatant by inverting the tubes and remove the remaining medium by washing the sediment with 50 mL sterile H_2O and centrifuge the cells as described above.
6. Remove the supernatant completely and then resuspend the cell pellets in 1.5 mL of 1× TE/LiAc solution.
7. Collect the cell by centrifugation at high speed for 15 s. Resuspend the cell pellet in 600 μL of 1× TE/LiAc solution. The yeast cells are now in a competent state and ready for transformation.

3.1.2. Small-Scale Yeast Transformation

1. Prepare yeast competent cells (**Section 3.1.1**).
2. Combine 0.2 μg of the vector with 0.2 mg denatured herring testes carrier DNA in a fresh 1.5-mL tube.
3. Transfer 100 μL competent yeast cells to the DNA mixture and mix the tube by vortexing.
4. Add 600 μL of the PEG/LiAc solution to the transformation reaction and incubate the tube at 30°C for 30 min. Keep cells in solution by gently mixing every 10 min.
5. To increase the transformation efficiency, add 70 μL DMSO and mix the solution by inverting the tube.

6. Place the reaction in 42°C water bath for 15 min.
7. Cool the transformed cell suspension on ice for 2 min.
8. Sediment the cells by centrifugation at 13,000×*g* for 10 s and remove the supernatant.
9. Resuspend the cells in 0.5 mL sterile H_2O or 1× TE buffer.
10. Plate the transformants on appropriate selective agar plates.

3.1.3. Compensation of Leaky Expression of HIS3 Reporter Gene

The expression of the *HIS3* reporter gene is crucial for the success of the yeast one-hybrid screen. Unfortunately its expression is not fully controllable. Due to the presence of P_{min}*HIS3* promoter the *HIS3* reporter gene is transcribed even in the original pHis2 vector. This basal level may be increased after inserting a DNA fragment of the plant promoter of interest. Therefore each bait element must be tested separately for reporter gene expression level. The titration with competitive inhibitor 3-amino-1,2,4-triazole (3-AT) of the *HIS3* gene product is used to eliminate the background growth caused by leaky expression of *HIS3* gene.

1. Use the small-scale transformation protocol (*see* **Section 3.1.2**) to transform the bait element containing pHis2 vector into Y187 yeast strain cells and plate an aliquot of 10 μL on 150-mm SD/-Trp master plates.
2. Incubate the plates at 30°C until colonies appear.
3. Restreak several colonies on SD/-Trp/-His plates containing different 3-AT concentrations. Start with 10 mM and increase the 3-AT concentration up to 70 mM.
4. Analyse the growth ability of each clone on the plates after 7 days of incubation at 30°C (*see* **Note 1**). Clones showing no growth on plates with certain 3-AT concentration must be recovered from the master plate and stored as glycerol stock at −70°C for following screens.

3.2. Construction of cDNA Library for Recombinatorial Cloning

One essential precondition for successful identification of *cis*-element-interacting proteins or pure protein interactions is a good-quality cDNA library which should represent all genes expressed by the organism or the tissue of interest. Additionally the protein-encoding regions should be available as full-length molecules in the right codon reading frame to guarantee the proper function of putative interactors.

The guidelines given below provide the method to generate a highly diverse and full-length cDNA library from small amounts of purified total RNA or mRNA (7). In combination with prey vectors such as pGADT7-Rec2 or pGADT7-Rec, it is directly usable for yeast one- and two-hybrid screenings (Clontech).

3.2.1. SMART First-Strand cDNA Synthesis

SMART (*s*witching *m*echanism *a*t 5′-end of *R*NA *t*ranscript) technology is a PCR-based technique for cDNA library construction. A special oligo (dT) primer containing an additional CDS III sequence at its 5′-end is used as oligonucleotide for the first-strand synthesis. In the process of cDNA synthesis, MMLV (Moloney murine leukaemia virus) reverse transcriptase adds several deoxycytidines to the 3′-end of the cDNA strand independent of the template (8). This deoxycytidine region helps to anneal with the 3′-end of the SMART III primer. Once hybridized the MMLV reverse transcriptase switches the template and completes the first cDNA strand, containing a 3′-end complementary to the SMART III primer.

1. Purify either the total RNA or ideally poly(A)-tailed mRNA which is highly enriched in protein-coding transcripts with preferred method and test its quality by denaturing agarose gel electrophoresis (*see* **Note 2**). Consider thoroughly the plant growth condition that is optimal for RNA isolation, e.g. the tissue type and plant age, the stress regime, its duration and strength. In order to identify it in the screening, the proteins of interest must be expressed under the respective conditions.
2. The reverse transcription reaction has to be prepared in an RNase-free 250-μL tube, by adding the following:
   a. RNA (2.0 μL; 0.5 μg poly(A) mRNA or 2 μg total RNA).
   b. CDS III-extended primer (1.0 μL).
   c. RNase-free H_2O (1.0 μL).
3. Mix the components carefully and spin down the solution.
4. Denature the secondary structure of the RNA molecules by incubation at 72°C for 2 min and immediately cool the sample on ice for 2 min.
5. Combine the reaction with
   a. First-strand buffer (2 μL, 5×).
   b. DTT (1.0 μL, 20 mM).
   c. dNTP mix (1.0 μL).
   d. MMLV reverse transcriptase (1.0 μL).
6. Store the sample at 42°C for 10 min and add 1 μL SMART III oligonucleotide.
7. Perform the reverse transcriptase reaction at 42°C for 1 h. Terminate the first-strand synthesis by heat inactivation of MMLV reverse transcriptase by placing the reaction tube into a thermostat of 75°C for 10 min.
8. After cooling on ice, add 1 μL RNase H to the reaction. RNase H hydrolyses RNA in RNA–DNA hybrid molecules. Then incubate the sample at 37°C for further 20 min. The

constructed first-strand cDNA may be stored at −20°C for 2 months.

3.2.2. Second-Strand Synthesis

The second-strand cDNA synthesis consists of an ordinary two-step PCR reaction using 5′- and 3′-primers which are complementary to cDNA-flanking SMART III and CDS III regions. The desired number of PCR cycles for cDNA library amplification depends on the quality and amount of mRNA you started with. To keep the cDNA library diversity high, the number of amplification steps should be kept to a minimum. In our hands, experiments with a wide range of 16–30 amplification cycles still gave satisfactory results.

1. The second strand is produced by PCR:
   a. First-strand cDNA (5 μL)
   b. Sterile H_2O (70 μL)
   c. Advantage 2 PCR buffer (10 μL)
   d. dNTP mix (2 μL)
   e. 5′-PCR primer (2 μL)
   f. 3′-PCR primer (2 μL)
   g. GC-Melt solution (10 μL, 10×)
   h. Advantage 2 polymerase mix (2 μL, 50×)
2. Before starting the PCR reaction, mix the reaction gently and centrifuge the solution down.
3. Use the following two-step PCR program to amplify the second DNA strand (*x* denotes the amplification cycles usually between 16 and 30, see above):
   a. 30 s at 95°C
   b. 10 s at 95° C
   c. 6 min at 68° C
   } *x* cycles
   d. 5 min at 68°C
4. Check for sufficient cDNA second-strand amplification by loading 10 μL of the PCR reaction on 1.2% agarose gel besides 0.25 μg of a 1-kb DNA marker and separate the double-stranded cDNA at 130 V for 15 min. Keep the remaining PCR product on ice (*see* **Note 3**).
5. Remove DNA fragments caused by incomplete amplification and unspecific primer hybridization before continuing with the yeast one-hybrid screening. Therefore, use either a cDNA size fractionation column or separate the PCR product on 1.2% agarose gel and extract DNA fragments with sizes bigger than 400 bp.
6. Concentrate finally the purified double-stranded cDNA library in 20 μL H_2O by ethanol precipitation and store it at −20°C.

3.3. Yeast One-Hybrid Library Screening Protocol

To show the functionality of the described one-hybrid system, a 385-bp promoter region of stromal ascorbate peroxidase (*sAPX*) gene from *Arabidopsis thaliana* was chosen as bait and cloned into the pHis2 vector, tested for *HIS3* reporter gene autoactivation and finally screened against *A. thaliana* cDNA library using the protocol described below.

1. Prepare competent Y187 strain yeast cells containing the bait vector.
2. Denature a 50 μL aliquot of herring testes carrier DNA by boiling at 100°C for 5 min and cool it on ice immediately.
3. Combine the following components in a sterile 15-mL tube:
   a. 30 μL denatured herring testes carrier DNA (5 mg/mL) (*see* **Note 4**)
   b. 10 μL SmaI-hydrolysed pGADT7-Rec2 vector (0.5 μg DNA/μL)
   c. 20 μL purified ds cDNA
4. Transfer 600 μL competent cells to the DNA mixture and vortex the transformation reaction at low speed.
5. Add 2.5 mL PEG/LiAc solution and mix by gentle vortexing.
6. Incubate the cells for 45 min at 30°C. Mix the cells every 15 min by tapping to keep in solution.
7. For high transformation efficiency, add 160 μL DMSO to the solution and mix by thorough swirling.
8. Heat shock the cells in a 42°C water bath for 20 min. Mix the cells every 10 min to assure that they stay in solution.
9. Spin down the cells by centrifugation at 700×*g* for 5 min, discard the supernatant and resuspend the cells in 3 mL YPD liquid media.
10. After a 90-min recovery period at 30°C with 170 rpm shaking, collect the cells by centrifugation at 700×*g* at room temperature for 5 min.
11. Remove the complete supernatant and resuspend the cells in 6 mL NaCl solution.
12. Spread aliquots of 150 μL on 150 mm Ø Petri plates containing SD/-Leu/-His/-Trp with optimal 3-AT concentration agar media.
13. In order to determine the transformation efficiency of cDNA library, plate also each of the 1:10, 1:100 and 1:1,000 dilutions of the culture on 150-mm SD/-Leu and SD/-Leu/-Trp plates.

14. Incubate the plates at 30°C for 5 days and recover growing clones to verify the interaction.
15. To quantify the transformation efficiency, count the colonies on 1:10, 1:100 and 1:/1,000 SD/-Leu/-Trp dilution plates. Use the following formula to determine the number of screened clones (*see* **Note 5**):

$$\frac{\text{Colonies on SD/-Leu/-Trp (multiplication point) dilution (multiplication point) 6ml}}{\text{volume plated (mL)}} = \text{screened clones}$$

In the case of our promoter screening experiment a set of 21 colonies grew on SD/-Leu/-Trp/-His + 3-AT selective plates after 5 days of incubation. To exclude false positives we followed the positive interaction verification test as described below (**Section 3.5**).

3.3.1. Bait Construction for Yeast Two-Hybrid Screen

Investigations of protein–protein interactions with the two-hybrid system require the construction of a bait vector. The full-length coding cDNA of the bait protein has to be cloned in-frame downstream of the GAL4 BD into the pGBKT7 vector. Follow steps below to construct a two-hybrid system bait element.

1. Determine the coding sequence of your target protein and design primers with restriction sites on 5′- and 3′-ends for cloning into pGBKT7 vector. Check for preservation of codon reading frame.
2. Amplify the sequence by standard PCR reaction and purify the fragments using PCR purification kit.
3. Digest the PCR product and the pGBKT7 vector with appropriate restriction endonucleases and purify them as described above.
4. Insert the protein-coding sequence into the pGBKT7 vector by ligation reaction overnight.
5. Use the complete ligation reaction for transformation into *E. coli* DH5α strain and plate the transformants on LB agar plates containing 50 μg/mL kanamycin and incubate the plates overnight at 37°C.
6. Check grown colonies for the presence of the bait element by performing a colony PCR.
7. Prepare 5 mL liquid culture inoculated with positive clones and extract the vector for further confirmations like vector PCR and sequencing. Prepare a glycerol stock by adding sterile glycerol to final concentration of 25% and store aliquots at −75°C.
8. Sequence the bait element using sequencing primer and check the sequence and correct the reading frame of the bait element.

3.3.2. HIS3 Auto-expression in AH109 Yeast Strain

The reporter gene *HIS3* that is usually used in the two-hybrid system is under the control of the GAL4 transcription activator. A basal expression of the gene often leads to a significant number of false-positive clones. Therefore, similar to the one-hybrid system, the autoactivation of each gene should be tested and if necessary the leakiness must be suppressed by addition of 3-AT (*see* **Note 6**).

1. Transform the AH109 yeast strain cells with the pGBKT7 bait vector containing the protein of interest using the small-scale transformation protocol (**Section 3.1.2**).
2. Restreak AH109 growing clones on SD/-Trp/-His + 3-AT agar plates. Optimize the 3-AT concentration required to suppress the basal expression of the *HIS3* gene.
3. Seal the plates with parafilm and incubate them at 30°C for 1 week.
4. Based on the colony growth on SD/-Trp/-His + 3-AT selective plates, determine the 3-AT concentration sufficient to suppress the activity of the *HIS3* gene product. Use this inhibitor concentration for your two-hybrid screens.

3.4. Large-Scale Yeast Transformation

1. Prepare 50 mL SD/-Trp medium in a 250-mL flask and inoculate with a single yeast colony harbouring the constructed bait vector.
2. Grow the culture with shaking at 30°C for 16 h. Warm up 200 mL SD/-Trp liquid media in the incubator.
3. Centrifuge the overnight culture, discard the supernatant and transfer sufficient cells into prewarmed 200 mL SD/-Trp medium to get the OD_{600} between 0.2 and 0.3.
4. Incubate the culture at 30°C with 200 rpm shaking for at least two cell divisions which takes about 4–5 h.
5. Prepare the following transformation mix in a sterile 50-mL tube:
   a. PEG 50% (v/v), 7.2 mL
   b. LiAc (1.0 M), 1.08 mL
   c. Single-stranded carrier DNA (5 mg/mL) (*see* **Note 4**), 1.5 mL
   d. cDNA library (pAct2) (40 μg) + H_2O, 1.02 mL
6. Collect the cells in sterile 50-mL tubes by centrifugation at 700×*g* for 5 min at room temperature and discard the supernatant.
7. Remove the medium by washing the pellets in 50 mL sterile H_2O and repeat the centrifugation step as described above.

8. Resuspend each cell pellet in 10 mL H_2O, pour the cells in a single tube and collect them by centrifugation at 700×*g* at room temperature for 5 min.
9. Discard the supernatant completely and resuspend the cells thoroughly by adding the transformation mix.
10. Incubate the cells at 30°C for 45 min. To keep the cells in solution, gently mix the reaction every 15 min.
11. Place the cells in 42°C water bath for 20 min and mix every 10 min.
12. Collect the cells by centrifugation at 700×*g* for 5 min at 20°C and discard the supernatant.
13. Resuspend the transformants in 20 mL sterile H_2O and plate 400 μL aliquots on 150-mm Ø plates containing SD/-Trp/-Leu/-His + optimal 3-AT concentration.
14. Determine the transformation efficiency by plating 100 μL of 1:100 and 1:1,000 dilutions on SD/-Trp and SD/-Trp/-Leu agar plates.
15. Seal the plates with parafilm and incubate the plates for 7 days at 30°C (*see* **Note 7**).
16. Collect growing clones and proceed with confirming the interaction (**Section 3.5**).

3.5. Strategies to Confirm Positive Interactions

In the case of the one-hybrid screening, the positive DNA–protein interaction and in the two-hybrid assay the protein–protein interplay should enable the growth of colonies on selective SD/-Leu/-Trp/-His + 3-AT agar plates within 7 days. As already mentioned the described methods are very sensitive and according to many reports the majority of primary screened clones show false-positive signals. Depending on the screening type, follow the appropriate instruction to eliminate the false-positive clones (**Fig. 10.4**).

3.5.1. Test of Positives from Primary Yeast One-Hybrid Screen

Rescue fast-growing clones and replate them on SD/-Leu/-His/-Trp plates with increasing 3-AT amounts (**Note 8**), starting with previously determined optimal concentration. Unfortunately, not every growing colony represents a real positive interaction. According to our experience, a high number of replated primary clones produce very small colonies or fail to grow at all (**Fig. 10.5**) (*see* **Note 9**). To verify the DNA–protein interaction in rescued clones, reproduce the result by repeated vector transformation (*see* **Note 10**). First extract the prey protein-encoding vector from yeast cells using "extraction of prey vectors" method (**Section 3.5.2.2**). Retransform the vector again into yeast cells strain harbouring previously used bait element. Use the original pHis2 prey vector as negative control.

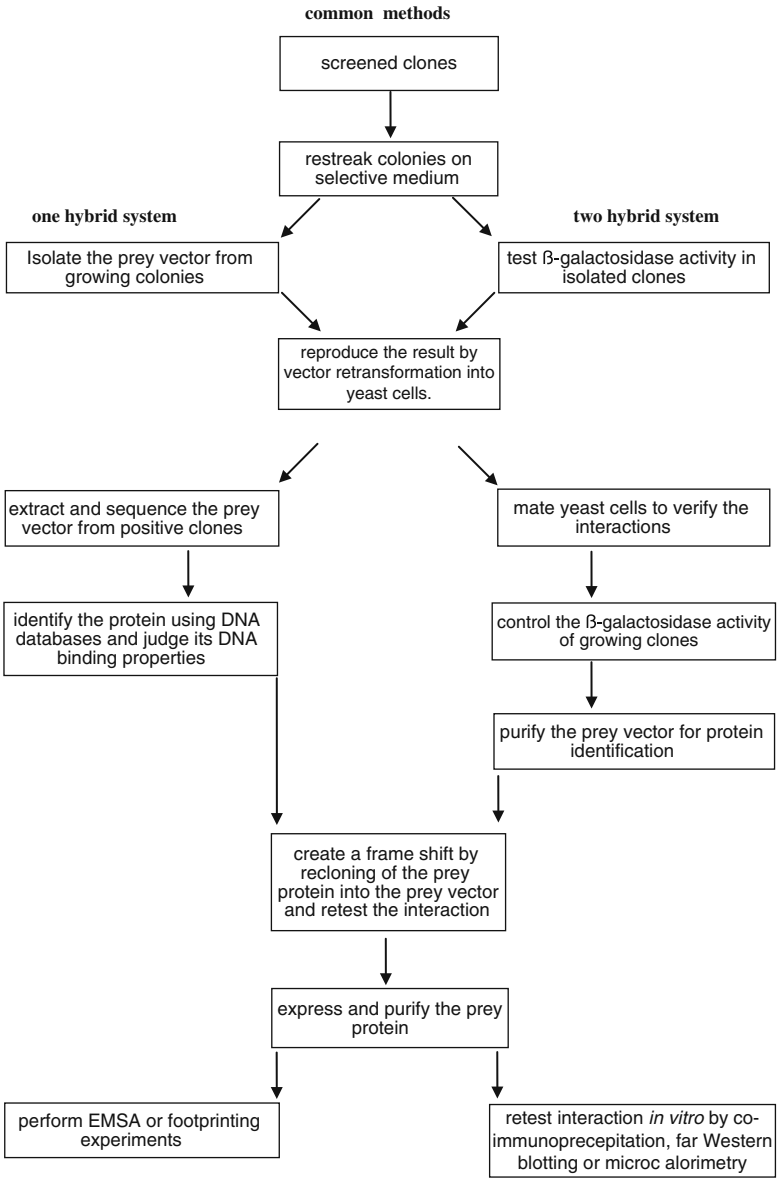

Fig. 10.4. Workflow to isolate true-positive interaction partners among rescued clones in one- and two-hybrid screenings.

Plate the transformants on agar plates containing SD/-Leu/-Trp/-His + optimal 3-AT concentration and incubate them at 30°C for 5 days. This second in vivo selection will decrease the number of clones with putative interactions. Among 21 rescued clones showing positive interaction with the sAPX promoter region of interest, only clone 21 was able to grow after the retransformation into yeast. To target the region containing the putative *cis*-element inside the sAPX promoter fragment, split the

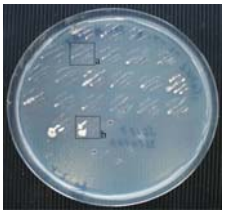

Fig. 10.5. In the one-hybrid screen using an sAPX promoter fragment as bait, 21 clones showing positive protein–DNA interaction were restreaked on SD/-Leu/-His/-Trp +3-AT agar plate. For interaction verification by retransformation analysis, prey vectors from growing clones 1, 11, 14, 15 and twice clone 21 were extracted and sequenced. The dotted squares labelled with (*a*) and (*b*) represent two individual restreaks: (*a*) with little growth of a false-positive and (*b*) vigorous growth of a true-positive interaction.

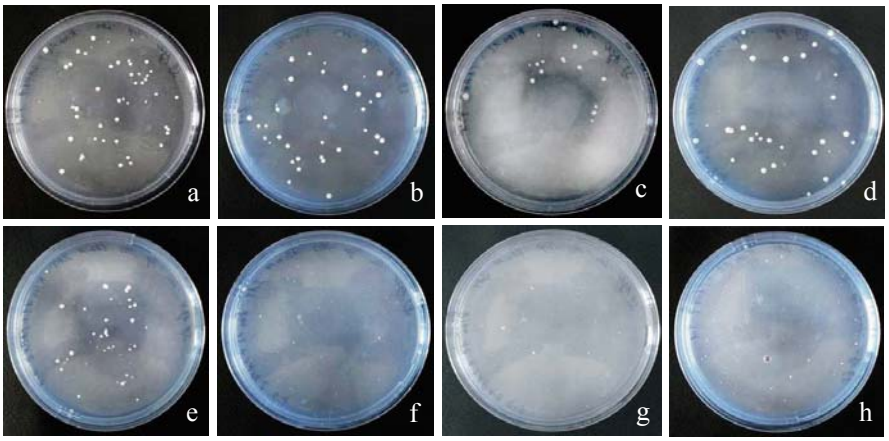

Fig. 10.6. Result of the one-hybrid screen with four subfragments of the sAPX promoter region. The control transformation for each fragment was plated on SD/-Trp/-Leu agar plates (**a–d**). The DNA–protein interaction was screened on SD/-Trp/-His/-Leu + 30 mM 3-AT selective plates (**e–h**). A positive interaction was observed between a *cis*-element within the first subfragment of the sAPX promoter region (**e**) as seen by colony growth.

bait element into four fragments with overlapping ends and clone separately into pHis2 vector. For each subfragment, perform a one-hybrid screen (**Fig. 10.6**).

The purified prey vector from clone 21 was sequenced and the results were used for further in silico studies (*see* **Note 11**). The nucleotide and amino acid sequences were analysed by comparing with NCBI blast and database tools (http://blast.ncbi.nlm.nih.gov/Blast.cgi).

Analysis of the amino acid sequence revealed a known DNA-binding domain and classified the protein as an ANAC transcription factor. The final proof for the DNA–protein interaction has to be done in vitro. The identified putative prey protein must be expressed and purified. Use the electrophoretic mobility shift assay (EMSA) or DNA footprinting technique to prove the interaction between the target DNA element and the identified DNA-binding protein.

3.5.2. Test of Positives from Primary Yeast Two-Hybrid Screening

The protein–protein interaction specificity of growing clones can be tested by restreaking the colony on SD/-Leu/-His/-Trp/-Ade + increasing 3-AT concentration containing 150-mm Ø agar plates. Due to the fact that GAL4 transcription activator also controls the *ADE2* gene expression of the AH109 yeast strain, the false-positive colonies develop reddish coloured phenotype on L-adenine-lacking SD/-Leu/-His/-Trp/-L-Ade agar medium. Strong interaction between the bait and the prey activates the *ADE2* reporter gene and turns the colony colour to white.

3.5.2.1. β-Galactosidase Filter Lift Assay

In AH109 yeast strain, the *lacZ* reporter gene is controlled by the GAL4 transcription activator. Positive bait–prey interaction activates the expression of the *lacZ* gene and leads to accumulation of β-galactosidase. This enzyme is able to cleave β-D-galactosides with a diverse range of aglycone groups. The cleavage takes place between the glycosyl oxygen and the anomeric partner molecule. In the case of synthetic X-Gal (5-bromo-4-chloro-3-indolyl-β-D-galactoside) as substrate, the hydrolase reaction produces D-galactose and the easily detectible blue-coloured 5-bromo-4-chloro-indigo molecules (9). The following protocol was adapted from Clontech laboratories:

1. Pre-wet a round filter paper of suitable size to cover the entire Petri dish surface with Z-buffer/X-Gal solution.
2. Place an identical but clean filter carefully on SD/-Leu/-His/-Trp/-Ade + 3-AT plates. Make sure that clones of each colony are transferred on the filter. For subsequent identification of positive clones, mark the filter position on the Petri dish.
3. Using forceps transfer the filter with clones in liquid nitrogen and freeze it for 20 s.
4. Remove the filter from liquid nitrogen and place it with clone side up on the presoaked Z-buffer/X-Gal filter (*see* **Note 12**).
5. Incubate the filter at 30°C for 8 h. Clones with positive protein–protein interaction should be revealed by the development of blue colour.
6. Blue-coloured clones indicate the expression of the *LacZ* reporter gene. Rescue these colonies from the original plate and grow them on separate SD/-Leu/-His/-Trp/-Ade + 3-AT agar plates.

3.5.2.2. Extraction of Prey Vectors from Yeast

The protocol described below provides a simple and reliable method for vector extraction from yeast cells.

1. Inoculate a single yeast clone into 5 mL SD/-Leu liquid medium and grow at 30°C with shaking overnight.

2. Centrifuge for 20 s at 13,000×*g* to sediment the cells. Remove the medium, wash the cells twice with 1 mL sterile H_2O and once with rescue buffer.
3. Resuspend the yeast cells in 25 μL lysis buffer and incubate at 37°C for 1 h.
4. Add 25 μL of 10% SDS solution and incubate at room temperature for a further 1 min.
5. Add 100 μL of 7.5 M ammonium acetate to the reaction and place it at −70°C for 20 min.
6. Thaw the reaction slowly on ice and centrifuge it at 13,000×*g* at 4°C for 15 min.
7. Transfer the DNA-containing supernatant into a fresh 1.5-mL tube and add 300 μL isopropanol. Precipitate the DNA on ice for 20 min.
8. Centrifuge at 13,000×*g* at 4°C for 15 min and aspirate the complete supernatant.
9. Wash the DNA with 300 μL of 70% ethanol. Remove ethanol and dry the DNA in air at room temperature.
10. Resuspend the DNA in 10 μL H_2O. Transform the extracted DNA into *E. coli* DH5 strain and grow the transformants on LB–ampicillin plates for 16 h.
11. Pick several *E. coli* clones and extract the prey vector by standard mini-plasmid preparation protocol.

3.5.2.3. Mating of Yeast Cells

For sexual reproduction, *S. cerevisiae* forms haploid vegetative cells which can differentiate into gametes. The gametes are specified by the harboured *MAT* allele, i.e. either *MAT*a or *MAT*α mating types. As response to *MAT*a and *MAT*α, the cells in their haploid state produce mating pheromone which differentiates the matable gametes. Only *MAT*a and *MAT*α gametes are able to mate and form *MAT*a/α diploid yeast cell (10).

In order to prove that identified protein–protein interaction is true, researchers utilize the yeast mating process to introduce the bait and prey vectors into one cell during sexual reproduction and screen for interaction on suitable selective agar plates.

1. Transform the Y187 *MAT*α strain with the bait vector. Transform also the extracted prey vectors separately into AH109 *MAT*a yeast strain. Use the small-scale protocol for both transformation experiments (**Section 3.1.2**). Incubate the bait and prey transformants on SD/-Trp and SD/-Leu agar medium, respectively, for 4 days at 30°C.
2. Combine one colony from each plate in 0.5 mL YPDA medium.
3. Resuspend the cells by vortexing and incubate them at 200 rpm shaking for 24 h.

4. Control the mating result by plating the cells on double dropout SD/-Leu/-Trp agar plates. For interaction analysis, plate the mating culture also on SD/-Ade/-Leu/-His/-Trp + 3-AT agar medium.
5. Incubate the plates at 30°C for 4–5 days.
6. Rescue the growing colonies and perform the β-galactosidase filter lift assay to verify the protein–protein interaction (**Section 3.5.2.1**).

3.5.3. Further Protein–Protein Interaction Tests

Sequence the prey vector which enabled from the positive interaction with the protein of interest and analyse the sequence for putative interaction regions. Change the reading frame of the prey cDNA by subcloning into the prey vector and repeat the two-hybrid screen with modified prey element. Switch finally to in vitro tests suitable to reveal the protein–protein interactions like plasmon resonance, pull-down assays with antibodies, overlay Western blots and isothermal titration calorimetry.

4. Conclusions

Yeast one- and two-hybrid screens are routinely used in molecular biology and stress research. The search for "yeast AND hybrid AND Arabidopsis" in the Science Citation index gives 761 hits (19 Dec 2008, less than 10% false hits not dealing with interaction studies). Many of these studies deal with abiotic stress responses and have provided novel information on protein networks in plant cell signalling. For example, Tardif et al. (11) have analysed the protein interaction network associated with abiotic stress response and development in wheat. From 97 interactions of 73 proteins identified in an intensive yeast two-hybrid screen, 21 could be confirmed by bimolecular fluorescence complementation (BIFC) in vivo. A review on interaction studies is available from Uhrig (12). Once interesting pairs of interacting proteins are being identified, in vitro and in vivo studies must address the biochemical and physiological significance of these interactions for plant development and acclimation.

5. Notes

1. Under normal conditions the basal level of expressed *HIS3* gene product can be inhibited by 3-AT. If inhibition is not achieved even with more than 70 mM 3-AT, check the

following parameters: (i) Were more than one pHis2 bait vector introduced into one cell? (ii) Is the excessive growth caused by high amount of plated cells? To solve the problem, perform a new transformation with less vector and plate a small volume of transformants on SD/-Leu/-His/-Trp + 3-AT medium. In very rare cases it is not possible to adjust the appropriate 3-AT concentration. Then a redesign of the bait element is unavoidable, for example, by further truncation.

2. The RNA used for the cDNA library construction should be intact and contain full-length mRNAs. The characteristic band pattern of total RNA sample, caused by ribosomal RNA molecules, must appear on denaturing agarose gel. A weak smear from lower to higher molecular mass is also a sign for good mRNA quality. Accumulation of small molecules on the gel indicates degradation of the RNA. In that case, prepare a new RNA sample before starting.
3. After cDNA library synthesis, a smear in the range between 0 and up to 8 kb should appear in the agarose gel. If the smear is weak or completely missing, incubate the reaction in the thermocycler for additional cycles.
4. Use small aliquots of herring testes carrier DNA. Denature the DNA by boiling at 100°C for 5 min and cool it immediately on ice. Do not use the same aliquot more than five times.
5. The performed yeast transformation protocol should generate at least 3×10^5 independent transformants on SD/-Leu/-Trp control plates. If the transformation efficiency is less, then try again using a young colony for competent cell preparation.
6. Some bait proteins, especially transcription factors, can cause some trouble in two-hybrid screenings because of their own AD domains. They may be able to activate the transcription of the reporter gene and make the 3-AT adjustment impossible. In this case, subclone the bait into the prey vector like pAct2 and the putative interaction partner into the bait vector pGBKT7. Test the new bait for autoactivation.
7. Colonies which appear later on the plate highly probably are false positives which grow due to a leaky expression of the *HIS3* reporter gene.
8. Clones with true-positive interactions can deal with high 3-AT concentrations. By increasing the 3-AT concentration on selective plates, the interaction strength can be estimated.

9. Skip colonies with sizes smaller than 1 mm. Based on our experience these clones are also false positives.
10. For interaction verification via retransformation, use the small-scale transformation protocol.
11. It can happen that the insertion of the coding sequence of a putative interaction partner causes a frameshift relative to the GAL4 AD domain. Statistically only one out of six protein-coding cDNA sequences is inserted in-frame with the GAL4 AD domain (13). Studies show that yeast cells at least in some cases are able to switch the reading frame and restore the reading frame during translation (14).
12. Avoid the formation of bubbles between both filters. Ensure that the Z-buffer/X-Gal solution is transferred on the upper filter.

References

1. Fields, S. and Song O. (1989) A novel genetic system to detect protein–protein interactions. *Nature* **340**, 245–246.
2. Laughon, A., Driscoll, R., Wills, N., and Gesteland, R.F. (1984) Identification of two proteins encoded by the *Saccharomyces cerevisiae* GAL4 gene. *Mol Cell Biol* **4**, 268–275.
3. Paravicini, G. and Friedli, L. (1996) Protein–protein interactions in the yeast PKC1 pathway: Pkclp interacts with a component of the MAP kinase cascade. *Mol Gen Genet* **251**, 682–691.
4. Bhaumik, S.R., Raha, T., Aiello, D.P., and Green, M.R. (2004) In vivo target of a transcriptional activator revealed by fluorescence resonance energy transfer. *Genes Dev* **18**, 333–343.
5. Ito, H., Fukuda, Y., Murata, K., and Kimura, A. (1983) Transformation of intact yeast cells treated with alkali cations. *J Bacteriol* **153**, 163–168.
6. Gietz, R.D. and Schiestl, R.H. (2007) High-efficiency yeast transformation using the LiAc/SS carrier DNA/PEG method. *Nat Protoc* **2**, 31–34.
7. Wellenreuther, R., Schupp, I., Poustka, A., and Wiemann, S. (2004) SMART amplification combined with cDNA size fractionation in order to obtain large full-length clones. BMC *Genom* **5**, 36.
8. Ni, W.-S., Lei, Z.-Y., Chen, X., Oliver, D.J., and Xiang, C.-B. (2006) Construction of a plant transformation-ready expression cDNA library for *Thellungiella halophila* using recombination cloning. *J Integr Plant Biol* **49**, 1313.
9. Serebriiskii, I.G. and Golemis, E.A. (2000) Uses of lacZ to study gene function: evaluation of β-galactosidase assays employed in the yeast two-hybrid system. *Anal Biochem* **285**, 1–15.
10. Wittenberg, C. and La Valle, R. (2003) Cell-cycle-regulatory elements and the control of cell differentiation in the budding yeast. *Bioessays* **25**, 856–867.
11. Tardif, G., Kane, N.A., Adam, H., Labrie, L., Major, G., Gulick, P., Sarhan, F., and Laliberte, J.F. (2007) Interaction network of proteins associated with abiotic stress response and development in wheat. *Plant Mol Biol* **63**, 703–718.
12. Uhrig, J.F. (2006) Protein interaction networks in plants. *Planta* **224**, 771–781.
13. Van Criekinge, W. and Beyaert, R. (1999) Yeast two-hybrid: state of the art. *Biol Proced Online* **2**, 1–38.
14. Stahl, G., Bidou, L., Rousset, J.P., and Cassan, M. (1995) Versatile vectors to study recoding: conservation of rules between yeast and mammalian cells. *Nucleic Acids Res* **23**, 1557–1560.

Chapter 11

Functional Characterization of Water-Deficit Stress Responsive Genes Using RNAi

Muthappa Senthil-Kumar, Makarla Udayakumar, and Kirankumar S. Mysore

Abstract

In response to water-deficit stress, plants alter expression of thousands of genes and as a result, cellular, physiological, and biochemical processes are modified. Understanding the functional role of water-deficit stress-responsive genes is important in order to develop stress-tolerant plants. RNA interference (RNAi) technology is one of the potential reverse genetics tool for assessing the functional significance of these genes. We describe here the protocols for developing stable gene knockdown lines for stress-induced genes using RNAi. In addition, stress imposition method that allows plants to experience gradual acclimation stress is enumerated. Further, precautions that should be taken while developing RNAi lines and during stress imposition are discussed.

Key words: Drought stress, functional genomics, gene silencing, RNAi, stress imposition protocol.

1. Introduction

The mechanism of molecular responses of higher plants to water-deficit stress has been well studied (1). Several water-deficit, stress-induced genes have been identified and sequence information is available in the form of expressed sequence tags (ESTs) and/or genomic sequence. However, functional relevance of genes corresponding to many of these ESTs and genomic sequences from diverse stress cDNA databases is yet to be studied (2). Therefore, developing novel tools and approaches for functional analyses of these water-deficit stress-related genes are critical. Although gene expression profiling experiments can provide clues, the functional relevance of genes in imparting stress tolerance in plants can be studied only by functional genomic

R. Sunkar (ed.), *Plant Stress Tolerance*, Methods in Molecular Biology 639,
DOI 10.1007/978-1-60761-702-0_11,

approaches involving either gene overexpression or downregulation. RNA interference (RNAi) technology using constructs transcribing self-complementary hairpin RNA is one of the reverse genetics approaches to downregulate genes in plants (3, 4). The process of post-transcriptional gene silencing (PTGS) by RNAi can be divided into few steps. It is initiated by the production of double-stranded RNA, which is recognized and cleaved by a nuclease, DICER, to produce 21–23-nucleotide small interfering RNAs (siRNAs). These siRNAs are incorporated into the enzyme complex, named RNA-induced silencing complex that is responsible for sequence-specific degradation of corresponding endogenous homologous mRNAs in the cytoplasm (3–5).

1.1. Advantages of RNAi and Use of Heterologous Gene Fragments for Silencing

In contrast to transient gene silencing methods in plants like virus-induced gene silencing (VIGS), RNAi technology leads to stable silencing that can be inherited. Unlike mutagenesis methods, RNAi silencing can be made inducible. These attributes can be used to study genes crucial for water-deficit stress tolerance. A single RNAi construct can silence all members of a gene family, making it possible to characterize genes with redundant copies in the genome. Further, recent reports on efficient use of heterologous gene fragments for silencing their orthologs (6, 7) in transformation-efficient species will extend the application of RNAi-mediated reverse genetics to characterize genes from transformation-recalcitrant plant species.

1.2. Use of RNAi to Study Abiotic Stress Tolerance

Stable gene-silenced lines developed through RNAi technology are particularly useful to analyze the role of genes showing altered expression during abiotic stress. Apart from a prominent study showing the role of free proline in salt tolerance in tobacco cells, several studies used RNAi as a tool to assess relevance of abiotic stress-induced genes (8, 9). RNAi has also been used to develop commercial water-deficit-tolerant crop plants (10). One of the advantages of RNAi in stress studies is its ability to develop plants with varying levels of silencing that can be used to relate transcript levels of stress-responsive genes to degree of stress tolerance. Hence RNAi is an excellent approach to dissect water-deficit stress tolerance mechanisms.

1.3. Analyses of Stress Tolerance Require Well-Established Stress Protocols

There is a need for the assessment of stress tolerance of transgenic plants using appropriate stress protocols (11, 12). Characterization of water-deficit stress-regulated genes using gene downregulation approaches require optimum stress imposition that can clearly distinguish between wild-type and silenced plants. Along with this, appropriate stress effect quantification methods are important for realistic evaluation of gene of interest (GOI). Further, biphasic stress treatments involving mild acclimation stress followed by severe stress that can assess basal and acquired

tolerance are useful to better understand the functional relevance of stress-regulated genes (13).

Present challenge of water-deficit stress studies is to bridge the gap between agronomic or physiological field experiments with the basic research using green house-grown model plants. In this chapter we enumerate the methods and discuss relevant aspects that can better bridge this gap. We also discuss examples that can be of assistance to researchers in designing stress experiments that are suitable for genetic studies and rapid screening of stable transgenic plants modified to confer water-deficit stress tolerance.

This chapter is aimed to provide procedures to perform the following with specific reference to the model plant tobacco (*Nicotiana tabacum*):

- To develop RNAi constructs to silence water–deficit stress-regulated genes.
- To develop and confirm stable RNAi transgenic plants.
- To perform water-deficit stress imposition in gene-silenced plants.
- To quantify stress effects in RNAi plants.

2. Materials

2.1. Developing RNAi Constructs

2.1.1. RT-PCR and BP Reaction

1. Gene-specific primers with attB sites added.
2. Omniscript Reverse Transcription Kit (Qiagen, Inc., Valencia, CA, USA).
3. Total RNA (2 μg) isolated using RNeasy Plant Mini Kit (Qiagen).
4. BP reaction kit, pDONR 207 plasmid (150 ng), and proteinase K (Invitrogen Corporation, Carlsbad, CA, USA).
5. JM109 (Promega, Madison, WI, USA) *Escherichia coli* cells and LB medium (Q-BIOgene, Irvine, CA, USA) with gentamicin (12.5 mg/L).
6. NanoDrop spectrophotometer (Thermo Scientific, Wilmington, DE, USA).

2.1.2. LR Reaction

1. Plasmids (150 ng each) of entry clone from BP reaction and destination RNAi vector pK7GWIWG2(I).
2. LR reaction kit and proteinase K (Invitrogen).
3. *Agrobacterium* strain EHA105 and LB medium (Q-BIOgene) with rifampicin (25 mg/L) and kanamycin (50 mg/L).

2.1.3. Confirmation of Cloning

1. Three sets of primers (a) attB1 (forward) and attB2 (reverse); (b) destination vector promoter (CaMV35S forward) and attB2 (reverse); (c) destination vector terminator (CaMV35S forward) and attB2 (reverse).
2. Suitable gene-specific primers and attB1–attB2 sequencing primers to sequence PCR products.

2.2. Agrobacterium-Mediated Plant Transformation for Developing Stable RNAi Lines in Tobacco

1. *Agrobacterium* (strain EHA105) containing suitable RNAi construct.
2. Half-strength Murashige and Skoog (MS) medium (Caisson Laboratories, Inc., North Logan, UT, USA).
3. Co-cultivation medium: MS + 0.2 mg/L NAA + 2 mg/L BA.
4. Selection medium: MS + 0.2 mg/L NAA + 2 mg/L BA + 100 mg/L kanamycin + 300 mg/L cefotaxime.

2.3. Confirmation of RNAi Lines

2.3.1. Confirmation of Genetic Transformation by PCR

1. Genomic DNA of wild-type, vector control, and RNAi plants isolated using DNeasy Plant Mini Kit (Qiagen).
2. PCR primers attB1 and attB2; *nptII* gene-specific forward and reverse primers.

2.3.2. Quantitative RT-PCR to Study Downregulation of Endogenous Gene

1. Total RNA (2 μg) from wild-type, vector control, and RNAi plants isolated using RNeasy Plant Mini Kit (Qiagen).
2. Omniscript Reverse Transcription Kit (Qiagen).
3. SYBR Green (DyNAmo SYBR Green qPCR Kit; Finnzymes, Finland) and related accessories to perform real-time RT-qPCR (Opticon2; MJ Research, Watertown, MA, USA).

2.4. Water-Deficit Stress Imposition

1. WP4 dew point potentiometer (Decagon Devices, Inc., Washington DC, USA) for soil water potential measurements.
2. Weighing balance or mini lysimeter with rain out shelter facility for gravimetric studies.
3. About 40-day-old wild-type, vector control, and RNAi plants planted on suitable potting medium.

2.5. Quantification of Stress Effects

2.5.1. Relative Water Content (RWC)

Leaf punch (cork borer) (1 cm diameter) and de-ionized water.

2.5.2. Cell Membrane Stability (CMS)

De-ionized water and conductivity meter Orion 555A (Thermo Electron Corporation, Waltham, MA USA).

2.5.3. Cell Viability

Triphenyltetrazolium chloride (TTC) test (EMD Chemicals, Inc., Gibbstown, NJ, USA), 50 mM sodium phosphate buffer (pH 7.4), 2-methoxyethanol (Sigma Aldrich, Inc., St. Louis, MO, USA), and spectrophotometer (UV 2450; Shimadzu Corporation, Kyoto, Japan).

3. Methods

3.1. Developing RNAi Constructs

3.1.1. RT-PCR and BP Reaction

1. Perform RT-PCR to synthesize first-strand cDNA from total RNA using oligo$(dT)_{15}$ primers. Partial sequences (300–350 bp) of GOI should be PCR amplified using specific primers along with attB1 and attB2 sites from total cDNA pool. More details are described in Ref. [14] and also *see* **Notes 1**, **2,** and **8**. For stress-only-induced genes, cDNA should be made from water-deficit stress-experiencing leaves.
2. Clone the PCR products into pDONR 207 by BP Clonase-mediated recombination reaction by incubating reaction mix at room temperature (21°C) overnight (12 h). Follow the manufacturer's instructions to set up the reaction mix.
3. Stop the reaction by treating with proteinase K and transform (about 3–5 μL) into JM109 cells by following heat-shock method of bacterial transformation.
4. Plate the culture on LB agar plates containing gentamicin (12.5 mg/L). Colonies will appear in about 16 h of incubation at 37°C.
5. Select colony containing correct entry clones by performing colony PCR with gene-specific primers.
6. Isolate plasmid, quantify using NanoDrop, and proceed with LR reaction.

3.1.2. LR Reaction

1. Mobilize the gene fragments of GOI from entry clone into gateway ready pK7GWIWG2(I) RNAi vector (15) by LR Clonase-mediated recombination reaction by following manufacturer's protocol. This gateway cloning will facilitate cloning gene fragments in sense and antisense orientation intervening with a spacer (intron) which is already provided in the destination vector.

2. Transform about 5–7 μL of LR reaction product to EHA105 cells by following electroporation method of bacterial transformation.

3.1.3. Confirmation of Cloning

1. Verification of cloning correct fragment of DNA is necessary. This can be done by PCR amplification with attB and promoter/terminator primer combination. Perform independent PCR reactions using three different sets of primers and select the transformed colony that tested positive in all three reactions.
2. Sequence PCR products and perform NCBI–BLAST analyses to ensure specificity of amplified genes.
3. Clone partial sequence of a green fluorescent protein (GFP) by following above said protocols into pK7GWIWG2(I). This construct can be used to develop vector control (mock) plants. We suggest readers to refer Ref. (14) for detailed methods for selection of gene fragment and target RNAi vector development.

3.2. Agrobacterium-*Mediated Plant Transformation for Developing Stable RNAi Lines in Tobacco*

1. Collect healthy leaves from the wild-type tobacco plants and surface sterilize by using 0.1% $HgCl_2$ for 3 min. Rinse with sterile water for 5–6 times. Perform all further steps under aseptic conditions.
2. Cut the leaves into small segments (avoid midrib and veins) and incubate on the MS medium for 2 days.
3. Inoculate leaf segments with *Agrobacterium* harboring respective RNAi construct for 5 min with moderate shaking. Blot dry on sterile tissue paper and co-cultivate for 2 days in co-cultivation medium. Wash the leaf segments, blot on tissue paper, and incubate on selection medium for 30 days.
4. During this period the shoots produced from explants can be subcultured at 10-day interval into fresh selection medium. Grown-up shoots can be transferred to half-strength basal MS medium for rooting.
5. Putative T_0 transgenic plants with 3–4 leaves can be hardened and grown in green house until maturity. Perform PCR with suitable primers to confirm integration of RNAi construct.
6. Collect the seeds from T_0 plants, sterilize, and germinate on MS medium supplemented with 100 mg/L kanamycin.
7. Transfer only healthy seedlings (T_1 generation) to green house. Also the segregation can be assessed at this generation.

3.3. Confirmation of RNAi Lines

3.3.1. Confirmation of Genetic Transformation by PCR Analyses

1. Isolate genomic DNA from T_1 generation plants and perform PCR with attB1 and attB2 primers and plant selection marker (*nptII*) gene-specific primers. Amplification of *Actin* gene can serve as loading control. Use only PCR-positive plants for further experiments. To rule out *Agrobacterium* contamination, PCR with virulence (*vir*) gene-specific primers can be done.
2. Perform southern blotting for further confirmation and to study integration pattern of RNAi construct (this step is optional).

3.3.2. Quantitative RT-PCR to Study Downregulation of Endogenous Gene

1. Isolate total RNA from wild-type, vector control, and selected RNAi lines (T_1 generation) and perform RT reaction to synthesize first-strand cDNA using oligo$(dT)_{15}$ primers.
2. Perform real-time RT-qPCR with SYBR Green by following manufacturer's protocol. Primers can be designed to anneal to a region of targeted transcript outside of sequence cloned in RNAi vector.
3. Relative transcript expression ratio of respective genes can be assessed from C_t values (16). Use elongation factor 1-α gene expression as internal standard for normalization (*see* **Notes 3** and **8**).

3.4. Water-Deficit Stress Imposition

1. Grow the young seedlings under well-watered condition in green house having temperature range of 20–22°C with daytime relative humidity (RH) of around 60% and 12 h photoperiod with light intensity ranging from 400 to 600 μmol/m^2/s. Supplement with artificial light if natural light does not meet this requirement.
2. Transfer plants (about 30-day old) to green house conditions having temperature range from 22°C to 25°C with daytime RH of around 40% and 12 h photoperiod with mid-day light intensity ranging from 1,000 to 1,200 μmol/m^2/s. Maintain all plants at 100% field capacity (FC) for 10 more days until imposition of water-deficit stress. These green house environmental conditions are maintained until end of stress imposition period.
3. Arrange adequate number of plants from wild-type, vector control, and RNAi transgenic line in two batches with several subsets. Maintain one batch of plants at 100% FC and impose water-deficit stress to other batch of plants. Impose water-deficit stress by gradually withholding irrigation. Monitor soil moisture regimes gravimetrically by weighing the pots twice a day, morning and evening. Also

establish a correction factor for water loss due to direct soil evaporation by maintaining a pot without plant.

4. Decrease the soil water status gradually over 1 week until it is reduced to 50% of FC (acclimation treatment). Then divide three subsets of plants containing at least 10 replicates each and impose severe stress for each set at 60%, 40%, and 20% FC, respectively, for 3–7 days by replenishing exact amount of water lost through transpiration.
5. In parallel, maintain a set of non-acclimated plants by directly exposing them to severe stress levels without acclimation. The non-acclimated plants can be used to assess basal tolerance. Plants exposed to acclimation followed by severe stress can be used to assess acquired stress tolerance.
6. Analyze the plants for stress effects. *See* **Fig. 11.1** for details (*see* **Note 4**).

3.4.1. Recovery Response

1. After stress period, re-water all plants to 100% FC and maintain it for 3–7 days (short-term observations) and 1 month (to study stress effects on reproductive stage).
2. Analyze plants for recovery response. *See* **Figs. 11.1** and **11.2** for details.

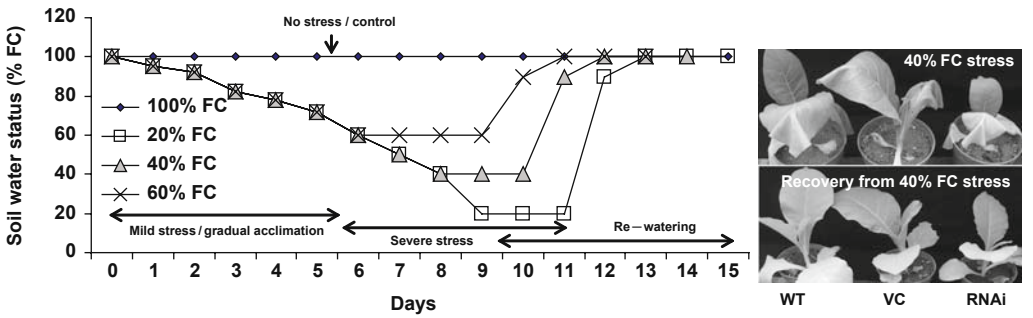

Fig. 11.1. General stress imposition protocol for studying water-deficit stress effects in tobacco plants. Water-deficit stress is imposed by gradually withholding water to plants. Initially about 40-day-old plants are subjected to acclimation in such a way that soil water status is reduced from 100% to 50% FC over a period of 6–7 days. Later plants are subjected to different severe stress levels (for example, 60%, 40% or 20% FC) for 3 days (or more). During this period, if the silenced gene(s) has a role in stress tolerance, the RNAi plants might show early or late wilting compared to wild-type (WT) and vector control (VC). *Right top panel* photograph shows marginal wilting phenotype of early light-inducible protein (*ELIP*)-downregulated RNAi tobacco plant. To study recovery phenotype, stressed plants are re-watered to 100% FC in two stages. *Right bottom panel* photograph shows recovery response of re-watered *ELIP* gene-downregulated RNAi tobacco plant. *ELIP* data is reproduced with permission from Senthil-Kumar (2007). Analysis of several physiological, biochemical, and molecular parameters is done independently during acclimation and severe stress periods and also after re-watering. Note that these protocols need to be customized prior to experimentation using wild-type plants. This figure is a simulation conceived based on the data presented in Senthil-Kumar (2007). FC, field capacity; *x*-axis shows days after plants are subjected for stress experiment. For example, age of plant at day 0 would be ~40 days.

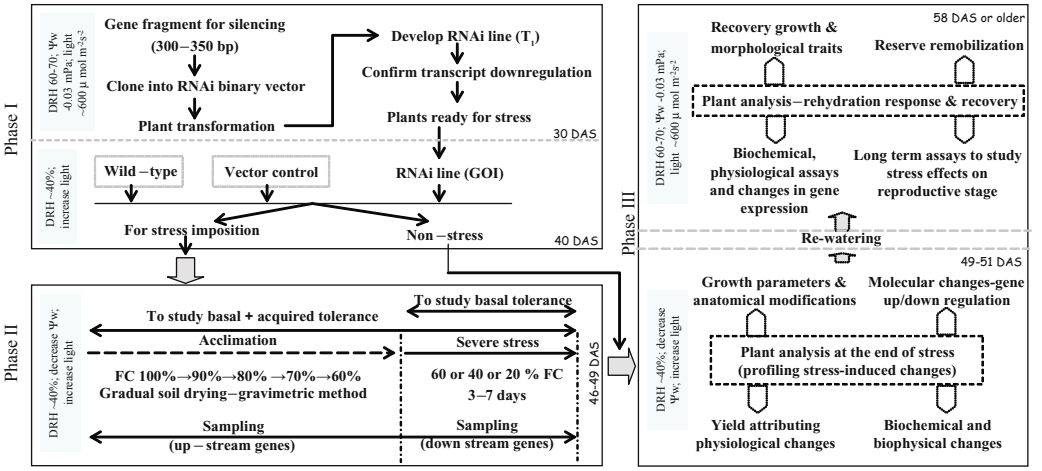

Fig. 11.2. Flow diagram showing steps involved in the characterization of water-deficit, stress-induced genes using RNAi. *Phase I, development of RNAi line*: Appropriate fragment of gene to be silenced or its homolog is identified and cloned into a suitable RNAi vector. This vector is transformed into plant and stable knockdown lines are developed. Plants confirmed for silencing are raised in appropriate soil medium along with wild-type and vector control plants. A subset of these plants subjected to stress imposition and other set are maintained under non-stress conditions. *Phase II, stress imposition*: Gradual soil drying is done in such a way that plants undergo acclimation stress followed by specific severe stress. During this period, moisture content in plant tissue reduces gradually to reach physiologically severe stress levels. Duration and intensity of stress vary with the plant species and the type of gene under study. Plants subjected to acclimation followed by severe stress and directly exposed to severe stress are separately maintained. *Phase III, plant analyses*: Plants are re-watered to 100% FC to assess recovery response. Plant analyses at this stage can reveal functional role of GOI during rehydration response, especially the ones related to re-allocating resources to different organs. GOI, gene of interest; FC, field capacity; DRH, daytime relative humidity; Ψw, soil water potential; DAS, days after sowing.

3.5. Quantification of Stress Effects

3.5.1. Relative Water Content (RWC)

1. Collect leaf discs (1 cm diameter) from stress (at the end of stress period) and non-stress plants during midday. Determine fresh weight.
2. Float leaf discs on de-ionized water for 5 h at 22–25°C and determine turgid weight.
3. Dry leaf discs and determine dry weight.
4. Calculate RWC (%) using the following formula: [(fresh weight–dry weight)/(turgid weight–dry weight)] × 100
5. At a given stress level, if silenced plants have altered RWC compared to wild-type plants, then the gene under study has some relevance in imparting stress tolerance.

3.5.2. Cell Membrane Stability (CMS)

1. Collect leaf discs (1 cm diameter) from stress (at the end of stress period) and non-stress plants during midday.
2. Rinse leaf discs to remove solutes leaking at cut end surface and incubate (about five per replication) in de-ionized water for 8 h at 22–25°C.

3. Record initial solute and ion leakage readings of stress (T_1) and non-stress (C_1) leaf discs using conductivity meter.
4. Boil leaf discs in same solution for 30 min or perform autoclaving. Cool down and record final reading for stress (T_2) and non-stress (C_2) samples using conductivity meter.
5. Calculate CMS using the following formula: CMS (%) = (1–(T_1/T_2)] / (1–(C_1/C_2)] × 100.
6. At a given stress level, if silenced plants have altered CMS compared to wild-type plants, then the gene under study has some relevance in imparting stress tolerance.

3.5.3. Cell Viability

1. Collect leaf discs (1 cm diameter) from stressed (at the end of stress period) and non-stressed plants.
2. Prepare triphenyltetrazolium chloride (TTC) solution by dissolving 0.4% of TTC in 50 mM sodium phosphate buffer.
3. Gently shake freshly obtained leaf discs in TTC solution at room temperature for 5 h.
4. Wash leaf discs to remove unbound formazan and boil with 5 mL of 2-methoxyethanol till dryness.
5. Extract bound TTC using 2-methoxyethanol and record absorbance at 485 nm using UV-2450 UV–visible spectrophotometer.
6. At a given stress level, if silenced plants have altered absorbance values (less cell viability) compared to wild-type plants, then the gene under study has some relevance in imparting stress tolerance.

3.5.4. Phenotypic Observations

All through the stress period, observe silenced and control plants for phenotypes such as leaf wilting, drooping, yellowing, and senescence. Observe changes in growth and reproductive parameters during recovery.

This section deals with only few examples of quantification methods. For realistic stress effect assessment, the researcher is expected to perform more assays (*see* **Notes 5** and **6**). Some useful suggested readings about these methods are given in the reference section (6, 13, 17, 18). Further, all the data from stressed plants should be normalized with corresponding non-stress plants (*see* **Note 7**). Assessing changes in stress-associated genes including genes involved in signaling pathways, transcription, ion/water transport, ubiquitin-mediated protein degradation, nutrient uptake, senescence, ROS scavenging, and detoxification would be beneficial. Also, assessing changes in stress-associated metabolites like osmoprotectants, polyamines, and carbon metabolism would be useful.

4. Notes

1. One of the limitations of RNAi is off-target gene silencing due to high degree of homology within a small stretch of DNA (21–23 nucleotides) between the target gene and other genes in plant genome. Off-target silencing can complicate interpretation of the results. Therefore, selection of appropriate gene fragment to make RNAi construct is necessary. Xu et al. (19) has developed a software (http://bioinfo2.noble.org/RNAiScan.htm) that can predict possible off-targets of the gene fragment used for silencing and can be used to make better RNAi constructs to prevent unintended silencing (19). On the contrary, if a family of closely related genes is targeted for silencing, this software can also be used to select gene fragment in the conserved region while designing RNAi constructs (7).
2. The pK7GWIWG2(I) vectors described in Ref. (15) are widely used to develop RNAi constructs. This RNAi gateway-compatible vector with choice of promoter, intron, and plant selection marker can be obtained from VIB Department of Plant Systems Biology, Ghent University, Belgium (http://www.psb.ugent.be/gateway/). Apart from these, several other vectors including the ones that employ conventional cloning strategies are also available (14, 20).
3. Effect of silencing may vary for individual transformants. Hence plants selected for water-deficit stress experiments should be confirmed for degree of silencing and comparison should be made among those showing similar levels of gene downregulation. RNAi plants with a wide range of silencing are useful to select plants that look normal during non-stress condition.
4. *Precautions to be taken during water-deficit stress imposition*: Determining severity of stress, duration of stress, method used to impose stress, and parameters to be measured are important aspects for better understanding the functional role of silenced genes (6). Following two major precautions during stress experiments will help researchers to obtain reliable results.

   Plant material and soil or potting medium characteristics: Uniform aged plants with similar leaf area index (LAI) should be used for all experiments. This will minimize variation in stress levels due to differential plant transpiration and soil evaporation. Planting the wild-type, vector control, and RNAi lines in same container or mini lysimeter adopting simple randomized complete block design (RCBD) will avoid any position effect and variation due to soil characteristics. Potting medium should be such that FC can be gradually

decreased facilitating not more than 2–3% reduction in leaf RWC per day during stress. Normally a natural soil or an artificial medium that has water-holding capacity (WHC) and porosity (φ) range of 30–40% and 40–60%, respectively, can be a good choice for stress experiments. In addition, knowledge about physical properties like bulk and particle density of potting medium is recommended. More importantly, interpretation of stress levels as soil moisture content or FC should be accompanied by its corresponding water potential measurements. For example, at 100% and 40% FC, red soil and sand mix (1:1) hold water at negative potential ($-\Psi w$) of approximately 0.03 and 0.8 mPa, respectively.

Environmental conditions: Vapor pressure deficit (VPD) necessitates plant to draw more water from the potting medium favoring stress imposition. Hence maintaining RH and air temperature range that can create adequate VPD to drive transpiration water loss is important. In addition, maintaining higher midday light intensity and stimulating natural variations in the green house will help in optimum stress imposition. Preferably observations and sample collection should be performed during midday when the silenced plant possibly show transient lower leaf wilting phenotype (6).

5. *Other methods for inducing dehydration or desiccation stress*: Apart from stress imposition at whole plant level, osmotic stress can also be induced, in vitro, using PEG. Excised leaf discs, young seedlings, and seeds can be used for these assays. Assessing desiccation response of leaves by estimating leaf water loss in detached leaves is also a useful method.
6. *Quantification techniques*: Techniques for precise estimation of physiological changes along with supporting information from biochemical analyses in the silenced plant are important to dissect role of GOI. We suggest the researchers to include some of the following techniques or growth parameters as a baseline to compare results between wild-type and silenced plant. Selection of parameters depends on the type of plant species and preliminary information available for the gene under study.
   a) *Physiological analyses*: Assess relative growth rate, net assimilation rate, specific leaf area, stem–leaf ratio, root length, root–shoot ratio, and leaf ash contents during vegetative growth stage. Apart from this, canopy temperature, photosynthetic rate, transpiration rate, light saturation, CO_2 compensation point, other gas exchange parameters, solute potential, tissue water potential, osmotic adjustment, chlorophyll florescence, and carbon isotope discrimination are also useful parameters.

During reproductive stage, yield-attributing parameters like number of days took to 50% flowering, pollen viability, total biomass, and grain or leaf drop are important.

b) *Biochemical analyses*: Estimation of cell death, reactive oxygen species, lipid peroxidation, enzyme activity, chlorophyll degradation, anthocyanin content, content of other anti-oxidants, incorporation of [^{35}S]methionine into total protein, and cuticular wax content will be useful. Also profiling of protein expression pattern, primary, and secondary metabolites may place the gene in a specific pathway.

7. *Interpretation of results to assign functional relevance to the silenced gene*: All the silenced plants should have normal phenotype and maintain basic metabolic function. Stress imposition to already sick plant may not identify the role of silenced gene in water-deficit stress. In addition, maintaining appropriate positive and negative controls will help to compare the results. For example, including an RNAi line silenced for a well-characterized gene already implicated in imparting water-deficit stress tolerance (for example, late embryogenesis abundant, LEA) can serve as positive control. Further, stress levels should be such that most of the silenced plants experience higher water-deficit stress effects to produce visible symptoms that can be distinguished from wild-type plants. RNAi approach can provide only preliminary role of the silenced gene during water-deficit stress. Hence, other supporting approaches like gene overexpression are necessary to fully understand the functional role of the GOI during water-deficit stress.

8. *General rule of thumb during experimentation*: Use of sensitive transcript quantification techniques like real-time RT-qPCR requires proper internal controls and many replications. DNase treatment of RNA is a must before analyzing samples. Determine RNA quality using Agilent Bioanalyzer 2100 (Foster City, CA, USA) or a similar equipment and run the PCR products on gel.
   - Transforming LR reaction mix directly to *Agrobacterium* might give some false positives and hence needs PCR confirmation of transformed colonies.
   - Both plasmids of pDONR and destination vectors should be made fresh and quality should be checked before using it for BP or LR reactions.
   - Maintain a positive control and empty vector control in all PCR and RT-PCR reactions.
   - Rooting of antibiotic resistant tobacco plants during transformation with kanamycin selection often varies. We

suggest standardizing lethal dose of kanamycin prior to the experiment. Use half strength MS medium for better rooting.

References

1. Ramanjulu, S. and Bartels, D. (2002) Drought- and desiccation-induced modulation of gene expression in plants. *Plant Cell Environ* **25**, 141–151.
2. Seki, M., Kamei, A., Yamaguchi-Shinozaki, K., and Shinozaki, K. (2003) Molecular responses to drought, salinity and frost: common and different paths for plant protection. *Curr Opin Biotechnol* **14**, 194–199.
3. Small, I. (2007) RNAi for revealing and engineering plant gene functions. *Curr Opin Biotechnol* **18**, 148–153.
4. Matthew, L. (2004) RNAi for plant functional genomics. *Compar Funct Genom* **5**, 240–244.
5. Travella, S., Klimm, T.E., and Keller, B. (2006) RNA interference-based gene silencing as an efficient tool for functional genomics in hexaploid bread wheat. *Plant Physiol* **142**, 6–20.
6. Senthil-Kumar, M., Ramegowda, H.V., Hema, R., Mysore, K.S., and Udayakumar, M. (2008) Virus-induced gene silencing and its application in characterizing genes involved in water deficit stress tolerance. *J Plant Physiol* **165**, 1404–1421.
7. Senthil-Kumar, M. (2007) Functional characterization of peanut water deficit stress-induced genes: an approach based on virus-induced gene silencing (VIGS) and RNAi [PhD thesis]. Bangalore: University of Agricultural Sciences.
8. Mittler, R., Kim, Y., Song, L., Coutu, J., Coutu, A., Ciftci-Yilmaz, S., Lee, H., Stevenson, B., and Zhu, J.-K. (2006) Gain- and loss-of-function mutations in Zat10 enhance the tolerance of plants to abiotic stress. *FEBS Lett* **580**, 6537–6542.
9. Tateishi, Y., Nakagawa, T., and Esaka, M. (2005) Osmotolerance and growth stimulation of transgenic tobacco cells accumulating free proline by silencing proline dehydrogenase expression with double-stranded RNA interference technique. *Physiol Plant* **125**, 224–234.
10. Yang Wang, J.Y., Kuzma, M., Chalifoux, M., Sample, A., McArthur, C., Uchacz, T., Sarvas, C., Wan, J., Dennis, D.T., McCourt, P., and Huang, Y. (2005) Molecular tailoring of farnesylation for plant drought tolerance and yield protection. *Plant J* **43**, 413–424.
11. Verslues, P.E., Agarwal, M., Katiyar-Agarwal, S., Zhu, J., and Zhu, J.K. (2006) Methods and concepts in quantifying resistance to drought, salt and freezing, abiotic stresses that affect plant water status. *Plant J* **45**, 523–539.
12. Jones, H.G. (2007) Monitoring plant and soil water status: established and novel methods revisited and their relevance to studies of drought tolerance. *J Exp Bot* **58**, 119–130.
13. Senthil-Kumar, M., Kumar, G., Srikanthbabu, V., and Udayakumar, M. (2007) Assessment of variability in acquired thermotolerance: potential option to study genotypic response and the relevance of stress genes. *J Plant Physiol* **164**, 111–125.
14. Travella, S. and Keller, B. (2009) Down-regulation of gene expression by RNA-induced gene silencing. In *Transgenic Wheat, Barley and Oats*, Volume 478 (Jones, H.D. and Shewry, P.R. eds.). Methods in Molecular Biology, Humana Press, Springer, New York, pp. 185–199.
15. Karimi, M., Inze, D., and Depicker, A. (2002) GATEWAY^{TM} vectors for *Agrobacterium*-mediated plant transformation. *Trends Plant Sci* **7**, 193–195.
16. Pfaffl, M.W. (2001) A new mathematical model for relative quantification in real-time RT-PCR. *Nucleic Acids Res* **29**, 45.
17. Towill, L.E. and Mazur, P. (1975) Studies on the reduction of 2,3,5-triphenyl tetrazolium chloride as a viability assay for plant tissue cultures. *Can J Bot* **53**, 1097–1102.
18. Tripathy, J.N., Zhang, J., Robin, S., Nguyen, T.T., and Nguyen, H.T. (2000) QTLs for cell-membrane stability mapped in rice (*Oryza sativa* L.) under drought stress. *Theor Appl Genet* **100**, 1197–2202.
19. Xu, P., Zhang, Y., Kang, L., Roossinck, M.J., and Mysore, K.S. (2006) Computational estimation and experimental verification of off-target silencing during post-transcriptional gene silencing in plants. *Plant Physiol* **142**, 429–440.
20. Helliwell, C.A. and Waterhouse, P.M. (2005) Constructs and methods for hairpin RNA-mediated gene silencing in plants. In *Methods Enzymol*, Volume 392 ed. (Engelke, D.R. and Rossi, J.J., eds.). Academic Press, pp. 24–35.

Chapter 12

Difference Gel Electrophoresis as a Tool to Discover Stress-Regulated Proteins

Jenny Renaut

Abstract

Two-dimensional electrophoresis is a powerful tool to explore the plant proteome and to unravel changes in protein expression between samples. However, the acquisition of images on which thousands of spots may be resolved has some weak points, as always pointed out by scientists working with gel-free techniques, such as the lack of reproducibility. Nowadays, this inconvenience can be bypassed by the use of a technique known as "difference gel electrophoresis" or DIGE. This technique requires the labelling of proteins by fluorochromes before their separation on 2DE gels. This technique may be applied to a wide array of plant stress studies. Providing accurate quantitative results, differentially abundant spots are usually subjected to tryptic digestion and identified using electrospray ionization, matrix-assisted laser desorption/ionization-time of flight-MS and/or tandem MS.

Key words: Two-dimensional electrophoresis (2DE), quantitative approach, DIGE, protein abundance, plant stress.

1. Introduction

Proteomics, i.e. the study of the protein complement of the genome (1), is one of the numerous high-throughput techniques of the post-genome era, such as transcriptomics, metabolomics, phenomics, taking advantage of the completion of several sequenced genomes (e.g. *Arabidopsis*, rice, poplar) (2–4). As proteins are directly related to the function of phenotype of plants, proteomic techniques are more and more used in the plant biology field. It can be divided into two important types of techniques: the gel-based approach (e.g. 2DE) and the gel-free analyses (e.g. LC-MS/MS), each presenting advantages and inconveniences. Moreover, a majority of the results are still provided by the use of classical 2DE [*see* (5) for a review]. A

R. Sunkar (ed.), *Plant Stress Tolerance*, Methods in Molecular Biology 639,
DOI 10.1007/978-1-60761-702-0_12,

traditional workflow of 2DE includes the extraction of proteins, their separation by 2DE, the staining of the gels, the software-based analysis and finally the cutting of the spot out of the gel before the identification by mass spectrometry and database search. At the beginning of this decade, a new technique called difference gel electrophoresis (DIGE) offered to the proteomists to make a step forward in the quantification results (6, 7), reducing gel-to-gel variations drastically by sample multiplexing on the gels.

2. Materials

In our laboratory, the equipment comes mainly from GE Healthcare, but many other suppliers with equivalent equipment can also be considered.

2.1. Sample Preparation

1. Reswelling tray (GE Healthcare, Uppsala, Sweden).
2. Rehydration buffer: 7 M urea, 2 M thiourea, 0.5/2% Pharmalyte or IPG buffer, 0.002% bromophenol blue, 2% 3-((3-cholamidopropyl)dimethylammonium)-1-propanesulphonate (CHAPS).
3. pH test strips 4.5–10.0 pH, resolution: 0.5 pH unit (Sigma Aldrich).
4. CyDyes (Cy2, Cy3 and Cy5) stock solution: Add 25 μL dimethylformamide (DMF, less than 3 months old) to 25 nmol of dye.
5. Labelling buffer: 7 M urea; 2 M thiourea; 4% CHAPS; 30 mM Tris (*see* **Note 1**).
6. Stopping solution: 10 mM lysine.

2.2. Isoelectrofocusing

1. Sample buffer (2×): 7 M urea, 2 M thiourea, 4% CHAPS, 2% (v/v) ampholyte, 2% (w/v) dithiothreitol (DTT) (*see* **Notes 1** and **2**).
2. IPGphor (GE Healthcare, Uppsala, Sweden) or similar electrophoresis apparatus.
3. Manifold, paper wicks, sample cups.
4. Immobilized pH gradient strips: Gels strips may have different lengths and pH gradients. In the present example, we present the protocol for IPG strips of 24 cm on a pH gradient of 4–7.
5. Mineral oil (e.g. dry strip cover fluid; GE Healthcare).

2.3. Second Dimension

1. Dalt twelve Gel Caster (GE Healthcare, Uppsala, Sweden).
2. Displacing solution: 0.375 M Tris–HCl (pH 8.8), 50% (v/v) glycerol, trace of bromophenol blue.

3. Acrylamide stock solution: 30.8% (30% acrylamide, 0.8% *N,N′*-bisacrylamide). This solution can be adjusted for different applications.
4. Homogenous solution for gels: 12.5% T acrylamide stock solution, 1.5 M Tris–HCl (pH 8.8), 0.1% (w/v) sodium dodecyl sulphate (SDS), 0.1% (w/v) ammonium persulphate (APS), 0.01% (v/v) tetramethylethylenediamine (TEMED).
5. Low-fluorescence glass plates.
6. Bind-Silane solution: 80% (v/v) ethanol, 0.2% (v/v) glacial acetic acid, 0.01% (v/v) Bind-Silane (γ-methacryloxypropyltrimethoxysilane).
7. Fluorescent reference markers.
8. Equilibration buffer: 6 M urea, 50 mM Tris–HCl (pH 8.8), 30% glycerol, 2% SDS.
9. Agarose sealing solution: 25 mM Tris base, 192 mM glycine, 0.1% SDS, 0.5% agarose, 0.002% bromophenol blue.
10. Running buffer: 250 mM Tris base, 1.92 M glycine, 2% (w/v) SDS.
11. Ettan Dalt twelve (GE Healthcare, Uppsala, Sweden) or Protean Plus Dodeca cell (Bio-Rad).
12. Typhoon 9400 (GE Healthcare, Uppsala, Sweden).
13. Fixing solution: 40% (v/v) ethanol, 1% (v/v) glacial acetic acid.
14. Ettan Spot Handling Workstation (GE Healthcare, Uppsala, Sweden).

2.4. Handling of Spots and Peptide Extraction

1. Ninety-six-well polypropylene microplates (v-shaped; NUNC).
2. Washing solution: 50% (v/v)methanol (MS grade), 50 mM ammonium bicarbonate
3. Acetonitrile (75%, v/v, MS Grade).
4. Trypsin solution: 5 μg/mL Trypsin Gold (mass spectrometry grade; Promega) in 20 mM ammonium bicarbonate.
5. Peptide extraction solution: 50% (v/v) acetonitrile, 0.1% (v/v) trifluoroacetic acid (TFA).
6. Sample-spotting solution: 50% (v/v) acetonitrile, 0.1% (v/v) TFA.
7. Matrix solution: α-cyano-4-hydroxycinnamic acid (10 mg/mL in sample-spotting solution).

3. Methods

The first step of DIGE is, of course, the extraction of the proteins from the sample. Many extraction methods can be used and before the introduction of DIGE in the experimental set-up, it is important to optimize the extraction protocol and the sample handling to avoid interfering substances (lipids, phenolics, nucleic acids, etc.). Some references for protein extraction methods using TCA/acetone precipitation, hot SDS and/or phenol extraction, respectively, are given (8–10). However, a protocol should be optimized for individual studies. Fractionation steps to isolate, e.g. chloroplasts, mitochondria, nuclei or membranes (11–13), can precede these different methods.

The labelling reaction between the CyDyes and the proteins is based on the formation of a covalent bond between the lysine residues of the proteins and the *N*-hydroxysuccinimidyl ester reactive group. The CyDyes have been designed to have approximately the same mass (around 500 Da) and to carry a positive charge to replace the intrinsic positive charge of the lysine. This will thus ensure that the p*I* of the protein is not modified and its mass barely changed, although it may be visible in the low molecular mass range.

Once the extraction has been optimized, the proteins from different samples are quantified, labelled, separated and compared (*see* **Note 3**). It is of primary importance to correctly plan the experimental design, the number of samples needed, the homemade solutions and the time needed for the different steps. **Fig. 12.1** presents a chronological scheme grouping the different steps that will be described here below.

3.1. Preparation of Samples for Labelling

1. Before starting the labelling, IPG strips have to be rehydrated. Four-hundred and fifty microlitres of rehydration solution containing ampholytes of pH 4–7 (24 cm) is placed in each lane of the reswelling tray. The IPG strip can be placed in the lane with or without the light plastic cover protecting the gel itself, with the gel side down. The gel is covered with mineral oil to avoid drying and crystallization of urea. This step has to be carried out overnight or at least 10 h.
2. The extracted proteins are resolubilized in the labelling buffer. The high concentration of urea allows the denaturation of proteins in order to obtain all the proteins present in one conformation before their separation.
3. Reconstitution of CyDye with DMF (dimethylformamide): An anhydrous solution of DMF (>99.8% purity) has to be

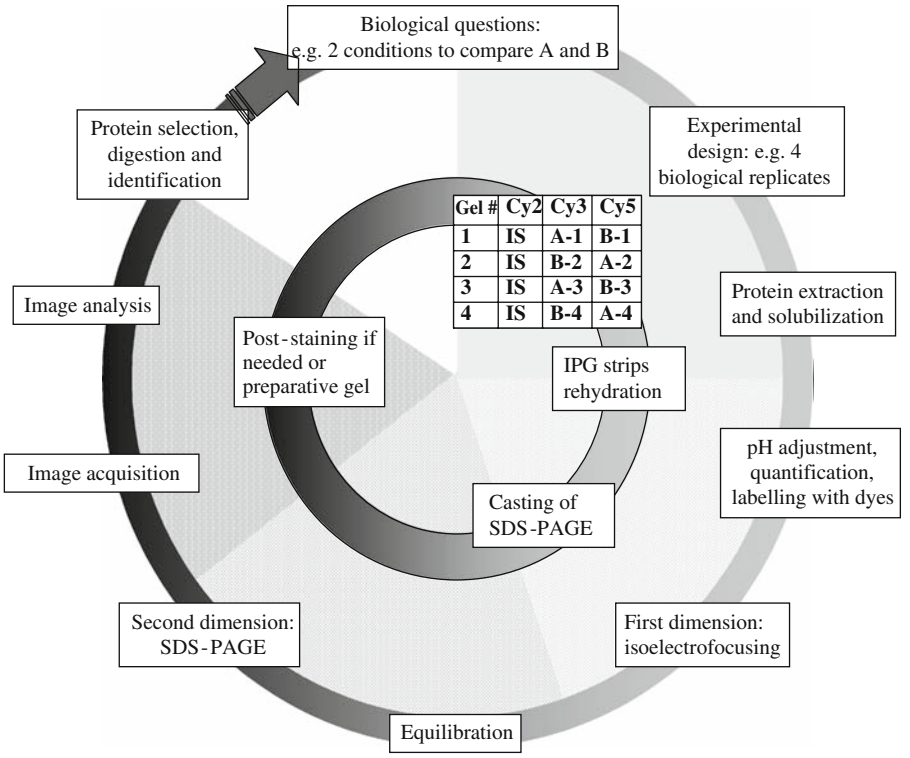

Fig. 12.1. Chronological scheme of a DIGE experiment over several days. An important step is the planning of the experiment itself (number of replicates, table with the labelling tags to respect the dye swap, number of gels to be rehydrated, casted, and so on). In parallel, IPG strips are rehydrated overnight to efficiently prepare the first dimension. The next day, after extraction of the protein according to your optimized method and solubilization in the appropriate buffer, the pH of the solution is adjusted prior to quantification and labelling. This being done, the first dimension can be started and the casting of the SDS-PAGE performed. The next morning, after completion of the IEF, IPG strips are equilibrated and placed on top of the SDS-PAGE to start the second dimension. Once the blue dye front has reached the bottom of the gels, images can be acquired and processed to unravel differentially expressed proteins before their identification.

used (*see* **Note 4**). To prepare a stock solution of dyes, the adequate volume of DMF is added to the tube containing the CyDye to reach the concentration of 1 nmol/μL. This solution may be kept for 2 months at −20°C.

4. The solution containing the proteins has to be equilibrated at a pH between 8.0 and 9.0, the optimum pH for the reaction between the CyDye and the proteins being 8.5. A first test of pH can be done with 0.5 μL of solution on pH paper and the adjustment is done by using NaOH solutions (0.1 or 1 M depending on the starting pH of the protein solution).
5. Before the labelling and after the pH adjustment, the contents of the protein sample have to be quantified. Several methods are available from different companies (Bio-Rad, GE Healthcare, Sigma, etc). Most of these methods are

based on a short protocol of precipitation before the quantification by colorimetry. The optimal concentration for the labelling reaction is around 5 μg/μL.

6. An example of experimental design is presented in **Fig. 12.1**. Thirty micrograms of protein is labelled for each sample by Cy3 and Cy5, and the internal standard is prepared with an equal part of each sample, before the labelling with Cy2, classically used for the internal standard (*see* **Note 5**).
7. Each CyDye is added to the Eppendorf tube containing the protein solution. The ratio of 400 pmol/μL of dye to 50 μg of protein has to be respected to optimize the labelling reaction, i.e. in our laboratory, 0.24 μL of dye solution is added to each tube containing 30 μg of protein solution. After vortexing and a short centrifugation to concentrate the solution at the bottom of the tube, the mixture is incubated for 30 min on ice in the dark.
8. After 30 min of incubation, 1 μL of stopping solution is added and the mixture is vortexed and incubated again for 10 min on ice in the dark.
9. The labelled samples can be stored at −80°C (for up to 3 months) or be used directly (*see* **Note 6**).

3.2. First-Dimension Separation: Isoelectrofocusing

1. The labelled samples have to be combined in one tube before the loading; each gel should contain 30 μg of protein labelled with Cy3, a second sample of 30 μg labelled with Cy5 and 30 μg of internal standard labelled with Cy2.
2. The volume of each combination has to be set at 120 μL before cup loading by adding 2× sample buffer solution containing DTT and ampholytes.
3. The rehydrated IPG strips are removed from the reswelling tray and transferred, gel side up, into the manifold properly positioned on the IPGphor system.
4. Electrode paper wicks, wetted with de-ionized water, are placed at the end of the IPG strips. Electrode is set on top of these papers before the positioning of the cup. It is important that the electrode wires are in contact with the paper.
5. IPG strips have to be covered with mineral oil to avoid drying during the first-dimension run. Pour around 100 mL on top of the gels into the manifold (*see* **Note 7**).
6. The combination of the three samples (labelled with Cy3, Cy5 and internal standard, respectively) is loaded in the cup. Before starting the electrophoretic run, the samples have to be covered with mineral oil, still to avoid dehydration and the formation of urea crystals in the cups.

7. The electrophoretic run can be started: in this example, the conditions of the run are the following at 20°C: 100 V for 2 h, 300 V for 3 h, 1,000 V for 6 h, a gradient step up to 8,000 V during 3 h and a constant step at 8,000 V to reach 60,000 V h with a maximum current setting of 50 μA/strip.
8. If the IPG strips are not used directly after the IEF run, they can be stored at −80°C between plastic sheets and maintained horizontally.

3.3. Second-Dimension Separation: SDS-PAGE

1. Casting of the gels between low-fluorescence glass plates: The glass plates are placed in the gel caster. The homogeneous solution for gels is first cooled (4°C) and degassed before addition of APS and TEMED. These last two compounds catalyse the polymerization of the gels and thus can be added directly only before casting. This solution is poured into the gel caster, and 1 mL of water-saturated butanol is added on top of each gel. The polymerization must be performed for at least 4 h.
2. Before the second dimension, the IPG strips are equilibrated in a buffered solution containing SDS (*see* **Note 8**), saturating the proteins in the IPG strips with negative charges to allow the mass-dependent separation of the protein in the second-dimension gel. A first step is carried out in equilibration buffer containing 1% DTT (w/v) for 15 min and then a second step with the equilibration buffer complemented with 2.5% (w/v) iodoacetamide to avoid formation of random S–S (*see* **Note 9**).
3. After equilibration, IPG strips are deposited on top of the SDS-PAGE and then sealed with hot agarose solution.
4. The gels are put in the electrophoresis vertical tank "Ettan Dalt twelve" and the running buffer is poured into the tank. The second-dimension run is started either for several hours (first 30 min at 1.5 W per gel, then 17 W per gel for 5 h) or overnight (first 30 min at 1.5 W per gel, then 2.5 W per gel for the night) at 20°C until the dye front reaches the bottom of the gels.

3.4. Image Acquisition and Analysis

1. When the gels are taken out of the SDS-PAGE tank, they are thoroughly rinsed with water (*see* **Note 10**) and dried with paper before the image acquisition in a scanner with three different lasers –or lasers able to combine three adequate wavelengths of emission and excitation – (here a Typhoon imager). Images are acquired by using three different lasers at 488, 532 and 633 nm (excitation wavelengths) and 520, 590 and 680 nm (emission wavelengths) for Cy2-, Cy3- and Cy5- labelled proteins, respectively (thus, three images per gel, corresponding to the two samples and the internal standard) (*see* **Note 11**).

2. After image acquisition, the first step for the image analysis is the detection of the spots. Softwares dedicated to DIGE image analysis are able to detect the spots simultaneously on the three images obtained from the same gel. One of the main advantages of the DIGE is the use of the internal standard for the gel-to-gel matching (as the same sample is run on all the gels from the experiment) but also for the normalization among the different gels. This feature helps the future analysis of the different gels and the comparison of the protein abundances. After the gel-to-gel matching, powerful statistical analyses can be achieved on thousands of spots present in all the gels (14, 15).
3. Once proteins of interest for the experiment have been selected on the basis of statistical analysis, the next step is the excision of the protein from a preparative gel (i.e. a gel containing more than 90 μg of proteins to obtain enough material for MS spectra acquisition). Depending on the excision mode (automated or manual), the use of Bind-Silane-coated glass plate has to be considered. A gel containing more or less 300 μg of proteins is run; the IEF step is performed on the same pH range, but with an increased amount of total volt per hour (e.g. ±90,000 V h for 24 cm on a pH 4–7). The SDS-PAGE is carried out in the same conditions. This preparative gel is then stained with Coomassie blue or a fluorescent post-migration stain (*see* **Note 12**).
4. After the scanning of the preparative gel and matching with analytical ones, a pick list is generated and used with the automated picker (e.g. here the Ettan Picker; GE Healthcare). Excised gel plugs are collected in microplates and used for protein identification protocols (*see* **Note 13**).
5. In this example, the protocol described is automatically performed on the Ettan Spot Handling Workstation (GE Healthcare), composed of an Ettan Picker, a digester and a spotter, in a closed cabinet to avoid contamination with keratin, for example (*see* **Note 14**). The digestion is performed in a temperature-controlled closed microplate tower. Washing steps aiming at removing interfering substances on the gel plugs such as Coomassie blue, excess of SDS (providing high background on the MS spectra) are then performed with the washing solution (150 μL, two or three times for 20 min depending on the intensity of the staining if Coomassie blue has been used). A solution of 75% acetonitrile is then added in the microplate wells for 30 min, then removed and the gel plugs are left to dry at room temperature.

6. Protein contained in the gel plug is digested by the addition of trypsin or another proteinase; here 6 μL of trypsin solution is added to the dried gel piece, the microplate is covered and the digestion is performed at 37°C for 4 h.
7. Extraction of peptides: 35 μL of peptide extraction solution is added in the well at the end of the digestion step and the supernatant is recuperated in a new microplate. This step is repeated twice and the supernatant pooled with the previous one. Peptides are then concentrated by drying.
8. Peptides are resuspended in 3 μL sample-spotting solution and mixed in the microplate wells. Then, 0.7 μL of this mixture is put on a MALDI target, and 0.7 μL of matrix solution is added on top (with three mixing strokes in the spotter needle before final deposition).
9. Once the peptides are on the MALDI target, the instrument is calibrated with a mixture of known peptides and the acquisition of spectra (MS and MS/MS) is started.
10. The data acquired on the mass spectrometer are used for identification searches in a protein databases. Several types of software may be used for automated and manual interpretation of the results. A non-exhaustive list of the web sites offering this feature is given here:
    a. http://fasta.bioch.virginia.edu/fasta_www2/fasta_list2.shtml
    b. http://www.matrixscience.com/search_form_select.html
    c. http://prospector.ucsf.edu/
    d. http://www.expasy.org/tools/popitam
    e. http://phenyx.vital-it.ch/pwi/login/login.jsp

The MS spectrum provides a list of masses corresponding to peptides generated during the digestion of the protein. The MS/MS spectra allow the sequence of amino acids from a specific peptide selected for fragmentation. The obtained masses and sequences are compared with existing databases. After identification, literature survey is usually requested to link the results obtained to the initial biological question. More information about MS can be found in the following selection of excellent reviews: general mass spectrometry (16) in plants (17, 18) and in non-model plants (19).

3.5. Additional Features of DIGE in Proteomics

Difference gel electrophoresis can be applied not only to the classical 2D electrophoresis techniques but also to e.g. Blue Native-PAGE (20). In this case, the multiplexing technique is applied for example to protein complexes extracted from chloroplasts. This method is used to unravel the composition of the protein complexes (e.g. specific subunit stoichiometry, assembly). In the

BN-PAGE technique, the proteins are solubilized in their native state with appropriate non-denaturating detergents (such as digitonin or dodecylmaltoside) and coupled with Coomassie blue G, which brings negative charge on the protein and ensure the migration towards the anode (21, 22). Protein complexes are then separated according to their mass, then the lanes are treated with SDS under reducing conditions before a second separation based again on their mass, but in denaturing conditions (SDS-PAGE). CyDyes can be added to the proteins complexes prior to the first dimension.

4. Notes

1. Urea and thiourea help the solubilization of proteins.
2. Dithiothreitol (DTT) preserves the fully reduced state of denatured, unalkylated proteins.
3. The classical colorimetric method of Bradford (23) cannot be used for protein quantification, as the components of the labelling solution interfere with the Bradford solution (e.g. the high concentration of urea, detergent).
4. The DMF solution should not be contaminated with water, which degrades DMF to amine compounds. Select a DMF solution of $\leq$0.005% H_2O, $\geq$99.8% of purity, and this solution should be replaced at least every 3 months.
5. A dye swap is always recommended to avoid preferential labelling.
6. Optionally, the labelling reaction can be checked on a small SDS-PAGE on some of the samples before running the complete series of DIGE.
7. When the mineral oil covers the gels, check that there is no leakage (no oil in the sample cups).
8. Sodium dodecyl sulphate (SDS) denatures proteins and forms negatively charged protein–SDS complexes.
9. Iodoacetamide alkylates thiol groups on proteins, preventing their reoxidation during electrophoresis. Protein reoxidation during electrophoresis can result in streaking and other artefacts. Iodoacetamide also alkylates residual DTT to prevent point streaking and other silver-staining artefacts.
10. In the above text, if it is not mentioned otherwise, "water" means double-distilled water.
11. If it is not possible to scan all the gels at the same day, they can be stored at 4°C for 48 h without variation in the signal and the position on the gel. For longer storage periods, the

gels have to be fixed in fixing solution and then kept at 4°C. Before scanning, leave the gels on the bench for a while to reach room temperature (as the temperature impacts the signal intensity).

12. Preparative gels, containing high amount of proteins, can be prepared separately for the identification of proteins. In this case, we recommend either to prepare an important amount of proteins coming from the different conditions or to run one preparative gel per sampling condition. In this case, the labelling step is omitted and the gel is stained with Coomassie or another fluorescent solution (Sypro Ruby, Lava Purple or others). At least 300 μg have to be loaded on the IPG strips, and the time for IEF has to be extended (for a 24-cm gel, pH 4–7, the recommended value to reach is 90,000 V h). It is also recommended to use Bind-Silane-coated glass plates to facilitate the picking (by avoiding shrinking or deformation of the gels).
13. Care is needed with the microplates; digestion carried out in microplates from several suppliers has resulted in the presence of polymers in the mass spectra, rendering the MS/MS spectra unreadable.

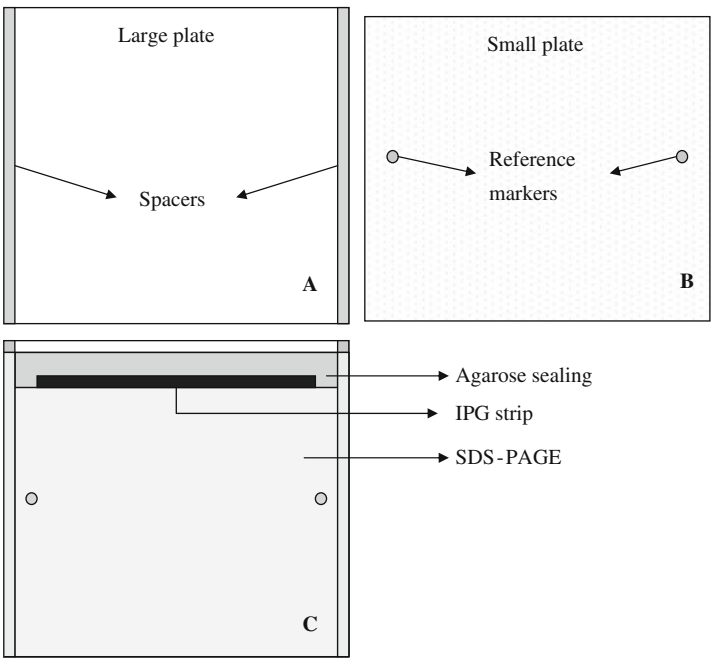

Fig. 12.2. Preparation of the glass plates and final assembled gel "sandwich". **(a)** Large plate with the spacers; **(b)** smaller plate coated with Bind-Silane. Reference markers have been put on the glass plate and covered with Bind-Silane (position: in the median of the height and not on the spacers!). **(c)** Final assembling of the two glass plates showing the reference markers and the IPG strip position sealed with the agarose solution on top of the gel of the second dimension (SDS-PAGE gel).

14. If the preparative gels are stained with fluorescent dyes and/or used for picking with the Ettan Spot picker or the Spot Handling Workstation, reference markers must be placed on the Bind-Silane-coated plate as shown in **Fig. 12.2**.

References

1. Wilkins, M.R., et al. (1995) Progress with proteome projects: why all proteins expressed by a genome should be identified and how to do it. *Biotechnol Gene Eng Rev* **13**, 19–50.
2. The Arabidopsis Genome Initiative (2001) Analysis of the genome sequence of the flowering plant *Arabidopsis thaliana*. *Nature* **408**, 796–815.
3. International Rice Genome Sequencing Project (2005) The map-based sequence of the rice genome. *Nature* **436**, 793–799.
4. Tuskan, G.A., et al. (2006) The genome of black cottonwood, *Populus trichocarpa* (Torr. & Gray). *Science* **313**, 1596–1604.
5. Jorrin, J.V., Maldonado, A.M., and Castillejo, M.A. (2007) Plant proteome analysis: a 2006 update. *Proteomics* **7**, 2947–2962.
6. Skynner, H., et al. (2002) Alterations of stress related proteins in genetically altered mice revealed by two-dimensional differential in-gel electrophoresis analysis. *Proteomics* **2**, 1018–1025.
7. Alban, A., et al. (2003) A novel experimental design for comparative two-dimensional gel analysis: two-dimensional difference gel electrophoresis incorporating a pooled internal standard. *Proteomics* **3**, 36–44.
8. Saravanan, R.S. and Rose, J.K.C. (2004) A critical evaluation of sample extraction techniques for enhanced proteomic analysis of recalcitrant plant tissues. *Proteomics* **4**, 2522–2532.
9. Carpentier, S.C., et al. (2005) Preparation of protein extracts from recalcitrant plant tissues: an evaluation of different methods for two-dimensional gel electrophoresis analysis. *Proteomics* **5**, 2497–2507.
10. Delaplace, P., et al. (2006) Potato tuber proteomics: comparison of two complementary extraction methods designed for 2-DE of acidic proteins. *Proteomics* **6**, 6494–6497.
11. Rolland, N., et al. (2006) A versatile method for deciphering plant membrane proteomes. *J Exp Bot* **57**, 1579–1589.
12. Zabrouskov, V., Giacomelli, L., van Wijk, K.J., and McLafferty, F.W. (2003) A new approach for plant proteomics: characterization of chloroplast proteins of *Arabidopsis thaliana* by top-down mass spectrometry. *Mol Cell Proteomics* **2**, 1253–1260.
13. Keech, O., Dizengremel, P., and Gardeström, P. (2005) Preparation of leaf mitochondria from *Arabidopsis thaliana*. *Physiol Plant* **124**, 403–409.
14. Fenselau, C. (2007) A review of quantitative methods for proteomic studies. *J Chromatogr B* **855**, 14–20.
15. Gottlieb, D.M., Schultz, J., Bruun, S.W., Jacobsen, S., and Sondergaard, I. (2004) Multivariate approaches in plant science. *Phytochemistry* **65**, 1531–1548.
16. Aebersold, R. and Mann, M. (2003) Mass spectrometry-based proteomics. *Nature* **422**, 198–207.
17. Baginsky, S. (2009) Plant proteomics: concepts, applications, and novel strategies for data interpretation. *Mass Spectr Rev* **28**, 93–120.
18. Glinski, M. and Weckwerth, W. (2006) The role of mass spectrometry in plant systems biology. *Mass Spectr Rev* **25**, 173–214.
19. Carpentier, S.C., et al. (2008) Proteome analysis of non-model plants: a challenging but powerful approach. *Mass Spectr Rev* **27**, 354–377.
20. Reisinger, V. and Eichacker, L.A. (2007) How to analyze protein complexes by 2D Blue Native SDS-PAGE. *Proteomics* **7 (S1)**, 6–16.
21. Reisinger, V. and Eichacker, L.A. (2008) Solubilization of membrane protein complexes for blue native PAGE. *J Proteom* **71**, 277–283.
22. Braun, R.J., Kinkl, N., Beer, M., and Ueffing, M. (2007) Two-dimensional electrophoresis of membrane proteins. *Anal Bioanal Chem* **389**, 1033–1045.
23. Bradford, M.M. (1976) A rapid and sensitive method for the quantitation of microgram quantities of protein utilizing the principle of protein-dye binding. *Anal Biochem* **72**, 248–254.

Chapter 13

Thiol–Disulfide Redox Proteomics in Plant Research

Meenakumari Muthuramalingam, Karl-Josef Dietz, and Elke Ströher

Abstract

Abiotic stresses often cause metabolic imbalances which affect cellular redox homeostasis and alter the rate of reduction state of functional and regulatory protein thiols and the rate of reactive oxygen species release. Excessive displacement from redox equilibrium causes oxidative damage to cell structures and may elicit cell death. The understanding of the cell response to progressive stress must include knowledge on the thiol redox state of specific proteins. This chapter describes selected gel-based biochemical methods (i) to identify thiol–disulfide redox proteins that undergo major redox-dependent conformational changes by 2D redox SDS-PAGE and (ii) to determine the thiol redox state of proteins by sequential blocking and labeling with *N*-ethylmaleimide and methoxypolyethylene glycol maleimide-5000 (mPEG-Mal-5000). Both sets of methods provide experimental information that defines the redox proteome of the cell.

Key words: 2D electrophoresis, acrylamide gel electrophoresis, maleimide labeling, redox proteome analysis, thiol protein.

1. Introduction

In general, the thiol group of the amino acid cysteine is one of the main redox centers found in biologically important peptides and proteins. Alteration of its redox state provides a decisive mechanism to regulate functional features of specific proteins, thereby affecting the entire cell. Posttranslational thiol modifications include intra- and intermolecular disulfide formation, and also *S*-nitrosylation, and alter protein functions, e.g., enzyme activities and binding properties for interaction partners (1). In the plant cell, protein thiols are reduced by electron donors ultimately linked to NAD(P)H, ferredoxin, and

R. Sunkar (ed.), *Plant Stress Tolerance*, Methods in Molecular Biology 639,
DOI 10.1007/978-1-60761-702-0_13,

glutathione and oxidized by electron acceptors, particularly by reactive oxygen species (2, 3). Thiol oxidation is stimulated under oxidizing conditions that occur in cells subjected to abiotic or biotic stress and may be considered as a prime and central metabolic response to stress which is used for feedback regulation via different signaling cascades, aiming at readjusting redox homeostasis (4). Depending on the midpoint redox potential of the target thiols, thiol modifications are early responses. In later stages of stress, other amino acid residues are oxidized as well (5). Thus monitoring the thiol state of proteins provides important information needed to assess the actual redox state and link it to the cellular response to specific stress. Since peptide and protein thiols represent functional groups with defined reactivity, chemicals and probes are at hand to covalently bind to the cysteinyl sulfur atom and, thereby, to block and/or mark reduced protein thiols. Well-characterized thiol-reactive groups are iodoacetamide and maleimide, often coupled to fluorescent or isotopically labeled probes, or to linear polymers to ease the detection. The diagonal 2D redox SDS-PAGE enables the identification of redox proteins that alter their electrophoretic mobility as a consequence of redox-dependent conformational changes (6, 7). This method works best with subfractions of tissues and fractionated protein extracts and also with membrane proteins (7, 8).

2. Materials

2.1. Blocking and Labeling of Free Thiols

1. Dithiothreitol (DTT, 1 M) should be prepared fresh in aqueous buffer of pH 7.0 (*see* **Note 1**).
2. Copper(II) chloride ($CuCl_2$) stock solution: 1 mM in water.
3. Hydrogen peroxide (H_2O_2) stock solution: 10 mM in water.
4. *N*-Ethylmaleimide stock (NEM, 2 M) solution is prepared in 100% ethanol. Working solutions are prepared by further dilution in labeling buffer.
5. Methoxypolyethylene glycol maleimide-5000 (mPEG-Mal-5000, 25 mM) (Fluka, Seelze, Germany) stock was prepared directly in labeling buffer just prior to use. Working solutions are prepared by further dilution in labeling buffer.
6. Labeling buffer: 6 M urea, 200 mM Bis–Tris (pH 6.5), 0.5% (w/v) SDS, 10 mM EDTA (*see* **Note 2**) frozen in (500 μL) aliquots for single use at −80°C (*see* **Note 3**). Just prior to use, the labeling buffer is supplemented with 100 mM NEM or 2–5 mM mPEG-Mal (*see* **Note 4**).
7. Incubator at 25°C.

8. Trichloroacetic acid (TCA) solution (100%, w/v). Stored in dark bottle at 4°C (*see* **Note 5**). The following dilutions are prepared:
   a. Ice-cold 20% (v/v) TCA solution, stored in dark bottle at 4°C.
   b. Ice-cold 10% (v/v) TCA solution, stored in dark bottle at 4°C.
   c. Ice-cold 5% (v/v) TCA solution, stored in dark bottle at 4°C.

2.2. Non-reducing SDS-Polyacrylamide Gel Electrophoresis (SDS-PAGE)

1. Stacking gel buffer (4×): 0.5 M Tris–HCl, pH 6.8. Store at 4°C.
2. Thirty percent (w/v) acrylamide/bisacrylamide solution (ratio 37.5:1) (Roth, Karlsruhe, Germany) (*see* **Note 6**).
3. *N*,*N*,*N*′,*N*′-Tetramethylethylenediamine (TEMED) (Sigma-Aldrich, Seelze, Germany), store at room temperature (RT).
4. Ammonium persulfate (APS) solution (10%): prepare 100 mg in 1 mL water. Store at 4°C and prepare fresh weekly.
5. Isopropanol (100%) to overlay the separating gel to ensure a flat surface and to exclude oxygen during polymerization.
6. Running buffer (10×): 125 mM Tris, 960 mM glycine, 0.5% (w/v) SDS. Store at room temperature. For 1× running buffer, add 100 mL of 10× running buffer to 900 mL ultrapure H_2O.
7. Unstained molecular weight marker: PageRuler™ Unstained Protein Ladder (Fermentas, St. Leon-Rot, Germany).
8. SDS electrophoresis system: chamber, comb, set of glass plates, spacer, rubber gum, clamps, power supply, cables. A Hamilton syringe to apply the samples and additional 10-mL syringe fitted with a 20-gauge needle to wash the wells after removing the comb.
9. Loading buffer (5×): 225 mM Tris–HCl (pH 6.8), 5% (w/v) SDS, 50% glycerol, 0.05% bromophenol blue (without reducing agent). Store at room temperature.

2.3. Diagonal 2D Redox SDS-PAGE

2.3.1. Preparation of Extracts for Diagonal 2D Redox SDS-PAGE: Reduction/Oxidation and Subsequent Blocking of Free Thiol Groups

1. Protein extract, e.g., isolated and fractionated chloroplasts, at a concentration of 3.5 mg/mL.
2. Buffer stock solutions: 1 M Tris–HCl (pH 7.5), 1 M Tris–HCl (pH 8.0). Dilutions are made from the stock solutions and the pH values are adjusted if necessary.
3. Dithiothreitol (DTT) stock solution: 1 M in 1 M Tris–HCl, pH 7.5 (*see* **Note 1**).

4. Hydrogen peroxide (H_2O_2) stock solution: 100 mM in water.
5. Iodoacetamide (IA) (Fluka, Seelze, Germany) stock solution: 1 M prepared in 1 M Tris–HCl, pH 8.0 (*see* **Note 7**).
6. Incubator at 25°C.

2.3.2. Preparation and Running the Second Dimension of the Diagonal 2D Redox SDS-PAGE

Similar to **Section 2.2**.

Additional:

1. Glass plates for the second dimension: To simplify the attachment of the excised gel segment (corresponding to a lane of first dimension) for the second dimension, it is recommended to use either (a) a set of notched glass plates, which consists of one rectangular piece of glass plus complementary piece of the same size with a cut made on the top edge leaving two "ears," one on each corner which additionally aids at fixing the gel lane or (b) a set of hinged spacer plates with one of the glass plates approximately 1.5–2 cm shorter than the other.
2. Comb with 1 cm broad teeth, can be self-made from Teflon plates (*see* **Note 8**).
3. Blue cap tubes (50 mL) or similar tubes for incubation of the gel slices after the first dimension.
4. Roller mixer (*see* **Note 9**).
5. Sharp new razor blade to cut the gel slice corresponding to one complete lane.
6. Loading buffer (1×): 800 mL deionized H_2O supplemented with 200 mL of 5× loading buffer.
7. Dithiothreitol (DTT).
8. Iodoacetamide (IA).
9. Agarose sealing solution: 0.5% (w/v) agarose solution, 0.01% (w/v) bromophenol blue in 1× loading buffer. Heat the solution in the microwave or on a heating stirrer until the agarose is melted. Dispense in aliquots and store at 4°C.

2.4. Detection and Analysis

All solutions are prepared with high-quality ultrapure water, as impurities have a strong effect on silver staining.

2.4.1. Silver Staining

1. Fixation solution: 50% (v/v) ethanol (*see* **Note 10**), 12% (v/v) acetic acid, 38% (v/v) H_2O.
2. Washing solution: 50% (v/v) ethanol.
3. Sensitizer stock solution: 2 g $Na_2S_2O_3 \cdot 5\ H_2O$ in 100 mL H_2O.
4. Sensitizer solution: 5 mL sensitizer stock solution in 495 mL H_2O.

5. Staining solution: 0.2% (w/v) $AgNO_3$ in H_2O, store in dark at RT.
6. Developer stock solution: 0.4 g $Na_2S_2O_3 \cdot 5\ H_2O$ in 100 mL H_2O.
7. Developer: 60 g Na_2CO_3, 1 mL developer stock solution, add H_2O to 1 L.
8. Stopping solution: same as fixation solution.
9. Formaldehyde (37%).
10. Horizontal shaker.

2.4.2. MALDI-TOF Analysis

1. Sharp scalpel.
2. Reaction tubes (1.5 mL), 96-well microtiter plates (depending on the number of spots to be analyzed).
3. Washing solution A: 0.1% (w/v) trifluoroacetic acid/60% (v/v) acetonitrile (*see* **Note 11**).
4. Washing solution B: 50% (v/v) acetonitrile.
5. Washing solution C: 50% (v/v) acetonitrile/50 mM NH_4HCO_3.
6. Washing solution D: 50% (v/v) acetonitrile/10 mM NH_4HCO_3.
7. Trypsin: 0.013 mg sequencing grade trypsin in 10 mM NH_4HCO_3, pH 8.0 (Promega, Mannheim, Germany).
8. Buffer: 10 mM NH_4HCO_3, pH 8.0.
9. Matrix: α-Cyano-4-hydroxycinnamic acid (Sigma-Aldrich, Seelze, Germany).
10. MALDI-TOF mass spectrometer: Biflex III matrix-assisted laser desorption/ionization-time of flight (MALDI-TOF)–MS (Bruker, Bremen, Germany).
11. Software that uses the MS data to identify proteins from primary sequence databases, e.g., MASCOT software (Matrix Science, London, UK).

3. Methods

Redox-dependent posttranslational modifications enable, disable, and modulate protein functions. The involved cysteinyl thiol groups undergo inter- or intramolecular disulfide bond formation with adjacent thiol groups and are oxidized to sulfenic, sulfinic, or sulfonic acid derivatives or *S*-nitroso groups. These thiol modifications change steric properties, charge distribution, protein conformation, and thereby function.

In order to analyze proteins regulated via defined redox-dependent modifications, methods are needed to identify such proteins, to arrest the thiol redox state in situ, to label the thiol groups, and to visualize the protein reduction state. Most of the methods aim at identifying redox-regulated thiol groups, especially those prone to oxidation to sulfenic acid, based on the sequential labeling with thiol-specific reagents, such as maleimide- or iodoacetamide-coupled substances (**Fig. 13.1**). Such a method is presented in the first part of this chapter (summarized in **Fig. 13.2**). The second part focuses on proteins undergoing major conformational changes due to redox-mediated processes. A special 2D SDS-PAGE technique facilitates their identification.

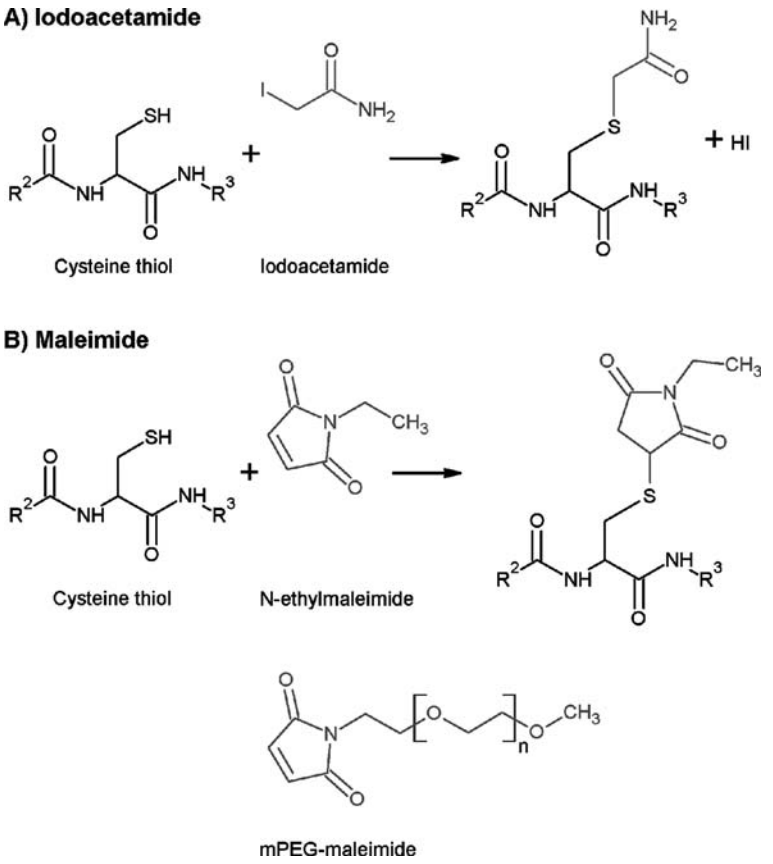

Fig. 13.1. Reaction of the amino acid cysteine with thiol-specific reagents. Thiol-specific reagents generally act on the thiolate anion of the cysteinyl residue. (**a**) Iodoacetamide and therewith coupled substances react irreversibly with thiol groups to form a stable thioether bond through a substitution reaction. (**b**) The maleimide group of *N*-ethylmaleimide and other derivatives react by nucleophilic attack of the thiolate ion through an addition reaction. The derivative methoxypolyethylene glycol (mPEG) maleimide increases the molecular mass of the labeled protein depending on the length of the polymer, thereby shifting the protein migration within SDS-PAGE analysis. R2 and R3 are the neighboring ends of the peptide chains.

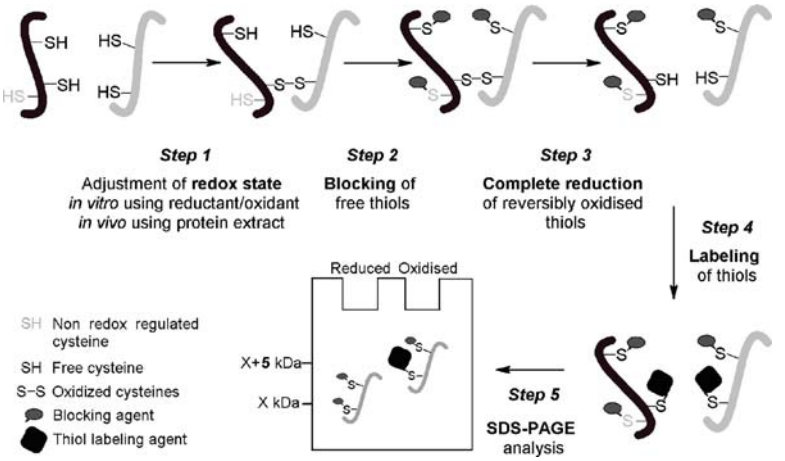

Fig. 13.2. Detection of redox-regulated proteins via a sequential labeling strategy. Step 1 includes the adjustment of redox state using either the enzymatic system (e.g., thioredoxin or glutaredoxin system) or artificial reductants (e.g., dithiothreitol) or oxidants (e.g., hydrogen peroxide and copper chloride). In step 2, free thiol groups are blocked using alkylating reagents (e.g., iodoacetamide, *N*-ethylmaleimide) under denaturing conditions. Subsequently, proteins are completely reduced with reductants in step 3. The newly freed thiol groups are labeled via thiol-specific reagents like mPEG-maleimide-5000 in step 4. The introduced molecular mass increase of about 5 kDa enables the detection of thiol-containing protein via SDS-PAGE analysis in step 5.

3.1. Labeling and Detection of Free Thiols

3.1.1. Adjustment of Redox State of the Proteins (Step 1)

1. Protein concentration: Purified protein is adjusted to a concentration of 0.1 mg/mL in 50 mM Tris–HCl, pH 7.5.
2. Complete reduction is achieved by addition of 20 μL of 1 M DTT (final concentration 100 mM DTT) to 180 μL of protein extract and incubation at 25°C for 60 min.
3. Oxidation is achieved by addition of 20 μL of 10 mM H_2O_2 or 1 mM $CuCl_2$ (final concentrations: 1 mM H_2O_2 and 100 μM $CuCl_2$, respectively) to 180 μL of protein extract and incubation at 25°C for 60 min.

3.1.2. Labeling of Free Thiols (Step 2)

1. Add 25 μL ice-cold 100% (w/v) TCA to quench the thiol–disulfide reaction and to remove excess reducing/oxidizing agent via precipitation (*see* **Note 12**). Mix well by vortexing and incubate on ice for at least 30 min.
2. The precipitated proteins are obtained by centrifugation at 20,000×*g* at 4°C for 15 min (*see* **Note 13**).
3. Remove the supernatant completely and wash the pellets with 500 μL ice-cold 10% (v/v) TCA.
4. Vortex briefly and centrifuge for 2 min at 20,000×*g* to pellet the proteins. Carefully remove the wash solution completely without disturbing the pellet.

5. Add 250 μL ice-cold 5% (v/v) TCA solution and vortex briefly.
6. Centrifuge at 20,000×*g* for 2 min to pellet the proteins. Carefully remove the wash solution completely without disturbing the pellet.
7. Thoroughly resuspend the pellet in 180 μL of labeling buffer containing 100 mM NEM (171 μL labeling buffer plus 9 μL of 2 M NEM) by vortexing (*see* **Notes 2** and **14**).
8. The alkylation is performed at 25°C in the dark for 60 min.
9. The reaction is stopped by addition of 180 μL ice-cold 20% (v/v) TCA (*see* **Note 15**).
10. Mix well by vortexing and the precipitation is performed for 30 min on ice.
11. The precipitated proteins are centrifuged at 20,000×*g* for 15 min at 4°C.
12. Repeat steps 3–6.

3.1.3. Complete Reduction of Thiols (Step 3)

1. Dissolve the pellet in 180 μL of labeling buffer supplemented with 100 mM DTT (162 μL labeling buffer plus 18 μL of 1 M DTT) to reduce all reversible thiol modifications such as disulfide bonds and sulfenic acid residues (*see* **Note 14**). Mix by vortexing.
2. Incubate the samples at 25°C for 1 h to ensure complete reduction.
3. The reaction is stopped by adding 180 μL of ice-cold 20% (v/v) TCA (*see* **Note 15**).
4. The precipitation is performed on ice for 30 min.
5. Repeat steps 3–6 of **Section 3.1.2**.

3.1.4. Labeling of Newly Reduced Thiols (Step 4)

1. Thoroughly dissolve the protein pellet in 180 μL of labeling buffer supplemented with the labeling reagent mPEG-Mal-5000 (**Fig. 13.3**).
2. The typical labeling reaction contains 0.1 mg/mL reduced protein in labeling buffer supplemented with mPEG-Mal-5000 at a molar ratio of 1:250 (thiol:mPEG-Mal).
3. The labeling reaction is performed at 25°C in dark for 1 h.
4. The reaction is stopped and excess labeling reagent is quenched by addition of 2 μL of 1 M DTT in labeling buffer (final concentration 10 mM DTT) (*see* **Note 16**).
5. The samples are supplemented with 5× loading buffer (180 μL sample plus 45 μL of 5× loading buffer).

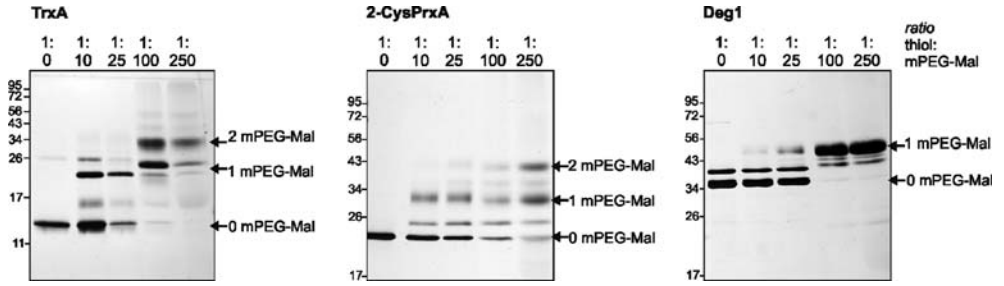

Fig. 13.3. Site-directed protein modification. SDS-PAGE analysis of the heterologously expressed and purified proteins *Escherichia coli* thioredoxin A (TrxA), *Arabidopsis thaliana* 2-cysteine peroxiredoxin A (2-CysPrxA), *A. thaliana* Deg1 protease (Deg1) after titration with increasing molar ratios of thiol-specific modification reagent. The extent of modification was quantified after SDS-PAGE analysis and subsequent silver staining. Proteins were chosen according to the position of the redox-active cysteines: In the case of TrxA, one of the two active sites of cysteines is on the surface, whereas the second one is more buried. Accordingly, binding of the first mPEG-Mal to the exposed Cys occurs at very low mPEG-Mal concentrations, while binding to the second is visualized by further shifting only at a ratio $\geq$100:1 (mPEG-Mal to protein thiols). The two active cysteines of 2-CysPrxA are buried within its dimeric structure. The band corresponding to the unlabeled protein nearly completely disappears and labeling is completed at a ratio $\geq$250:1. For the protease Deg1, a ratio of $\geq$100:1 is sufficient to completely label the single cysteine. It has to be mentioned that the double band detected without labeling reagent had already been described before (8). The cysteine is accessible only in the conformation represented by the lower band, which interestingly corresponds to the active protease (8). The acrylamide concentration was changed according to the size of the analyzed proteins: 16% for TrxA and 12% for 2-CysPrxA and Deg1.

6. The labeled proteins are analyzed using non-reducing SDS-PAGE. The percentage is chosen according to the molecular mass of the protein of interest.
7. The proteins can be detected by any of the staining techniques applicable to SDS-PAGE analysis, for example, via silver staining (see below). In more complex protein mixtures or extracts, immunodetection after Western blotting allows for the identification of the redox state of specific proteins.

3.2. Non-reducing SDS-PAGE (Step 5)

1. These instructions assume the use of an SDS-PAGE system with gels of 18 cm (width) × 10 cm (height) × 1 mm (thickness). The volumes can be easily adapted to other formats.
2. Thoroughly clean all components of the gel electrophoresis system (e.g., the glass plates, spacers, and comb) with 70% ethanol and a lint-free tissue (e.g., Kimwipes).
3. Assemble the system according to the manufacturer's recommendations.
4. Prepare 15 mL of 12% separating gel by mixing 3.7 mL separating gel buffer with 6 mL acrylamide solution (*see* **Note 6**), 5.2 mL water, 100 μL APS solution, and 14 μL TEMED. The polymerization process will start as soon as APS and TEMED have been added. Avoid formation of air bubbles.

5. Pour the gel between the plates carefully, overlay with 1 mL 100% isopropanol, and wait until the gel is polymerized (takes approximately 30 min).
6. Pour off the isopropanol and rinse twice with distilled water. Remove the water completely using a lint-free tissue.
7. Prepare 5 mL of 6% stacking gel by mixing 1.25 mL stacking gel buffer with 1 mL acrylamide solution, 2.65 mL water, 50 μL APS solution, and 5 μL of TEMED.
8. Pour the stacking gel and carefully insert the comb, avoid introduction of air bubbles.
9. Once the stacking gel is polymerized (~20 min), assemble the gel electrophoresis system by attaching the gel to the chamber and fill the reservoir chambers with 1× running buffer. After removing the comb, wash the wells with 1× running buffer using a 10-mL syringe fitted with a 20-gauge syringe needle.
10. Centrifuge the samples supplemented with loading buffer for 5 min at 17,000×*g* at room temperature to pellet any insoluble matter.
11. Reducing agents and boiling are omitted in this protocol as remaining disulfide bonds should be maintained.

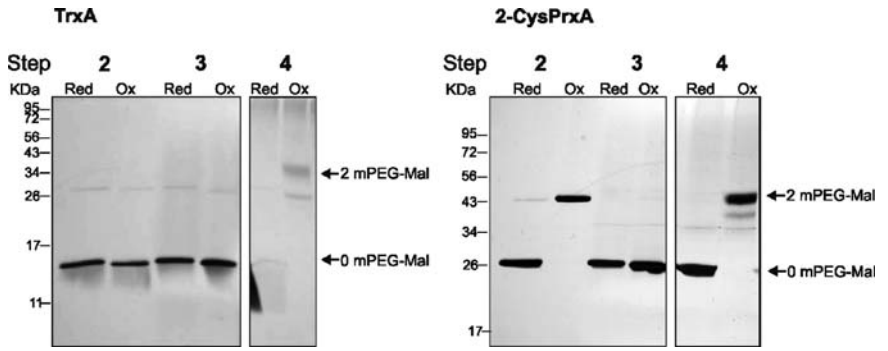

Fig. 13.4. Detection of redox-sensitive thiol groups of *E. coli* thioredoxin A (TrxA) and *A. thaliana* 2-cysteine peroxiredoxin A (2-CysPrxA) using the sequential labeling strategy. Heterologously expressed and purified proteins were employed to optimize the labeling method. After the initial reduction (Red) and oxidation (Ox) with 100 mM DTT and 100 μM $CuCl_2$, respectively, aliquots of steps 2–4 were taken and subjected to non-reducing SDS-PAGE analysis and subsequent silver staining. For TrxA and 2-CysPrxA, complete reduction and oxidation can be linked to conformational changes and concomitant changes in electrophoretic mobility. Oxidized TrxA is more compact due to intramolecular disulfide bond formation and the molecular mass of oxidized 2-CysPrxA increases due to dimer formation. Blocking of reduced thiol groups in step 2 is confirmed, as the band pattern corresponds to the reduced and oxidized state, respectively. Complete reduction of both proteins in step 3 is indicated by the migration behavior as reduced and oxidized protein, respectively. Subsequently, only newly reduced thiol groups are labeled, which is confirmed by the banding pattern obtained after step 4. For TrxA 16% and for 2-CysPrxA 12% acrylamide concentrations are used for the separation, depending on their molecular masses. It should be noted that the band identified after step 2 (ox) corresponds to the 2-Cys Prx dimer. The same band is seen after step 4 (ox) below the strong mPEG-Mal-labeled band.

12. Carefully apply 10 μL of sample (approximately corresponding to 1 μg) per well using the Hamilton syringe.
13. Run the gel at constant current (60 mA) until the running front reaches the bottom.
14. Visualize the proteins via silver staining (see below). An example of the results produced is shown in **Fig. 13.4**.

3.3. Diagonal 2D Redox SDS-PAGE

3.3.1. Preparation of Extracts: Adjustment of Redox State and Subsequent Blocking of Free Thiol Groups

1. If necessary, protein extracts are concentrated to 3.5 mg protein/mL using Amicon centrifugation units (cutoff 3 kDa; Millipore, Schwalbach, Germany) according to the manufacturer's recommendations.
2. Protein extract (180 μL) in 50 mM Tris–HCl (pH 7.5) is completely reduced by addition of 20 μL of 1 M DTT or oxidized by addition of 20 μL of 100 mM H_2O_2 (final concentration 100 mM DTT and 10 mM H_2O_2, respectively) (*see* **Note 17**).
3. The sample is mixed by vortexing and incubated for 30 min at 25°C.
4. In order to prevent thiol reshuffling, e.g., re-oxidation, 22 μL of 1 M iodoacetamide is added (final concentration 100 mM) (*see* **Note 18**).
5. The sample is mixed by vortexing and incubated at 25°C in the dark for 30 min.
6. Reaction is stopped by addition of 55 μL of 5× loading buffer followed by gel electrophoretic separation (see below).

3.3.2. Diagonal 2D Redox SDS-PAGE Electrophoresis

1. These instructions assume the use of an SDS-PAGE system with gels 18 cm (width) × 20 cm (height) × 1 mm (thickness). The volumes can be easily adapted to other formats.
2. Prepare 30 mL of 12% separating gel by mixing 7.4 mL separating gel buffer with 12 mL acrylamide solution, 10.4 mL water, 200 μL APS solution, and 28 μL TEMED, avoid formation of air bubbles (*see* **Note 6**). Pour the gel, overlay with 1 mL of 100% isopropanol, and wait until the gel is polymerized (takes approximately 30 min) (*see* **Note 19**).
3. Pour off the isopropanol and rinse the surface of the separating gel twice with distilled water. Remove the water completely using a lint-free tissue.
4. Prepare 10 mL of 6% stacking gel solution by mixing 2.5 mL stacking gel buffer with 2 mL acrylamide solution, 5.3 mL water, 100 μL APS solution, and 10 μL of TEMED, avoid formation of air bubbles.

(a) Pour the stacking gel and carefully insert the comb, avoid introduction of air bubbles.

(b) The stacking gel for the second dimension SDS-PAGE is prepared without a comb; instead prepare stacking gel of 1 cm height but do not completely fill the assembled glass plates with stacking gel, spare 0.3–0.5 cm to trap the gel section afterward.

5. Add running buffer to the upper and the lower chambers of the gel unit and wash the wells with running buffer using a 10-mL syringe fitted with a 20-gauge needle.
6. Slowly load 250 μL of each sample (corresponding to about 500 μg protein) in each well (*see* **Note 20**).
7. Protein samples are subjected to electrophoresis at 40 mA constant current for approximately 4 h (*see* **Note 21**).
8. Stop the electrophoresis when the running front reaches the bottom.
9. Disassemble the electrophoresis system and carefully excise the gel sections corresponding to single lanes using a sharp razor blade aided with a ruler (e.g., the spacer) positioned along the markings made during the gel run. The stacking gel is discarded (*see* **Note 22**).
10. Prepare 10 mL of 1× loading buffer supplemented with 100 mM DTT (154.3 mg in 10 mL of buffer) per gel lane in a 50-mL blue cap tube.
11. Carefully place the gel lane in the blue cap tube. Avoid contact of the gel lane with dry surfaces.
12. Incubate for 15 min on the roller mixer at RT (*see* **Note 23**). Discard the buffer; be careful not to lose the gel.
13. Wash the gel by adding 20 mL of 1× running buffer to remove excess DTT from the surface of the gel and the tube. Discard the buffer; be careful not to lose the gel.
14. Add 10 mL of 1× loading buffer supplemented with 100 mM IA (184.96 mg in 10 mL of buffer) per gel lane and tube.
15. Incubate for 15 min on the roller mixer at RT (*see* **Note 23**). Discard the buffer; be careful not to lose the gel.
16. Washing is achieved by adding 20 mL of 1× running buffer to remove excess IA from the surface of the gel and the tube.
17. Lay the SDS-PAGE prepared for the second dimension horizontally on the table with the eared glass plate on top pointing to the experimenter (*see* **Note 24**).

18. Apply the gel section horizontally on top of the stacking gel and push it gently between the glass plates until it has contact with the stacking gel (*see* **Note 22**). Avoid trapping air bubbles.
19. Molecular weight marker is applied by pipetting 5 μL on a 0.4 cm × 0.4 cm Whatman paper (0.34 mm thick). The piece is picked up with forceps and applied to the top surface of the stacking gel next to one end of the applied gel section.
20. The gel and the piece with the molecular weight marker can be fixed on top of the gel using 1 mL agarose sealing solution. Slowly distribute the sealing solution using a 1 mL pipette. Allow agarose sealing solution to solidify and assemble the electrophoresis system.
21. Electrophoresis is performed in the second dimension at constant current of 50 mA per gel for about 14 h, e.g., in a Hoefer gel apparatus.
22. Protein spots are detected using silver staining (see below) or stained with colloidal Coomassie according to the method of Chan et al. (9). An example of the results produced is shown in **Fig. 13.5b**.

3.4. Detection and Analysis

3.4.1. Silver Staining (Modified According to Blum et al. (10))

1. These instructions are designed for an SDS-PAGE system with gels of 18 cm (width) × 10 cm (height) × 1 mm (thickness). If other dimensions are utilized, volumes have to be adjusted in order to ensure complete coverage of the gel with the solutions during the different steps of the silver staining procedure.
2. All equipments must be cleaned with detergent and rinsed thoroughly with water, as detergents can interfere with silver staining.
3. Put the gel in a clean staining container with 50 mL fixation solution supplemented with 35 μL of 37% formaldehyde (*see* **Notes 22, 25**, and **26**).
4. Agitate for at least 15 min on a shaker at room temperature.
5. Discard fixation solution and wash the gel in 50% (v/v) ethanol three times for 10 min on a shaker at RT.
6. Discard ethanol, add sensitizer solution, and shake the box by hand for 60 s. Take care that the gel is covered by solution also on the top surface. Since the gel is hydrophobic due to previous washing with ethanol, it will not be covered evenly by the sensitizer when agitated only on the shaker.
7. Discard the sensitizer solution and wash the gel with ultrapure water two times for 20 s (prolongation will lead to

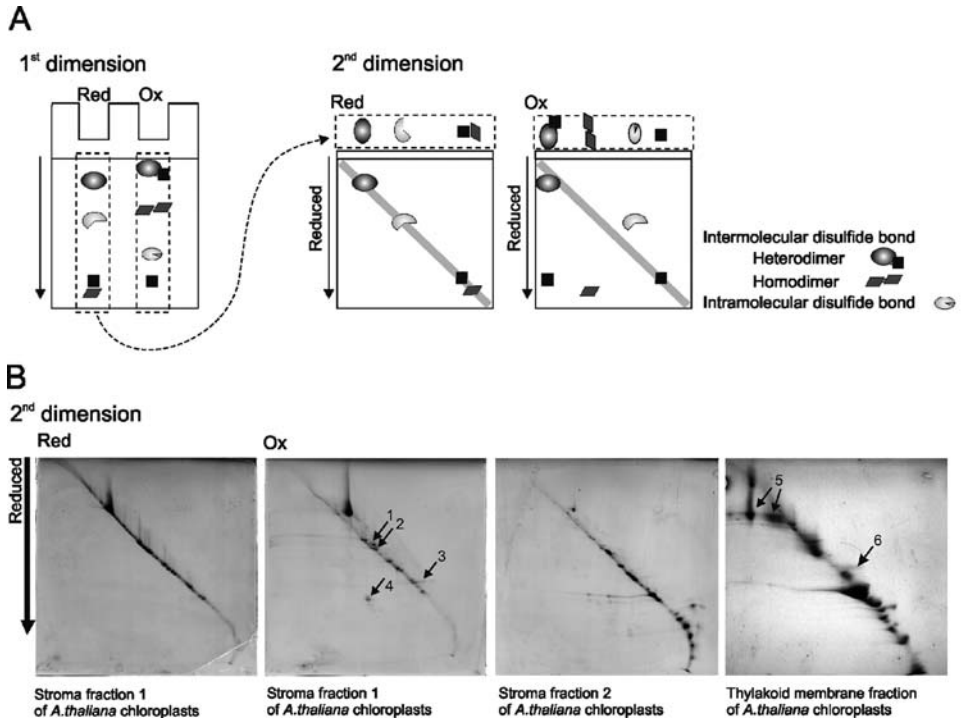

Fig. 13.5. Diagonal 2D redox SDS-PAGE. **(a)** Schematic presentation of the method. Oxidized and reduced proteins are separated using non-reducing SDS-PAGE. Sections corresponding to a complete lane of the first dimension are cut out and horizontally applied to the second dimension gel for SDS-PAGE after complete reduction and alkylation. Disulfide bonds are solved and the proteins migrate according to their molecular masses. Proteins previously engaged in intermolecular bonds migrate faster and proteins containing intramolecular disulfide bonds migrate slower after reduction and are detected below and above the diagonal, respectively. (**b)** Exemplary results obtained with diagonal 2D redox SDS-PAGE. The indicated fractions of isolated chloroplasts from *A. thaliana* were separated. Protein extracts were reduced with 100 mM DTT or oxidized with 10 mM H_2O_2 as described in Ref. (8). Altogether, 74 proteins were identified utilizing this approach, e.g., the spots highlighted by arrows are identified as follows: 1, phosphoribulokinase (PRK) (At1g32060); 2, chloroplast glyceraldehyde 3-phosphate dehydrogenase A (GAPA) (At3g26650); 3, β-carbon anhydrase 1 (CA1) (At3g01500); 4, 2-cysteine peroxiredoxin (At3g11630); 5, photosystem I apoprotein A1 (ArthCp022); 6, photosystem II protein D1 (ArthCp002).

decreased sensitivity of the staining). Shake by hand constantly.

8. Discard water completely and add 50 mL staining solution supplemented with 35 μL of 37% formaldehyde (*see* **Notes 26** and **27**).
9. Agitate for at least 30 min on a shaker at room temperature.
10. Discard the staining solution and wash the gel with ultrapure water twice for 20 s to remove staining solution from the surface of the gel and the container. Shake by hand constantly.
11. Discard water completely and add 50 mL developer supplemented with 35 μL of 37% formaldehyde (*see* **Note 26**).

12. Shake by hand constantly until the intensities of the bands and the contrast are satisfactory.
13. Discard the developer solution completely.
14. Add fixation solution to stop the developing process.
15. Incubate for 10 min on the shaker.
16. Discard the fixation solution, replace with fresh fixation solution, and incubate for 1 h or overnight before preparing for long-term storage in 1% (v/v) acetic acid solution or drying of the gel.

3.4.2. In-Gel Tryptic Digest and Mass Spectrometric Analysis

1. Prearrangement: 1.5 mL reaction tubes and/or 96-well microtiter plates used for collecting the excised protein spots and for aliquoting trypsin.
2. Carefully excise protein spots of interest from the gel with minimum gel volume using a clean scalpel.
3. Place the gel pieces in either a well of a microtiter plate or a reaction tube.
4. Wash gel slices with 150 μL washing solution A by incubating on a shaker for 5 min.
5. Discard the solution completely.
6. Add 150 μL washing solution B and incubate on the shaker for additional 30 min.
7. Discard the solution completely.
8. Add 150 μL washing solution C and incubate on the shaker for additional 30 min.
9. Discard the solution completely and let the gel pieces dry entirely until they become completely white, either in a vacuum centrifuge or overnight in the fume hood.
10. Rehydrate the gel pieces in 15 μL trypsin solution at 4°C for 1 h (*see* **Note 28**).
11. Digest at 37°C for 12–16 h.
12. Store the reaction in this state at −20°C or proceed immediately.
13. Mix the solution containing the released peptides with the matrix α-cyano-4-hydroxycinnamic acid at a 3:2 ratio.
14. The mass spectrum can be obtained, e.g., on a Biflex III matrix-assisted laser desorption/ionization-time of flight (MALDI-TOF)–MS (Bruker, Bremen, Germany), and the subsequent annotation of the peptide mass fingerprints is performed, e.g., by the MASCOT software (Matrix Science, London, UK). The subsequent search can be performed in the National Center for Biotechnology Information (NCBI) protein database.

The methods described in this chapter rely on equipments available in most biochemical and molecular laboratories and, in addition, on access to a proteome facility. The gel-based methods can be adapted to determine the redox midpoint potential by incubation in redox buffer of defined ratios of reduced to oxidized dithiothreitol (DTT_{red}/DTT_{ox}) either by quantification of redox-dependent gel shifts (8) or using labeling techniques as described here. Fluorescence-based probes also enable to monitor redox-dependent thiol modifications (6). The two-dimensional difference gel electrophoresis (2D-DIGE) is a powerful technique to sensitively and fluorometrically quantify thiol modifications under stress and is described in another chapter of this book. DIGE depends on sensitive but expensive labeling compounds and scanning equipment. Following the identification by redox proteomics, the significance of the redox environment for the functionality of proteins needs to be established, e.g., by activity tests and protein interaction studies, in combination with site-directed mutagenesis of the affected cysteines or reverse genetics approaches.

4. Notes

1. DTT (1 M) in water is acidic with a pH value around 5.0. DTT is highly prone to oxidation by air, a process promoted also by multiple freeze–thaw cycles. Therefore, aliquots for single use can be prepared and stored at -20°C, but it is strongly recommended to prepare DTT solutions fresh prior to usage.
2. The reaction of maleimide groups as present in NEM and mPEG-Mal with thiol groups is more specific in the pH range between 6.5 and 7. Therefore the pH value has to be controlled tightly during all steps. At least for the first time the pH should be checked with pH indicator strips. High urea and SDS concentrations are utilized to achieve complete reaction between the thiol group and the thiol-specific reagent (either within the blocking or the labeling step). The achieved complete denaturation of the proteins permits access even to buried thiols. Buffer is modified from a protocol, utilizing iodoacetamide derivates (11).
3. In aqueous solutions, urea degrades to cyanate and ammonium. In the presence of heat, cyanate can carbamylate proteins, an unwanted modification which often leads to

confusing results after mass spectrometric analysis as peptides with unexpected retention times and masses occur. This process is inhibited at −80°C.

4. The optimum concentration of mPEG-Mal-5000 depends on the amount of thiol groups either derived from the amino acid sequence of the purified protein or determined for protein extracts and is best around a 1:250 ratio of thiol to mPEG-Mal-5000 (**Fig. 13.3**). But this should be optimized/checked for each single protein, as the increase in size per each bound mPEG-Mal molecule might exceed the theoretical value of 5 kDa. The mPEG-Mal molecule itself is bulky and highly solvated, thereby possibly inhibiting complete saturation of the protein with SDS and altering the separation behavior. A titration with different molar ratios of labeling reagent to thiol group enables to assign the number of labeled thiols to the bands visualized in the gel.
5. TCA is a strong acid and should be handled with care while working with solid TCA or solutions.
6. Acrylamide is a potent neurotoxin and is absorbed through the skin. Take appropriate safety measures (gloves, fume hood, and mask), particularly if weighing solid acrylamide/bisacrylamide and while working with the solutions and gels.
7. The reaction of iodoacetamide with thiol groups is more specific at a pH between 7.5 and 8. Therefore the pH has to be controlled tightly during all steps. At least prior to the first experiment the pH should be checked with pH indicator strips.
8. Wells generated from 1 cm teeth allow application of sample volumes up to 250 μL. Higher volumes can be applied but require wider wells and with increasing width the handling of the gel section after the first dimension gets difficult.
9. To keep the volume of the buffer small, the roller mixer is needed to ensure complete coverage of the gel slice during the incubation of the gel sections with buffer supplemented with DTT or IA.
10. Denatured ethanol also works for all steps of the silver staining procedure and is much cheaper than pure ethanol.
11. As acetonitrile is harmful, solutions with acetonitrile should be stored in a fume hood.
12. Thiol groups of excess reductant compete with protein thiols for attachment of thiol-reactive labels such as maleimide or iodoacetamide. Therefore, excess reductant must be

removed before the labeling procedure, but simultaneously care has to be taken to prevent thiol reshuffling, e.g., re-oxidation. These two prerequisites make TCA precipitation to be the preferred precipitation method when it comes to analysis of redox-mediated processes. The acidic environment ensures protonation of the thiol groups and thereby inhibits oxidation.

13. Place the tube in the centrifuge in the same orientation during the entire procedure. The pellet remains on the same side of the tube after each centrifugation. This will minimize loss of protein pellet during centrifugation and washing.
14. It is recommended to prepare a master mix, sufficient for all samples, with 10% additional volume in order to compensate for reagent loss.
15. It is important to use 20% (v/v) TCA instead of a smaller volume of 100% (v/v) TCA to dilute the high urea and SDS concentrations in the labeling buffer which might otherwise prevent proper precipitation of the proteins.
16. The unbound mPEG-Mal-5000 may distort the protein migration; hence excess labeling reagent must be removed. In addition already a minor fraction of unlabeled protein might be oxidized during the SDS-PAGE, leading to confusing banding pattern that is difficult to interpret. The presence of DTT prevents the re-oxidation.
17. Some proteins are prone to overoxidation, therefore different concentrations and possibly also different oxidizing agents should be tested, e.g., copper chloride.
18. Besides iodoacetamide, *N*-ethylmaleimide can be employed for alkylation of free thiol groups. Some thiol groups reveal differential accessibility toward the two reagents, presumably due to the different thiol-specific reactive groups. Thereby, analyzing complex protein extracts often necessitates a compromise regarding the completeness of blocking and labeling, a fact that supports the recommendation to utilize reagents derived from the same reactive group for both steps.
19. Altering the acrylamide concentration may improve separation of proteins of interest; however, in any case the acrylamide concentrations of both dimensions must be identical.
20. The amount of protein depends on the detection method, i.e., staining and identifying of the protein spots, and can be adjusted accordingly. Sample volumes larger than 250 μL

require broader wells which subsequently lead to broader gel lanes. This makes the handling and the attachment of the gel section of the first dimension to the gel of the second dimension difficult.

21. The position of the single lanes should be marked during the gel run. This eases proper cutting of the gel slice to separate neighboring lanes after the electrophoretic separation.
22. Wet the gloves and all surfaces which make contact with the gel with running buffer; otherwise the gel section might stick to them and break, making the handling of the gel difficult and in the case of the diagonal 2D redox SDS-PAGE electrophoresis, the separation is often unsatisfactory.
23. Do not prolong the incubation time since the SDS might slowly wash out the proteins from the gel.
24. Preparation of the second dimension is easier when the assembled glass plates containing the gel are slightly lifted at the site where the gel lane of the first dimension has to be applied.
25. Wear clean powder-free gloves at all times and do not press the gels as this also produces background.
26. Never add formaldehyde directly on the gel, as this produces background. Mix formaldehyde and the corresponding solutions in a separate container just prior to use. In general, the stock solution has to be renewed from time to time as oxidation can occur, and especially cold temperatures lead to precipitation of trioxymethylene. As formaldehyde is a hazardous substance, care has to be taken for proper disposal.
27. As silver nitrate is a hazardous substance, care has to be taken for proper disposal.
28. If the gel piece is not completely covered with solution after complete rehydration, additional buffer has to be added.

Acknowledgment

The own cited work was supported by the Deutsche Forschungsgemeinschaft. M.M. acknowledges support by a fellowship of the NRW International Graduate School of Bioinformatics and Genome Research.

References

1. Ghezzi, P. (2005) Oxidoreduction of protein thiols in redox regulation. *Biochem Soc Trans* **33,** 1378–1381.
2. Meyer, A.J. and Hell, R. (2005) Glutathione homeostasis and redox-regulation by sulfhydryl groups. *Photosynthesis Res* **86,** 435–457.
3. Meyer, Y., Siala, W., Bashandy, T., Riondet, C., Vignols, F., and Reichheld, J.P. (2008) Glutaredoxins and thioredoxins in plants. *Biochim Biophys Acta* **1783,** 589–600.
4. Dietz, K.J. (2008) Redox signal integration: from stimulus to networks and genes. *Physiol Plant* **133**, 459–468.
5. Jones, D.P. (2008) Radical-free biology of oxidative stress. *Am J Physiol* **295**, C849–C868.
6. Ströher, E. and Dietz, K.J. (2006) Concepts and approaches towards understanding the cellular redox proteome. *Plant Biol* **8**, 407–418.
7. Winger, A.M., Taylor, N.L., Heazlewood, J.L., Day, D.A., and Millar, A.H. (2007) Identification of intra- and intermolecular disulphide bonding in the plant mitochondrial proteome by diagonal gel electrophoresis. *Proteomics* **7**, 4158–4170.
8. Ströher, E. and Dietz, K.J. (2008) The dynamic thiol–disulphide redox proteome of the *Arabidopsis thaliana* chloroplast as revealed by differential electrophoretic mobility. *Physiol Plant* **133**, 566–583.
9. Chan, H.L., Gharbi, S., Gaffney, P.R., Cramer, R., Waterfield, M.D., and Timms, J.F. (2005) Proteomic analysis of redox- and ErbB2-dependent changes in mammary luminal epithelial cells using cysteine- and lysine-labelling two-dimensional difference gel electrophoresis. *Proteomics* **5**, 2908–2926.
10. Blum, H., Beier, H., and Gross, H.J. (1987) Improved silver staining of plant proteins, RNA and DNA in polyacrylamide gels. *Electrophoresis* **8**, 93–99.
11. Leichert, L. I. and Jakob, U. (2004) Protein thiol modifications visualized in vivo. *PLoS Biol* **2**, e333, doi:10.1371/journal.pbio.0020333.

Chapter 14

Cloning of Stress-Responsive MicroRNAs and other Small RNAs from Plants

Jose Luis Reyes, Catalina Arenas-Huertero, and Ramanjulu Sunkar

Abstract

In plants, small RNA (microRNAs and other endogenous small RNAs)-guided target gene expression is vital for a wide variety of biological processes including adaptation to stress conditions. Identification of stress-regulated microRNAs or other classes of endogenous small RNAs advances our understanding of post-transcriptional gene regulation important for plant stress tolerance. This chapter describes a detailed step-by-step protocol for cloning of small RNAs. Following 5′ and 3′ adapter ligation to the purified small RNAs, cDNA will be synthesized using reverse transcription, which will be further amplified using a polymerase chain reaction. The resulting small DNA fragments can be either cloned and sequenced using traditional sequencing method or subjected to direct high-throughput pyrosequencing or sequencing-by-synthesis technology.

Key words: Abiotic stress, microRNAs, small RNAs, cloning, post-transcriptional gene regulation.

1. Introduction

MicroRNAs are small 20- to 23-nt-long RNA molecules that regulate mRNA expression at the post-transcriptional level in plants and animals (1). This regulation is based on RNA–RNA base pairing between the miRNA and its target mRNA that results in mRNA cleavage and degradation or a block in its translation. Due to the extensive base pairing between miRNA and mRNA, degradation is more commonly found in plants (2), although translation inhibition has been observed (3). Identification of target mRNAs is largely based on this fact and has allowed extensive analysis of miRNA function in diverse plants.

R. Sunkar (ed.), *Plant Stress Tolerance*, Methods in Molecular Biology 639,
DOI 10.1007/978-1-60761-702-0_14,

Although miRNA gene prediction has been successfully used, cloning and sequencing of small RNA molecules found in the RNA population of plant tissues is the preferred method if one is to identify miRNAs that are altered under certain conditions, such as drought or salt stress. Thus, sequencing of miRNAs has become an essential tool for plant biologists studying this and other phenomena. Its use to identify stress-regulated miRNAs has been exemplified in plants such as *Arabidopsis*, rice, and poplar (4–6). Here we describe a detailed methodology for small RNA cloning, based on previously published procedures (7, 8). Small RNA cloning protocol was developed specifically to capture Dicer products that carry a 5′-phosphate and 3′-hydroxyl termini. General RNA degradation products will carry a 5′-hydroxyl terminus. Small RNAs are initially isolated from total RNA by gel electrophoresis. Oligonucleotide adapters are then added at the 5′- and 3′-ends to prime reverse transcription and subsequent PCR amplification (**Fig. 14.1**). The protocol presented here is specifically applied for cost-effective, high-throughput sequencing

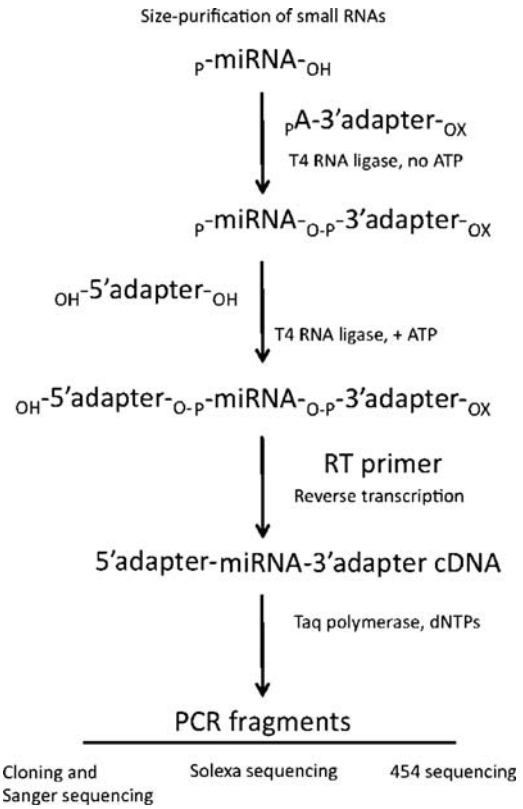

Fig. 14.1 Diagrammatic representation of the steps leading to small RNA cloning. Individual steps with the essential reagents used are shown along the path indicated by arrows. At the end of the procedure there are three alternative outcomes, depending on the purpose of the library obtained.

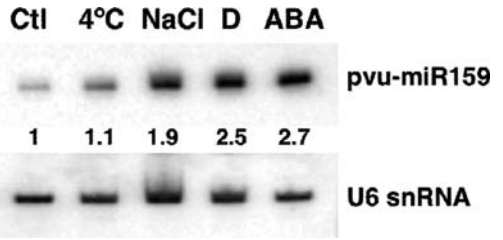

Fig. 14.2. Stress-responsive miR159 expression analysis in *Phaseolus vulgaris* (common bean; Pvu-miR159). One of the miRNAs identified by sequencing of *P. vulgaris* small RNAs obtained from stressed seedlings corresponds to miR159a. Northern blot analysis of *P. vulgaris* seedlings exposed to different conditions for 48 h, including well-irrigated control (Ctrl), cold (4°C), 100 mM NaCl, drought (D), and ABA 100 μM treatment, confirms its expression under stress conditions. Detection of U6 snRNA was used as a loading control.

technologies such as sequencing-by-synthesis. This method can generate several millions of reads, which also facilitates the identification of stress-regulated miRNAs using direct sequencing of small RNAs from unstressed and stressed samples (**Fig. 14.2**). The protocol can also be applied to other high-throughput sequencing technologies such as pyrosequencing (454) by replacing the 5′ and 3′ adapters and correspondingly the RT-PCR primers.

2. Materials

2.1. Isolation and Preparation of RNA for Denaturing Gel Electrophoresis

1. TRIzol Reagent (Invitrogen).
2. Chloroform.
3. Isopropanol.
4. Ethanol (80%).
5. DEPC-treated water or RNase-free Milli-Q pure water, sterile.
6. Deionized formamide solution (50%, in Milli-Q water).
7. Acrylamide (15%):Bisacrylamide (19:1) solution containing 8 M urea.
8. Ammonium persulfate (50% solution).
9. TEMED.
10. TBE (0.5×).

2.2. Size Selection and Recovery of Small RNAs

1. Siliconized microcentrifuge tubes (BioPlas) or low-retention microcentrifuge tubes (Fisher).
2. Formamide loading buffer: 98% (w/v) deionized formamide, 10 mM EDTA (pH 8.0), 0.02% (w/v) xylene cyanol, 0.02% (w/v) bromophenol blue.

3. Decade RNA markers (Ambion) labeled with T4 polynucleotide kinase and [^{32}P-γ]ATP as directed by the manufacturer.
4. Rotating shaker (rotisserie) for microcentrifuge tubes.
5. Elution solution (0.3 M NaCl).
6. TBE buffer (0.5×): 50 mM Tris, 50 mM boric acid, 1 mM EDTA.
7. Electrophoresis chamber to cast and run 20-cm × 16-cm × 1.5-mm (length × width × thickness) vertical polyacrylamide gels.
8. PhosphorImager or X-ray film.
9. Glycogen (20 μg/μL; Invitrogen).
10. Fluorescent labels.

2.3. Ligation

1. 3′ Solexa DNA Adapter (24 nt, DNA oligonucleotide). 5′-rAppTCGTATGCCGTCTTCTGCTTGTddC-3′.

2.3.1. 3′ Adapter Ligation

2. The oligonucleotide is adenylated at the 5′-end (rApp), and the 3′-end is blocked (ddC) (*see* **Note 1**).
3. 3′ Ligation buffer 10×, [500 mM Tris–HCl (pH 7.5), 100 mM $MgCl_2$, 100 mM DTT, 600 μg/mL BSA].
4. T4 RNA ligase (NEB).

2.3.2. 5′ Adapter Ligation

1. 5′ Solexa RNA Adapter (26 nt, custom RNA oligonucleotide). 5′-rGrUrUrCrArGrArGrUrUrCrUrArCrArGrUrCrCrGrArCrGrArUrC-3′.
2. 5′ Ligation buffer 10×, [500 mM Tris–HCl (pH 7.5), 100 mM $MgCl_2$, 100 mM DTT, 600 μg/mL BSA, 10 mM ATP].
3. T4 RNA ligase (NEB).

2.4. RT-PCR

1. Solexa RT primer (21 nt, DNA oligonucleotide), 5′-CAAGCAGAAGACGGCATACGA-3′.

2.4.1. Reverse Transcription

2. SuperScript III Reverse Transcriptase (Invitrogen).
3. First-strand buffer (5×).
4. DTT solution (0.1 M).
5. dNTP solution (2.5 mM).
6. KOH (150 mM)/20 mM Tris base solution.
7. HCl solution (150 mM).

2.4.2. PCR Amplification of cDNA

1. Forward primer: Small RNA PCR Primer (44 nt, DNA oligonucleotide), 5′-AATGATACGGCGACCACCGACAGGTTCAGAGTTCTACAGTCCGA-3′.

2. Reverse primer: Solexa RT primer (see reverse transcription).
3. PCR buffer 10×, [200 mM Tris–HCl (pH 8.4), 500 mM KCl, 20 mM $MgCl_2$].
4. Taq polymerase.

2.5. Gel Purification of PCR Product

1. NuSieve®GTG® LMP (low melting point) agarose 2% gels in 1× TAE buffer.
2. 25-Bp DNA ladder (Invitrogen).
3. TAE buffer (1×): 40 mM Tris-acetate (pH 8.4), 1 mM EDTA (pH 8.0).
4. DNA loading buffer (6×) [30% glycerol, 0.02% (w/v) xylene cyanol, 0.02% (w/v) bromophenol blue].
5. Thermal cycler.
6. Tris-buffered phenol, pH 7.9.

2.6. Cloning of PCR Fragments

1. TOPO TA cloning kit (Invitrogen) including *Escherichia coli* TOP10 chemical competent cells.
2. LB growth solid medium including ampicillin (100 μg/mL) or kanamycin (50 μg/mL).

3. Methods

3.1. Isolation and Preparation of RNA for Denaturing Gel Electrophoresis

1. Purify total RNA with TRIzol reagent following the manufacturer's directions. We typically start with a volume equivalent to 0.5 mL of liquid nitrogen-ground tissue per milliliter of TRIzol reagent. During RNA isolations, low-retention microcentrifuge tubes should be used during all steps and the RNA pellet should be washed with 80% ethanol (not 70% ethanol) (*see* **Notes 2** and **3**).
2. Dissolve the RNA pellet in 50–100 μL of 50% formamide solution.
3. Determine RNA concentration and purity by UV absorbance using a Nanodrop apparatus. Formamide does not interfere with UV reading. Test the integrity of the RNA sample by resolving 1 μg of total RNA in a 1.5% agarose gel in 1× TAE buffer (*see* **Note 4**).
4. The starting amount of total RNA for the library should be in the range of 200–300 μg. Keep the concentration in the range of 3–5 μg/μL. Keep the RNA sample on ice at all times or store at −20°C until used. Proceed to next step.

3.2. Size Selection and Recovery of Small RNAs

1. Prepare a 15% polyacrylamide/8 M urea/0.5× TBE gel (20 cm × 16 cm × 1.5 mm, length × width × thickness) with a six-well comb: two small wells (5 mm width) on both ends for size markers and four larger wells (30 mm width) in the middle for samples.
2. Pre-run the gel in 0.5× TBE buffer at constant 25 mA for 20 min.
3. Dilute the RNA sample with one-sixth volume of formamide loading buffer.
4. Heat at 65°C for 5 min. Just before loading the samples, rinse the wells with 0.5× TBE using a syringe to remove urea eluted from the gel into the wells.
5. Load 50–100 μg of total RNA sample in each well.
6. Load 10 μL of Ambion Decade RNA markers on the side wells.
7. Run the gel in 0.5× TBE at constant 25 mA until the bromophenol blue migrates to two-thirds of the gel.
8. Remove the gel from the plates and place fluorescent labels at four corners of the gel. Then wrap the gel with saran wrap to expose to a PhoshorImager screen. Allow 5–10 min to expose and then develop. Alternatively, the gel can be exposed to an X-ray film for autoradiography; note that appropriate time should be considered for film exposure (4°C, 30–40 min). Place visible marks on the gel to allow for accurate alignment between the gel and the image or the film. This step is critical to ensure correct identification of the acrylamide fragments to cut from the gel.
9. Align the image obtained from the PhosphorImager or X-ray film with the gel and excise the bands corresponding to around the 20-nt band marker (19–25 nt) into 2.0-mL siliconized/low-retention microcentrifuge tubes using clean one-edge razor blades.
10. Determine the weight of the gel piece.
11. Add two or three volumes of 0.3 M NaCl and rotate in a rotating shaker (rotisserie) at 4°C overnight. Large bands can be divided into small 3- to 5-mm-wide fragments to facilitate elution. It is not necessary to crush the polyacrylamide bands.
12. Recover the eluate to a new tube and add 1 μl glycogen (20 μg/μL; Invitrogen) to 400 μL elution solution. The volume recovered might be less than the initial volume added due to absorption by the polyacrylamide bands.
13. Add three volumes of 100% ethanol and mix by gentle shaking.

14. Incubate at −20°C for 1 h.
15. Spin at 18,000×*g* for 15 min at 4°C and wash the pellet with 100% ethanol.
16. Spin at 18,000×*g* for 1 min at 4°C and remove the residual ethanol. If necessary, remove the remaining liquid by centrifuging and using a 0.02-mL pipette.
17. Let stand for 1 min and dissolve RNA pellet in 13 μL of water and proceed to next section.

3.3. Adapter Ligation

3.3.1. 3′ Adapter Ligation

1. Set up the following reaction:

19- to 25-nt small RNA fraction	13 μL
100 μM 3′ adenylated DNA adapter	1 μL
10× 3′ Ligation buffer (no ATP)	2 μL
DMSO	2 μL
T4 RNA ligase	2 μL
Final volume	20 μL

2. Incubate at 37°C for 1 h
3. Proceed to next section.

3.3.1.1. Gel Purification of 3′ Ligated Small RNAs

1. Prepare a 15% polyacrylamide/urea gel with 5-mm-wide wells and 1.5 mm in thickness, as in step 1 of **Section 3.2**.
2. Pre-run the gel in 0.5× TBE buffer at constant 25 mA for 20 min.
3. Mix small RNA ligation reaction with an equal volume of formamide loading buffer.
4. Heat at 65°C for 5 min. Just before loading the samples, rinse the wells with 0.5× TBE using a syringe to remove urea eluted from the gel into the wells.
5. Load 10 μL of Ambion decade markers on both sides (*see* **Note 5**).
6. Load 3′ ligation samples in the middle lane and keep at least one empty well between two different samples.
7. Run the gel in 0.5× TBE at constant 25 mA until the bromophenol blue reaches three quarters of the gel.
8. Expose plastic-wrapped gel to a PhosphorImager screen or to an X-ray film as described above for the first polyacrylamide gel (steps 8 and 9 from **Section 3.2**).
9. Align the image with the gel and excise the appropriate size bands [corresponding to 3′ adapter ligated to small RNAs, i.e., 23+(1–25) nt] into 2-mL low-retention microcentrifuge tubes using a clean razor blade.

10. Determine the weight of the gel piece.
11. Add two to three volumes of 0.3 M NaCl and rotate at 4°C overnight in rotisserie.
12. Transfer the eluate to a new low-retention microcentrifuge tube and add 1 μL glycogen (20 μg/μL; Roche).
13. Add three volumes of 100% ethanol. Mix by gentle shaking
14. Incubate at −20°C for 1 h.
15. Spin at 18,000×*g* for 15 min at 4°C and wash the pellet with 100% ethanol.
16. Spin at 18,000×*g* for 1 min at 4°C and remove the residual ethanol with a pipette.
17. Spin again and remove the remaining liquid with a 0.02-mL pipette and dissolve the pellet in 13 μL of water.
18. Proceed to next section.

3.3.2. 5′ Adapter Ligation

1. Set up the following reaction:

3′ Adapter ligated small RNAs	13 μL
100 μM 5′ RNA adapter	1 μL
10× T4 RNA ligase buffer	2 μL
DMSO	2 μL
5 units/μL T4 RNA ligase	2 μL
Final volume	20 μL

Incubate at 37°C for 1 h.

2. Proceed to next section.

3.3.2.1. Gel Purification of 5′ Ligated Small RNAs

1. Prepare a 15% polyacrylamide/urea gel (1.5 mm thickness, as in previous sections) with a 20-well comb (each well 5 mm width).
2. Pre-run the gel in 0.5× TBE buffer at constant 20 mA for 20 min.
3. Mix 5′ ligation reaction with equal volume of formamide loading buffer.
4. Heat at 65°C for 5 min. Just before loading the samples, rinse the wells with 0.5× TBE using a syringe to remove urea eluted from the gel into the wells.
5. Load 10 μL of Ambion decade markers on both sides.
6. Load 5′ ligation samples and keep at least one empty well between two different samples.
7. Run the gel in 0.5× TBE at constant 25 mA until the bromophenol blue reaches the bottom of the gel.

8. Expose the gel wrapped with saran wrap to a PhosphorImager screen or an X-ray film.
9. Align the image with the gel and excise the bands around the 70-nt marker band (corresponding 26+23+[19–25] nt) into 2-mL low-retention microcentrifuge tubes.
10. Determine the weight of the gel piece.
11. Add two to three volumes of 0.3 M NaCl and rotate at 4°C overnight in rotisserie.
12. Transfer the eluate to a new low-retention microcentrifuge tube and add 1 μL glycogen (20 μg/μL; Roche) to it.
13. Add three volumes of 100% ethanol.
14. Incubate at −20°C for 1 h.
15. Spin at 18,000×*g* for 15 min at 4°C and wash the pellet with 100% ethanol.
16. Spin at 18,000×*g* for 1 min at 4°C and remove the residual ethanol.
17. Spin and remove residual liquid with a 0.02-mL pipette and dissolve the pellet with 10.5 μL of water.
18. Proceed to next step.

3.4. RT-PCR

3.4.1. Reverse Transcription

1. Set up the following reaction:

3' and 5' ligated RNA product	10.5 μL
100 μM Solexa RT primer	0.5 μL
Final volume	11 μL

   Incubate at 72°C for 2 min.
2. Spin at 12,000×*g* for 1 min at room temperature.
3. Cool on ice for 2 min.
4. Add the following reagents.
   Four microliters of 5× first-strand buffer
   One microliter of 0.1 M DTT
   Three microliters of 2.5 mM dNTPs
   One microliter of SuperScript III Reverse Transcriptase (Invitrogen).
5. Incubate at 50°C for 1 h.
6. To remove RNA, add 40 μL of 150 mM KOH/20 mM Tris base and incubate for 10 min at 90°C. Neutralize solution by addition of 40 μL of 150 mM HCl. The final pH of the solution should be 8–9.

3.4.2. PCR Amplification of cDNA

1. Set up the following PCR mix in two tubes:

RT reaction (**Section 3.4.1**)	10 μL
100 μM small RNA PCR primer	0.5 μL
100 μM Solexa RT Primer	0.5 μL
10× PCR buffer	5 μL
20 mM $MgCl_2$	5 μL
2.5 mM dNTPs (each)	5 μL
Water	23 μL
Taq polymerase	1 μL
Final volume	50 μL

2. Place in a thermal cycler with a heated lid.
3. Run the following PCR program:

94°C	2 min
94°C	30 s
54°C	30 s
72°C	30 s
72°C	2 min

4. Monitor the reaction starting at cycle 12 and every other cycle from there on removing 2 μL aliquots (*see* **Note 6**).
5. Resolve the PCR products in a 2% agarose gel.
6. Determine the optimal cycle number to obtain product accumulation in the linear range of amplification (*see* **Note 7**).
7. Repeat PCR with selected number of cycles using 50 μL reaction volume.

3.5. Gel Purification of PCR Product

1. Pre-warm phenol (pH 7.9) at room temperature.
2. Prepare a 2% NuSieve®GTG® agarose gel containing 1 μg/mL ethidium bromide.
3. Add 10 μL of 6× DNA loading buffer to each PCR tube.
4. Load 1 μg of 25-bp DNA ladder in a separate lane.
5. Load 60 μL of PCR product and keep at least one well empty between two different samples.
6. Run gel in 1× TAE buffer at constant 100 V until bromophenol blue reaches three-fourth of the gel length.

7. Visualize the bands with a long-wave UV lamp and excise the DNA band with a clean razor blade into a pre-weighed 2.0-mL Eppendorf tube.
8. Add 100 μL of 0.6 M NaCl per 100 mg of gel slices.
9. Incubate at 50°C for 10 min mixing the tube every couple of minutes to ensure complete melting of the agarose.
10. Add one volume of pre-warmed phenol (pH 7.9), vortex for 15–30 s and spin at 18,000×*g* for 5 min.
11. Transfer the aqueous phase to a fresh 1.5-mL Eppendorf tube.
12. Add one volume of phenol:chloroform:isoamyl alcohol (25:24:1, pH 8.0), vortex for 15–30 s and spin at 18,000×*g* for 15 min.
13. Transfer the aqueous phase to a fresh 1.5-mL Eppendorf tube.
14. Add one volume of chloroform:isoamyl alcohol (24:1), vortex for 15–30 s and spin at 18,000×*g* for 15 min.
15. Transfer the aqueous phase to a fresh 1.5-mL Eppendorf tube.
16. Add 2.5 volumes of 100% ethanol and incubate at −20°C for 1 h.
17. Spin at 18,000×*g* for 15 min at 4°C, wash with 70% ethanol.
18. Spin at 18,000×*g* for 2 min at 4°C, remove the residual ethanol.
19. Air dry and dissolve in 20 μL water.
20. Measure the concentration using a Nanodrop. The library of PCR products is ready for high-throughput sequencing using Solexa technology (*see* **Note 8**).

3.6. Cloning of PCR Fragments

1. Thaw competent cells on ice, warm SOC medium and warm LB-Amp plates.
2. Set up the following reaction:

PCR product (5–10 ng)	2 μL
Water	2 μL
Salt solution	1 μL
TOPO vector	1 μL
Final volume	6 μL

3. Mix the reaction gently and incubate at room temperature for 30 min to 1 h.

4. Cool on ice for 5 min.
5. Transfer 2 μL of cloning reaction into a vial of One Shot TOP10 chemically competent *E. coli* and mix gently. Do not mix by pipetting up and down.
6. Incubate on ice for 30 min.
7. Heat shock the cells at 42°C for 30 s.
8. Immediately cool on ice for 3 min
9. Add 250 μL of room temperature SOC medium.
10. Cap the tube tightly and shake the tube at 200 rpm for 1 h at 37°C.
11. Spread 50–100 μL on a pre-warmed LB-Amp plate and incubate overnight at 37°C.
12. Isolate plasmid DNA from 50–100 clones from each library for sequencing.

4. Notes

1. The 3' adapter oligonucleotide is blocked at its 3′-end (ddC) to avoid spurious ligation to other (5′) end of the adapter (self-ligation). Other chemistries are available from different companies.
2. RNA isolation is carried out with TRIzol reagent that gives consistent yields and does not exclude small RNAs. Other procedures, especially those using purification columns, exclude small RNAs in the total RNA fraction as the small RNAs are retained in the column. Low-retention microcentrifuge tubes should be used during RNA isolation to minimize binding of the small RNA molecules to the tube.
3. The RNA pellet should be washed with 80% ethanol, not with 70% ethanol. Washing with 70% ethanol may partially solubilize the small RNAs and thus may reduce the small RNA yield.
4. The integrity of the RNA sample is crucial for making a successful small RNA library. Always check RNA integrity by running total RNA using 1% agarose gel to visualize sharp 26S and 18S ribosomal RNA. Small degraded RNA fragments from highly abundant larger ribosomal or other messenger RNAs are the main source of contaminating sequences in small RNA libraries.
5. Use of an RNA marker such as Ambion Decade RNA ladder is sufficient to monitor the small RNAs ligated with the

adapters. DNA oligonucleotides cannot be used as markers since their migration is different from that of RNA oligonucleotides.

6. The PCR reaction has to be monitored closely. Since adapter-to-adapter ligation is possible, and such ligated products can be amplified in the PCR step. These products can be separated from the small RNA ligated with the adapters by running on 3% agarose gel.
7. PCR amplification of the small RNA ligated to adapters can carry other molecules undesirable during cloning. Other more easily amplifiable sequences can be also overrepresented, thus one should ensure that the PCR amplification is in the linear range.
8. Prior to high-throughput sequencing, a small number of clones should be confirmed by standard Sanger sequencing to determine the success of small RNA cloning. Approximately 50–100 independent clones are sufficient to estimate the result of the cloning procedure.

Acknowledgments

Support for the research in R.S. laboratory was provided by the Oklahoma Agricultural Experiment Station. Support for CAH and JLR was provided by funding from DGAPA-UNAM (IN-227706) and from CONACyT, Mexico (J48740).

References

1. Bartel, D.P. (2004) MicroRNAs: genomics, biogenesis, mechanism, and function. *Cell* **116**, 281–297.
2. Addo-Quaye, C., Eshoo, T.W., Bartel, D.P., and Axtell, M.J. (2008) Endogenous siRNA and miRNA targets identified by sequencing of the *Arabidopsis* degradome. *Curr Biol***18**, 758–762.
3. Brodersen, P., Sakvarelidze-Achard, L., Bruun-Rasmussen, M., et al. (2008) Widespread translational inhibition by plant miRNAs and siRNAs. *Science* **320**, 1185–1190.
4. Zhou, X., Wang, G., Sutoh, K., Zhu, J.K., and Zhang, W. (2008) Identification of cold-inducible microRNAs in plants by transcriptome analysis. *Biochem Biophys Acta* **1779**, 780–788.
5. Lu, S., Sun, Y.H., and Chiang, V.L. (2008) Stress-responsive microRNAs in *Populus*. *Plant J***55**, 131–151.
6. Zhao, B., Liang, R., Ge, L., et al. (2007) Identification of drought-induced microRNAs in rice. *Biochem Biophys Res Commun* **354**, 585–590.
7. Lu, C., Meyers, B.C., and Green, P.J. (2007) Construction of small RNA cDNA libraries for deep sequencing. *Methods* **43**,110–117.
8. Lagos-Quintana, M., Rauhut, R., Lendeckel, W., and Tuschl, T. (2001) Identification of novel genes coding for small expressed RNAs. *Science* **294**, 853–858.

Chapter 15

An Array Platform for Identification of Stress-Responsive MicroRNAs in Plants

Xiaoyun Jia, Venugopal Mendu, and Guiliang Tang

Abstract

MicroRNAs (miRNAs) are approximately 22-nucleotide (nt)-long non-coding RNAs that play a key role in plant development and abiotic stresses. We have developed a simple but effective array platform for profiling plant miRNAs from various plant species. The array is composed of 188 non-redundant miRNA probes that can detect both conserved and species-specific miRNAs from most plant species, including *Arabidopsis*, rice, and poplar. In this chapter, we describe a protocol for developing the miRNA array platform, which can be used to identify stress-responsive miRNAs in diverse plant species. Profiling of miRNAs in tobacco seedlings exposed to different abiotic stress conditions has revealed that a number of miRNAs, miR398, miR399, miR408, miR156, miR164, and miR168, were responsive to stresses. This comprehensive and easy-to-follow protocol will be useful for studying roles of miRNAs in plant stress response.

Key words: Abiotic stress, microRNAs, microRNA array, small RNA blot analysis.

1. Introduction

MicroRNAs (miRNAs) are a novel class of endogenous small RNAs that play a key role in gene regulation at post-transcriptional level in plants and animals (1). Since the first cloning of plant miRNAs in 2002 from *Arabidopsis* (2–4), many miRNAs and their target genes have been identified in diverse plants species. Most miRNAs appear to play fundamental roles in

The first two authors contribute equally to this work.

R. Sunkar (ed.), *Plant Stress Tolerance*, Methods in Molecular Biology 639,
DOI 10.1007/978-1-60761-702-0_15, © Springer Science+Business Media, LLC 2010

plant development (5, 6). However, a subset of them was found to play pivotal roles in plant responses to abiotic stresses (7, 8). The initial evidence for the role of miRNAs in plant abiotic stress tolerance came from the identification of miR398 that targets two Cu/Zn superoxide dismutases (SODs) (9, 10), as well as from cloning of small RNAs in stress-treated plants (9–13) and analyzing the expression of small RNAs from samples of stressed plants (14–16) by various methods such as micro-array technology (17). In this chapter, we describe a protocol for developing the miRNA array platform, which can be used to identify stress-responsive miRNAs in diverse plant species. Further, we show that a subset of the most conserved miRNAs is induced or suppressed by different types of abiotic stresses in tobacco. The altered expression of miRNA profiles from the array analysis was further validated using small RNA blot analysis, indicating the reliability of our miRNA array. Thus, the detailed protocol offered here should be useful in various miRNA studies in plants.

2. Materials

2.1. The Overall Design of a Simple miRNA Array Platform

1. MicroRNA data base (miRBase: http://microrna.sanger.ac.uk/sequences/).
2. DNA oligonucleotide probes complementary to 188 selected miRNAs and probes for four external controls, MAC2 (ATGGACCCGTCTACAGAGGCA), MAC3 (ATCCGGGGCTGCCGGCTTCGA), MAC4 (AGCTAGTCCTGGAACCCGGCA), and MAC5 (ATCTCCCCAAGAAAGCCGGCA), where MAC represents miRNA array control, that are synthesized by Integrated DNA Technologies (IDT).
3. Hybond N^+ nylon membrane (Amersham).
4. A high-throughput array probe printing robot (Genetix Qpix2).
5. UV cross-linker (Ultra-Violet Products).
6. SSPE (20×): 3 M NaCl, 0.25 M NaH_2PO_4, and 0.02 M EDTA, adjust to pH 7.4.

2.2. Preparation of Plant Material and Stress Treatments

1. Three-week-old plants grown on MS (Murashige and Skoog) media at 24°C with 16 h of light and 8 h of dark in aseptic Magenta boxes.
2. NaCl.
3. Abscisic acid (ABA).

2.3. Array Assay

2.3.1. RNA Preparation

1. TRIzol (Invitrogen).
2. Chloroform.
3. Isopropanol.
4. Cold ethanol (100%).
5. Cold ethanol (80%).
6. RNase-free water.
7. Nanodrop1000^{TM} spectrophotometer (Nanodrop Technologies).
8. Formamide loading dye: 98% (w/v) deionized formamide, 10 mM EDTA (pH 9.0), 0.025% (w/v) xylene cyanol, 0.025% (w/v) bromophenol blue.
9. SequaGel System (National Diagnostics).
10. TEMED (*N*,*N*,*N*′,*N*′-tetramethylethylenediamine).
11. APS (Ammonium persulfate, 10%).
12. TBE buffer (20×).
13. Vertical Gel Electrophoresis Apparatus (GIBCO-BRL Model V16).
14. Gel elution buffer (100 mM Tris–HCl, pH 7.5; 300 mM NaCl; 10 mM EDTA).
15. Glycogen (20 mg/mL; Roche).
16. External control RNAs: Four synthetic 21-nt small RNA oligos UGCCUCUGUAGACGGGUCCAU (40 fmol), UCGAAGCCGGCAGCCCCGGAU (20 fmol), UGCCGGGGUUCCAGGACUAGCU (10 fmol), and UGCCGGCUUUCUUGGGGAGAU (5 fmol) are used as external control RNAs that are complementary to external control probes MAC2, MAC3, MAC4, and MAC5, respectively.

2.3.2. Small RNA Dephosphorylation

1. Antarctic phosphatase (AP) (New England Biolabs).
2. Antarctic phosphatase (AP) buffer.
3. RNasin (40 U/μL; Promega).

2.3.3. Prehybridization

1. SSPE (20×): 3 M NaCl, 0.25 M NaH_2PO_4, and 0.02 M EDTA, adjust to pH 7.4.
2. SSC (20×): 3 M NaCl and 0.3 M sodium citrate, adjust to pH 7.0.
3. Denhardt's reagent (50×): 1% (w/v) Ficoll (type 400; Pharmacia), 1% (w/v) polyvinylpyrrolidone, 1% (w/v) bovine serum albumin (Fraction V; Sigma).
4. Formamide.
5. SDS (10%).

6. Herring sperm DNA (10 mg/mL; Invitrogen).
7. Array membrane.
8. Hybridization bottles.
9. Hybridization oven.

2.3.4. RNA Labeling, Purification of the Radiolabeled Samples, and the Hybridization

1. Radiochemicals: [γ-^{32}P]adenosine triphosphate ([γ-P^{32}] ATP) (6,000 Ci/mmol, $\geq$10 mCi/mL, NEN or ICN).
2. T4 polynucleotide kinase (PNK, 10,000 U/mL; New England Biolabs).
3. T4 polynucleotide kinase buffer (10×): 700 mM Tris–HCl (pH 7.6), 100 mM $MgCl_2$, 50 mM DTT.
4. Formamide loading dye: 98% (v/v) deionized formamide, 10 mM EDTA (pH 8.0), 0.025% (w/v) xylene cyanol, 0.025% (w/v) bromophenol blue.
5. Sephadex G-25 chromatography column (Roche Applied Science).

2.3.5. Membrane Washing

1. SSC (20×): 3 M NaCl and 0.3 M sodium citrate, adjust to pH 7.0.
2. SDS (10%).
3. Prepare washing buffer (2× SSC and 0.1% SDS).

2.3.6. Array Image Output and Analysis

1. PhosphorImager screen.
2. PhosphorImager scanner (Typhoon 9400; Molecular Dynamics).
3. ImageQuant TL software (GE Health Care).

2.4. Small RNA Blot Analysis

1. The RNA preparation (*see* **Section 2.3.1**).
2. Trans-Blot Semi-Dry Electrophoretic Transfer Cell apparatus (Bio-Rad).
3. Hybond N$^+$ nylon membrane (Amersham).
4. Whatman paper (3 MM).
5. SSPE (20×): 3 M NaCl, 0.25 M NaH_2PO_4, 0.02 M EDTA, adjust pH to 7.4.
6. UV cross-linker (Ultra-Violet Products).
7. Prehybridization, RNA labeling, purification of the radiolabeled sample, hybridization, and membrane washing (*see* **Sections 2.3.3**, **2.3.4**, and **2.3.5**).

2.5. Probe Stripping

1. SSC (20×): 3 M NaCl and 0.3 M sodium citrate, adjust to pH 7.0.
2. SDS (10%).

3. Methods

High-quality RNA preparation is a key step to begin miRNA array analysis (*see* **Note 1**).

3.1. The Overall Design of a Simple miRNA Array Platform

More than 959 miRNAs have been identified in plants and mature miRNA sequences are highly conserved across the plant kingdom (18). miRNAs are divided into different families and some family members (paralogs) differ only by one or two nucleotides. Thus, cross-hybridization between the miRNAs and their probes is inevitable. Single-nucleotide mutation and cross-hybridization experiments showed that miRNAs with a stretch of less than 18 continuous identical nucleotides have no cross-hybridization and specific probes are needed for each of them. On the other hand, miRNAs with a stretch of more than 18 continuous identical nucleotides will have cross-hybridization with their probes, and thus only one probe is necessary to detect their additive signals (19). Following this principle and based on the known sequence information of miRNAs from miRNA database (http://microrna.sanger.ac.uk/sequences/), a total of 188 miRNA antisense DNA oligos for known miRNAs was selected, which cover the available (August 2006) conserved and unique plant miRNAs from different plant species (20). Since there is no standard internal control to normalize the expression among different treatments, we designed four external control probes (MAC2–5). The corresponding four synthetic external control RNAs complementary to the external control probes were added to the total RNA. This helps monitor the loss of small RNAs during extraction and purification, as well as normalize the array data. Any loss of small RNAs would be represented by the loss of external control signals. The overall designing steps of the miRNA array platform are outlined as the following:

1. Analyze the sequences of the entire plant miRNAs from miRNA database (miRBase: http://microrna.sanger.ac.uk/sequences/) using an Excel spreadsheet.
2. Select the conserved miRNAs that have a stretch of more than 18 continuous identical nucleotides and design one probe for each of such highly conserved miRNA clusters; select those unique miRNAs that have a stretch of less than 18 continuous identical nucleotides and design specific probe for each of them. The miRNAs we selected in this chapter were based on the miRBase that was available in August 2006.
3. Design and synthesize 188 miRNA antisense DNA oligos.
4. Design and synthesize four unique external controls.

5. Design the array map (*see* **Table 15.1**) in a 16 row × 12 column format so that the 188 miRNA probes and the four external control small RNA probes can be printed on the array membrane. All the miRNA probes and the control probes are printed in duplicate inside each cell of the array map in a reasonable space area to detect high, medium, and low levels of endogenous miRNAs simultaneously with easy quantification.
6. Spot about 0.25 pmol of each probe in duplicate onto a Hybond N^+ membrane using a printing robot such as the Genetix QPix2.
7. UV cross-link the spotted membrane twice with $1{,}200 \times 100$ $\mu J/cm^2$ for half a minute each time, before and after floating the membrane on a 2× SSPE buffer with the probe side up.

3.2. Preparation of Plant Material and Stress Treatments

1. Grow the tobacco plants (*Nicotiana tabacum*) on MS media with 3% sucrose at 24°C with 16 h of light and 8 h of dark in aseptic Magenta boxes.
2. Remove the plants from the Magenta boxes and expose them to air under the same light and temperature conditions until the plants lost 30% of fresh weight for dehydration treatments.
3. Immerse the plant roots in the Magenta boxes with MS liquid media containing 300 mM NaCl for 4 h for salt (NaCl) stress treatment.
4. For ABA treatment, immerse the plant roots in the Magenta boxes with MS liquid media containing 100 μM abscisic acid (ABA) for 3 h.
5. Place the Magenta boxes containing plants at 4°C and 45°C for 1 h for cold and heat treatments, respectively.
6. Take 1 g of non-stressed and stressed tobacco leaves and flash freeze them in liquid N_2.

3.3. Array Analysis

3.3.1. RNA Preparation

1. Chill the mortar and pestle with liquid Nitrogen.
2. Grind 1 g of each of the following leaf samples, non-stressed, dehydrated, NaCl-stressed, ABA-treated, cold-stressed, and heat-stressed, in liquid N_2 to fine powder with the pre-chilled mortars and pestles.

3.3.1.1. Total RNA Isolation

3. Immediately transfer the powder of each sample to another ice–cold, pre-chilled mortar and pestle and homogenize it by grinding the sample in 4 mL TRIzol (Invitrogen) for at least 2 min.

Table 15.1

	1	2	3	4	5	6	7	8	9	10	11	12
A	athmiR156a	osamiR162a	athmiR168a	mtrmiR171	ptcmiR319i	osamiR396a	mtrmiR399d	athmiR414	osamiR437	ptcmiR474b	ptcmiR481b	osamiR810
B	osamiR156k	osamiR162b	sofmiR168b	osamiR171a	athmiR390a	osamiR396d	ptcmiR399h	osamiR415	osamiR438	ptcmiR474c	ptcmiR482	osamiR811a
C	athmiR156h	athmiR163	osamiR169e	osamiR171b	athmiR391	ptcmiR397b	ptcmiR399l	athmiR415	osamiR439h	ptcmiR474a	osamiR528	osamiR812a
D	ptcmiR156k	athmiR164a	ptcmiR169x	zmamiR171c	osamiR393b	ptcmiR397c	athmiR400	athmiR416	osamiR440	ptcmiR475b	osamiR529	osamiR813
E	sbimiR156e	ptcmiR164f	athmiR169a	zmamiR171f	athmiR394a	athmiR397b	athmiR401	osamiR416	osamiR441c	ptcmiR475d	osamiR530	osamiR814a
F	athmiR157a	sbimiR164c	zmamiR169d	osamiR171i	athmiR395b	athmiR398a	athmiR402	athmiR417	osamiR442	ptcmiR475c	osamiR531	osamiR815a
G	athmiR158a	osamiR164c	osamiR169d	osamiR171g	ptcmiR395a	osamiR398b	athmiR403	osamiR417	osamiR443	ptcmiR476a	osamiR535	osamiR816
H	athmiR159a	athmiR165a	osamiR169n	osamiR171h	osamiR395t	osamiR399a	athmiR404	athmiR418	osamiR444	ptcmiR476c	pptmiR533	osamiR817
I	sofmiR159e	athmiR166a	osamiR169q	athmiR171c	mtrmiR395a	osamiR399h	athmiR405a	osamiR418	osamiR445d	ptcmiR477a	pptmiR534	osamiR818a
J	ptcmiR159f	osamiR166i	ptcmiR169ab	ptcmiR172i	osamiR395c	ptcmiR399d	athmiR406	athmiR419	osamiR446	ptcmiR478e	pptmiR536	osamiR819a
K	ptcmiR159e	osamiR166l	osamiR169p	ptcmiR172g	mtrmiR395b	athmiR399e	athmiR407	osamiR419	athmiR447c	ptcmiR478a	pptmiR537a	osamiR820a
L	athmiR160a	ptcmiR166p	athmiR169g*	athmiR172b*	osamiR395a	ptcmiR399k	osamiR408	athmiR420	athmiR447b	ptcmiR478m	pptmiR538c	osamiR821a
M	osamiR160f	athamiR167a	ptcmiR169z	athmiR173	osamiR395u	ptcmiR399j	sofmiR408e	osamiR420	ptcmiR472a	ptcmiR479	osamiR806a	MAC2
N	ptcmiR160h	ptcmiR167h	ptcmiR169y	osamiR319a	osamiR395v	osamiR399k	osamiR413	athmiR426	ptcmiR472b	ptcmiR480a	osamiR807a	MAC3
O	ptcmiR160g	osamiR168a	ptcmiR169aa	athmiR319a	osamiR395w	osamiR399j	athmiR413	osamiR426	ptcmiR473b	ptcmiR480b	osamiR808	MAC4
P	athmiR161	osamiR168b	athmiR170	gmamiR319c	ptcmiR396f	zmamiR399b	osamiR414	osamiR435	ptcmiR473a	ptcmiR481d	osamiR809a	MAC5

4. Transfer the 4 mL into four 1.5-mL tubes with 1 mL in each tube.
5. Keep the sample at room temperature for 5 min to permit the complete dissociation of nucleoprotein complexes.
6. Add 0.2 mL chloroform to each tube, close the cap well, and shake vigorously for 1 min.
7. Keep the sample at room temperature for another 5 min.
8. Spin the sample for 15 min at 16,000×*g* at 4°C to allow the mixture to separate into a lower red, phenol–chloroform phase, an interphase, and a colorless upper aqueous phase.
9. Carefully take the upper aqueous phase (containing total RNA) to a fresh, RNase-free, 1.5-mL tube without touching the interphase (*see* **Note 2**).
10. Add 0.5 mL isopropanol to each tube containing the upper aqueous phase and mix them well.
11. Place the tubes at −20°C overnight to precipitate the total RNA.
12. Centrifuge for 15 min at 16,000×*g* at 4°C.
13. Carefully remove the supernatant, add 0.5 mL 80% cold ethanol, and centrifuge for 10 min at 16,000×*g* at 4°C.
14. Remove the supernatant carefully using a pipette.
15. Vacuum dry the RNA pellet for 1–3 min.
16. Dissolve the RNA pellet in 15–40 μL RNase-free water or formamide (depending on the size of the pellet) and then pool the total RNA from four tubes (*see* **Note 3**). It is better to prepare 100 μg of total RNA for array and 20–25 μg for small RNA blot analysis in the formamide loading buffer immediately to prevent RNA degradation. RNA in sample buffer (formamide loading dye) can be stored by keeping at −80°C for future use.
17. Measure RNA concentration as micrograms per microliter using Nanodrop.

3.3.1.2. Gel Preparation for Small RNA Enrichment and Purification

1. Clean the gel plates with detergent and rinse the plates well with tap water.
2. Assemble the plates with 3-mm-thick spacers.
3. Prepare 15% denaturing PAGE gel solutions (SequaGel-National Diagnostics) as follows: 60 mL concentrate, 30 mL diluent, 10 mL of 10× buffer, 0.04 mL TEMED (*N*,*N*,*N*′,*N*′-tetramethylethylenediamine) and 0.6 mL of 10% APS.
4. Pour the mixed solution between the gel plates (*see* **Note 4**).

5. Insert the comb immediately into the gel.
7. Wait for 20–30 min for the gel solution to polymerize.
8. Prepare the 0.5× TBE (running buffer) by diluting the 20× TBE.
9. Carefully remove the comb once the gel is polymerized.
10. Rinse the wells using running buffer with the help of a 3-mL syringe fitted with a 22-gauge needle.
11. Assemble the gel system with the gel running unit.
12. Add the running buffer to the upper and lower chambers of the gel unit.
13. Pre-run for 1 h at a constant 20 W power.

3.3.1.3. Running the Gel to Separate RNA Samples

1. Mix 100 μg of total RNA in the sample buffer with 5 μL external control siRNAs, which is a mixture of different amounts (40, 20, 10, and 5 fmol) of synthetic 21-nt control RNAs that were complementary to four MAC probes.
2. Use 21–24-nt labeled synthetic RNA oligos as markers (*see* **Section 3.3.4** for 5′-end labeling using T4 polynucleotide kinase).
2. Denature the RNA mixture in the sample buffer by boiling the samples at 95°C for 3 min.
3. Stop the pre-running and rinse the gel wells again for sample loading.
4. Load the RNA samples into the wells (*see* **Note 5**).
5. Mark the sample number on the glass plate so that each sample identity is recognized for later steps.
6. Run the loaded samples at a constant power of 20–25 W for about 1 h 40 min until the front dye (blue dye) has reached the bottom of the gel (*see* **Note 6**).
7. Stop the running.

3.3.1.4. Gel Purification of Small RNAs

1. Disassemble the gel apparatus and take away one of the glass plates and leave the gel on the other glass plate.
2. Insert florescent labels at the four corners of the gel and cover the gel together with the glass plate with a saran wrap.
3. Expose the gel to an X-ray film for 3–5 min and develop the film.
4. Overlay the gel on the X-ray film and place it on a light box (light source coming from below the X-ray film and glass plate).
5. Mark the position of 21 and 24 nt on the gel.

6. Cut the gel fragment between 21 and 24 nt into small squares (not too small, about 12 pieces).
7. Recover the small RNAs by soaking the gel slice in 1–2 mL of gel elution buffer shaking overnight on a rotor at room temperature.
8. Remove samples from the rotor and centrifuge at 16,000×*g* briefly at room temperature.
9. Transfer the elution buffer that contains the small RNAs to a fresh 2-mL tube and spin for 5 min at 16,000×*g* to remove the gel pieces, if any.
10. Take out the clean supernatant to a new 1.5-mL Eppendorf tube.
11. Add 1 μL glycogen (20 mg/mL) per milliliter of eluted sample solutions and mix them thoroughly by gentle vortexing.
12. Divide the supernatant into four tubes. Add three volumes of −20°C chilled absolute ethanol, mix well, and precipitate the small RNAs overnight at −20°C.
13. Spin at 16,000×*g* for 15 min at 4°C.
14. Carefully remove the supernatant and keep the pellet.
15. Add 1 mL of 80% cold ethanol and wash the pellet at 16,000×*g* at 4°C for 10 min.
16. Discard the supernatant with a pipette and do not disturb the small RNA pellet (*see* **Note 7**).
17. Vacuum dry the RNA pellet briefly for 1 min.
18. Dissolve completely the pellets of each small RNA sample from the four tubes using a total volume of 51 μL RNase-free water.
19. Take 1 μL of the small RNA sample to measure the concentration using a Nanodrop.

3.3.2. Removal of the Monophosphate from the 5′-End of the Small RNAs

Plant miRNAs contain a monophosphate at their 5′-ends and it is necessary to remove it using a phosphatase (i.e., Antarctic phosphatase; New England Biolabs) before labeling the small RNAs with [γ-P^{32}]ATP using polynucleotide kinase (PNK).

1. Prepare the following dephosphorylation reaction mixture: 6 μL Antarctic phosphatase (AP) buffer (10×), 1 μL RNasin, 2 μL Antarctic phosphatase (AP), up to 50 μL small RNA, use water to make up to 60 μL.
2. Mix them gently using a pipette.
3. Incubate at 37°C for 1 h.
4. Inactivate the phosphatase by keeping at 65°C for 10 min.

3.3.3. Array Prehybridization

1. Prepare hybridization buffer (10 mL/array) for prehybridization: in 10 mL volume, add 5 mL of 100% formamide, 2.5 mL of 20× SSPE, 1 mL of 50× Denharts, 0.5 mL of 10% SDS, 0.08 mL of 10 mg/mL sperm DNA (denatured), and 0.92 mL H_2O.
2. Put the array membrane in a small hybridization tube with the probe face opposite to the wall of the hybridization tube. Label the bottle with the name of your sample and mark the array membrane series number.
3. Add the hybridization buffer and rotate in hybridization oven at 37°C for at least 2 h.

3.3.4. Small RNA Labeling

1. After dephosphorylation, label the small RNAs (60 μL) by adding the following: 7.5 μL of 10× PNK buffer, 2 μL polynucleotide kinase (PNK), 1 μL RNasin (40 U), 4 μL [γ-P^{32}]ATP, 0.5 μL water to make a volume of 75 μL.
2. Incubate at 37°C for 1 h to label the small RNAs.

3.3.5. Purification of the Radiolabeled Sample and the Hybridization

The labeled samples will be purified by passing through a G-25 spin column (Roche) and monitored for labeling efficiency with GM counter (*see* **Notes 8** and **9**).

1. Take a G-25 column and remove air bubbles inside the matrix by mixing thoroughly with the buffer.
2. Remove the top cap first and then the bottom cap.
3. Put it in a 15-mL tube with a collection tube inside.
4. Spin the column at 2,000×*g* for 1 min at room temperature.
5. Discard the effluent and spin the column again at 2,000×*g* for 2 min.
6. Replace the collection tube with a new tube.
7. Mark the sample name on the column and the collection tube.
8. Load the radiolabeled small RNAs onto the G25 column right in the middle of the matrix without touching the matrix behind a radioactive shield.
9. Transfer the loaded column to a 15-mL capped tube and tighten the cap behind a shield.
10. Spin the column at 2,000×*g* for 2 min and collect the purified labeled small RNAs using a fresh 1.5-mL tube. Check the labeling efficiency with GM counter by reading the counts for the eluted labeled RNA and the free isotope inside the column. The labeling efficiency should be over 50% (*see* **Note 10**).

11. Mark the sample name on the tube that contains the labeled small RNAs. Use the labeled small RNAs immediately for hybridization or store it at −20°C for future hybridization use.
12. Add the labeled small RNAs directly to the prehybridization solution without a direct touch of the array filter after 2 h of prehybridization.
13. Mix well the labeled small RNAs with the prehybridization buffer and continue the hybridization overnight.

3.3.6. Membrane Washing

1. Pre-warm the washing buffer (2× SSC containing 0.1% SDS) at 37°C.
2. Transfer the hybridization solution containing the labeled small RNAs to a 50-mL capped falcon tube, tighten the cap, mark the sample name, and store it in a shield box in a −20°C freezer for future backup use.
3. Rinse the membrane in the hybridization bottle with 15 mL pre-warmed washing buffer (*see* **Note 11**).
4. Wash the array membrane in the hybridization bottle with 30 mL washing buffer for 2–3 times for 20 min each.
5. Check the membrane for background with a GM counter monitor. If the background is too high, wash the membrane again until the background is reasonably low.
6. Wrap the membrane using saran wrap, label the sample name, and expose it to a PhosphorImage screen overnight or longer.

3.3.7. Document the Array Picture, Signal, and Array Analysis

3.3.7.1. Signal Detection and Documentation

The PhosphorImager screen will be scanned using a PhosphorImager scanner (Typhoon 9400; Molecular Dynamics). Array picture output and quantification will be performed using ImageQuant software (Amersham Biosciences). An example of the representative array images of the control and the different abiotic stress-treated tobacco plants is shown in **Fig. 15.1** (*see* **Note 12**).

3.3.7.2. Data Normalization

The intensities of duplicate spots on each array image will be averaged. To compare the miRNA expression profiles between different tissues, external controls will be used for array data normalization. The external controls will be used to remove system-related variations (e.g., amount variations, process-related loss of small RNAs or signals, variations in labeling signal strength, and signal gain differences between scanners) so that biologically relevant variations could be faithfully revealed. An example of the quantified data of miRNA profiling under different abiotic stress conditions in tobacco is shown in **Table 15.2**.

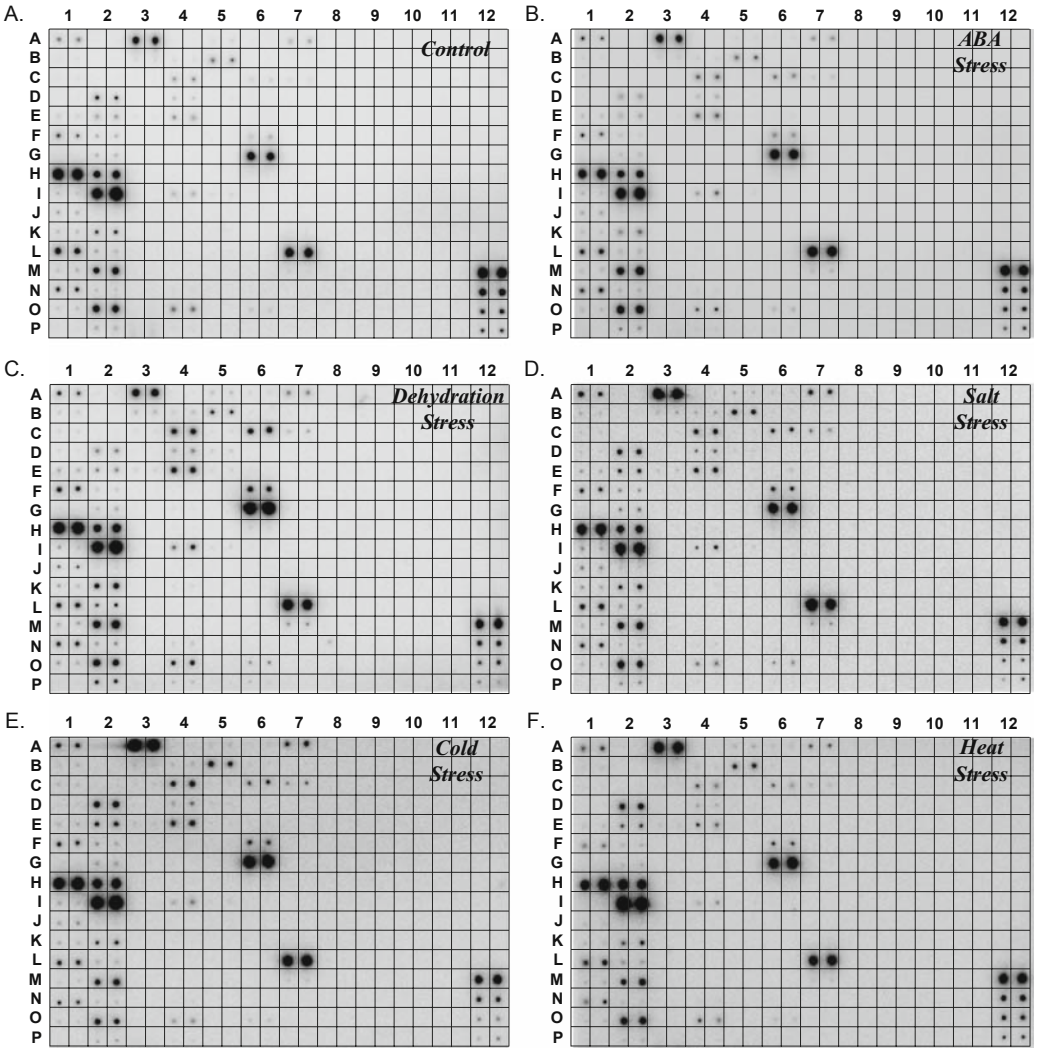

Fig. 15.1. MicroRNA array of the control and the abiotic stress-treated tobacco plants. Total RNA was extracted from the stress-treated and control plants. One hundred micrograms of total RNA was used for each array. The extracted small RNA was 5′-end labeled and probed against the spotted antisense DNA oligos on the membrane. (**a)** Control; (**b)** abscisic acid stress (100 μM for 3 h); (**c)** dehydration stress – 30% loss of fresh weight; (**d)** salt stress (300 mM for 4 h); (**e)** cold stress (4°C for 1 h); (**f)** heat stress (45°C for 1 h).

3.4. Small RNA Blot Analysis

The differentially expressed miRNAs under different stress treatments will be further validated by small RNA blot analysis. **Fig. 15.2** shows a small RNA blot validation of the stress-responsive miRNAs in tobacco. The detailed steps for small RNA blot validation are as follows:

1. Total RNA for small RNA blot validation should be from the same batch for the array analysis (for total RNA isolation, *see* **Section 3.3.1.1**).

Table 15.2
Quantified data of miRNA expression profile under different stress conditions

Series No.	miRNA	Control	ABA	Dehydration	Salt	Cold	Heat
1	athmiR156a	1	1.22	2.73	5.77	6.90	2.95
2	athmiR157a	1	1.09	4.10	2.87	4.20	1.59
3	athmiR164a	1	0.56	1.27	5.02	7.85	3.74
4	ptcmiR164f	1	0.81	2.22	5.19	9.00	3.08
5	osamiR166l	1	1.04	4.29	2.68	2.75	1.93
6	ptcmiR166p	1	0.83	2.68	2.65	2.46	1.92
7	ptcmiR167h	1	1.58	2.83	2.90	2.41	2.06
8	athmiR168a	1	1.17	1.75	6.31	5.68	2.28
9	osamiR171b	1	2.15	8.80	7.81	11.37	2.69
10	zmamiR171c	1	1.39	5.50	6.70	9.83	3.66
11	zmamiR171f	1	2.23	8.30	7.55	10.82	2.71
12	athmiR171b	1	1.61	5.03	3.97	4.85	2.00
13	ptcmiR319i	1	0.81	2.59	6.15	9.29	4.18
14	athmiR390a	1	1.10	2.27	5.44	7.21	3.16
15	ptcmiR397b	1	3.01	22.47	10.75	14.82	4.76
16	athmiR398a	1	1.97	9.52	5.75	9.84	3.56
17	osamiR398b	1	1.81	6.01	4.46	8.26	3.42
18	osamiR399j	1	1.01	2.25	3.02	2.07	1.50
19	mtrmiR399d	1	1.40	3.61	8.29	13.07	3.52
20	ptcmiR399l	1	1.31	3.59	8.46	11.76	3.88
21	osamiR408	1	1.90	3.53	4.10	3.90	1.57
22	sofmiR408e	1	1.26	2.62	3.57	2.90	1.50

MicroRNA profiling under different abiotic stress conditions along with a control. Data were normalized using the average of four membrane array external controls. MicroRNAs with a minimum of twofold changes in three of the five abiotic stresses were selected.
ABA, abscisic acid (100 μM, 3 h); dehydration stress (30% loss of fresh weight); salt stress (NaCl 300 mM, 4 h); cold stress (4°C, 1 h), and heat stress (45°C, 1 h).

2. Separate 20–25 μg of total RNA on a sequencing gel (sequencing gel preparation and the gel running as described in **Sections 3.3.1.2** and **3.3.1.3**).
3. Stop the gel running and visualize the RNA quality by staining the gel with ethidium bromide and documenting the gel picture.
4. Transfer the RNAs from the gel to a Hybond N^+ membrane using a semi-dry electrotransfer apparatus (Bio-Rad).
5. Rinse the Hybond N^+ membrane containing RNAs with 2× SSPE (pH 7.4).

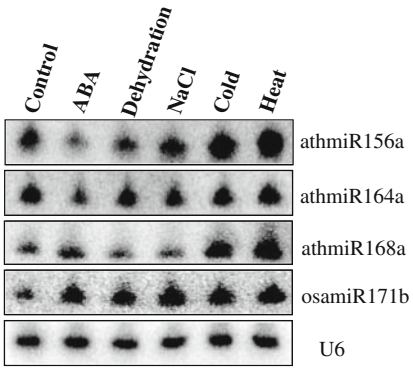

Fig. 15.2. Validation of the stress-responsive miRNAs using small RNA blot analysis in tobacco. Total RNA (25 μg) was used for the blot analysis for the control and the stress-treated tobacco leaves. Though the small RNA blot is from tobacco RNA, the miRNAs are named based on the detected sequence from ath (*Arabidopsis thaliana*) and osa (*Oryza sativa*).

6. Cross-link the RNAs to the membrane using a UV cross-linker at 1,200 × 100 μJ/cm^2 for 1 min.
7. Prehybridize the membrane for at least 2 h as described in **Section 3.3.3**.
8. Hybridize the membrane with a radiolabeled antisense DNA probe of a selected miRNA and wash the membrane to have a clean background (for probe labeling, purification, hybridization, and the membrane washing, *see* **Sections 3.3.4**, **3.3.5**, and **3.3.6**).
9. Expose the membrane to a PhosphorImager screen and document the radioactive signal (*see* **Section 3.3.7.1.**).

3.5. Probe Stripping

Once a satisfactory result is obtained, the membrane of the array or the small RNA blot can be stripped and used for another hybridization.

1. Prepare 500 mL stripping buffer containing 0.1× SSC and 0.5% SDS.
2. Boil the stripping buffer.
3. Put the membrane containing isotope probes inside the stripping buffer.
4. Let it cool down to room temperature.
5. Repeat the above steps, if necessary.
6. Wrap the membrane using a saran wrap and expose it to a PhosphorImage screen for confirming the stripping is complete (*see* **Note 12**).

4. Notes

1. RNA integrity is critical for these experiments. Special care should be taken during RNA preparation. All containers and RNA-extracting equipment should be prepared RNase free by DEPC treatment or by baking them overnight. Always wear gloves while handling RNA.
2. While transferring the aqueous phase, make sure that you are not touching the interphase.
3. RNA is much more stable in formamide.
4. Avoid air bubble formation while pouring the gel.
5. Load the RNA samples onto the wells before the gel temperature cools down.
6. While running radiolabeled samples, electrophoresis should be performed in an area designated for radioactive work behind a protective shield.
7. Extreme care is required as the pellet may go with the supernatant while removing supernatant from the tube in which small RNAs are precipitated. It is hard to see the small RNA pellet if small quantity of RNA is used.
8. All these steps should be done with extreme care and behind a radioactive protective shield. When you are working with radioisotopes, always wear appropriate protective wears such as eye glasses and gloves.
9. Only well-labeled samples should be used for hybridization with the array membrane.
10. Signal from the eluted labeled RNA should be higher than that from the free isotope inside the column.
11. Do not let your membranes stand longer than 2 min without adding the washing buffer. Otherwise, you will not be able to wash away the array background and ruin your array membrane.
12. The array membrane can be re-used for many times. If you want to reuse the array membrane, never let the membrane dry out. After hybridization, the probe can be stripped and the membrane can be wrapped using a saran wrap while it is still moist and can be stored at 4°C.

Acknowledgments

G.T. is supported by the Kentucky Tobacco Research and Development Center (KTRDC), the USDA-NRI grants 2006-

35301-17115 and 2006-35100-17433, the NSF MCB-0718029 (Subaward No. S-00000260), and an award from the Kentucky Science and Technology Corporation under Contract # KSTC-144-401-08-029.

References

1. Tang, G., Tang, X., Mendu, V., Jia, X., Chen, Q.J., and He, L. (2008) The art of microRNA: various strategies leading to gene silencing via an ancient pathway. *Biochim Biophys Acta* **1779**, 655–662.
2. Llave, C., Kasschau, K.D., Rector, M.A., and Carrington, J.C. (2002) Endogenous and silencing-associated small RNAs in plants. *Plant Cell* **14**, 1605–1619.
3. Park, W., Li, J.J., Song, R.T., Messing. J., and Chen, X.M. (2002) CARPEL FACTORY, a Dicer homolog, and HEN1, a novel protein, act in microRNA metabolism in *Arabidopsis thaliana*. *Curr Biol* **12**, 1484–1495.
4. Reinhart, B.J., Weinstein, E.G., Rhoades, M.W., Bartel, B., and Bartel, D.P. (2002) MicroRNAs in plants. *Gene Dev* **16**, 1616–1626.
5. Jones-Rhoades, M.W., Bartel, D.P., and Bartel, B. (2006) MicroRNAs and their regulatory roles in plants. *Annu Rev Plant Biol* **57**, 19–53.
6. Voinnet, O. (2009) Origin, biogenesis, and activity of plant microRNAs. *Cell* **136**, 669–687.
7. Sunkar, R., Chinnusamy, V., Zhu, J., and Zhu, J.K. (2007) Small RNAs as big players in plant abiotic stress responses and nutrient deprivation. *Trends Plant Sci* **12**, 301–309.
8. Shukla, L.I., Chinnusamy, V., and Sunkar, R. (2008) The role of microRNAs and other endogenous small RNAs in plant stress responses. *Biochim Biophys Acta* **1779**, 743–748.
9. Sunkar, R. and Zhu, J.K. (2004) Novel and stress-regulated microRNAs and other small RNAs from *Arabidopsis*. *Plant Cell* **16**, 2001–2019.
10. Sunkar, R., Kapoor, A., and Zhu J.K. (2006) Posttranscriptional induction of two Cu/Zn superoxide dismutase genes in *Arabidopsis* is mediated by downregulation of miR398 and important for oxidative stress tolerance. *Plant Cell* **18**, 2051–2065.
11. Jones-Rhoades, M.W. and Bartel, D.P. (2004) Computational identification of plant MicroRNAs and their targets, including a stress-induced miRNA. *Mol Cell* **14**, 787–799.
12. Lu, S., Sun, Y.-H., Shi, R., Clark, C., Li, L., and Chiang, V.L. (2005) Novel and mechanical stress-responsive microRNAs in *Populus trichocarpa* that are absent from *Arabidopsis*. *Plant Cell* **17**, 2186–2203.
13. Katiyar-Agarwal, S., Gao, S., Vivian-Smith, A., and Jin, H. (2007) A novel class of bacteria-induced small RNAs in *Arabidopsis*. *Genes Dev* **21**, 3123–3134.
14. Reyes, J.L. and Chua, N.H. (2007) ABA induction of miR159 controls transcript levels of two MYB factors during *Arabidopsis* seed germination. *Plant J* **49**, 592–606.
15. Zhao, B., Liang, R., Ge, L., Li, W., Xiao, H., Lin, H., Ruan, K., and Jin, Y. (2007) Identification of drought-induced microRNAs in rice. *Biochem Biophys Res Commun* **354**, 585–590.
16. Zhang, Z., Wei, L., Zou, X., Tao, Y., Liu, Z., and Zheng, Y. (2008) Submergence-responsive microRNAs are potentially involved in the regulation of morphological and metabolic adaptations in maize root cells. *Ann Bot* **102**, 509–519.
17. Liu, H.-H., Tian, X., Li, Y.-J., Wu, C.-A., and Zheng, C.-C. (2008) Microarray-based analysis of stress-regulated microRNAs in *Arabidopsis thaliana*. *RNA* **14**, 836–843.
18. Zhang, B., Pan, X., Cannon, C.H., Cobb, G.P., and Anderson, T.A. (2006) Conservation and divergence of plant microRNA genes. *Plant J* **46**, 243–259.
19. Tang, X., Gal, J., Zhuang, X., Wang, W., Zhu, H., and Tang, G. (2007) A simple array platform for microRNA analysis and its application in mouse tissues. *RNA* **13**, 1803–1822.
20. Griffiths-Jones, S., Saini, H.K., van Dongen, S., and Enright, A.J. (2008) miRBase: tools for microRNA genomics. *Nucl Acids Res* **36**, D154–D158.

Part III

Antioxidant Enzymes and Metabolites

Chapter 16

Spectrophotometric Assays for Antioxidant Enzymes in Plants

Sathya Elavarthi and Bjorn Martin

Abstract

Reactive oxygen species (ROS) are formed in biological systems as part of normal metabolism. Adverse environmental factors like drought stress result in increased levels of ROS that are detrimental to the plant (1, 2). To avoid damage caused by these excess ROS, plants have developed elaborate mechanisms to manage them at sustainable levels. Enzymes play an important role in lowering the ROS levels and helping avoid oxidative stress. Superoxide dismutase, catalase, ascorbate peroxidase, and glutathione reductase play a vital role in combating oxidative stress. Measuring these enzyme activities spectrophotometrically provides researchers an easy and precise way to study and understand an important part of the defense against oxidative stress. In this chapter we provide details of the assays we used to determine the enzyme activities spectrophotometrically. Antioxidant enzyme responses to moderate water-deficit stress were studied. All enzyme assays were conducted using wheat leaf tissue.

Key words: Antioxidant enzymes, ascorbate peroxidase, catalase, glutathione reductase, oxidative stress, superoxide dismutase.

1. Introduction

Plants are frequently exposed to oxidative stresses that are caused by both biotic and abiotic factors. Under stress, enormous amounts of reactive oxygen species (ROS) are produced that can cause peroxidation, resulting in damage to cell membranes, protein oxidation, enzyme inhibition, and strand breakage in nucleic acids (3). Plants have developed elaborate mechanisms to detoxify these ROS and in these mechanisms, enzymes play a very important role (4). Major ROS scavenging enzymes in plants include

R. Sunkar (ed.), *Plant Stress Tolerance*, Methods in Molecular Biology 639,
DOI 10.1007/978-1-60761-702-0_16,

superoxide dismutase (SOD), catalase (CAT), ascorbate peroxidase (APX), and glutathione reductase (GR) (5).

Transgenic wheat lines containing a bacterial *mtlD* gene for mannitol biosynthesis were used in this study (6). Mannitol has been shown to protect plants from oxidative stress damage by scavenging hydroxyl radicals (7). The antioxidant enzyme activities of transgenic lines containing the enzyme mannitol-1-phosphate dehydrogenase (*mtlD*) targeted to cytosol (TA2 lines) and chloroplasts (TA5 lines) along with a transgenic control (*pahc20*) and wild type (Bobwhite) were determined under well-watered and water-deficit conditions. Moderate water-deficit stress was imposed on the plants over a 30-day period starting at the jointing stage of the plants and the antioxidant enzyme responses to stress were studied **(Fig. 16.1**). The stress levels were controlled by measuring volumetric water content of the pots using time domain reflectometry (TDR).

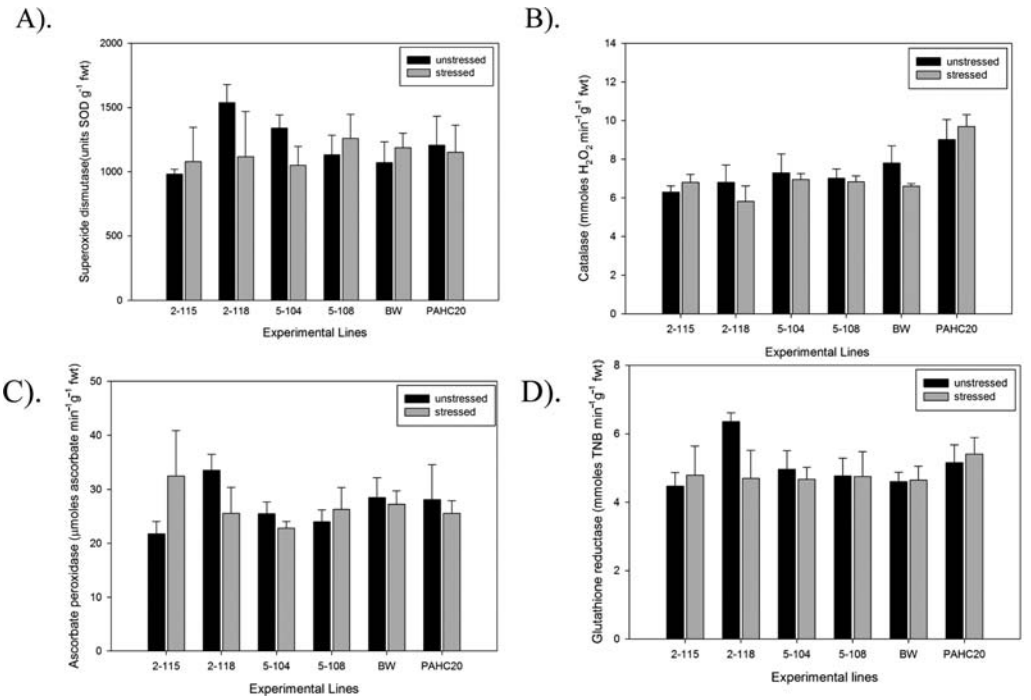

Fig. 16.1. Superoxide dismutase (SOD), catalase (CAT), ascorbate peroxidase (APX), and glutathione reductase (GR) activities were determined on wheat leaf samples from both well-watered and stressed plants. Samples were collected from Bobwhite (wild type), *pahc20* (transgenic control), 2-115, 2-118 [mannitol-1-phosphate dehydrogenase (*mtlD)* targeted into cytosol], and 5-104, 5-108 (*mtlD* targeted into chloroplast) after 30 days of stress. The enzyme activities were determined spectrophotometrically and expressed as units SOD per gram fresh weight (SOD), millimoles H_2O_2 per minute per gram fresh weight (CAT), micromoles ascorbate per minute per gram fresh weight (APX), and millimoles TNB per minute per gram fresh weight (GR).

1.1. Superoxide Dismutase (SOD)

1. SODs are metalloproteins that catalyze the dismutation reaction of two superoxide free radicals to one molecule of O_2 and one molecule of H_2O_2.
2. SODs occur in different isoforms with different metal cofactors.
3. SODs are considered the first line of defense against damage by the superoxide radical (8).
4. Superoxide free radicals are generated in vitro, especially in the presence of bright light.
5. Nitroblue tetrazolium (NBT), which is a yellow compound, is reduced to blue monoformazon by the superoxide radical.
6. SOD activity is quantified based on the competitive inhibition of NBT reduction by the superoxide radical. At near-neutral pH, the dismutation rate of superoxide radicals increases 1,000-fold in the presence of SOD.

1.2. Catalase (CAT)

1. CAT is a heme protein that catalyzes the decomposition of H_2O_2 into H_2O and O_2.
2. CAT is present in the cytosol and in peroxisomes.
3. Rapid decomposition of H_2O_2 in the cell reduces the likelihood of formation of the highly reactive hydroxyl radical through metal-catalyzed Fenton and Haber-Weiss reactions.
4. The decomposition of H_2O_2 in the presence of CAT is followed as a decrease in absorbance at 240 nm.
5. CAT activity is measured as the decrease in absorbance per unit time.

1.3. Ascorbate Peroxidase (APX)

1. Ascorbate-specific peroxidases play an important role in decomposition of H_2O_2 generated both in the chloroplasts and in the cytosol.
2. APXs are distributed in stroma, thylakoids, microbodies, cytosol, and mitochondria (9).
3. Ascorbate acts as the electron donor for the decomposition of H_2O_2 in the cell.
4. The enzyme activity is assayed by measuring the rate of decrease in absorbance of ascorbate at 290 nm.

1.4. Glutathione Reductase (GR)

1. GR is a NADPH-dependent enzyme that catalyzes the reduction of oxidized glutathione (GSSG) to reduced glutathione (GSH) (10).
2. GR helps to maintain a high ratio of GSH/GSSG as part of the ascorbate–glutathione cycle, thus playing an important role in cell metabolism (11).

3. The activity of GR is measured by following the reduction of 5,5′-dithio-bis-(2-nitrobenzoic acid) (DTNB) to 2-nitro-5-thiobenzoic acid (TNB) by GSH.
4. The increase in absorbance per unit time at 412 nm due to the formation of TNB is determined using a spectrophotometer.

2. Materials

2.1. Hardware and Crude Leaf Extract

1. A UV/Vis spectrophotometer.
2. Quartz/clear plastic disposable cuvettes.
3. Liquid nitrogen.
4. Mortar and pestle.
5. Refrigerator for storing buffers.
6. Fresh leaves.
7. Potassium phosphate buffer (0.2 M, pH 7.0) containing 0.1 mM EDTA.

2.2. Superoxide Dismutase (SOD)

1. Potassium phosphate buffer (50 mM, pH 7.8) with 2 mM EDTA (*see* **Notes 1–4**).
2. L-Methionine (30 mg/mL).
3. NBT hydrochloride (1.41 g/mL).
4. Triton-X100 (1%, w/v).
5. Riboflavin (0.044 g/mL).
6. Pure SOD from Sigma.

2.3. Catalase (CAT)

1. Potassium phosphate buffer (50 mM, pH 7.0) (*see* **Notes 1–4**).
2. H_2O_2 solution (30 mM).

2.4. Ascorbate Peroxidase (APX)

1. Potassium phosphate buffer (50 mM, pH 7.0) (*see* **Notes 1–4**).
2. Ascorbic acid solution (100 mM).
3. H_2O_2 solution (100 mM).

2.5. Glutathione Reductase (GR)

1. Potassium phosphate buffer (50 mM, pH 7.8) with 2 mM EDTA (*see* **Notes 1–4**).
2. DTNB solution (3 mM).
3. NADPH solution (10 mM).
4. GSSG solution (10 mM).

3. Methods

3.1. Crude Leaf Extract for Antioxidant Enzyme Assays

1. Fresh leaf tissue was collected from stressed and well-watered plants of both transgenic and control lines.
2. Approximately 200 mg of leaf tissue was weighed and ground to a fine powder in liquid nitrogen using a pre-cooled mortar and pestle.
3. The exact weight of each powdered sample was determined before it was thoroughly homogenized in 1.2 mL of 0.2 M potassium phosphate buffer (pH 7.8 with 0.1 mM EDTA).
4. The samples were centrifuged at 15,000×*g* for 20 min at 4°C.
5. The supernatant was removed, the pellet resuspended in 0.8 mL of the same buffer, and the suspension centrifuged for another 15 min at 15,000×*g*.
6. The combined supernatants were stored on ice and used to determine different antioxidant enzyme activities (*see* **Notes 5** and **6**).

3.2. Superoxide Dismutase (SOD)

1. Total SOD activity was assayed using a modified NBT method (11) (*see* **Note 7**).
2. The 2 mL assay reaction mixture contained 50 mM phosphate buffer (pH 7.8) containing 2 mM EDTA, 9.9 mM L-methionine, 55 μM NBT, and 0.025% Triton-X100.
3. Forty microliters of diluted (2×) sample and 20 μL of 1 mM riboflavin were added and the reaction was initiated by illuminating the samples under a 15 W fluorescent tube (12).
4. During the 10-min exposure, the test tubes were placed in a box lined with aluminum foil.
5. The box with the test tubes was placed on a slowly oscillating platform at a distance of approximately 12 cm from the light source.
6. Duplicate tubes with the same reaction mixture were kept in the dark and used as blanks.
7. Absorbance of the samples was measured immediately after the reaction was stopped at 560 nm (*see* **Note 8**)
8. The enzyme activity (grams per fresh weight) of a sample was determined from a standard curve obtained by using pure SOD.

3.3. Catalase (CAT)

1. CAT activity was determined according to Aebi and Lester (13) (*see* **Notes 1–4**).

2. The decomposition of H_2O_2 was followed as a decrease in absorbance at 240 nm in a UV/Vis spectrophotometer.
3. The 3 mL assay mixture contained 2 mL leaf extract (diluted 200 times in 50 mM potassium phosphate buffer, pH 7.0) and 10 mM H_2O_2.
4. The extinction coefficient of H_2O_2 (40 mM^{-1} cm^{-1} at 240 nm) was used to calculate the enzyme activity that was expressed in terms of millimoles of H_2O_2 per minute per gram fresh weight).

3.4. Ascorbate Peroxidase (APX)

1. APX activity was assayed using a modified method of Nakano and Asada (14) (*see* **Notes 1–4**).
2. APX activity was determined from the decrease in absorbance at 290 nm due to oxidation of ascorbate in the reaction.
3. The 1 mL assay mixture contained 50 mM potassium phosphate buffer (pH 7.0), 0.5 mM ascorbate, 0.5 mM H_2O_2, and 10 μL of crude leaf extract (*see* **Note 9**).
4. H_2O_2 was added last to initiate the reaction, and the decrease in absorbance was recorded for 3 min.
5. The extinction coefficient of 2.8 mM^{-1} cm^{-1} for reduced ascorbate was used in calculating the enzyme activity that was expressed in terms of millimole of ascorbate per minute per gram fresh weight.

3.5. Glutathione Reductase (GR)

1. GR activity was assayed according to Smith et al. (15) (*see* **Notes 1–4**).
2. The increase in absorbance at 412 nm was measured when DTNB was reduced to TNB by GSH in the reaction.
3. Ten microliters of leaf extract was used in the assay along with 0.75 mM DTNB, 0.1 mM NADPH, and 1 mM GSSG in a total of 1 mL assay volume (*see* **Notes 9** and **10**).
4. GSSG was added last to initiate the reaction and the increase in absorbance was recorded for 3 min.
5. The extinction coefficient of TNB (14.15 M^{-1} cm^{-1}) was used to calculate the activity of GR that was expressed in terms of millimole TNB minute per gram fresh weight.

4. Notes

1. Unless otherwise stated, all buffers/solutions were prepared using Millipore water and stored at 4°C until they were used.

2. Store buffers at 4°C and bring them to room temperature before the experiment except NADPH and GSSG, which should be maintained at 4°C at all times prior to use.
3. Quartz cuvettes were used for assays using UV wavelengths and clear plastic disposable cuvettes were used for assays in the visible range.
4. For all assays, care must be taken to avoid air bubbles forming in the cuvettes before making absorbance measurements.
5. The crude leaf extract was prepared fresh daily from leaf tissue and all assays were conducted within a few hours.
6. The crude leaf extract should at all times be kept on ice.
7. All solutions for SOD assay should be at room temperature for optimal enzyme activity.
8. Absorbance readings for SOD samples should be taken as soon as the assay is stopped, because the blue formazon will quickly start precipitating out, resulting in errors.
9. Ascorbic acid in the APX assay and GSSG in the GR assay should always be kept on ice.
10. The NADPH stock solution can be stored at −20°C and reused for up to a week. Thawed stock solution should be kept on ice until used.

Acknowledgments

The authors would like to thank Dr. Kalpalatha Melmaiee and Shraddha Vadvalkar for valuable suggestions and help in the critical review of the chapter.

References

1. Asada, K. (1999) The water–water cycle in chloroplasts: scavenging of active oxygens and dissipation of excess photons. *Annu Rev Plant Physiol Plant Mol Biol* **50**, 601–639.
2. Borsani, O., Díaz, P., Agius, M.F., Valpuesta, V., and Monza, J. (2001) Water stress generates an oxidative stress through the induction of a specific Cu/Zn superoxide dismutase in *Lotus corniculatus* leaves. *Plant Sci* **161**, 757–763.
3. Allen, R.D. (1995) Dissection of oxidative stress tolerance using transgenic plants. *Plant Physiol* **107**, 1049–1054.
4. Khanna-Chopra, R. and Selote, D.S. (2007) Acclimation to drought stress generates oxidative stress tolerance in drought-resistant than susceptible wheat cultivar under field conditions. *Environ Exp Bot* **60**, 276–283.
5. Loggini, B., Scartazza, A., Brugnoli, E., and Navari-Izzo, F. (1999) Antioxidative defense system, pigment composition, and photosynthetic efficiency in two wheat cultivars subjected to drought. *Plant Physiol* **119**, 1091–1100.
6. Abebe, T., Guenzi, A.C., Martin, B., and Cushman, J.C. (2003) Tolerance of

mannitol-accumulating transgenic wheat to water stress and salinity. *Plant Physiol* **131**, 1748–1755.
7. Shen, B., Jensen, R.G., and Bohnert, H.J. (1997) Mannitol protects against oxidation by hydroxyl radicals. *Plant Physiol* **115**, 527–532.
8. Wang, F.-Z., Wang, Q.-B., Kwon, S.-Y., Kwak, S.-S., and Su, W.-A. (2005) Enhanced drought tolerance of transgenic rice plants expressing a pea manganese superoxide dismutase. *J Plant Physiol* **62**, 465.
9. Yoshimura, K., Yabuta, Y., Ishikawa, T., and Shigeoka, S. (2000) Expression of spinach ascorbate peroxidase isoenzymes in response to oxidative stresses. *Plant Physiol* **123**, 223–234.
10. Schaedle, M. and Bassham, J.A. (1977) Chloroplast glutathione reductase. *Plant Physiol* **59**, 1011–1012.
11. Beyer, W.F. and Fridovich, I. (1987) Assaying for superoxide dismutase activity: some large consequences of minor changes in conditions. *Anal Biochem* **161**, 559–566.
12. Giannopolitis, C.N. and Ries, S.K. (1977) Superoxide dismutases: I. Occurrence in higher plants. *Plant Physiol* **59**, 309–314.
13. Aebi, H. and Lester, P. (1984) Catalase in vitro. *Meth Enzymol*,121–126.
14. Nakano, Y. and Asada, K. (1981) Hydrogen peroxide is scavenged by ascorbate-specific peroxidase in spinach chloroplasts. *Plant Cell Physiol* **22**, 867–280.
15. Smith, I.K., Vierheller, T.L., and Thorne, C.A. (1988) Assay of glutathione reductase in crude tissue homogenates using 5,5′-dithiobis(2-nitrobenzoic acid). *Anal Biochem* **175**, 408–413.

Chapter 17

Affinity Purification and Determination of Enzymatic Activity of Recombinantly Expressed Aldehyde Dehydrogenases

Hans-Hubert Kirch and Horst Röhrig

Abstract

Aldehydes are highly reactive and ubiquitous molecules involved in numerous biochemical processes and physiological responses. Many biologically important aldehydes are metabolized by the superfamily of NAD(P)$^+$-dependent aldehyde dehydrogenases [aldehyde:NAD(P)$^+$ oxidoreductases, EC 1.2.1, ALDH]. Here we describe a straightforward protocol for purification of soluble recombinantly expressed ALDH enzyme based on metal affinity chromatography and the subsequent determination of enzymatic activity using aldehydic substrates, which is assayed spectrophotometrically at 340 nm by conversion of NAD(P)+ to NAD(P)H.

Key words: Aldehyde dehydrogenase (ALDH), enzymatic activity, immobilized metal affinity chromatography (IMAC), oxidoreductase, recombinant expression.

1. Introduction

Aldehydes are intermediate metabolites in a variety of fundamental biochemical pathways and are generated during the metabolism of amino acids, carbohydrates, lipids, biogenic amines, vitamins, and steroids (1, 2). Aldehydes can also be generated in response to a variety of environmental stresses such as salinity, desiccation, cold, and heat shock (3, 4). Due to their chemical reactivity, many aldehydes are highly toxic at physiological concentrations (5, 6). Aldehyde dehydrogenases (ALDHs) (EC 1.2.1.3 and EC 1.2.1.5) represent a protein superfamily of NAD(P)$^+$-dependent enzymes that oxidize a wide range of endogenous and exogenous aliphatic and aromatic aldehydes to the corresponding carboxylic acid (7, 8). Currently, 555 genes encoding ALDH proteins have been identified throughout all

R. Sunkar (ed.), *Plant Stress Tolerance*, Methods in Molecular Biology 639,
DOI 10.1007/978-1-60761-702-0_17,

taxa (9), with diverse biochemical properties (10, 11). A first and important major step in elucidating the physiological function of a certain ALDH is to verify its enzymatic activity. Usually it can be very difficult and time consuming to determine ALDH activity in vivo because of the high number of other oxidoreductases in a cell that would affect the specific measurement of ALDH activity. Thus, initial ALDH enzymatic activity is frequently analyzed using recombinantly expressed proteins and purified enzyme fractions. Several alternatives exist for recombinant protein expression and purification of the recombinantly expressed proteins in general (12) and soluble active NAD^+-dependent dehydrogenases like ALDH enzymes in particular (13–15). Expression of ALDH proteins as His-tag fusions in *Escherichia coli* and purification of soluble, active enzyme by metal affinity chromatography are relatively cheap and very powerful tools for the expression and single-step purification of recombinant proteins (16) and can easily be established in every molecular biology laboratory. Enzymatic activity of the purified fractions can then be determined with a simple assay protocol.

2. Materials

2.1. Bacterial Culture and Lysis

1. Luria–Bertani (LB) medium (Lennox) was purchased as a ready-to-use medium and contains 1% (w/v) tryptone, 0.5% (w/v) yeast extract, and 0.5% (w/v) NaCl at pH 7.0.
2. Kanamycin is dissolved as 50 mg/mL stock solution (Kan^{50}) in $H_2O_{deion.}$ and then added to the medium as required.
3. IPTG (isopropyl-β-D-thiogalactopyranoside) is prepared as 1 M stock solution in $H_2O_{deion.}$ and can be stored at −20°C.
4. Lysozyme (Sigma, St. Louis, MO) should be prepared freshly as 100 mg/mL stock solution in buffer A.

2.2. ALDH Affinity Purification

1. Buffer A: 50 mM HEPES/NaOH (pH 7.4), 300 mM NaCl, 5 mM imidazole, 10% (v/v) glycerol, 0.1% (v/v) Triton X-100, 1.5 mM β-mercaptoethanol (add fresh) (*see* **Note 1** and **2**).

   Buffer B: 50 mM HEPES/NaOH (pH 7.4), 300 mM NaCl, 20 mM imidazole, 10% (v/v) glycerol, 0.1% (v/v) Triton X-100, 1.5 mM β-mercaptoethanol (add fresh) (*see* **Note 1** and **2**).

   Buffer C: 50 mM HEPES/NaOH (pH 7.4), 300 mM NaCl, 250 mM imidazole, 10% (v/v) glycerol, 0.1% (v/v) Triton X-100, 1.5 mM β-mercaptoethanol (add fresh) (*see* **Notes 1** and **2**).

   Strip buffer (4×): 400 mM EDTA, 2 M NaCl, 80 mM Tris–HCl (pH 7.9).

2. Concentrated stabilization solution: 80% (v/v) glycerol, 1 mM NAD, 12 mM DTT; β-NAD (Roche, free acid) can be prepared as 25 mM stock solution in $H_2O_{deion.}$ and stored at −20°C. DTT should always be added freshly.
3. In order to determine the concentration of purified ALDH in the fractions, the quantitative Bradford protein assay (17) (reagent prepared by Bio-Rad) can be used with bovine serum albumin (BSA) as standard.

2.3. SDS-Polyacrylamide Gel Electrophoresis (SDS-PAGE) and Protein Detection

1. Acrylamide gel stock solutions: 1.5 M Tris–HCl (pH 8.8), 1 M Tris–HCl (pH 6.8), 10% (v/v) SDS, 10% (v/v) ammonium persulfate (APS), 30% acrylamide (containing 0.8% bisacrylamide), TEMED (*N*,*N*,*N*′,*N*′-tetramethylethylenediamine; Sigma, St. Louis, MO). Acrylamide is toxic when unpolymerized. So, gloves should be worn during preparation and handling of the gel solutions to minimize the risk of skin exposure.
2. Separating gel solution: 0.375 M Tris–HCl (pH 8.8), 10% acrylamide, 0.1% SDS.
3. Stacking gel solution: 0.125 M Tris–HCl (pH 6.8), 4% acrylamide, 0.1% SDS.
4. Laemmli (18) buffer (2×): 4% SDS, 20% glycerol, 100 mM Tris (pH 6.8), 0.2% bromophenol blue, 0.2 M DTT (added freshly before use).
5. Running buffer: 25 mM Tris, 192 mM glycine, 0.1% SDS (pH 8.3). pH should not be adjusted.
6. Fixation solution: 10% (v/v) acetic acid, 40% (v/v) methanol.
7. Dye stock solution (500 mL): ammonium sulfate (50 g), 85% phosphoric acid (6 mL), 5% (w/v) Coomassie blue G250 solution (10 mL), fill up to 500 mL with $H_2O_{deion.}$. Prepare the colloidal Coomassie stain by mixing four parts of dye stock solution with one part of methanol prior to use. The dye Coomassie blue G250 complexes with basic amino acids and has a detection range of 8–50 ng per protein band (19). The colloidal properties of Coomassie blue G250 prevent the dye from penetrating the gel, eliminating the requirement for long de-staining periods.

2.4. ALDH Enzyme Assay

1. Na pyrophosphate (0.2 M), adjust pH with phosphoric acid.
2. Aldehyde (1 M; most common saturated and unsaturated C-3 to C-12 aldehydes are commercially available from Sigma) in ethanol (*see* **Note 3**).
3. To prepare the substrate solution, add 20 mg β-NAD (Roche, free acid) to 10 mL of 0.2 M Na pyrophosphate

(of appropriate pH), and bring solution to 20 mL with sterile H_2O. Add 5 μL of 1 M aldehyde to 5 mL of this solution to achieve a 1 mM aldehyde solution. Dilute the 1 mM aldehyde solution with the substrate solution to achieve the desired final substrate concentrations.

3. Methods

The pET His-tag System was used herein, because it is an easy-to-use system for the cloning and expression of recombinant proteins in *E. coli*. Based on the T7 promoter-driven system originally developed by Studier and colleagues (20), the pET System has been used to express thousands of different proteins. In pET vectors, target genes are cloned under the control of strong bacteriophage T7 transcription and translation signals, and expression is induced by providing a source of T7 RNA polymerase in the host cell. Purification of soluble recombinant protein is performed by immobilized metal affinity chromatography (IMAC) using the chelating ligand nitrilotriacetic acid (NTA) as a matrix. If NTA is charged with Ni^{2+} ions, the matrix occupies only four of the six ligand-binding sites in the coordination sphere of the nickel ion, thus leaving two sites free to interact with the His-tag. Elution of His-tagged proteins from the Ni–NTA matrix can easily be done with imidazole. The imidazole ring is part of the structure of histidine and competes with the His-tag for binding to the Ni–NTA matrix.

3.1. Induction of E. coli Cultures Expressing a Recombinant ALDH

1. Inoculate 10 mL LB+Kan^{50} with a single colony from the plate.
2. Grow overnight at 37°C with vigorous shaking.
3. Inoculate 100 mL LB+Kan^{50} with 2–5 mL of overnight culture in 500-mL Erlenmeyer flasks.
4. Grow cells at 37°C until OD_{600} ~0.5–0.6.
5. Pre-incubate culture for 30 min at 24°C.
6. Induce with 0.1 mM IPTG for 3 h at 24°C with vigorous shaking (*see* **Note 4**).
7. Pellet cells by centrifugation (3,000×*g*, 4°C, 20 min) (*see* **Note 5**).

3.2. Immobilized Metal Affinity Chromatography (IMAC) of Recombinant ALDH

1. Re-thaw cells (if frozen) on ice and resuspend completely in 5 mL buffer A.
2. Add lysozyme (freshly prepared) to 1 mg/mL and incubate on ice for 30 min.

3. Sonificate cell suspension until solution gets translucent (6 × 20 s, microtip output setting 3).
4. Centrifuge for 30 min at 4°C at maximum speed (20,000×*g*).
5. Filter the supernatant (0.45 μm) to get rid of any insoluble cell debris. Remove an aliquot for electrophoresis (10 μL). This is the pre-column sample (F0).
6. Prepare pre-packed His-column (1 mL bed volume) for purification by washing the column with 3 bed vol. $H_2O_{deion.}$, followed by 5 bed vol. 1× charge buffer (50 mM $NiSO_4$) and 3 bed vol. buffer A.
7. Load clear cell lysate on the column (the flow-through can be re-loaded for a higher efficiency) and collect an aliquot of the final flow-through for electrophoresis (10 μL) after 2 mL of the sample have run through the column (sample FT). Wash the column with 10 bed vol. buffer A and 8 bed vol. buffer B.
8. Elute purified His-tag protein with buffer C (in twelve 250 μL fractions) into 1.5-mL reaction tubes already containing 250 μL of concentrated stabilization solution (*see* **Note 6**). Remove an aliquot (10 μL) of fractions F1–F8 for electrophoresis (*see* below)
9. The resulting enzyme solution is stable and can be frozen at −80°C.
10. Regenerate the column by washing with ≥3 bed vol. 1× strip buffer (4× = 400 mM EDTA, 2 M NaCl, 80 mM Tris–HCl, pH 7.9).
11. Wash the column by adding 5 bed vol. $H_2O_{deion.}$ followed by 5 bed vol. 20% ethanol.
12. Store the column at 4°C.
13. Measure the protein content (e.g., by using Bradford assay) and store the purified protein at −80°C (aliquoted in small amounts to avoid loss of activity due to repeated freeze and re-thawing cycles).
    (a) Mix the sample or the protein standard with H_2O in an Eppendorf tube.
    (b) Add 0.2 mL of Bradford dye reagent concentrate and vortex briefly.
    c) Measure the $OD_{595\ nm}$ after 5 min to 1 h versus reagent blank.
    d) Plot $OD_{595\ nm}$ versus concentration of standards and determine the unknown protein concentrations from the standard curve.

14. Check the purity of the eluted protein by loading a small amount of the purified fractions [F0, FT, and F1–F81 (10 μL each)] on an SDS-PAGE. **Figure 17.1** shows a typical purification pattern of a recombinantly expressed aldehyde dehydrogenase from the resurrection plant *Craterostigma plantagineum*. Please note that although the His-tag affinity purification is very specific, the purified fractions still can contain marginal contaminations from unspecifically binding proteins or other proteins containing consecutive His residues (*see* **Note 7**).

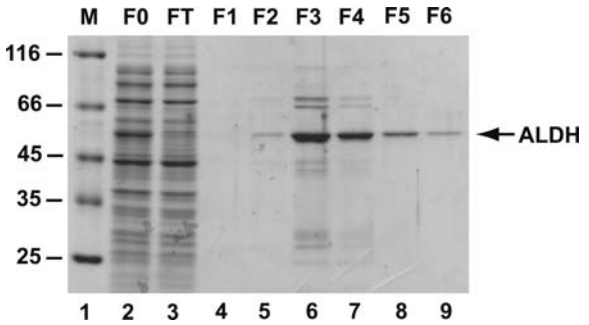

Fig. 17.1. Single-step purification of 6×His-CpALDH on a Ni^{2+}-charged His-Bind resin. Binding of proteins as well as washing and elution of matrix-bound proteins was performed as described in the text. Proteins in binding buffer before (F0) and after chromatography (FT) were analyzed together with the eluted fractions (F1–F6, please note that here 500 μL protein fractions were collected) by 12% SDS-PAGE and stained with Coomassie.

3.3. SDS-PAGE

1. These instructions assume the use of a Biometra gel system, but the method can easily be adapted to other formats. In this experiment a discontinuous 10% separating/4% stacking gel is used to monitor the purification of ALDH proteins.
2. Clean the gel plates, dry, and then join the plates together to form the cassette. Clamp the cassette in a vertical position.
3. Mix the components of the 10% gel (9 mL) in a 14-mL Sarstedt tube. Add 10% APS (90 μL) and TEMED (3.6 μL) as the last components and gently mix the solution. The addition of TEMED will initiate the polymerization reaction, so it is advisable to work quickly at this stage.
4. Pour the separating gel mixture carefully into the gel cassette until it reaches a position of 1.5 cm from the cutaway edge of the glass plate.
5. To ensure that the gel polymerizes with a smooth surface, very carefully pour H_2O from both edges into the cassette.

The H_2O will spread across the surface without adverse mixing. Leave the gel to set for at least 1 h.

6. When the separating gel has set, prepare the stacking gel solution (3 mL) without APS and TEMED.
7. Pour off the overlaying H_2O from the separating gel and carefully dry the gel surface with a piece of Whatman paper. Do not touch the gel surface.
8. Add 10% APS (30 μL) and TEMED (3 μL) to the stacking gel solution and carefully mix the solution.
9. Add the stacking gel solution to the gel cassette until the solution reaches the cutaway edge of the gel plate. Place the well-forming comb into this solution without introducing air bubbles and leave it to set. The refractive index change around the comb indicates that the gel has set.
10. After the gel has set, carefully remove the comb from the stacking gel and then rinse out any unpolymerized acrylamide solution from the wells using electrophoresis buffer. Remove the sealing belt of the gel cassette. Fill up the bottom reservoir with electrophoresis buffer and assemble the cassette in the electrophoresis chamber. Fill up the top and bottom reservoirs and remove any bubbles caught under the gel.
11. Proteins to be analyzed on an SDS-PAGE must first be boiled in sample buffer containing 0.2 M DTT and SDS. Mix samples F0, FT, and F1–F8 (10 μL each) with 10 μL of 2× Laemmli buffer. Heat all samples for 10 min at 95°C. Centrifuge for 5 min in an Eppendorf centrifuge (20,000×*g* at room temperature) to remove insoluble material. Samples can now be loaded onto the gel. Run the gel at 10 mA when the proteins move through the stacking gel and increase the current to 25 mA when the dye front enters the separating gel. Continue electrophoresis until bromophenol blue reaches the bottom of the separating gel.
12. After running the gel, dismantle the apparatus by opening the gel plates and discarding the stacking gel. Place the separating gel in fixation solution and gently agitate the gel on an orbital shaker for at least 1 h in a plastic dish. Remove the fixative and wash the gel three times with H_2O (10 min per wash). After the third wash, stain the gel overnight with the colloidal Coomassie (~100 mL per gel) by shaking with gentle agitation. Destain the gel with H_2O on the next day. As the H_2O colors, discard it and wash the gel with fresh H_2O until protein bands are at the desired contrast against the background of the gel.

3.4. ALDH Enzyme Assay

Enzymatic activity is assayed spectrophotometrically at 340 nm by conversion of NAD(P)+ to NAD(P)H at room temperature in 1 mL total volume. The assay buffer contains 100 mM sodium pyrophosphate at an optimal pH (*see* **Note 8**), 1.5 mM $NAD(P)^+$, and various concentrations of aldehyde substrate. The enzyme reaction is initiated by adding the purified protein. For calculations, the extinction coefficient for NAD(P)H = 6.22 cm^{-1} mM^{-1} is used.

1. Pipette 1 mL of the substrate solution into a quartz glass or disposable UV-plastic cuvette (Brand, Germany) and set the UV spectrophotometer at 340 nm to zero.
2. Initiate the reaction by adding the purified ALDH protein. After addition of the ALDH protein, directly seal the cuvette with parafilm, mix the sample, and reset the spectrophotometer to zero. Observe aldehyde metabolism continuously for at least 5 min at 340 nm. Take OD values after 0.5, 1, 2, 3, 4, and 5 min. Take care that the addition of a certain amount of protein results in a linear progression of the OD; if this is not the case, test different amounts of the enzyme.
3. Use different amounts of the substrate (e.g., 0.1, 0.2, 0.3, 0.4, 1 mM, or other concentrations of aldehyde) for the enzymatic reaction and keep all other parameters constant.

4. Notes

1. Do not autoclave solutions. Rather prepare with sterile $H_2O_{deion.}$ and filter sterilize (0.45 μm).
2. Usually sodium phosphate or phosphate–citrate buffers at a pH 7–8 are recommended as buffer system for the His-tag affinity purification, because buffers with secondary or tertiary amines (like Tris or HEPES) can reduce nickel ions. However, in our hands, the 50 mM HEPES/NaOH buffer at pH 7.4 worked well for purification, but the concentration should not exceed 100 mM. β-Mercaptoethanol is added at a low concentration to all purification buffers to prevent disulfide cross-linkages.

   A very nice description of the method and detailed troubleshooting guide for His-tag affinity purification can be found in the QIAexpressionist™ handbook for high-level expression and purification of 6×His-tagged proteins (http://www1.qiagen.com).
3. Aldehyde substrate solubility in aqueous solution decreases rapidly with increasing chain length. Thus, for mid- to long-chain aldehydes the highest soluble final concentration

in the assay buffer must be determined for each individual aldehyde, and the solution should stay clear even over longer time periods. It is also important that the substrate assay solution does not contain more than 1% ethanol. Pipetting of low volumes (1–20 μL) of concentrated, pure aldehyde solutions can be difficult due to the low viscosity. Thus, care should be taken to assure that the volume pipetted is as exact as possible. In addition, most aldehydes are toxic at high concentrations and generate a significant and intense smell in the laboratory. So gloves should be worn when diluting aldehyde substrates and stock solutions should be diluted only under an extractor hood. Finally, because the 1 M aldehyde stock solutions in ethanol are not stable over longer time periods, they always should be prepared freshly.

4. Because in our experience, recombinantly expressed ALDHs preferentially form inclusion bodies when expressed at high levels in bacteria under normal growth conditions, induction temperature of bacterial cultures and concentration of IPTG are critical to obtain high amounts of soluble protein for purification. Thus, induction should take place under reduced metabolic conditions and may have to be optimized for each individual protein. In most cases 3 h of induction is sufficient for high-yield protein expression, but optimal induction time may have to be optimized depending on the protein to be overexpressed.
5. Pelleted cells optionally can be frozen and stored at −20°C for several weeks without yield loss.
6. The enzyme is unstable in buffer C. Upon storage at −80°C and repeated thawing and re-freezing, more than 50% of activity is usually lost within a short time period. To avoid this, eluted protein in buffer C is adjusted to 45% glycerol, 0.5 mM NAD, and 6 mM DTT with concentrated stabilization solution. Dilution of the enzyme solution should be done only with stabilization buffer [25 mM HEPES/NaOH (pH 7.4), 150 mM NaCl, 45% (v/v) glycerol, 0.05% (v/v) Triton X-100, 0.5 mM NAD, 6 mM DTT].
7. Binding and wash buffers used in this protocol already contain low concentrations of imidazole and β-mercaptoethanol to minimize binding of contaminating proteins to the Ni–NTA matrix and to reduce disulfide bonding. Further increase in purity may be achieved by increasing the salt concentration or the concentration of non-ionic detergents. Furthermore, the imidazole concentration in buffer B may be increased up to 50 mM. Since this may lead to elution of the recombinant 6×His protein, the column effluent should be tested for the presence of the recombinant protein by SDS-PAGE analysis.

8. Most ALDHs have a pH optimum at basic pH between 8.5 and 9.5. Thus, for initial activity measurements, it is sufficient to use a pyrophosphate buffer at pH 9. However, for determination of enzymatic constants, the pH optimum of the purified enzyme should be verified experimentally. A pyrophosphate buffer can be used between pH 8 and 9.5. At a pH below 8, phosphate or Tris buffer systems may be used for activity measurements.

References

1. Vasiliou, V., Pappa, A., and Petersen, D. R. (2000) Role of aldehyde dehydrogenases in endogenous and xenobiotic metabolism. *Chem Biol Interact* **129**, 1–19.
2. O'Brien, P.J., Siraki, A.G., and Shangari, N. (2005) Aldehyde sources, metabolism, molecular toxicity mechanisms, and possible effects on human health. *Crit Rev Toxicol* **35**, 609–662.
3. Barclay, K.D. and McKersie, B.D. (1994) Peroxidation reactions in plant membranes effects of free fatty acids. *Lipids* **29**, 877–882.
4. Bartels, D. (2001) Targeting detoxification pathways: an efficient approach to obtain plants with multiple stress tolerance? *Trends Plant Sci* **6**, 284–286.
5. Lindahl, R. (1992) Aldehyde dehydrogenases and their role in carcinogenesis. *Crit Rev Biochem Mol Biol* **15**, 11–26.
6. Esterbauer, H., Schauer, R.J., and Zollner, H. (1991) Chemistry and biochemistry of 4-hydroxynonenal, malondialdehyde and related aldehydes. *Free Radic Biol Med* **11**, 81–128.
7. Vasiliou, V., Bairoch, A., Tipton, K.F., and Nebert, D.W. (1999) Eucaryotic aldehyde dehydrogenase (*ALDH*) genes: human polymorphisms, and recommended nomenclature based on divergent evolution and chromosomal mapping. *Pharmacogenetics* **9**, 421–434.
8. Perozich, J., Nicholas, H.B., Jr., Wang, B.-C., Lindahl, R., and Hempel, J. (1999) Relationships within the aldehyde dehydrogenase extended family. *Prot Sci* **8**, 137–146.
9. Sophos, N.A. and Vasiliou, V. (2003) Aldehyde dehydrogenase gene superfamily: the 2002 update. *Chem Biol Interact* **143–144**, 5–22.
10. Kirch, H.H., Bartels, D., Wei, Y., Schnable, P.S., and Wood, A.J. (2004) The *ALDH* gene superfamily of Arabidopsis. *Trends Plant Sci* **9**, 371–377.
11. Marchitti, S.A, Brocker, C., Stagos, D., and Vasiliou, V. (2008) Non-P450 aldehyde oxidizing enzymes: the aldehyde dehydrogenase superfamily. *Expert Opin Drug Metab Toxicol* **4**, 697–720.
12. Arnau, J., Lauritzen, C., Petersen, G.E., and Pedersen, J. (2006) Current strategies for the use of affinity tags and tag removal for the purification of recombinant proteins. *Protein Expr Purif* **48**, 1–13.
13. Rose, J.P., Hempel, J., Kuo, I., Lindahl, R., and Wang, B.C. (1990) Preliminary crystallographic analysis of rat class 3 ALDH. *Proteins* **8**, 305–308.
14. Hempel, J., Kuo, I., Perozich, J., Wang, B.C., Lindahl, R., and Nicholas, H. (2001) Aldehyde dehydrogenase: maintaining critical active site geometry at motif 8 in the class 3 enzyme. *Eur J Biochem* **268**, 722–726.
15. Pappa, A., Estey, T., Manzer, R., Brown, D., and Vasiliou, V. (2003) Human aldehyde dehydrogenase 3A1 (ALDH3A1): biochemical characterization and immunohistochemical localization in the cornea. *Biochem J* **376**, 615–623.
16. Van Dyke, M.W., Sirito, M., and Sawadogo, M. (1992) Single-step purification of bacterially expressed polypeptides containing an oligo-histidine domain. *Gene* **111**, 99–104.
17. Bradford, M.M. (1976) A rapid and sensitive method for the quantification of microgram quantities of protein utilizing the principle of protein–dye binding. *Anal Biochem* **72**, 248–254.
18. Laemmli, U.K. (1970) Cleavage of structural proteins during the assembly of the head of maize bacteriophage T4. *Nature* **227**, 680–685.
19. Neuhoff, V., Arold, N., Taube, N., and Ehrhardt, W. (1988) Improved staining of proteins in polyacrylamide gels including isoelectric focusing gels with clear background at nanogram sensitivity using Coomassie Brilliant Blue G-250 and R-250. *Electrophoresis* **9**, 255–262.
20. Studier, F.W., Rosenberg, A.H., Dunn, J.J., and Dubendorff, J.W. (1990) Use of T7 RNA polymerase to direct expression of cloned genes. *Meth Enzymol* **185**, 60–89.

Chapter 18

Determination and Detection of Reactive Oxygen Species (ROS), Lipid Peroxidation, and Electrolyte Leakage in Plants

Niranjani Jambunathan

Abstract

Reactive oxygen species or intermediates are formed by the incomplete reduction of oxygen. Organisms living in aerobic environment generate various kinds of reactive oxygen species (ROS) molecules, such as superoxide ($\bullet O_2^-$), hydrogen peroxide (H_2O_2), hydroxyl radical (OH^-), singlet oxygen, and lipid hydroperoxides. ROS are highly reactive molecules and are extremely unstable, so detection of ROS relies on measuring the end products that are formed when they react with particular substances. The end products can be measured by changes in their fluorescence, color, or luminescence. ROS causes lipid peroxidation wherein the lipids in the cell membranes are damaged. Lipid peroxidation is usually quantified using a colorimetric assay. When ROS concentrations reach a certain threshold, it activates a programmed cell death response in the cells. This is quantified by measuring the amount of ion leakage. ROS such as superoxide and hydrogen peroxide have been detected traditionally by staining techniques. Superoxide anion is detected with nitroblue tetrazolium (NBT) and hydrogen peroxide by Diaminobenzidine tetrahydrochloride (DAB) staining. In this chapter, methods for determining total ROS and lipid peroxidation assay, histochemical staining techniques for superoxide and H_2O_2 molecules are described.

Key words: DAB, DCFDA, ion leakage, lipid peroxidation, NBT, ROS, stress.

1. Introduction

One of the most commonly used dyes for determining total ROS is 2′, 7′-dichlorofluorescein (H_2DCF). Esterified H_2DCFs are permeable to cell membranes, thus can enter the cells freely. Inside the cells, they are deacetylated by intracellular esterases and are trapped. Non-fluorescent H_2DCF then gets oxidized by ROS molecules to highly fluorescent 2′, 7′-dichlorofluorescein (DCF). Depending on experimental material, the rate of DCF formation can be monitored by fluorometer, fluorescence microscopy. Several ROS detection probes are available from Molecular

R. Sunkar (ed.), *Plant Stress Tolerance*, Methods in Molecular Biology 639,
DOI 10.1007/978-1-60761-702-0_18,

Probes (Invitrogen) and BACHEM that are suitable for live cell imaging. DCFDA is popular way of determining total ROS in any system (1, 2).

Histochemical staining for superoxide anion in leaf tissue is based on the ability of cells to reduce NBT (3). NBT specifically reacts with superoxide and forms a purple/blue formazan precipitate (4). Hydrogen peroxide is usually detected in leaves of plants by using DAB as substrate. A marked brown polymerization product is formed by the reaction of DAB with hydrogen peroxide.

Lipid peroxidation is the process where ROS remove electrons from the lipids in the cell membranes thereby damaging the cells. This process occurs in three stages: initiation, propagation, and termination (5). During initiation phase, hydroxyl, alkoxyl, peroxyl radicals abstract the first hydrogen atom. Phospholipids containing polyunsaturated fatty acids are susceptible to peroxidation as they contain multiple double bonds and the methylene group that lies within is prone to abstraction of hydrogen atom. The initial reaction with polyunsaturated fatty acids produces a lipid radical. The lipid radical produced abstracts hydrogen from neighboring fatty acids to produce lipid hydroperoxide (LOOH) and a second lipid radical. The LOOH undergoes reductive cleavage by reducing metals and produces alkoxyl radical. Both alkoxyl and peroxyl radicals create a chain reaction by abstracting additional hydrogen atoms.

Thiobarbituric acid (TBARS) assay is the most widely used for determining lipid peroxidation (6). During the process of lipid peroxidation, the malondialdehyde (MDA) is formed by the decomposition of polyunsaturated fatty acids which reacts with thiobarbituric acid. This controlled reaction is quantified colorimetrically. In plants, a modified TBARS method has been adopted (7).

ROS is often considered as an important modulator of plant programmed cell death (PCD). Quantification of programmed cell death due to biotic or abiotic elicitors is commonly assayed by measuring ion leakage from the damaged cell. Depending on the type of treatment, the ion leakage experiment can be done with detached leaves or whole rosette (as in *Arabidopsis*).

2. Materials

2.1. Total ROS Estimation Using DCFDA

1. VersaFluor fluorometer (Bio-Rad, Hercules, CA).
2. 2′,7′-Dichlorofluorescein diacetate (*see* **Notes 1–3**).
3. 10 mM Tris–HCl, pH 7.2.
4. Parafilm.

5. DMSO.
6. Bradford reagent (used for protein quantification).
7. Refrigerated centrifuge.

2.2. Histochemical Staining Technique for ROS Detection

1. Vacuum infiltrator.
2. Nitroblue tetrazolium chloride (0.1% (w/v) NBT prepared in 10 mM sodium azide, 50 mM potassium phosphate, pH 6.4.
3. Diaminobenzidine tetrahydrochloride (1 mg/mL DAB solution, pH 3.8).
4. Ethanol.
5. Fixer solution (3:1:1 ethanol: lactic acid: glycerol).
6. Glass slide.
7. Cover slips.
8. Camera.

2.3. Lipid Peroxidation Assay

1. Spectrophotometer.
2. Thiobarbituric acid (0.5% TBA).
3. 0.1% TCA (20% stock solution).
4. Centrifuge.

2.4. Ion Leakage Assay to Quantify Cell Death

1. Conductivity meter (Model 2052 digital conductivity meter (VWR)).
2. Test tubes.
3. Autoclave.

3. Methods

3.1. Total ROS Estimation Using DCFDA

1. Before starting the experiment, turn on the fluorometer and set the instrument at medium gain.
2. Harvest control and treated tissue and grind nearly 100 mg of tissue in liquid nitrogen.
3. Place the ground tissue powder in pre-weighed 2 mL tube with 1 mL of 10 mM Tris–HCl, pH 7.2.
4. Centrifuge at 12,000×*g* for 20 min at 4°C.
5. Transfer the supernatant to a fresh 2 mL tube.
6. If supernatant is not clear, spin at 12,000×*g* for 10 min at 4°C to collect any debris.

7. Blank the instrument with 10 mM Tris–HCl, pH 7.2 (1 mL).
8. Take 100 μL of supernatant and dilute with 900 μL of 10 mM Tris–HCl, pH 7.2.
9. Arrange samples in an order (do not work with more than 10 samples at a time). Add 10 μL of 1 mM DCFDA (final concentration will be 10 μM) to the first sample, after 45 s or 1 min add 10 μL of DCFDA to the next sample. Continue this for the rest of the samples. As soon as you add DCFDA to the tube, vortex and incubate all your samples in dark for 10 min. Information on making and handling of DCFDA solution is provided in notes section (*see* **Notes 1–3**).
10. Control: Add 100 μL of plant extract + 900 μL of Tris–HCl, pH 7.2, invert and mix (use a parafilm), and read the values in fluorometer. The readings fluctuate initially but become stable in few seconds (you have to press print button at this point). This is the background fluorescence. Deduct this value from all your readings.
11. Measure the fluorescence values of samples treated with DCFDA. The readings fluctuate and are stable in few seconds (you have to press print at this point). This is the ROS fluorescence of your samples.
12. Maintain the same order of samples and take readings at 1 min interval.
13. Estimate protein concentration in all samples using Bradford reagent.
14. Express the ROS as relative fluorescence units/mg of protein extract.
15. To rule out doubts about H_2DCFDA not being completely specific to ROS follow instructions provided (*see* **Note 4**).

3.2. Histochemical Staining Technique for ROS Detection

3.2.1. Determination of Superoxide Anion Radicals by Histochemical Detection Technique (4)

1. Excise the leaves and immerse the leaves with abaxial side up in 100 mL of staining solution containing 0.1% (w/v) NBT, 10 mM sodium azide, 50 mM potassium phosphate, pH 6.4.
2. Vacuum infiltrate the leaves by building a vacuum (~100–150 mbar for 1 min). Release the vacuum gently and repeat the procedure 2–3 times until the leaves are completely infiltrated.
3. Incubate the leaves in 10 mL of staining solution (0.1% NBT) for 15 min.
4. Incubate the infiltrated leaves at ambient temperature under cool fluorescent light for 20 min.

5. Stop the reaction with 95% ethanol.
6. Remove the chlorophyll by series of ethanol washes. Add fresh ethanol every wash. The green chlorophyll comes out with every wash; continue until you see a clear leaf. Leaves can be also de-stained with 96% (v/v) ethanol under heating at 40°C.
7. Superoxide ions react with NBT and appear as blue stain. The stained leaves can be photographed.

3.2.2. H_2O_2 Detection by DAB Staining (8)

1. Immerse the detached leaves in staining solution containing 1 mg/mL DAB solution, pH 3.8 (*see* **Note 5**)
2. Vacuum infiltrate the leaves at nearly 100–150 mbar for 1 min. Release the vacuum gently and repeat the procedure 2–3 times until the leaves are completely infiltrated (*see* **Note 6**).
3. Incubate the leaves in plastic box for 5–6 h under high humidity conditions till brown precipitates are observed.
4. Chlorophyll can be removed by repeated washes with ethanol or leaves can be de-stained with 96% (v/v) ethanol under heating at 40°C.
5. Stained leaves can be fixed with solution of 3:1:1 ethanol: lactic acid: glycerol and photographed.

3.3. Lipid Peroxidation Assay

1. Homogenize nearly 200 mg of treated and control tissue in 4 mL of 0.1% TCA.
2. Centrifuge the extract at 10,000×*g* for 15 min.
3. Collect the supernatant, and mix 1 mL of supernatant with 2 mL of 20% TCA and 2 mL of 0.5% TBA.
4. Heat the mixture at 95°C for 30 min in a fume hood (*see* **Note 7**) and later cool on ice.
5. Read the absorbance of supernatant at 532 nm and 600 nm. A_{600} is the nonspecific absorbance and is subtracted from the values for A_{532}.
6. Calculate the concentration of MDA using Beer–Lambert's equation (extinction coefficient of MDA is 155 mM^{-1} cm^{-1}).

3.4. Ion Leakage Assay to Quantify Cell Death

1. Ion leakage occurs well before programmed cell death is visible. Hence several time points after initiation of the treatment can be considered for ion leakage quantification. Calibrate the conductivity meter based on manufacturer's instruction.
2. Cut out uniform leaf discs with a sharp cork borer from several plants. Transfer the leaf discs to a test tube containing

5 mL of distilled water. Similarly, leaf discs from control plants will be excised and transferred to a test tube containing 5 mL of distilled water.

3. Leave the tubes in a shaker for 4 h at room temperature.
4. Measure the conductivity in the solution by inserting the probe of the conductivity meter into the solution (*see* **Note 8**). This represents the ion leakage from the leaf discs (Reading1).
5. Autoclave the solution containing the leaf discs.
6. After the liquid cools down, measure the conductivity of the solution. This represents the total ions present in the leaf discs (Reading2).
7. Ion leakage is represented as the percentage of total ions released (Reading1/Reading2 × 100).
8. Compare the percentage of ion leakage between the treated and the control leaves.

4. Notes

1. DCFDA (MW: 487.3) stock solution: Make an original stock of 100 mM DCFDA in DMSO.
2. DCFDA is light sensitive. Cover the tubes containing the solution with aluminum foil to prevent light exposure.
3. Prepare a working stock of 1 mM DCFDA in DMSO. Work with the working stock at room temperature and protected from light.
4. H_2DCFDA has been indicated to be not completely specific for ROS. To rule out this doubt, it is a good idea to perform measurements on equal aliquots with catalase (300 Units/mL) added in one of them and subtracting the catalase insensitive background from experimental value.
5. A low pH of 3.8 is necessary for proper solubilization of DAB.
6. During vacuum infiltration, it is important to release the vacuum gently to enable better infiltration of leaves.
7. Boiling the mixture in fume hood helps in preventing the spread of bad odor.
8. Depending on the model of conductivity meter used, the volume of water used for assaying will vary.

References

1. Joo, J.H., Wang, S., Chen, J.G., Jones, A.M., and Fedoroff, N.V. (2005) Different signaling and cell death roles of heterotrimeric G protein (alpha) and ß subunits in the Arabidopsis Oxidative stress response to Ozone. *Plant Cell* **17**, 957–970.
2. Mahalingam, R., Jambunathan, N., Gunjan, S.K., Faustin, E., Weng, H., and Ayoubi, P. (2006) Analysis of oxidative signalling induced by ozone in Arabidopsis thaliana. *Plant Cell and Environ* **29**, 1357–1371.
3. Jabs, T., Dietrich, R.A., and Dangl, J.L. (1996) Initiation of runaway cell death in an Arabidopsis mutant by extracellular superoxide. *Science* **273**, 1853–1856.
4. Doke, N. (1983) Involvement of superoxide anion generation in the hypersensitive response of potato tuber tissues to infection with an incompatible race of *Phytopthora infestans* and to the hyphal wall components. *Physiol Plant Pathol* **23**, 345–357.
5. Catala, A. (2006) An overview of lipid peroxidation with emphasis in outer segments of photoreceptors and the chemiluminescence assay. *Int J Biochem Cell Biol 38*, 1482–1495.
6. Yagi, K. (1998) Simple assay for the level of total lipid peroxides in serum or plasma. *Methods Mol Biol* **108**, 101–106.
7. Dhindsa, R.S., Plumb-Dhindsa, P., and Thorpe, T.A. (1981) Leaf senescence: correlated with increased levels of membrane permeability and lipid peroxidation, and decreased levels of superoxide dismutase and catalase. *J Exp Bot* **32**, 93–101.
8. Thordal-Christensen, H., Zhang, Z.G., Wei, Y.D., and Collinge, D.B. (1997) Subcellular localization of H_2O_2 in plants. H_2O_2 accumulation in papillae and hypersensitive response during the barley-powdery mildew interaction. *Plant J* **11**, 1187–1194.

Part IV

Osmotic Adjustment and Ion Measurements

Chapter 19

Quantification of Water Stress-Induced Osmotic Adjustment and Proline Accumulation for *Arabidopsis thaliana* Molecular Genetic Studies

Paul E. Verslues

Abstract

For the genetic potential of model systems such as *Arabidopsis thaliana* to be most effectively used to understand drought resistance, reliable and rapid protocols are needed for laboratory study of phenotypes relevant to stress responses in the field. Osmotic adjustment, the amount of additional solutes accumulated by plants under water stress, is often measured in drought physiology studies and requires quantification of both relative water content and solute content (osmotic potential) of the plant tissue. Water stress also elicits high levels of proline accumulation. Protocols are presented here to measure both of these parameters in *Arabidopsis* seedlings that have been exposed to controlled water stress treatments using polyethylene glycol–agar plates. For the ninhydrin-based assay of proline, a protocol for performing the assay in 96-well format to increase sample throughput is presented.

Key words: *Arabidopsis*, drought, osmotic adjustment, osmoregulation, proline assay, polyethylene glycol, relative water content, water relations.

1. Introduction

The availability of water is a key determinant of crop yields and the distribution of plant species across different environments. Understanding the genetic and molecular basis of plant responses to water limitation depends upon accurate phenotypic analysis. For agronomists studying drought, the phenotype of ultimate interest is usually harvestable yield and for environmental biologists the ability of a plant species to establish itself in a harsh environment is often the key data.

R. Sunkar (ed.), *Plant Stress Tolerance*, Methods in Molecular Biology 639,
DOI 10.1007/978-1-60761-702-0_19,

For plant physiologists and molecular biologists interested in drought stress, the situation is both simpler and more complex. It is simpler in that we can break down plant stress response into a collection of discreet phenotypes, such as changes in gene expression or content of a specific hormone or solute, and study these changes in the controlled environment of the laboratory. It is perhaps more complex in that we must at some point determine how the detailed molecular mechanisms discovered in laboratory experiments fit into the context of overall stress resistance. At the same time, the use of genetics means that we often must examine a large number of lines to find the gene, polymorphism, or other factor that can ultimately give us new insight into stress resistance at the whole plant level. Thus, the speed and the convenience with which a particular trait can be analyzed are also considerations in designing molecular genetic studies of water stress.

Because of the many genetic and genomic resources available, these experiments are often done using the model plant *Arabidopsis thaliana*. However, working with *Arabidopsis* does impose some constraints on stress experiments, particularly because of its small size. Previously, some important considerations for laboratory stress experiments, particularly those involving *Arabidopsis*, have been discussed (1). This includes the need to know the water status (water potential) of the plant tissue or the growth media. Such measurements of water status allow the severity of the stress imposed to be precisely known so that experimental data can be interpreted and results accurately compared between different sets of experiments. Another key factor for *Arabidopsis* seedling experiments is to avoid adding sugars to the growth media. Addition of sugar alters abscisic acid responses as well as more generally altering metabolism in a manner that is unlikely to reflect the status of plants growing in dry environments where photosynthesis, and thus carbon supply, is limited because of stomatal closure. In addition, use of low molecular weight solutes such as mannitol to impose low water potential should be avoided as these solutes cause plasmolysis instead of cytorrhysis and are often taken up by the plant in longer term experiments. A system of using PEG-infused agar plates that avoided these problems and allowed *Arabidopsis* seedlings to be exposed to controlled severities of low water potential stress has been described (1, 2).

In *Arabidopsis* research, seed germination, root growth, expression of certain stress-regulated genes, and control of stomatal opening and closing have been the most common stress-related phenotypes examined. Understanding of these phenotypes has contributed greatly to our overall understanding of water stress responses. However, it is also important to note that there are other water stress responses which have been of keen interest to agronomists and physiologists but have been less studied in *Arabidopsis*. One of these is osmotic adjustment. Osmotic

adjustment is the active accumulation of solutes inside the plant cell to maintain a favorable osmotic gradient to minimize water loss or allow continued water uptake (3). Osmotic adjustment is a specific type of the more general phenomenon of osmoregulation which all cells must use to control their volume and/or turgor (4). Quantification of osmotic adjustment requires measurement of both solute content (osmotic potential) and water content of the plant tissue so that passive changes in solute concentration caused by volume changes (measured as the change in relative water content) can be accounted for (3). Another important water stress response is the accumulation of free proline. Proline can accumulate to osmotically significant concentrations, especially when one considers that it is largely confined to the relatively small volume of the cytoplasm (5, 6). Thus, proline accumulation can contribute to osmotic adjustment. However, proline accumulation and changes in proline metabolism are also likely to affect plant stress tolerance via additional, as yet unclear, mechanisms related to the metabolism of proline or protective effects of proline itself (7).

Measurement of osmotic adjustment and proline accumulation is not new. Osmotic adjustment has been extensively used by agronomists and plant physiologists in field studies (3, 8–10). However, osmotic adjustment has not been studied in *Arabidopsis*, despite the potential to use this model system to determine the molecular mechanisms controlling osmotic adjustment. Likewise, proline accumulation has been often described and is known to be highly regulated. However, its function in stress resistance remains unclear, making proline accumulation a promising basis for molecular genetic studies (2, 7). The contribution of this chapter is to bring together a robust and reproducible experimental system for low water potential treatment of *Arabidopsis* seedlings with methods for measuring osmotic adjustment and proline accumulation that have been optimized for use with *Arabidopsis*. In this way the genetic resources of *Arabidopsis* can be better deployed to understand these key water stress responses.

2. Materials

2.1. Osmotic Adjustment

1. Square Petri dishes (120 mm × 120 mm, 17 mm deep; Greinier Bio-One #688-102).
2. Nylon mesh.
3. PEG-8000 (Sigma P2139).
4. Single-well tray with same footprint as a 96-well plate (Nunc Omnitray or equivalent).

5. Cotton cloth cut to 96-well size.
6. Benchtop centrifuge capable of spinning microplates.
7. Ninety-six-well plate lids.
8. Sealable plastic boxes.
9. Instrument to measure osmotic potential: We currently use a Psypro system with C-52 sample chambers from Wescor (Logan, UT). A vapor pressure osmometer from Wescor would also be suitable as would other instruments capable of measuring osmotic potential (osmolality) of small sample volumes.

2.2. Proline Assay

1. Library tubes/racks (Labcon, Petaluma, CA).
2. Grinding beads (BioSpec, Bartlesville, OK).
3. Bead beater. We use a Retsch Mixer Mill MM301. Other bead beaters or grinding samples with microfuge pestles are alternatives.
4. Glass sample tubes (1.5 mL; Alltech, Deerfield, IL).
5. Heat-resistant 96-well holder for the glass tubes (in our case a custom-built aluminum holder is used).
6. Acidic ninhydrin solution: Dissolve 2.5 g ninhydrin (triketohydrindene hydrate; Sigma N4876) in 60 mL glacial acetic acid at ~70°C. Then add 40 mL of 6 M phosphoric acid.
7. Water bath capable of holding temperature of 95–100°C.
8. Clear sealing film (type used for PCR plates).
9. Plate+ glass-coated microplates (Sun-SRI, Rockwood, TN).
10. Optional: microplate stir apparatus (VP Scientific, San Diego, CA).
11. Microplate reader.

3. Methods

3.1. Osmotic Adjustment

The procedure for growing seedlings and imposing stress by transfer to PEG-infused plates is similar to previous descriptions (1) with a couple of exceptions. First, we get more consistent results when using media where the amount of external salts or other low molecular weight solutes is kept low. Typically this is one-quarter-strength MS media with 2 mM MES buffer. As for all of our experiments, no sugar of any kind is added to the media. Also, because a number of seedlings need to be grown while

avoiding clumping that would interfere with the assay, larger sized plates are used. These are then compatible with using standard microplate holders to spin the mesh and seedlings to remove adhering liquid which would interfere with obtaining accurate seedling weights.

The typical format for an experiment is to test two genotypes on six water potential treatments ranging from −0.2 to −2.0 MPa. For each genotype, four relative water content measurements (prepared using two PEG–agar plates) are performed for each water potential treatment. Thus, we typically do these experiments using sets of 24 plates. Seedlings are collected from the same PEG–agar plates for measurement of osmotic potential. The combined data are then used to calculate osmotic adjustment.

1. Cut mesh pieces (~12 cm × 5.5 cm) to cover one-half of the square plates (12 cm × 12 cm). Place mesh between pieces of foil to autoclave.
2. Prepare one-quarter MS, 2 mM MES media. For one set of 24 plates, 1 L of media containing 1.1 g of MS salts and 0.4 ml of MES (adjusted to pH 5.7 using KOH) and 15 g of agar will be needed . Autoclave media, foil wrapped mesh pieces and a separate bottle with a small quantity of 1% agar in water. Pour 24 agar plates and allow to cool.
3. After the agar plates have solidified, place two pieces of mesh side-by-side onto each plate (this will give two measurements per plate). Put a small volume (~100 μL) of hot 1% agar on the mesh and spread with a glass rod to stick the mesh to the plates.
4. Aliquot and sterilize an appropriate amount of seed. Approximately 100–150 seeds will be needed for each plate and typically 8 or 12 plates are prepared for each genotype being tested. After the seeds are sterilized, use a sterile toothpick or pipette to place seed on the plates. Take care that the seed is spread out well so that the seedlings grow mostly in a single layer and not in clumps (**Fig. 19.1a**). Use micropore tape to secure the plate lids.
5. Stratify at 4°C for 3 days and then transfer the plates to a growth chamber. Incubate plates vertically in a growth chamber (so that seedlings grow on top of the mesh) for 7 days. Typical growth conditions are 23°C with continuous light (80–100 $\mu mol/m^2/s$). Keep the humidity in the growth chamber as high as possible to minimize drying of the plates. In our case, we keep the plates inside a large plexiglass box inside of the growth chamber. To maintain high humidity, the box has a layer of water directly below the rack holding the agar plates.

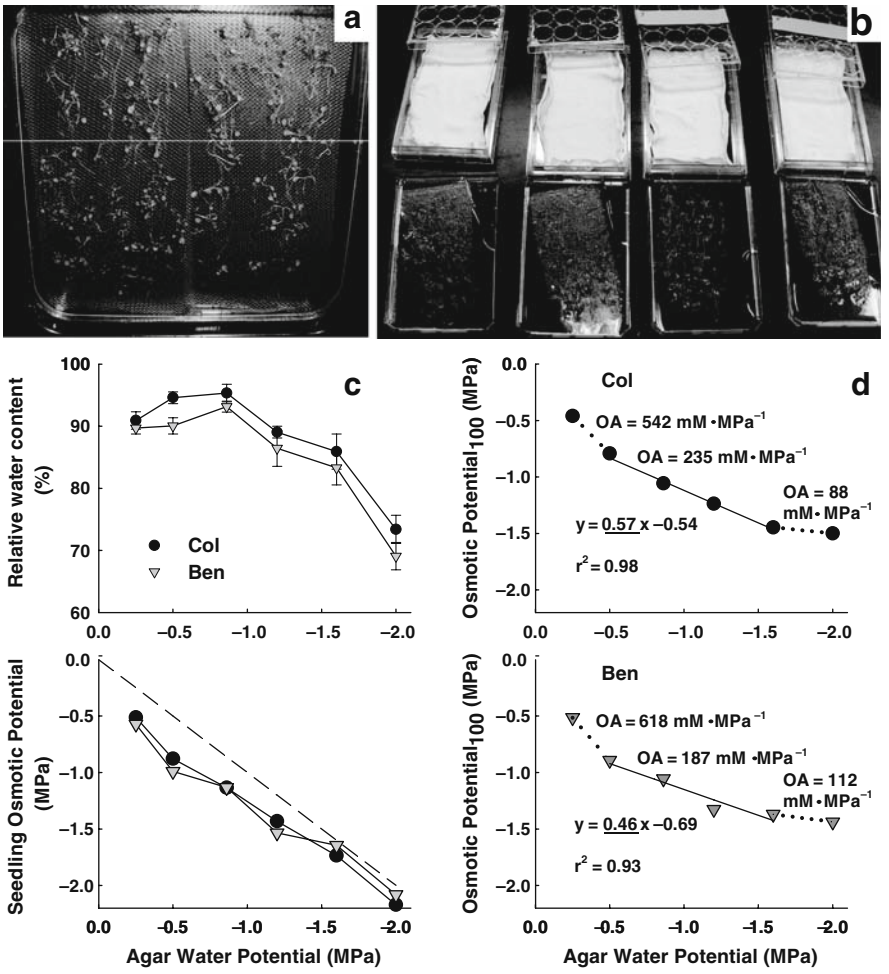

Fig. 19.1 Measurement of osmotic adjustment in *Arabidopsis* seedlings. **(a)** Seedlings growing on 12 cm × 12 cm square plate. Note the nylon mesh on the surface of the agar which allows the seedlings to be transferred from one plate to another and supports the seedlings during the RWC measurement. **(b)** Flat trays and lids used for processing samples for the RWC measurement. Mesh pieces and seedlings have just been spun to remove adhering liquid and the fresh weight recorded. The picture shows the mesh and seedlings being transferred to trays containing cold water for rehydration and subsequent measurement of the hydrated weight. **(c)** Relative water content (RWC) and osmotic potential data for Columbia (Col) and Bensheim (Ben) ecotypes. Seven-day-old seedlings were transferred to the indicated water potentials and data collected 3 days later. Data are combined from two independent experiments. RWC data are means ± S.E. ($n = 8$) and osmotic potential data are means of two. **(d)** Osmotic adjustment data for Col and Ben. For each ecotype, osmotic potential$_{100}$ and a regression line fit for the data from agar water potentials −0.5 to −1.6 MPa were calculated. Equations of the regression lines are shown and the underlined slope values indicate the osmotic adjustment (MPa · MPa^{-1}). These slope values were also converted to millimolar solute concentrations for both the middle water potentials and the highest water potentials (−0.2 to −0.5 MPa) and lowest water potentials (−1.6 to −2.0 MPa). OA, osmotic adjustment.

6. On the fifth or sixth day after transfer of plates to the growth chamber: Prepare PEG–agar plates. This essentially follows previously described procedures (1) except that the low solute media described above (one-quarter MS, 2 mM MES) is used. Because of the reduced amount of buffer in

Table 19.1
Preparation of PEG overlay solutions to use in preparing PEG–agar plates (for osmotic adjustment experiments) and mannitol solutions of equivalent water potentials

Water potential (MPa)	Starting volume of one-quarter MS, 2 mM MES media (ml)[a]	Amount of PEG to add (g)	pH adjustment[b]	Amount of mannitol (g) to make solution of equivalent water potential[c] (grams of mannitol per 250 ml water)
−0.25	N.A.[d]	N.A.	N.A.	4.6
−0.5	250	62.5	Two drops of 1 M KOH	9.1
−0.7	250	100	No pH adjustment needed	13.7
−1.2	200	110	Three drops of 1.5 M HCl	21.6
−1.6	150	105	Four drops of 1.5 M HCl	30.1
−2.0	150	120	Five drops of 1.5 M HCl	35.0

[a]The volumes shown indicate the *starting* volume of solution needed before adding the PEG. Significant volume expansion will occur when PEG is added. Do not adjust the final volume.
[b]These are working guidelines for our laboratory and should be checked by new users. Note that when measuring the pH of concentrated PEG solutions, extra time must be allowed for pH equilibration because of the high viscosity.
[c]These solutions are used to saturate the cloth squares that the mesh and seedlings are placed on after removal from the agar plates. Using these solutions ensures that excess liquid on the outside of the seedlings can be removed by centrifugation, while there is no water uptake or water loss from the seedlings.
[d]A PEG overlay solution is not needed for the −0.25-MPa treatment. The surface of these agar plates can instead be wetted with a small volume of water just before seedling transfer as this will make it easier to place the mesh and seedlings on the plate properly.

this media, the pH must be adjusted after adding the PEG. In a typical experiment, four plates of each water potential are prepared (*see* **Table 19.1** for amounts of PEG solution to prepare and pH adjustment).

To prepare PEG–agar plates:

a. Prepare 1 L of media with agar as described in **step 2** and adjust pH to 5.7. Prepare a second liter of media with the MS salts and MES buffer but without adding agar or adjusting the pH. Aliquot this media into 500-mL plastic beakers as shown in **Table 19.1**. Add a stir bar to each beaker.

b. Autoclave the media. From the autoclaved agar media, pipette 40 mL of media into each of 24 of the 12 × 12 square Petri dishes and allow to cool. Note that this must be done by pipetting instead of pouring as the

volume must be precisely controlled. For the autoclaved liquid media, add PEG-8000 to each beaker as shown in **Table 19.1**. Stir to dissolve the PEG (best done when media is still hot). After the media has cooled, adjust the pH following the guidelines in **Table 19.1** (*see* **Notes 1** and **2**).

c. Pipette 60 mL of PEG solution onto the solidified agar of each plate. Prepare four plates for each water potential treatment. Wrap the stacks of plates in plastic wrap and incubate for at least 12–24 h before use.

7. When seedlings have grown for 7 days, transfer them to the PEG–agar plates. Pour off part, but not all, of the PEG overlay solution from a PEG–agar plate; use forceps to lift the mesh and seedlings off their original plate; place mesh on the PEG plate and make sure that all parts of it are in contact with the PEG–agar, drain off the remaining PEG as completely as possible. Use micropore tape to secure the plate lids and place plates back into the growth chamber, again in the vertical position, for an additional 3 days.

8. Set up four (or eight) flat-bottom trays (the size of 96-well plates) by placing in each one 2 layers of cotton cloth squares moistened with mannitol solution of same water potential as the PEG–agar plate (*see* **Table 19.1**). This prevents the seedlings from being dehydrated or rehydrated while still allowing excess liquid on the outside of the seedlings to be absorbed into the cloth. Be sure to squeeze out the cloth well before placing in the tray so that there is no excess liquid.

9. Remove plates from the growth chamber and drain off any PEG solution that may have collected in the bottom of the plate (it is best to keep the plates vertical until the mesh/seedlings are removed). Collect seedlings for osmotic potential measurement by picking them off the plates with forceps and sealing them in a microfuge tube. Collect sufficient seedlings to yield 30–40 μL of cell sap (see below). Freeze these samples for later analysis.

   A sample of the PEG–agar can also be collected at this time to use for water potential measurement (*see* **Note 3**).

10. Remove mesh and remaining seedlings from the PEG–agar plate and place on top of the mannitol solution-moistened cloth (*see* **Fig. 19.1b**). Place lids on the trays and spin at 100–150×*g* for 1.5 min in a refrigerated benchtop centrifuge. In this and subsequent steps, minimize the amount of time the seedlings are uncovered.

11. Remove from centrifuge and weigh each mesh with seedlings (fresh weight) (*see* **Note 4**). Take care to

perform this measurement quickly so that the seedlings do not dry out.

12. Put mesh and seedlings in a 96-well plate lid and add enough cold water to cover the entire mesh and seedlings (**Fig. 19.1b**) and incubate for 8–12 h at 4°C.
13. Repeat steps 8–12 for each water potential treatment. Rewet the cloth pieces with the appropriate mannitol solution each time samples of a different water potential treatment are processed.
14. Prepare trays with moistened cloth again (this time the cloth is moistened with water since all the seedlings have been equilibrated with water, squeeze out excess liquid from the cloth after processing each round of seedlings).
15. Remove mesh and seedlings from water and place into tray on top of the cloth. Be sure to get all of the seedlings transferred as some may have come loose from the mesh.
16. Spin at 100–150×*g* for 1.5 min and reweigh the mesh and seedlings (hydrated weight).
17. Wrap mesh and seedlings in foil and dry overnight in a 60°C oven.
18. Weigh mesh and seedlings again (dry weight).
19. Calculate RWC using the following formula:
(Fresh weight–dry weight/hydrated weight–dry weight)
Note that the weight of the mesh is included in all of the measurements. *See* **Fig. 19.1c** for typical relative water content data.
20. Measure osmotic potential. Freeze and thaw the seedlings and grind with a microfuge pestle. Spin down the insoluble cell debris and measure the osmotic potential of the cell sap following the instructions for the instrument in use. See **Fig. 19.1c** for typical osmotic potential data. We typically collect one sample for osmotic potential measurement from each treatment but perform several replicate measurements of that sample to improve the accuracy of the data.
21. The RWC data are then combined with the osmotic potential to calculate the osmotic potential at full hydration (osmotic potential$_{100}$ = osmotic potential × RWC) and overall osmotic adjustment. Because a range of PEG concentrations were tested, the osmotic potential$_{100}$ can be used to generate a regression line. The slope of this line gives the amount of osmotic adjustment (in MPa · MPa^{-1}). The osmotic adjustment in megapascals can then be converted to solute concentration using the van't Hoff equation [$\psi_s = -RTC$, where ψ_s is the osmotic potential (MPa); R the gas constant (0.0083143 MPa L/mol/K];

T the absolute temperature (°C + 273); and *C* the molar solute concentration] (1, 11). Under ideal behavior, a 1 MPa decrease in osmotic potential is equivalent to an approximately 400 mM increase in solute concentration. While there may be deviation from ideal behavior in the concentrated solution inside the cell, this calculation nonetheless gives us a convenient method to compare the overall amount of solutes accumulated in osmotic adjustment to the measured concentrations of individual solutes (2).

Fig. 19.1 shows the osmotic adjustment calculation for two ecotypes of *Arabidopsis*: Columbia (Col) and Bensheim (Ben). These two *Arabidopsis* ecotypes are essentially identical in both their RWC and osmotic potential after exposure to a range of water potential treatments (**Fig. 19.1c**). Therefore, the calculated osmotic adjustment was also similar for both ecotypes. For both ecotypes, there was a linear relationship between osmotic potential$_{100}$ and agar water potential over the range of −0.5 to −1.6 MPa (**Fig. 19.1d**). The slopes of these regression lines indicated that Col and Ben differed by less than 10% in their osmotic adjustment. Both accumulated around 50% of the amount of solutes needed to fully compensate for the decreasing agar water potential (underlined values in **Fig. 19.1d**). Note that between the two highest water potentials tested (−0.2 and −0.5 MPa), both ecotypes exhibited a very high level of osmotic adjustment, more than enough to compensate for the decreased water potential. Consequently, both relative water content and, perhaps, turgor remained high or even increased. Conversely, between the two lowest water potentials (−1.6 and −2.0 MPa), there was a more dramatic decrease in relative water content (**Fig. 19.1c**), probably a loss of turgor, and a low level of osmotic adjustment (**Fig. 19.1d**), indicating that the seedlings were reaching the limit of their ability to adjust to the decreasing water potential. Note that although these experiments do not directly measure turgor, the difference between the water potential of the agar media and the osmotic potential of the seedlings indicates the possible magnitude of turgor in the seedlings. It must be taken with some caution however as it assumes water potential equilibrium between the seedlings and the agar media (which can be true as long as transpiration is minimal) and can be affected by even small changes in the water potential of the media. Overall, by using this type of analysis, it is possible to very precisely define the osmotic adjustment and osmoregulatory properties of *Arabidopsis* seedlings. This is useful in testing mutants and ecotypes hypothesized to differ in osmotic adjustment or other stress responses.

3.2. Proline Accumulation

The ninhydrin-based proline assay has been widely used following the procedure described by Bates et al. (12). Proline can be measured after transfer of seedlings to PEG–agar plates prepared as described above or as described previously (1). Salt and other stress treatments as well as exogenous ABA also induce proline accumulation (but at a lower level than the water stress treatments described here). These treatments can be investigated in a similar manner by transferring seedlings from control plates to treatment plates. Because fewer seedlings are needed for proline assay, the seeds are usually plated on small strips of mesh which makes moving the seedlings between plates convenient while still allowing samples to be collected easily. The protocol presented here describes how to process proline samples in 96-well format for improved convenience and throughput of the assay.

1. Prepare a rack of library tubes for sample collection by adding 2–3 grinding balls into each tube that will be used for sample collection (leave the first row empty as this will be needed for the standard curve later).
2. Remove seedlings (20–100 mg depending on the expected proline content) from plate, blot lightly if any liquid is adhering, and record the fresh weight. Transfer into an appropriate tube of the 96-well plate and freeze on liquid nitrogen or dry ice.
3. Extract the samples by adding 400–500 μL of water to each tube. Grind samples using a bead beater.
4. Spin down the samples using a benchtop centrifuge (1,000×*g* or greater for more than 5 min). Transfer an aliquot (10–100 μL, depending on the expected proline concentration) of each sample to a glass tube in the aluminum sample block (*see* **Fig. 19.2a**). If more than one replicate is to be assayed for each sample, set up more than one of the aluminum sample blocks. Add water to bring the total volume in each tube to 100 μL.
5. Set up blank tubes and standard curve from 0.012 to 0.10 μmol of proline (five points assayed in duplicate) in the first row of the 96-well block. Typically this is done using varying amounts of a 1 mM proline stock solution.
6. Move the sample block/tubes into a fume hood and add 200 μL of glacial acetic acid followed by 200 μL of acidic ninhydrin solution to each tube. Cover the tubes with an adhesive sealing film (the type usually used for PCR plates).
7. Incubate in a 95–100°C water bath for 1 h (*see* **Note 5**).
8. After the tubes have cooled, add 500 μL of toluene to each using a dispenser bottle (*see* **Note 6**). Mix the two phases either by pipetting up and down or using a microplate

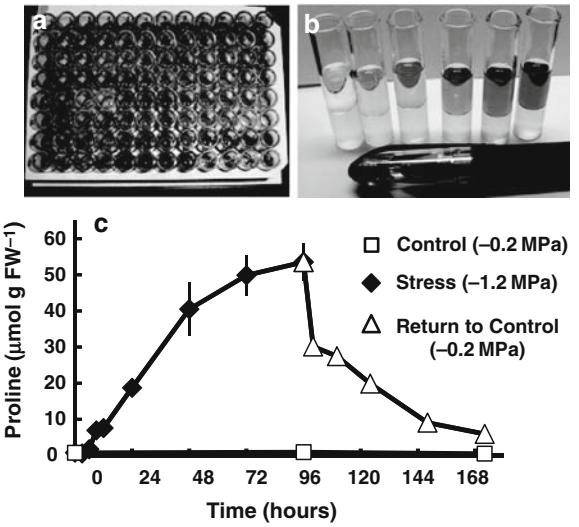

Fig. 19.2. Ninhydrin-based assay of proline in 96-well format. **(a)** A plate of proline samples in a custom-built aluminum sample block and glass tubes shown here after the incubation at 95–100°C that completes the reaction of ninhydrin with proline. **(b)** Proline standard curve after addition of toluene, mixing and phase separation (from left to right: 0, 0.0125, 0.025, 0.050, 0.075, and 0.1 micromolar proline per tube). A pen is shown for scale. **(c)** Representative proline data for *Arabidopsis* (ecotype Columbia). Seven-day-old seedlings were transferred from −0.2 to −1.2 MPa at time 0 and then transferred back to −0.2 MPa at 96 h. Data are means ± SE ($n = 3$). Note that the control level of proline is 0.7 μmol/ g FW. Thus transfer of seedlings to −1.2 MPa caused a greater than 70-fold increase in proline content over the course of 96 h.

stir apparatus. The red color should partition into the top (toluene) phase (**Fig. 19.2b**).

9. Transfer 200 μL of the top (toluene) phase to the corresponding well in a glass-coated microplate. Filter tips can be used to protect the pipettor. It is essential that this transfer be performed without disturbing the interface between the aqueous and toluene phases. A cloudy appearance of the samples after transfer means that the aqueous/toluene interface has been disturbed and the absorbance readings will be erroneously high.
10. Cover the microplate with clear sealing film (to protect both experimenter and plate reader from toluene). Read A_{515} promptly using a plate reader. After the data are recorded, the assay tubes and microplate can be cleaned and reused by rinsing thoroughly with 95% ethanol.
11. Use the standard curve and sample weights to calculate the amount of proline in each sample.

    Typical proline data for experiments where 7-day-old seedlings are transferred from control plates to −1.2 MPa PEG–agar plates for 96 h followed by transfer back to

control conditions is shown in **Fig. 19.2c**. Proline accumulates steadily after transfer to −1.2 MPa and reaches a near maximal level by 96 h. One of the advantages of the PEG–agar plate system is that the water potential is constant over time, thus allowing both the initial response to stress and longer term, more steady state, responses to be studied. After transfer back to −0.2 MPa, proline decreases gradually back to the control level. The seedlings are fully viable and resume growth after transfer back to −0.2 MPa; thus the decrease in proline seen is because of its controlled catabolism. Thus, another advantage of the PEG–agar plate system is the ability to study both dehydration and rehydration responses in a controlled manner.

4. Notes

1. PEG–agar plates must be allowed to equilibrate for more than 12 h before use. Thus, these plates must be prepared on the fifth or sixth day after transfer of the seeds to the growth chamber in step 5. It is not recommended to prepare PEG–agar plates more than 48 h in advance because even slight drying of the plates can change the water potential significantly and lead to inconsistent data.
2. PEG should not be autoclaved. Autoclaving changes the PEG and causes the water potential of the solution to change (13). Even though the PEG solutions may not be completely sterile after the PEG is added, we have little or no problem with contamination as long as plate preparation and seedling transfer is done inside a laminar flow hood. It should also be noted that PEG does not behave as an ideal solute, thus water potentials of PEG solutions cannot be calculated from the van't Hoff equation but must instead be determined empirically.
3. In osmotic adjustment experiments it is advisable to collect samples of the agar at the end of the experiment to check that no drying of the media or other problem has occurred to cause the water potential of the plate to deviate from the expected value. We find that as long as the PEG–agar plates are used promptly after they are prepared and are handled in a consistent manner, there is little deviation in the water potential (within ± 0.1 MPa of the values shown in **Table 19.1**). Thus, the check of agar water potential can be omitted for routine experiments once the experimental system is well established.

4. We find that after collecting the fresh weight data, allowing the seedlings to rehydrate for longer than 12 h leads to inconsistent data, while less than 6 h may not be enough to fully rehydrate seedlings exposed to the more severe stress treatments. Timing of the experiments should be planned accordingly.
5. The proline assay tubes must stay sealed during the heating step to avoid having water condense inside the tubes.
6. Toluene is volatile and toxic and all procedures using toluene should be done under a fume hood or in a closed container. Toluene also attacks most plastics, which necessitates the use of glass tubes and glass-coated microplates for all steps involving toluene.

Acknowledgments

I thank Dr. Sandeep Sharma and Nagaraj Kumar for comments on the procedures and Shu-ya Chiang and Wei-ju Chen for assistance in the laboratory. Work in the Verslues laboratory is supported by Academia Sinica and the National Science Council of Taiwan.

References

1. Verslues, P.E., Agarwal, M., Katiyar-Agarwal, S., Zhu, J.H., and Zhu, J.K. (2006) Methods and concepts in quantifying resistance to drought, salt and freezing, abiotic stresses that affect plant water status. *Plant J* **45**, 523–539.
2. Verslues, P.E. and Bray, E.A. (2004) LWR1 and LWR2 are required for osmoregulation and osmotic adjustment in *Arabidopsis*. *Plant Physiol* **136**, 2831–2842.
3. Zhang, J., Nguyen, H.T., and Blum, A. (1999) Genetic analysis of osmotic adjustment in crop plants. *J Exp Bot* **50**, 292–302.
4. Wood, J.M. (1999) Osmosensing by bacteria: signals and membrane-based sensors. *Microbiol Mol Biol Rev* **63**, 230–262.
5. Leigh, R.A., Ahmad, N., and Wyn Jones, R.G. (1981) Assessment of glycine betaine and proline compartmentation by analysis of isolated beet vacuoles. *Planta* **153**, 34–41.
6. Voetberg, G.S. and Sharp, R.E. (1991) Growth of the maize primary root at low water potentials. III. Role of increased proline deposition in osmotic adjustment. *Plant Physiol* **96**, 1125–1130.
7. Hare, P.D., Cress, W.A., and van Staden, J. (1999) Proline synthesis and degradation: a model system for elucidating stress-related signal transduction. *J Exp Bot* **50**, 413–434.
8. Lilley, J.M., Ludlow, M.M., McCouch, S.R., and Otoole, J.C. (1996) Locating QTL for osmotic adjustment and dehydration tolerance in rice. *J Exp Bot* **47**, 1427–1436.
9. Robin, S., Pathan, M.S., Courtois, B., Lafitte, R., Carandang, S., Lanceras, S., Amante, M., Nguyen, H.T., and Li, Z. (2003) Mapping osmotic adjustment in an advanced back-cross inbred population of rice. *Theor Appl Genet* **107**, 1288–1296.
10. Teulat, B., This, D., Khairallah, M., Borries, C., Ragot, C., Sourdille, P., Leroy, P., Monneveux, P., and Charrier, A. (1998) Several QTLs involved in osmotic adjustment trait variation in barley (*Hordeum vulgare* L.). *Theor Appl Genet* **96**, 688–698.

11. Taiz, L. and Zeiger, E. (1991) *Plant Physiology*. Redwood City, CA: Benjamin Cummings Publishing Company.
12. Bates, L.S., Waldren, R.P., and Teare, I.D. (1973) Rapid determination of free proline in water-stress studies. *Plant Soil* **39**, 205–207.
13. van der Weele, C.M., Spollen, W.G., Sharp, R.E., and Baskin, T.I. (2000) Growth of *Arabidopsis thaliana* seedlings under water deficit studied by control of water potential in nutrient-agar media. *J Exp Bot* **51**, 1555–1562.

Chapter 20

Methods for Determination of Proline in Plants

Edit Ábrahám, Cecile Hourton-Cabassa, László Erdei, and László Szabados

Abstract

Accumulation of proline in higher plants is an indication of disturbed physiological condition, triggered by biotic or abiotic stress condition. Free proline content can increase upon exposure of plants to drought, salinity, cold, heavy metals, or certain pathogens. Determination of free proline levels is a useful assay to monitor physiological status and to assess stress tolerance of higher plants. Here we describe three methods suitable for determination of free proline content. The isatin paper assay is simple and is suitable to assay proline content in large number of samples. The colorimetric measurement is quantitative and provides reliable data about proline content. The HPLC-based amino acid analysis can be employed when concentration of all amino acids has to be compared.

Key words: Amino acid profile, colorimetric assay, HPLC, isatin, ninhydrin, proline.

1. Introduction

Proline accumulation has been first observed in wilting perennial ryegrass (1) and was later found to be one of the common physiological responses of higher plants when they are exposed to a number of environmental stresses (2–5). Proline accumulation has been reported in plants exposed to high salinity (6–8), drought (9, 10) water stress (11), heavy metals (12, 13), cold (14, 15), hypoxia (16, 17), UV irradiation (18), and pathogen infection (19, 20).

Proline has been proposed to act as an important compatible osmolyte and osmoprotective compound, acting as molecular chaperone in osmotic adjustment and protection of cellular structures, proteins, and membranes during osmotic stress. Proline can protect proteins by stabilizing their structures and

R. Sunkar (ed.), *Plant Stress Tolerance*, Methods in Molecular Biology 639,
DOI 10.1007/978-1-60761-702-0_20,

preventing aggregation during refolding (21, 22). Proline was shown to alleviate inhibition of different enzymes by heavy metals (23). Proline is considered as a scavenger of reactive oxygen species (ROS) able to reduce the damage of oxidative stress induced by drought, high salinity, heavy metals, or UV irradiation (18, 24–26). *p5cs1* mutants are deficient in stress-induced proline accumulation and has higher ROS accumulation, enhanced oxidative damage, and reduced activity of enzymes of the ascorbate–glutathione detoxification cycle during salt stress, suggesting that proline is important to protect plant cells against oxidative damage by stabilizing key cellular detoxification mechanisms (27) Enhanced proline biosynthesis was suggested to stabilize redox potential and $NAD(P)^+/NAD(P)H$ ratios during stress conditions (28).

In higher plants, proline is synthesized from glutamate and ornithine but the levels of free proline are also controlled catabolically. Proline biosynthesis through the glutamate pathway is catalyzed by a bifunctional delta-1-pyrroline-5-carboxylate synthetase (P5CS) enzyme that yields pyrroline-5-carboxylate (P5C) from glutamate in a two-step reaction (29). The intermediate product P5C is further reduced to proline by the 1-pyrroline-5-carboxylate reductase (P5CR) enzyme (30, 31). Activity of P5CS represents a rate-limiting step of proline biosynthesis and is controlled at the level of P5CS transcription and through feedback inhibition of P5CS by proline (32–34). Recent data suggest that difference in intracellular compartmentalization of the P5CS1 and P5CS2 isozymes in *Arabidopsis* can be important in the control of proline biosynthesis (27). In the catabolic pathway, proline is oxidized to glutamate through two steps in the mitochondria. The first and rate-limiting reaction of proline catabolism is catalyzed by proline dehydrogenase (PDH) that converts proline to P5C (35, 36). Subsequently, P5C is oxidized to glutamate by P5C-dehydrogenase (P5CDH) (37, 38). Reciprocal regulation of *P5CS* and *PDH* genes plays a key role in the control of proline levels during and after osmotic stress (35, 36, 39).

Proline levels can be engineered by modulating either the biosynthetic or the catabolic pathways in transgenic plants or mutants. Increasing the rate of proline biosynthesis or blocking proline oxidation can lead to proline accumulation, while suppression of proline biosynthesis results in proline deficiency. As P5CS is the rate-limiting step in proline accumulation, while PDH controls proline degradation, these enzymes (or their coding genes) were the most common targets of modifications. Overexpression of the *Vigna P5CS* gene under the control of the *CaMV35S* promoter leads to 10–18 times increase in proline levels (40). Overexpression of the feedback-insensitive mutant of the *Vigna P5CS* enzyme (P5CSF129A) leads to a further twofold increase in proline levels (25). Enhanced proline levels lead to increased salt

tolerance and reduction of oxidative damage. Overexpression of *P5CS* genes was used to enhance proline accumulation in other species such as *Petunia hybrida* (10) and *Medicago truncatula* (41). Antisense expression of proline dehydrogenase in transgenic *Arabidopsis* suppressed proline degradation, leading to proline accumulation and improved salt and cold tolerance (42). On the other hand, antisense expression of the *Arabidopsis P5CS1* gene leads to reduced proline levels which lead to hypersensitivity to osmotic stress and developmental defects (43). Inhibition of proline accumulation was achieved in *Arabidopsis* mutants, where T-DNA insertions inactivated the *P5CS* genes (27). Reduction of free proline levels could be achieved by antisense expression of the *P5CR* gene in transgenic soybean plants, which leads to drought and heat stress hypersensitivity (44).

Although numerous published results confirm the beneficial effect of proline accumulation in protecting plants during diverse stress conditions, it is also apparent that proline accumulation does not represent an exclusive condition for stress tolerance. The capacity to accumulate proline was not correlated with salt tolerance in different barley varieties (45). *Arabidopsis* mutants, characterized by high proline accumulation, may have enhanced cold and drought tolerance (46) or can be hypersensitive to salt stress (47). Under certain conditions, proline is even toxic to plants. In proline dehydrogenase (*pdh*) mutants and transgenic plants expressing antisense *PDH* cDNA constructs, impaired proline degradation resulted in severe toxicity (48, 49). Therefore, it is still an open question as to how proline accumulation influences particular regulatory pathways in complex stress responses (50, 51). Nevertheless, it is noteworthy that free proline levels are higher in halophyte species such as *Thellungiella halophila* than in closely related glycophyte species (52–55). These results indicate that high proline accumulation in halophytes can contribute to adaptation to saline environment.

Data on proline accumulation can therefore provide valuable information on the physiological status of the plants. Determination of free proline levels can be a very useful assay to monitor physiological status and/or stress tolerance of higher plants. Here we describe three procedures, each with different complexity, to determine free proline levels. The isatin paper assay is a simple method and is suitable for testing proline content in large number of samples. The colorimetric measurement is the standard quantitative method which provides reliable data about proline content. The HPLC-based amino acid analysis is used when concentration of all amino acids has to be compared.

1.1. Proline Determination with Isatin Paper Assay

Isatin (1H-indole-2,3-dione) was employed as a visualizing agent giving different colors with amino acids in thin-layer and paper chromatography (56). Boctor (57) demonstrated that the

reaction between isatin and proline is suitable to quantitatively determine the amount of proline in a protein hydrolysate and biological fluids. Isatin is a highly specific color reagent for the proline, forming a blue derivative, pyrrole blue. Intensity of the blue color correlates with proline concentration. The characteristic blue coloration can therefore be used for rapid determination of free proline in biological samples. Other amino acids present in biological samples usually do not interfere with the result of free proline quantitation. This method is simple, fast, and is suitable to estimate proline content in large number of samples (**Fig. 20.1**). Although not frequently used, utility of proline determination with isatin has been demonstrated in several papers (57–60).

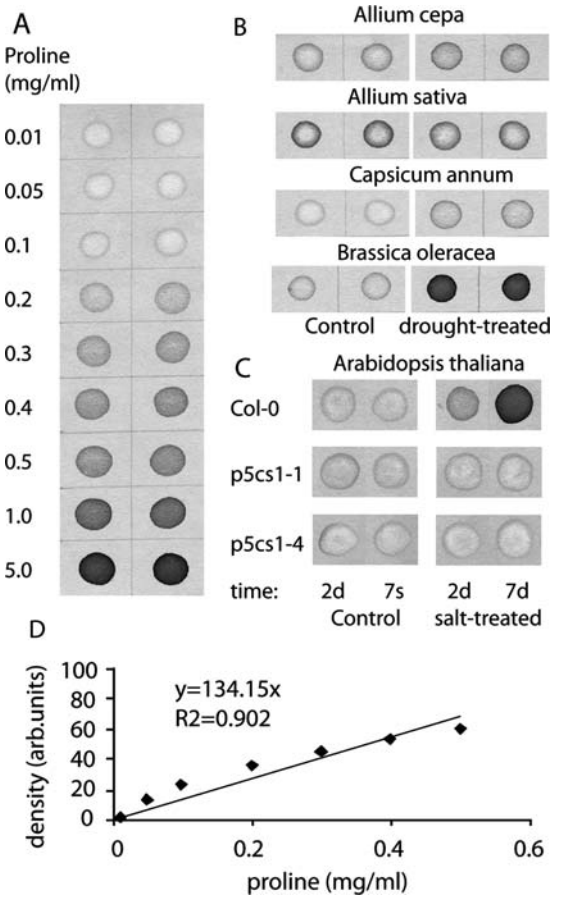

Fig. 20.1. Determination of proline levels with the isatin method. **(a)** Isatin color reaction series with 0–5 mg/mL proline standard solutions. **(b)** Testing proline content in different plant species subjected to 7-week drought. **(c)** Proline accumulation in wild-type and *p5cs1* mutant *Arabidopsis* plants treated with saline solutions (0.2 M for 2 or 7 days). **(d)** Calibration curve for semiquantitative analysis of proline content.

1.2. Proline Determination with Colorimetric Assay

Proline content of plant tissues can be determined by several methods. In 1952, Chinard (61) published that at acidic pH, ninhydrin can form a red product with proline and ornithine which can be used for the estimation of the concentration of these amino acids in pure solution. The ninhydrin-based colorimetric assay has been improved by Bates (62) more than 30 years ago and became the standard method for many laboratories to determine proline content. This assay is simple, reliable, is quantitative, does not need sophisticated instrumentation or expensive reagents, and has been tested for numerous plants. The original method have been modified and downscaled in order to handle higher number of samples and to use the standard equipment of molecular biology and biochemistry laboratories (**Fig. 20.2**).

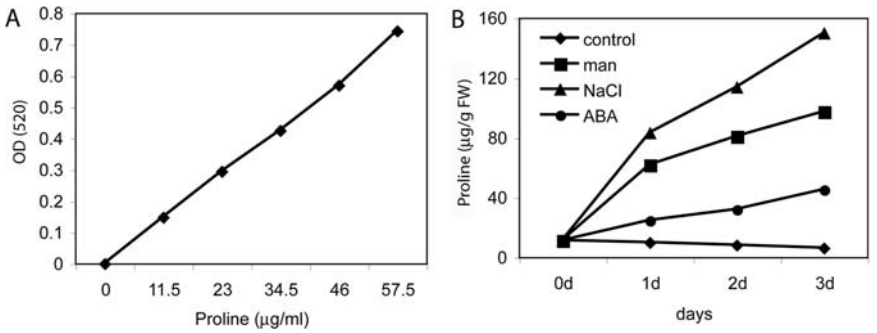

Fig. 20.2. Determination of proline content by acid ninhydrin method. **(a)** Calibration curve of the standard proline solutions. **(b)** Proline accumulation in 2-week-old wild-type *Arabidopsis* Col-0 seedlings treated with 100 mM NaCl, 200 mM mannitol, or 10 µM ABA.

1.3. Amino Acid Determination with HPLC

The amino acid content of biological samples can be determined by reverse-phase, high-performance liquid chromatography (HPLC) combined with detection by UV and/or fluorescent and/or mass spectroscopy. Here, we describe a protocol, modified from Noctor and co-workers (63), used for fluorescent detection when amino acids are derivatized with *o*-phthalaldehyde (OPA) in the presence of mercaptoethanol, a mixture that reacts with primary amines to form highly fluorescent products (64). The HPLC method is more sensitive for detecting a large range of amino acids than are methods using fluorescamine and ninhydrin (65). This method is suitable for the detection of imino acids such as proline and hydroxyproline. In that case, chloramine-T and sodium borohydride should be added to samples in order to produce proline and hydroxyproline derivatives that can react with OPA reagent (66). This method is useful to compare all amino acid content but needs quite sophisticated instrumentation.

2. Materials

2.1. Proline Determination with Isatin Paper Assay

1. Isatin solution: 1 g isatin dissolved in 100 mL methanol, 2.5 mL glacial acetic acid. Use freshly prepared solution.
2. Chromatography paper or Whatman 3MM filter paper.
3. Isatin paper: Impregnate chromatography paper or Whatman 3MM filter paper with the isatin solution. Air dry the impregnated papers on air for 1 h. Papers can be stored in dark for a few weeks.
4. Ethanol solution (20%).
5. L-Proline: prepare standard proline solutions of different concentrations (0–5 mg/mL).
6. Microcentrifuge.
7. Oven heated to 90°C.
8. Scanner or digital camera (optional).

2.2. Proline Determination with Colorimetric Assay

1. Sulfosalicylic acid (3%): Dissolve 3 g 5-sulfosalicylic acid (2-hydroxy-5-sulfobenzoic acid) in 80 mL distilled water and make up to 100 mL. Solution can be stored at room temperature for weeks.
2. Acidic ninhydrin: 1.25 g ninhydrin (1,2,3-indantrione monohydrate), 30 mL glacial acetic acid, 20 mL of 6 M orthophosphoric acid, dissolve by vortexing and gentle warming. Solution can be stored at 4°C for up to 1 week.
3. Phosphoric acid solution (aqueous solution of 85% orthophosphoric acid).
4. Glacial acetic acid.
5. Toluene.
6. L-Proline.
7. Microcentrifuge.
8. Spectrophotometer.
9. Quartz cuvettes.

2.3. Amino Acid Determination with HPLC

1. Cold 100% ethanol.
2. α-Aminobutyrate (120 μM, dissolved in distilled water).
3. Column: C18-Gemini 5μ 110A-250 × 4.
4. HPLC: Beckman Coulter.
5. Analysis software: 32 K Software (System Gold HPLC).

3. Methods

3.1. Proline Determination with Isatin Paper Assay

1. Harvest the samples, measure their fresh weight, and use approximately 100 mg for a reaction. Alternatively snap freeze the samples in liquid nitrogen. When necessary, samples can be stored at −80°C (*see* **Note 1**).
2. Add 20% ethanol (10 μL/mg fresh weight) and grind the plant material.
3. Centrifuge samples for 5 min at room temperature using benchtop centrifuge with maximum speed (14,000×*g*).
4. Drop 10 μL solution to the isatin paper, dry the paper for 30 min.
5. Incubate the isatin paper with dried samples at 90°C for 20 min to develop the blue color. Intensity of the blue color correlates with proline content.
6. For recording and for subsequent semiquantitative evaluation, scan or photograph the image. Optional: remove the yellow color of the isatin paper by washing it in 50% ethanol for several minutes.
7. Use densitometry to generate semiquantitative data. Freely available softwares such as ImageJ or NIH Image softwares are suitable for densitometry and to generate quantitative data (http://rsb.info.nih.gov/ij).
8. To compare proline content of the samples to a reference, prepare a proline concentration series in 20% ethanol (0–5 mg/mL) and perform the isatin reaction with 10 μL samples as indicated above.
9. Compare color intensities of the samples to the standard reactions. For semiquantitative measurements, prepare a calibration curve with the reference reactions, scan the images, quantitate the intensities, and compare the values of the calibration curve to the values of the samples.

3.2. Proline Determination with Colorimetric Assay

1. Harvest the samples, measure their fresh weight, and use approximately 100 mg for a reaction. Alternatively snap freeze the samples in liquid nitrogen. When necessary, samples can be stored at −80°C (*see* **Note 2**).
2. Add 3% sulfosalicylic acid (5 μL/mg fresh weight) and grind the plant material. Keep the tubes on ice until finishing with all samples.
3. Centrifuge samples for 5 min at room temperature using benchtop centrifuge with maximum speed.

4. Prepare the reaction mixture in a separate tube: 100 μL of 3% sulfosalicylic acid, 200 μL glacial acetic acid, 200 μL acidic ninhydrin (*see* **Note 3**).
5. Add 100 μL from the supernatant of the plant extract, mix the tubes well. To avoid high pressure and accidental opening of the tubes in subsequent reaction, you can puncture the lid of the microcentrifuge tube with a needle.
6. Incubate the tubes at 96°C for 60 min (*see* **Note 4**).
7. Terminate the reaction on ice.
8. Extract the samples with toluene: Add 1 mL toluene to the reaction mixture, vortex the samples for 20 s, and leave on the bench for 5 min to allow the separation of the organic and water phases. Use gloves to handle the tubes during extraction (*see* **Notes 5** and **6**).
9. Remove the chromophore containing toluene into a fresh tube.
10. Measure the absorbance at 520 nm using toluene as reference. The proline concentration can be determined using a standard concentration curve and calculated on fresh weight basis (usually expressed as microgram per gram FW or micromole per gram FW).

3.3. Amino Acid Determination with HPLC

3.3.1. Extraction of Amino Acids

1. Freeze 100 mg plant material in liquid nitrogen and grind it in a mortar with 2 mL cold ethanol.
2. Transfer the solution into a 2 mL microcentrifuge tube, mix well, transfer 1 mL into new microcentrifuge tube, and save the rest for chlorophyll measurement (see below).
3. Add 1 mL of 120 μM α-aminobutyrate (dissolved in distilled water) and mix well.
4. Incubate the mixture at 70°C for 5 min.
5. Incubate the mixture at 4°C for 1 h.
6. Centrifuge in cooled microcentrifuge at 14,000×*g* for 30 min at 4°C.
7. Collect supernatants and dispense into 200 μL aliquots.
8. Vacuum dry samples in a SpeedVac for 2 h, then freeze and store them at −80°C.
9. For analysis, thaw samples, add 1.2 mL distilled water, and mix at room temperature for 1 h.
10. Centrifuge in cooled microcentrifuge at top speed and 4°C for 30 min.
11. Collect supernatant and centrifuge it as in step 10.
12. Dilute the supernatant 10 times for HPLC analysis.

3.3.2. Measurement of Chlorophyll Content

Use extract from the protocol above (step 2 of **Section 3.3.1**).

1. Mix 200 μL sample with 1 mL cold ethanol, mix well.
2. Incubate the mixture at 4°C for 1 h.
3. Centrifuge samples in cooled microcentrifuge at 14,000×*g* for 5 min at 4°C.
4. Collect supernatant and use it to determine chlorophyll content.
5. Measure the OD of the supernatant in spectrophotometer at $\lambda_{645\ nm}$ and $\lambda_{663\ nm}$.
6. Calculate the chlorophyll content as follows:
   $A_{663} = A_{663}$ ChlA + A_{663} ChlB
   $A_{645} = A_{645}$ ChlA + A_{645} ChlB
   where A is the absorbance; ChlA is chlorophyll A; and ChlB is chlorophyll B.

For each chlorophyll, the absorbance $A = \varepsilon lC$, where ε is the specific absorption coefficient of the chlorophyll considered, l is the light path, 1 cm, and C is the chlorophyll concentration.

For chlorophyll A, ε values are 82.04 at 663 nm and 17.75 at 645 nm. For chlorophyll B, ε values are 9.27 at 663 nm and 45.6 at 645 nm (with ε expressed in L/g cm).

$C_a = 12.7A_{663} - 2.63A_{645}$

$C_b = 22.9A_{645} - 4.68A_{663}$

where C_a is the chlorophyll A concentration and C_b is the chlorophyll B concentration, both expressed in mg/L.

3.3.3. High-Performance Liquid Chromatography

1. OPA powder is dissolved in HPLC-grade methanol in order to produce a 0.4 M solution (*see* **Note 7**).

3.3.3.1. Derivatization with o-Phthalaldehyde (OPA)

2. The final derivatization OPA reagent is prepared as follows: 0.9 mL sodium tetraborate (pH 9.5 with NaOH), 0.1 mL of 0.4 M OPA, 20 μL 2-mercaptoethanol.
3. Equal volumes of OPA reagent and sample are mixed at room temperature for 1 min for derivatization to occur.
4. Ten microliters of the derivatized sample is immediately injected into the HPLC column.

3.3.3.2. Chromatography:

OPA derivatives are separated at room temperature using sodium phosphate elution buffers.

Buffer A is 20 mM sodium phosphate (pH 6.8): HPLC-grade methanol 90:10 (v/v). Buffer B is 20 mM sodium phosphate (pH 6.8): HPLC-grade methanol 40:60 (v/v).

Elution:

0–5 min: 100% buffer A (isocratic step).

5–45 min: linear gradient 0–30% buffer B.

Table 20.1
Amino acid analysis of Col-0 wild-type and *p5cs1* mutant *Arabidopsis* plants

Amino acids	p5cs1–1		p5cs1–2		p5cs1–3		p5cs1–4		Col. wt	
	Control	NaCl	Control	NaCl	Control	NaCl	Control	NaCl	Control	NaCl
Ala	1.31	2.98	1.17	3.91	1.30	1.41	1.18	1.75	1.11	1.75
Arg	4.56	4.85	6.51	2.52	6.12	5.77	5.13	2.61	5.42	4.98
Asn	20.74	22.56	21.13	15.02	19.32	15.32	21.23	14.71	20.37	15.50
Asp	2.72	3.86	2.74	3.65	2.80	2.30	2.96	3.29	2.66	2.71
Gln	45.50	36.76	40.31	45.44	38.16	37.27	40.18	41.94	44.76	36.98
Glu	8.20	9.17	8.21	9.47	9.49	8.15	8.89	9.38	7.43	7.45
Gly	1.74	0.43	2.49	1.47	3.65	1.21	2.47	1.43	2.73	2.27
His	0.56	0.69	0.60	0.73	0.60	0.61	0.59	0.63	0.54	0.58
Ile	0.24	0.29	0.25	0.24	0.24	0.24	0.23	0.20	0.18	0.17
Leu	0.25	0.27	0.26	0.27	0.23	0.26	0.24	0.22	0.19	0.19
Lys	0.32	0.33	0.35	0.28	0.35	0.40	0.34	0.25	0.25	0.24
Met	0.12	0.14	0.15	0.15	0.16	0.16	0.15	0.11	0.14	0.12
Norleu	0.05	0.06	0.08	0.06	0.11	0.13	0.09	0.09	0.05	0.07
OHPro	0.12	0.11	0.13	0.09	0.12	0.12	0.14	0.08	0.11	0.10
Orn	0.29	0.11	0.34	0.11	0.42	0.61	0.27	0.23	0.22	0.33
Phe	0.24	0.33	0.32	0.25	0.30	0.33	0.32	0.27	0.20	0.21
Pro	0.56	0.68	0.36	0.99	0.38	0.61	0.38	1.05	0.93	8.83
Ser	8.46	11.33	8.75	10.13	10.70	18.42	9.12	15.60	8.41	12.60
Thr	0.96	1.53	1.06	1.60	1.14	1.26	1.05	1.36	0.90	0.98
Trp	0.15	0.14	0.22	0.13	0.24	0.32	0.24	0.21	0.14	0.16
Tyr	0.15	0.14	0.17	0.13	0.16	0.18	0.16	0.13	0.12	0.11
Val	0.58	0.87	0.58	0.76	0.56	0.61	0.56	0.58	0.48	0.54

Amino acid content of 3-week-old plantlets was analyzed by the HPLC method. Plants were treated with or without 200 mM NaCl in liquid culture for 24 h prior to analysis as described (27). Amino acid contents are shown as percentage of the total amino acid pool. Note that 10 times increase of proline is detected in salt-treated, wild-type plants, while only 2–3 times increase is detected in the *p5cs1* mutants.

45–80 min: linear gradient 30–100% buffer B.

80–110 min: 100% buffer B.

110–120 min: linear gradient 100–0% buffer B.

3.3.3.3. Detection

Fluorescent derivatives are detected by spectrofluorometer with excitation at 340 nm and emission 455 nm.

3.3.3.4. Standards

Purified amino acids are individually dissolved in 0.1 N HCl to give 2.5 mM stock solutions that can be stored at −20°C for up to 1 month. Two hundred and fifty micromolar solutions are used for derivatization with OPA and injection. For derivatization, equal volumes of OPA reagent and amino acid solution are mixed at room temperature for 1 min and 10 μL of this mix is immediately injected into the HPLC column. Samples and standards can be co-injected to precisely identify each peak in the elution profiles of the sample.

3.3.3.5. Analysis of Results

It is important to check that there is a linear relationship between the amount of standard injected and the fluorescence yield (i.e., peak areas) before analyzing the results.

1. Identify sample peaks with reference to standards.
2. Peak areas are quantified using "System Gold Pic Integration Software."
3. For each amino acid, content is calculated for 1 mg of fresh plant material or for 1 μg of chlorophyll (**Table 20.1**). Alternatively, relative amounts of amino acids can be calculated as percentage of total amino acid content.

4. Notes

1. The isatin method offers a semiquantitative measurement of proline content, which is not as precise as the ninhydrin colorimetric method.
2. Determine carefully the fresh weight of samples. If the samples are wet, drain off as much excess liquid as you can but do not dry plant samples. Make at least five parallel samples for each treatment and measurement.
3. Although in the original protocol of Bates, boiling water is used for the ninhydrin reaction (62), dry heating blocks adjusted to 96°C can be employed and it is more convenient to incubate microcentrifuge tubes. Care should be taken with the accumulating pressure inside the tubes. Puncture the tubes, which allows evaporation and prevents high pressure in the tube and opening of the lids.
4. Use rubber gloves when handling the reaction tubes. Ninhydrin is very reactive.

5. As toluene damages the plastic cuvettes, quartz glass cuvettes should be used to measure absorbance with spectrophotometer.
6. Toluene is harmful and highly flammable; handling of toluene should be done in chemical hood.
7. OPA and derivatization solution must be prepared on the day of use to avoid loss of fluorescence and filtered through 0.45 μm Millipore filters to avoid column clog up.

Acknowledgments

This work was supported by OTKA grant no. F-68598, TéT grant no. ZA-16/2007, and EU grant no. FP6-020232-2. Edit Abrahám was supported by the Janos Bolyai Fellowship of the Hungarian Academy of Sciences.

References

1. Kemble, A.R. and MacPherson, H.T. (1954) Liberation of amino acids in perennial ray grass during wilting. *Biochem J* **58**, 46–59.
2. Rhodes, D., Handa, S., and Bressan, R.A. (1986) Metabolic changes associated with adaptation of plant cells to water stress. *Plant Physiol* **82**, 890–903.
3. Delauney, A.J. and Verma, D.P.S. (1993) Proline biosynthesis and osmoregulation in plants. *Plant J* **4**, 215–223.
4. Kavi Kishor, P.B., Sangam, S., Amrutha, R.N., Laxmi, P.S., Naidu, K.R., Rao, K.R.S.S., Rao, S., Reddy, K.J., Theriappan, P., and Sreenivasulu, N. (2005) Regulation of proline biosynthesis, degradation, uptake and transport in higher plants: its implications in plant growth and abiotic stress tolerance. *Curr Sci* **88**, 424–438.
5. Verbruggen, N. and Hermans, C. (2008) Proline accumulation in plants: a review. *Amino Acids* **35**, 753–759.
6. Ahmad, I., Wainwright, S.J., and Stewart, G.R. (1981) The solute and water relations of *Agrostis stolonifera* ecotypes differing in their salt tolerance. *New Phytol* **87**, 615–629.
7. Fougere, F., Le Rudulier, D., and Streeter, J.G. (1991) Effects of salt stress on amino acid, organic acid, and carbohydrate composition of roots, bacteroids, and cytosol of Alfalfa (*Medicago sativa* L.). *Plant Physiol* **96**, 1228–1236.
8. Armengaud, P., Thiery, L., Buhot, N., Grenier-De March, G., and Savouré, A. (2004) Transcriptional regulation of proline biosynthesis in *Medicago truncatula* reveals developmental and environmental specific features. *Physiol Plant* **120**, 442–450.
9. Newton, R.J., Sen, S., and Puryear, J.D. (1986) Free proline changes in *Pinus taeda* L. callus in response to drought stress. *Tree Physiol* **1**, 325–332.
10. Yamada, M., Morishita, H., Urano, K., Shiozaki, N., Yamaguchi-Shinozaki, K., Shinozaki, K., and Yoshiba, Y. (2005) Effects of free proline accumulation in petunias under drought stress. *J Exp Bot* **56**, 1975–1981.
11. Huang, A.H. and Cavalieri, A.J. (1979) Proline oxidase and water stress-induced proline accumulation in spinach leaves. *Plant Physiol* **63**, 531–535.
12. Mehta, S.K. and Gaur, J.P. (1999) Heavy-metal-induced proline accumulation and its role in ameliorating metal toxicity in *Chlorella vulgaris*. *New Phytol* **143**, 253–259.
13. Chen, C.T., Chen, L., Lin, C.C., and Kao, C.H. (2001) Regulation of proline accumulation in detached rice leaves exposed to excess copper. *Plant Sci* **160**, 283–290.
14. Draper, S.R. (1972) Amino acid changes associated with low temperature treatment of *Lolium perenne*. *Phytochemistry* **11**, 639–641.
15. Naidu, B.P., Paleg, L.G., Aspinall, D., Jennings, A.C., and Jones, G.P. (1991) Amino acid and glycine betaine accumulation in

cold-stressed wheat seedlings. *Phytochemistry*, **30**, 407–409.
16. Kuo, C.G. and Chen, B.W. (1980) Physiological responses of tomato cultivars to flooding. *J Am Soc Hort Sci* **105**, 751–755.
17. Aloni, B. and Rosenshtein, G. (1982) Effect of flooding on tomato cultivars: the relationship between proline accumulation and other morphological and physiological changes. *Physiol Plant* **56**, 513–517.
18. Saradhi, P.P., Alia Arora, A.S., and Prasad, K.V.S.K (1995) Proline accumulates in plants exposed to UV radiation and protects them against UV induced peroxidation. Biochem Biophys Res Commun, **209**, 1–5.
19. Meon, S., Fisher, J.M., and Wallace, H.R. (1978) Changes in free proline following infection of plants with either *Meloidogyne javanica* or *Agrobacterium tumefaciens*. *Physiol Plant Pathol,* **12**, 251–256.
20. Fabro, G., Kovács, I., Pavet, V., Szabados, L., and Alvarez, M.E. (2004) Proline accumulation and AtP5CS2 gene activation are induced by plant–pathogen incompatible interactions in *Arabidopsis*. *Mol Plant Microbe Interact* **17**, 343–350.
21. Samuel, D., et al. (2000) Proline inhibits aggregation during protein refolding. *Protein Sci* **9**(2), 344–352.
22. Terao, Y., Nakamori, S., and Takagi, H. (2003) Gene dosage effect of L-proline biosynthetic enzymes on L-proline accumulation and freeze tolerance in *Saccharomyces cerevisiae*. *Appl Environ Microbiol* **69**, 6527–6532.
23. Sharma, S.S., Schat, H., and Vooijs, R. (1998) In vitro alleviation of heavy metal-induced enzyme inhibition by proline. *Phytochemistry* **49**, 1531–1535.
24. Smirnoff, N. and Cumbes, Q.J. (1989) Hydroxyl radical scavenging activity of compatible solutes. *Phytochemistry* **28**, 1057–1060.
25. Hong, Z., Lakkineni, K., Zhang, Z., and Verma, D.P.S. (2000) Removal of feedback inhibition of delta(1)-pyrroline-5-carboxylate synthetase results in increased proline accumulation and protection of plants from osmotic stress. *Plant Physiol.* **122**, 1129–1136.
26. Alia, Mohanty, P., and Matysik, J. (2001) Effect of proline on the production of singlet oxygen. *Amino Acids* **21**, 195–200.
27. Székely, G., Abrahám, E., Cséplo, A., Rigó, G., Zsigmond, L., Csiszár, J., Ayaydin, F., Strizhov, N., Jásik, J., Schmelzer, E., Koncz, C., and Szabados, L. (2008) Duplicated P5CS genes of *Arabidopsis* play distinct roles in stress regulation and developmental control of proline biosynthesis. *Plant J* **53**, 11–28.
28. Hare, P. and Cress, W. (1997) Metabolic implications of stress induced proline accumulation in plants. *Plant Growth Reg* **21**, 79–102.
29. Hu, C.A., Delauney, A.J., and Verma, D.P.S. (1992) A bifunctional enzyme (delta 1-pyrroline-5-carboxylate synthetase) catalyzes the first two steps in proline biosynthesis in plants. *Proc Natl Acad Sci USA,* **89**, 9354–9358.
30. Delauney, A.J. and Verma, D.P.S. (1990) A soybean gene encoding delta 1-pyrroline-5-carboxylate reductase was isolated by functional complementation in *Escherichia coli* and is found to be osmoregulated. *Mol Gen Genet* **221**, 299–305.
31. Verbruggen, N., Villarroel, R., and Van Montagu, M. (1993) Osmoregulation of a pyrroline-5-carboxylate reductase gene in *Arabidopsis thaliana*. *Plant Physiol* **103**, 771–781.
32. Zhang, C.S., Lu, Q., and Verma, D.P.S. (1995) Removal of feedback inhibition of delta 1-pyrroline-5-carboxylate synthetase, a bifunctional enzyme catalyzing the first two steps of proline biosynthesis in plants. *J Biol Chem* **270**, 20491–20496.
33. Yoshiba, Y., Kiyosue, T., Katagiri, T., Ueda, H., Mizoguchi, T., Yamaguchi-Shinozaki, K., Wada, K., Harada, Y., and Shinozaki, K. (1995) Correlation between the induction of a gene for delta 1-pyrroline-5-carboxylate synthetase and the accumulation of proline in *Arabidopsis thaliana* under osmotic stress. *Plant J* **7**, 751–760.
34. Strizhov, N., Abrahám, E., Okrész, L., Blickling, S., Zilberstein, A., Schell, J., Koncz, C., and Szabados, L. (1997) Differential expression of two P5CS genes controlling proline accumulation during salt-stress requires ABA and is regulated by ABA1, ABI1 and AXR2 in *Arabidopsis*. *Plant J* **12**, 557–569.
35. Peng, Z., Lu, Q., and Verma, D.P.S. (1996) Reciprocal regulation of delta 1-pyrroline-5-carboxylate synthetase and proline dehydrogenase genes controls proline levels during and after osmotic stress in plants. *Mol Gen Genet* **253**, 334–341.
36. Verbruggen, N., Hua, X.J., May, M., and Van Montagu, M. (1996) Environmental and developmental signals modulate proline homeostasis: evidence for a negative transcriptional regulator. *Proc Natl Acad Sci USA,* **93**, 8787–8791.
37. Forlani, G., Scainelli, D. and Nielsen, E. (1997) [delta]1-Pyrroline-5-carboxylate

dehydrogenase from cultured cells of potato (purification and properties). *Plant Physiol* **113**, 1413–1418.
38. Deuschle, K., Funck, D., Forlani, G., Stransky, H., Biehl, A., Leister, D., van der Graaff, E., Kunze, R., and Frommer, W.B. (2004) The role of [delta]1-pyrroline-5-carboxylate dehydrogenase in proline degradation. *Plant Cell* **16**, 3413–3425.
39. Kiyosue, T., Yoshiba, Y., Yamaguchi-Shinozaki, K., and Shinozaki, K. (1996) A nuclear gene encoding mitochondrial proline dehydrogenase, an enzyme involved in proline metabolism, is upregulated by proline but downregulated by dehydration in *Arabidopsis*. *Plant Cell* **8**, 1323–1335.
40. Kishor, P., Hong, Z., Miao, G.H., Hu, C.A.A., and Verma, D.P.S. (1995) Overexpression of [delta]-pyrroline-5-carboxylate synthetase increases proline production and confers osmotolerance in transgenic plants. *Plant Physiol* **108**, 1387–1394.
41. Verdoy, D., Coba de la Peña, T., Redondo, F.J., Lucas, M.M., and Pueyo, J.J. (2006) Transgenic *Medicago truncatula* plants that accumulate proline display nitrogen-fixing activity with enhanced tolerance to osmotic stress. *Plant Cell Environ* **29**, 1913–1923.
42. Nanjo, T., Kobayashi, M., Yoshiba, Y., Kakubari, Y., Yamaguchi-Shinozaki, K., and Shinozaki, K. (1999) Antisense suppression of proline degradation improves tolerance to freezing and salinity in *Arabidopsis thaliana*. *FEBS Lett* **461**, 205–210.
43. Nanjo, T., et al. (1999) Biological functions of proline in morphogenesis and osmotolerance revealed in antisense transgenic *Arabidopsis thaliana*. *Plant J* **18**, 185–193.
44. De Ronde, J.A., et al. (2004) Photosynthetic response of transgenic soybean plants, containing an *Arabidopsis* P5CR gene, during heat and drought stress. *J Plant Physiol* **161**, 1211–1224.
45. Chen, Z., et al. (2007) Compatible solute accumulation and stress-mitigating effects in barley genotypes contrasting in their salt tolerance. *J Exp Bot* **58**, 4245–4255.
46. Xin, Z. and Browse, J. (1998) Eskimo1 mutants of *Arabidopsis* are constitutively freezing-tolerant. *Proc Natl Acad Sci USA* **95**, 7799–7804.
47. Liu, J. and Zhu, J.K. (1997) Proline accumulation and salt-stress-induced gene expression in a salt-hypersensitive mutant of *Arabidopsis*. *Plant Physiol* **114**, 591–596.
48. Mani, S., et al. (2002) Altered levels of proline dehydrogenase cause hypersensitivity to proline and its analogs in *Arabidopsis*. *Plant Physiol* **128**, 73–83.
49. Nanjo, T., et al. (2003) Toxicity of free proline revealed in an *Arabidopsis* T-DNA-tagged mutant deficient in proline dehydrogenase. *Plant Cell Physiol* **44**, 541–548.
50. Hare, P., Cress, W., and van Staden, J. (1999) Proline synthesis and degradation: a model system for elucidating stress-related signal transduction. *J Exp Bot* **50**, 413–434.
51. Maggio, A., et al. (2002) Does proline accumulation play an active role in stress-induced growth reduction? *Plant J* **31**, 699–712.
52. Taji, T., et al. (2004) Comparative genomics in salt tolerance between *Arabidopsis* and *Arabidopsis*-related halophyte salt cress using *Arabidopsis* microarray. *Plant Physiol* **135**, 1697–1709.
53. Inan, G., et al. (2004) Salt cress. A halophyte and cryophyte *Arabidopsis* relative model system and its applicability to molecular genetic analyses of growth and development of extremophiles. *Plant Physiol* **135**, 1718–1737.
54. Kant, S., et al. (2006) Evidence that differential gene expression between the halophyte, *Thellungiella halophila*, and *Arabidopsis thaliana* is responsible for higher levels of the compatible osmolyte proline and tight control of Na+ uptake in *T. halophila*. *Plant Cell Environ* **29**, 1220–1234.
55. Ghars, M.A., et al. (2008) Comparative salt tolerance analysis between *Arabidopsis thaliana* and *Thellungiella halophila*, with special emphasis on K(+)/Na(+) selectivity and proline accumulation. *J Plant Physiol* **165**, 588–599.
56. Smith, I. (1953) Colour reactions on paper chromatograms by a dipping technique. *Nature* **171**, 43–44.
57. Boctor, F.N. (1971) An improved method for colorimetric determination of proline with isatin. *Anal Biochem* **43**, 66–70.
58. Elliott, R.J. and Gardner, D.L. (1976) Proline determination with isatin, in the presence of amino acids. *Anal Biochem* **70**, 268–273.
59. Erdei, L. (2003) *Final Report to the PHARE CBC Project No. HU-0009-03-01-014 L.* (Erdei, ed.). University of Szeged, Szeged, pp. 37–63.
60. Grainger, D.J. and S. Aitken (2004) A microtitre format assay for proline in human serum or plasma. *Clin Chim Acta* **343**, 113–118.
61. Chinard, F.P. (1952) Photometric estimation of proline and ornithine. *J Biol Chem* **199**, 91–95.
62. Bates, L.S., Waldren, R.P., and Teare, I.D. (1973) Rapid determination of free

proline for water-stress studies. *Plant Soil* **39**, 205–207.
63. Noctor, G. and Foyer, C.H. (1998) Simultaneous measurement of foliar glutathione, gamma-glutamylcysteine, and amino acids by high-performance liquid chromatography: comparison with two other assay methods for glutathione. *Anal Biochem* **264**, 98–110.
64. Hanczko, R., et al. (2007) Advances in the *o*-phthalaldehyde derivatizations. Comeback to the *o*-phthalaldehyde–ethanethiol reagent. *J Chromatogr A* **1163**, 25–42.
65. Benson, J.R. and Hare, P.E. (1975) *o*-Phthalaldehyde: fluorogenic detection of primary amines in the picomole range. Comparison with fluorescamine and ninhydrin. *Proc Natl Acad Sci USA*, **72**, 619–22.
66. Cooper, J.D.H., Lewis, M.T., and Turnell, D.C. (1984) Pre-column *o*-phthalaldehyde derivatization of amino acids and their separation using reversed-phase high-performance liquid chromatography. I: Detection of the imino acids hydroxyproline and proline. *J Chromatography* **285**, 484–489.

Chapter 21

A New Method for Accurately Measuring Δ^1-Pyrroline-5-Carboxylate Synthetase Activity

Elodie Parre, Jacques de Virville, Françoise Cochet, Anne-Sophie Leprince, Luc Richard, Delphine Lefebvre-De Vos, Mohamed Ali Ghars, Marianne Bordenave, Alain Zachowski, and Arnould Savouré

Abstract

Proline is a key factor in plant adaptation to environmental stresses. The Δ^1-pyrroline-5-carboxylate synthetase catalyzes the first committed step and the rate-limiting step for proline biosynthesis in both plants and mammals. This enzyme catalyzes the reduction of glutamate to pyrroline-5-carboxylate in two sequential steps including the phosphorylation and the reduction of its precursor. Several methods were established to assay P5CS activity but however none of them are fully reliable. Therefore, we developed a new simple and reliable assay which is based on the quantification of Pi. This assay allowed us to determine the optimal pH, the apparent K_m and V_m of P5CS with regard to ATP and glutamate.

Key words: Δ^1-Pyrroline-5-carboxylate synthetase, proline, gamma-glutamyl kinase activity, glutamic -semialdehyde dehydrogenase activity, enzyme kinetics, water stress.

1. Introduction

The Δ^1-pyrroline-5-carboxylate synthetase (P5CS; EC. 2.7.2.11/1.2.2.41) is a key enzyme involved in the synthesis of the amino acid proline in both mammals and plants. Proline level is tightly regulated by its de novo synthesis and degradation. Glutamate, a precursor of proline synthesis in the cytosol, is first phosphorylated to gamma-glutamyl phosphate, which is then reduced to glutamate semialdehyde (GSA) by a bifunctional ATP- and NAD(P)H-dependent P5CS enzyme that consists of two domains, an N-terminal gamma-glutamyl kinase (gamma-GK)

R. Sunkar (ed.), *Plant Stress Tolerance*, Methods in Molecular Biology 639,
DOI 10.1007/978-1-60761-702-0_21, © Springer Science+Business Media, LLC 2010

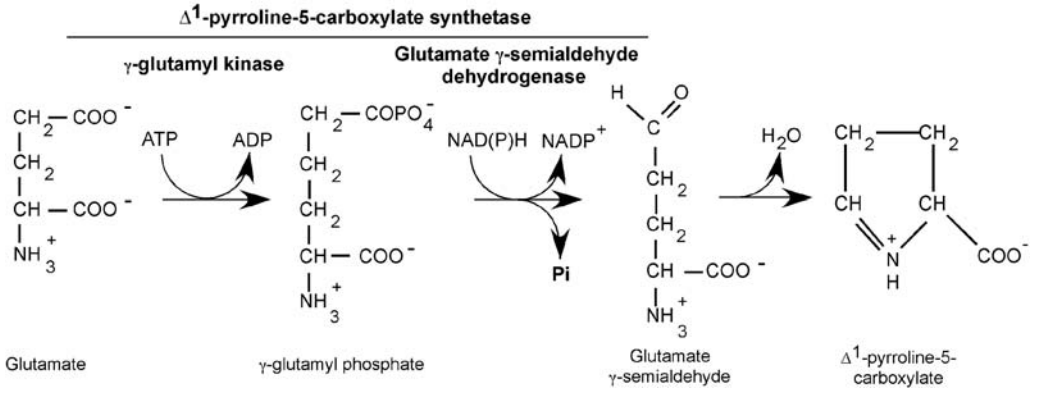

Fig. 21.1. Δ^1-Pyrroline-5-carboxylate synthetase catalyzes the first step in proline biosynthesis from glutamate.

domain and a C-terminal GSA dehydrogenase domain (**Fig. 21.1**) (1–3). GSA spontaneously cyclizes to P5C, which is finally reduced to proline by the P5C reductase (P5CR). In prokaryotes and lower eukaryotes like *Saccharomyces cerevisiae*, the P5CS activity is carried out by a complex of distinct gamma-GK and GSA dehydrogenase enzymes.

Besides the fact that proline is essential for primary metabolism, several other roles have been postulated for this amino acid in plants. Proline accumulation is a widespread response to water stress to which it may play a role as an osmolyte. Proline may also act as a chaperone to protect macromolecules from degradation (4), as a sink for energy and reducing power (5), as a transient source of carbon and nitrogen (5), or as a hydroxyl radical scavenger (6). Upon relief from stress, proline is rapidly oxidized by the sequential action of two mitochondrial enzymes proline dehydrogenase and P5C dehydrogenase to produce glutamate.

In this context, development of an accurate, reliable, and simple method for measuring P5CS activity is of considerable interest. Several methods have been used to assay P5CS activity. The most commonly used method involved the incorporation of labeled glutamate into proline (7, 8). Another method was also reported based on the P5CS reverse reaction (9). Indeed GSA reductase activity was measured by phosphate-dependent reduction of $NADP^+$, using P5C as the substrate.

Here, we describe a new method to measure the specific P5CS activity based on the quantification of inorganic phosphate. Indeed, Pi is formed after the phosphorylation of glutamate to -glutamyl phosphate by the gamma-GK activity of P5CS and its reduction by the GSA dehydrogenase activity. Pi determination is based on a malachite green colorimetric assay (10–12). This method is sensitive enough, requires small amount of biological material, and does not use any radiolabeled compounds.

2. Materials

2.1. Plant Material and Treatments

2.1.1. Plant Material

Arabidopsis thaliana Heynh. ecotype Columbia seeds were surface sterilized and grown on 0.5× Murashige and Skoog (MS) agar medium (13) in 14-cm-diameter Petri dishes as described previously (14–16). After an overnight period at 4°C to break dormancy, seedlings were grown for 12 days at 22°C under continuous light with a luminosity of 60 µmol photons/m^2/s.

2.1.2. Treatments

Twelve-day-old seedlings were removed from 0.5× MS agar plates and transferred onto 0.5× MS liquid medium supplemented or not with 321 mM mannitol. After 24 h treatment, seedlings were collected, immediately frozen in liquid nitrogen, and stored at −80°C until further analysis.

2.2. P5CS Enzyme Activity

1. Extraction buffer: 1 mM ethylenediaminetetraacetic acid (EDTA; Sigma-Aldrich), 5 mM $MgCl_2$, 10 mM dithiothreitol (DTT; Sigma-Aldrich), 1× protease inhibitor cocktail (Roche), 10 mM 3-(*N*-morpholino)propanesulfonic acid (MOPS; Sigma–Aldrich), pH 7.5 (*see* **Note 1**). Prepare freshly and store at 4°C.
2. Activity buffer: 1 mM EDTA, 50 mM KCl, 3 mM $MgSO_4$, 10 mM MOPS (pH 7.5). Prepare freshly and keep at 4°C.
3. Solution of ammonium heptamolybdate: Add carefully 32 mL H_2SO_4 to 100 mL H_2O on ice under a fume hood. Dissolve 3.7 g ammonium molybdate (Sigma-Aldrich) in 50 mL H_2O. Mix the two solutions and add H_2O qsp 200 mL. Store at room temperature away from light.
4. Solution of malachite green: Dissolve 1 g polyvinyl alcohol in 50 mL H_2O. Filter the solution and add 18.5 mg malachite green (Sigma-Aldrich) to it. Mix well and store in dark at room temperature.
5. NADPH (20 mM), 50 mM ATP, and 200 mM DDT are freshly prepared in water for each experiment and kept at 4°C.
6. Glutamate (1 M) is prepared in water and stored as single-use aliquots at −20°C.

3. Methods

The gamma-glutamyl phosphate is a labile intermediate that requires P5CS phosphorylation and reduction activities to be tightly coordinated (**Fig. 21.1**). This feature was not taken into

account in previous studies, which might explain why P5CS activity assays were so elusive. Therefore, this P5CS assay was based on both kinase and reductase activities.

The success of this method most probably depends upon the concurrent and nonlimiting provision of both ATP and NADPH in order to avoid any restriction in either the kinase or the reductase activity of P5CS. This assay is specific and sensitive enough for measurement of P5CS activity in plant tissue.

3.1. P5CS Soluble Extract

1. *Arabidopsis* leaves or roots (from 0.5 g up to 1 g fresh matter) are ground in a mortar at 4°C in 2 mL of extraction medium.
2. The homogenate is centrifuged at 20,000×*g* for 15 min at 4°C.
3. The supernatant is then recovered and centrifuged again at 154,000×*g* for 30 min at 4°C.
4. The supernatant is desalted by elution through a PD10 column (GE Healthcare) pre-equilibrated with activity buffer at 4°C.
5. Protein content is determined according to Bradford (17) using BSA as standard.

3.2. P5CS Activity Measurement

1. For each sample, four time points should be prepared with or without glutamate.
2. The reaction mix is prepared as follows: 60 μg protein, activity buffer pH 7.5, 10 mM DTT, 0.5 mM NADPH, 30 μL antiphosphatase inhibitor cocktail (Sigma-Aldrich), and 60 mM glutamate mix if needed (*see* **Note 2**).
3. ATP (2.5 mM) is added to start the reaction, the final volume of the reaction mix being 1 mL (*see* **Note 3**).
4. For one sample, the reaction is incubated for 0, 10, 20, or 30 min at room temperature.
5. For each time point, 100 μL of the reaction is removed and put in a tube containing 700 μL water and 200 μL ammonium heptamolybdate solution in order to stop the reaction.
6. When all the reactions are stopped, 200 μL malachite green solution is added. The mix is incubated at room temperature during 30 min in order to reveal Pi.
7. Pi released from the P5CS activity is measured at 623 nm with a spectrophotometer.
8. P5CS activity is assessed by calculating the difference between the amount of Pi released in the presence and in the absence of glutamate. The amount of released

Pi is obtained from a standard curve obtained with 0–40 nmol Pi using a 50 μM dipotassium phosphate solution incubated for 30 min in the phosphate coloration buffer (*see* steps 4–6). The P5CS activity is expressed in μmoles released Pi per hour per gram of fresh weight (*see* **Note 4**).

9. For the determination of the optimal pH of the P5CS activity, 60 mM MES in a range of pH from 6 to 6.5, 60 mM MOPS for pH up to 7, and 60 mM Bicine buffer for higher pHs were used. The pH of the activity buffer was measured before and after the reaction. As shown in **Fig. 21.2**, an optimum pH was observed at 7.5 in mannitol-treated seedlings.

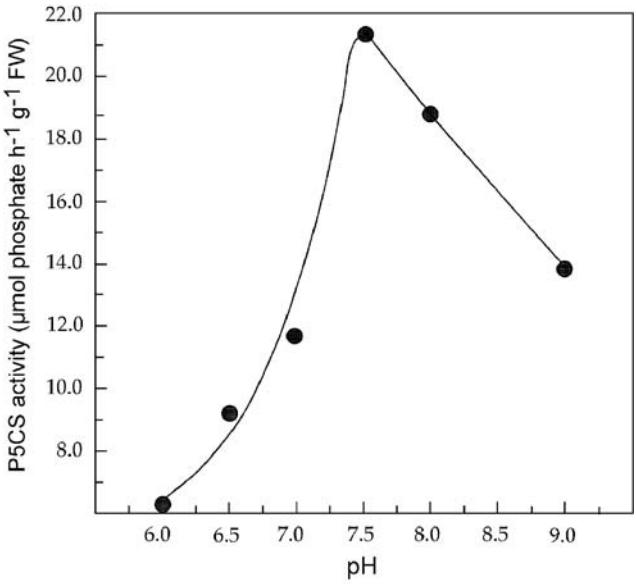

Fig. 21.2. P5CS activity shows an optimal pH activity at 7.5 with soluble proteins extracted from 12-day-old *Arabidopsis* leaves.

10. To characterize P5CS enzymatic properties, detailed kinetic studies were undertaken. The initial rates for Pi formation were determined as a function of ATP concentrations, while glutamate substrate concentration was fixed. As seen in **Fig. 21.3**, using the Eadie–Hofstee transformation of the substrate concentration vs. reaction velocity, we determined an apparent K_m of 1.5 mM for ATP.
11. The effect of substrate concentration on velocity was analyzed. As observed in **Fig. 21.4**, the velocity of the reaction increases dramatically as the glutamate concentration increases. From these plots, we concluded that the P5CS enzyme from mannitol-treated plants is characterized by

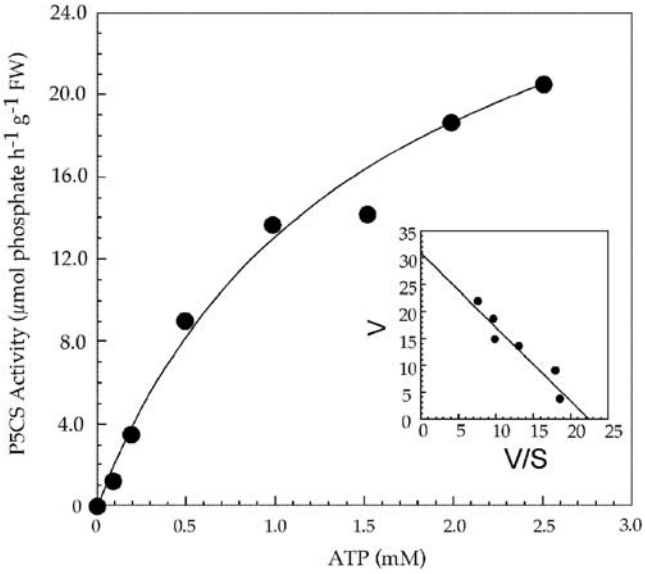

Fig. 21.3. K_m and V_m values of P5CS for ATP. Enzyme activity was assessed with soluble proteins from 12-day-old *Arabidopsis* leaves treated for 24 h with 321 mM mannitol. In the inset is presented Eadie–Hofstee transformation of the substrate concentration vs. reaction velocity (v) to measure the K_m for the hydrolysis of ATP catalyzed by P5CS. Reaction velocity was plotted against velocity divided by substrate concentration (v/[S]) and linear regression analysis performed.

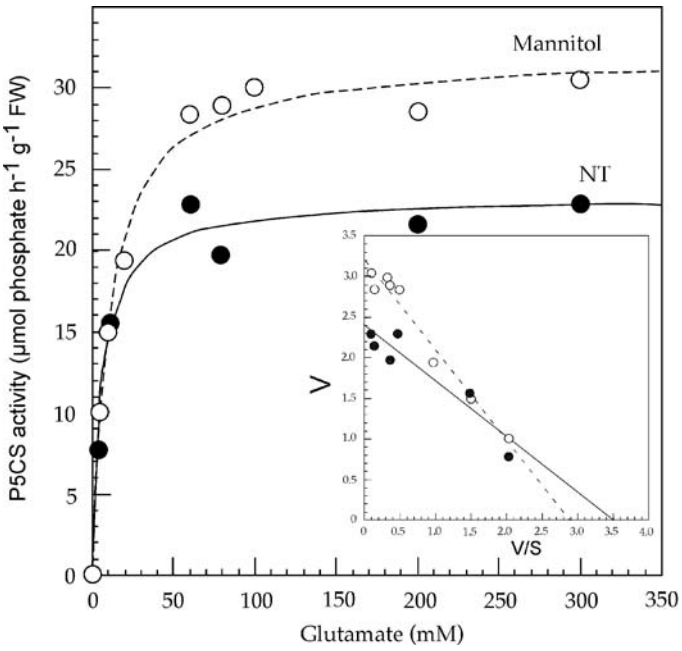

Fig. 21.4. K_m and V_m values of P5CS for glutamate. P5CS activity was assayed from *Arabidopsis* seedlings treated for 24 h with either MS/2 medium (NT) or 321 mM mannitol. In the inset is presented Eadie–Hofstee transformation of the substrate concentration vs. reaction velocity (v) to measure the K_m for glutamate as indicated in **Fig. 21.3**.

an apparent K_m of 8 mM and a maximum rate of reaction (V_{max}) of 32,000 nmol Pi/h/g FW for glutamate. A lower V_{max} for P5CS, 23,000 nmol Pi/h/g FW for glutamate, was observed from extracts isolated from non-stressed plants, while the K_m of the enzyme was not statistically different from the nontreated one.

4. Notes

1. This method is based on the determination of Pi. Contamination by phosphate should be prevented in all steps. Therefore, gloves should be worn in all steps of the protocol and all solutions should be prepared in ultrapure water.
2. It is essential to wash all the tubes with Decon Decomatic (Decon Laboratories Limited) and to carefully rinse them with ultrapure water to avoid any phosphate contamination. Another possibility is to use disposable crystal tubes, at least for the enzymatic assay.
3. After each step, vortex to mix well.
4. It is more accurate to express P5CS activity in μmoles Pi per hour per gram of fresh weight in plant samples subjected to water stress. It is also possible to express data in μmoles Pi per hour per mg of proteins.

Acknowledgments

E.P. was supported by a Ph.D. grant from the French "Ministère de l'Education Nationale, France" and M.A.G. by a grant from the French "Ministère des Affaires Etrangères" (French Embassy, Tunis).

References

1. Hu, C.A., Delauney, A.J., and Verma, D.P. (1992) A bifunctional enzyme (delta 1-pyrroline-5-carboxylate synthetase) catalyzes the first two steps in proline biosynthesis in plants *Proc Natl Acad Sci USA* **89**, 9354–9358.
2. Savouré, A., Jaoua, S., Hua, X.-J., Ardiles, W., Van Montagu, M., and Verbruggen, N. (1995) Isolation, characterization, and chromosomal location of a gene encoding the Δ^1-pyrroline-5-carboxylate synthetase in *Arabidopsis thaliana*. *FEBS Lett* **372**, 13–19.
3. Yoshiba, Y., Kiyosue, T., Katagiri, T., et al. (1995) Correlation between the induction of a gene for Δ^1-pyrroline-5-carboxylate synthetase and the accumulation of proline

in *Arabidopsis thaliana* under osmotic stress. *Plant J* **7**, 751–760.
4. Diamant, S., Eliahu, N., Rosenthal, D., and Goloubinoff, P. (2001) Chemical chaperones regulate molecular chaperones in vitro and in cells under combined salt and heat stresses. *J Biol Chem* **276**, 39586–39591.
5. Hare, P. and Cress, W. (1997) Metabolic implications of stress induced proline accumulation in plants *Plant Growth Reg* **21**, 79–102.
6. Matysik, J., Alia, A., Bhalu, B., and Mohanty, P. (2002) Molecular mechanisms of quenching of reactive oxygen species by proline under stress in plants *Curr Sci* **82**, S525–532.
7. Wakabayashi, Y., Iwashima, A., Yamada, E., and Yamada, R. (1991) Enzymological evidence for the indispensability of small intestine in the synthesis of arginine from glutamate. II. *N*-Acetylglutamate synthase. *Arch Biochem Biophys* **291**, 9–14.
8. Smith, R.J., Downing, S.J., Phang, J.M., Lodato, R.F., and Aoki, T.T. (1980) Pyrroline-5-carboxylate synthase activity in mammalian cells. *Proc Natl Acad Sci USA* **77**, 5221–5225.
9. Zhang, C.S., Lu, Q., and Verma, D.P. (1995) Removal of feedback inhibition of delta 1-pyrroline-5-carboxylate synthetase, a bifunctional enzyme catalyzing the first two steps of proline biosynthesis in plants. *J Biol Chem* **270**, 20491–20496.
10. Anner, B. and Mossmayer, M. (1975) Rapid determination of inorganic phosphate in biological systems by a highly sensitive photometric method. *Anal Biochem* **65**, 305–309.
11. Baykov, A., Evtushenko, O., and Avaeva, S. (1988) A malachite green procedure for orthophosphate determination and its use in alkaline phosphatase-based enzyme immunoassay. *Anal Biochem* **171**, 266–270.
12. Geladopoulos, T., Sotiroudis, T., and Evangelopoulos, A. (1991) A malachite green colorimetric assay for protein phosphatase activity. *Anal Biochem* **192**, 112–116.
13. Murashige, T. and Skoog, F. (1962) A revised medium for rapid growth and bio assays with tobacco tissue culture. *Physiol Plant* **15**, 473–497.
14. Parre, E., Ghars, M.A., Leprince, A.S., et al. (2007) Calcium signaling via phospholipase C is essential for proline accumulation upon ionic but not nonionic hyperosmotic stresses in *Arabidopsis. Plant Physiol* **144**, 503–12.
15. Thiery, L., Leprince, A.S., Lefebvre, D., Ghars, M.A., Debarbieux, E., and Savouré, A. (2004) Phospholipase D is a negative regulator of proline biosynthesis in *Arabidopsis thaliana*. *J Biol Chem* **279**, 14812–14818.
16. Verbruggen, N., Villarroel, R., and Van Montagu, M. (1993) Osmoregulation of a pyrroline-5-carboxylate reductase gene in *Arabidopsis thaliana*. *Plant Physiol* **103**, 771–781.
17. Bradford, M.M. (1976) A rapid and sensitive method for the quantitation of microgram quantities of protein utilizing the principle of protein–dye binding. *Anal Biochem* **72**, 248–254.

Chapter 22

Extraction and Analysis of Soluble Carbohydrates

Niels Maness

Abstract

Soluble sugars are a universal component of most living organisms and a fundamental building block in biosynthetic processes. It is no wonder that both qualitative and quantitative changes in carbohydrates often accompany plant's responses to stress. Depending on the speed of onset of stress, plant tissues can exhibit rapid and very site-specific shifts in their soluble carbohydrate pool – rapid and precise tissue collection and stabilization are necessary if analytical results are to truly represent the sugar composition at the instant of harvest. Since soluble carbohydrates are, by definition, soluble in the cell's aqueous environment, they may be analyzed directly from liquids obtained from plants or they may require extraction from the plant matrix. During extraction and prior to analysis, steps should be taken to avoid change in form or quantity of sugars by endogenous active enzyme conversion or by contaminating microbial growth. Many procedures for soluble sugar analysis exist; the choice of the most appropriate analytical protocol is ultimately dictated by the depth of information required to substantiate findings for a particular purpose.

Key words: Colorimetric sugar assay, glucose, GC, fructose, fructan, HPLC, soluble sugars, sucrose, starch.

1. Introduction

Soluble carbohydrates are perhaps the most fundamental metabolic pool in plants. Derived from carbon dioxide during the dark reaction of photosynthesis and utilized as precursors for numerous compounds required to maintain plant health and even signaling molecules for stress-induced source–sink response (1), soluble carbohydrates indeed play a substantial role in higher plant development. Localized changes in quantity and form of soluble carbohydrates are often associated with plant stress. These changes may be due to increased or decreased sugar biosynthesis, conversion of starch or other storage forms to soluble sugars, breakdown of cell wall polysaccharides, and/or changes in the

R. Sunkar (ed.), *Plant Stress Tolerance*, Methods in Molecular Biology 639,
DOI 10.1007/978-1-60761-702-0_22,

rate of sugar transport. Some transgenic plants accumulate sugar alcohols which are thought to increase cell osmotic potential and increase stress tolerance (2).

In order to validate and document the interaction of soluble sugar content with plant stress interaction, plant tissues must first be stabilized so that further changes in sugar quantity or identity are not imposed during tissue harvest. Sugars must then be extracted from the plant tissue in a stable form, at high enough concentration to accommodate the analytical procedure. Sugar identity and quantity can then be determined by a number of analytical techniques. This chapter will attempt to outline various methods used for soluble sugar determination from a variety of plant tissue types, highlighting techniques applicable for sample acquisition and stabilization, sugar extraction, and sugar analysis. Although the focus of this chapter is on soluble sugars, some methods for starch and fructan extraction and analysis are included since these oligomers/polymers may be hydrolyzed in response to stress and thus change the soluble sugar pool in given higher plant tissues.

2. Materials

2.1. Sample Acquisition and Stabilization

1. Liquid samples can be obtained directly from very high water tissues (fruits and fruit vegetables) by homogenizing or otherwise expressing liquid from a pre-cooled sample (*see* **Note 1**). Common homogenizers include Waring® blenders (Waring Corp., Torrington, CT), Omni Mixer homogenizers (Omni International, Marietta, GA), and Polytron probe (Brinkmann Instruments, Inc., Westbury, NY). Ground samples may be filtered through one to several layers of Miracloth® (Calbiochem; EMD Chemicals, Inc., La Jolla, CA) or through a clean sintered glass funnel, or may be obtained as a supernatant following centrifugation. Low-volume juice samples (vascular exudates, etc.) may be collected into pulled borosilicate glass capillary tubes (*see* **Note 2**), sealed, and frozen with liquid nitrogen (3).
2. Common lyophilizers for medium to large samples include cabinet-type systems with shelf temperature control (Millrock Technology, Inc., Kingston, NY) or manifold systems (Labconco Corp., Kansas City, MO). Cabinet-type systems are best suited for drying tissues, while manifold systems are best suited for drying liquids. Small-volume liquid samples may be lyophilized using a centrifugal lyophilizer such as a Speed Vac® (Savant, Farmingdale, NY).
3. Mechanical convection ovens should maintain high air flow for rapid temperature transfer into a tissue at 90°C. Oven

temperature should not exceed 95°C. Samples should be placed inside a labeled heat-resistant container (paper bags are appropriate) and then immediately into the forced draft oven at 90°C (*see* **Note 3**) for no longer than 90 min.

2.2. Sample Homogenization and Sugar Extraction

1. Liquid samples may not require further treatment prior to analysis except appropriate dilution and filtration, or lyophilization if further stabilization is desired. If enzyme inactivation is desired, heat a known volume of the sample to not higher than 95°C for no longer than 60 min.
2. If tissue samples preserved by freezing are to be processed without lyophilization, they may be pre-processed for extraction by powdering or directly homogenized with a wet grinder. Tissue powdering is done using a ceramic mortar and pestle (Coors Tek, Golden, CO) with the mortar bowl on dry ice or in a shallow dry ice:acetone bath. Frozen tissues may be directly homogenized in extraction solvent [water (*see* **Note 4**) or ethanol (*see* **Note 5**)] with one of the wet grinders indicated in **Section 2.1**, step 1. Sample:solvent ratio should be 1:10 (w/v) to accommodate adequate grinding. Grinding may be done directly in the same centrifuge tube used for extraction. Sonication can be achieved by placing the grinding vessel into a sonication water bath or by placing a clean sonication probe into the ground sample (Branson, Danbury, CT) while it is held on ice.
3. Dry tissues are typically ground to a fine powder prior to extraction. If tissue pieces are small enough (or can be readily broken by hand to obtain smaller pieces) to pass through the opening of a UDY cyclone mill (UDY Corp., Fort Collins, CO), they can be ground in one step to pass a 1-mm screen (*see* **Note 6**). If samples are too large to pass through the cyclone mill opening, they may need to be reduced in particle size. Waring-type blenders (Waring Corp., Torrington, CT) or a Wiley mill (Thomas Scientific, Swedesboro, NJ) may be used for small sample quantities; Hammer mills (Schutte-Buffalo Hammer Mill, LLC, Buffalo, NY) may be used for larger sample quantities.
4. If the sugar content of a high oil substrate [10% (w/w) oil or higher] is to be measured, oil should first be removed with diethyl ether (*see* **Note 7**) and then sugars can be extracted quantitatively with the solvent of choice. Use a Waring blender (Waring Corp., Torrington, CT) to pregrind the sample in three bursts of not more than 20 s each.
5. A refluxing tube (pulled glass or a long Pasteur pipette) can be inexpensively fit into a rubber stopper to fit a 50-mL centrifuge tube or through a silicon insert to fit the inside of an open top, screw-on lid for a 2 dram vial to

accommodate ethanol vapor re-condensation during boiling ethanol extraction (*see* **Note 8**). Vapors from boiling ethanol are cooled during travel up the tube enough to re-condense into a liquid. Liquid ethanol then drips back into the extraction system.

6. If determination of both soluble sugar and starch concentration is desired on the same sample, the pellet from ethanol sugar extraction (but not water extraction) can be used for starch determination (*see* **Note 9**).
7. A mixture of 2% (w/v) amyloglucosidase and 0.5% (w/v) α-amylase (Sigma Chemical Co., St. Louis, MO) is prepared in 0.1 M sodium acetate buffer (pH 4.5). If stored at 4°C, this reagent is stable for at least 1 week. Commercial amyloglucosidase preparations may contain substantial glucose which necessitates co-incubation and analysis of a blank with each set of starch hydrolysates to correct for the contaminating glucose in each determination.

2.3. Sample Analysis

1. Soluble sugars may be concentrated by evaporation of a known volume of the extraction solvent. This is done typically in vacuo with a Speed Vac® (Savant, Farmingdale, NY) but can be done under a steam of nitrogen gas. Typically the sample is brought to dryness and may be stored in a freezer prior to analysis (*see* **Note 10**).
2. Sample dilution should be done just prior to analysis (*see* **Note 10**). Assure that liquids are equilibrated to room temperature prior to dilution since liquid density is impacted by temperature. Following dilution in water, samples should not be stored for more than 5 days at 4°C prior to analysis.
3. If a non-hydrolyzing colorimetric reducing sugar assay via Nelson–Somogyi reagent or a similar assay is used and both reducing and non-reducing sugars are to be quantitated, the assay should be performed on one sample without pretreatment to account for resident reducing sugars, then non-reducing sugars (disaccharides, oligosaccharides, or polysaccharides) are converted to monomeric reducing sugars, and the assay is redone (*see* **Note 11**). Nelson–Somogyi reagents are prepared as follows:
   A) Prepare copper reagent in three steps:
      Reagent A: Dissolve 100 g sodium sulfate, 12.5 g anhydrous sodium carbonate, 10 g sodium bicarbonate, and 12.5 g sodium potassium tartrate in 400 mL water and bring to 500 mL volume. If the solution is cloudy, filter through Whatman no. 1 filter paper.

      Reagent B: Dissolve 3 g copper sulfate pentahydrate in 5 mL water, add one drop of concentrated sulfuric acid, and bring to 20 mL volume.

Copper working solution: Add 4 mL of reagent B to 96 mL of reagent A. This solution is stable for at least 3 weeks at room temperature.

B) Prepare arsenomolybdate reagent in three steps:
Dissolve 25 g ammonium molybdate in 400 mL water and add 25 mL concentrated sulfuric acid and mix.

Dissolve 3 g sodium arsenate heptahydrate in 25 mL water.

Add the sodium arsenate heptahydrate solution to the ammonium molybdate solution and bring to 500 mL volume. Heat at 50–60°C to dissolve completely, if necessary. This stock solution is stable for at least 2 weeks at room temperature.

Arsenomolybdate working solution: Dilute the above stock solution 1:5 with water just prior to use. This working solution is stable for 1 week at 4°C.

4. If a hydrolyzing colorimetric assay is used (anthrone), no distinction between monomeric reducing sugars and other linked sugars can be made; results reflect total sugar and approximate weight of linked carbohydrates cannot be determined.

   Prepare anthrone reagent by mixing 100 mg anthrone with 100 mL ice-cold 72% sulfuric acid. Store anthrone reagent in the dark at 4 °C. This solution is stable for up to 2 months.

5. Enzymatic sugar assays give more specific information about reducing and non-reducing sugars because enzymes are specific to individual sugars (*see* **Note 12**). Like colorimetric assays, they usually require only a spectrophotometer as analytical equipment. If disaccharides, oligosaccharides, or polysaccharides are of interest, in most cases they must be hydrolyzed to monosaccharides to accommodate analysis (*see* **Note 11**). The enzymatic analytical method described in **Section 3** uses a Boehringer Mannheim/R-Biopharm test combination for sucrose/glucose/fructose for approximately 20 assays.

   Enzyme substrates and buffers required for analysis are prepared as follows:

   a) Solution 1 contains 0.5 g lyophilisate of citrate buffer and 720 U of invertase (β-fructosidase); once diluted with 10 mL redistilled water (*see* **Note 18**), the solution should have a pH of 4.6 and is stable for 4 weeks at 2–8°C. Solution should be brought to room temperature before use.

   b) Solution 2 contains about 7.2 g of powder comprised of triethanolamine buffer, 110 mg NADP, 260 mg ATP, and magnesium sulfate; once diluted with 45 mL

redistilled water, the solution should have a pH of 7.6 and is stable for 4 weeks at 2–8°C. Solution should be brought to room temperature before use.

c) Suspension 3 contains about 1.1 mL suspension of 320 U of hexokinase and 160 U of glucose-6-phosphate dehydrogenase. This suspension is used undiluted and is stable for 3–4 weeks at 4°C.

d) Suspension 4 contains about 0.6 mL suspension of 420 U of phosphoglucose isomerase. This suspension is used undiluted and is stable for 3–4 weeks at 4 °C.

6. Gas chromatographic sugar assays require that monosaccharides be first derivatized to make them volatile. Common procedures are trimethylsilylation (TMS) (4) or formation of alditol acetates (5). TMS sugars chromatograph as multiple peaks of repeatable relative responses; alditol acetates chromatograph as single peaks. For most plant tissues inositol is an acceptable internal standard. Disaccharides, oligosaccharides and polysaccharides must first be methanolized to monosaccharide constituents and then derivatized. Polysaccharide sugar linkages vary in susceptibility to cleavage; conditions which result in quantitative conversion for α-1,4-glucose may not be sufficient for quantitative conversion of β-1,4-glucose or of uronic acid linkages.

A) Methanolic HCl preparation: To 10 mL HPLC grade methanol, add 2.1 mL acetyl chloride drop-wise with vigorous stirring. Store in securely capped vials in 2–5 mL aliquots in a freezer; allow solution to warm to room temperature before opening. Solution is stable for 3 weeks stored frozen or 1 week at room temperature.

B) Trisilylation reagent: Prepare a 1:1:5 (v/v/v) mixture of hexamethyldisilazane:trimethylchlorosilane:pyridine [or dilute TriSil (Pierce Chemical Co., Rockford, IL) with dry pyridine].

7. The various high-performance liquid chromatography (HPLC) procedures used for sugar analysis can be categorized by separation and/or detection requiring moderate pH versus those which require high pH (pH 11 or higher). HPLC is suitable for monomeric to polymeric sugar analysis. Most sugar columns operating at moderate pH are packed with cation exchange resin and may use water, acetonitrile:water, or dilute buffer as mobile phase. Guard columns typically last for up to 300 injections for most sample types (6). Ethanol extracts may be injected directly onto these columns after appropriate dilution. Bio-ethanol yields can be assessed along with soluble sugar residue in a single injection. Most detectors are non-selective (refractive

index or light scattering), vary in sensitivity, and may not be suitable for mobile phase gradients. Sugar columns operating at high pH via varying sodium hydroxide concentrations in the mobile phase (*see* **Note 13**) separate sugars based on ion exchange. The molarity of sodium hydroxide impacts mobile phase pH, which in turn impacts the degree of protonation of sugar hydroxyl groups. Guard columns tend to last for over 300 injections unless samples contain a high amount of particulates. Ethanol extracts must be dried and re-dissolved in water or mild buffer solution prior to injection (*see* **Notes 10** and **14**). Detection is typically by pulsed electrochemical detection (PED). With the appropriate wave form, PED can be selective for sugars and is more sensitive than refractive index. Gold working electrodes may be purchased in disposable or non-disposable styles – non-disposable electrodes are most economical for common sugar analyses. Most monosaccharide/disaccharide separations can be done isocratically; larger oligomeric or polymeric carbohydrates usually require a gradient of either increasing sodium hydroxide concentration or increasing buffer salt concentration, with sodium hydroxide concentration held constant.

A) Removal of phenolic compounds with a C18 Sep-Pak® (Waters Associates, Milford, MA) syringe cartridge:
   a) Precondition cartridge by applying at least 2 mL of HPLC methanol through the cartridge.
   b) Equilibrate cartridge with at least 4 mL water, then blow out remaining water with air from an empty syringe.
   c) Apply extract in water and rinse with one to two additional volumes of water.
   d) Utilize the cartridge effluent for sugar analysis.

B) Potential waveform for pulsed electrochemical detection of carbohydrates:

Time (s)	Potential (V)	Integration
0.00	0.05	
0.20	0.05	Begin
0.40	0.05	End
0.41	0.75	
0.60	0.75	
0.61	−0.15	
1.00	−0.15	

3. Methods

Within any given plant tissue, soluble sugars are in a state of flux with various metabolic cycles and with storage pools. It is important to separate the tissue of interest and stabilize it as rapidly as possible to preserve the sugars in the form and quantity they were in at the instant of harvest. Metabolism may be suspended by freezing or stopped by heat inactivation; dense tissues may need to be dissected to allow rapid thermal penetration. Soluble sugars in certain high water tissues or plant exudates may be directly analyzed following particulate removal via centrifugation or filtration. More frequently, sugars are extracted from frozen or dried tissues using water or ethanol. Tissues are first ground (non-dried tissues are powdered while still frozen or ground with wet grinders in extraction buffer; pre-dried tissues are ground with dry mills prior to extraction) and then extracted with the appropriate solvent. Multiple extractions are necessary for quantitative sugar recovery. If sugar content of high oil tissues [5–10% (w/w) oil or higher] is to be determined, lipids can first be extracted with diethyl ether (*see* **Note 7**) and then sugars can be extracted. Extraction with boiling 95% (v/v) ethanol allows extraction of soluble sugars and subsequent hydrolysis and analysis of starch content. For extraction of oligomeric sugars such as fructans, ethanol concentration should be reduced to no more than 70% (v/v) ethanol.

The depth of information needed in the determination of soluble sugars impacts the choice of an analytical protocol. Relatively simple colorimetric assays can be used to evaluate concentration of reducing and non-reducing sugars, but these assays do not provide information regarding individual sugar concentration and tend to be less sensitive than other assays. Enzymatic assays provide specific sugar concentration and require the use of relatively inexpensive laboratory instrumentation but require multiple readings to evaluate sugar concentration and can be labor intensive. Gas chromatographic assays provide information regarding numerous sugars in a single run and are sufficiently sensitive for most applications but require sample derivatization prior to analysis and may not be appropriate for quantitative analysis of oligomeric sugars. Absolute quantization of all sugars may be difficult to achieve because sugar derivatization may be incomplete for certain sugars. HPLC allows sensitive characterization of the presence and quantity of numerous sugars in a single run; most detectors do not require derivatization of sugars prior to injection and separations may be optimized to evaluate concentration of monomeric to oligomeric sugars if the appropriate extraction solvent was used.

3.1. Sample Acquisition and Stabilization

1. Samples acquired in liquid form should be cooled on ice (*see* **Note 1**) prior to juice acquisition to slow metabolic conversions. To assure homogeneity in sugar content, pre-cooled tissue samples of adequate size to be representative of the tissue in question can be weighed and then ground with a blender to release cellular liquids. Maintenance of cold temperatures during grinding is essential to avoid excessive sugar metabolic conversion; a Waring® blender must be placed inside a cold room, whereas the container with sample for Omni Mixer or Polytron grinding may be placed into an ice bath to maintain cold sample temperature. Juice samples of a known volume can be obtained as filtrates or as supernatants after centrifugation (3,000–10,000×*g* is sufficient) and should be either immediately analyzed or placed inside a sealable plastic ampoule and frozen with liquid nitrogen, then stored inside a freezer (–20°C minimum, –80°C recommended). Frozen liquid samples can be further stabilized by heat treatment or with lyophilization. If lyophilization is to be conducted, shell freezing increases surface area and decreases drying time.
2. Samples acquired in solid form should be excised with a clean, sharp instrument and then stabilized by rapid freezing with liquid nitrogen and stored in a freezer as indicated for liquid samples or heat inactivated, dried (*see* **Note 3**), and then stored inside a freezer to await dry grinding and extraction. Tissues should be dissected into smaller pieces (1–3 cm) to allow rapid thermal transmission through the tissue. Frozen tissue samples may be directly homogenized and extracted or lyophilized and stored frozen to await dry grinding and extraction. Prior to extraction, samples should be removed from the freezer and allowed to thaw to room temperature prior to opening of the storage container to prevent moisture condensation onto the tissue surface. Since enzymes may still be active, tissue processing is continued soon after thawing.
3. Non-liquid samples to be preserved by heat should be held at 90°C for a maximum of 90 min (minimum of 60 min) to stop enzymatic sugar conversion in the tissue and then dried at 70°C or lower for an additional 12–36 h to a constant weight (*see* **Note 3**). Prolonged tissue exposure to 90°C beyond 90 min can cause complexation reactions of sugar with other tissue components (especially proteins and phenolic compounds) and should be avoided. Samples should be stored in a freezer after drying to await dry grinding and extraction.

3.2. Sample Homogenization and Sugar Extraction

1. Frozen samples can be pre-ground to a powder in the frozen state or they may be ground in extraction buffer with a wet homogenizer. Tissue powdering is conducted on a cold surface to maintain the tissue in a frozen state throughout the powdering process to prevent excessive tissue water thaw, which would cause a change in the form of the powder to a gum. If the entire sample were weighed just prior to freezing, it can be quantitatively transferred into an extraction container using a small volume of extraction buffer. Frozen tissues may also be placed into extraction solvent [water (*see* **Note 4**) or ethanol (*see* **Note 5**)] and homogenized with a wet grinder. The homogenizer should be rinsed with a minimal volume of grinding solvent back into the ground sample to accommodate quantitative sugar recovery and prevent contamination with the next sample. If water is used as extraction solvent, an additional rinse with 95% ethanol helps prevent protein or microbial contamination between samples.
2. Pre-dried samples are ground to a fine powder with a UDY mill (UDY Corp., Fort Collins, CO) prior to extraction. After grinding, the samples are either immediately extracted or stored frozen inside a brown bottle.
3. For "typical" reducing and non-reducing soluble sugars (monomeric and most dimeric sugars), boiling 95% (v/v) ethanol serves as the extraction solvent. Accurately weigh 100–400 mg dry ground or frozen wet sample into a round–bottom, plastic 50-mL centrifuge tube. Add 15–20 mL 95% (v/v) ethanol, cap with a one-hole rubber stopper equipped with a glass reflux tube (*see* **Note 8**), mix and place into a water bath set at 85°C. Observe liquid for initiation of boiling and incubate in boiling ethanol for 20 min. Uncap tubes and centrifuge at 10,000×*g* for 10 min. Decant the supernatant into a volumetric flask and repeat extraction three more times. If determination of starch content is desired, after decanting the fourth 95% (v/v) ethanol supernatant into the volumetric flask, proceed with starch digestion or overlay the centrifugal pellet with 95% (v/v) ethanol, cap the tubes with a rubber stopper, and store at 4°C for up to 2 weeks. The ethanol extracts can be held at room temperature for up to 2 weeks prior to analysis; storage at 4°C helps prevent ethanol evaporation during storage. This process can be easily scaled down to a 2 dram vial (*see* **Note 8**), using 20–80 mg of sample and 4 mL extraction solvent and decanting the extraction supernatant into a 20- or 25-mL volumetric flask. Water can be used for extraction of soluble sugars using the same basic procedure outlined above except that the samples are incubated at 60°C rather

than 85°C, centrifugal speeds of 20,000–30,000×*g* (rather than 10,000×*g* for the ethanol procedure) are necessary for an equivalent pellet, and samples should be stored for no more than 5 days at 4°C prior to analysis. Since starch may be partially solubilized during water extraction, the pellet after water extraction is not suitable for subsequent starch determination.

4. Starch determinations should be done on samples after soluble sugar removal [sugar removal should have been done with 95% (v/v) ethanol]. If samples were overlaid with ethanol, uncap and evaporate the ethanol prior to proceeding (*see* **Note 9**). Add 10 mL water to samples in a 50-mL centrifuge tube (2 mL water for samples in 2 dram vials) and mix. Include two or three blank tubes, handled exactly the same as those containing sample. Incubate the samples at 90°C with intermittent mixing for 30 min to gelatinize starch. Allow samples to cool to room temperature, then add 10 mL of 0.2 M sodium acetate, pH 4.5 (2 mL for 2 dram vials). Add 1 mL of amyloglucosidase and α-amylase (200 μL for 2 dram vials), mix well, and stopper tubes. Incubate at room temperature for 1–2 h to allow α-amylase to pre-digest the gelatinized starch, then incubate at 55°C for 16–24 h (*see* **Note 15**). Allow tubes to cool and then centrifuge at 30,000×*g* for 10 min. Decant supernatant into a volumetric flask (volume may be the same as for sugar extraction or it may differ depending on the amount of starch in the tissue), add 10 mL water (2 mL for 2 dram vials) to the pellet, mix well, and incubate at 60°C for 10 min. Repeat centrifugation and re-extract with water two more times. Bring volumetric flasks to volume with water and store the starch extracts and blanks at 4°C for up to 5 days to await analysis.
5. If co-analysis of fructans with soluble sugars is desired, use of 70% (v/v) ethanol with 0.05% calcium carbonate (to prevent pH drop during extraction) as extraction buffer is common. Perform extractions while boiling as indicated in **Section 3.2**, step 3 for 95% (v/v) ethanol extraction. Bring solution to volume with 70% (v/v) ethanol.
6. If the sugar content of a tissue containing more than 10% (w/w) of oil is desired, lipid extraction of the tissue should precede sugar extraction (*see* **Note 7**). Grind with a Waring® blender, place the ground material on a clean, flat surface, and separate out any particles greater than 1 mm. The remainder of the sample can then be accurately weighed (target weight depends on expected sugar content) and extracted with diethyl ether (ratio of 1:10 for sample weight versus diethyl ether volume) with stirring for 20 min.

Centrifuge at between 3,000 and 10,000×*g* and decant supernatant into a clean, pre-weighed container. Repeat the extraction three more times for quantitative oil removal. Evaporate diethyl ether from the extract and weigh the container for gravimetric oil content determination. Completely evaporate diethyl ether from the sample residue and proceed with sugar extraction as described in step 3 of this section. If boiling 95% (v/v) ethanol is used as extraction solvent, starch analysis can proceed following sugar extraction, as described in step 4 of this section.

3.3. Sample Analysis

3.3.1. Colorimetric Non-hydrolyzing Assay (Nelson–Somogyi Procedure)

There are a number of procedures used for colorimetric determination of reducing sugars which do not hydrolyze sugar linkages in the sample. A very common procedure is the Nelson–Somogyi procedure (7). Since no sugar linkages are hydrolyzed, the procedure will not detect non-reducing sugars such as sucrose, but sucrose and like sugars can be hydrolyzed with acid or preferably enzymatic treatment; the yield of monomeric reducing sugars can then be detected and quantitated using the procedure. Since different sugars react with the reagent to give differing absorbance and thus different standard curves, a standard containing the same sugar(s) expected in the sample should be used and base results relative to the sugar(s) chosen as standard. This procedure has been scaled for use of microplates, which greatly increases the number of samples that can be run (8).

1. Prepare a sugar standard solution at 100 μg/mL water (*see* **Note 16**). This solution is stable for 1 week at 4°C.
2. Add 1 mL of aqueous sample (or of appropriate dilutions of the sugar standard solution) to a test tube. Add 1 mL water (or appropriate sample buffer) to triplicate tubes to serve as reagent blank.
3. Add 0.5 mL copper working solution and mix.
4. Heat at 100°C for 10 min and cool to room temperature.
5. Mix well, then add 3 mL arsenomolybdate working solution and allow to stand at room temperature for 10 min.
6. Mix well and measure absorbance of blue to dark blue samples, blanks, and standards at 520 nm.
7. Calculate reducing sugar concentration relative to the sugar(s) chosen as standard, from the standard curve for each run. Subtract the average of blank absorbance from samples and standards.

3.3.2. Colorimetric Hydrolyzing Assay (Anthrone Procedure)

As with non-hydrolyzing colorimetric sugar assays, many procedures exist for colorimetric determination of sugars which do hydrolyze sugar linkages in the sample. The anthrone procedure (9) can be used to determine total sugars but will not yield

specific information on the amount of reducing sugars in a sample if other sugars are hydrolyzed and subsequently contribute to the colorimetric response. The anthrone procedure has found utility for determination of starch content (if starch is present in a relatively pure form) (10). Choose sugars for use in standards which are representative of those expected in samples and present results relative to the sugar(s) chosen for standards (*see* **Note 16**).

1. Prepare a sugar standard solution at 100 μg/mL or a starch standard solution at 1 mg/mL (*see* **Note 16**). This solution is stable for 1 week at 4°C.
2. Add 1 mL of aqueous sample (or of appropriate dilutions of the sugar standard solution) to a test tube. Add 1 mL water (or appropriate sample buffer) to triplicate tubes to serve as reagent blank.
3. Add 4 mL ice-cold anthrone reagent to all tubes (*see* **Note 17**), vortex, and place at 100°C for exactly 10 min.
4. Place tubes into an ice bath and rapidly cool.
5. Mix well and read absorbance of green to dark green blanks, standards, and samples at 630 nm.
6. Calculate total sugar concentration relative to the sugar(s) chosen as standard, from the standard curve for each run. Subtract the average of blank absorbance from samples and standards.

3.3.3. Enzymatic Sugar Determination

Enzymatic sugar determinations have an advantage over colorimetric assays in being sugar specific and may be more sensitive than standard colorimetric assays. In most cases a stoichiometric enzyme product other than the sugar is measured spectrophotometrically. Enzyme substrates are provided in excess to assure completion of enzyme reaction. Once the user has confirmed quantitative conversion of a standard within a range of concentrations, standards need not be run with each set of samples. Samples must contain sugars within the specified range of concentration; too much sugar may overwhelm substrate concentration and cause deviation in the stoichiometric relationship required for quantification. A number of enzymatic sugar assays are available. The assay demonstrated here is from Boehringer Mannheim/R-Biopharm and is taken from the R-Biopharm Enzymatic Bioanalysis and Food Analysis handbook using test kits. A number of sugar assays are available; glucose, fructose, and sucrose quantization via stoichiometric NADPH formation by glucose-6-phosphate dehydrogenase will be demonstrated. Glucose is converted to glucose-6-phosphate by hexokinase and then glucose-6-phosphate is converted to gluconate-6-phosphate with stoichiometric production of NADPH from NADP, which is measured against a co-incubated

blank solution spectrophotometrically at 340 nm. Fructose is converted to fructose-6-phosphate by hexokinase and then isomerized to glucose-6-phosphate by phosphoglucose isomerase and quantified in the same reaction mixture as above. Sucrose is hydrolyzed into glucose and fructose by invertase and then glucose is quantified as above in a separate cuvette.

1. Warm sample extracts (ethanol or water) to room temperature and mix well before pipetting.
2. Conduct glucose/fructose assay in the same spectrophotometer cuvette as follows (*see* **Note 12**):
   a) Add 1.9 mL redistilled water, followed by 1.0 mL solution 2 and mix (*see* **Note 19**).
   b) Add 0.100 mL sample or blank [95% (v/v) ethanol or water, depending on the extraction solvent] and mix.
   c) Read and record the time zero absorbance of sample and blank solutions at 340 nm.
   d) Start glucose reaction by adding 20 μL of suspension 3 to sample and blank cuvettes and mix.
   e) Read and record absorbance after 15 min or after sample absorbance becomes static.
   f) Start fructose conversion to glucose and coupled glucose reaction by adding 20 μL of suspension 4 to sample and blank cuvettes and mix.
   g) Read and record absorbance after 15 min or after sample absorbance becomes static.
3. Conduct sucrose assay independent of the glucose/fructose assay by first mixing 0.2 mL solution 1 (invertase in citrate buffer) with 0.100 mL sample or blank, then follow steps a–e outlined in step 2 above.
4. Calculations are based on ΔA values, where $\Delta A = (A_{\text{after enzyme addition}} - A_{\text{prior to enzyme addition}})$ for cuvettes containing sample $- (A_{\text{after enzyme addition}} - A_{\text{prior to enzyme addition}})$ for cuvettes containing blank solution. For determination of glucose, this would be A from step e of step 2 above – A from step c of step 2 above; for fructose this would be A from step g of step 2 above – A from step e of step 2 above.

The general calculation for sugar concentration (c) is as follows:

$$c = ((V \times \text{MW})/(\varepsilon \times d \times v \times 1{,}000)) \times \Delta A$$

where

V is the final reaction volume (mL),

v is the sample volume (mL),

MW is the molecular weight of sugar being assayed (180.16 g/mol for glucose or fructose; 342.3 g/mol for sucrose),

D is the light path length (1 cm),

ε is the extinction coefficient for NADPH at 340 nm = 6.3 l/mmol/cm.

For glucose, $c = ((3.020 \times 180.16)/(6.3 \times 1.00 \times 0.100 \times 1{,}000)) \times \Delta A = 0.864 \times \Delta A$.

For fructose, $c = ((3.040 \times 180.16)/(6.3 \times 1.00 \times 0.100 \times 1{,}000)) \times \Delta A = 0.869 \times \Delta A$.

For sucrose, $c = ((3.020 \times 342.3)/(6.3 \times 1.00 \times 0.100 \times 1{,}000)) \times \Delta A = 1.641 \times \Delta A$.

3.3.4. Gas Chromatographic Sugar Determination

Sugar determination by gas chromatography requires that the sugars in extracts first be dried and then derivatized to make the sugars volatile enough for travel down a gas chromatography column. The two most common derivatives used for sugar analysis are trimethylsilylation (TMS; 4) or alditol acetates (11). Although TMS derivatives for most sugars chromatograph as multiple peaks, which makes data entry more complicated, the ratio of peak area units from each sugar is constant and can thus be used as a qualitative identification of sugars within a sample. Sugar-reducing ends are first methanolized with methanolic HCl and the monomeric sugars are then trimethylsilylated. If dimeric, oligomeric, or polymeric sugars are present, they will be converted into their monomeric constituents and information regarding their concentration will be lost. The TMS procedure is thus not a method of choice for quantifying sucrose or maltose in the presence of glucose and fructose, but it can be useful for quantifying starch if soluble sugars were removed in a prior step and glucose-containing oligomeric or polymeric carbohydrates which are susceptible to cleavage by methanolic HCl are substantially absent (*see* **Note 5**). The TMS procedure provides sugar composition information but does not yield the confirmation from which they originated.

1. To a 1 or 2 dram screw cap glass vial, add a volume of sugar extract containing approximately 50 μg sugar to a volume of inositol containing 100.0 nmol inositol (used as internal standard) and completely dry under a stream of nitrogen gas (*see* **Note 20**).
2. Place vials into a vacuum desiccator over P_2O_5 for at least 3 h at room temperature.
3. Add 0.40 mL methanol, that is, 1.5 M HCl and 0.10 mL methyl acetate, to each vial and securely cap vials with a Teflon-lined screw cap (*see* **Note 21**).

4. Place vials into a dry block heater at 80°C for 15 min, retighten screw caps, and incubate overnight (*see* **Note 22**).
5. Allow vials to cool, remove the screw caps (*see* **Note 22**), then add 3–6 drops of *t*-butanol, and evaporate their contents under a gentle stream of nitrogen gas at room temperature (*see* **Note 23**). Dry vial contents to one concentrated spot in the vial versus many spattered dry spots to accommodate the TMS step.
6. Add 25 μL of trimethylsilylation reagent to each vial, making sure that the reagent comes in contact with the dry sample.
7. Securely cap each sample and incubate at room temperature for at least 15 min but no more than 2 h.
8. Dry the reagent with a gentle stream of nitrogen gas at room temperature and add 100 μL isooctane just when dryness is achieved.
9. Inject 1 μL sample via cool, on-column injection onto a DB-1 fused silica capillary column (0.25 mm × 30 m, 0.25 μm film thickness; J and W Scientific, Folsom, CA) equipped with an FID detector using helium as a carrier gas. Oven temperature program is as follows:
   a) Start at 105°C for 2 min.
   b) Increase temperature to 160°C at 10°C/min and hold for 4 min.
   c) Increase temperature to 200°C at 1°C/min and hold for 5 min.
   d) Increase temperature to 290°C at 10°C/min and hold for 5 min to clean contamination.
   e) Cool to 105°C and hold for 10 min prior to a subsequent injection.
10. Sugar peaks are identified by co-elution with authentic standards and calculations are based on sugar responses (area units) relative to inositol response (area units) using an internal standard procedure and compared to previously run sugar standards:
    ((area units of sugar in sample/area units of 100 nmol inositol in sample)/(area units of 100 nmol of sugar in standard/ area units of 100 nmol inositol in standard)) × 100 nmol = nanomoles of sugar in sample.

The nanomoles of sugar in the sample is equivalent to the nanomoles of sugar per unit volume initially dried down prior to methanolysis and can be calculated back to concentration of sugar per extract volume or per unit weight of the original sample (*see* **Note 24**).

3.3.5. HPLC Sugar Determination

HPLC is perhaps the most popular and most powerful means for soluble sugar analysis. Most procedures do not require derivatization of sugars and many allow direct injection of extracts. Procedures differ based on the mode of sugar separation and detection. Two differing protocols will be presented: one based on weak ionic interaction using water or acetonitrile:water as mobile phase and refractive index as detection and the other based on relatively strong ion exchange using an isocratic or a gradient of sodium hydroxide as mobile phase and pulsed electrochemical detection (gold working electrode).

HPLC can be used for quantification of simple monomeric sugars but is also capable of yielding quantitative and qualitative information for dimeric sugars and up to polysaccharides. While polysaccharide analysis is beyond the scope of this chapter, procedures do exist for their analysis via HPLC.

The Biorad Aminex® (Biorad Laboratories, Hercules, CA) series of HPLC columns have been in use for sugar analysis since the early 1980s and are still popular for certain uses today. Two of the more popular sugar columns today are the HPX 87C and HPX 87P. A third column the HPX 87H is popular for combined organic acid, ethanol, and sugar separations. Aminex® columns are usually stainless steel in construction and have resin-based packings, usually require elevated temperatures (up to 85°C) for optimum peak resolution, and have moderate maximum pressure limits (1,500 psi). The typical mobile phase for the sugar columns is adequately degassed HPLC water (*see* **Note 4**) and the HPX 87C column can be used for direct injection of either water or ethanol extracts (*see* **Note 25**). They should be protected with the appropriate pre-column(s) which will generally withstand 300–350 injections before they need to be replaced. Detection can be done with various methods, the most simple of which is refractive index (RI).

1. Appropriately dilute extract with extraction solvent or reconstitute a dried sample in degassed water.
2. Remove particulates by filtration through a 0.45-μm filter or by centrifugation. If extract has excessive quantities of phenolics of other dissolved impurities, preprocess by flowing through a C18 Sep-Pak (or equivalent) syringe cartridge.
3. Place sample into an autosampler or use a manual injector with a 20-μL injection loop.
4. Overfill the injection loop by applying at least 50 μL of sample prior to injection onto an HPX 87P (or HPX 87H; 300 mm × 7.8 mm; BioRad Laboratories, Hercules, CA) column contained inside a heated jacket at 85°C for the HPX 87P or 60°C for the HPX 87H.

5. Inject the sample onto the column with water as eluent for the HPX 87P and 0.05 M sulfuric acid as eluent for the HPX 87H columns at a flow rate of 0.6 mL/min, using a refractive index detector with column eluent in the reference cell (*see* **Note 26**). Larger sugars elute first with the HPX 87C (6), HPX 87P (**Fig. 22.1**), and HPX 87H (**Fig. 22.2**) columns in the order of sucrose (or cellobiose), glucose, then fructose.

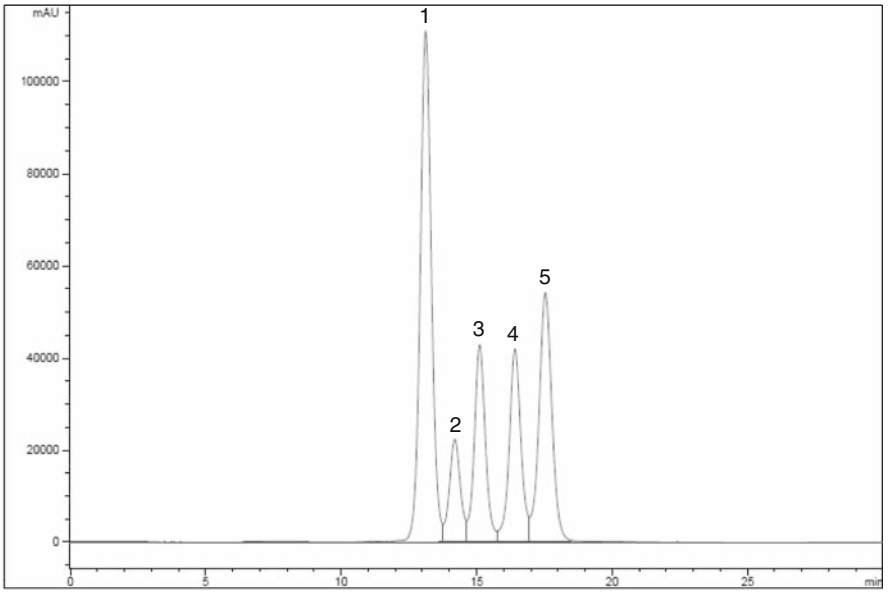

Fig. 22.1. BioRad HPX 87P HPLC chromatogram of standards for glucose (1), xylose (2), galactose (3), arabinose (4), and fructose (5). Sugars were injected in 20 μL (1.12 μmol glucose, 0.33 μmol xylose, 0.46 μmol galactose, 0.53 μmol arabinose, and 0.67 μmol fructose) and chromatography was conducted at 85°C using degassed water as elution buffer at a flow rate of 0.6 mL/min. Sugars were detected using a refractive index detector with water as reference. (Chromatogram courtesy of Mark Wilkins, Biosystems and Agricultural Engineering Dept., Oklahoma State University.)

6. Note pressure periodically and change guard columns when pressure starts to climb 200–300 psi above nominal operating pressure. Guard column(s) should last for 300–350 injections. If guard columns must be replaced substantially more often, filter or pre-clean samples as indicated in **Section 2**.
7. Certain samples may be very high in one sugar (sucrose, for example) and low in other sugars (glucose and/or fructose, for example). If quantification of all sugars is of interest, run the sample in different dilutions in order to prevent exceeding the linear range of quantification for each sugar.
8. If collection of fractionated sugars is of interest, attach a fraction collector with the smallest length of tubing practical. Use a low internal diameter (i.d.) tubing (usually matching the i.d. of the tubing running between the column and the

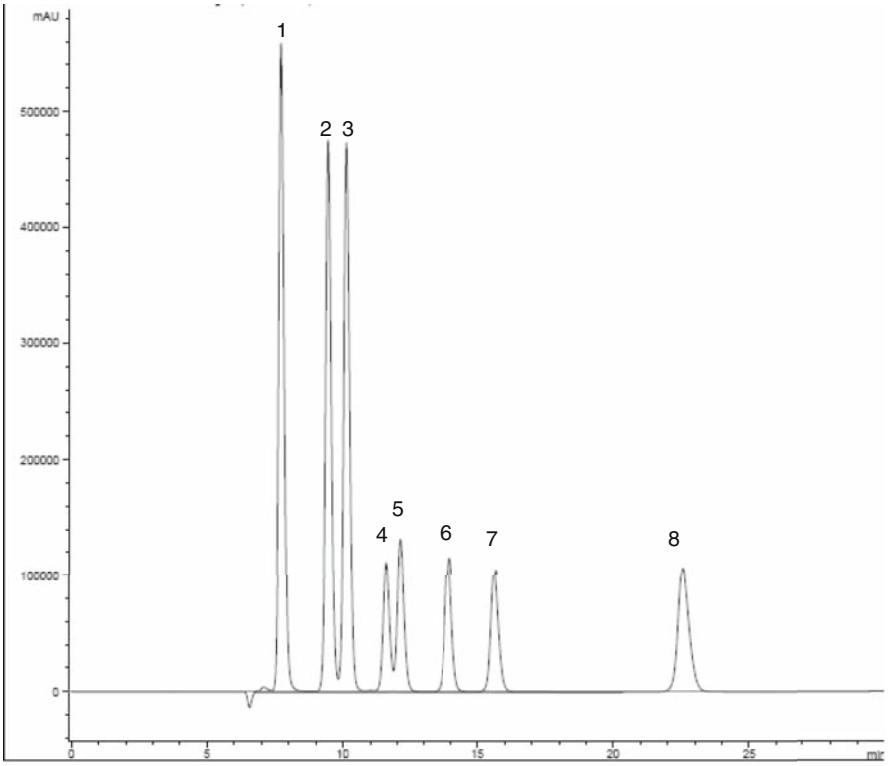

Fig. 22.2. BioRad HPX 87H HPLC chromatogram of standards for cellobiose (1), glucose (2), xylose (3), succinic acid (4), xylitol (5), glycerol (6), acetic acid (7), and ethanol (8). Sugars and organic acids were injected in 20 μL (1.23 μmol cellobiose, 2.40 μmol glucose, 3.20 μmol xylose, 1.71 μmol succinic acid, 0.81 μmol xylitol, 1.76 μmol glycerol, 5.04 μmol acetic acid, and 10.2 μmol ethanol) and chromatography was conducted at 60°C using 0.05 M sulfuric acid as elution buffer at a flow rate of 0.6 mL/min. Peaks were detected using a refractive index detector with 0.05 M sulfuric acid as reference. Although sucrose may be partially hydrolyzed in the elution buffer, if it were present, it would essentially co-elute with cellobiose. (Chromatogram courtesy of Mark Wilkins, Biosystems and Agricultural Engineering Dept., Oklahoma State University.)

detector is sufficient). Calculate the volume contained in the tubing to estimate when sugars will reach specific tubes in the fraction collector.

9. Calculations are usually done using the external standard procedure and utilizing standard sugar responses run with each batch of samples. A new standard set should be run at least daily (if not more frequently) to account for any drift in detector response. From the appropriate standard runs, calculate results for each sugar as

   (Area units of sugar in sample / concentration of sugar in sample) = (area units of sugar in standard/known concentration of sugar in standard)

   Concentration of sugar in sample = ((area units of sugar in sample × known concentration of sugar in standard)/area units of sugar in standard)

Note that units of concentration of sugar in the standard are used for the sample. Account for sample dilution and initial sample weight to calculate the quantity of sugar in the original sample prior to extraction.

The Dionex CarboPac® (Dionex Corp., Sunnyvale, CA) PA series of columns (PA1, PA10, PA100, PA200) are popular for many sugar separation applications, ranging from simple sugars to polysaccharides. The MA1 column is more useful for sugar alcohol and some pentose sugar separations. CarboPac® columns are made from a polymer material similar to Peak® and packings are resin based and are especially well suited for high pH. Most applications do not require elevation of column temperature, flow rates are typically 1.0 mL/min (MA1 is typically 0.6 mL/min), and maximum pressures range from 2,000 to 4,000 psi. Elution buffer contains variable concentrations of sodium hydroxide (*see* **Note 13**) and is thus very alkaline in pH. The high pH causes hydroxyl groups on sugars to be variably de-protonated, which induces a negative charge for the sugar. Reproducibility in degree of charge is regulated by sodium hydroxide ionic strength of the elution buffer, which is more commonly applied during a run of glucose, fructose, and sucrose isocratically (**Figs. 22.3** and **22.4**). Reproducibility in elution time is better accommodated using a gradient of increasing sodium hydroxide concentration to prevent carbonate buildup on the column (*see* **Note 13**). More complex carbohydrate separations (fructans, inulins, etc.) can be accommodated with sodium acetate gradient, usually with sodium hydroxide concentration held constant (**Figs. 22.5** and **22.6**). The mode of separation for the CarboPac® columns is ion exchange. For simple sugars, ionic strength of the elution buffer sodium hydroxide is usually relative low, in the range of 20–100 mM and most separations can be achieved under isocratic conditions. Most gradients of sodium hydroxide do not exceed 200 mM, and most

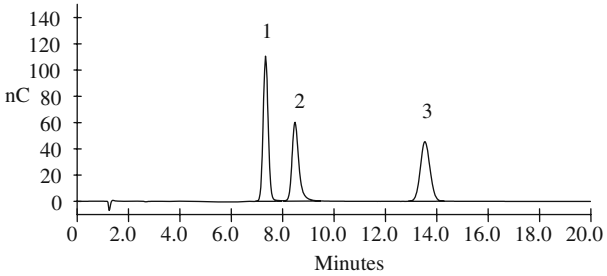

Fig. 22.3. Dionex PA1 HPLC chromatogram of standards for glucose (1), fructose (2), and sucrose (3). Sugars were injected in 50 μL (4 nmol each) and chromatography was conducted at ambient temperature using 20 mM NaOH as isocratic elution buffer at a flow rate of 1 mL/min. Sugars were detected using a pulsed electrochemical detector using the standard potential waveform indicated in **Section 2**.

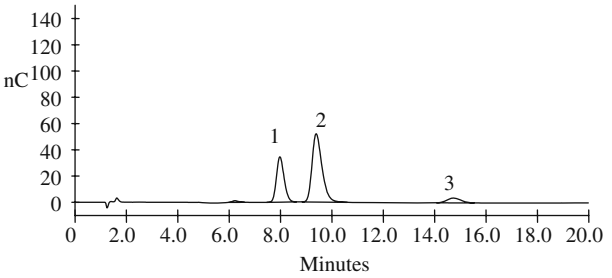

Fig. 22.4. Dionex PA1 HPLC chromatogram of mature "Sugartime" watermelon juice. Watermelon mesocarp tissue was ground with a Polytron blender and centrifuged for 10 min at 3,000×*g*. Juice (50 μL) was diluted to 100 mL with HPLC water. Run conditions and sugar peak elution patterns were identical to those described for the standards in **Fig. 22.3**. Note that the elution of sugars in this figure is earlier than that in the standard run shown in **Fig. 22.3** due to carbonate buildup on the column.

gradients involving sodium acetate are conducted in 100 mM sodium hydroxide. Samples should be in water prior to injection. Pre-columns should be used, packed with the same resin as the analytical column. Typically, the pre-columns last for up to 600 injections; at times the inlet frit can become clogged but can be easily replaced. Detection is typically by pulsed electrochemical detection (PED), using a gold working electrode. Sugars at high pH are oxidized at the surface of the gold electrode and detected by a difference in potential caused by the oxidation. The oxidized material is cleaned from the gold surface by changing the electrical potential. The sequence of potentials can be changed and optimized for the sugars of interest under set operating conditions and is referred to as the detector "waveform." Probably the most universal CarboPac® column is the PA1, and the following procedure will include its use.

1. Appropriately dilute extract with water or reconstitute a dried sample in degassed water.
2. Remove particulates by filtration through a 0.45-μm filter or by centrifugation. If extract has excessive quantities of phenolics of other dissolved impurities, preprocess by flowing through a C18 Sep-Pak (or equivalent) syringe cartridge.
3. Place sample into an autosampler or use a manual injector with a 20-μL injection loop.
4. Overfill the injection loop by applying at least 50 μL of sample prior to injection onto a CarboPac® PA1 column (4 mm × 250 mm; Dionex Corp., Sunnyvale, CA) at ambient temperature.
5. Inject the sample onto the column with 20 mM sodium hydroxide as eluent for glucose/fructose/sucrose separations or a gradient from 40 mM sodium hydroxide to 500 mM sodium acetate in 100 mM sodium hydroxide for

fructan separations, at a flow rate of 1.0 mL/min, using pulsed electrochemical detection. For most applications, the monosaccharide/disaccharide recommended waveform is sufficient for simple sugar detection. Smaller (less charge dense) sugars elute first with the PA1 column in the order of glucose, fructose, lactose, sucrose, and higher degree of polymerization (DP) sugars (**Figs. 22.3**, **22.4**, **22.5**, and **22.6**; melezitose may be used as an internal standard for plant fructan extracts).

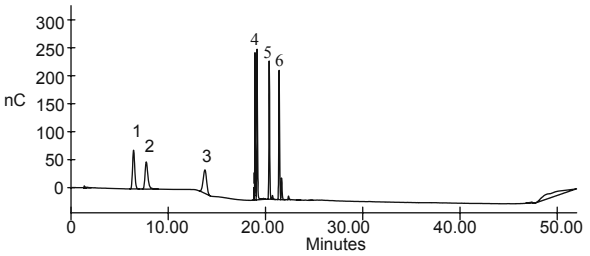

Fig. 22.5. Dionex PA1 HPLC chromatogram of standards for glucose (1), fructose (2), sucrose (3), raffinose, and 1-kestose (4) [degree of polymerization (DP) = 3; raffinose is the first twin peak and 1-kestose is the second twin peak in peak 4], nystose (5) (DP = 4), and 1-fructofranosylnystose (6) (DP = 5). Sugars were injected in 50 μL (4 nmol each for glucose, fructose, and sucrose; 12 nmol each for raffinose, 1-kestose, nystose, and 1-fructofranosylnystose) and chromatography was conducted at ambient temperature using a gradient as follows: 40 mM NaOH from 0 to 10 min, 40–100 mM NaOH from 10 to 11 min, 100 mM NaOH to 100 mM NaOH plus 500 mM sodium acetate from 11.5 to 41.5 min, 100 mM NaOH plus 500 mM sodium acetate to 100 mM NaOH from 45 to 46 min, 100 mM NaOH back to 40 mM NaOH from 46.5 to 47 min. Flow rate was 1 mL/min. Sugars were detected using a pulsed electrochemical detector using the standard carbohydrate potential waveform indicated in **Section 2**.

6. Run standards before and after every 12–15 sample injections for isocratic glucose, fructose, and sucrose separations. Following the last standard run, remove any carbonate buildup from the column with a sodium hydroxide gradient as follows (*see* **Note 13**):
   a) Increase sodium hydroxide concentration from 20 to 500 mM in 5 min.
   b) Hold for 5 min.
   c) Decrease sodium hydroxide concentration from 500 to 20 mM in 2 min.
   d) Hold for at least 5 min prior to starting the next series of sugar injections.
7. Note pressure periodically and change guard column when pressure starts to climb from 500 to 800 psi above nominal operating pressure. Oftentimes the guard column inlet frit becomes clogged and its replacement can bring pressure back to nominal operating conditions. Guard column

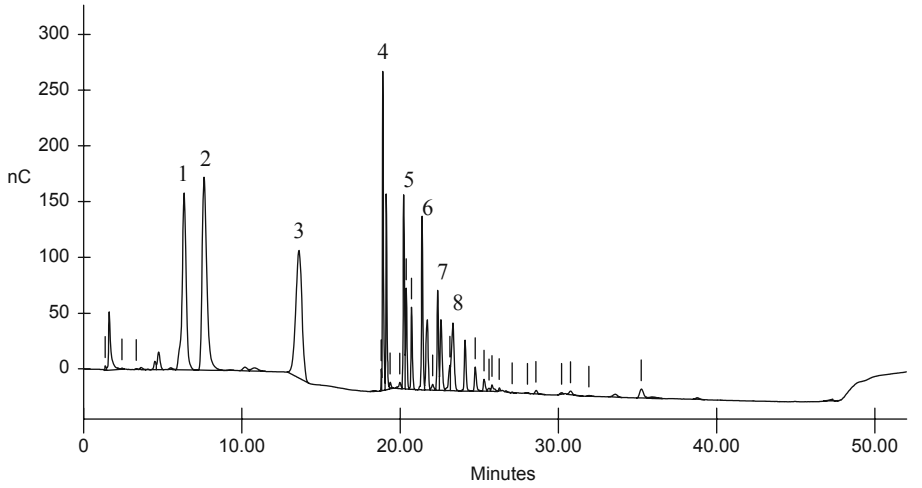

Fig. 22.6. Dionex PA1 HPLC chromatogram of fructans extracted from a short-day onion. Lyophilized onion tissue was homogenized with 70% ethanol plus 0.05% (w/v) sodium carbonate and extracted with boiling. A 1 mL aliquot was dried and reconstituted with 100 μL water and chromatography was conducted at ambient temperature at a flow rate of 1 mL/min. Glucose (1), fructose (2), sucrose (3), melezitose and raffinose (4) (first large twin peak is melezitose, added at 6.2 nmol as internal standard, and second smaller twin peak is raffinose), degree of polymerization (DP) 4 peaks (5), DP 5 peaks (6), DP 6 peaks (7), and DP 7 peaks (8). Other peaks in the series were of sequentially increasing DP. Chromatographic and gradient elution conditions were identical to those indicated in **Fig. 22.5**. Sugars were detected using a pulsed electrochemical detector using the standard carbohydrate potential waveform indicated in **Section 2**.

should last for at least 600 injections. If the inlet frit for the guard column must be replaced substantially more often, filter samples or centrifuge at a higher speed/longer duration to remove particulates. If degradation in performance beyond nominal operation is noted too frequently, it means that the packing has been prematurely fouled by sample contaminants which should be removed prior to injection with an appropriate Sep-Pak or equivalent syringe cartridge.

8. Certain samples may be very high in one sugar (sucrose, for example) and low in other sugars (glucose and/or fructose, for example). If quantification of all sugars is of interest, run the sample in different dilutions in order to prevent exceeding the linear range of quantification for each sugar.
9. Calculations are similar to those presented for the Aminex® columns. Even if internal standard procedure (calculated as outlined for GC sugars) is used, run a new set of standards often to account for changes in performance during the course of that sugar series. This is especially important if excessive column carbonate buildup occurs since peak retention time and resolution may be impacted enough to shift standard peak response (compare **Fig. 22.3** with **Fig. 22.4**).

4. Notes

1. Never place sample directly onto ice since water from ice can cause excessive sample contamination. Instead, place samples into a clean labeled water-resistant, non-insulating container (freezer bag or ampoule with a sealable lid), seal it, and then place into ice. Layer the container with ice to assure most rapid cooling.
2. Glass capillary tubes can be heated by the flame from a Bunsen burner or a soldering torch, pulled, and the glass broken to a fine point to allow juice collection from a very small area or used to puncture into and collect juice from a liquid-containing tissue zone (3). The fine point also accommodates rapid juice flow into the capillary tube by capillary action.
3. Preservation of samples by heat killing is acceptable for simple sugar (glucose, fructose, sucrose, etc.) and starch stabilization but high temperatures may be detrimental to heat-labile sample components such as enzymes, antioxidants, pigments, and low molecular weight volatile compounds. If co-determination of these compounds is anticipated, preservation by freezing is recommended. If preservation with heat is acceptable, cut bulky or high water-containing tissues (stems, fruits, woody tissues) into smaller pieces to accommodate rapid heat transfer and enzyme inactivation in the tissue.
4. Unless stated otherwise, water used for extraction or mixing of reagents has a resistivity of 18.2 MΩ cm and total organic content of less than five parts per billion. If water is used for extraction, inclusion of 0.05% (w/v) of sodium azide will help prevent microbial contamination. If water is used as HPLC elution solvent, degas with vacuum or by extensive sparging with chromatographic grade helium.
5. Non-denatured ethanol should be used for sugar extraction. For glucose, fructose, and sucrose determination, extraction with 95% (v/v) boiling (solution held at above 78°C; 80–85°C is typical) ethanol prevents solubilization of starch and many other oligomeric or polymeric sugars and allows separate extraction of soluble sugars from starch. For extraction of fructans and other oligomeric sugars, reducing ethanol concentration to 70% (v/v) may be necessary to accommodate quantitative extraction. Use of the highest concentration of ethanol deemed appropriate for extraction of sugars of interest is advisable to denature enzymes which could otherwise metabolize the sugars

and alter their concentration. Higher ethanol concentration also inhibits microbial growth and thus prevents sugar use by contaminating microorganisms.

6. The size of the round inlet for a cyclone mill is typically less than 2–3 cm in diameter, and a spring-loaded rubber ball may be depressed over the inlet to halt air flow through the mill during sample bottle detachment and reattachment. Clear sample bottles are typically supplied with the mill; brown screw top glass bottles (120 mL) fit the mill and can be used in place of the clear bottles. Brown glass has an added advantage of discouraging microbial growth. Since bottles are typically stored in a freezer to await sample extraction, tape labels should slightly overlap to avoid label loss caused by water condensation and loss of adhesion to the glass surface during re-warming.
7. Oils can interfere with sugar extraction and cause incomplete extraction as well as a non-volatile oily residue which can interfere with subsequent sugar analysis. Since oils and many other lipids are essentially universally soluble in diethyl ether, and sugars and other hydrophilic substances are essentially universally insoluble in diethyl ether, oil content can be determined and the extraction residue can then be used for quantitative sugar extraction. In our experience a sample can be pre-extracted with diethyl ether [sample:extractant ratio of 1:10 (w/v)] four consecutive times, followed by extraction with boiling 95% (v/v) ethanol [sample:extractant ratio of 1:10 (w/v)] four consecutive times to yield >98% recoveries of both oil and sugar.
8. Reflux tubes should extend prior to tapering about 10–12 cm past the top of the tube stopper or vial closure to allow enough distance for vapor cooling and recondensation. The bottom of the tube should extend about 2 cm into the extraction vessel to allow dripping of fresh ethanol into the extraction system without contacting either the bottom of the closure or the sides of the extraction vessel. A tapered end provides resistance to free vapor exchange into the atmosphere and thus encourages condensation upon cooling. The tapered end should be otherwise open to the atmosphere to allow pressure release and prevent pressurization of the vessel during extraction. Pasteur pipettes are typically about the right length to allow cooling/re-condensation of ethanol vapors if used with a 2 dram vial. These pipettes are insufficient in length to fit through a standard rubber stopper into a 50-mL centrifuge tube and are too fragile to be pushed through the hole in the stopper. Thicker glass tubing of about the same outer dimension as a Pasteur pipette can be used if tapered at a

sufficient length to accommodate the added length of the single-hole stopper.

9. If immediate processing for starch determination is not conducted, overlay the top of the pellet with 95% ethanol, seal, and place samples at 4°C. This step helps prevent microbial contamination; storage at 4°C also reduces evaporation of the ethanol. Just prior to starch processing, warm samples at 80°C to allow ethanol to vaporize.
10. Prior to drying, record the total extract volume and the aliquot volume used for drying. Sugars are most stable for storage in a dry form but should be stored in subdued light in a freezer. Certain analytical protocols [high-performance anion exchange pulsed electrochemical detection (HPAE-PED), for example] are not compatible with ethanol and ethanol must be evaporated to accommodate the analytical protocol. During re-hydration with water, samples may be warmed to 60°C and vortexed to assure total solubilization prior to quantitative transfer into a volumetric flask.
11. The Nelson–Somogyi reducing sugar assay, and most of the derivations thereof, reacts with the sugar-reducing end and results in a change in absorbance or transmittance of the assay solution. The chosen standard should be representative of sugars to be assayed and standard curves should be checked for linearity within the range of concentrations to be assayed. This type of assay does not accurately quantitate most dimeric (sucrose, maltose), oligomeric (fructans, small starch or cell wall fragments), or polymeric (starch, cell walls, etc.) sugars. These sugars must be degraded to their monomeric forms (enzymatic hydrolysis results in definable end products; acid hydrolysis is non-specific, may degrade the sugars, and some sugar linkages may be more resistant to hydrolysis than others) and then the reducing sugar assay redone. To convert the results from monomeric sugars back to a weight of oligo- or polymeric sugars, the weight of water added when the sugar was hydrolyzed to its monomeric form must be subtracted. For starch, multiply the weight of glucose by 0.90 to account for its dehydrated form in the polymeric molecule.
12. Enzymatic sugar assays depend on completion of reaction with specific sugars, which can be checked with an assay for linearity within the range of sugar concentrations to be analyzed. Since some procedures allow determination of multiple sugars in the same test solution (such as glucose/fructose/sucrose test combinations), use of disposable cuvettes allows for multiple readings of the same solution and saves time. Check that the cuvette is

recommended for use at the wavelength of your assay and be sure during placement of the cuvette into the spectrophotometer that it is aligned properly within the light path. Plastic ordure swords fit nicely into most square cuvettes which can be used for mixing the reaction solution after component additions.

13. Dissolved carbonates in the mobile phase will bind to the chromatographic column and cause a loss of chromatographic resolution and efficiency. Water used for the mobile phase and for sample dilution prior to injection should be sparged exhaustively with chromatographic grade helium to displace dissolved carbon dioxide and should be stored under a blanket of helium to avoid any additional exposure to carbon dioxide. Sodium hydroxide solutions for the mobile phase should be prepared using carbonate-free water from commercially available 50% sodium hydroxide (w/w) solutions rather than from sodium hydroxide pellets since the pellets are commonly covered with a layer of sodium carbonate which would serve as a source of contamination. Depending on how often the 50% sodium hydroxide solution is opened to the atmosphere, replace it at regular intervals (monthly under moderate use) to avoid introduction of substantial quantities of carbonate into the mobile phase.
14. Direct injection of samples with high ethanol concentration causes a large and tailing peak at the beginning of the run which may mask sugar alcohol and certain monosaccharide response. Ethanol can be dried relatively quickly using vacuum-assisted drying or under a stream of nitrogen gas. Reconstitute the sample just prior to dilution and HPLC injection in carbonate-free water, prepared as directed in **Note 13**.
15. During incubation at 55°C, gas pressure inside the centrifuge tube may build up to a sufficient level to pop the rubber stopper off the tube. Securing the stoppers with a rubber band around a single tube or a wooden stick across several tubes will prevent stopper loss during incubation.
16. Colorimetric procedures such as Nelson–Somogyi or anthrone give varying results depending on the sugar being analyzed and absorbance values can change from run to run. For preparation of a standard curve, use the reducing sugar most prevalent in the samples to be analyzed and prepare standards in the same buffer as used for samples. Run a new standard curve with each set of samples. If the Nelson–Somogyi assay is used to quantitate enzyme activity, it is common to terminate the reaction by addition of

the copper working solution immediately followed by incubation at 100 °C. If the anthrone procedure is used for starch determination, use either glucose (multiply results by 0.9 to account for the dehydrated form of glucose in the starch molecule) or starch as standard (no correction needed).

17. Since the anthrone reagent contains a very high concentration of sulfuric acid, it is quite viscous and may be difficult to pipette. Exercise care when adding high acid concentrations to water. The solution will become very hot and may react violently upon vortexing.
18. Redistilled water can be prepared by distilling house reverse osmosis or distilled water. Distilling particularly removes any trace metal contamination which can interfere with enzyme sugar assays. Collect and store redistilled water in glass or sturdy plastic containers and avoid conveyance or storage in metallic pipes or containers.
19. While the Boehringer–Mannheim procedure published by Rhone-Biopharm suggests addition of sample and buffer prior to redistilled water addition, we have found that for certain samples, absorbance values deviated from linearity and gave elevated sugar results unless water was added first to dilute buffer prior to sample addition.
20. Drying solvents under nitrogen gas should be conducted inside an appropriate fume hood to prevent organic vapors from entering the laboratory air.
21. During methanolysis, methanol, catalyzed by HCl, is added across glycosidic bonds and reducing ends of free sugars to form methyl glycosides. Methyl acetate is added to scavenge any water formed during the reaction from the solution to prevent hydrolysis of the methyl glycosides.
22. As the vials heat up, the screw caps will sometimes loosen and allow methanol to evaporate. This would cause HCl to increase in concentration and damage the sugars as well as remove methanol needed for the formation of methyl glycosides. Retightening of the screw caps helps to prevent evaporation of the methanolysis solution; use of heat-resistant gloves protects hands from burns and affords some protection in case vials break during tightening. If vials have dried during incubation, discard the sample.
23. *t*-Butanol should be stored in a warm place to ensure that it remains liquid. It is added to co-evaporate with HCl, helping to remove HCl during evaporation without degrading the sugars.

24. Absolute recovery of sugars in TMS results cannot always be assured – to verify sugar recovery and correct for any sugar losses, either include a monomeric sugar during extraction which is not present in the sample and correct for recovery or conduct a recovery trial by spiking a sample prior to extraction with approximately 25% (w/w) of the sugar expected in the sample and compare analytical results to unspiked samples as follows:
((Sugar concentration in spiked sample – sugar concentration in native sample)/concentration of sugar added as spike) × 100 = percentage recovery.
25. Column re-equilibration for subsequent injections is substantially less if samples are injected in water versus 95% (v/v) ethanol. For determination of glucose, fructose, and sucrose, system re-equilibration time was 17 min for extracts in water versus 40 min for extracts in 95% (v/v) ethanol (6).
26. Baseline stability is optimized when the reference cell liquid is changed on a regular basis. Usually changing the reference solution every 3 days to each week is sufficient; if excessive baseline drift is noted, change the reference solution more often with well-equilibrated column effluent.

Acknowledgments

The author would like to thank Dr. Mark Wilkins for contributing chromatograms used for **Figs. 22.1** and **22.2** of this chapter and Ms. Donna Chrz for technical assistance. This work was supported by the Oklahoma Agricultural Experiment Station, private grants, and by USDA grant 2006-34150-16891.

References

1. Roitsch, T. (1999) Source–sink regulation by sugar and stress. *Curr Opin Plant Biol* **2**,198–206.
2. Abebe, T., Guenzi, A.C., Martin, B., and Cushman, J.C. (2003) Tolerance of mannitol-accumulating transgenic wheat to water stress and salinity. *Plant Physiol* **131**, 1–8.
3. Maness, N.O. and McBee, G.G. (1986) Role of placental sac in endosperm carbohydrate import in sorghum caryopses. *Crop Sci* **26**, 1201–1207.
4. Chapman, G.W. and Horvat, R.J. (1989) Determination of nonvolatile acids and sugars from fruits and sweet potato extracts by capillary GLC and GLC/MS. *J Agric Food Chem* **37**, 947–950.
5. Hoebler, C., Barry, J.L., David, A., and Delort-Laval, J. (1989) Rapid acid hydrolysis of plant cell wall polysaccharides and simplified quantitative determination of their neutral monosaccharides by gas–liquid chromatography. *J Agric Food Chem* **37**, 360–367.

6. McBee, G.G. and Maness, N.O. (1983) Determination of sucrose, glucose and fructose in plant tissue by high-performance liquid chromatography. *J Chromatogr* **264**, 474–478.
7. Nelson, N. (1944) A photometric adaptation of the Somogyi method for the determination of glucose. *J Biol Chem* **153**, 375–380.
8. Green III, F., Clausen, C.A., and Highley, T.L. (1989) Adaptation of the Nelson–Somogyi reducing-sugar assay to a microassay using microliter plates. *Anal Biochem* **182**, 197–199.
9. Morris, D.L. (1948) Quantitative determination of carbohydrates with Dreywood's anthrone reagent. *Science* **107**, 254–255.
10. Clegg, K.M. (1956) The application of the anthrone reagent to the estimation of starch in cereals. *J Sci Food Agric* **7**, 40–44.
11. Albersheim, P., Nevins, D.J., English, P.D., and Karr, A. (1967) A method for the analysis of sugars in plant cell-wall polysaccharides by gas–liquid chromatography. *Carbohydr Res* **5**, 340–345.

Chapter 23

Measuring Soluble Ion Concentrations (Na^+, K^+, Cl^-) in Salt-Treated Plants

Rana Munns, Patricia A. Wallace, Natasha L. Teakle, and Timothy D. Colmer

Abstract

The control of Na^+ and Cl^- uptake from soils, and the partitioning of these ions within plants, is an essential component of salinity tolerance. Genetic variation in the ability of roots to exclude Na^+ and Cl^- from the transpiration stream flowing to the shoot has been associated with salinity tolerance in many species. The maintenance of a high uptake of K^+ is also essential, so measurements of Na^+, K^+ or Cl^- are frequently used to screen for genetic variation in salinity tolerance. As these ions are not bound covalently to compounds in cells, they can be readily extracted with dilute acid. Na^+ and K^+ can be measured in a dilute nitric acid extract using a flame photometer, by atomic absorption spectrometry or by inductively coupled plasma (ICP)–atomic emission spectrometry. Cl^- can be measured in the same acid extract with a chloridometer or colorimetrically using a spectrophotometer.

Key words: Sodium, potassium, chloride, ion extraction, ion analyses, salinity.

1. Introduction

The control of Na^+ and Cl^- transport is a critical requirement for salinity tolerance in plants. If excessive amounts of Na^+ or Cl^- enter plants, these ions typically rise to toxic levels in the older transpiring leaves. Because leaves evaporate about 50 times more water than they retain, Na^+ and Cl^- will quickly reach high concentrations there, unless the roots can restrict the movement of these ions into the transpiration stream. Salt-tolerant plants should therefore exclude most of the NaCl in the soil solution, ideally 98% (1). On the other hand, accumulation of a certain amount of Na^+ or Cl^- in leaves is essential for osmotic

R. Sunkar (ed.), *Plant Stress Tolerance*, Methods in Molecular Biology 639,
DOI 10.1007/978-1-60761-702-0_23,

adjustment. The partitioning of Na^+ and Cl^- into the vacuole, accompanied by the accumulation of K^+ or organic solutes in the cytoplasm, is an important mechanism of salinity tolerance for halophytes (2). Genetic variation in the accumulation of Na^+ and Cl^- is associated with salinity tolerance in many species. The maintenance of a high K^+/Na^+ ratio in the cytoplasm is also essential (3).

Some of the genes controlling Na^+ uptake and transport have been cloned (3), but much more remains to be learnt about the control of Na^+ and Cl^- concentrations in various compartments and transport of these ions at the intracellular, cellular, organ and long-distance transport levels. There is therefore a frequent need to measure the concentrations of Na^+, K^+ and Cl^- in various plant organs and tissues, both in the search for natural variation and the analysis of transgenic lines. Considerations of experimental design, of the time frame measurements should be taken, and the critical tissues to be sampled, are given in the accompanying chapter in this volume (4).

At any one time, the concentration of Na^+ will vary from leaf to leaf and between locations within a single leaf. The concentration is always less in younger than older leaves (5). As ion concentrations continually change with time in individual leaves (5, 6), it is important, when comparing differences in Na^+ uptake between different genotypes, to take the leaves at the same stage of development or at the same period of exposure to the NaCl (7). A leaf blade at a defined stage of development is the recommended tissue to sample, for example in wheat, leaf 3 at 10 days after emergence (7). The concentrations may be quite different in different leaf parts: between base and tip of a leaf blade (8), between blade and petiole (9) or between blade and sheath (6, 8). These differences are not fixed in time. The gradients in Na^+ and K^+ along a leaf change with age of the leaf both in degree and in direction (8).

In plant cells, Na^+, K^+ and Cl^- are largely present in soluble form and can be recovered with a dilute (0.5 M) acid extract (10). Protons displace the ionic bonds between Na^+ and K^+ to the negative charges on proteins and other macromolecules, and if nitric acid (HNO_3) rather than hydrochloric acid (HCl) is used, the NO_3^- replaces the ionic bonds between Cl^- and macromolecules. A conventional acid digest, using concentrated nitric acid at about 150°C, which completely solubilizes the plant tissue, is unnecessary to extract these three ions as they are not bound to cell constituents by covalent bonds.

To measure Na^+ and K^+, three atomic spectroscopy techniques are currently in use in various laboratories: flame photometry, atomic absorption spectrometry and inductively coupled plasma–atomic emission spectrometry (known as ICP). The latter is often the preferred method as it can measure a number of

elements simultaneously and over a very wide concentration range but is more expensive and confined to well-equipped analytical laboratories.

All three instruments operate under a similar principle. Solutions are aspirated into the excitation region where high-temperature atomization sources (flame or plasma) provide energy, which excites the electrons in atoms to higher energy levels. Energy is released by the electron as it returns to its original state. These energies are detected as light at a particular wavelength. The fundamental characteristic of this process is that each element absorbs and emits energy at specific wavelengths peculiar to its chemical composition. The intensity of the energy emitted at the chosen wavelength is proportional to the concentration of that element in the aspirated solution. By determining which wavelengths are absorbed or emitted by a sample and by measuring their intensities in relation to a reference standard, the concentrations of elements in the sample can be calculated.

Flame photometry is an atomic emission method for the routine detection of Na^+ and K^+. It uses a readily available hydrocarbon gas such as propane. Optical filters select the emission wavelength for the element. A calibration curve is made with solutions of known concentration, and comparison of emission intensities of samples to those of standard solutions allows quantitative analysis of the element of interest in the solution.

Atomic absorption spectrometry is a more sensitive analytical method. It uses the absorption of light to measure the concentration of specific atoms. A hollow cathode lamp of the element being measured is used as the light source. A mixture of air and acetylene produces a high-temperature flame into which samples are introduced. The atoms in the sample absorb light from the source and the electrons move to higher energy levels. A light detector set at a particular wavelength (monochrometer) measures the light absorbed by that element.

An inductively coupled plasma (ICP) is a very high-temperature excitation source (7,000 K) that ionizes atoms. Coupled with a high-resolution atomic emission spectrometer, it is used for quantitative, simultaneous measurement of a large range of elements. Samples are aspirated into the plasma gas (argon). The high temperature provides sufficient energy to enable the excited atoms to move to higher energy levels. When the atoms decay, they emit characteristic light, which is detected simultaneously using polychromators and multiple detectors or camera chips.

To measure Cl^-, the most common instrument is a chloridometer, which titrates the Cl^- with Ag^+ released from a silver wire. The principles of operation of the chloridometer are that Ag^+ is released at a constant rate as current is passed between a

pair of silver generator electrodes. Cl^- in the sample solution precipitates with the generated Ag^+ as AgCl. After all the Cl^- in the sample have precipitated, there is a steady increase in Ag^+ in solution that produces an increasing current through a pair of silver indicator electrodes. In the presence of an increase in indicator current, a relay will be activated, and a timer, which runs concurrently with Ag^+ generation, is automatically stopped (amperometric indication). As the rate of generation of Ag^+ is constant, the amount of Cl^- precipitated from the sample is proportional to the elapsed time. Thus, solutions with higher amounts of Cl^- take a longer time to reach the endpoint, and Cl^- is quantified by making a standard curve to relate time to known concentrations of Cl^- in standard solutions.

If a chloridometer is not available, Cl^- can be measured by a colorimetric "ferricyanide" method. Thiocyanate ion is liberated from mercuric thiocyanate by the formation of soluble mercuric chloride. In the presence of ferric ion, free thiocyanate ion forms a highly coloured ferric thiocyanate (11).

It is possible to measure Cl^- with a "Cl^--specific electrode", but details are not presented here.

The reliability of these techniques, like all analytical methods, relies on the use of appropriate standards, blanks, reference samples and spikes. A blank is an assay unit taken through all the same procedures, but lacking any plant tissue, so as to check for any background contamination. A reference sample is a plant tissue, verified to contain a known nutrient concentration, taken through the procedure with each batch of samples so as to determine reliability of each set of analyses over time. A spike is the addition of a known amount of the compound being analysed to a selected group of tissue extracts so that percent recovery can be determined.

2. Materials

2.1. Laboratory Items

1. HNO_3 A.R. grade.
2. NaCl A.R. grade.
3. KCl A.R. grade.
4. Distilled or de-ionized water.
5. Volumetric glassware (1 L and 100 mL).
6. Measuring cylinder (50 mL), pipettes.
7. Analytical balance.

8. Plastic tubes (10 mL) with screw tops.
9. Oven set at 60–70°C or shaker at room temperature.

All glassware should be washed in dilute nitric acid so that it is free of ions.

2.2. Sample Preparation

The dilute acid extraction based on Hunt (10) can be varied in detail depending on the amount of tissue and whether it is thin or soft and therefore readily permeated by the acid, or whether it is bulky or fibrous and should be ground first.

2.2.1. Leaf Blades

The surface of the leaves should be rinsed in distilled water if there is concern that the surface might be contaminated by handling or by splashing of saline solution. If the concentration of ions on a fresh weight or a water basis is required, the leaves should be weighed fresh by handling with forceps or rubber gloves and then placed in small envelopes or vials and dried in an oven at 60°C–70°C for 2 days. Individual leaf blades can be extracted in whole and the extract sampled directly for analysis (*see* **Notes 1** and **2**).

2.2.2. Roots

The surface of roots should be rinsed in solution, but quickly as there will be rapid efflux of Na^+ from the apoplast and epidermal cells. Two 10-s dips in 10 mM $CaNO_3$ is recommended. If the roots have been in high concentrations of salt (over 150 mM NaCl), it is advisable to rinse them in "iso-osmotic solutions" so as to avoid turgor loss due to osmotic shock. Organic osmotica such as sorbitol, mannitol, or high molecular weight PEG have been used by various laboratories to make iso-osmotic solutions. $CaNO_3$ should again be present. It is difficult to get a true fresh weight of roots without adhering solution on the one hand or damage due to heavy blotting on the other hand. Roots are then placed in small envelopes or vials and dried in an oven at 60°C–70°C for 2 days. Individual roots can also be extracted in whole and the extract sampled directly for analysis (*see* **Notes 1** and **2**).

Whole shoots or leaves of woody perennials need to be chopped into small pieces or ground, and the extract should be filtered or centrifuged before an aliquot is taken for analysis.

2.3. Grinding

Large or woody samples should be ground to a fine powder to achieve a homogenous representative sample for ion analysis.

1. Vials and metal spatula for collecting sample from grinder.
2. Dust mask.
3. Ear plugs.
4. Safety glasses.
5. Air-tight bags with desiccant for storing samples.

3. Methods

3.1. Dilute Acid Extraction

1. Make up 1 L of 0.5 M nitric acid with HNO_3 and distilled or de-ionized (e.g. Milli-Q) water. In a fume cupboard, add about 900 mL of distilled water to a 1-L volumetric flask, then 31.9 mL of concentrated HNO_3 using a graduated pipette to which a hand-held suction device is fitted, or a 50-mL measuring cylinder. Do not use your mouth to suck the concentrated acid into the pipette. Mix by stopping the flask and inverting several times, slowly. Add sufficient distilled water to make up to the 1 L mark. Always add the acid to water, as mixing the two is an exothermic reaction and it can "spit" if mixed the other way round.
2. Weigh out approximately 100 mg of dried and ground plant tissue into a tared 10-mL plastic tube and record the exact weight. Alternatively, place a pre-weighed leaf into the 10-mL tube. Add 10 mL of 0.5 M HNO_3.
3. For smaller samples of plant tissue, extraction volumes should be reduced: For 20–50 mg, use 5 mL and for <20 mg, use 2.5 mL. For samples larger than 100 mg, use 50-mL plastic tubes and increase the volume of dilute acid accordingly, i.e. for 200 mg, use 20 mL, etc.
4. Include "blanks" consisting of only the dilute acid and no tissue at the start and end of each set, as well as any time a new source of dilute acid or vials is used.

   Include reference material with known ion concentrations and prepare as per experimental samples. A number of organizations – NIST (USA), IAEA, BCR (Europe) and ASPAC (Australia) – supply dried plant tissue with certified concentrations of Na^+, K^+ and Cl^-.
5. Tightly screw on the lids for all samples and shake well to suspend all plant materials in the dilute acid. Place all vials tightly in a box and place on a shaker for 2 days at room temperature. Alternatively place in an oven at 80°C for 1 h. Mix by inverting tube once during that time and once after cooling.
6. After extraction, allow solid material to settle to the bottom of the vial. For dilutions, pipette from the middle of the extract, being careful not to take any solid or suspended material. Samples should be filtered or centrifuged if necessary.
7. Dilute extracts using only distilled or Milli-Q water.

3.2. Flame Photometer

3.2.1. Standards

For Na and K: Make up a stock of 50 μg/mL K^+(e.g. use KCl) and Na^+(e.g. use NaCl) and dilute accordingly to make up 0, 0.5, 1, 2.5, 5, 10, 15, 20 and 25 μg/mL standards of Na^+ and K^+. Ensure that the salts used are dry (e.g. oven dry at 60°C). Alternatively, standards can be purchased from commercial suppliers.

3.2.2. Dilutions

The dilution needed for the extracts will vary depending on the salt concentration of the growth medium, the tissue being analysed and the plant species being studied. The dilutions are required to provide samples with K^+ and Na^+ within the range of the standard curve. The following is an approximate guide for leaf tissue from a non-halophyte grown in 100 mM NaCl. We recommend always doing "trial" dilutions for each treatment, tissue and species before diluting all extracts.

1. K^+: Dilute controls 1:100 in a total of 10 mL, e.g. 100 μL of extract plus 9,900 μL of Milli-Q water. Dilute saline samples 1:50.
2. Na^+: Controls will often not need diluting but then should be run with standard solutions in the same matrix (i.e. 0.5 M nitric acid), as the standard curve shifts. Dilutions of 1:5 would typically enable standards in water to be used. Dilute saline samples 1:10 to 1:50, depending on which tissue is being assayed (e.g. Na^+ is higher in older leaves), in a total volume of at least 2 mL.

The following instructions were developed based on experience with Corning (model 410) and Jenway (model PFP7) flame photometers, but the overall approach should, with some modifications, be applicable to other instruments.

3.2.3. Operation

1. Ensure that the U tube is full of water (check by giving a squeeze) and make sure that the nebulizing tube is in a beaker full of de-ionized (DI) water. (Make sure that this tube is always in DI water between samples.)
2. Turn on air, gas, power switch. Hold the ignition switch until the flame is strong.
3. Set to Na or K.
4. Allow 30 min for the machine to warm up and stabilize.
5. Aspirate the most concentrated standard first (10 μg/mL K^+, 25 μg/mL Na^+) and adjust the coarse and fine tuning dials to display ~150 for Na^+ and ~100 for K^+.
6. Aspirate the 0 μg/mL standard and use the blank dial to adjust to 0. Aspirate all standards and obtain a linear standard curve.

7. Aspirate samples until a steady reading is obtained. Approximately every 10 samples repeat one of the standards so as to check that the machine has not drifted. Redo standard curve when drift has occurred (or about every hour).
8. When finished, leave tube in DI water for about 10 min, then turn off switch, gas, then air, followed by the power.

3.2.4. Calculating Concentrations

1. Convert the readings from the flame photometer to micrograms per millilitre using the standard curve.
2. Convert micrograms per millilitre into micromole per gram DW = (concentration in micrograms per millilitre × dilution factor, e.g. 100 for 1:100 dilution × volume of dilute acid extract, e.g. 10 mL) / (DW of tissue used in extraction × MW of ion 39.098 for K^+ and 22.99 for Na^+).

3.3. Atomic Absorption Spectrometry

1. Remove about 3 mL of solution from each tube and place in clean 10-mL tubes and give to operator with blanks.
2. Construct a spreadsheet with the weight of sample and the expected approximate concentration for each sample range as dilutions will need to be done. The operator needs to know whether the samples are controls (in which case a 1:10 dilution may be done) or salt-treated plants (in which case a 1:100 or 1:500 dilution will need to be done). The operator has standards in the range of 0–2 μg/mL. Tell the operator that you need K^+ and Na^+ as two separate measurements need to be made.
3. Calculate as above (step 2 of **Section 3.2.4**).

3.4. ICP

1. Remove about 3 mL of solution from each tube and place in clean 10-mL tubes and give to the operator with blanks. The operator has standards in the range of 0–1,000 μg/mL, which means that dilutions are not needed. Tell the operator which ions you need (*see* **Note 3**).
2. Calculate as above (step 2 of **Section 3.2.4**).

3.5. Chloridometer

3.5.1. Reagents

1. Nitric/acetic acid reagent (0.4 M HNO_3 and 40% acetic acid): Add 25.6 mL concentrated nitric acid to about 500 mL Milli-Q water in a 1-L volumetric flask. Add 400 mL glacial acetic acid slowly to the flask, stirring as you add, and then make up to 1 L. The final concentration in the titration vials should be 0.1 M nitric acid and 10% acetic acid.
2. Gelatin reagent: Dissolve 0.62 g dry gelatin in 100 mL of boiling Milli-Q water in a beaker. Dispense into 25-mL containers and store in fridge for up to 6 months. Bring back to room temperature before using.

3.5.2. Standards

Make up 0, 0.1, 0.3, 0.5, 0.7 and 1 mM Cl^- standards (e.g. use NaCl).

3.5.3. Dilutions

Add volumes of extracts required to give sample dilutions so that Cl^- falls in the range of the standard curve. Examples of dilutions for K^+ and Na^+ are given above.

3.5.4. Operation

The following protocol is for older machines (e.g. Buchler–Cotlove Chloridometer 662201). For newer models (e.g. Sherwood 926), the reagents and principles are the same, except a smaller volume of extract (e.g. 20 μL or 100 μL) is added directly to a 100 mL solution containing the reagents, which needs replacing only every 20 samples.

1. Clean all electrodes thoroughly with silver polish, and rinse, before turning on the machine.
2. Set the range of the machine to medium (0–0.5 mM) unless low concentrations are expected (i.e. less than 0.1 mM), then use the low range.
3. Switch the machine on and after 10 s stop the stirrer by manual shut off. Set titration switch to titrate, move adjustable red pointer to coincide with the indicator black pointer. A click will be heard as the relay is activated. Move the red pointer to about 20 μA (black one will follow).
4. Allow 30 min for machine to warm up.
5. Prepare sample vials: Add 3 mL of diluted extract (or blank or standard), 1 mL nitric/acetic acid reagent and 200 μL of gelatin reagent to glass vials.
6. Condition the electrodes by titration of three blanks (3 mL of blank plus reagents as above). Place the vial into the metal holder and raise so that solution covers the electrodes and the vial fits over the plastic housing above the electrodes. Turn titration switch to adjust. Wait for the black needle to fall to a stable value of <5 μA (will probably take until the third blank). When it does fall below 5, move the red pointer to 10 μA above the black pointer (i.e. about 15). Ensure before each sample that there is a difference of about 10 μA between the red and black needles. Turn the titration switch to titrate. Record the time when the timer shuts off and reset this between samples.
7. Run all the standards to generate a standard curve of time vs millimolar of Cl^-.
8. Run all samples, blanks and reference tests.
9. If the machine is left for >5 min, then another blank must be measured to make sure that the black needle is falling below 5 μA. Run a check standard approximately every 20

samples to check for any drift. If there is drift, it is likely that the electrodes need cleaning with silver polish. Turn off the instrument prior to cleaning electrodes.

10. To re-use glass vials, rinse with DI water and dry with paper towels (*see* **Note 4**).

3.5.5. Calculating Concentrations

1. Convert the readings in seconds to Cl^- concentrations in millimolar using the standard curve.
2. Convert millimolar Cl^- in samples into micromolar per gram DW = (concentration in micromol × dilution factor, e.g. 100 for 1:100 dilution × volume of acid extract, e.g. 10 mL) / (DW of tissue extracted).

3.6. Colorimetric Determination of Cl (Ferricyanide Method)

Ferric thiocyanate absorbs strongly at 480 nm. The calibration fits a second-order polynomial (12).

3.6.1. Reagents

1. Stock mercuric thiocyanate solution: Dissolve 4.17 g $Hg(SCN)_2$ in about 500 mL methanol, dilute to 1,000 mL with methanol, mix and filter through filter paper. *Caution*: Mercuric thiocyanate is toxic. Wear gloves!
2. Stock ferric nitrate solution: Dissolve 202 g $Fe(NO_3)_3 \bullet 9H_2O$ in about 500 mL distilled water, then carefully add 25 mL concentrated HNO_3. Dilute to 1,000 mL with distilled water and mix. Filter through paper and store in an amber bottle.
3. Combined colour reagent: Add 150 mL stock $Hg(SCN)_2$ solution to 150 mL stock $Fe(NO_3)_3$ solution. Mix and dilute to 1,000 mL with distilled water.
4. Stock chloride solution: Dissolve 1.6482 g NaCl, dried overnight at 140°C, in distilled water and dilute to 1,000 mL; 1.00 mL solution is equivalent to 1.00 mg Cl.

3.6.2. Standard Chloride Solutions

1. Prepare a set of chloride standards in the desired concentration range, such as 1, 2, 5, 10, 20, 40, 60, 80, 100, 140, 200 mg/L, using stock chloride solution and making to volume with 0.5 M HNO_3 extractant. N.B. Remember to include some acid blanks.
2. To make up this standard set using 100-mL volumetric flasks, pipette 100 μL, 200 μL, 0.5 mL, 1.0 mL, 2 mL, 6 mL, 8 mL, 10 mL, 14 mL and 20 mL of the standard chloride solution and make up to the mark with 0.5 M HNO_3.

3.6.3. Method

1. Pipette 1 mL of the standard chloride solutions, the samples and blanks into labelled plastic tubes. Pipette 3 mL of com-

bined colour reagent into each tube and mix. The absorption of the resulting colour is measured using a spectrophotometer with the wavelength set at 480 nm.

2. Prepare a standard calibration curve by plotting the measured absorption against the chloride concentration in the standards. Use this curve to determine the chloride concentration of the samples.
3. Report only those values that fall between the lowest and the highest calibration standards. Samples exceeding the highest standard should be diluted and reanalysed.
4. If the supernatant of extracted samples is highly coloured, they may be clarified, before adding the colour reagent, by adding some washed activated carbon, shaking, then filtering. Ensure that a couple of blanks are similarly treated and measured.
5. Report results in milligrams of Cl per litre (*see* **Note 4**).
6. Convert to millimolar Cl and then into micromolar per gram DW (see 3.5.5).

4. Notes

1. A decision must be made to present ion concentrations on a water basis (mM) or dry weight basis (μmol/g DW or mmol/g DW). The water content (amount of water per gram dry weight) is quite different for different parts of a leaf. In monocotyledonous species, the sheath has higher water content than does the blade; in dicotyledonous species, the blade usually has a high water content than does the petiole. Calculation on a water content or a fresh weight basis is therefore not valid for a whole shoot, so ions should be expressed on a dry weight basis.
2. Some laboratories have measured ion concentrations in expressed sap from leaves (13), but as critical toxicity values have been determined on a dry weight basis (14), and as sap ion concentrations can change with changes in water content as well as ion content, this method has not been widely adopted. The method is valid for ion ratios, such as K^+/Na^+, but caution is needed if comparing different treatments as leaf water content can change markedly with different salinity treatments.
3. A wide range of elements in plant tissue can be analysed with ICP-AES. However, this simple dilute acid extraction is not recommended when a complete elemental analysis is required. It has been found that there is incomplete recovery

for some elements, particularly those elements which play a structural role in the plant or are present in a relatively insoluble form. Performing a complete, conventional elemental analysis requires the plant tissue to be digested in concentrated nitric acid or a mixture of nitric/perchloric acids at high temperature (15).

4. It is important to ensure that hazardous chemical waste is disposed of in a manner that complies with local regulations.

References

1. Munns R. (2005). Genes and salt tolerance: bringing them together. *New Phytol* **167**, 645–663.
2. Flowers, T.J. and Colmer, T.D. (2008). Salinity tolerance in halophytes. *New Phytol* **179**, 945–963.
3. Munns, R. and Tester, M. (2008). Mechanisms of salinity tolerance. *Annu Rev Plant Biol* **59**, 651–681.
4. Munns, R. (2009). Approaches to identifying genes for salinity tolerance, and the importance of time scale (this volume).
5. Rivelli, A.R., James, R.A. Munns, R., and Condon, A.G. (2002). Effect of salinity on water relations and growth of wheat genotypes with contrasting sodium uptake. *Funct Plant Biol* **29**, 1065–1074.
6. Lacerda, C.F., Cambraia, J., Oliva, M.A., Ruiz, H.A., and Prisco, J.T. (2003). Solute accumulation and distribution during shoot and leaf development in two sorghum genotypes under salt stress. *Environ Exp Bot* **49**, 107–120.
7. Munns, R. and James, R.A. (2003). Screening methods for salinity tolerance: a case study with tetraploid wheat. *Plant Soil* **253**, 201–218.
8. James, R.A., Davenport, R.J., and Munns, R. (2006). Physiological characterization of two genes for Na^+ exclusion in durum wheat, *Nax1* and *Nax2*. *Plant Physiol* **142**, 1537–1547.
9. Prior, L.D., Grieve, A.M., and Cullis, B.R. (1992). Sodium chloride and soil texture interactions in irrigated field grown sultana grapevines. II. Plant mineral content, growth and physiology. *Aust J Agric Res* **43**, 1067–1083.
10. Hunt, J. (1982). Dilute hydrochloric acid extraction of plant material for routine cation analysis. *Commun Soil Sci Plant Anal* **13**, 49–55.
11. AWWA, APHA. (1998). *Standard Methods for the Examination of Water and Wastewater*, 18th ed. AWWA, APHA. Method 4500 Cl^-.
12. Pruefer, A. (2001) *Determination of Chloride by Flow Injection Colorimetry (Mercuric Thiocyanate Method)*. Lachat Instruments QuikChem Method 10-117-07-1-B.
13. Gorham, J., Bristol, A., Young, E.M., and Wyn Jones, R.G. (1991). The presence of the enhanced K/Na discrimination trait in diploid *Triticum* species. *Theoret Appl Genet* **82**, 729–736.
14. Reuter, D.J. and Robinson, J.B. (2007) *Plant Analyses: An Interpretation Manual*, 2nd ed. CSIRO Publishing, Collingwood, Australia.
15. Zarcinas, B.A., Cartwright, B., and Spouncer, L.R. (1987) Nitric acid digestion and multi-element analysis of plant material by inductively coupled plasma spectrometry. *Commun Soil Sci Plant Anal* **18**, 131–146.

Subject Index

R. Sunkar (ed.), Plant Stress Tolerance, Methods in Molecular Biology 639,
DOI 10.1007/978-1-60761-702-0,

E

F

G

H

I

K

L

M

N

O

P

Q

R

S

T

U

V

W

Z